This document is made available through the declassification efforts and research of John Greenewald, Jr., creator of:

The Black Vault

The Black Vault is the largest online Freedom of Information Act (FOIA) document clearinghouse in the world. The research efforts here are responsible for the declassification of hundreds of thousands of pages released by the U.S. Government & Military.

**Discover the Truth** at: **http://www.theblackvault.com**

AD-A131 869   PROCEEDINGS OF INTERNATIONAL WORKSHOP ON ATMOSPHERIC   1/4
ICING OF STRUCTURES (..(U) COLD REGIONS RESEARCH AND
ENGINEERING LAB HANOVER NH  L D MINSK JUN 83
UNCLASSIFIED   CRREL-SR-83-17   F/G 8/12   NL

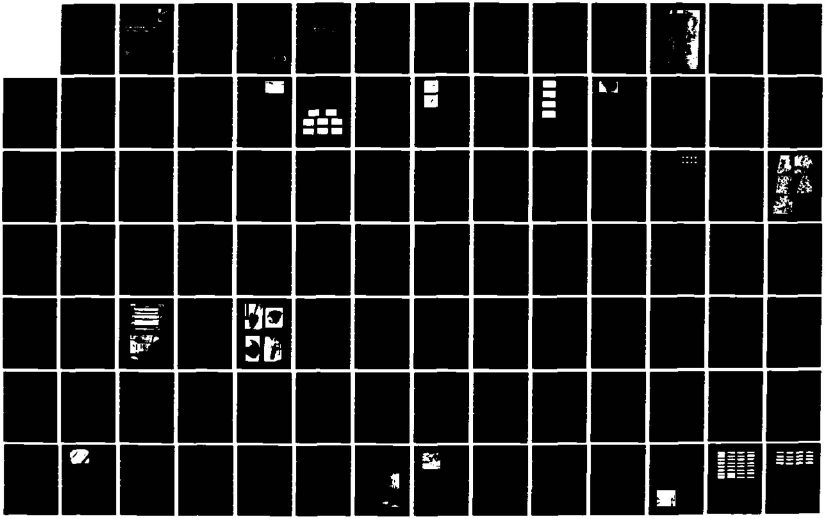

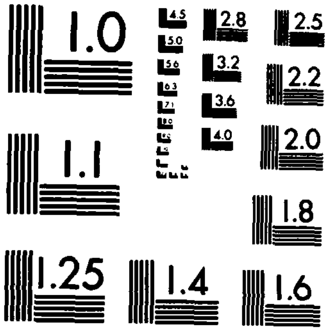
1.0
4.5
5.0
5.6
6.3
7.1
8.0
2.8
3.2
3.6
4.0
2.5
2.2
2.0
1.1
1.8
1.25
1.4
1.6

MICROCOPY RESOLUTION TEST CHART
NATIONAL BUREAU OF STANDARDS-1963-A

ADA131869

⑫

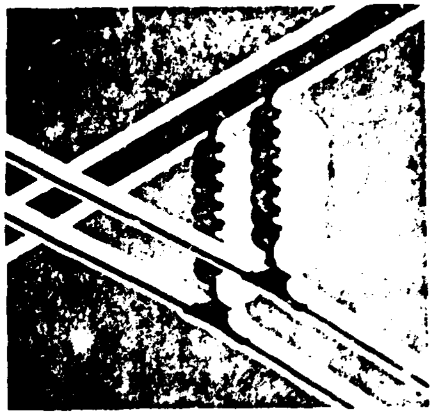

## Proceedings of First International Workshop

# ATMOSPHERIC ICING OF STRUCTURES

### Special Report 83-17

DTIC
AUG 2 1983
A

DTIC FILE COPY

**US Army Corps of Engineers**
Cold Regions Research & Engineering Laboratory

**EPRI** Electric Power Research Institute

83 08 19 034

①

# COMPONENT PART NOTICE

THIS PAPER IS A COMPONENT PART OF THE FOLLOWING COMPILATION REPORT:

(TITLE): Proceedings of International Workshop on Atmospheric Icing of Structures (1st) Held at Hanover, New Hampshire on 1-3 June 1982.

(SOURCE): Cold Regions Research and Engineering Lab., Hanover, NH.

TO ORDER THE COMPLETE COMPILATION REPORT USE AD-A131 869.

THE COMPONENT PART IS PROVIDED HERE TO ALLOW USERS ACCESS TO INDIVIDUALLY AUTHORED SECTIONS OF PROCEEDINGS, ANNALS, SYMPOSIA, ETC. HOWEVER, THE COMPONENT SHOULD BE CONSIDERED WITHIN THE CONTEXT OF THE OVERALL COMPILATION REPORT AND NOT AS A STAND-ALONE TECHNICAL REPORT.

THE FOLLOWING COMPONENT PART NUMBERS COMPRISE THE COMPILATION REPORT:

| AD#: | TITLE: |
|---|---|
| AD-P001 666 | Measurement of Water Droplet Distributions in an Icing Wind Tunnel by Holography. |
| AD-P001 667 | Contribution to the Modeling of the Ice Accretion Process: Ice Density Variation with the Impacted Surface Angle. |
| AD-P001 668 | Icing Research on Mount Washington, New Hampshire. |
| AD-P001 669 | Mechanisms for Ice Bonding in Wet Snow Accretions on Power Lines. |
| AD-P001 670 | Attempts Toward Estimating Ice Loadings Based on General Climatological Data. |
| AD-P001 671 | Icing of Cables. |
| AD-P001 672 | Numerical Simulation of Ice Accretion on Cables. |
| AD-P001 673 | Design and Testing of a Lagrangian Computer Model for Simulating Time-Dependent Rime Icing on Two-Dimensional Structures. |
| AD-P001 674 | Aspects of Freezing Rain Simulation and Testing. |
| AD-P001 675 | Ice as an Influence on Compact Line Phase Spacing. |
| AD-P001 676 | Adhesion of Ice on Aluminum Conductor and Crystal Size in Surface Layer. |
| AD-P001 677 | How Effective are Icephobic Coatings? |
| AD-P001 678 | Adhesion of Ice from Helicopter Rotor Blades: Preliminary Work. |
| AD-P001 679 | Aircraft Icing Research at NASA. |
| AD-P001 680 | Studies of High-Speed Rotor Icing under Natural Conditions. |
| AD-P001 681 | Ice Treeing under DC and AC Electric Fields at Different Intensities of Accretion. |
| AD-P001 682 | The Impact of Falling Ice on Elastic Structures. |
| AD-P001 683 | Estimation of Combined Ice and Wind Load on Overhead Transmission Lines. |
| AD-P001 684 | Application of a Block Copolymer Solution to Ice-Prone Structures. |
| AD-P001 685 | Ice-Phobic Coatings Applied to Saline-Ice-Covered Whip-Type Antennas. |
| AD-P001 686 | The Effect of Meteorological Parameters on Rime Formation in Finland. |
| AD-P001 687 | Determining Atmospheric Parameters during Ice Accretion from the Microstructure of Natural Ice Samples. |
| AD-P001 688 | Icing Cloud Microstructure from in situ Measurements. |
| AD-P001 689 | Surface Icing Research at AFGL. |

# COMPONENT PART NOTICE (CON'T)

| AD#: | TITLE: |
|---|---|
| AD-P001 690 | Field Measurements of Combined Icing and Wind Loads on Wires. |
| AD-P001 691 | An Application of Dendrochronology to the Determination of the Recurrence of Severe Ice Storms. |
| AD-P001 692 | Damages of Structures due to Ice and Wind. |
| AD-P001 693 | Icing Related Problems, Effect of Line Design and Ice Load Mapping. |
| AD-P001 694 | Ice Accumulation on Tall Radio and TV Towers in Finland. |
| AD-P001 695 | Icing and Combined Wind and Ice Design Loadings for Transmission Lines in Remote Areas. |
| AD-P001 696 | Predicting Ice and Snow Loads for Transmission Line Design. |
| AD-P001 697 | Iceload Measurements and Design Practice. |
| AD-P001 698 | Measurement of Ice Accretion on Overhead Transmission Line Conductors. |
| AD-P001 699 | Extreme Glaze and Rime Ice Loads in Southern California. Part 1. Rime. |
| AD-P001 700 | Extreme Glaze and Rime Ice Loads in Southern California. Part 2. Glaze. |
| AD-P001 701 | Field Research on the Galloping of Iced Conductors: A Status Report. |
| AD-P001 702 | Development of an Ice and Snow Load Transducer to Simulate Transmission Line Loading. |
| AD-P001 703 | Experience Concerning Ice Loads on Overhead Lines in Austria. |
| AD-P001 704 | Methods of Calculating Icing Loads on Overhead Lines as Spatial Constructions. |

Accession For
NTIS GRA&I ☒
DTIC TAB ☐
Unannounced ☐
Justification
By
Distribution/
Availability Codes
Avail and/or
Dist Special
A

DTIC
ELECTE
AUG 31 1983
S D
A

This document has been approved for public release and sale; its distribution is unlimited.

# Proceedings of
# First International Workshop

# ATMOSPHERIC ICING
# OF STRUCTURES

1 – 3 June 1982
Hanover, New Hampshire

L.D. Minsk, Editor

United States Army, Corps of Engineers
Cold Regions Research and Engineering Laboratory

Electric Power Research Institute

CRREL Special Report 83-17
June 1983

# Preface

The accumulation of ice in its various forms on structures has long been recognized as a significant and costly problem for both industry and government world-wide. Though many efforts have been made to understand the mechanics of ice accretion and to improve designs of structures to ameliorate the effects of ice, and some of these efforts have been described in technical meetings, heretofore there has not been a conference that specifically dealt with this subject and that brought together scientists and engineers from the many disciplines participating in this work. Recognition of this by the Electric Power Research Institute (EPRI), the research arm of the United States' utility industry, and by CRREL, representing the U.S. Government's interests, led to the planning for an international workshop. An organizing committee was formed to solicit and screen contributed papers. Members of this committee were:

Joe Pohlman, consultant (representing EPRI).

Jean Laflamme, Hydro-Quebec, Montreal, Quebec, Canada.

Magnar Ervik, Elektrisitetsforsyningens Forskningsinstitutt (EFI) (The Norwegian Research Institute of Electricity Supply).

L. David Minsk, U.S. Army Cold Regions Research and Engineering Laboratory.

The purpose of this First International Workshop on Atmospheric Icing of Structures was to bring together scientists, engineers and managers from industrial and military organizations from around the world that have an interest in the accretion of ice on structures. The presumption underlying the use of "First" in the title of the workshop is that this meeting would demonstrate the need for continued exchange of ideas, of reports of work accomplished and of future plans, and further identification of research areas requiring particular attention.

The 39 papers from 10 countries presented at the workshop were organized into four technical sessions representing the various aspects of structural ice accretion studies underway. Topics included:

| | |
|---|---|
| Session 1 | Basic research;<br>Physics of ice accretion;<br>Simulation and modeling, |
| Session 2 | Design-oriented research, |
| Session 3 | Meteorological measurements and damage observations; and |
| Session 4 | Iceload measurements and design practices, |

In addition, in view of this first forum on the subject, a fifth session was held to discuss the accomplishments of this first workshop, to expose gaps in the knowledge of atmospheric ice accretion processes, and to lay plans for the future. This proceedings volume includes the camera-ready reports furnished by all the authors, a transcription of tape-recorded discussions following some of the papers, and the transcript of the final review and planning session.

A conference of this size is not the product of one person. In addition to the recognition that the members of the organizing committee are due for their efforts, special thanks are extended to Phil Landers of EPRI, and to the following members of the CRREL staff: Ben Yamashita and David Langlois for handling arrangements, and Donna Murphy for production of this proceedings volume.

L.D. Minsk
U.S. Army Cold Regions Research and
Engineering Laboratory
Proceedings Editor

Ac sion For
NT GRA&I ☒
TAB ☐
ounced ☐
fication
By
Distribution/
Availability Codes
Avail and/or
Dist Special
A
DTIC
COPY
ED

CONTENTS

Page

Preface------------------------------------------------ ii

Registration list-------------------------------------- ix

SESSION 1: BASIC RESEARCH (Jean Laflamme, Chairman)---------- 1

Physics of Ice Accretion---------------------------------- 1

Measurement of water droplet distributions in an icing wind tunnel by holography, E.M. Gates------------------------ 3

Contribution to the modeling of the ice accretion process: Ice density variation with the impacted surface angle, M. Bain and J.F. Gayet---------------------------------- 13

Icing research on Mt. Washington, N.H., J.B. Howe------------ 21

Mechanisms for ice bonding in wet snow accretions on power lines, S.C. Colbeck and S.F. Ackley-------------------- 25

Simulation and Modeling---------------------------------- 31

Attempts toward estimating ice loadings based on general climatological data, M. Ervik and S.M. Fikke------------ 33

Icing of cables, B.W. Smith and C.P. Barker------------------ 41

Numerical simulation of ice accretion on cables, P. McComber- 51

The design and testing of a Lagrangian computer model for simulating time-dependent rime icing on two-dimensional structures, M.M. Oleskiw and E.P. Lozowski-------------- 59

Aspects of freezing rain simulation and testing, J.R. Stallabrass------------------------------------------------ 67

SESSION 2: DESIGN-ORIENTED RESEARCH (Magnar Ervik, Chairman)- 75

Ice as an influence on compact line phase spacing, J.R. Stewart------------------------------------------------ 77

Adhesion of ice on aluminum conductor and crystal size in the surface layer, J.L. Laforte, C.L. Phan, B. Félin and R. Martin------------------------------------------------ 83

How effective are icephobic coatings?, L.D. Minsk------------ 93

Abhesion of ice from helicopter rotor blades: Preliminary work, H.H.G. Jellinek and I. Chodak-------------------- 97

Aircraft icing research at NASA, J.J. Reinmann, R.J. Shaw and W.A. Olsen, Jr.------------------------------------ 103

Studies of high-speed rotor icing under natural conditions, K. Itagaki, G.E. Lemieux, H.W. Bosworth, J. O'Keefe and G. Hogan------------------------------------------------ 117

Ice treeing under DC and AC electric fields at different intensities of accretion, L.C. Phan, J.L. Laforte and D.D. Nguyen------------------------------------------------ 125

The impact of falling ice on elastic structures, J.R. Murat and L. Lainey------------------------------------------- 135

Estimation of combined ice and wind load on overhead transmission lines, P. McComber, R. Martin, G. Morin and L.V. Van ------------------------------------------------ 143

Page

Application of a block copolymer solution to ice-prone structures, B. Hanamoto---------- 155
"Ice-phobic" coatings applied to saline-ice-covered whip-type antennas, E.A. Thowless---------- 159
A review of the effect of ice storms on the power industry (abstract), W.B. Bendel and D. Paton---------- 163

SESSION 3: METEOROLOGICAL MEASUREMENTS AND DAMAGE OBSERVATION (L. David Minsk, Chairman)---------- 165

The effect of meteorological parameters on rime formation in Finland, L. Makkonen and K. Ahti---------- 167
Determining atmospheric parameters during ice a-cretion from the microstructure of natural ice samples, J.L. Laforte, C.L. Phan, D.D. Nguyen and B. Félin---------- 175
Icing cloud microstructure from in situ measurements, J.F. Gayet and M. Bain---------- 185
Surface icing research at AFGL, P. Tattelman---------- 195
Field measurements of combined icing and wind loads on wires, J.W. Govoni and S.F. Ackley---------- 205
An application of dendrochronology to the determination of the recurrence of severe ice storms, B. Félin and J. Rivest---------- 217
Damages of structures due to ice and wind, S. Plazinic and N. Miljkovic---------- 225
Icing related problems, effect of line design and ice load mapping, Eu.P. Nikiforov---------- 239

SESSION 4: ICELOAD MEASUREMENTS AND DESIGN PRACTICES (Béatrice Félin, Chairman)---------- 247

Ice accumulation on tall radio and TV towers in Finland, Y. Jaakkola, J. Laiho and M. Vuorenvirta---------- 249
Icing and combined wind and ice design loadings for transmission lines in remote areas, M.C. Richmond---------- 261
Predicting ice and snow loads for transmission line design, E.J. Goodwin, III, J.D. Mozer, A.M. DiGioia, Jr. and B.A. Power---------- 267
Iceload measurements and design practice, S.M. Fikke, K. Schjetne and B.D. Evensen---------- 277
Measurement of ice accretion on overhead transmission line conductors, S.G. Krishnasamy---------- 291
Extreme glaze and rime ice loads in Southern California: Part I--Rime, J.H. Mallory and D.C. Leavengood---------- 299
Extreme glaze and rime ice loads in Southern California: Part II--Glaze, J.H. Mallory and D.C. Leavengood---------- 309
Field research on the galloping of iced conductors: A status report, J.C. Pohlman and D. Havard---------- 319
Development of an ice and snow load transducer to simulate transmission line loading, N.W. Brodie and D.E. Franklin---------- 327
Experience concerning ice loads on overhead lines in Austria, H. Schauer and W. Hammerschmid---------- 335
Methods of calculating icing loads on overhead lines as spatial constructions, T.N. Golikova, B.F. Golikov and D.S. Savvaitov---------- 341

Page

SESSION 5: PLANNING OF FUTURE ATMOSPHERIC ICING RESEARCH (J. Pohlman, Chairman)---------------------------- 347

Discussion by All Attendees

Summary------------------------------------------------------- 349

COLD REGIONS
RESEARCH & ENGINEERING
LABORATORY
U.S. ARMY
CORPS OF ENGINEERS

# FIRST INTERNATIONAL WORKSHOP ON ATMOSPHERIC ICING OF STRUCTURES

1-3 June 1982

## Registration List

Dr. William B. Bendel, Manager of Permitting Operations, Environmental
Research and Technology, Inc., 696 Virginia Rd., Concord, MA 01742. (617)
369-8910.

Richard L. Berry, Head, Building and Construction Research Unit,
Atmospheric Environment Service, 4905 Dufferin St., Downsview, Ontari
Canada M3H 5T4. (416) 667-4917.

Michel Boutteau, Chef du Departement Exploitation, Électricité de Fra
Service du Transport, 22, 30 Avenue de Wagram, Paris, France 75008. (
764.85.09.

N.R. Cuer, Assistant Chief Transmission Engineer (Design), Kennedy &
Donkin, Premier House, Woking, Surrey, England GU21 1DG. Woking (04862)
5900.

Magnar Ervik, Chief Engineer - Senior Research Office, Norwegian Research
Institute of Electricity Supply, c/o EFI, Sem Saelandsv. 11, 7034
Trondheim-NTH, Norway. (Int) 47-75-32520.

Bjorn Dag Evensen, Senior Engineer, Norwegian Water Resources and
Electricity Board, State Power Systems, Middelthuns GT. 29, Oslo 3,
Norway. 02-469800.

Béatrice Félin, Group Leader - Meteorology, Hydro-Québec, 855 E.
Sainte-Catherine, Montréal, QC, Canada H2L 4P5. (514) 289-5086.

Svein M. Fikke, Meteorologist, Norwegian Research Institute of Electricity
Supply, Sem Saelandsv. 11, 7034 Trondheim - NTH, Norway. 2-60-5090.

P.J. Florio, Assistant Professor, New Jersey Institute of Technology, 323
Hight St., Newark, NJ 07102. (201) 645-5451.

Douglas E. Franklin, Mechanical Research Engineer, B.C. Hydro, 12388-88
Ave., Surrey, British Columbia, Canada V3W 7R7. (604) 591-0240.

Edward M. Gates, Associate Professor, Department of Mechanical Engineering,
University of Alberta, Edmonton, Alta., Canada T6G 2G8. (403) 432-5180.

Jean-Francois Gayet, Ingénieur, Laboratoire Associé de Météorologie
Physique, Université de Clermont II, Complexe Scientifique des Cézeaux,
B.P. 45, Aubière, France 63170. (73) 26.41.10.

Jay Gonzalez, Research Engineer, ARCO Oil and Gas Company, Plano, Texas. (214) 422-6506.

Edwin J. Goodwin, Senior Project Engineer, Pennsylvania Power & Light Co., Two North Ninth St., Allentown, PA 18101. (215) 770-4695.

John B. Howe, Staff Engineer, Mt. Washington Observatory, Gorham, NH 03851. (603) 466-3388.

Yrjö Jaakkola, Head of Planning, Masts and Antennas, Finnish Broadcasting Co., Päijänteentie 18, 00550 Helsinki 55, Finland. 358/0/4016592.

Dr. H.H.G. Jellinek, Research Professor, Clarkson College, Potsdam, NY 13676. (518) 768-2394.

Dr. S. (Samy) Krishnasamy, Engineer - Structures, Ontario Hydro, 800 Kipling Ave., Toronto, Ontario, Canada M8Z 5S4. (416) 231-4111.

Jean Laflamme, Assistant Manager, Hydro-Québec, 855 E. Ste-Catherine, Montréal, Québec, Canada H2L 4P5. (514) 289-5089.

Jean-Louis Laforte, Professor, Université du Québec à Chicoutimi, 555, chemin St-Thomas, Chicoutimi, Quebéc, Canada G7H 2P9. (418) 545-5403.

Dr. Luc Lainey, Research Associate, École Polytechnique, Montréal, Québec, Canada H3C 3A7. (514) 344-4613.

Phil Landers, Project Manager, EPRI, P.O. Box 10412, Palo Alto, CA 94303. (415) 855-2307.

David C. Leavengood, Manager of Atmospheric Sciences, Engineering-Science, 125 W. Huntington Dr., P.O. Box 538, Arcadia, CA 91006. (213) 445-7560.

Dr. E.P. Lozowski, Professor, University of Alberta, Edmonton, Alberta, Canada T6G 2H4. (403) 432-5672.

Jack R. Maison, Director, Department of Structural Research, Southwest Research Institute, P.O. Drawer 28510, San Antonio, Texas 78284. (512) 684-5111.

Lasse Makkonen, Institute of Marine Research, P.O. Box 16, SF-00141, Helsinki 14, Finland. 90 651566.

Richard C. Martin, Group Leader, Hydro-Quebéc, 855 East Ste-Catherine, Montréal, Québec, Canada H2L 4P5. (514) 289-5084.

Pierre McComber, Professor, Université du Québec à Chicoutimi, 555, chemin St-Thomas, Chicoutimi, Québec, Canada G7H 2P9. (418) 545-5296.

John D. Mozer, Engineering Manager, GAI Consultants, Inc., 570 Battey Rd., Monroeville, PA 15146. (412) 856-6400.

Jon W. Nauman, Oceanographer, DOI - Minerals Management Service, 800 A Street, Anchorage, Alaska 99501. (907) 271-4303.

Dr. Myron M. Oleskiw, Research Meteorologist, INTERA Environment Consultants Ltd., P.O. Box 5487, Station A, Calgary, Alberta, Canada T2H 1X9. (403) 253-8895.

Dr. William Olsen, Research Engineer, NASA-Lewis Research Center, 21000 Brookpark Rd., Cleveland, Ohio 44012. (216) 433-4000.

Dr. Jacob Patnaik, Engineering Section, U.S. Coast Guard (G-EVC), 2100 2nd Street, N.W., Washington, D.C. 20593. (202) 426-1314.

Dr. C. Luan Phan, Professor, Université du Québec à Chicoutimi, 555, chemin St-Thomas, Chicoutimi, Québec, Canada G7H 2P9. (418) 545-5289.

Joe C. Pohlman, Consulting Engineer, P.O. Box 15098, Pittsburgh, PA 15237. (412) 366-0066.

B.A. Power, President, Weather Engineering Corporation of Canada, Ltd., P.O. Box 2060, Dorval, Quebec, Canada H9S 3K7. (514) 636-0293.

C.B. Rawlins, Technical Consultant, ALCOA Conductor Products Co., P.O. Box 150, Massena, NY 13662. (315) 764-4235.

M.C. Richmond, Manager, Meteorology Department, Meteorology Research, Inc., 464 West Woodbury Rd., Altadena, CA 91001. (213) 791-1901.

Charles E. Smith, Assistant Research Program Manager, Minerals Management Service, 620 National Center, Reston, VA 22092. (703) 860-7865.

Hilda J. Snelling, Assistant Chief, Engineering Meteorology Section, U.S. Air Force Environmental Technical Applications Center, Scott Air Force Base, IL 62225. (618) 256-3641/5008; AV 638-3641/5008.

James R. Stallabrass, Senior Research Officer, National Research Council of Canada, Montreal Rd., Ottawa, Canada K1A 0R6. (613) 993-2371.

James R. Stewart, Senior Engineer, Power Technologies, Inc., P.O. Box 1058, Schenectady, NY 12301. (518) 374-1220.

Paul Tattelman, Meteorologist, U.S. Air Force Geophysics Laboratory, Hanscom Air Force Base, Bedford, MA 02368. (617) 861-5957.

Eric Thowless, Electrical Engineer, Naval Ocean Systems Center, Code 8122, San Diego, CA 92152. (714) 225-2646; AV 933-2646.

Matti Vuorenvirta, Head of Mast Engineering, Finnish Broadcasting Company, Päijänteentie 18, 00550 Helsinki 55, Finland. 358/0/441141.

Robert Whapham, Manager, Laboratory Operations, Preformed Line Products Company, 660 Beta Dr., Mayfield Village, Ohio 44143. (216) 461-5200.

Participating personnel from:

U.S. Army Cold Regions Research and Engineering Laboratory, 72 Lyme Rd., Hanover, NH 03755 (603) 646-4100; AV 684-4100; FTS 836-4100.

Stephen F. Ackley, Chief, Snow & Ice Branch, Ext. 4258
Dr. Andrew Assur, Chief Scientist, Ext. 4237.
Hazen (Bill) Bosworth, Physical Science Technician, Ext. 4416.
Dr. Samuel Colbeck Jr., Geophysicist, Ext. 4257.
Guenther Frankenstein, Chief, Ice Engineering Research Branch, Ext. 4343.
John W. Govoni, Physical Science Technician, Ext. 4268.
Ben Hanamoto, Research General Engineer, Ext. 4276.
Col. Wayne A. Hanson, Commander and Director, Ext. 4200.
Dr. Kazuhiko Itagaki, Research Physicist, Ext. 4255.
George E. Lemieux, Research Physicist, Ext. 4255.
L. David Minsk, Research Physical Scientist, Ext. 4474.
Albert F. Wuori, Chief, Experimental Engineering Division, Ext. 4405.

# SESSION 1: BASIC RESEARCH

## Physics of Ice Accretion

AD P001666

# MEASUREMENT OF WATER DROPLET DISTRIBUTIONS IN AN ICING WIND TUNNEL BY HOLOGRAPHY

E.M. Gates Department of Mechanical Engineering,
University of Alberta

The standard methods for determining liquid water content and water droplet size distribution are the single rotating cylinder and the oil slide technique respectively. With the development of laser technology several other techniques have been introduced, namely: light scattering and holography. The advantages of the holography method is that in a single measurement both the liquid water content and the droplet size distribution can be determined. The holography technique however has some serious disadvantages. Aside from the expense involved, the reduction of the data is tedious and involves some judgment. Also, a good image of any water droplet is obtained only over a range of distances from the film plane which is a function of droplet size. This is a particularly serious handicap when examining the smaller droplets (∿ 10 micrometers diameter).

The results of a preliminary comparison between the rotating cylinder and oil slide measurements with those obtained by holography show good agreement for liquid water contents, but indicate the oil slide technique over-predicts the median volume diameter.

Start

## INTRODUCTION

Water droplet populations in the atmosphere and in facilities for simulating atmospheric icing are characterized by two parameters: (i) water mass per unit volume of air (liquid water content (LWC)) and (ii) some measure of the droplet size distribution - normally the median volume diameter (MVD). At the icing wind tunnel (FROST*) at the University of Alberta these quantities have been measured by the single rotating cylinder and the oil slide methods, respectively. With the development of laser technology, several more sophisticated instruments for making these measurements have been introduced. Since these new techniques do not intrude into the flow, but instead depend upon sensing various properties of light scattered from a droplet as it passes through a laser beam, it would appear that these methods would be more advantageous to use and quite possibly more accurate. In particular, of these techniques, holography seems to provide the ultimate instrument. For in a single measurement, a permanent record of the droplets in a volume of the test fluid is obtained. From this record, which can be played back at the investigator's leisure, the liquid water content and the droplet size and spatial distributions can be determined. If the laser can be double pulsed, the droplet velocity can be obtained. And, in addition, under conditions of temperature, air speed and water loading where the rotating cylinder cannot be used (i.e. above the Ludlam limit), the holography method is still applicable. However, holography does have some serious disadvantages which makes its general use impractical.

In this report a holographic system for measuring water droplets in the test

---

* Acronym for Facility of Research on Solidification and Thawing.

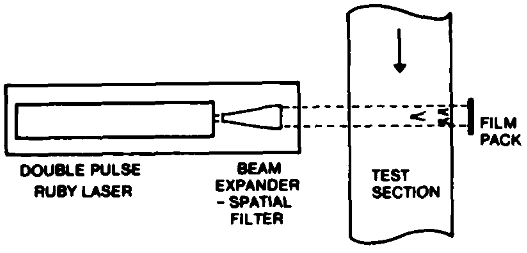

(a) HOLOCAMERA

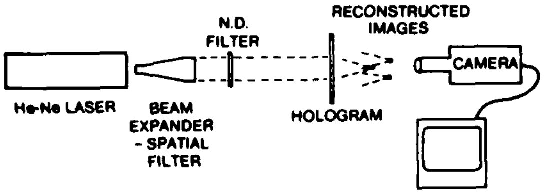

(b) RECONSTRUCTOR

Figure 1. Schematic drawings showing the components of the holocamera and the reconstruction system.

section of an icing wind tunnel will be described. The advantages and disadvantages of the system will be discussed and some preliminary results of a comparison with rotating cylinder and oil slide measurements will be presented.

## DESCRIPTION OF EQUIPMENT

### Holography

Holographic determination of the water droplet distribution involves a two-step process. In the first step the interference pattern produced by the addition of light scattered by a droplet and an undisturbed reference beam is recorded on a special high resolution film. The film is then developed producing a hologram which, in the second step of the procedure, is reconstructed to produce a three-dimensional image of the original droplet.

Following the example of the initial studies in this area (see Wuerker, 1975, or Thompson, 1978), in-line or on-axis holography was used. In addition to being a mechanically straightforward arrangement, it imposes a less stringent requirement on the coherence of the recording beam. It was also decided that a lensless system with a collimated recording beam would be used. This choice was made because it has been shown by Parrent Jr. and Reynolds, 1965, that an in-line, lensless system employing plane waves provides the maximum resoolution. Also, in a lensless system the magnification is constant through the depth of the sample volume, whereas in a system employing a lens it varies and hence makes sizing the particles more difficult. The experimental arrangements for both recording and reconstructing the holograms are shown schematically in Figure 1 and in Figure 2 a photograph of the recording system is presented.

Figure 2. A photograph of the arrangement of the equipment at the FROST tunnel.

In the recording system a KORAD K1QDH pulsed ruby laser provides a 10 mJ, 30 nanosecond, $TEM_{00}$ mode pulse. This beam then passes through a combined spatial filter-beam expander producing a collimated beam 4.5 cm in diameter which was then directed through the test section of the tunnel. The interference pattern produced by the addition of the light scattered by droplets and unscattered light was then recorded on film. In the experiments reported here Agfa-Gevaert 8E75 and 10E75 holographic film plates were used. Processing of these plates was carried out according to a procedure summarized in Collier, Burckhardt and Lin. Neutral density filters were used to control film density to be near 1 or somewhat greater.

Reconstruction of the hologram was carried out with the equipment illustrated in Figure 1(b). The output of a 5 mw He-Ne laser was passed through a beam expander-spatial filter to provide a collimated beam to illuminate the hologram. The image of the reconstructed droplet was then focussed onto an RCA Neuvicon camera, which is particularly sensitive in the red end of the visible spectrum, and the image displayed on a TV monitor. Focussing of the droplet image and sweeping out of the sample volume was accomplished by mounting the hologram on a x-y-z translational unit and moving the hologram. By use of the contrast and brightness controls on the monitor and neutral density filters in the illuminating beam the monitor display could be adjusted to maximize droplet visibility. Overall magnification varied between approximately 100 to 250 depending upon the objective used to image the particle onto the camera.

### Rotating Cylinder and Oil Slide

The water droplet population in the test section was also sampled with the rotating cylinder and the oil slide methods. For the rotating cylinder a 2.46 mm diameter cylinder with a sample length of 5.08 cm was used. The cylinder was rotated at approximately 1 Hz and the sample time was normally 60 seconds. Calculation of the liquid water content was carried out employing the recent recommendations of Stallabrass (1978) and median droplet diameters obtained from the holography measurements.

Droplet size distributions were obtained by the oil slide technique. Shell Omala 85 oil was spread over a 3 mm x 10 mm slide which was then exposed to the flow by sliding it past a 3 mm diameter aperture. The slide was then photographed at a magnification of approximately 60. The developed film was then projected onto a screen and the droplets were sized by direct measurement on the screen.

### Resolution of Holographic System

To determine the resolution of the current holographic system, holograms were made of a microscope slide containing polystyrene spheres of 100, 32 and 10 micron diameter. Photographs of the monitor display of the reconstructed images of these particles are given in Figure 3. At a plate to particle distance of 1.5 cm all three sizes of spheres are clearly distinguishable. At 13 cm the 100 micron spheres are still quite distinct, but the boundaries of the 30 micron spheres have become indistinct

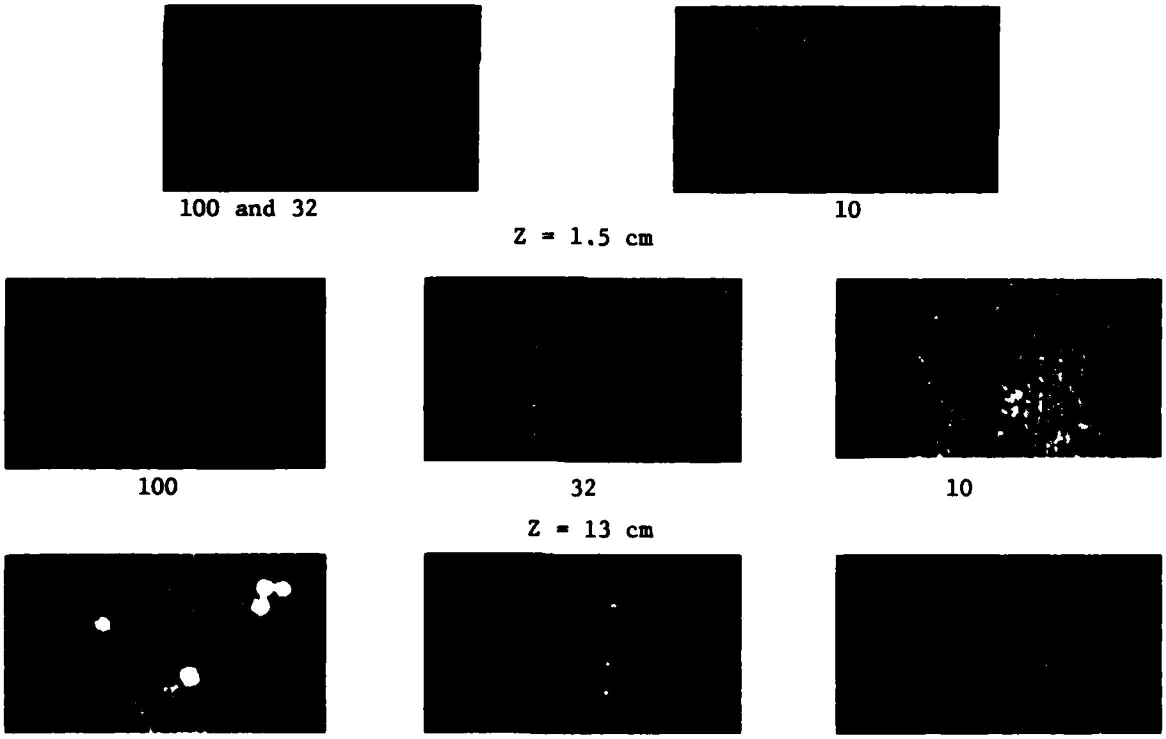

100 and 32

10

Z = 1.5 cm

100

32

10

Z = 13 cm

100

32

10

Z = 26 cm

Figure 3. Photographs of the reconstructed images of 10, 32 and 100 micron diameter polystyrene spheres recorded at various film to particle distances.

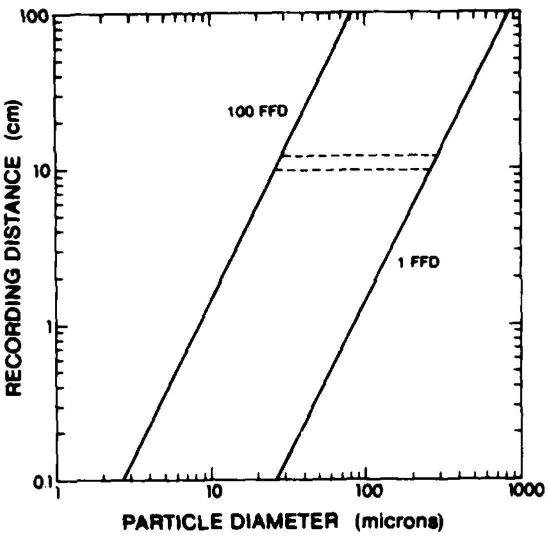

Figure 4. An estimate of the maximum and minimum distances at which a droplet may be resolved with the current holographic system.

and the 10 micron spheres and dirt particles are only detectable as bright points of light against the background. At 26 cm the 100 micron spheres no longer have distinct boundaries, the 30 micron spheres are only detectable and 10 micron spheres are not visible. Hence, for each droplet size, there is an upper bound upon the film to droplet distance at which an acceptable record of the droplet can be made. Expressing the recording or stand-off distance in terms of far-field distances (FFD- the ratio of the square of the droplet diameter to the wavelength of the illuminating beam) a plot has been prepared in Figure 4 giving the depth of field limitations. It was found that an upper bound of 100 FFD suggested by Pitlak et al (1976) agreed well with the present findings. Since the deterioration of the image is gradual, the 100 FFD boundary is not an absolute recording distance, but provides a guideline. Note also in Figure 4 that a minimum distance of at least one FFD is required for the droplet to be in the Fraunhofer region.

This upper bound on the recording distance produces a severe limitation for the lensless system. It would be desirable to be able to detect droplets of at least 10 microns diameter. From Figure 4 then the maximum recording distance must be only a few centimeters. For the FROST tunnel, which has a working area with an octagonal cross section of 45.6 cm across flats, this restriction requires the sample be taken close to the test section wall and far from the section centerline. Pavitt et al (1970) encountered the same problem and discussed many of the factors influencing the resolution of the system. They concluded that the spatial resolution of the illuminating beam was probably the limiting factor. In the present geometry a spatial resolution of approximately 4 cm is required to adequately record a 10 micron particle on the tunnel centerline. The results of the test summarized in Figure 3 suggest that the present system has a spatial resolution of about 1.5 cm.

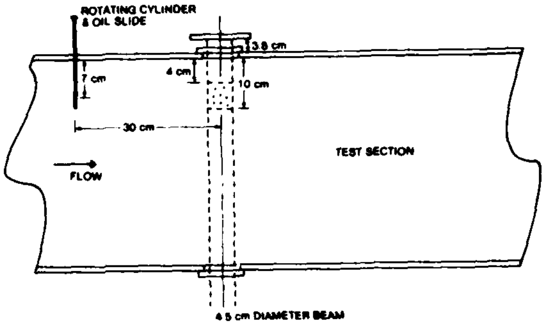

Figure 5. A schematic drawing showing the sampling positions for each instrument.

## EXPERIMENTAL ARRANGEMENT & PROCEDURES

To compare the measurements of the holographic system with those of the rotating cylinder and the oil slide each instrument must sample the same region in the working section. For the holographic system a compromise had to be made in establishing the limits of volume to be sampled. Near the test section wall small droplets can be resolved, but the droplet population will not be representative of the flow as a whole. Far from the wall a more representative droplet population will be obtained, but the minimum resolvable droplet diameter increases. The limits for the sample volume are defined in Figure 5. During the reconstruction of the hologram a volume 2.5 cm in length and 1 cm square centered at 7 cm from the wall was sampled. This results in a recording distance that varied between 9.5 and 12 cm. From Figure 4 this suggests that droplets in the 25-30 micron diameter range are the smallest that can be resolved. This estimate is

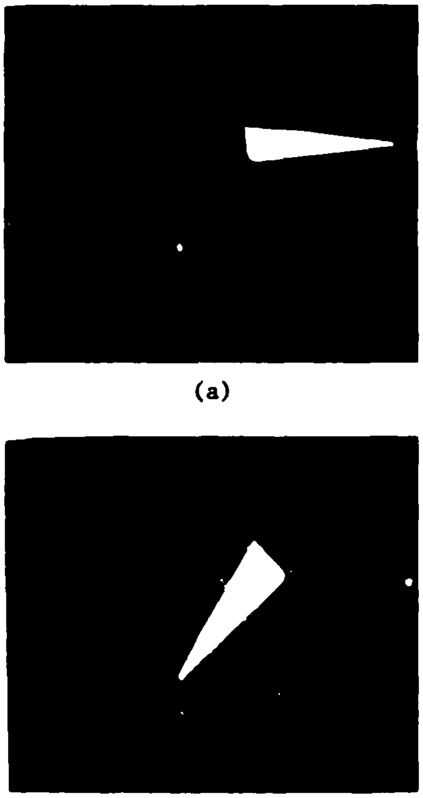

(a)

(b)

Figure 6. Photographs of the reconstructed images of two water droplets. In photograph (a) the droplet in focus is 30 microns in diameter and the out of focus droplet is 40 microns. In photograph (b) the 40 micron droplet has been brought into focus. The recording distance was about 10 cm.

somewhat pessimistic and it was found that droplets in the 15-20 micron range could be reliably detected. In Figure 6 photographs of the monitor display of the reconstructed images of 30 and 40 micron droplets are presented. These droplets are located near the midpoint of the volume, i.e. approximately 10 cm from the film plane.

The sampling region for the oil slide and the rotating cylinder was located 30 cm upstream of that for the holographic system. The aperture of the oil slide and the center of the sampling length of the rotating cylinder were located 7 cm from the wall corresponding to the center of the reconstructed sample volume.

At the time of preparation of this report only some very preliminary results are available. The results reported here correspond to two nominal water loadings: 0.5 and 1.0 gm/m$^3$. Both tests were carried out with an air speed of 30 m/s and an air temperature of -10°C. The procedure in each case was to first make at least three measurements each with the rotating cylinder and oil slide. Four holograms were then recorded and again a series of oil slide and cylinder measurements were taken. In the reconstruction of the holograms the number of droplets counted per hologram varied between 50 and 300, but averaged at approximately 150. Similarly, for the oil slides, the number of droplets varied between 80 and 300 per sample, but averaged 180.

## COMPARISON OF RESULTS

### Liquid Water Content

A comparison between estimates of the liquid water content determined from the holographic reconstruction with those from the rotating cylinder is made in Figure 7. (Note the low values of LWC compared to nominal settings indicate most of the droplets are not close to the wall). At each test condition six rotating cylinder measurements were taken and then averaged to obtain the horizontal coordinate in the graph. These measurements were reasonably consistent varying ± 4% from the average. On the other hand there is a great deal of scatter in the holographic data. This scatter is due to some limitations of the holographic system and also some limitations of the operation of the FROST tunnel. The scatter is mainly attributable to the combination of the short duration time of the holographic sampling with the observation that air speed and water droplet distribution do vary somewhat in time. The rotating cylinder measurement takes place over a sufficiently long period of time (60 seconds) that the variations average. Hence, the holographic measurement gives values for the LWC that are both above and below the rotating cylinder value. In this case then, if a sufficient number of samples are taken and the results averaged, the correct average value will be arrived at. At this time only four samples per run are available, but if they are averaged it can be seen in Figure 7 that the agreement with the rotating cylinder values is reasonably good.

Another factor which contributes to the spread of the data is the size of the sampling volume (2.5 cc). This limitation arises because of the rather lengthy time required to count and size the droplets at the overall magnification of 250X used in the reconstruction. (It takes approximately one half day to "read" a 2.5 cc

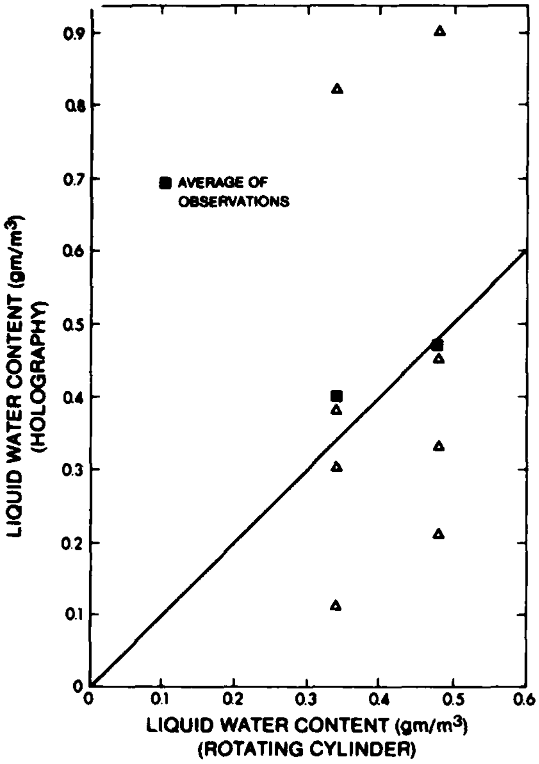

Figure 7. A comparison of water liquid contents determined by holography and by the single rotating cylinder.

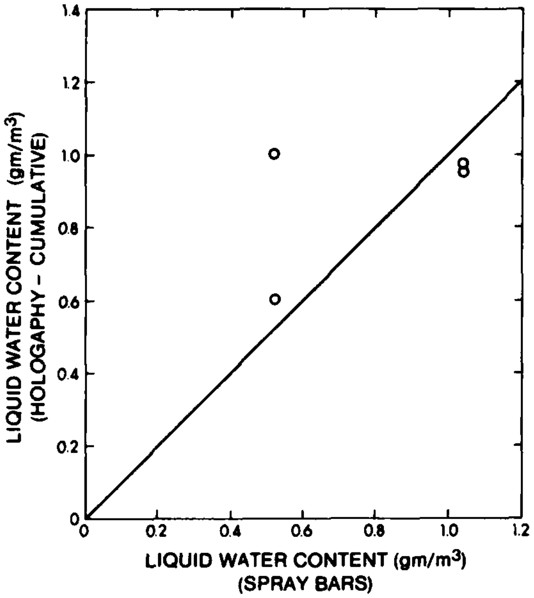

Figure 8. A comparison of the nominal liquid water content with that determined by holography

volume). The small size, however, leads to an inaccurate estimate of the volume concentration of the larger droplets since it is so low (much less than 0.5 per cc for droplets above 50 microns diameter). And, since it does not require too many large droplets to change the liquid water content, a poor estimate of large drop concentration will noticeably influence the liquid water content.

To obtain a better estimate of the large droplet concentrations the overall magnification was reduced to approximately 100X and a volume 1 cm square and extending from 10 cm to 30 cm from the tunnel wall was sampled. Over this volume (20 cc) the smallest droplet that could be reliably detected was 30 microns diameter. The results from the large volume sample for droplets over 40 microns diameter were combined with the average results from the small sample volume for droplets between 15 and 40 microns diameter to provide an estimate for the LWC in the test section. Since no rotating cylinder measurements at the tunnel center line were taken, the holographic results are compared in Figure 8 with a nominal LWC calculated from the water flow rate at the spray bars and assuming a uniform distribution over the tunnel cross-section. The agreement is very good at the high loading, but at the lower loading the holography results are above the values predicted from the water flow rates. Again at this time the data is too limited to draw any conclusion from this study, but a similar comparison reported by Hunt, 1978, suggests a bias on the holography system to over predict the LWC.

Another factor that influences the determination of the LWC from holography is that the droplet diameter cannot always be specified accurately. An accurate estimate depends upon the clear definition of the droplet boundary against the background. For droplets at many far field distances from the film at the time of recording the reconstructed image is not always distinct. This is particularly true for the smaller droplets (see Figure 3 for example), but as can be seen in Figure 9 is a less serious problem with the larger droplets. Since a 10 percent error in droplet diameter produces a 33 percent error in droplet volume, the sizing could pose a problem. This problem was handled by putting the droplets into 5 or 10 micron wide bins, using an average volume diameter for the bins and counting many droplets.

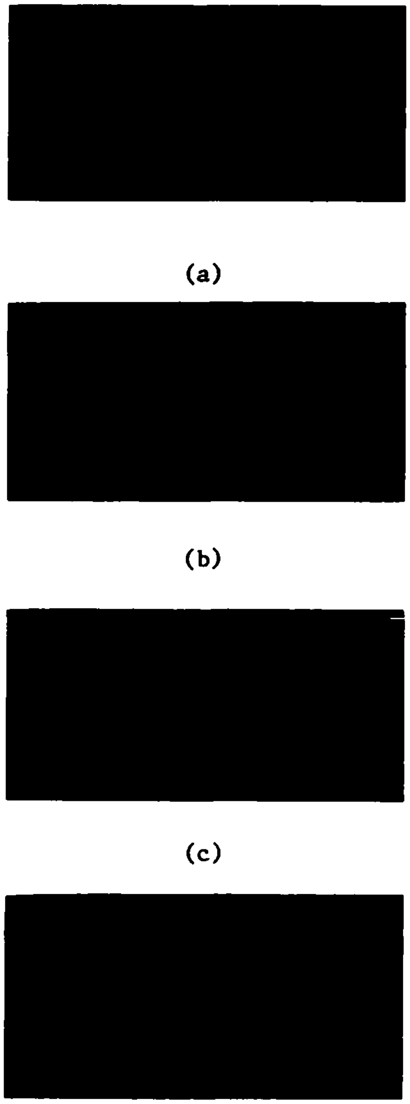

(a)

(b)

(c)

(d)

Figure 9. A sequence of photographs showing a 60 micron diameter droplet coming into and out of focus.

Median Volume Diameter

A comparison between the values of the median volume diameter estimated by holography and the oil slide is shown in Figure 10. It is readily apparent that the oil slide method gives a systematically larger estimate than the holography. A comparison of droplet size distributions in Figure 11 shows that the discrepancy is attributable to a greater number of large droplets measured on the oil slide (see Figure 12). As the holographic system gives reasonable agreement with the rotating cylinder estimate of LWC, it seems the

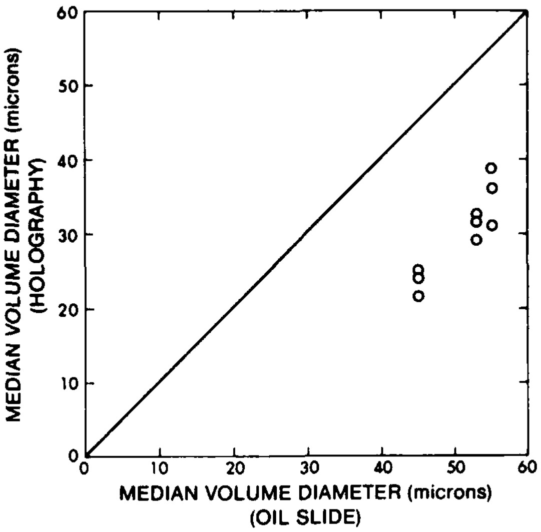

Figure 10. A comparison of the volume median diameter determined by holography with that determined by the oil slide method.

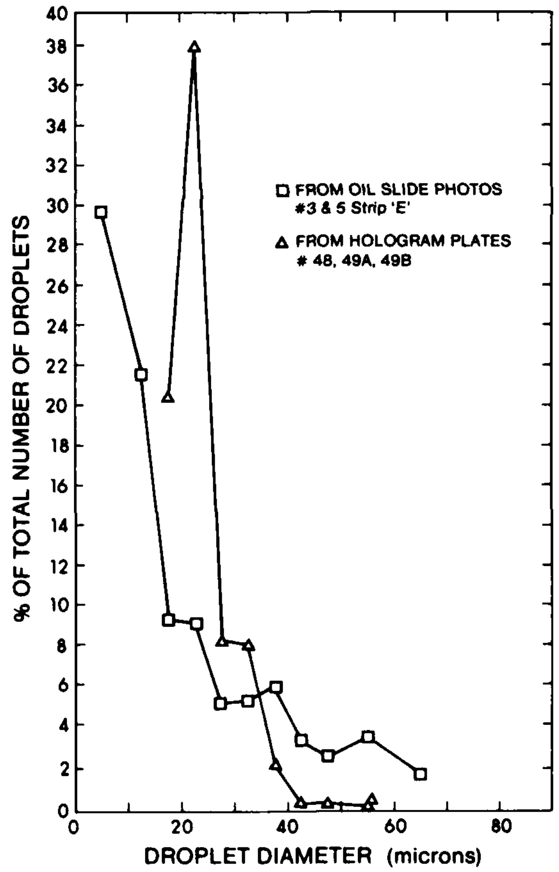

Figure 11. A comparison of the distribution of water droplet sizes determined by holography and by oil slide.

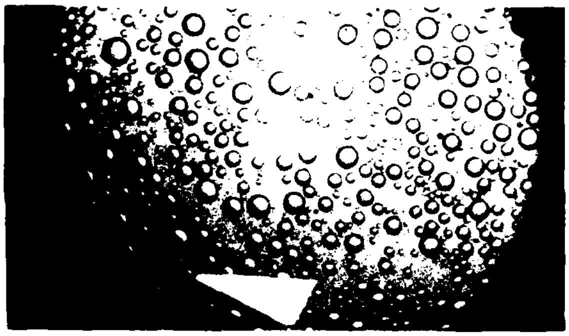

Figure 12. A photograph of droplets collected on the oil slide. The indicated droplet is 30 microns in diameter.

oil slide is providing an overestimate of the MVD. Keller, 1978, has reported the same overestimate when comparing the oil slide with light-scattering-type counters. The main problem with the oil slide appears to be evaporation and coalescence of the smaller droplets giving a bias towards the larger diameters.

## CONCLUSION

The holography method for estimating water droplet populations has the advantage that in a single measurement the droplets occupying a particular volume can be recorded. Play back of this record allows determination of liquid water content, median volume diameter, spatial distribution of the droplets and droplet velocity if a multiple pulsing capability is present. However, the depth of field over which a droplet can be recorded is a function of the droplet size. For the present icing facility this requires the addition of a lens if droplet populations near the tunnel centerline are to be sampled. To obtain reasonable estimates of droplet concentrations at least two volumes must be sampled (a small volume for the more numerous small droplets and a large one for the less numerous large droplets). Further, reduction of the data is extremely tedious and requires some judgment. Consequently the use of a holography system as a regular method for characterizing the droplet population in an icing facility is impractical.

Although only preliminary data has been obtained, comparison with the rotating cylinder appears to show good agreement on estimates of LWC, but comparisons of median volume diameter suggests the oil slide method overestimates the value. (By about a factor of 1.6-1.8 in the present case).

## ACKNOWLEDGEMENT

This work was supported by the National Research Sciences and Engineering Research Council Canada.

## REFERENCES

Collier, R.J., C.B. Burckhardt and L.H. Lin, "Optical Holography", London: Academic Press, 1971.

Hunt, J.D., "Engine Icing Measurement at the AEDC", AGARD Conference Proceedings 236 - Icing Testing for Aircraft Engines.

Keller, R.G., "Measurement and Control of Simulated Environmental Icing Conditions in an Outdoor, Free Jet, Engine Ground Test Facility", AGARD Conference Proceedings. No. 236 - Icing Testing for Aircraft Engines.

Parrent Jr., G.G. and G.O. Reynolds, "Resolution Limits of Lensless Photography", S.P.I.E. Journal, Vol. 3, 1965, pp. 219-220.

Pavitt, K.W., M.C. Jackson, R.J. Adams and J.T. Bartlett, "Holography of Fast Moving Cloud Droplets", J. of Phys. E., Sci. Instr., Vol. 3, No. 12, December 1970, pp. 971-975.

Pitlak, R.T., R. Page and N.P. Selvin, "Limitations of Transmission Holography in Particle Analysis", Holosphere, August 1976, Vol. 5, No. 8.

Stallabrass, J.R., "An Appraisal of the Single Rotating Cylinder Method of Liquid Water Content Measurement", National Research Council Canada, Low Temperature Laboratory, Report LTR-LT-92, Nov. 1978.

Thompson, B.J., "Applications of Holography", Rep. Prog. Phys., V. 41, 1978.

Wuerker, R.F., "Particle and Flow Field Measurements by Laser Holography", Conference on the Engineering Uses of Coherent Optics, University of Strathclyde, April 8-11, 1975.

## DISCUSSION

Gates: Droplets tend to spread out as they're caught on the oil. I found a magnification factor of something like 1.5 quite appropriate for that.

Stallabrass: We've used the oil slide method for a number of years. We observed lensing effects as long as the oil film is the same order... Technique is still important. Another error in technique I noticed from your photograph is you have far too many droplets on the slide. The tendency then is for adjacent droplets to coalesce. This will again give you larger droplets than you really have.

Gates: I chose this particular slide because it had the most water drops on it. Normally they have quite a bit fewer. I think I noted in the paper approximately 150, something like that, the average number I counted. I was extremely worried about evaporation that seemed to be taking place while I was trying to focus it.

Stallabrass: Yes, this depends on the type of oil you're using - it's necessary to be very selective.

Olsen: Oil is a black mark. In fact there is very little of the stuff around. You have a little vial of it? That's the last of the good oil.

Question: What type of oil is this?

Stallabrass: Shell [XM]

Gates: I have a quart of that.

Stallbrass: At one time it had a surface activator in it.

AD P001667

# CONTRIBUTION TO THE MODELING OF THE ICE ACCRETION PROCESS

## Ice Density Variation with the Impacted Surface Angle

M. Bain Laboratoire Associé de Météorologie Physique,
J.F. Gayet Univ. Clermont II B.P. 45, 63170 Aubière, France

Abstract

Icing measurements were carried out in natural winter clouds with an instrumented wind tunnel set up at the top of the Puy de Dôme (1500 MLS).

The microphysical data (liquid water content, droplet spectra) were obtained by using the PMS ASSP 100. The ice density was measured on a rotating cylinder and the ice deposit of the cross section was photographed on a fixed cylinder.

The density measurements ranging from 300 to 900 kg m$^{-3}$during the experiment are in agreement with Macklin's results (1962). The profile of the ice deposit is compared to the profile predicted by the model of Lozowski et al.(1979), which consider a fixed density.

We propose to improve this model by taking into account the ice density variation with the angle of impact on the cylinder. This calculation is based on Macklin's results (above mentioned) and on the determination of the local impact speed by using the result of Langmuir et al. (1946). The ice density variation with the angle depends on various parameters : pressure, temperature, air speed, liquid water content and especially on the droplet distribution.

This improvement is not sufficient to explain some observed profiles ; this may be attributed to the fact that the model is not time dependent.

## I - INTRODUCTION

In winter 1981, icing measurements were carried out in an instrumented wind-tunnel set up at the "Observatory of Puy de Dôme" which is located at the top of the Puy de Dôme mountain (1500 m MSL). The purpose of this experiment was to verify the relations between the ice accretion characteristics on cylinders and the meteorological parameters, namely, air temperature, air speed, liquid water content, droplet diameter, etc.

A numerical model (Lozowski et al., 1979) was used to simulate the profiles of the ice cap. The purpose of this paper is to compare the observed and the predicted profiles and to try to explain the differences, in order to improve the model.

## II - EXPERIMENTAL PROCEDURE

The open wind-tunnel is used when the Observatory is surrounded by clouds. The inflow of cloudy air is sampled in a cross-sectional area of 20 x 30 cm. The air speed ranges from 17 to 25 m s$^{-1}$.

The following probes are set up in the working section :

- a PMS (*) ASSP-100 for the measurement of cloud droplet spectra ($3 \leqslant D \leqslant 45$ µm) ;
- a PMS 2D-C providing particle images having dimensions from 25 to 800 µm ;
- two icing cylinders (22.5 mm diameter), one fixed and the other rotating (15 rpm) ;
- a thermometer and a Pitot tube for the measurements of air temperature and velocity respectively.

The microphysical data are recorded at a 1 Hz frequency.

Once the accretion on a cylinder has grown to a noticeable size under quasi-

---

(*) PMS : Particle Measuring Systems, Boulder, Co.

homogeneous cloud microstructure (controlled on a real-time display) the wind-tunnel is stopped. The ice density is deduced from the mass and deposit thickness measurements on the rotating cylinder and the cross section of the ice profile on the fixed cylinder is photographed.

During the whole experiment, which included 45 tests, various meteorological conditions were encountered. The outside temperature ranged from - 2 to - 9°C, the cloud liquid water content and median volume diameter calculated from the ASSP data ranged from 0.05 to 0.3 g $m^{-3}$ and from 7 to 23 µm respectively. The ice water content was evaluated from the 2D-C images and varied from 0.0 to 0.1 g $m^{-3}$.

## III - COMPARISON BETWEEN THE EXPERIMENT AND THE MODEL OF LOZOWSKI et al.

This model requires as input parameters the values of the cylinder diameter, the air speed, the temperature, the liquid water content, the ice particle content and the size distribution of the cloud droplets. The steady state heat balance equation is solved with a 5° angle intervals around the cylinder surface, and the model deduces the local equilibrium surface temperature, the ice fraction of the impinging and runback water substance, and the local rate of icing. The unfrozen liquid with any entrained ice particles is allowed to runback from a 5° sector to the next, starting from the stagnation line and participating in the local heat exchange. The diffusivity of heat is neglected in the cylinder and in the ice deposit. Any unfrozen water at a polar angle of 90° is assumed to be shed into the air stream.

Under mixed accretion conditions, the model assumes an ice sticking efficiency value based on thermodynamic considerations only, such that ice particles can stick to a wet surface, but not to a dry one.

The thickness of the ice deposit is deduced from the evaluation of the ice growth flux in each sector, by using the next formula :

$$h = R.\Delta t/\rho.\cos(\theta) \qquad (1)$$

with R the ice growth flux, Δt the time duration of the simulation, ρ the ice density and θ the angle.

For all the wind tunnel tests, the ice deposit grew under dry conditions and the profiles predicted by the model of Lozowski et al. have an elliptical shape.

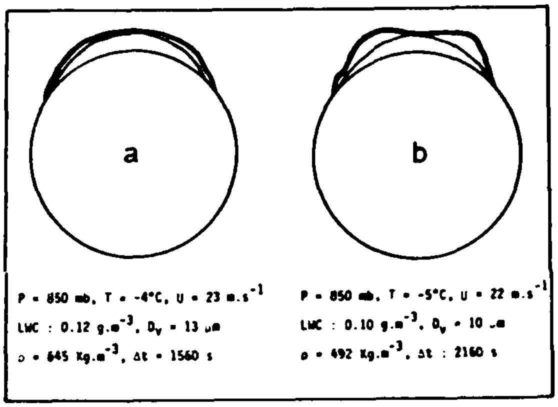
a
b
P = 850 mb, T = -4°C, U = 23 m.s⁻¹
LWC : 0.12 g.m⁻³, Dv = 13 µm
ρ = 645 Kg.m⁻³, Δt = 1560 s
P = 850 mb, T = -5°C, U = 22 m.s⁻¹
LWC : 0.10 g.m⁻³, Dv = 10 µm
ρ = 492 Kg.m⁻³, Δt : 2160 s

Fig. 1 : Comparison between the observed (thick line) and predicted (thin line) profiles.

Two examples of comparison are presented in Figures 1-a and 1-b. The thick curve corresponds to the observed profile on the fixed cylinder and the thin curve to the predicted profile (*). The meteorological characteristics (pressure P, temperature T, air speed U, liquid water content LWC, median volume diameter $D_v$, ice density ρ and experimental duration Δt) are also reported in the Figures.

Fig. 1-a indicates a good agreement between the two profiles whereas Fig.1-b shows a noticeable difference. Since in this case, the observed profile presents a flat front surface in contrast to the elliptical predicted profile. It may be noticed than the time duration of the simulation is higher than in the previous case.

In order to explain this disagreement two reasons may be pointed out :

- the ice density used in the model is considered as constant for the whole deposit, and equal to 890 kg $m^{-3}$ ; while the measured density varies from about 300 to 900 kg $m^{-3}$ ;
- the model is not time dependent and does not take into account the change of the collection efficiency with the time evolution of the profile through the modification of the flow pattern.

This second point is not fully considered in this work, but is under present investigation and we focus our attention preliminarily on the density variation with the cylinder angle.

---

(*) The thickness of ice is plotted in the direction parallel to the free air stream direction ; the heat transfert coefficient for a rough surface is assumed.

## IV - FORMULATION OF THE DENSITY VARIATION WITH THE ANGLE

### 1) Experimental results on the ice density on the rotating cylinder

Our density measurements from the rotating cylinder are displayed in Figure 2 versus (- rVo/Ts) as suggested by Macklin(1962) where : r is the median volume radius of the cloud droplet spectra, Vo the speed of impact of the droplet on the stagnation line and Ts the mean temperature of the riming cylinder.

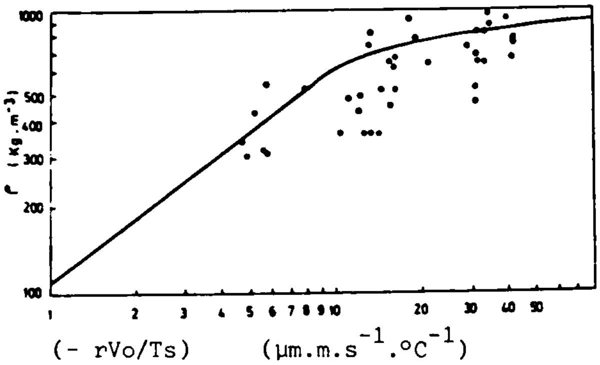

Fig. 2 : Ice density on the rotating cylinder versus the ratio (- rVo/Ts). The curve from Macklin's results is also plotted.

- The impact speed on the stagnation line Vo is obtained from the curves of Langmuir and Blodgett.

- The surface temperature is calculated from the heat balance equation at the riming surface of the cylinder.

We have also reported in Figure 2 the curve corresponding to the best fit of the data set obtained by Macklin. Our measurements are in rather good agreement with Macklin's curve. For the parameterization of the variation of the ice density, we use the formulation suggested by Macklin when (- rVo/Ts) is less than 10 :

$$\rho = 110\ (- rVo/Ts)^{0.76}\ \mathrm{kg\ m^{-3}}$$

For (- rVo/Ts) ranging from 10 to 60, we propose the following expression :

$$\rho = 10^{3}\ (-rVo/Ts)\ /(-rVo/Ts + 5.61)\ \mathrm{kg\ m^{-3}}$$

which approximates Macklin's curve to an accuracy better than 7 %. This formula is chosen due to the finite density limit when the ratio (-rVo/Ts) reaches large values. We take a constant value of $\rho$ = 917 k $\mathrm{kg^{-3}}$ for (- rVo/Ts) greater than 60.

### 2) Determination of the local impact speed and the local surface temperature versus the angle θ on the fixed cylinder.

In order to express the local density of the ice on the fixed cylinder : $\rho(\theta)$ as a function of :

$$\left(- \frac{r\ Vr\ (\theta)}{Ts\ (\theta)}\right)$$

the above formulas are used together with:

- Ts ($\theta$) the surface temperature of the angle ($\theta$) determined by a local heat energy balance, as proposed by Lozowski et al.;

- Vr ($\theta$) the local impact speed taken as the radial component (perpendicular to the surface) of the droplet speed calculated at the angle ($\theta$).

To determine Vr ($\theta$) we proceed as follows :

a) obtain a relationship for the impact speed on the stagnation line, Vo, from the curves of Langmuir and Blodgett ;

b) calculate the droplet speed V ($\theta$) with the assumption that this parameter is a linear function of cos.($\theta$) from the value Vo at $\theta = 0°$ to $V_M = 1.05$ U at $\theta = \theta_M$, with U the true air speed in the undisturbed flow (from Langmuir) ;

c) express the local impact speed as Vr ($\theta$) = V ($\theta$) cos.($\alpha$) where $\alpha$ is the angle between the radius direction and the tangent to the trajectory of the droplet at the point of impact, as shown in Figure 3. Three possible droplet trajectories are plotted, for $\theta = 0°$ , for any $\theta$, and for $\theta = \theta_M$, with the corresponding impact speed ; Vr(0) = Vo, Vr($\theta$) = V($\theta$) cos. ($\alpha$), Vr($\theta_M$) = 0.

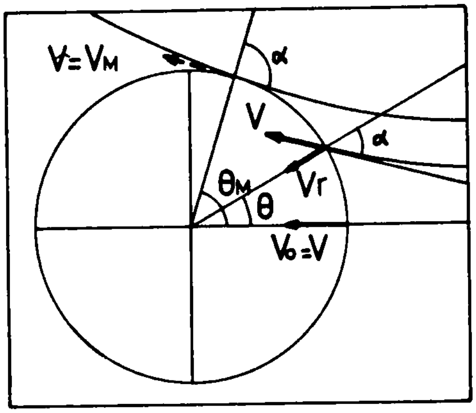

Fig. 3 : Droplet trajectories with the corresponding droplet speed (dotted arrow) and local impact speed (thick line arrow).

Figure 4 shows the local impact speed Vr, determined by the three steps described above, plotted versus the angle θ. The parameters used in the calculation are : the pressure (P = 850 mb), the air temperature (T = - 10°C), the air speed (U = 20 m $s^{-1}$), the liquid water content (LWC = 0.5 g $m^{-3}$) and the droplet diameter (D = 15 μm).

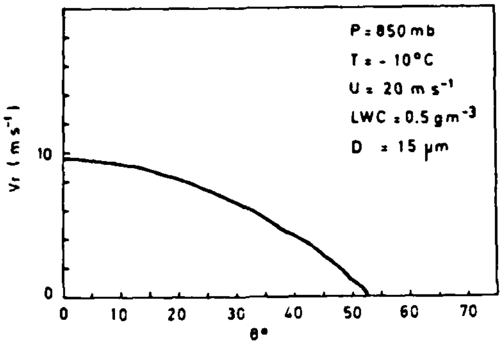

Fig. 4 : Local impact speed (radial component) versus the angle of impact on the cylinder.

Under these conditions, Vr decreases from Vo = 9.8 m $s^{-1}$ to $Vr(\theta_M)$ = 0 m $s^{-1}$, at the maximum impinging angle which is $\theta_M$ = 53°.

Figure 5 illustrates the variation of the surface temperature Ts versus the angle θ, which is obtained from the model of Lozowski et al. The parameters used are the same as in Figure 4. The local surface temperature decreases from Ts (0) = - 5.2°C at the stagnation line to $Ts(\theta_M)$ = - 9.9°C at the maximum impinging angle.

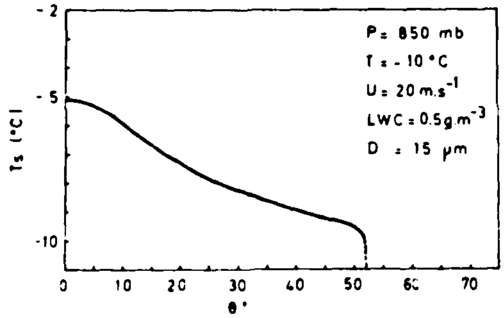

Fig. 5 : Surface temperature versus the angle around the cylinder, calculated by using the model of Lozowski et al.

3) Formulation of the ice density

To take into account the real droplet spectrum, we assume that the local ice density ρ(θ) is a mean value of the discrete densities induced by each of the droplet categories weighted by the liquid water content of these droplets :

$$\rho(\theta) = \frac{\sum_{j=1}^{15} \rho_j(\theta) \times G_j(\theta) \times f_j \times m_j}{\sum_{j=1}^{15} G_j(\theta) \times f_j \times m_j} \qquad (2)$$

The index j characterises the droplet diameter category ; and ranges from 1 to 15 when the corresponding droplet diameter ranges from 3 to 45 μm.

- $m_j$ is the liquid water mass of a droplet of diameter dj.

- $f_j$ is the fraction of the total concentration consisting of the $j^{th}$ size category.

- $G_j(\theta)$ is the local collection efficiency of droplets of diameter dj.

- $\rho_j(\theta)$ is the local density calculated for the $j^{th}$ category impinging at the angle θ.

It is assumed that freezing is an individual process for droplets and that droplets remain approximately spherical on freezing. This assumption is valid if the impact speed and the surface temperature are moderately low ; under these conditions the ice density ranges from 100 to 700 kg $m^{-3}$ (Macklin, 1962). For high impact speed and surface temperatures near 0°C, this assumption is no longer justified but the above formula is still valid because, for all droplet categories, the ice density reaches the maximum value of 917 kg $m^{-3}$.

4) Result concerning the ice density variation with the angle.

Figure 6 shows the ice density variation versus the angle on the cylinder calculated with the following parameters : pressure (P = 850 mb), temperature (T = - 10°C), air speed (U = 20 m $s^{-1}$), liquid water content (LWC = 0.5 g $m^{-3}$).

The cloud droplet spectrum is indicated in the upper right corner of the Figure. The vertical scale is the frequency distribution of the concentration ; each size category is 3 μm wide and is plotted horizontally from 3 to 30 μm.

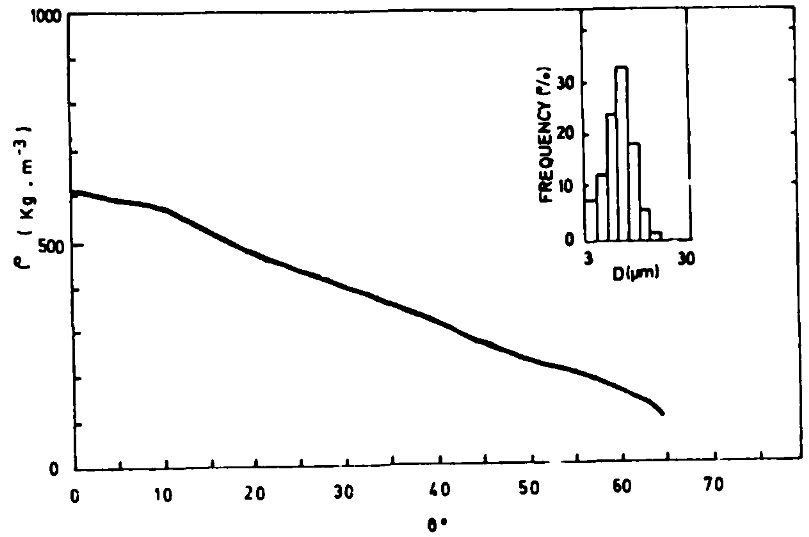

Fig. 6 : Ice density variation with the cylinder angle.

The median volume diameter is 13 μm. Figure 6 shows that the ice density decreases from 605 kg m$^{-3}$ at the stagnation line value, to 110 kg m$^{-3}$ at the maximum impinging angle $\theta_M$ = 65°.

## V - EFFECT OF THE DENSITY VARIATION ON THE PREDICTED PROFILE

### 1) Sensitivity to the droplet spectrum

The ice density variation depends on various parameters, pressure, temperature, air speed, liquid water content, and droplet distribution. The role of each parameter has been studied, and we focus our attention in this paper on the influence of the droplet spectrum.

Figures 7 and 8 illustrate the results of simulations performed for various droplet spectra ; the other parameters are identical with those of Figure 6. Three spectra (a, b, c) are displayed in the upper right corner of Figure 7. The median volume diameters are 9 μm, 13 μm and 23 μm respectively. These values are representative of the range of spectra encountered during the measurements. The corresponding curves of the ice density variation are also labelled (a), (b), (c).

The simulated profile calculated for case (a), (b), (c) are reported with the thick line in Figure 8. The thin line corresponds to simulations with a fixed density (890 kg m$^{-3}$) as proposed by Lozowski et al. The most important difference between the two simulations concerns the thickness of the ice deposit.

For case (a), the calculated density is about three times smaller than the fixed density ; then the thickness of ice is three times larger.

The shape of the ice deposit changes from sharp-pointed for case (a), to flat for case (b), and to elliptical for case (c), when the median volume diameter varies from 9, to 13 and to 23 μm respectively. This means that a flat deposit is observed for a specific droplet spectrum (median volume diameter equal to 13 μm in this case), when the other parameters are fixed. From Figure 7, we notice that the flat deposit is forecasted (case b) when the decrease of the ice density with the angle is "quasi-linear" ; by contrast the curves (a) and (c) show a lower decrease than curve (b).

### 2) Comparison between the new predicted profiles and the observed profiles

Figures 9 and 10 display the ice density variation with the angle and the predicted profiles respectively, for the experimental measurements presented in Figure 1-a and 1-b.

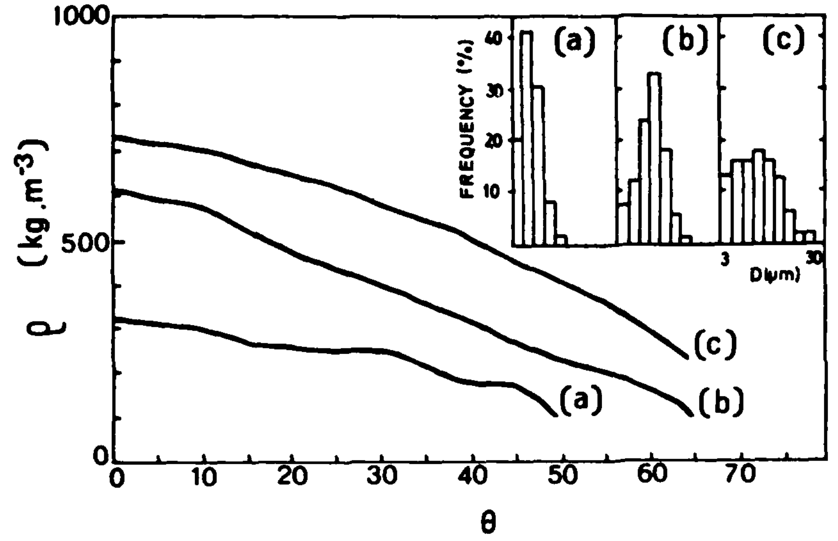

Fig. 7

Ice density variation with the cylinder angle for various cloud droplet spectra.

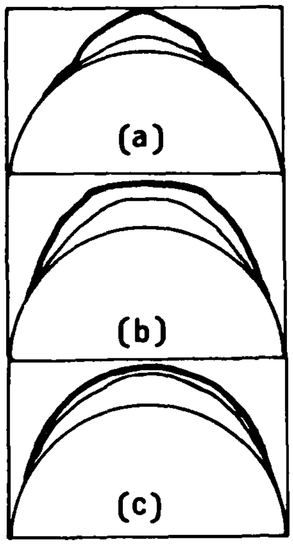

Fig. 8

Simulated profiles for a duration Δt = 10 mn.

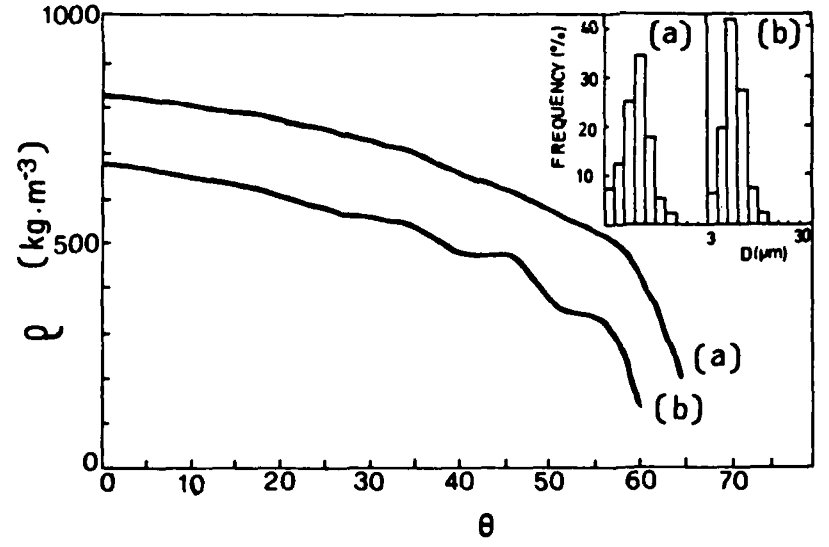

Fig. 8

Ice density versus the cylinder angle calculated for curves a and b with the parameters described in Fig. 1-a and b respectively.

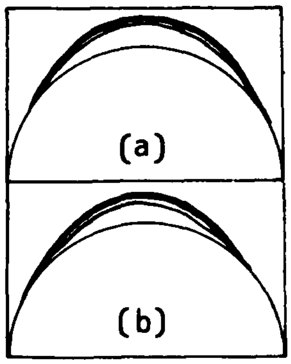

Fig. 10

Simulated ice profiles.

Figure 9 indicates that the ice density decreases slowly from the stagnation line to the angle $\theta = 55°$ from 815 to 500 kg $m^{-3}$ for case (a) and from 662 to 333 kg $m^{-3}$ for case (b) respectively. Then the ice density decreases quickly to the values 185 and 113 kg $m^{-3}$ for the angle 65° (case a) and 60° (case b) respectively.

From Figure 10, the simulated profiles obtained with a variable density is larger than with the constant density (890 kg $m^{-3}$), but they still have an elliptical shape which is not observed during the experiment. We notice that the decrease of the ice density is not quasi linear and the most important density variations are in the sectors where the ice growth fluxes are the smallest.

This result seems to indicate that the ice density variation cannot explain the differences between the shape of the observed ice deposit of Figure 1-b and the predicted shape of Figure 7-b.

As suspected in Section III, the ice density variation is not the only effect involved in the flattening and widening of a profile. In order to produce a realistic result, this effect has to be taken into account at the same time as a local collection efficiency variation due to the time evolution of the profile. In fact, these effects are linked ; a variation in the local collection efficiency $G_j(\theta)$ induces a local density variation (see Eq. 2) and changes the profile inducing a new variation in the collection efficiency and so on.

Ackley et al.(1979) indicate a decrease of the total collection efficiency of small droplets impinging on an elliptical profile with the increase of the eccentricity. For any observed profile the calculations are more difficult than for the elliptical shape and have not yet been done.

Moreover, it is difficult to guess the effect of this variation because the local collection efficiency $G_j(\theta)$ is involved first in the evaluation of the local ice density, directly in Eq. 2 and also indirectly through the surface temperature $Ts(\theta)$ used to express $\rho_j(\theta)$, and secondly in the determination of the ice growth flux R (see Eq. 1) on which the plot of the ice profile depends.

It must be pointed out that for the previous examples presented in Figures 9 and 10 the droplet spectra used in the simulation are the spectra measured by the PMS ASSP-100. Pinnick et al. (1981) show that the droplet size measured by the probe is inaccurate for a diameter less than 8 μm, this corresponds to the first three channels of the probe. The small error in the measured spectra may contribute to the disagreement between the observed and the simulated profile.

## VI - CONCLUSION

Experiments on icing have been performed on rotating and fixed cylinders in a wind-tunnel. Ice density measurements on the rotating cylinder indicate a rather good agreement with Macklin's results and lead us to use his formulation of ice density as a function of : (- rVo/Ts).

The profiles of the ice deposits on the fixed cylinder are compared to the results of simulations by using a model developed by Lozowski et al. In order to improve this simulation we have introduced the ice density variation as a function of the cylinder angle.

This calculation is found to be very sensitive to the cloud droplet spectrum. In some cases this calculation leads to the simulation of a flat profile of the ice deposit, but in other cases this new formulation is not sufficient and it seems necessary to take into account, at the same time, the time evolution of the profile. Continuation of the work described in this paper is under consideration at present.

## Acknowledgements

The authors would like to express their appreciation to Professor Soulage for his guidance during the period of this study, to Professor Coulman for his comments on the manuscript and to Doctor Pointin for helpful discussions.

We are indebted to Doctor Ramond, Director of the "Institut de Physique du Globe" of Clermont-Ferrand for having allowed us to use the Observatory at the summit of the Puy de Dôme to set up our experiments.

Thanks are due to the L.A.M.P.'s technical staff.

This research is supported by the "Direction des Recherches et Etudes Techniques" under the contract n°81.34.646.

## References

Ackley, S.F. and K. Templeton, 1979 : "Computer modeling of atmospheric ice accretion", CRREL, report 79.4.

Langmuir, I. and K.B. Blodgett, 1946 : "A mathematical investigation of water drop trajectories", Collected works of I. Langmuir, Pergamon Press, 335-393.

Lozowski, E.P., J.R. Stallabrass and P.F. Hearty, 1979 : "The icing of an unheated non-rotating cylinder in liquid water droplet-ice crystal clouds", NRCC report LTRC.LT 96.

Macklin, W.C., 1962 : "The density and structure of ice formed by accretion", Quart. J. Roy. Met. Soc., 88, 30-50.

Pinnick, R.G. D.M. Garvey and L.D. Duncan, 1981 : "Calibration of Knollenberg FSSP light scattering counters for measuremen of cloud droplets", J. Appl. Met., 20, 1049-1057.

## DISCUSSION

**Lozowski:** ... where the functional relationship comes from. It wasn't clear what your f'(rV/T) was - where it came from and where in particular the normal components of droplet velocity came from.

**Gayet:** These result since air velocity vs median volume radius and speed means of temperature. The ice variation vs the ... we must first calculate the temperature and speed and when we have the two parameters ... and droplet radius we use this formulation to calculate the air velocity, when this term ranges from 1-10 we use that, when this term ranges from 10-16 we use this one and when this term is greater than 16 we choose a constant ice. Now to express v,t we use your model and to calculate the local .. speed we take the right hand column. For example for θ we get zero.

**Phan:** My question concerns the value of the liquid water content which is 0.1 g/m$^3$. It seems to me that is a little small. Is this the average value you observe in the icing cloud?

**Gayet:** The values of liquid water content which are introduced into the model were measured with the PMS probe, and the values were not very large of course, but generally these measurements were made in the middle or near the base of the cloud. You see, they were capped clouds on the mountain, and the liquid water content of capped clouds is not very large. This is a natural cloud.

**Olsen:** Did you attempt to correlate the ice density with the freezing fraction from Lozowski's model?

**Gayet:** With our experiment, with low water content the ice growth was dry in all the tests. We had no runback, no runoff. We suppose that all the droplets freeze on the ice thickness. The model of Lozowski predicts for all experiments elliptical profile.

AD P001668

# ICING RESEARCH ON MT. WASHINGTON, N.H.

J.B. Howe Mt. Washington Observatory, Gorham, N.H.

## CLIMATE

Mt. Washington, N.H., 100 km northeast of Hanover, has been described as an island of sub-arctic climate in the temperate zone. Annual average temperature is -3°C, and the record high and low are 22° and -44°C. Daily normal temperatures are below freezing from mid-October to early May. The summit is in clouds approximately 55% of the time, and structures are coated with a meter or more of rime for most of the winter. Annual snowfall averages 625 cm.

The mountain is famous for its high winds; average wind speed during the winter months is about 65 km/hr (40 mph). During April 1982, for example, there were 14 days when gusts exceeded 160 km/hr (100 mph), and for one period of 55 hours there were continuous gusts over that speed. Of course the world record speed of 370 km/hr (231 mph) was measured by the Mt. Washington Observatory in April 1934.

## HISTORY OF ICING RESEARCH

The Mt. Washington Observatory was founded in 1932 as a private, non-profit corporation. For the first few years icing research was confined to practical matters, such as how to make radio antennas and anemometers survive. During the late 1930's scientific work was begun by Cunningham, Howell, and Charles Brooks, among others. Irving Langmuir and Vincent Schaefer of General Electric came to the mountain in 1943 to study precipitation static for the U.S. Air Force, but soon switched to icing and cloud physics research when they found that they were unable to keep their antennas ice-free. Langmuir's involvement resulted in his work on droplet trajectory theory and the perfection of the rotating multicylinder method for measuring cloud liquid-water content and droplet size. Schaefer's work on the mountain led directly to his invention of cloud seeding, and the Observatory was involved in some of the early weather modification experiments such as Project Cirrus and Project Overseed.

In the mid-1940's the Air Force became interested in Mt. Washington's potential as a site for aircraft icing studies. In the late 1940's the U.S. Navy and U.S. Air Force began icing tests of jet engines and aircraft components, and this grew into a large-scale effort, with living quarters for 50 people, a laboratory building with three test cells, and a helicopter test site. Also during this time techniques of winter transportation on the mountain were developed. The large Air Force facility ceased operations about 1960 and was torn down in 1967.

## RECENT WORK

Since that time the only winter residents of the mountain have been the television station engineers and the

Observatory staff. For many years the home of the Observatory was a two-story wood frame building about 100 m southwest of the summit. In 1980 we moved into much roomier quarters at one end of the new Sherman Adams Building, a steel and concrete structure built the by the State of New Hampshire for the Mt. Washington State Park.

The Observatory has a contract with the National Weather Service to operate a first-order weather station, and has also continued to do research work, including occasional projects in icing and cloud physics. During the past few years we have worked with CRREL on the rotor icing and wire icing projects to be reported on at this Workshop, and at present we are engaged in a study of ice detector performance for CRREL.

## INSTRUMENTATION

Two instruments which the Observatory uses in icing conditions may be of general interest to workshop participants.

Our anemometer is a standard aircraft pitot-static tube mounted on a heated, vaned hub; the pressure signal is recorded mechanically on a draft recorder. This system does require some personal attention, but it gives us better than 99% reliability. Total pressure from the pitot is led to a sealed-cistern barometer and a sealed microbarograph for station pressure measurement, since empirical studies showed this to give good agreement with nearby radiosonde observations. (The Bernoulli effect causes a decrease in static pressure over the summit.

For measuring cloud liquid-water content (LWC) and droplet size we still consider the rotating multicylinder to be the most reliable and accurate instrument available, although we occasionally use oil-coated slides for size measurement. We use a set of six cyliders ranging in diameter from about 2 mm to 76 cm.

The multicylinder method has enjoyed a mixed reputation, so it is necessary to explain our reasons for relying on it. It is true that problems may arise with the technique when it is used at aircraft speeds, or in wind tunnels with artificial fog, or wherever the temperature is only a few degrees below freezing. Of course we do not suffer from the first two kinds of problems, but warm temperatures, which may result in run-off of unfrozen water, are a definite hazard. However, this brings out a very important point: problems with the multicylinder method are almost always apparent to the operator and in many cases the problems can be properly allowed for during data reduction. Of course one cannot make valid corrections for severe run-off, so this remains a limitation of the method. Other limitations or disadvantages are:

1) At low wind speeds (below about 30 km/hr) and/or with very small droplets the two or three largest cylinders may have spotty collections or none at all; with data from only three or four cylinders accuracy is reduced.

2) Exposures last for 10 to 30 minutes and thus represent integrations over several kilometers of cloud, which may be undesirable.

3) Some manual dexterity is required, and the data reduction procedure is rather laborious.

4) Although the results of an exposure appear to specify the droplet size distribution, actually the method is quite insensitive to the parameter and will not even identify bimodal distributions except in extreme cases such as fog with drizzle.

Advantages of the multicylinder method include:

1) Equipment is simple and inexpensive.

2) The method is foolproof, in the sense that problems which may affect accuracy are easily recognized.

3) Accuracy over a broad range of conditions is estimated to be from 5% to 10% in both LWC and droplet size.

The original droplet trajectory studies by Langmuir and Blodgett (1964), which are the foundation of the multicylinder method, were done on a differential analyzer. They were repeated by Brun et al. (1955) of the NACA, using a mechanical analog, and more recently on a computer of McComber and Touzot (1981) using the method of finite elements. There are no significant differences among the results of these three studies. Howell (1952) investigated the accuracy of the multicylinder method and the effect of differences in the design of the instruments themselves.

## REFERENCES

Brun, R.J., W. Lewis, P.J. Perkins and J.S. Serafini (1955) Impingement of cloud droplets on a cylinder and procedure for measuring liquid-water content and droplet sizes in supercooled clouds by rotating multicylider method. NACA Report 1215.

Howell, W.E. (1952) Comparison of three multicylinder icing meters and critique of the multicylinder method. NACA Tech. Note 2708.

Langmiur, I. and K.B. Blodgett (1964) A mathematical investigation of water dropet trajectories. Tech. Rept. No. 5418, Air Materiel Command, AAF.

McComber, P. and G. Touzot (1981) Calculation of the impingement of cloud droplets in a cylinder by the finite-element method. Jour. Atmos. Sci., 38, 1027-1036.

## DISCUSSION

Félin: I would like to know if you have tested the Rosemount ice detector?

Howe: Yes, we have, in fact we're testing a couple of them for CRREL. We also ran tests on them when I was with the Air Force facility in the 50's. The project is going on now so I haven't analyzed the data. The results should be available around the end of the summer when we finish the analysis.

Fikke: We had a Rosemount detector in a similar place like Mt. Washington where we experienced very extreme ice loads. There we have seen that the Rosemount ice detector is covered by an ice cap, so when it is really icy it does not register at all.

Howe: That's very true. We've had that experience. If you want to measure icing with a Rosemount ice detector, except for very brief episodes, you have to be able to deice it. Perhaps, it could very easily be done if you have the power available. The trouble is some of the ice collects on the support structure and around the box-there are various models of ice detectors.

Power: Some of the early work on the median drop size diameters from Mt. Washington showed a value I think of around 14 microns diameter. Would you say that still holds for the typical bottom cap size?

Howe: Yes - that's a good average. If I had to guess before hearing your figure, I would have said about 12 microns. But of course, it is a cap cloud normally. It may be a cap cloud imbedded in general cloud structure, but it may not be quite typical of the free atmosphere.

Ervik: I have a question - you mentioned anemometers you have tested and tried to develop a new one. Do you think it's reliable?

Howe: The one we use?

Ervik: Yes.

Howe: Well, reliable in the sense that it keeps free of ice, or reliable in the sense that it gives an accurate reading when it is free of ice?

Ervik: When it is free of ice.

Howe: Well, yes. The only problem is, it was wind-tunnel tested - the pitot-static tube must pass an Army-Navy test for error due to angle out of the wind. The only problem with it is - oh, yes and our instrument has been tested in the wind tunnel -it's not quite the same as on an aircraft because the size of the hub affects the static pressure. This correction is made, but the problem with it is when the wind is turbulent it's vaning, gusty, it's spending a lot of time pointing out of the wind. I mean way out of the wind, and that may drop the average reading.

Fikke: I'm asking because we always have troubles with our anemometers, so I don't rely on wind being measured during ice periods.

Félin: How good is this anemometer at low wind speeds?

Howe: Not too good, but we don't have very many of those (laughter).

AD P001669

# MECHANISMS FOR ICE BONDING IN WET SNOW ACCRETIONS ON POWER LINES

S.C. Colbeck, USACRREL*
S.F. Ackley, USACRREL

## ABSTRACT

## INTRODUCTION

The adhesion of wet snow to power lines and other structures is particularly troublesome because a large mass accumulation can occur quickly. Even at temperatures above freezing, substantial wet snow accumulations can occur on power lines when the snowfall is accompanied by strong winds.

While the formation of these accretions is generally understood, important unknowns in the accretion process are how the accretion maintains its form and what the forces are that hold the it together. The adhesive mechanism is of considerable importance because of our need to understand and control wet snow accretions. Important applications include the clear writing of design criteria, impact statements, and documents with legal ramifications such as insurance policies. A recent settlement between a utility and an insurance company over wet snow induced damage indicates how the lack of understanding about this phenomenon can be expensive ($4.3 million).

In this particular case, an insurance policy excluded damages caused by "ice formation on overhead transmission lines." The utility challenged this exclusion when wet snow accumulated onto overhead conductors which fell into a generator substation, destroying generating capacity.

The technical argument eventually hinged on whether "freezing," i.e. the change from liquid phase (water) to solid phase (ice) occurred after the snow was deposited on the lines. It was commonly believed that insubfreezing external conditions either sensible or evaporative heat loss was necessary to cause ice bonding, i.e. freezing, in the accretion. Neither subfreezing air temperatures (cooling by sensible heat loss) nor subfreezing dew points (evaporative cooling losses) occurred consistently during the period of the accretion. One side in the dispute contended that freezing was not taking place in the accretions on the lines and that capillary forces (liquid-solid surface tension forces) were a plausible explanation of what keeps the accretion together and growing. The technical literature is also confusing on this point.

Kemp (1980) and Ryder (1981) have proposed that evaporative cooling (subfreezing dew point even in the absence of subfreezing air temperature) explains the adhesion of wet snow, although this seems highly unlikely, as explained by Makkonen (1981). Wakahama, Kuroiwa and Gato (1977) even observed an increase in the adhesive force with liquid water content thus proving that evaporative cooling is not a comprehensive explanation of the phenomenon, if indeed it is even an explanation. We first review the growth and compaction processes in wet snow accretions, and then argue that interparticle bonding (freezing) is a necessary feature of these accretions.

---

* U.S. Army Cold Regions Research and Engineering Laboratory, Hanover, N.H.

Finally, we explain how this bonding or freezing mechanism can take place in the absence of subfreezing external conditions.

## GROWTH OF WET SNOW ACCRETIONS

Wakahama (1979) demonstrated the effectiveness of wind in causing the accretion to roll, turning the snow mass in such a way that the accretion builds uniformly around the line. Figure 1 shows the accretion process on wires for low and high winds.

The wind action is necessary for the accumulation of a symmetrical deposit which is less likely to shed by self-rupture than an asymmetrical deposit. The wind is apparently responsible for packing the snow grains with a high density as well. This packing process is particularly enhanced in high winds since the shape of the accretion gives a partial airfoil form to the wire/accretion composite. Wind forces then lift the accretion and hold it for a longer period into the wind. The impact forces of snow particles and wind drag then continue to pack the accretion onto the wire.

The snow densities obtained during accretion on a power line are normally much higher (0.5-0.9 $\mathrm{Mg/m^3}$) than the densities of snow on the ground during the same period (<0.4 $\mathrm{Mg/m^3}$). Once the accretion has built completely around the wire (Fig. 1), an additional densification factor comes into play, that is, the role of the wire as a stress riser contributing to the packing in the accretion. In this case, wind forces exert a drag on the wire/accretion composite in the horizontal direction (per unit length) as

$$F_D = C_D \, \rho_{air} \, D \, v^2 \qquad (1)$$

where $C_D$ is the drag coefficient, $\rho_{air}$ the density of air, D the total diameter of the wire and accretion, and v the wind velocity.

This drag force is balanced by the tension in the wire and acts roughly in the contact area of the wire. The average packing stress $\bar{\sigma}$ on the snow is, as derived in the Appendix,

$$\bar{\sigma} = \frac{4}{\pi^2} \frac{F_D}{r} \qquad (2)$$

where r is the wire radius.

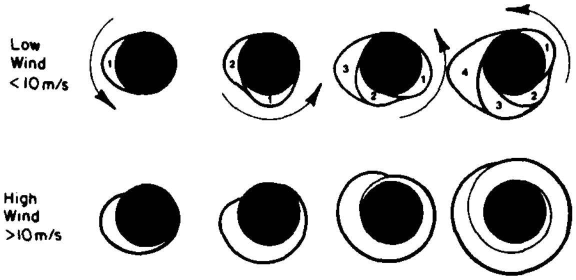

Figure 1. Accretion process of wet snow on a wire for low and high winds (after Wakahama, 1979). For high winds, lift forces develop and "hold" the accretion into the wind, increasing the packing density.

A similar relation exists in the vertical direction where the weight of the entire accretion is supported by a compactive stress acting along the top surface of the wire and is balanced by the tension in the wire.

It is well known that wet snow is easily compressed (Colbeck, 1979a), especially at larger liquid water contents. Accretions on wires can there fore build to much higher densities than snow on the ground. This happens through a combination of the accretion process and wire reaction forces to wind drag and gravity, which act through the relatively small contact area on the wire surface when compared to the total cross-sectional area of the wet snow accretion.

## THE NECESSITY FOR INTERPARTICLE BONDING IN WET SNOW ACCRETIONS

Some mechanical considerations relying on the observations of wet snow accretions are invoked to demonstrate that interparticle forces (ice bonding or freezing) are necessary. Without ice bonding the only plausible explanation for interparticle adherence is surface tension force (capillary force) caused by the contact of liquid water and ice particles. While these attractive forces are considerable, one of their important features is that they are strong in tension but have negligible strength in shear. The absence of shear strength would limit the shape of an accretion on a line to arrangements where the interparticle forces were only compressive or tensile. Since the observed forms are cylindrical, we quickly see that considerable shear forces develop within the accretion due to both the horizontal reaction of the wire to the wind and the vertical reaction of the wire to gravity. Using capillary forces alone, snow accretions could only take the form that a wet sand accretion would take if packed around a wire. In the absence of wind this form would be a pile of sand on top (theoretically at the angle of repose), and a small amount ("beard") hanging below, such that all the intergranular forces were tensile.

The cylindrical accretions commonly observed with wet snow exhibit considerable strength in shear by resisting both gravity and wind forces against the reaction of the wire. The most plausible explanation, given that these accretions are formed by successive impacts of wet snow particles, is that large shear strengths are the consequence of solid-solid bonding (freezing) between the individual particles.

Laboratory and field evidence indicates also that these cylindrical wet snow accretions occur at above-freezing temperatures. We offer some evidence and explanation for this behavior in the next section.

## ICE BONDING IN THE ABSENCE OF SUBFREEZING EXTERNAL CONDITIONS

There is no need to resort to arguments about external cooling (either evaporative or sensible) in order to account for the strength (especially shear) of wet snow accretions. The development of interparticle adhesion through the evolution of ice-to-ice grain boundaries is a normal, in fact unavoidable, consequence of the accumulation of wet snow on an object.

Figure 2 is a sequence of photographs taken during and after a wet snow storm which caused considerable disruption of electrical power service in our area. These photographs are of samples taken from snow on the ground and not from snow packed by wind on a power line, but the grain-bonding mechanisms are the same. The major difference between the low density snow on the ground and the high density, wind-packed snow accretion is that the large forces on a power line immediately bring the ice particles into close contact. This accelerates both the densification process and the formation of grain boundaries; thus the development of interparticle strength occurs more quickly on power lines than on the ground.

The sequence in Figure 2 shows the rounding of the ice grains and their rapid growth as larger particles grow at the expense of smaller particles. Both of these processes are driven by the melting temperature - radius of curvature relation,

$$T_m = -\frac{1}{L\rho_i}\frac{2\sigma}{r} \tag{3}$$

where L is the latent heat of fusion, $\rho_i$ is the density of ice, $\sigma$ is the solid-liquid interfacial energy, and r is the mean curvature. The grain growth mechanism is described in more detail in Colbeck (1973) and in Raymond and Tusima (1979).

The evolution of grain boundaries is also shown in Figure 2 where grain clusters are shown to develop simultaneously with the growth and rounding of the grains. In low density seasonal snow a grain cluster generally consists of a number of tightly packed grains. Accordingly, the density of an individual cluster is quite high, while the snow density is low because the clusters are loosely bonded to their neighbors. The reasons for the formation of the high density clusters were explained in Colbeck (1979b) and can best be visualized by Figure 3. The arrangement of water, air and ice grains shown in Figure 3 is that necessary to minimize the surface free energy. The large grain boundaries shown in Figure 3 are not only stable, but are necessary. Any arrangement of ice particles at the liquid contents normally found in freely draining snow requires ice-to-ice bonding for thermodynamic reasons. Accordingly, it is unnecessary to argue that the strength of wet snow is explained by capillary forces; furthermore, ice grains bonded only by liquid menisci are unstable thermodynamically and will be replaced by grain boundaries (see Colbeck, 1979b). It is equally superfluous to argue about external cooling. External cooling is difficult to prove and unnecessary in any case; the formation of grain clusters and the associated grain boundaries provides the strength observed in wet snow.

As the density of wet snow increases above about 0.6 $Mg/m^3$, the

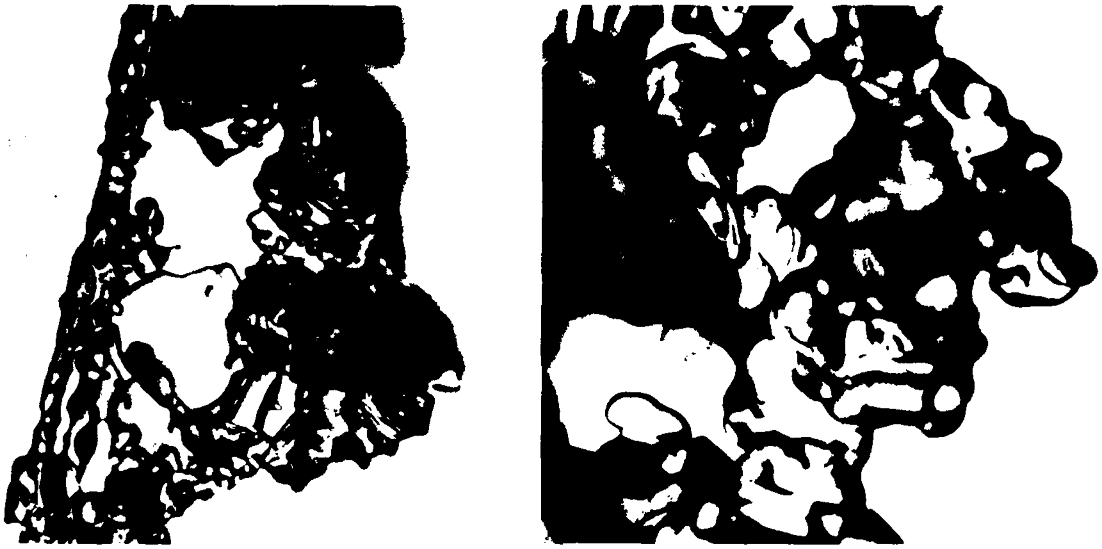

a. Fresh snowflake (T ≈ 2°C).

b. 5 hours old.

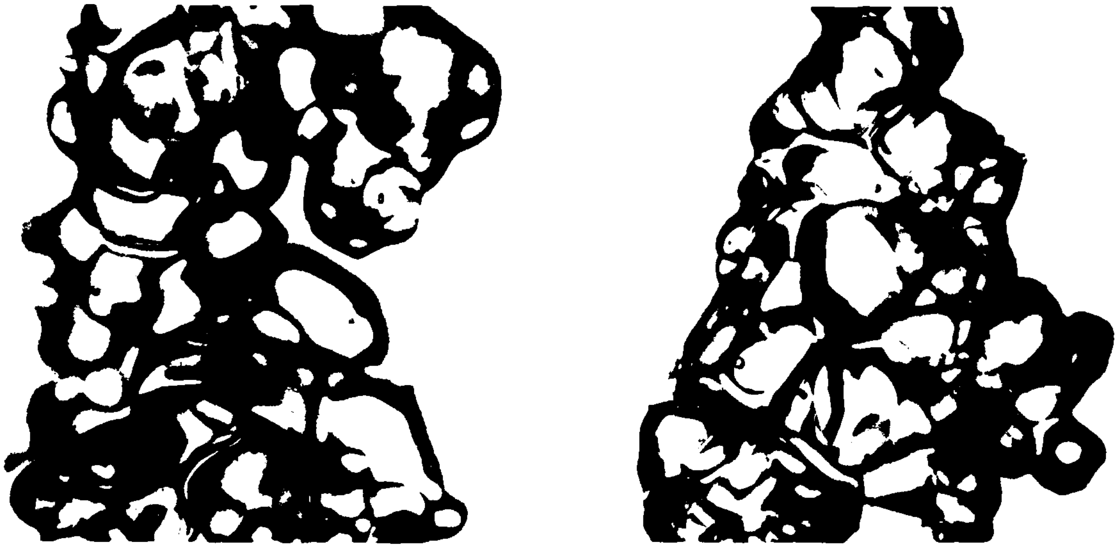

c. 10 hours old.

d. 28 hours old.

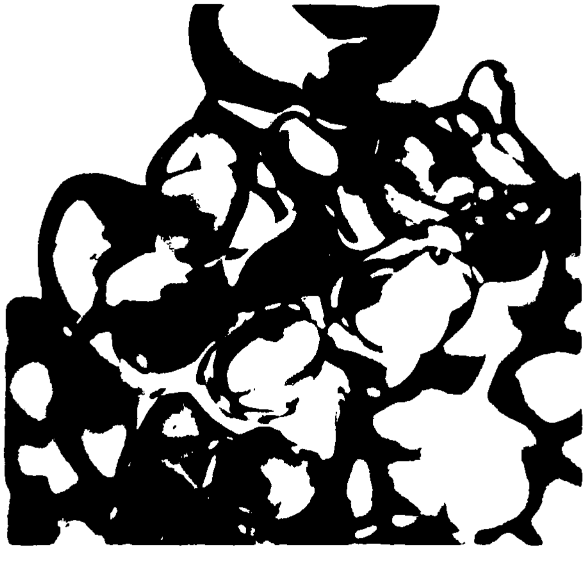

e. 53 hours old.

Figure 2. A series of photographs taken during a wet snow storm which led to major power outages in the Hanover, N.H., area on 25 Feb 1981. The temperature throughout this period was above freezing. The individual ice grains in e) are about 1 mm in size and all photographs have the same scale.

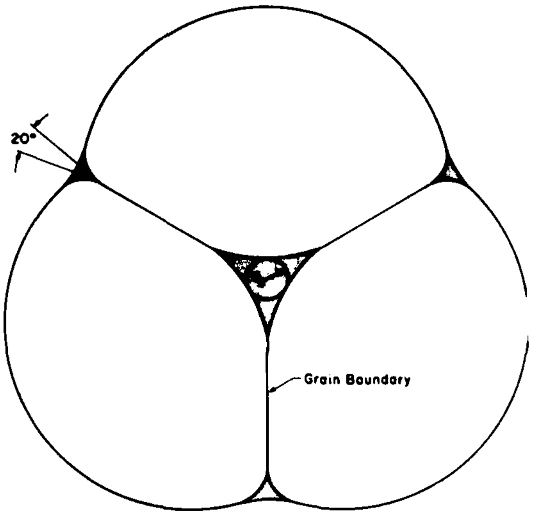

Figure 3. The basic three grain cluster in wet snow. The shaded area is liquid water and air surrounds the figure (from Colbeck, 1979).

strength increases as well. At about that density, the individual grain clusters disappear as the ice grains establish a continuous network of interconnected grains throughout the snow mass. This closer contact among the grains, and the increased density of grain boundaries associated with it, are due to the close packing requirements of well rounded particles at a higher density. In the snow cover on the ground these higher densities take months to achieve unless many meters of wet snow accumulation occur. On power lines, in the presence of high winds, the forces are sufficient to cause high accretion densities and the large specific grain boundary areas. Thus only a few hours is required to develop high strength, simultaneously with grain growth and grain rounding, in wet snow on power lines.

## REFERENCES

Colbeck, S.C., 1973. Theory of wet snow metamorphism. Research Report 313, USACRREL, Hanover, N.H.

Colbeck, S.C., 1979a. Sintering and compaction of snow containing liquid water. Phil. Mag. A39(1), 13-32.

Colbeck, S.C., 1979b. Grain clusters in wet snow, J. Colloid and Interface Sci. 72(3), 371-84.

Kemp, A.K., 1980. The formation of ice on electrical conductors during heavy falls of wet snow, Meteor. Mag. 109, 69-74.

Makkonen, L., 1981. The heat balance of wet snow, Meteor. Mag. 110, 82.

Raymond, C.F. and K. Tusima, 1979. Grain coarsening of water-saturated snow. J. Glaciol. 22(86), 83-106.

Ryder, P., 1981. Comment on the heat balance of wet snow, by L. Makkonen, Meteor. Mag. 110, 83.

Wakahama, G., D. Kuroiwa, and K. Gato, 1977. Snow accretion on electric wires and its prevention. J. Glaciol. 19(81), 479-87.

Wakahama, G., 1979. Experimental studies of snow accretion on electrical lines developed in a strong wind, J. Nat. Disaster Sci. 1(1), 21-23.

## APPENDIX

A wet snow accretion on a wire with a drag force per unit length $F_D$ is shown in Figure A1. We assume there is no ice bonding to the wire so there are no shear or tensile forces between the wire and snow. The snow is compacted against the wire by the compactive stress $\sigma_p$ ($\theta$) arising from the force normal to the wire F($\theta$). Both $\sigma_p$ and F vary with the angle $\theta$ and are related by

$$\Delta F = \sigma_p (r\Delta\theta) \qquad \text{(A1)}$$

where ($r\Delta\theta$) is the increment of area over which $\Delta F$ acts. We assume the compactive stress reaches a maximum value $\sigma_m$ at $\theta = \pi/2$ and varies according to

$$\sigma_p = \sigma_m \sin\theta \qquad \text{(A2)}$$

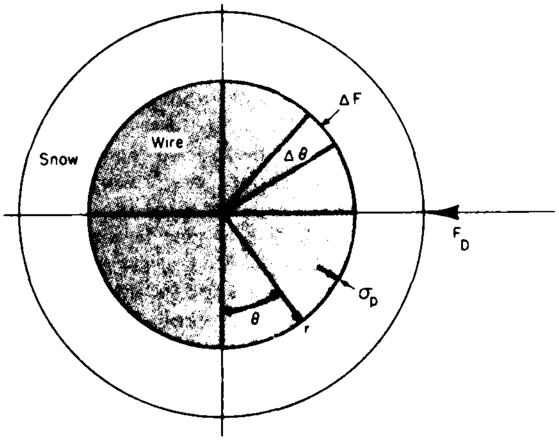

Figure A1. The cross-section of a wet snow accretion on a wire with a drag force $F_D$.

Then the average compactive stress $\bar{\sigma}$ is

$$\bar{\sigma} = \frac{2}{\pi} \sigma_m \qquad (A3)$$

The drag force $F_D$ is balanced by the compactive stress $\sigma_p$ when

$$F_D = \int_0^\pi \sigma_p \sin\theta \, (r d\theta) \qquad (A4)$$

Using Equations (A2) and (A3),

$$F_D = \frac{\pi}{2} r \bar{\sigma} \int_0^\pi \sin^2\theta \, d\theta \qquad (A5)$$

or

$$\bar{\sigma} = \frac{4}{\pi^2} \frac{F_D}{r} \qquad (A6)$$

DISCUSSION

Lozowski: What are the temperature limits to this effect? Presumably. if the air temperature is 70°F, you're not going to get wet snow and freezing on power lines, even if you have fog.

Colbeck: I think that the real question is how rapidly is the snow melting. If the snow is melting with sufficient speed and the liquid water content is sufficiently high, then at a very high liquid content, wet snow tends to be cohesionless spheres, and there would be no accretion on power lines. At low liquid contents, which are typically, say, below 10% by volume, then this geometry dominates; but you're right, at 70°, your're not going to get wet snow accretions. You can get wet snow accretions at temperatures which are above freezing.

Lowowski: How much above?

Ackley: If you have the compactive stresses and a supply of wet snow, you can make a snowball in this room. Right now. So there really is no temperature limit on that process, it's only in the context of whether the supply of wet snow is available, which probably has some upper limit, up around 5°C. But, for the purposes of making these wet snow accretions, the temperature is completely beside the point.

Schulson (Dartmouth): Do you know whether the surface energetics involved in the processes here are at all atmospheric sensitive? In other words, the liquid to solid interfacial energy - is it at all sensitive to the conditions of the atmospheric type of formation, and if so, will this model be dependent upon those conditions?

Colbeck: I'm not entirely sure what you're saying, but the thing which is important in determining this geometry are things like the contact angle, the free surface energies, the dihedral angle and the liquid-filled vein. The exact shape of this is going to be sensitive to all of the surface energies, the contact angle, the dihedral angle, etc. The shape is going to change with those values.

Schulson: You take those values to be more or less constant?

Colbeck: The contact angle is close to zero and the dihedral angle is 20°±10°. Now you know that from metallurgy, you get these liquid-filled veins, but they form a different kind of a figure in typical metals, because the dihedral angle in ice is something like 25°; at 40°, of course, these would be bigger, but the veins would still be there.

# Simulation and Modeling

AD P001670

# ATTEMPTS TOWARD ESTIMATING ICE LOADINGS BASED ON GENERAL CLIMATOLOGICAL DATA

Magnar Ervik The Norwegian Research Institute of Electricity Supply
Svein M. Fikke The Norwegian Research Institute of Electricity Supply

With reference to the development of a model to estimate ice loadings based on general climatological data, this paper presents the head lines of the work with atmospheric icing in Norway. Having a country with big climatic differences over short distances, effort has been put into systematizing all available information about heavy ice loadings in the past, general maintenance experiences and icing measurements in various parts of the country. In order to generate time series of ice loadings, the icing information must be correlated with general climatological data. As water content and droplet spectra of the cloud air are not measured regularly, it is supposed that they are correlated with other meteorological parameters. Some test results are presented.

## INTRODUCTION

In an earlier paper [1] the authors reported about a project on a model to estimate ice loading on transmission lines by use of general climatological data. In the concluding remark it is said that the aim of the project was:

"1. Obtaining an icing model of a certain quality to generate time series of ice loading at an arbitrary location/site as a base for using statistics of extremes. It is hoped that some topographical effects can be included in the model while it is anticipated that others have to be corrected for by direct inspection and judgement.

2. Introducing a program for continued maintenance and improvement of the model. This includes routines for ice measurements, observations and reporting as a feed back adjusting the model as well as taking into account new meteorological data not available at present."

In the following we will give an outline of the general parts of this program in order to discuss it with other workers in this field. We believe that such a program might form a base for further cooperation.

Some results obtained at the present stage, will also be reported.

## MAIN LINES OF THE PROGRAM

The main lines of the program is apparent from the aim: To generate time series on icing by use of general climatological data (see fig. 1)

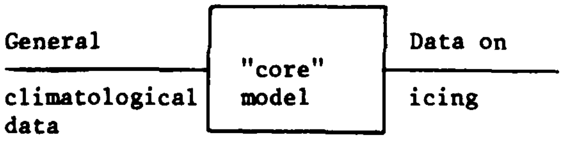

Fig. 1

The program can thus be divided in 3 main parts:

1. The formulation of a "core model.
2. Collecting and making available climatological data.
3. Carrying out icing measurements for control and improvement of the core model.

(The term "core model" has been used here to distinguish this part from the total program for which the term "icing model" has been used earlier.)

These three parts can be handled separately, although they currently have to be held together.

It is natural to mention the core model first since the possibility of converting weather data into icing data must be investigated first.

The basic requirement for such a model is the accessability to long enough time series of climatological data. Then we have to ask: Do we have the data needed to use the core model in its first version?

If we are in lack of data, we have to go back to the core model and try to modify it or build into it a part to convert available data into not available data.

The icing data based on direct measurements are necessary to control the model during the development stage, but also during its normal use to make improvements possible.

If there is any discrepancy between measured and calculated icing data, we have to investigate the reason for this.

Altogether the program will be an iteration process where the three main parts influence each other:

- The core model must take into account the climatological data *available today* with long enough time series. It should be modified if not consistent with available (measured) data on icing if these are reliable.
- The climatological data needed should be made available. If necessary own measurements should be initiated for future use. The possibility of cooperation with national meteorological institutions should be investigated.
- The work with the two first parts will indicate what we should be looking for when planning and carrying out ice-measurements.

In the next chapters some further comments will be made on the three parts of the program.

## THE CORE MODEL

### Physics of icing

There are mainly two atmospheric processes which cause icing.

Firstly, cloud droplets freeze immediately upon impact. Depending mainly upon the collection rate and temperature, the resulting icecover is (hard) rime (dry growth) or glaze (wet growth).

Secondly, supercooled rain or wet snow may cause icing mainly when falling into a surface freezing layer, or due to adhesion between the object and the free water in the wet snow. Freezing rain also results in glaze (wet growth) as above.

The parameters which govern the ice growth in the first case are therefore:

- liquid water content of the air
- distribution of droplet sizes
- air temperature
- windspeed relative to the perpendicular on the object

In the second case the important factors are:

- precipitation
- temperature of the object
- vertical temperature distribution
- wind

Due to the differences in physical processes, we may define the two mechanisms as:

- incloud icing

and - precpitation icing

### Accumulation models

The fundamental theory of accretion of cloud droplets as developed by Albrecht [3], demands knowledge of

- the content of liquid water in the air
- the distribution of droplet sizes

These parameters are not included in regular meteorological observations. Traditionally they have also been difficult to measure in areas where icing conditions are severe. For these reasons, the fundamental accretion theory has been only little used for practical dimensioning purposes. Another complicating element is that there are possibilities for the most severe icing conditions to be combinations of in-cloud icing and precipitation icing during the same storm or series of storms. Efforts have therefore been made to correlate iceloads directly to regular meteorological observations [1,4].

## METEOROLOGICAL DATA

### Observations

There are basicly two kinds of meteorological data:

1) Surface observations from ground stations.
2) Vertical soundings of the atmosphere.

Each are taken at regular hours and according to international standards.

The most relevant surface elements are:

- cloud amount
- height of cloud base
- air temperature
- wind
- prcipitation

From the soundings we get vertical profiles of:

- temperature
- humidity
- windspeed
- wind direction

These profiles help us to characterize the air mass and to indicate the thickness of the cloud cover in addition to the description of the physical state at any level of the atmosphere. The stability of the air is calculated from the temperature-profiles.

By analyzing synoptic soundings from a great area, fields of the parameters can be established for different heights, and the parameter value is known at any place of the field level.

### How to use the meteorological data

The cloud observations indicate the presence of droplets and the temperature of any height of the free atmosphere can be calculated. However, the the temperature must be adjusted for near surface conditions, and the representativity weakens with the distance away from the sounding station. Supposing the cloud to be a water cloud, as it is in most cases, an icing situation can thus be identified.

The icing intensity or accumulation rate must then be found by help of the parameters available. The intensity depends upon (among others):

- water content
- droplet sizes

However, these parameters are correlated with:

- temperature
- stability (vertical speeds)
- wind
- topography
- trajectories of the airstream

Thus it is possible to estimate water content and droplet sizes from the available parameters and calculate iceloadings for accretion models. Another possibility is to measure iceloadings directly and correlate these to the weather parameters. It is the latter procedure which is followed in Norway up to now.

In any case, measuring iceloadings directly and correlate these to the weather parameters is a possibility that should be used as a control as often as practical.

### Time series

Many nations have handled their data by computers for many years, and time series of 20-30 years or more are ready for computer calculations in some countries. If it is possible to achieve good correlations between the icing process and the climatological data, it is therefore possible to generate equal time series of iceloadings. In this way the probability distribution of iceloadings can be found.

### Some requirements for a meteorological data base

It is necessary to establish a data base for model development and maintenance. The meteorological data must *at least* consist of time series of:

- SURFACE OBSERVATIONS
  - air temperature
  - windspeed
  - wind-direction on the site (→ exposed sector)
  - maximum wind force between observation hours
  - cloud cover
  - base of cloud height
  - cloud type
  - amount of precipitation

- RADIOSONDE-DATA
  - height
  - temperature }
  - humidity } at fixed levels
  - wind }
  - significant levels for:
    - temperature
    - humidity
    - wind

All these data must be available up to at least 700 mb level.

If possible, there should also be access to analyzed fields of temperature, humidity and wind of a certain level representing the free atmosphere, e.g. the 850 mb level. The fields could be represented by gridpoint values. This would give higher accuracy for the estimation of the involved parameters at the site in question.

At last, a very valuable source of information are trajectories (previous paths) of air parcels reaching given points in the region. Such trajectories tell the "history" of the air mass, e.g. whether it is "maritime" or "continental". This is important for the estimation of the liquid water content and droplet size distribution.

The space and time resolutions are mainly determined by the distribution of radiosonde stations and their observing and recording programs. In many countries radiosonde-balloons are dropped every 12 hours (00 and 12 GMT), but in some cases they are dropped at 6 hour intervals. Surface stations make mainly 3-8 observations per day, though many airports observe every hour, or even half hour during most of the day. Proper use of such data may improve the time resolution of an icing model.

The vertical resolution depends upon the observation of cloud heights. The synoptic code for cloud base divides the heights in ten groups:

| code | height (m) | code | height (m) |
|---|---|---|---|
| 0 | 0-50 | 5 | 600-1000 |
| 1 | 50-100 | 6 | 1000-1500 |
| 2 | 100-200 | 7 | 1500-2000 |
| 3 | 200-300 | 8 | 2000-2500 |
| 4 | 300-600 | 9 | > 2500 |

However, especially airports have ceilometers, which give a much higher resolution of the heights.

## ICING MEASUREMENTS

### Background

For a long time ice loading measurements have been carried out. The relationship between climatological parameters and icing has been known very long, at least the main pattern. The combination of measured data and use of weather statistics has been applied for several years to select design loadings. This has been described in the companion paper [2].

### Data for the icing model

Within the icing model program,

icing measurements will still play an important role. However, the purpose of the icing measurements may have changed a bit as already mentioned in the chapter "Main lines of the program".

The impact of the icing model on icing measurements, or on collecting data on icing otherwise, is to systematize.

On the one hand this will give us a rather liberal attitude towards the measurements: Any kind of icing data may be accepted provided certain precautions are taken as to origin and reliability. We only ask:

- What is available?
- What is practical/cheap to obtain?
- What is possible to get?

On the other hand, if we are in a position to initiate new measurements, we would know better than before what we should be looking for and plan our tests accordingly.

### Data types as to icing

Different quantities expressing icing may be of intere .. Examples of these are:

- Icing intensity
- Rate of growth (on different objects)
- Accumulated ice deposit
- Ice loadings

### Icing data sources

Following sources supplying data on icing may be mentioned:

- Special measuring stations
- Observations/measurements at other installations
- Experience

The two first mentioned groups of sources include historical as well as current data collections. They may also give several data types including meteorologic ones - or they can be confined to a single quantity. Also they may give a high time resolution, up to continuous measurements - or they give a few values a year (e.g. extreme load measurements).

There is also a large amount of icing data, more or less easily available from practical experience. Boldfaced experience like breakdowns or other damages due to excess loading, are representative sources in this group. However, a transmission line with a long history of no failure, is also a source that should not be overlooked.

## TEST RESULTS IN NORWAY

### Meteorological stations

The Norwegian Metorological Institute stores data from about 200 weather stations observing cloud heights according to the synoptic code. Additionally there are 80-90 climatic stations observing the amount of cloud cover. All stations observe such elements as temperature, wind and precipitation. These data are available partly from 1951 on, partly from 1957, stored on magnetic tapes. There are 4 radiosonde-stations in Norway, some with data from 1949.

### Icing observations

In (2) is given a survey of the test stations for icing observations in Norway. Two of the stations have been manned and have observed both icing and meteorological parameters. They have also been situated near synoptic weather stations, one in northern Norway (850-100 m a.s.l.) and the other in southeastern Norway (950 m a.s.l.). Observing periods have been 1971-78 and 1973-78 respectively.

### Model results

Table 1 shows 17 periods with measured loads above 20 kg/m or the season's extreme from the test station "Fagernesfjellet", near the city of Narvik in northern Norway. The measured loads are from the highest part of the station (1000 m a.s.l.). This part was separate from the observer's logde and was not accessible in bad weather. However, this part gave the highest loads and was exposed to a wider sector (SW-N).

The columns with model results show the dates where the model defines icing within the periods of observed icing. The totals of the iceloadings are also shown.

The greatest uncertainties in the measured values are linked with the inspeciton frequency of the test tubes and also with the ice density measurements. The model results are somewhat limited

TABLE 1: Calculated iceloadings during observed periods of icing at the test station "Fagernesfjellet" (1000 m a.s.l.). Model periods are terminated after 36 hours of no icing.

| OBSERVED | | CALCULATED BY MODEL | |
|---|---|---|---|
| Period | Iceload | Period | Iceload |
| 71-12-29 - 72-01-04 | 70 | 71-12-29 - 71-01-03 | 72 |
| 72-02-15 - 72-02-25 | 57 | 72-02-18, 72-02-22-24 | 42 |
| 72-03-10 - 72-03-16 | 38 | 72-03-13 | 12 |
| 72-03-21 - 72-03-25 | 52 | 72-03-18 - 72-03-22 | 54 |
| 72-12-30 - 73-01-05 | 27 | 72-12-30, 73-01-04-05 | 24 |
| 73-03-09 - 73-03-21 | 43 | 73-03-10-12, 73-03-14-15 | 66 |
| 73-11-25 - 73-11-30 | 25 | | 0 |
| 75-02-04 - 75-02-12 | 78 | 75-02-03 - 75-02-08 | 78 |
| 75-02-26 - 75-03-06 | 60 | 75-02-26-27, 75-03-03, 75-03-05 | 54 |
| 75-03-11 - 75-03-21 | 100 *) | 75-03-12-14, 75-03-18 | 30 |
| 76-02-18 - 76-03-04 | 12 | 76-02-15-18, 76-02-24-29,<br>76-03-04 | 102 |
| 76-11-16 - 76-11-25 | 30 | 76-11-17 - 76-11-21 | 54 |
| 77-01-03 - 77-01-10 | 27 | 76-01-05 - 76-01-07 | 30 |
| 77-02-11 - 77-02-15 | 24 | | 0 |
| 77-03-01 - 77-03-05 | 21 | 77-03-05 | 6 |
| 77-03-20 - 77-03-28 | 25 | 77-03-24 | 12 |
| 77-11-26 - 77-12-05 | 43 | 77-11-29 - 77-12-01 | 42 |

*) uncertain value

by the time resolution of 12 hours of the radiosonde-data. Introducing air mass characteristics, intermediate surface observations and analyzed field values of temperature and wind in the 850 mb level is supposed to improve the reliability of the model results.

Some discrepancies between observed and calculated iceloadings may be explained by e.g. ice falling off the tubes before inspection (76-03-04), or in some cases the layer has been accumulated by drifting snow (75-03-21).

REFERENCES:

(1) Ervik, M. and Fikke, S.M., "Ice Loadings on Transmission Line Conductors, Estimated by Use of General Climatological Data," Transactions on Power Apparatus and Systems. Vol. PAS-101,pp 1497-1503, June 1982

(2) Evensen B., Fikke S.M. and Schjetne K., "Iceload Measurements and Design Practices in Norway", First International Workshop on Atmospheric Icing of Structures, Hanover N.H. 1982.

(3) Albrecht F., "Theoretische Untersuchungen über die Ablagerungen von Staub aus strömmender Luft und ihre Anwendung auf die Theorie der Staubfilter", Physik. Zeitschrift XXXII, 48-56 (1931).

(4) Chaîné P.M, "In-Cloud Icing", Industrial Meteorology - Study V. Environment Canada. Toronto 1974.

DISCUSSION

Question: [...] to establish eventually ice loading maps for transmission lines throughout Norway, is this your basic goal?

Ervik: Maybe we will not go as far as to establish maps all over Norway, but we want to know what can be used each time we are designing a transmission line for that region and we now have a special project for the state model board to use our models [...] for a certain transmission line. But it's fitting that we do some tests and also to try to make our model better doing this work.

Assur: I have several questions. The first one: you are referring to calculated values, and I wonder whether the algorithms will be available which you used, which could be either theoretical or empirical, I don't know.

Ervik: They are a mixture of theoretical and empirical.

Assur: Are they going to be available?

Ervik: Yes, I think we could make them available.

Assur: Apparently, you have a tremendous amount of observational data, so the question is whether these observations will be available in a systematic fashion for other people to work on.

Ervik: Yes, I think we have them in our documents, we have them available, so it could be.

Assur: Two more questions. One of them-whether you have tried your model on observational data obtained from the TV tower in Moscow - that's rather well documented, both the actual icing and of course the weather data, that's available, we have it on microfiche.

Ervik: Well, I think we would like to try, we have not, of course.

Assur: But it would be a test in another environment.

Ervik: Yes.

Assur: And the last question - in your algorithm, what do you assume is the function of the wind speed?

Erivk: Well that's - as far as now, we had not - we have used it only as a ...

Assur: How does the wind speed affect the collection of icing?

Ervik: We have a problem by comparing our test data to wind, that above a certain wind speed, we will have a better fit than in the lower wind speed. So, of now, we have only -

Assur: Well, it is not proportional.

Ervik: No,no, no - it's not proportional.

Assur: Ackley and company here in our lab proved it is a sort of an exponential function, which, by the way, came out, also, of the observational data in Moscow. The functions, empirical or derived from the lab, are very similar, and I wonder what you are using. From the paper itself I have no lead.

Ervik: Well we - no, there's no lead in the paper. But what we actually used from the only stations where we tested it was to try with different levels of wind speed; below we said no ice, above there is ice.

Assur: Could you sort of sketch the way it looks according to your idea?

Ervik: Well, I don't think I have the material to sketch it here, but it's just an on-off process - the wind has just been used as an on/off factor. Below a certain value, we have said there is no icing, which is of course, not great. And above a certain wind speed...

Assur: What happens at extremely high wind speeds?

Ervik: We have not taken this into account. We know that what can happen is that maybe the wind will blow the ice off.

Assur: Without that, you have no solution.

Ervik: We have not defined the solution. We know that.

Assur: Then, of course there's the difficulty - Norway is very mountainous, you have the difficulty with climatological data in that you cannot really extrapolate very well.

Ervik: All your questions will show we have not solved all this too well but we are working on it. But it is an extrapolation of the ways used today when you just go out and do the terrain and then you try to fit some data. At least we now try to develop a model. It's not finished yet. But we try to systematize all the data later and see how they compare to what we measured.

Assur: You probably have the worst spot on earth, but ...

Ervik: The whole contribution here, is just to have them discussed and we will note all you have said, and try to work on it.

AD P001671

# ICING OF CABLES

B.W.Smith,B.A.,M.S.,FICE,
MASCE. Partner, Flint & Neill
Partnership.
C.P. Barker, B.Sc.,ACGI,
Senior Engineer, Flint &
Neill Partnership.

## ABSTRACT

Tests have been undertaken in a climatic chamber to examine ice formation on cables. The purpose of the tests was to investigate the build up of ice in relation to the torsional stiffness of cables as used in guyed mast construction.

The build up was simulated using an analytical approach and good agreement obtained between the test profiles and the computer model predictions. The analytical approach was then used to develop ice shapes for various cable parameters.

Comparison with ice shapes measured from a guyed mast also showed good agreement, enabling the ice intensity and distribution to be assessed. The paper describes the tests undertaken, the analytical approach adopted and the treatment generally used in the U.K. for assessing the static effects of ice on guyed masts.

## 1. INTRODUCTION

The collapse of the 1,250 ft. high guyed mast at Emley Moor in 1969 under conditions of icing focussed the attention of engineers concerned with the design of such structures on the problems of predicting ice loading on guyed masts.

The shape of the ice is of extreme importance in predicting the appropriate wind lift and drag coefficients for use in design, and in assessing the likely weights of ice on cables. The paper describes the development of a theoretical approach to the prediction of the ice shape on guyed cables; describes tests in a climatic chamber to verify the theory adopted; and compares the theoretical approach with samples of ice collected from the cables of the Emley Moor mast.

In the United Kingdom, the period during which ice forms are not sufficiently prolonged to assume that full ice loading occurs under conditions of maximum wind speeds. The appropriate combination of wind and ice for design criteria therefore needs to be carefully established.

A brief description of the current approach to wind and ice loading in the United Kingdom is given.

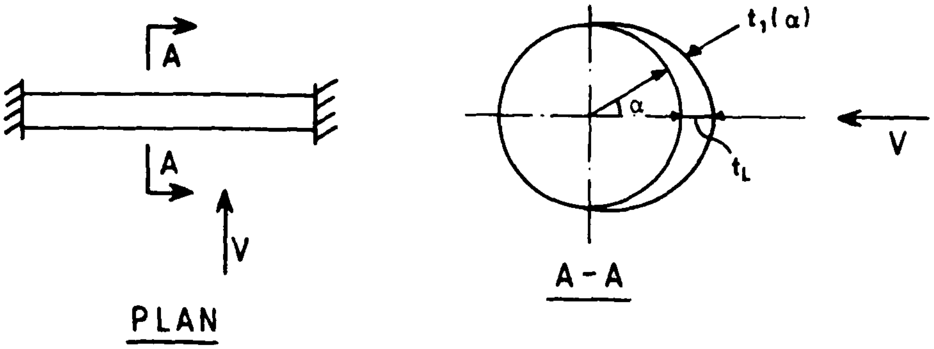

Fig.1: Prismatic Bar

## 2. THEORY

The formation of ice on cables is known to be dependent upon the orientation of the cable to the wind direction. In order to predict the likely patterns on the stays of guyed masts. which are each at a differing incidence to the wind, the likely form of the build-up of ice needs to be established. The following simplified theory provides a means of predicting the shape of the ice on cables inclined to the wind. The basis is divided into two parts. The first deals with the treatment of ice accretion on prismatic sections. The second deals with the interaction between the rate of ice accretion and the torsional stiffness of a finite length of cable.

### 2.1 Treatment of Ice Accretion on Prismatic Bars

Consider a torsionally stiff prismatic bar held on fixed supports at its ends, with the wind blowing horizontally, normal to the bar (see Fig.1).

The quantity of ice deposited by the wind will obviously be greatest on the front face of the cylinder.

It is assumed that ice will only be deposited on the front face, and the thickness will be proportional to the component of wind normal to each part of that face, hence

$$t_i(\alpha) = t_L \cos\alpha \qquad -90^\circ < \alpha < 90^\circ$$

where α = the angle between the surface point in question and a fixed point on the body surface, x

$t_L$ = maximum thickness applied in each lamina

$t_i(\alpha)$ = thickness of ice in the ith lamina at position α

For any further lamina the shape of the cross section is defined as the total shape of ice + cylinder after the application of the previous ice layer [R (α)] See Fig. 2.

After the application of i lamina the total body surface is defined by $R_i(\alpha)$, and the thickness of the next layer at any α is given by

$$t_i(\alpha) = t_L \cos\phi \qquad -90^\circ<\phi<90^\circ \quad (1)$$

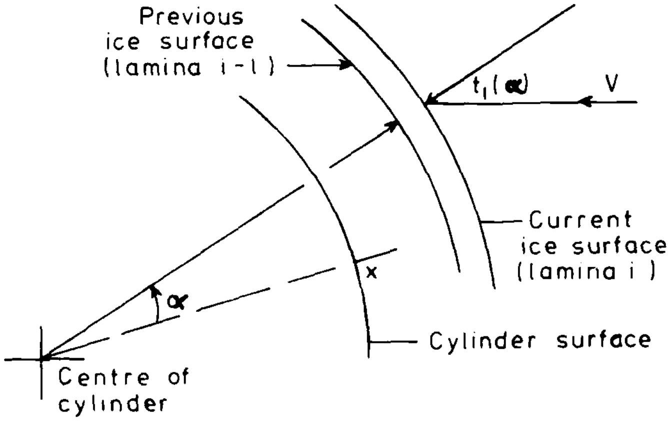
Previous ice surface (lamina i-1)
$t_1(\alpha)$
V
Current ice surface (lamina i)
x
α
Cylinder surface
Centre of cylinder

Fig 2 Build-up of ice

$\phi$ = angle between the wind and the normal to the total surface at the point in question.

In fact tests have shown that ice is accreted beyond $\phi = \pm 90^{o}$ and that $\pm\ 105^{o}$ would seem a more suitable value for use. Differing values of these limits can easily be incorporated by scaling in equation (1) above.

By repeating this process over and over again using suitably small values of $t_L$, realistic ice shapes may be produced.

## 2.2 Treatment of Ice Accretion on Cables.

When considering ice accretion on cables, the cable will rotate slightly between the applications of each ice layer, continuously accommodating the torque caused by the asymmetric shape. This section proposes a method for dealing with this interaction.

### 2.2.1 Relation between Torque and Deflections.

If we represent the cable by a lumped mass system (see Fig. 3), the centre of the cable and hence its stiffness is located at A, and the centroid of the ice at B.

Hence the applied torque per unit length, T, is given by

$$T = mg\bar{d}\sin\left[\tan^{-1}\left(\frac{\bar{x}}{\bar{y}}\right)\right]$$

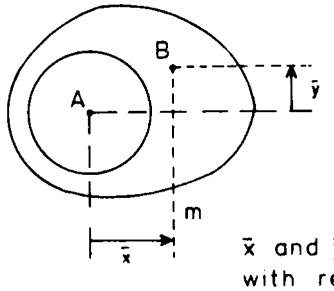

$\bar{x}$ and $\bar{y}$ define B with respect to A

m = mass of ice

$\bar{d} = \sqrt{[\bar{x}^2 + \bar{y}^2]}$

Fig. 3: Ice Build-up on Cable

But if this is rotated through $\Psi$ then T becomes

$$T = mg\bar{d}\sin\left[\tan^{-1}\left(\frac{\bar{x}}{\bar{y}}\right) + \Psi\right]$$

By ensuring that the lamina are very small, $\Psi$ can be kept small, hence for small $\Psi$ :-

$$T = mg\bar{d}\ \sin\left[\left(\tan^{-1}\left(\frac{\bar{x}}{\bar{y}}\right)\right) + \Psi\cos\left(\tan^{-1}\left(\frac{\bar{x}}{\bar{y}}\right)\right)\right] \quad . (2)$$

which can be rewritten as

$$T = a + b\ \Psi \quad . \quad . \ (3)$$

### 2.2.2 Allowance for Varying Deflection along Cable.

A finite element treatment can be adopted to allow for the variation of rotation along the cable.

The cable is split into a number of discrete lengths, with rotations, $\theta_i$, calculated at the node positions and the applied torques, $T_i$, found from effective lengths $L_i$. This may be seen in Fig.4.

The torque at node j is found by assuming $\theta_j$ to be constant along length $L_j$.

By using the normal stiffness method:

$$T = K\Theta \quad . \quad . \quad . \quad .(4)$$

T = vector of applied torques
K = stiffness matrix
$\Theta$ = vector of deflections (twists)

From equation (3) it may be seen that the applied torque is a function of the final position

$$\text{i.e,}\ T = A + B\Psi \quad . \quad . \quad .(5)$$

where A and B are matrices of the terms a and b found in Equation (3)

$\Psi$ is the vector of terms $\delta\theta$ the change in twist between the last lamina and the results of applying this lamina

$\Theta$ is the vector of final twists, i.e. $\Theta$ from last cycle plus $\delta\Theta$ (or $\Psi$) from this.

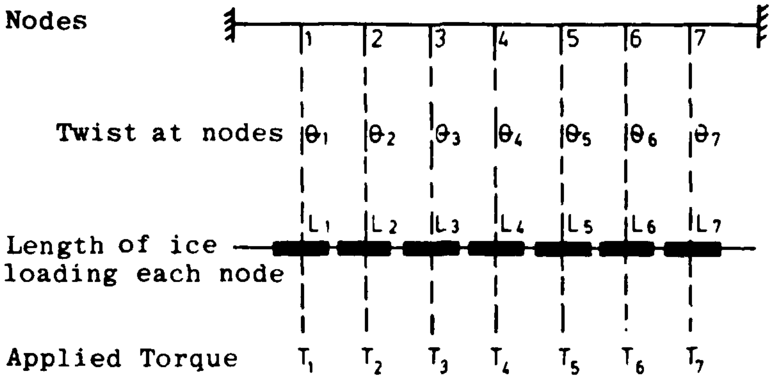
Nodes
1
2
3
4
5
6
7
Twist at nodes
θ1
θ2
θ3
θ4
θ5
θ6
θ7
Length of ice loading each node
L1
L2
L3
L4
L5
L6
L7
Applied Torque
T1
T2
T3
T4
T5
T6
T7

Fig. 4: Treatment along Length of Cable

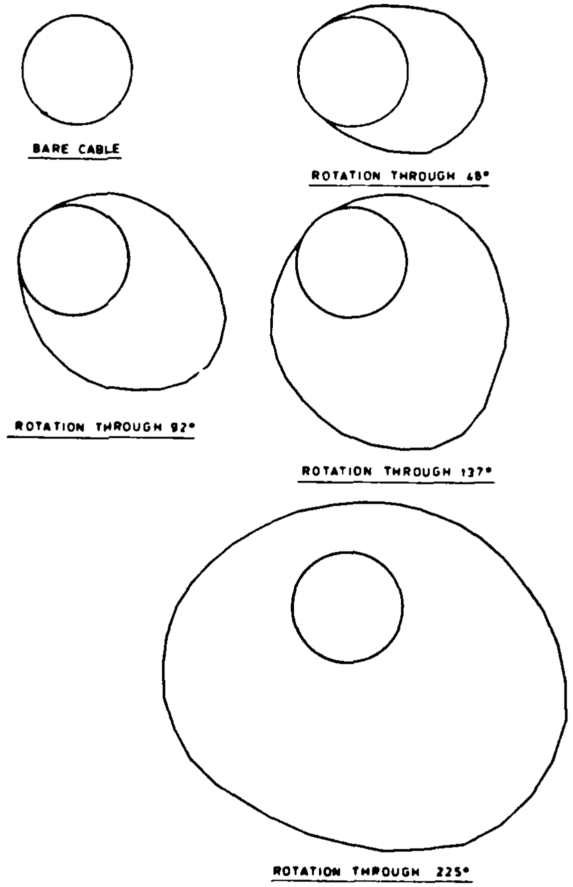
BARE CABLE
ROTATION THROUGH 48°
ROTATION THROUGH 92°
ROTATION THROUGH 137°
ROTATION THROUGH 225°

Fig. 5a. Predicted shape at centre of cable for stages in build up of ice.

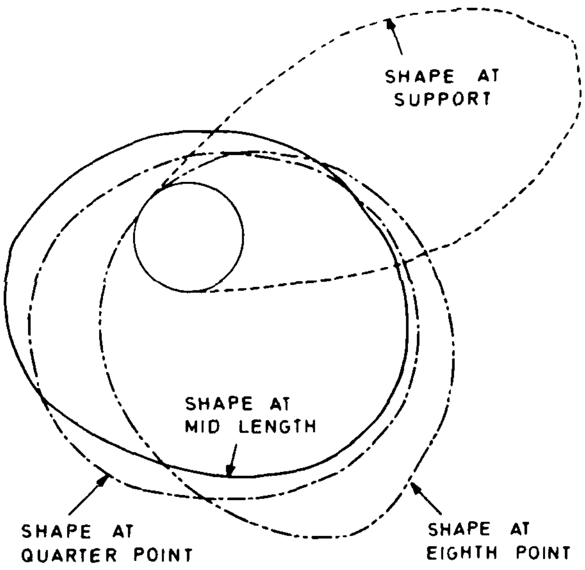
SHAPE AT SUPPORT
SHAPE AT MID LENGTH
SHAPE AT QUARTER POINT
SHAPE AT EIGHTH POINT

Fig. 5b. Predicted Shape along length of cable for centre rotation of 225°.

So $T = K(\Theta + \Psi)$

$$\Psi = K^{-1}T - \Theta$$

Substituting for T from (5)

$$\Psi = K^{-1}(A + B\Psi) - \Theta$$

$$\therefore (U - K^{-1}B)\Psi = K^{-1}A - \Theta$$

where U = unit vector.

Hence $$\psi_i = \delta\Theta_i \frac{\left[ K^{-1}A - \Theta \right]_i}{\left[ U - K^{-1}B \right]_i} \qquad (6)$$

Hence the change of twist due to the application of each lamina can be solved.

By repeating this process as each lamina is applied, not only can the varying twist down the cable be represented, but also the variation of shape. Examples of this treatment are shown in Fig. 5(a), which shows the shape derived at various rotations of a cable at its centre point, and the variation along the length of the cable for a centre rotation of 225° is shown in Fig. 5(b).

## 3. TESTS IN THE CLIMATIC CHAMBER.

### 3.1 General

To verify the approach developed, as outlined in (2) above, tests were carried out in the British Aircraft Corporation's climatic test chamber. This chamber is 7.6 metres in diameter and 15.2 metres in length, the atmosphere of which can be controlled to produce various conditions of temperature, humidity, barometric pressure, wind, rain, snow and ice. Environmental conditions within the chamber can be controlled over the temperature range -55°C to + 60°C, and winds of up to 20 metres per second can be generated, and humidity controlled to produce ice, snow or dry conditions.

### 3.2 Test Arrangements

In the tests undertaken to simulate icing on cables, the following models were of the most interest:

(i) a horizontal tube of 45 mm diameter, approximately 1.5 metres long, supported at its ends on needle bearings, allowing the tube to twist freely,

(ii) two inclined tubes positioned such that their axes of inclination were in the line of the wind, with one tube representing a windward stay and the other tube a leeward stay,

(iii) tubes mounted on torsional springs at their ends, providing variable rotational restraints. These are sketched in Fig. 6(a) and shown in Plate 1. The tubes were mounted at various incidence angles to the flow.

(iv) three tubes each approximately 1.3 metres long mounted horizontally on a steel wire of total length 8 metres, as shown in Fig. 6(b). The tubes were rigidly fixed to the wire whose diameter was chosen to represent the torsional

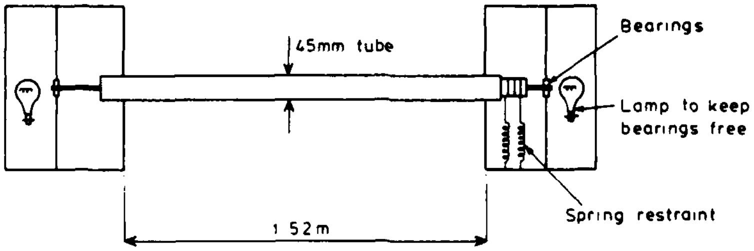

(a) Tubes mounted on torsional springs

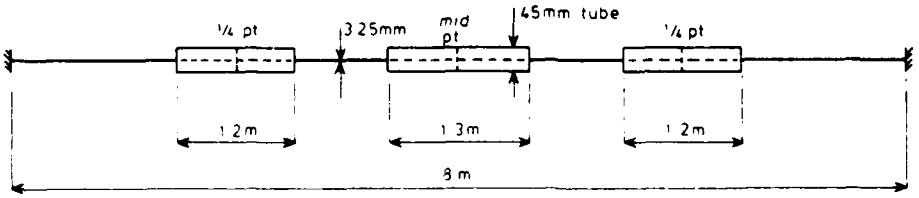

(b) Tubes mounted on steel wire

Fig. 6 Test Arrangement

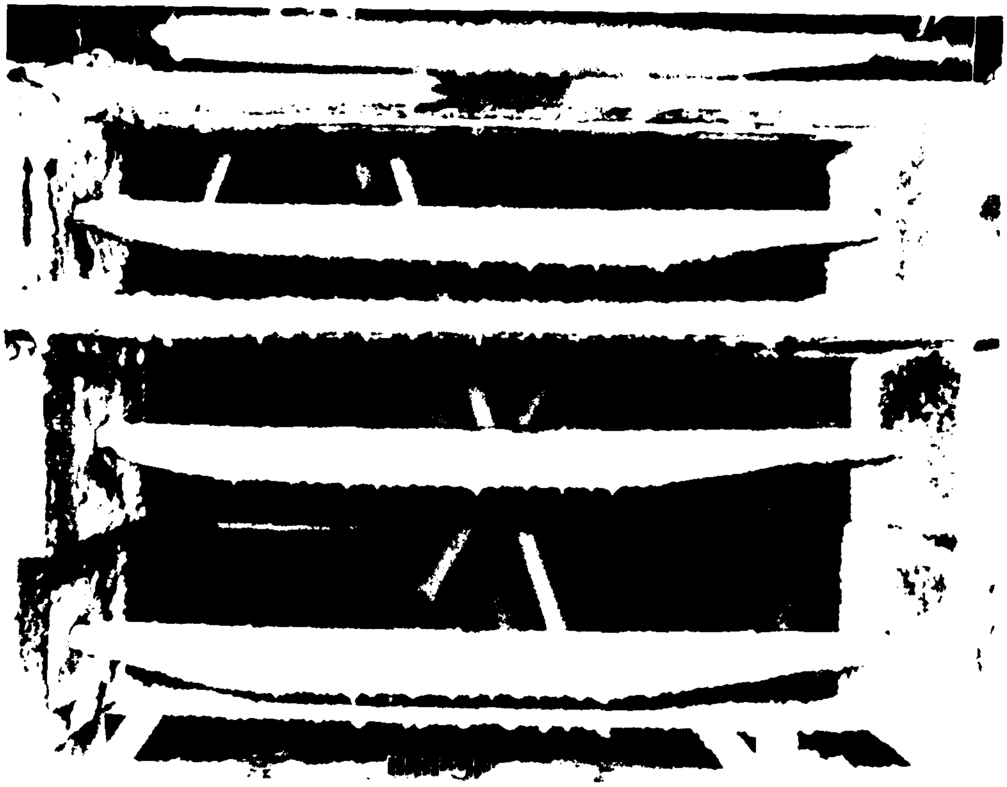

PLATE I  TUBES MOUNTED ON TORSIONAL SPRINGS

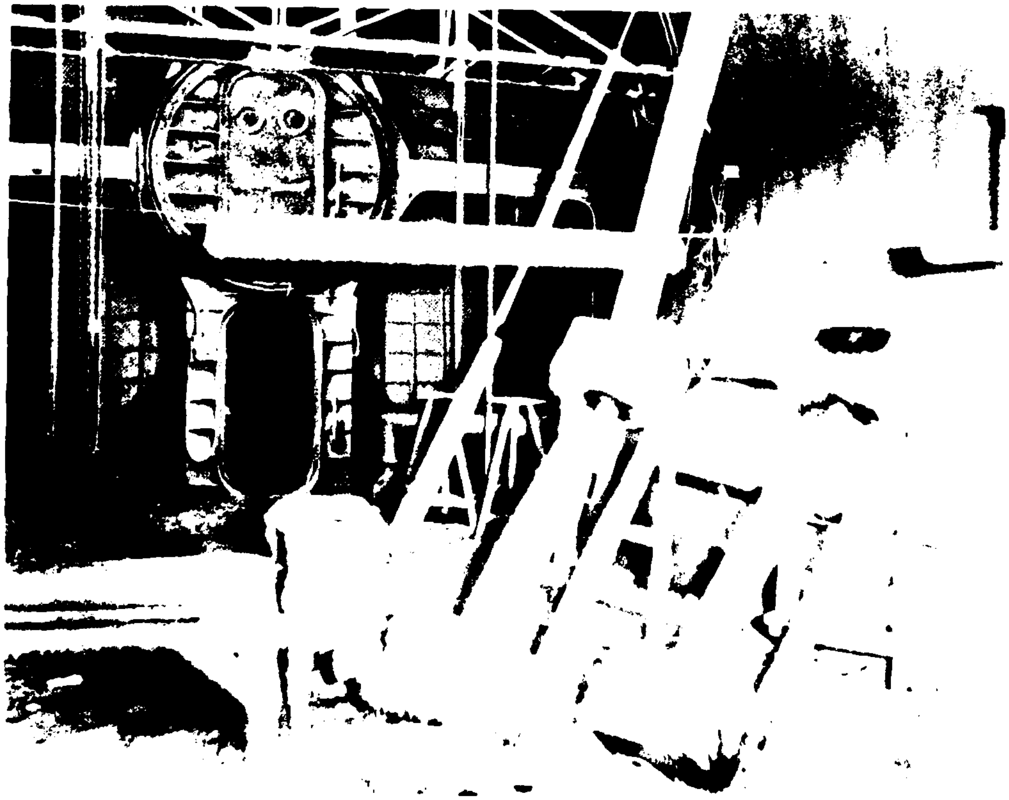

PLATE II  GENERAL ARRANGEMENT IN CLIMATIC CHAMBER

stiffness of a typical stay in a guyed mast. A general arrangement in the chamber is shown in Plate II.

## 3.3 Environmental Conditions during the tests.

Wind speed, measured prior to the tests using an anemometer, was kept at 8.5 metres per second throughout. The temperature was maintained at approximately -2°C, although on occasions it reduced to approximately -9°C.

Water vapour was introduced into the chamber through a four start spray. The temperature of the water, which had been passed through a heat exchanger, was measured at -2°C.

## 3.4 General Comments.

The stiffness of each of the torsional springs was measured to enable comparisons with theory to be made. No measurements were made of forces on the tubes but photographs and measurements of the shapes were recorded.

Measurements of density were made by taking various samples from the tubes and supporting steelwork,and generally a value of approximately 0.9 grams per c.c. was obtained. The formation of the ice appeared to be of a clear, glazed type adjacent to the tubes, followed by a more crystalline and opaque formation. The final surface was relatively rough with undulations about 8 mm deep and 16 mm long.

## 3.5 Results of test.

The tube which was free to rotate formed a sensibly uniform build-up of ice, and during the tests the tube rotated more than one revolution with a total thickness of the ice of approximately 15 mm.

In the tests on tubes with torsional springs, and on the tubes supported by the steel wire, ice build-up occurred initially on the windward face,until the weight of ice induced sufficient torsional moment to rotate the tube downward, allowing further ice to occur above that already formed. Measurements were made of the ice shape progressively throughout the tests,and typical cross sections are shown in Fig. 7 (a to d).

## 3.6 Summary

It was found that the climatic chamber could simulate icing conditions and produce a realistic accumulation of ice in a relatively short period of time. Simulation of the exact ice patterns observed in practice on masts was not achieved, but this was probably due to:

i) the tests being undertaken in a uniform wind speed,
ii) a sensibly uniform water condition being used throughout the tests.

The mechanism of twisting of the cables predicted by theory was borne out by the tests, as may be seen in Fig. 8. In addition, it was found that the rate of accretion appeared to be greater on smaller tubes and, on members inclined away from the wind (i.e.: the windward tube),the total ice accreted was greater.

## 4. ICE EXAMPLES FROM CABLES

Following the collapse of the Emley Moor mast, samples of ice found on snow covered ground were photographed and sketched. These samples were matched to the cables from which they broke away and, knowing the wind direction and slope of the cable, it was possible to predict from the theory developed, the general shape of the ice, and to compare it with the sketches of the samples.

A typical comparison is shown in Fig. 9, from which it may be seen that good agreement is obtained.

## 5. CODES OF PRACTICE AND SPECIFICATIONS ON THE U.K.

Current British Standards do not provide quantitative guidance for ice loadings of masts and towers. In the Draft British Standard Code of Practice for Lattice Towers, rules have been developed, and in current

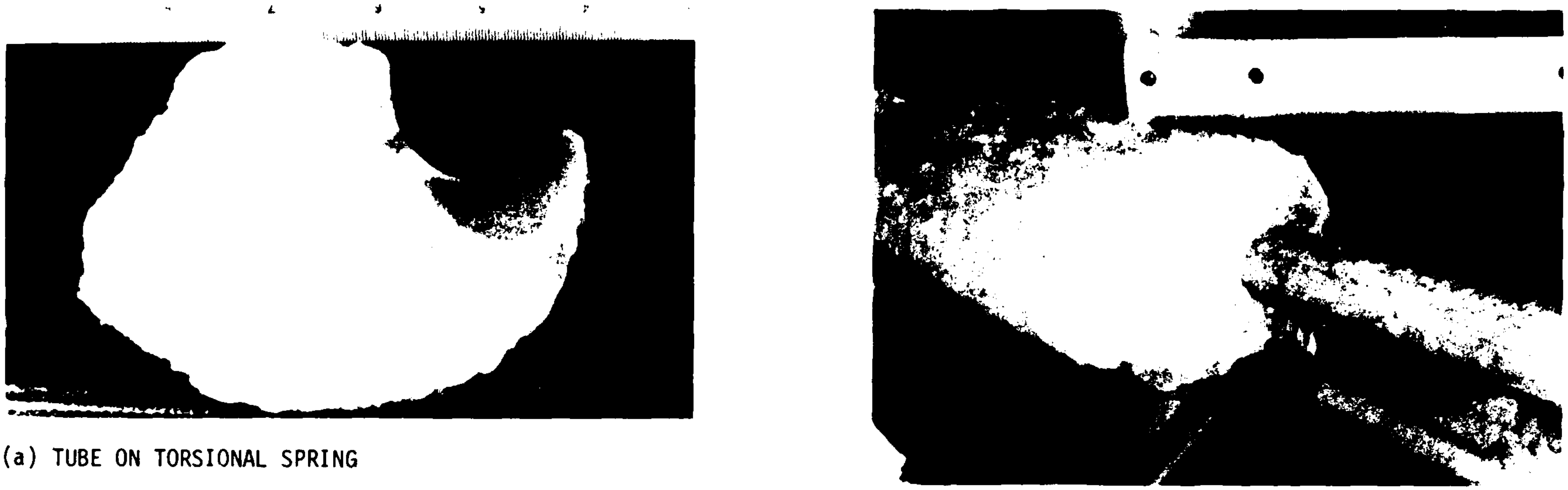

(a) TUBE ON TORSIONAL SPRING

(b) TUBE ON TORSIONAL SPRING

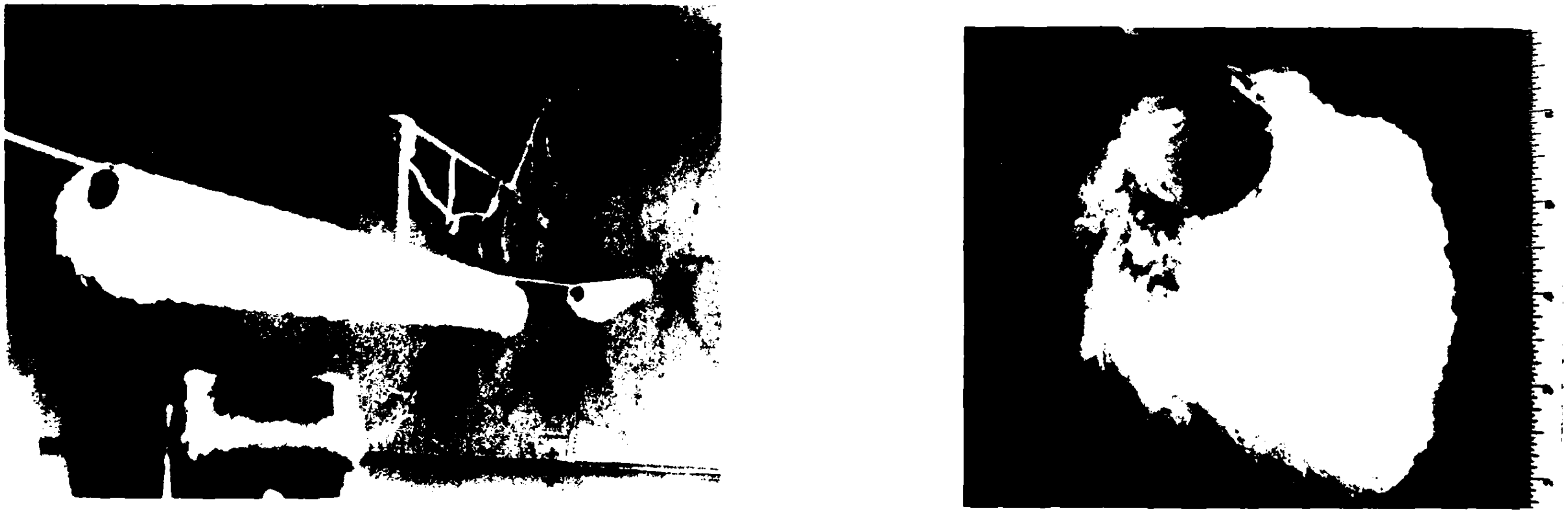

(c) TUBE SUPPORTED ON WIRE

(d) TUBE SUPPORTED ON WIRE

Fig. 7. TYPICAL CROSS SECTION FROM TESTS.

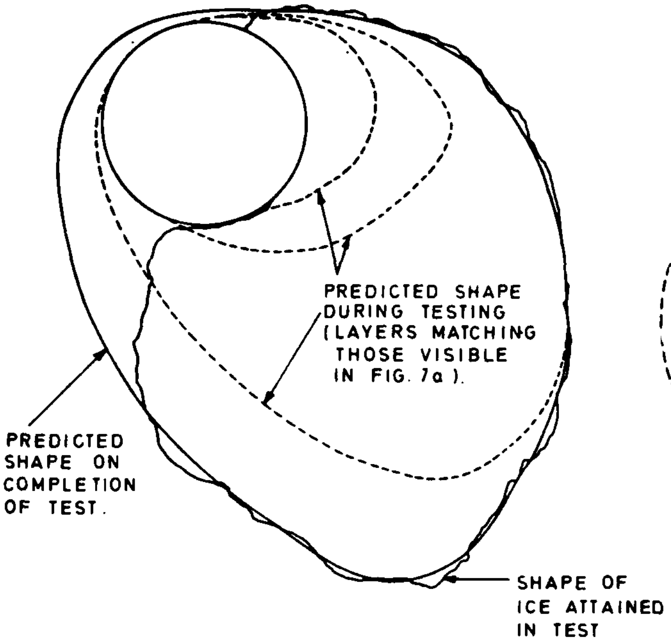
PREDICTED SHAPE DURING TESTING (LAYERS MATCHING THOSE VISIBLE IN FIG. 7a).
PREDICTED SHAPE ON COMPLETION OF TEST.
SHAPE OF ICE ATTAINED IN TEST

Fig. 8. Comparison of Theory with Tests from Climatic Chamber

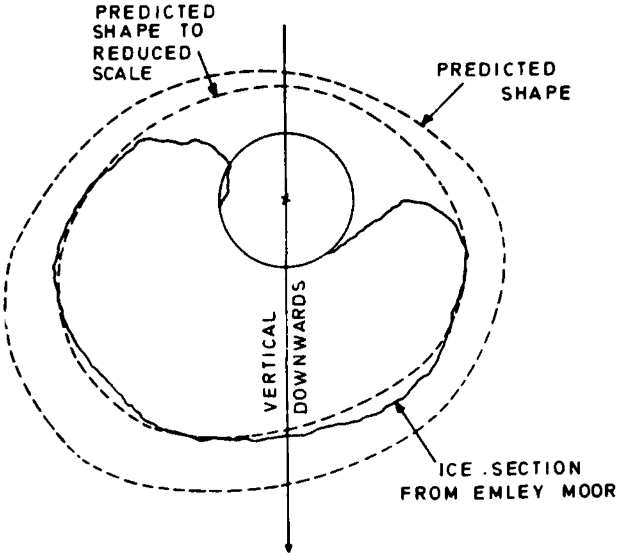
PREDICTED SHAPE TO REDUCED SCALE
PREDICTED SHAPE
VERTICAL
DOWNWARDS
ICE SECTION FROM EMLEY MOOR

Fig. 9. Comparison of Theory with Ice Samples from Guyed Mast.

specifications for Broadcasting Authorities in the United Kingdom, allowance is made for ice loading of cables for guyed structures. In these, account is allowed for asymmetric distribution of ice on the cables at any one level - generally the most critical condition, in severe icing, for the mast column design.

In the Draft Code of Practice allowance is made for variable ice intensity throughout the United Kingdom, on the basis of Meteorological data. The analyses of records at 23 stations of the average annual duration of occurrence of relative humidity exceeding 97% in combination with minimum daily air temperatures within the range -4°C to 0°C, was made. This analysis, combined with qualitative information obtained from the various sites, suggested that a reference ice thickness could be defined in a regional zoning map. Separate allowance is made in the Code for altitudes.

The probable combinations of ice thickness and density with wind speed, were also based on meteorological data. The wind speed coincident with the conditions deemed to permit icing was examined, from which it was found that the extreme coincident speed did not exceed 70% of the 50 year return value. The Meteorological Office have since considered that the 70% figure was an upper bound, but realised that the adoption of a lower wind speed would imply an effective return period less than two years, which could not be predicted with confidence.

## 6. SUMMARY

This paper has attempted to outline a procedure for predicting ice formation on cables, which has been verified by both climatic chamber tests and measurements of ice samples from a guyed mast.

This enables ice shapes to be derived from which wind coefficients could be determined from conventional models of the predicted shapes.

The procedure has been used in the development of current practice in the United Kingdom.

AD P001672

# NUMERICAL SIMULATION OF ICE ACCRETION ON CABLES

Pierre McComber    Université du Québec à Chicoutimi

Samples of ice accretions collected on cables of overhead transmission lines have shown evidence of twisting of the cable during icing. A method is presented to simulate numerically in two dimensions the accretion on a cable of a known torsional rigidity. The surface is approximated by one dimensional isoparametric quadratic elements. For each time step, the change in shape is calculated at each node from the droplet velocities; the surface is then interpolated to find the ice weight by integration; the equilibrium angle of rotation is found and finally the rotation of the shape is done numerically. Results of a numerical simulation for different torsional rigidities is presented. A larger rigidity makes the accretion shape more elliptical whereas it becomes more circular for a smaller rigidity. Results also indicate that twisting of the cable has a significant effect on the accretion shape obtained but has almost no influence on the accretion rate.

## INTRODUCTION

Atmospheric ice accretion on structures is presently being investigated by different research groups (1,2,3,4,5) to solve various environmental problems both experimentally and theoretically. One of these problems is related to the increasing importance of overhead transmission lines in northern regions where they are exposed to adverse weather conditions. Since data on the meteorological conditions prevailing during icing is difficult to obtain, research has been done on icing using wind tunnel simulation as well as numerical simulation.

Ice accretion samples collected on cables of overhead transmission lines have displayed shapes somewhat different from those obtained in wind tunnels on fixed conductors. In fact it has been known for some time that cables twist under the weight of ice. Recent grain structure analyses by Laforte and Nguyen (6) on field samples clearly show the accretion rotation during icing. A realistic numerical model to predict ice accretion shapes on cables has to provide for cable twisting and rotation of the shape with respect to wind direction. Icing has a cumulative effect so that a difference in shape is important at any time during accretion. As shown in Fig. 1, rotation can modify the accretion rate on a twisted cable.

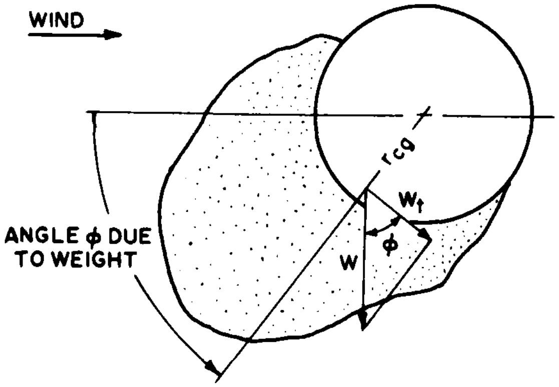

Fig. 1 Diagram of an ice accretion on a cable showing the angle of rotation

In the following sections, a method (is presented) to simulate numerically ice accretion on a cable, while taking into account the rotation of the accretion, is presented.

## GENERAL DESCRIPTION ON THE NUMERICAL SIMULATION MODEL

Figure 2 shows a block diagram of the numerical simulation procedure. Basically it consists of a loop making a time integration. At each iteration, calculations are made for a time interval $\Delta t$, during which simulation is done for a steady state.

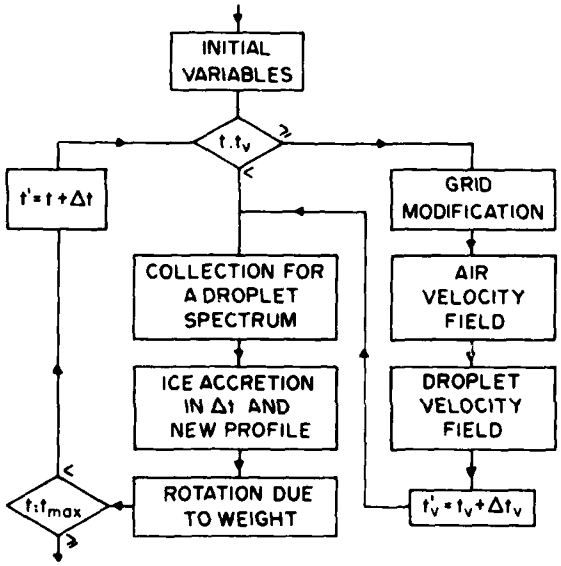

Fig. 2 Block diagram of the numerical simulation procedure

### Droplet velocity field

The first part of the simulation is a calculation of the droplet velocity field (7,8) around the changing shape of the accretion. However the droplet velocity field is only computed for longer time intervals $\Delta t_v > \Delta t$. This is justified by the fact that droplet collection is immediately affected by any small changes in the surface orientation, whereas droplet velocites are not influenced directly. Trajectories of droplets are changed through the effect of air-droplet drag. Also, the drag force has less effect on larger droplets because of their greater inertia ; these droplets make the largest contribution to the accretion. Since this part of the calculation involves the solution of non-linear equations by iteration for the two-dimensional droplet velocity field, it is relatively long and should therefore be made only when justified by the overall accuracy of the simulation.

### Ice accretion shape

When the droplet velocity field $\vec{V}$ has been evaluated, the local collection efficiency $\beta$ is calculated at any point on the accretion surface by the following equation:

$$\beta = \frac{\vec{V}\cdot d\vec{\ell}}{|d\ell|} = |V| \cos\psi \text{ for } \beta > 0 \qquad (1)$$

The geometry of the accretion surface is described in Fig. 3: $\psi$ is the angle between the droplet velocity vector and the surface direction vector $d\vec{\ell}/|d\ell|$. This angle can be evaluated by using: $\alpha = \tan^{-1}(V_y/V_x)$ and $\delta = \tan^{-1}(dy/dx)$:

$$\beta = |V| \cos(\pi/2-\delta+\alpha) \qquad (2)$$

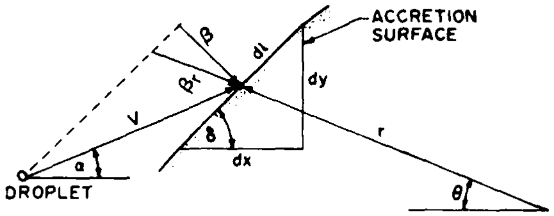

Fig. 3 Geometry of the ice accretion surface.

The droplet collection efficiency on the surface is a function of droplet diameter $d_j$, and can be calculated for a droplet diameter spectrum by adding the efficiency applicable to each droplet diameter $d_j$ in the spectrum:

$$\beta = \sum_j \beta_j(d_j) \qquad (3)$$

The local collection efficiency is related to the local intensity of accretion I by multiplying $\beta$ by the liquid water content w: $I = \beta w$. In the case of dry growth, the normal increment thickness per unit area is found by:

$$\Delta L = \beta\ w\ \Delta t/\rho_i \qquad (4)$$

which, if polar coordinates are used, is converted to a change in radius r by:

$$\Delta r = \frac{\Delta L}{\cos\left[\pi/2 - (\delta+\theta)\right]} \qquad (5)$$

This change in radius can be calculated at each point on the accretion surface and therefore yields the overall change in shape for a time interval $\Delta t$.

## ROTATION OF THE ICED CABLE

The rotation of the ice-covered cable under its weight is calculated in three steps: calculation of the weight and center of gravity of the ice-covered cable, calculation of the equilibrium angle of rotation $\phi$ and finally numerical rotation of the shape by an angle $\Delta\phi$.

### Calculation of the weight and center of gravity of the ice-covered cable.

The ice surface is an arbitrary shape varying at each time interval $\Delta t$. It is approximated by n one-dimensional isoparametric quadratic elements, as described in Fig. 4. Using this approach, the accuracy of the simulation can be improved by increasing the number of elements n. If $N_j(\xi_i)$ are the interpolation functions of the point $\xi_i$ on the reference element, the polar coordinates $(r_i, \theta_i)$ of this point on the surface is given by:

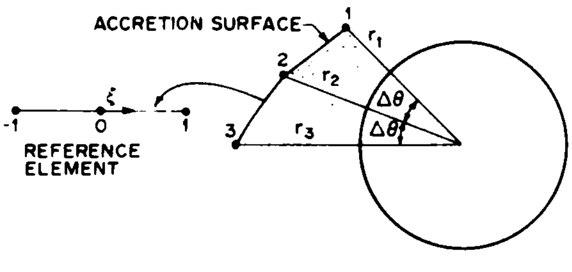

Fig. 4 Diagram of the interpolation element used on the accretion surface

$$r_i = \sum_{j=1}^{3} N_j(\xi_i) r_j ; \quad \theta_i = \sum_{j=1}^{3} N_j(\xi_i)\theta_j \qquad (6)$$

The integration on the reference element coordinate requires the use of $|d\theta/d\xi|$ which for this geometry is a constant found by: $|d\theta/d\xi| = \pi/n$.

The ice accretion volume per unit length of cable corresponds in two dimensions to the area $A_j$ between the accretion surface and the cable and is calculated for each element by:

$$A_j = \int_{-1}^{1} \frac{\left[r^2(\xi) - r_o^2\right]}{2} \left|\frac{d\theta}{d\xi}\right| d\xi \qquad (7)$$

The coordinates of the center of gravity $\bar{x}_j$, $\bar{y}_j$ of each element are found from the following equations:

$$\bar{x}_j\ A_j = \int_{-1}^{1} r(\xi) \cos\left[\theta(\xi)+\pi\right] \frac{\left[r^2(\xi)-r_o^2\right]}{2} \left|\frac{d\theta}{d\xi}\right| d\xi \qquad (8)$$

$$\bar{y}_j\ A_j = \int_{-1}^{1} r(\xi) \sin\left[\theta(\xi)+\pi\right] \frac{\left|r^2(\xi)-r_o^2\right|}{2} \left|\frac{d\theta}{d\xi}\right| d\xi \qquad (9)$$

Integration of these equations is done numerically using a Gauss integration procedure. If $w_c$ is the weight per unit length of the conductor and $\rho_i$ the ice density, then the total weight per unit length of the cable and accretion is:

$$w = \left(\sum_{j=1}^{n} \rho_i\ A_j\right) + w_c \qquad (10)$$

and overall center of gravity is located at $x_{cg}$ and $y_{cg}$:

$$x_{cg} = \sum_{j=1}^{n} \rho_i\ A_j\ \bar{x}_j/w \qquad (11)$$

$$y_{cg} = \sum_{j=1}^{n} \rho_i\ A_j\ \bar{y}_j/w \qquad (12)$$

### Calculation of the equilibrium angle, of the cable

To calculate the cable twisting angle a simplified model is considered, i.e. torsion in the middle of a rod supported at both ends and submitted to a distributed torque $w_t \cdot r_{cg}$. If k is the equivalent torsional rigidity constant in the center of a span of length L then, referring to Fig. 1, the equilibrium of torques requires:

$$L\, w \cos\phi\, r_{cg} = k\, \phi \qquad (13)$$

An example for a typical aluminium stranded cable [Bersimis conductor D = 3.49 cm, $w_c$ = 21.446 N/m], the product of the shear modulus and polar moment of inertia is GJ = 351.4 Nm²/rad. Since a distributed torque results in half the angle of rotation as compared with a concentrated torque, it is equivalent to a rigidity constant given by:

$$k = 2\left(\frac{GJ}{L/2}\right) = 23.05 \text{ Nm/rad} \qquad (14)$$

where L is taken to be 60.97 m for a subspan of a typical overhead transmission line.

Equation 13 for $\phi$ is a transcendental equation. For the solution, the angle of the center of gravity before rotation is used as the initial value $\phi_o$, then the Newton-Raphson method is used to find $\phi$ with the following recurrence equation:

$$\phi_{j+1} = \phi_j + (w\, L\, r_{cg} \cos\phi - k\,\phi)/(w\, L\, r_{cg} \sin\phi + k) \qquad (15)$$

Convergence of this equation gives the angle of the center of gravity $\phi_{cg}$ at equilibrium and the angle of rotation for the time step $\Delta t$ is given by:

$$\Delta\phi = \phi_{cg} - \phi_o \qquad (16)$$

Rotation of the ice-covered cable

To rotate the ice accretion shape, the new coordinates for each node are found from an interpolation between the adjacent nodes using for each element the same reference coordinate $\xi_r$:

$$\xi_r = \frac{\Delta\phi}{\pi/n} \qquad (17)$$

The interpolation is then made at $\xi_r$ using Equation (6) systematically at each node in succession.

## RESULTS OF A COMPUTER SIMULATION OF ICING ON A CABLE WITH ROTATION

The purpose of the numerical simulation presented in this section was to deterne the effect of cable twisting on the accretion shape: it was therefore done with some simplifying assumptions. The first one was to assume a large inertia for the supercooled droplets. In such a case, the droplet velocity is the same as the free stream air velocity V and it is not recomputed at each time interval. The second important assumption is a dry growth when the supercooled droplets impinge on the accretion surface. This condition can be justified for rime formation but would not be acceptable for glaze simulation.

Parameters chosen for the computer simulation were the following: free stream air velocity, 7.75 m/s; liquid water content w, 2.5 g/m³; air temperature, -11°C and accretion density $\rho_i$, 852 kg/m³.

Accretion shape on a fixed cable.

Figure 5 shows the result of the computation on a fixed cylinder 3.49 cm in diameter which approximates the shape of a Bersimis cable. The simulation was done for n = 16 elements around the cable and the accretion is shown by a linear interpolation between the 32 nodes around the cylinder. The time interval used for the integration was $\Delta t$ = 60 s.

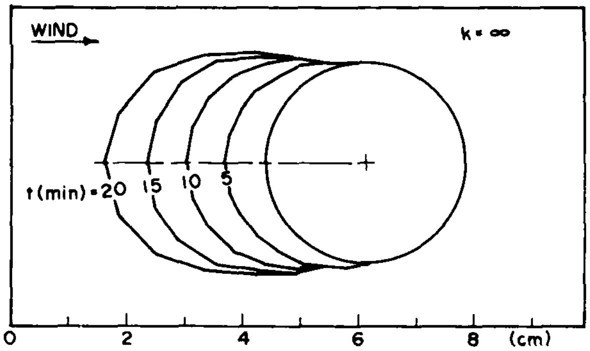

Fig. 5 Ice accretion on the front part of a fixed cylinder

The shape obtained is symmetrical with respect to the horizontal axis, i.e. the direction of the wind. The accretion weight being exclusively on the front part of the cylinder, it creates the torque responsible for the twisting when the cylinder is free to rotate.

Ice accretion with cable twisting.

Figure 6 gives results of a computer simulation when the cable is permitted to rotate around its center. The time interval chosen for the iteration is Δt = 60 s and the shape is drawn for 5 minute intervals. This simulation was done for an equivalent torsional rigidity constant k of 25.03 Nm/rad. This corresponds to the rigidity for distributed torque in the middle of a typical sub-span (L = 60.97 m) of a transmission line using a Bersimis cable. A sub-span is defined as the length of conductor between spacer-dampers on a four-conductor bundle.

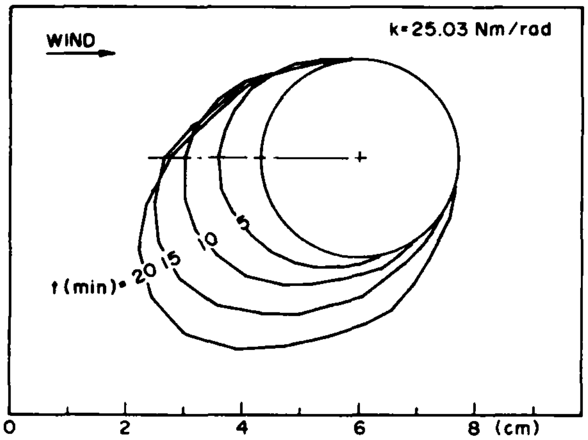

Fig. 6 Ice accretion on a twisted cable.

The combined effect of twisting and of accretion shown in Fig. 6 was a mass addition mostly on the front and lower portion of the conductor. The total angle of rotation of the cable for the 20 min simulation was 61.6°, and the angle of the center of gravity was 38.2° from the horizontal axis.

### Computer simulations with different rigidity constants.

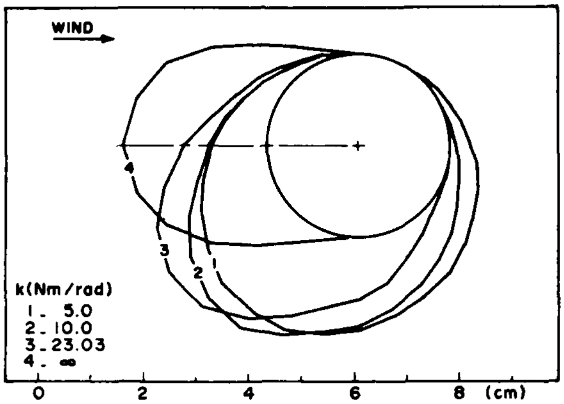

Fig. 7 Ice accretion after 20 min for different cable torsional rigidities.

The next four figures show results of computer simulations when the torsional rigidity constant k is varied. In Fig. 7 a comparison is made of accretion shapes obtained for three different torsional rigidity constants k of 5, 10 and 23.05 Nm/rad with the shape computed for a fixed cylinder (k = ∞). Whereas for k = ∞ the shape is approximately elliptical, as k decreases the shape becomes closer to being circular. Also the accretion mass builds up more on the bottom portion of the cylinder. Even though the twisting of the cable decreases slightly with time, always requiring more accretion weight for the same rotation $\phi$, it can be observed that eventually the ice surrounds the cylinder completely, at least for those conductors with a lower rigidity constant. Figure 8 displays this effect by showing the angle of twist $\phi$ as a function of time for different rigidities. For a similar time the twisting angle is inversely proportional to the rigidity. On the other hand, for a given rigidity the rotation is almost proportional to time t at first, but then the twisting rate $d\phi/dt$ tends to decrease for a longer simulation time. There is no doubt however that for lower rigidities the accretion surrounds the cable completely. This has a practical importance since an accretion surrounding the cable will take longer to detach from the cable when it melts.

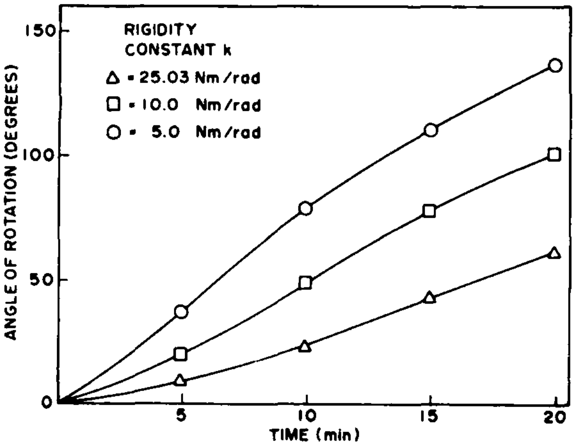

Fig. 8 Twisting angle of the cable as a function of time for different rigidities.

Figure 9 shows the angle of rotation of the center of gravity with respect to the horizontal axis. In order to maintain the equilibrium, this twisting moment angle will always be less than 90°. This maximum angle however is approached faster on lower rigidity cables.

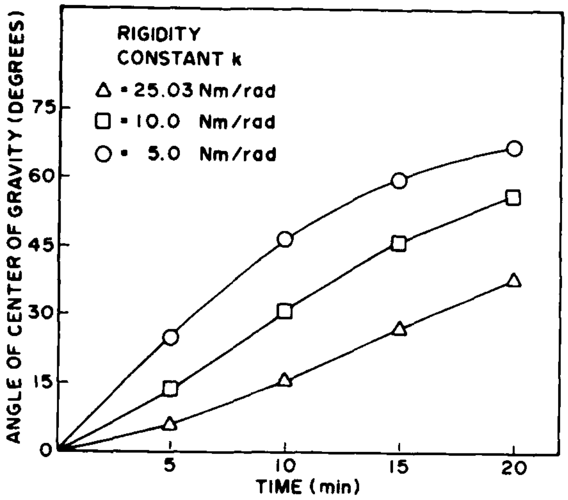

Fig. 9 Angle of the center of gravity as a function of time for different cable rigidities.

Figure 10 describes the accretion rate as a function of time for different rigidities. The accretion rate is largely responsible for the total load supported by transmission lines so it is interesting to analyse the effect the cable rigidity has on it. Unfortunately, results given in Fig. 10 are not conclusive. The more rigid cables have a smaller accretion rate early in the simulation but the rate increases afterward. The more flexible cables have a larger accretion rate at first but it decreases at a latter time. Therefore, at least for the time covered by this simulation, the difference in the accretion rate for various rigidities is small.

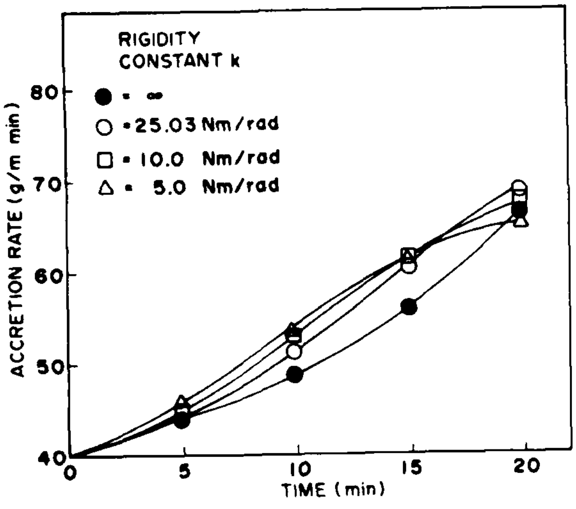

Fig. 10 Accretion rate as a function of time for different cable rigidities.

DISCUSSION

The torsional rigidity of a cable changes along its length L between supports. Equations 13 and 14 show that the rigidity constant is inversely proportional to L and the twisting moment ($L \cdot W_t \cdot r_{cg}$) is proportional to L. The twisting of a cable is expected to be approximately proportional to the square of the distance from the supports, reaching a maximum at the mid-span. A simulation aimed at determining the accretion weight on a transmission line would have to take into account this variation in rigidity.

Furthermore, the rigidity of a cable will also be affected by the presence of an ice accretion especially so when the ice surrounds the cable completely; the effect would undoubtedly increase the cable rigidity.

The computer simulation presented above does not include the effect of the collection efficiency on the accretion rate. This efficiency could modify the results particularly with respect to the accretion rate. Wind tunnel simulation on a fixed cylinder (8) indicates an almost constant accretion rate. If this were the case then the cable twisting would certainly increase the accretion rate significantly.

CONCLUSIONS

The twisting of cables during icing is an important factor to consider in the accretion shape obtained and should be an essential parameter of a realistic computer simulation of cable icing, at least as far as rime is concerned.

For a lower torsional rigidity constant the shape is more circular and the center of gravity becomes closer to the vertical line and to the location of the center of gravity of the bare cable, both effects resulting in a lower twisting moment developed by the accretion weight. For a more rigid cable, the accretion shape becomes more eccentric and elliptical in shape, both conditions making the cable vulnerable to adverse effects from aerodynamic forces.

The rate of ice accretion was not found to vary significantly at a given time when the rigidity of the cable was modified.

## ACKNOWLEDGEMENT

This work is supported by the Conseil National de la Recherche en Science et en Génie du Canada and by the Ministère de l'Education du Québec.

## REFERENCES

1. ACKLEY, S.F., TEMPLETON, M.K., ''Computer Modeling of Atmospheric Ice Accretion'' CRREL Rept. 79-4, March 1979.
2. LOZOWSKI, E.P., STALLABRASS, J.R., HEARTY, P.F., ''The Icing of an Unheated Non-rotating Cylinder in Liquid Water Droplet-ice Crystal Clouds'' N.R.C. Res. Rept. LTR-LT-96, February 1979.
3. LOZOWSKI, E.P., OLESKIW, M.M., ''Computer Simulation of Airfoil Icing without Runback'' AIAA paper 81-0402, 1981.
4. STALLABRASS, J.R., LOZOWSKI, E.P., ''Ice Shapes on Cylinders and Rotor Blades'' Symposium on Helicopter Icing, NATO Army Armaments Group, Panel X, London, November 1978.
5. MAKKONEN, L., ''Estimating Intensity of Atmospheric Ice Accretion on Stationary Structures'' J. of Applied Meteorology. Vol. 20, No. 5, May 1981.
6. LAFORTE, J.L., NGUYEN, D.D., ''Examen des échantillons de givre et de verglas pour l'année 1981''. Rept. submitted to Hydro-Quebec.
7. McCOMBER, P., TOUZOT, G., ''Calculation of the Impingement of Cloud Droplets in a Cylinder by the Finite Element Method''. J. Atmos. Sci. Vol. 38, May 1981, pp. 1028-1036.
8. McCOMBER, P., ''Numerical Simulation of Ice Accretion Using the Finite Element Method''. Proceedings of the 6th International Conference on Port and Ocean Engineering under Artic Conditions, Quebec, July 1981, pp. 1047-1056.

---

## DISCUSSION

Whapham: Was the wind always at a 0° angle with the horizontal?

McComber: Yes, from the left to the right.

Whapham: Did you look at the effects of the rotation with different wind angles of approach? Or do you feel that that would make any difference?

McComber: Well, again, I would say that this would be equivalent to a rotation independent of the weight. So, that could be done easily with this type of model.

Mozer: ... just to extend Bob Whapham's question, there is, of course, a vertical turbulence component in atmospheric [...] Will this model do the computations? The standard deviation is perhaps 10° or 5°, this sort of thing - a vertical angle.

McComber: No, the wind was taken to be steady, horizontal, and no allowance made for this.

Howe: Just a comment, in our experience on the mountain in an actual [installation], we had a 30 foot slack wire, to be commented on later, fixed at each end. What happens is, you get this spiral start, and then it oscillates. It twists about 180° and then it oscillates back and forth.

McComber: Well, eventually, with this type of numerical model could be included fairly easily, because it's just a rotation exactly like the one due to the weight, except it's done to take into account the variation of the wind. But it would be fairly easy to put, for example, the direction of the wind that would vary with [...] and this would not cause too much difficulty, in the numerical model. This is probably one advantage in this case of the numerical model versus a simulation in a tunnel.

Assur: Your last conclusion that the rate of accretion does not depend on rigidity is somewhat surprising, simply because if you have infinite rigidity you expose the short axis of an ellipse to the wind. Once you start to rotate, you expose the long axis.

McComber: This is the reason why I was very careful on this. I said for the condition that I've simulated, which is the fact that I have 100% collection efficiency, and therefore, in this case we solve [...] with the accretion of the fixed cylinder. In fact, the accretion rate increases because the shape extends a bit. In other words, it becomes larger than the original cylinder, which we know is not the case with lower collection efficiencies. Now I believe this is the reason why this simulation gives this result and this is why I was very careful to point out that this conclusion is linked with the condition of the simulation.

Ackley: In calculating the torsion that you put into this, you only consider gravity loads. Is that correct? In other words, you didn't consider the fact that you are now presenting a bluffer face to the wind, you've got an increased drag [...] which will tend to give you more twist in that direction?

McComber: This, of course, is not something easily calculated, to find exactly what would be the resulting torque from the drag. This will be eventually included in the model.

Assur: The accretion is more difficult.

McComber: Yes, the accretion is more difficult.

Question: (unintelligible)

McComber: Yes, well the comment I would make on this is that one of the purposes of predicting shape numerically is to eventually calculate the loads. We're planning to get to that stage later on. Of course, in order to predict the right load, we had to first start by predicting the right shapes, and we'll get the concentration of the wind loads later on.

AD P001673

# THE DESIGN AND TESTING OF A LAGRANGIAN COMPUTER MODEL FOR SIMULATING TIME-DEPENDENT RIME ICING ON TWO-DIMENSIONAL STRUCTURES

M.M. Oleskiw[1]   Division of Meteorology, Department of Geography,
E.P. Lozowski[2]   University of Alberta, Edmonton, Canada T6G 2H4

## ABSTRACT

A computer model has been developed which is capable of simulating time-dependent rime icing on arbitrary two-dimensional structures, in potential flow. The fast, Kennedy-Marsden algorithm is used to generate the potential flow field around the icing substrate. Lagrangian droplet trajectories are then calculated using a fourth-order integration procedure with a variable time step, which offers a good compromise between computing accuracy and computing time. Trajectory pairs are used to determine collision efficiencies. Knowing these and the impingement limits, a smooth interpolated collision efficiency curve is generated and used to estimate the growth of the accretion over a small time interval. The new accretion profile is then fitted using cubic splines, and the entire procedure is repeated as often as desired to generate subsequent accretion layers.

This paper describes many of the design considerations which went into the development of the model, to try to insure both its accuracy and efficiency. It also describes some of the tests which were made with existing experimental and theoretical data, in order to validate the model. Some initial results, which illustrate the potential and limitations of the model, are also presented.

## 1. INTRODUCTION

Modelling of a phenomenon such as icing serves a number of useful functions. It provides a framework for interpreting experimental measurements of icing. It permits making sensitivity tests to determine the relative importance of the physical phenomena and parameters which control the ice accretion. It also makes it possible to predict the nature and occurrence of icing under conditions other than those which have or can be simulated experimentally.

The goal of icing modelling is to simulate the ice accretion process in as complete a way as possible. The ultimate model must therefore include: (1) detailed calculations of the airflow and droplet trajectories, (2) an understanding of the physics of the impaction and freezing processes, (3) detailed computations of the spatially varying thermodynamics of the ice accretion, and (4) a consideration of the feedback effects of the time varying accretion shape and of changing environmental conditions on (1), (2) and (3).

No complete icing model presently exists, so far as the authors are aware. All currently available models are restricted in some way by making approximations in one or more of the four areas outlined above. These approximations are made either for convenience of computation, or more frequently because certain physical phenomena such as the flow around and the heat transfer to complicated icing shapes, are simply not understood at present. For accretion on a cylinder, Ackley and Templeton (1979), for example, include time-dependent effects but ignore the thermodynamics of the ice. Lozowski, Stallabrass and Hearty (1979) on the other hand, include accretion thermodynamics but ignore the time-dependent feedback effects.

---

[1] Present affiliation: Intera Environmental Consultants, Calgary, Alberta, Canada.

[2] Presently on Leave with: Ice Branch, Atmospheric Environment Service, Department of Environment, Ottawa, Canada K1A 0H3.

Accretion on more general two-dimensional shapes, with the emphasis on airfoils, has been recently addressed by Bragg, Gregorek and Shaw (1981), by Lozowski and Oleskiw (1981) and by Cansdale (1981). The first two of these models allow for time-dependence but ignore thermodynamics, while the third includes the thermodynamics (at least for airfoils) but it is not time dependent.

The purpose of this paper is to discuss the design and testing of the Oleskiw and Lozowski rime icing model more fully than has been done before. Complete details, including a listing of the computer program, are to be found in Oleskiw (1982), and in the forthcoming CRREL report #232.

## 2. DESIGN OF THE MODEL

As already mentioned, the model is restricted to a consideration of time-dependent rime icing. This restriction has been necessitated by the lack of adequate experimental or theoretical treatments of the heat transfer from two-dimensional iced structures. The authors feel that this deficiency is the fundamental obstacle to progress towards a more general time-dependent icing model including thermodynamics.

User input to the model includes the specification of the icing substrate, and of the environmental conditions. The model output consists of the potential flowfield around the substrate, the droplet trajectories, the local collision efficiency, ice accretion profiles, and accretion mass. The operation of the model is semi-automatic, inasmuch as the user must provide the program with certain assistance as the simulation proceeds. This assistance consists of such things as specifying certain error tolerances for the computations, and providing initial estimates for the automatic tangent trajectory finding procedure.

In principle, the model is capable of handling any two-dimensional shape as the icing substrate, so long as incompressible potential flow is a reasonable approximation to the actual air flow in the upwind region prior to droplet impingement. In practise, however, the authors have so far applied the model only to the icing of cylinders and airfoils. The shape of the icing substrate may be specified either by an analytical equation or by a set of surface point coordinates.

The potential flow is calculated by the Kennedy and Marsden (1976) surface vorticity technique, an efficient algorithm developed for multi-component airfoil design on small computers. Comparisons between the model-predicted flowfield and known analytical solutions for the cylinder and for a Joukowski airfoil, showed that very good agreement could be achieved with only about 40 surface vorticity elements (panels). The maximum velocity error was less than 2%, the largest values occurring in a relatively small domain adjacent to the airfoil surface.

The droplet trajectories for as many as five drop size categories are determined by numerically integrating their Lagrangian equations of motion. These equations (Pearcey and Hill, 1956) include a drag term, a gravity term (which was negligible) and a history term. The latter term is non-zero only if the droplet is accelerating. It can have a significant effect on the collision efficiency when the droplet trajectories are highly curved. The numerical integration is performed using the Runge-Kutta-Fehlberg variable time-step algorithm (Burden et al., 1978). The algorithm provides a good compromise between numerical accuracy and computational efficiency. This is a particularly important consideration because the computation of droplet trajectories is generally the most time-consuming part of the overall icing model.

In order not to waste time computing a lot of droplet trajectories which miss the icing substrate, a semi-automatic technique has been devised which iterates to find the tangent trajectories. Given an initial estimate of the tangent trajectory, which the user supplies, the program successively adjusts it, if it is a "miss" trajectory, until a "hit" trajectory is found. This trajectory is then adjusted until a miss occurs, and so on. The tangent trajectory can thus be found to within whatever error limits the user wishes to specify. Since the tangent trajectories determine the overall collection efficiency, E, this quantity is very well determined by the program.

A knowledge of the release ordinate (y) and the impingement location along the surface ($\ell$) for each trajectory leads to a graph of point values, ($y,\ell$). These points are fitted using a quintic Hermite spline interpolation. Differentiation of the fitted curve yields the local collision efficiency ($\beta$) as a function of distance along the substrate surface ($\ell$). This approach has the advantage that whereas there may be local errors in the estimation of $\beta$, the integrated area underneath the $\beta$ vs $\ell$ curve is conserved. Thus the overall collection efficiency, E, is not affected by local estimation errors in $\beta$. Comparisons of computed $\beta$ curves with experimental measurements in the literature show a most gratifying agreement. The curve-fitting procedure, however, can lead to spurious spatial oscillations in the $\beta$-curve. These in turn give rise to bumps on the accretion surface. The feedback effect of these artificial bumps on the flowfield, droplet trajectories, and subsequent accretions is unfortunately an unstable one. This phenomenon is at present the principal impediment to using the model to predict ice accretions over very long times.

Given the local collision efficiency, $\beta$, the growth of the ice accretion can be modelled only to the extent that the physics of the accretion and freezing processes is properly understood. Three important considerations are the heat transfers between the accretion and the airstream, the structure of the ice, particularly its density and growth direction, and the fate of any non-frozen surface water (e.g., splashing, surface flow or shedding). No current icing models simulate these processes adequately, at least in the general case. This is because few pertinent experimental results exist that can be applied in the models. Thus clearly defined experiments with the objective of investigating these problems are the sine-qua-non of future progress in icing modelling. The present model circumvents this lack of knowledge by making certain assumptions about the accretion physics which scientific intuition and a posterior analysis suggest are reasonable over a limited range of icing conditions.

The overriding assumption is that the heat transfer with the airstream is sufficient to cause all of the impinging water droplets to freeze at or very near their point of impact (rime icing). Thus the question of the detailed heat transfer can be sidestepped and the fate of non-frozen surface water is of no consequence because the freezing process takes place very quickly. Just how quickly the freezing of individual droplets takes place will determine the accretion density. If relatively slowly, the droplets will deform substantially before freezing and the ice is likely to contain few air spaces (though it may contain air bubbles which are rejected from the ice lattice as freezing proceeds). On the other hand, if freezing occurs relatively quickly, the droplets will tend to preserve their spherical shape and a loose rime structure with many small air spaces (rime feathers) is likely to result. Rime feathers tend to be fast growing and because of their shape, give rise to shadow regions of essentially zero collection efficiency between the feathers. Thus in the rime feather region, there are also large interstitial spaces, which can substantially reduce the local density of the ice accretion. There have been some attempts to measure the density of ice accretions (e.g., Macklin, 1962), but these are of limited applicability. Our attempts to use Macklin's density formulations were quite unsuccessful, compared with the rather simpler assumption of a constant ice accretion density. We have, therefore, made the constant density assumption in the model, using a value of 917 kg $m^{-3}$.

With the aid of these simplifying assumptions, it is possible to use the local collision efficiency data to calculate local ice thickness growth. The thickness of the ice accreted over a small but finite time interval is in turn calculated by simply extrapolating the initial growth rate over the time interval and taking into account the "curvature effect." The "curvature effect" is the tendency for the surface area of the accretion over a convex surface element, to increase with time. These thicknesses are plotted as points normal to the underlying surface elements with which they are associated. This set of points is then fitted using a cubic spline interpolated curve, which represents the model's estimation of the accretion surface at the end of the time interval. At present no smoothing is applied to this curve. The accretion profile is then plotted and accretion masses calculated.

By defining new vorticity elements on the uniced and iced portions of the substrate, the Kennedy-Marsden technique may once again be applied to compute the modified potential flow, and the entire procedure repeated to estimate yet another accretion profile following a second time interval. In principle this procedure may be repeated as often as desired. However, the limitations imposed by available computer time and the amplification of the spurious numerical bumps engendered by the curve fitting procedures, have so far limited the model extrapolation to about five time steps.

## 3. MODEL TESTING

The model testing comprises three aspects: testing the flowfield, testing the collision efficiencies, and testing the ice accretion profiles. In each case, comparisons have been made, between the model output and other appropriate experimental or theoretical results. Most of the testing of the model has been done for cylinders and airfoils, and these are the results which will be presented here.

A flowfield test was made using an uncambered Joukowski 12% airfoil of chord 0.711 m at an angle of attack of 4° with respect to a free stream of velocity 128.6 m $s^{-1}$. The model using 40 vorticity elements predicted velocities at a number of points upstream of the airfoil and adjacent to the airfoil surface. These were compared with the velocities given by the Joukowski analytical solution. The velocity errors were less than 0.01% at points more than one chord length upstream. For points adjacent to the airfoil surface, the maximum error was found to be 1.7% at a point just above the nose of the airfoil. In view of the fact that the relatively large velocity errors occur only near the airfoil surface where the droplets spend very little time, these results were considered acceptable. Thus all model simulations are performed with forty vorticity elements. Nevertheless it is possible to reduce the maximum velocity errors to less than 0.2% if desired by increasing the number of surface vorticity elements to 60 and judiciously distributing them around the airfoil in such a way that the greatest number occur near the leading edge.

Collision efficiency testing was accomplished using the computed results of Langmuir and Blodgett (1946) as the first comparison and the experimental results of Gelder et al. (1956) as the second. Table 1 compares the model predicted total collision efficiencies (E) and maximum local collision efficiencies at the stagnation line ($\beta_{max}$) with the corresponding Langmuir and Blodgett data for a cylinder under two rather different conditions. K and $\phi$ are Langmuir and Blodgett's non-dimensional inertia and impingement parameters respectively.

Table 1

*Comparison with Langmuir and Blodgett*

|  | K | $\phi$ | E% | $\beta_{max}$% |
|---|---|---|---|---|
| L & B | 16 | $5x10^4$ | 61.5 | 76.0 |
| PRESENT MODEL | 16 | $5x10^4$ | .61.1 | 77.7 |
| L & B | 0.5 | 100 | 12.7 | 32.0 |
| PRESENT MODEL | 0.5 | 100 | 18.2 | 37.5 |

The first case is one in which the total collision efficiency is relatively high, and here we agree well with the results of Langmuir and Blodgett. The second case, however, has a low total collision efficiency, and the discrepancy with the results of Langmuir and Blodgett is rather substantial. Part of this discrepancy is due to the effect of the history term in the droplet trajectory equation. Langmuir and Blodgett did not take this into account. Nevertheless if we ignore the history term in the model, the values of E and $\beta_{max}$ are reduced only to 15.7 and 35.0 respectively. This tendency for Langmuir and Blodgett's results to be lower than ours occurs in other low collision efficiency cases too. At present we do not have an explanation for it. We should mention, however, that the results of Brun and Mergler (1953) for low collision efficiency cases also demonstrate a similar discrepancy, i.e., the Langmuir and Blodgett figures seem to be somewhat low.

Figure 1 compares the model predicted local collision efficiency for a 15% Joukowski airfoil at 0° attack, with the wind tunnel results of Gelder et al. In their experiment, Gelder et al. used a drop size distribution similar to the Langmuir D distribution with a volume median diameter of 18.6 μm. The airfoil chord was 0.330 m and the free stream velocity 78.20 m $s^{-1}$. The model simulates all of the experimental conditions but one. Instead of a drop size distribution, a single drop size of 18.6 μm is used. Thus the model has too

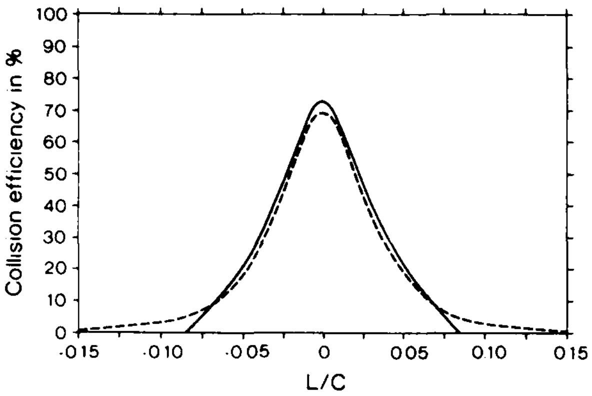

*Fig. 1. Local collision efficiency curves for a 15% Joukowski airfoil at 0° attack angle. Airfoil chord 0.33 m, free stream velocity 78.2 m s$^{-1}$. Dashed line - experimental results of Gelder. Solid line - present model results.*

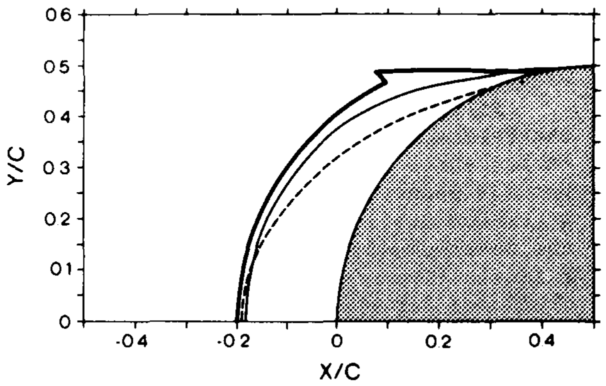

*Fig. 2. Accretion profiles on a 1" diameter cylinder. The air temperature was -15°C, the freestream airspeed 30.5 m s$^{-1}$, the liquid water content 0.82 g m$^{-3}$, the volume median droplet diameter 20 μm, and the accretion time 5 min. The heavy solid line is the experimental result of Lozowski, Stallabrass and Hearty (1979). The dashed line is their model prediction, while the light solid line is the profile predicted by the present model using a single 5 min. time step.*

many medium size drops and too few small and large ones. This fact notwithstanding, the comparison in Figure 1 is quite encouraging. The model impingement limits (points at which β goes to zero) are too narrow. This is exactly what we expected because the model doesn't have any large droplets to spread out the limits of impingement. On the other hand, the model's maximum local collision efficiency is too high, probably because the small droplets present in the experiment are being ignored. These two discrepancies tend to cancel each other when it comes to determining the total collision efficiency. The model value is 37.1% while Gelder et al. measured 37.8%.

These discrepancies which arise because a monodisperse drop size distribution has been used in the model can be rectified by using more drop size categories, but this increases the computational cost. Consequently, we have experimented within other approaches to making the β curve broader and squatter, i.e., more like the experimental curve. We have had some success with filtering the β curve, but will not go into detail about it here. Oleskiw (1982) gives complete results for this approach.

Testing of the model-predicted ice accretion profiles on a cylinder was accomplished by making comparisons with the theoretical and experimental results of Lozowski, Stallabrass and Hearty (1979). All cases are for a cylinder one inch in diameter. Figure 2 compares the model-predicted profile, using a single five minute time step to the experimental profile and to their model profile, which was also computed using a single time step. The experimental conditions were as follows: air temperature -15°C, free stream airspeed 30.5 m s$^{-1}$, liquid water content 0.82 g m$^{-3}$, volume median diameter of droplet size distribution approximately 20 μm. Once again, our model simulates all of the experimental conditions except the droplet size distribution. Instead a single 20 μm droplet size is used. The comparison between our model results and the experimental profile in Figure 2 is an encouraging one. The model seems to underpredict the growth slightly out to about 45°. This could be due to the rather high ice density used in the model. Beyond 45°, the model's underprediction is rather worse. The explanation here is likely that this is the region in which rime feathers grow, yielding an accretion full of air bubbles and spaces and of relatively low density. At present, the model is incapable of simulating this type of growth. The model of Lozowski et al., by comparison, yields a good prediction for the stagnation line growth but underpredicts the overall growth even more than the present model. The reason may have to do with the analytical fit which Lozowski et al. used to the Langmuir and Blodgett data for local collision efficiency. The fitting procedure did not necessarily conserve the total collision efficiency, thus giving rise to the possibility of a significant underprediction of the total profile area, such as we see in Figure 2.

Figure 3 shows the importance of the feedback between the changing substrate shape and the air and droplet fluxes, upon the development of the ice accretion profile. This figure compares the model-predicted accretion profile for a single five minute time step with that predicted for three time steps of 1.67 minutes each. The difference between the two profiles is quite striking showing the necessity of taking the feedback effects into account, and the value of a model such as the present time-dependent one in enabling one to do so.

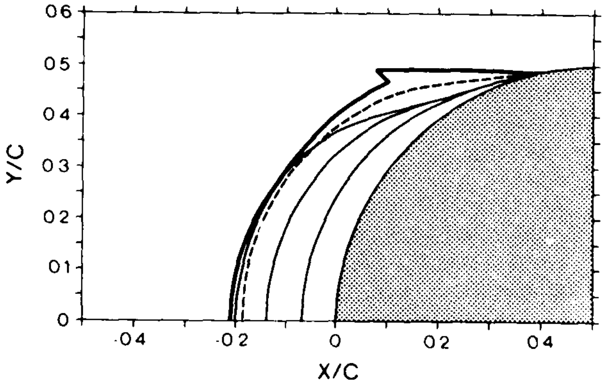

*Fig. 3. Accretion profiles on a 1" diameter cylinder. See Fig. 2 caption for experimental conditions. The heavy solid line is the experimental result of Lozowski, Stallabrass and Hearty (1979). The dashed line is the present model result using a single 5 min. time step. The sequence of three light solid lines are model predicted profiles at 1.67, 3.33, and 5.00 min., respectively, allowing for the effect of each successive layer on the airflow and droplet trajectories.*

The differences consist chiefly of a slight enhancement of the stagnation line growth and a reduction in the growth near the periphery. This occurs because with time the local collision efficiency at the stagnation line increases while the impingement limits defined in terms of distance along the surface are reduced. The net effect for the time-dependent case is a slightly better agreement with experiment near the stagnation line but worse agreement near the edges of the accretion. This lack of agreement near the edges should not be considered a drawback of the time-dependent model. It is expected because the model is not able to handle the physics of the low density rime feather accretion. The somewhat better agreement that occurs in this region in the single step case must therefore be viewed as rather fortuitous. If the growth were considered over a longer period than 5 minutes, it would be apparent that the time-dependent model generally predicts that the accretion will grow in a forward sense, while the one-step model would tend to predict far too much lateral spreading of the accretion.

Part of the reason for the difference between the single and multi-step accretions is the change in the local collision efficiency curve with time (Figure 4). However, even if this curve were independent of time, a difference with the single step case would still arise because the $\beta$ curve must be applied to a surface that is continuously moving forward, rather than to the underlying cylindrical surface as is the case in the single step model.

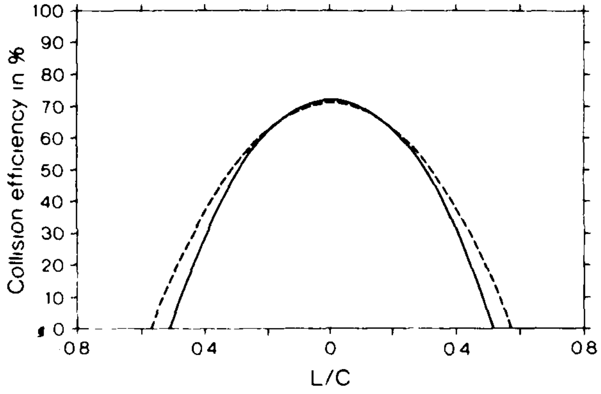

*Fig. 4. The local collision efficiency, $\beta$, as a function of non-dimensional distance around the substrate surface L/C, C being the cylinder diameter. The dashed line is for the first of the three 1.67 min. layers in Fig. 3, while the solid line is for the third layer.*

Instead of a monodisperse droplet size distribution, the model may take into account up to five drop-size categories. This tends to improve the model's predictions particularly as they concern the limits of impingement, which are ultimately determined by the largest droplets in the natural cloud. However, the use of discrete drop size categories in the model to simulate what is essentially a continuous natural distribution, has some drawbacks. The problem is most readily illustrated using two drop size categories for the case already considered. Figure 5 shows

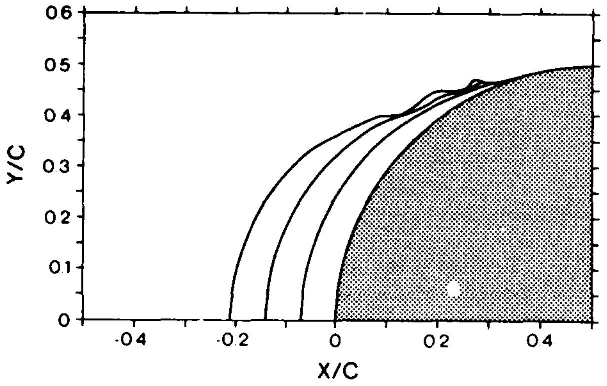

*Fig. 5. Accretion profiles on a 1" diameter cylinder at 1.67, 3.33, and 5.0 min. The conditions are given in the Fig. 2 caption, with one difference. In place of a 20 μm diameter monodisperse droplet distribution, a two-droplet size distribution is used, with droplets of diameter 27.0 μm and 14.4 μm, each comprising half the liquid water content.*

the accretion profile for a single 1.67 minute time step using 27.0 μm and 14.4 μm droplets, each category comprising half the total liquid water content. A careful inspection of this Figure shows a small kink in the profile near 60°. This kink occurs at the impingement limit for the smaller drops and it is an artificial phenomenon in the sense that it would not occur if a continuous distribution could be used in the model. Nevertheless, it gives rise to a slight depression in the surface of the first layer. Because of the feedback effect of this depression on the airflow, droplet trajectories and hence the local collision efficiency, this surface irregularity is amplified in the profiles of the second and third layers (Figure 5). This spurious "noise" on the surface eventually causes the program to crash and thereby limits the number of layers which can be accreted. We have had some success in controlling this problem by filtering the β-curves (see Oleskiw, 1982 for details). Nevertheless, at the present stage, this has not been entirely successful, and the model is therefore generally limited to accreting at most about five layers.

This limitation notwithstanding, the model performed well for time periods up to about 5 minutes at a recent intercomparison of aircraft icing models held at NASA Lewis on March 8, 1982. Further details concerning this intercomparison workshop are available from Dr. R.J. Shaw or Mr. J. Reinmann of NASA Lewis.

## 4. CONCLUSIONS AND RECOMMENDATIONS

On the basis of the foregoing presentation, the authors wish to draw the following points to the attention of the reader:

1. The present model is capable of producing realistic simulations of rime icing on two-dimensional objects over short periods (≤5 minutes, at an airspeed of ~30 m $s^{-1}$, and a liquid water content of ~1 g $m^{-3}$). Deficiencies occur in the simulation of the low density rime feather portion of the accretion. The major obstacles to producing simulations over longer time periods are computer time limitations and the uncontrolled amplification of spurious surface irregularities caused by curve fitting procedures and the use of a small number of discrete droplet size categories.

2. The present model is a distinct improvement over the time-independent model of Lozowski, Stallabrass, and Hearty (1979).

3. The principal impediment to further model development and generalization is a lack of sound experimental data concerning the physics of the accretion process. A detailed understanding of the heat transfers, the ice structure, and the fate of unfrozen surface water is required if any significant progress is to be made.

4. Because of the computational cost of calculating droplet trajectories, the model could be made more economical and hence more useful, if a more efficient procedure for trajectory calculation could be devised.

## 5. ACKNOWLEDGEMENTS

The authors are grateful for the research support provided by the Canadian Natural Sciences and Engineering Research Council under grant NSERC A8168, and by the U.S. Army Cold Regions Research and Engineering Laboratory under contract DACA89-79-C-0004. Sound advice, assistance, and encouragement were provided along the way by J.R. Stallabrass, E.M. Gates, S. Ackley and R.J. Shaw. We also thank P. Burge and L. Smith who typed the manuscript, and G. Lester and his staff who drafted the figures.

## 6. BIBLIOGRAPHY

Ackley, S.F. and M.K. Templeton, 1979: Computer modelling of atmospheric ice accretion. U.S. Army Cold Regions Research and Engineering Lab. Report CRREL 79-4, 36 pp.

Bragg, M.B., G.M. Gregorek, and R.J. Shaw, 1981: An analytical approach to airfoil icing. Amer. Inst. Aeronautics Astronautics, Paper #AIAA-81-0403, 17 pp.

Brun, R.J. and H.W. Mergler, 1953: Impingement of water droplets on a cylinder in an incompressible flow field and evaluation of rotating multicylinder method for measurement of droplet-size distribution, volume-median droplet size, and liquid-water content in clouds. NACA Tech. Note 2904.

Burden, R.L., J.D. Faires and A.C. Reynolds, 1978: *Numerical Analysis*. Prindle, Weber & Schmidt, 579 pp.

Cansdale, J.T., 1981: Helicopter rotor ice accretion and protection research. *Vertica*, 5, 357-368.

Gelder, T.F., W.H. Smyers, Jr., and V. von Glahn, 1956: Experimental droplet impingement on several two-dimensional airfoils with thickness ratios of 6 to 16 percent. NACA Tech. Note 3839.

Kennedy, J.L. and D.J. Marsden, 1976: Potential flow velocity distributions on multi-component airfoil sections. *Canadian Aeronautics and Space Journal*, 22, 243-256.

Langmuir, I. and K.B. Blodgett, 1946: A mathematical investigation of water droplet trajectories. In *Collected Works of I. Langmuir*. Pergamon Press, 10, 348-393.

Lozowski, E.P. and M.M. Oleskiw, 1981: Computer simulation of airfoil icing without runback. Amer. Inst. *Aeronautics Astronautics*, Paper AIAA-81-0402, 8 pp.

Lozowski, E.P., J.R. Stallabrass and P.F. Hearty, 1979: The icing of an unheated non-rotating cylinder in liquid water droplet-ice crystal clouds. Nat. Research Council Canada, Lab Report #LTR-LT-96, 61 pp.

Pearcey, T. and G.W. Hill, 1956: The accelerated motion of droplets and bubbles. *Aust. J. Phys.*, 9, 19-30.

Oleskiw, M.M., 1982: A computer simulation of time-dependent rime icing on airfoils. Unpublished Ph.D. Thesis, Division of Meteorology, University of Alberta, Edmonton, Canada.

DISCUSSION

Power: My question concerns the particular values of the parameters, the input parameters you used in your two diagrams as to how they might apply to transmission line. You use a 20 micron drop diameter, wind speed 30.5 meters/second, and liquid water content of 0.82 g/m$^3$. These values would seem to me to be all very high in relation to realistic transmission line conditions. Is there any problem with going to lower values?

Oleskiw: No,there aren't any problems at all. The particular values in these simulations were chosen because of the simulations essentially being involved with airfoil icing at the time, helicopter airfoil icing, and these model parameters can easily be changed to any reasonable value for which general assumptions like potential are valid. And, that being the case, the experiments will be redone for icing more peculiar to what you mentioned.

Howe: Perhaps this question is foolish, but is there any possibility that your spurious amplification problem is in fact the cause of the two-pronged growth in some cases?

Oleskiw: No, I don't think that's a foolish question at all. In fact, I think there's a very good possibility the spurious amplification in this particular case is actually the interesting feature of the model because if one was to assume that it was correct, that the collision efficiency curve has a kink in, it isn't because we only used two droplet sizes whereas in actual fact there is a continuum. But, if that collision efficiency curve is correct, then we would get those little spurious bumps, and that would lead to the allocation.

Howe: One of the first papers mentioned that with a broad droplet distribution you get a flatter [...]

Oleskiw: Yes, right, I agree with you that this amplification in itself is a useful thing, providing [...]

AD P001674

# ASPECTS OF FREEZING RAIN SIMULATION AND TESTING

J.R. Stallabrass National Research Council of Canada

## ABSTRACT

The paper examines first the available information on freezing rain and freezing drizzle in an attempt to define the applicable parameters, viz. temperature, precipitation rate (or liquid water content), drop size, and wind speed, in order to permit representative simulation and testing. Methods of measuring the simulated rain intensity and drop size are presented, and the problem of incomplete drop supercooling is addressed.

Methods of simulating freezing rain in the cold chambers and wind tunnels of the National Research Council of Canada are described, and the results of tests are used to illustrate various facets of the problem.

## INTRODUCTION

For most people a glaze storm may be regarded as little more than an inconvenience, perhaps causing them to be late for work, but its social and economic impact may be enormous. Chainé (1973) reports the following losses by electrical utilities in the Province of Quebec as the result of individual storms:

| | |
|---|---|
| 1961 | $ 5,000,000 |
| 1969 | $20,000,000 |
| 1972 | $ 3,000,000 |
| 1973 | $ 6,000,000 |

These are almost yearly events and were not exceptional storms such as that in Tennessee in 1951 (Harlin, 1952) that caused 25 deaths and 500 non-fatal accidents, and resulted in the following damage:

| | |
|---|---|
| Forests | $56,000,000 |
| Communication & power lines | 10,000,000 |
| Highways & streets | 15,000,000 |
| Fruit and nut trees | 4,000,000 |
| Buildings & plumbing | 4,300,000 |
| Livestock | 3,000,000 |
| Truck and grain crops | 1,600,000 |
| Transportation & business | several million |

In many cases, the damage or loss in such storms is caused by the direct ice weight and wind loading effects resulting for instance in the breaking of power or communication lines and the collapse of their supporting structures. In many other cases the losses result less dramatically; by delays in the transportation of goods or people caused by ice on the roads or iced-up windshields, delays of rail traffic caused by iced switch-points, the failure of outdoor electrical switch gear to function, arcing across iced insulator strings, the loss of communication caused by ice on antennae, the hazard to people and damage to property that can result from ice falling off tall buildings or structures, and the list goes on and on.

Freezing rain and drizzle result when snow, originating at higher altitude, first falls through a warm inversion layer, the temperature of which is above freezing, causing it to melt, and then, through a colder, subfreezing layer of sufficient thickness that the drops falling through it supercool. Figure 1 (taken from Werner, 1975) shows typical air temperature profiles during the occurrence of supercooled rain or drizzle.

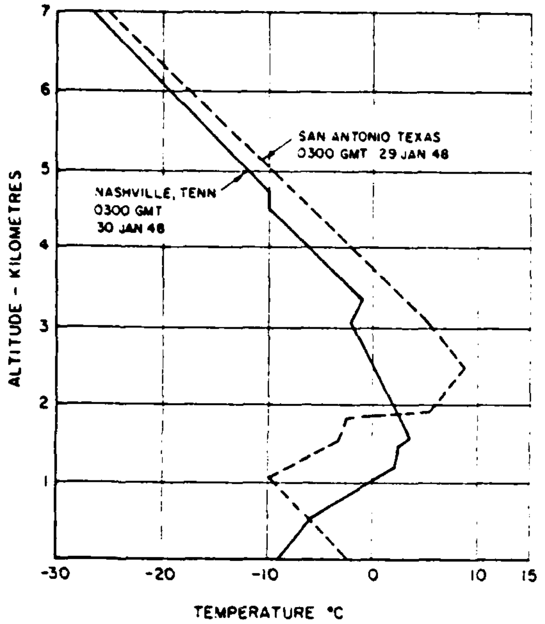

Figure 1. Typical temperature profiles during the occurrence of supercooled precipitation at the ground. (After Werner, 1975.)

In view of the severity of the problem, it seems remarkable that so little information on the characteristics of freezing rain and drizzle is available.

## SIGNIFICANT METEOROLOGICAL PARAMETERS

For the most part, the published data on freezing rain conditions have been assembled from the point of view of ice and contingent wind loads on structures and hence are concerned with the maximum amount of ice produced by an ice storm and the extremes of wind speed during the storm or in the 24-hr period following the storm.

This type of information may be adequate for setting up standards for the design of structures to withstand the added stresses imposed as a result of an ice storm, but *it does not* provide the information required for the design of thermal anti-icing systems, for the realistic simulation of freezing rain/drizzle conditions, nor for any application in which the rate of ice deposition or the fidelity of the ice shape or form is of importance.

The parameters of significance in these cases are the liquid water content (LWC), the effective drop size (D), the temperature (T), the relative humidity (RH), and the velocity (V). Not only is the range of values of these parameters required, but also their combination and probability of occurrence.

Such information is not generally available currently, and would require that the meteorological records of a region be analysed over many years to abstract the appropriate data and estimate return periods, etc.

Most of the raw data is readily obtained, but rain gauges ice up, with the result that normal hourly readings of precipitation amount are not available during ice storms. However, if precipitation rates are available, or can be deduced, they still have to be converted to liquid water content (LWC) values for design and test purposes. The fundamental relation, which requires a knowledge of the drop size distribution, is:

$$\mathrm{LWC} = \int_0^{D_{max}} R(D)/3.6\ V(D) \quad (\mathrm{g/m^3}) \qquad (1)$$

where R(D) is the contribution to the overall precipitation rate R in mm/h due to drops of diameter D and whose fall velocity is V(D) in m/s. Expression (1) is thus too cumbersome for normal use, but fortunately, a number of workers have derived empirical expressions relating LWC directly to the precipitation rate. These expressions differ with the type and character of rainfalls measured in their derivation. For rains originating above the freezing level, the expression due to Best (1950) is representative and is recommended:

$$\mathrm{LWC} = 0.072\ R^{0.88}. \qquad (2)$$

Similar empirical expressions for the median volume drop diameter of the distribution, as a function of precipitation rate, have been derived. Expression (3), given by Mason (1971), is recommended as giving reasonable compromise values of drop size (in mm), i.e.

$$D = R^{0.23}. \qquad (3)$$

Expressions (2) and (3) refer to rain at any temperature and intensity. Specifically, for freezing rain, an intensity of no greater than "moderate rain" (i.e. R ≈ 4 mm/h) is to be expected. As indicated earlier, data on freezing rain intensity is sparse, and in the absence of hourly rainfall rates it is usually necessary to determine mean precipitation rates for the complete storm period.

The earliest data of this sort was presented by Austin and Hensel (1956).

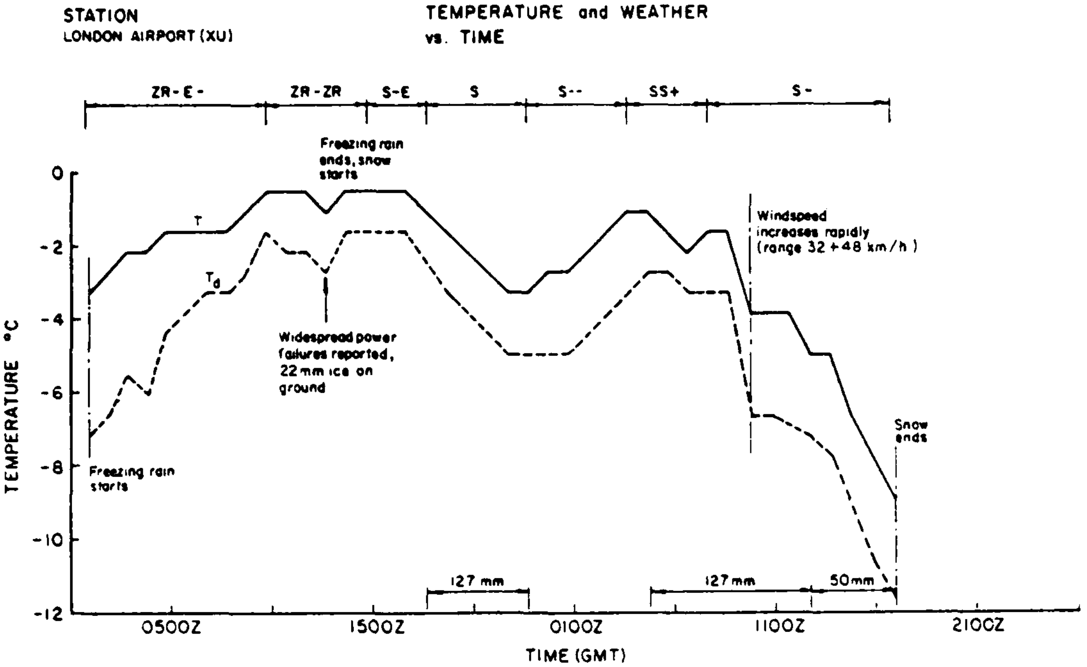

Figure 2. Chronology of freezing rain/snow storm at London, Ontario, 14-15 January 1968. (After Gee and Tozer, 1968.)

They indicated precipitation rates for a 3-year period as high as 2.0 mm/h at Yarmouth, Nova Scotia, and in the same order at Cape Harrison, Labrador. Two particularly well documented storms in Southern Ontario are reported by Thomas (1960) and by Gee and Tozer (1968). The storm of 13-15 January 1968 reported by Gee and Tozer resulted in about 26 mm of freezing rain at Toronto International Airport at an average rate of 2.4 mm/h, while at London Airport, 38 mm fell at an average rate of 2.7 mm/h. Figure 2, taken from Gee and Tozer, shows the chronology of the weather experienced at London on 14-15 January 1968.

In 1971, Bell Canada made a survey (Collins, 1971) of all freezing precipitation storms, with total precipitation greater than 2.5 mm, recorded at Toronto International Airport for the 10-year period 1957-1966. Twenty-three storms were identified. The greatest precipitation recorded was 24 mm, while the maximum precipitation rate was 4.8 mm/h. The minimum temperature recorded was -6.5°C, but the mean value for all storms was -0.4°C. The maximum and minimum values of storm mean windspeed were 14.9 m/s and 1.8 m/s, with a mean for all storms of 5.9 m/s. The lowest storm mean relative humidity was 83%.

Werner (1975) has derived the cumulative probability distributions of hourly precipitation rate for freezing rain and drizzle from data obtained in the northeastern United States, and compared them with a distribution derived by Lewis and Perkins (1958) for freezing rain over New England. From these, Werner has developed severity conditions as a function of temperature that are exceeded only 1 percent of the time (99th percentiles). These were based on the assumption that the 99th percentile precipitation rate (4.75 mm/h) occurred at 0°C and that the rate decreased linearly to zero at about -10.6°C, i.e.

$$R = 0.445T + 4.75 \qquad (4)$$

Werner then applied relations due to Marshall and Palmer (1948) to obtain the liquid water content and drop size. Figure 3 presents Werner's proposed relationships. These are probably the best available basis for design and test specifications currently available. It will be seen that the data for the various storms, quoted earlier, fall within the precipitation rate envelope.

Werner (1975) was concerned with the icing of helicopters in flight, and so did not consider contingent wind velocity. If, however, we are to consider the rate of icing, or the heat required to prevent the formation of ice on the vertical surfaces of a stationary structure, the wind velocity must be taken into consideration. The data of Austin and Hensel (1956) show that, at Gander, Newfoundland, average windspeeds during freezing

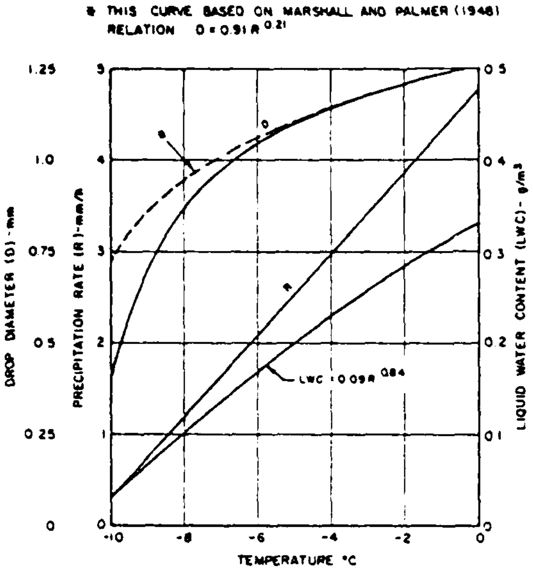

Figure 3. Proposed freezing rain severity as a function of temperature--99th percentile conditions. (Adapted from Werner, 1975.)

precipitation never exceeded 17.5 m/s, and only 3% of the time did they exceed 13 m/s. At Cape Harrison, Labrador and Yarmouth, Nova Scotia, the average windspeed never exceeded 13 m/s.

The data of Collins (1971) show that for the 10-year period studied at Toronto, the average wind velocity exceeded 10 m/s only once, when an average of 14.9 m/s was recorded for a 4-hour storm, i.e. 2% of the total duration of freezing precipitation.

Combining the data of Austin and Hensel with that of Collins, we find that all but 1-1/2% of the average hourly wind readings are contained within the velocity/temperature envelope defined by the relation:

$$V = 1.5T + 18 \quad (m/s) \qquad (5)$$

where T is the air temperature in °C.

Finally, because evaporative cooling affects the icing rate or the heat energy required to prevent ice formation, it is necessary to know the relative humidity. The air is frequently far from saturated during precipitation, as demonstrated by the dew point depression evident in Figure 2. The relative humidity climbed from 70% at the beginning of the storm to 91% by the time the freezing rain turned to snow.

Collins' (1971) data for Toronto reveals that 50% of the time in freezing precipitation the relative humidity was 95% or below, while 90% RH or below was experienced 20% of the time and 84% RH or lower occurred 5% of the time. It is therefore proposed that for design purposes a relative humidity of 85% be assumed.

## MEASUREMENT OF INTENSITY AND DROP SIZE

The methods of measurement that have been employed in the cold chambers and wind tunnels of the National Research Council of Canada are simple ones. Modern sophisticated instruments such as laser spectrographs or holography do not seem to be justified, since precise measurement of drop size is not critical (the impingement efficiency is high and not significantly affected by the range of drop sizes involved), and, as will be seen later, variations in the liquid water content are generally less significant than variations in temperature and velocity.

Generally, in cold chamber work, where wind velocity is low, it is simpler and more convenient to measure the precipitation rate. This may be done by placing an array of collectors (cylinders or trays) in the vicinity of the test article.

In the wind tunnel, where a known and constant wind velocity applies, the direct measurement of liquid water content is preferred. This is most easily done using a pitot sampling tube and measuring the amount of water collected in a given time. No attempt has been made to heat the measuring device because of the problem of evaporation loss, so that measurements are made above freezing and form the basis of calibrations for subsequent tests.

Drop size has been measured using a simple method attributed to Wiesner (1895). It consists of dusting a piece of standard filter paper with a water-soluble dye and exposing it to the rain. The size of the impinging raindrops is determined by the diameter of the colored stains they produce, and which are related to the drop diameters (D mm) by the following expression:

$$d = 4D^{1.36} \quad (mm).$$

The method is simple and cheap, but has the disadvantage that classification of the stains into size groups is a rather tedious procedure. However, a very quick visual indication of whether the drops are approximately of the desired size is obtained.

## DROP SUPERCOOLING

The temperature of rain drops is not likely to be in equilibrium with that of the air through which they are falling. However, because the divergence between the two temperatures will be unknown, the only logical course in trying to simulate freezing rain conditions is to try to reduce the difference as much as possible. First, it is necessary to cool the water being supplied to the rain nozzles to as close to the freezing point as possible. A good way of doing this, and which avoids the danger of freezing the water in the pipe, is to immerse the water supply line in an ice/water bath.

Next, since the remainder of the cooling has to be by convective and evaporative cooling from the raindrops themselves, their time of flight must be as long as possible. The nozzles should therefore be mounted as high as possible in the cold chamber or wind tunnel.

By using a suitable drop cooling expression, cooling curves for drops falling at their terminal fall velocity through saturated air have been calculated and are presented in Figure 4 to show the effect of initial water temperature on cooling time. The time required for the drops to reach any desired temperature, under the chosen conditions, is increased by 0.25 seconds (i.e. an additional metre of fall height) for every degree increase in initial water temperature.

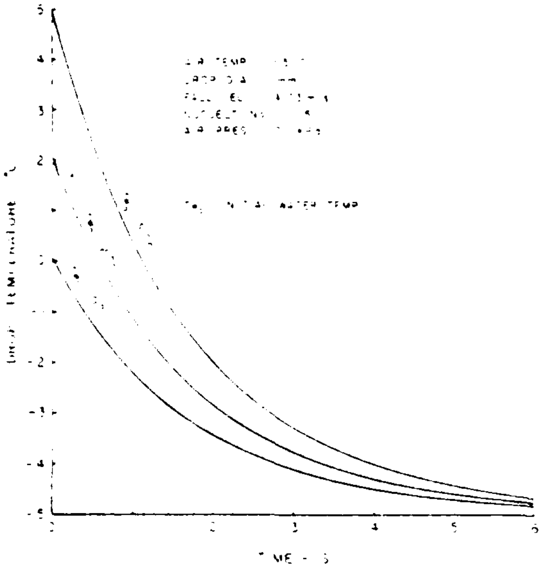

Figure 4. Effect of initial water temperature on the cooling time of 1-mm drops falling at terminal velocity through -5°C air.

## EFFECT OF VARIABLES ON RATE OF ICING

The effect that changes in the various icing parameters have on the rate of icing can be shown by performing a thermodynamic analysis of the icing process. The results of such an analysis for the stagnation point of a cylinder of 0.3 m diameter are shown in Figure 5. A set of standard conditions was chosen as shown, and each was varied in turn, while the others were held constant, except that, when the air temperature was the variable, the drop temperature was varied equally.

It is at once apparent from the figure that, as long as icing is in the wet growth regime, only two parameters are of primary significance, the air temperature and the velocity. However, should icing be occurring in the dry regime (i.e. at low temperature, low LWC, or low wind speed, when all the impinging water drops freeze in their immediate vicinity of impingement), the significant parameters are then the liquid water content and velocity, while the air temperature has no further effect on the rate of icing.

The transition between dry and wet growth (the Ludlam limit) is evident in Figure 5 by the knees in the velocity,

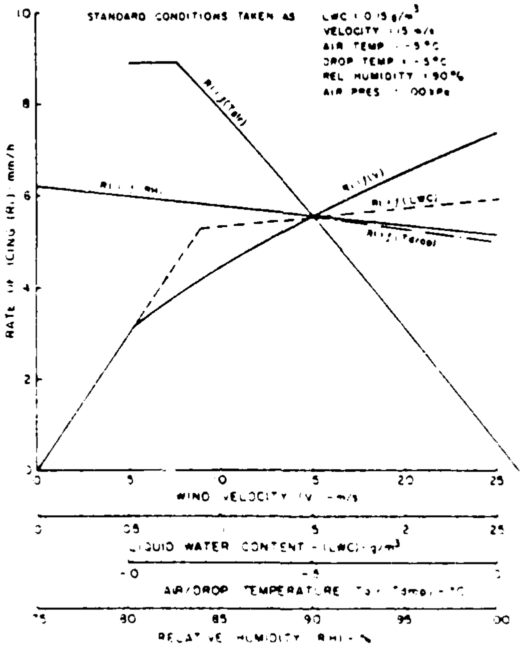

Figure 5. Rate of icing at the stagnation point of a 0.3-m-diameter cylinder, showing the effect of varying each parameter independently.

liquid water content and air temperature curves. In many circumstances, less attention need be paid to the drop temperature and the relative humidity than to the other test parameters, but their effects become more significant should conditions be close to the Ludlam limit or at locations removed from the cylinder stagnation region.

A similar thermodynamic analysis may be employed to estimate the power required for anti-icing a structure. The results of such an analysis made for the windshield of an automobile are shown in Figure 6. Under these conditions, the effects of variations in the liquid water content and drop temperature cannot be ignored, although they are less significant than effects caused by variations in temperature and speed.

## DROP PRODUCTION AND DISTRIBUTION

If water is ejected from a nozzle at the same velocity as the surrounding airstream, the diameter of the droplets produced has been found to be approximately twice the nozzle orifice diameter.

The area of dispersion from a stationary nozzle is small with a correspondingly high water concentration. One method of spreading the water over a larger area is to move the nozzle or nozzles every few minutes from one fixed position to another, so that over the course of the test the complete test object has received the correct average liquid water content.

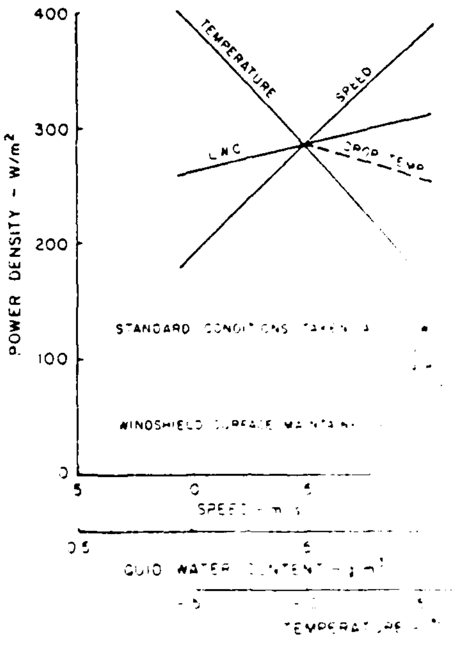

Figure 6. Heating load required to main- [illegible] automobile windshield ice-free in [illegible] rain conditions, showing effect [illegible] the primary parameters inde-

This method is not always convenient, and as a result a method of oscillating a nozzle about two orthogonal axes has been developed. A lateral to vertical oscillation rate in the ratio of 28 to 13 is being used, and the time for one complete cycle of the spray pattern, which has the form of a Lissajou figure, is 53 seconds. Both the lateral and vertical angular throws can be adjusted up to about ±30% so that a range of rectangular patterns can be provided as required.

This rain distributor has been used in cold chamber tests designed to develop a more realistic test of automobile windshield anti-icing performance. Good distribution over an area of 1 m$^2$ was achieved with only two nozzles.

The current "Windshield Defrosting and Defogging" test method is not representative of actual vehicular and environmental operating conditions. It represents a condition that exists only before a vehicle is driven, and under these circumstances most drivers will remove the ice with a scraper rather than wait for the defroster to melt the ice.

The object of the new test proposal was to test the performance of the windshield heater under simulated running conditions. A blower was used in the cold chamber to produce winds over the windshield area of at least 50 km/h. In addition, a dynamometer is proposed to apply the necessary road load, although one was not used during the evaluation tests.

Two types of tests were performed. The first run each day was a cold start [illegible], the car having been cold-soaked for [illegible] hours at -5°C. One minute after the [illegible] was started, rain delivery was [illegible], the blower was started and the [illegible] wipers were turned on, repre- [illegible] car leaving the garage. The [illegible] continued until the engine [illegible] normal operating temperatures, during which time the progress of ice [illegible] was recorded.

The other type of test, following the cold start test, was a 30-minute steady state test representing the warmed-up car driving in freezing rain conditions. Adequate driving visibility was to be demonstrated under specified conditions, those proposed being: temperature -5°C, speed 50 km/h, rain intensity 1 mm/h

Figure 7. Freezing rain test of car windshield de-froster system performance.

(LWC = 0.7 g/m$^3$), drop size 1 mm. Figure 7 shows such a test in progress.

## CONCLUSIONS

Although freezing rain has serious economic and social consequences for some part of northeastern North America almost every winter, very little information on its characteristics, other than the total thickness of the resulting ice, is available. On the basis of sources of information known to the author, it is proposed that, for design and test purposes, the rain intensity and wind velocity be based on the air temperature:

$$R = 0.445T + 4.75$$

$$V = 1.5T + 18$$

that the liquid water content and the drop diameter be based on the rain intensity:

$$LWC = 0.072R^{0.88}$$

$$D = R^{0.23}$$

that the relative humidity be assumed constant at 85%, and that the temperature range of occurrence be 0°C to -10°C.

Based on these relations, two test conditions are proposed as follows:

| | (a) | (b) |
|---|---|---|
| Air temp (°C) | -1 | -6 |
| Intensity (mm/h) | 4.0 | 2.0 |
| LWC (g/m$^3$) | 0.25 | 0.15 |
| Drop diam. (mm) | 1.0 | 1.0 |
| Wind velocity (m/s) | 16.5 | 9 |

These proposed relations and test conditions are put forward for consideration; however, they must be regarded as interim in view of the rather meagre amount of data on which they are based. As more data become available, modification can no doubt be made, in particular a recognition of regional differences would seem to be appropriate.

Because rain intensity and drop size are generally secondary parameters in their effects on icing rate or heat requirements for icing prevention, simple, unsophisticated methods of measuring these parameters in simulated rain are adequate. The temperature of the raindrops is also shown to be of lesser significance than the air temperature and velocity, but it is considered that attempts should be made to cool the drops as much as possible.

Uniform distribution of water at representative concentrations is difficult to achieve with stationary nozzles. The method of oscillating the nozzles about orthogonal axes has proved successful in giving a uniform distribution over a wide area.

## ACKNOWLEDGEMENTS

The author wishes to express his thanks to Mr. E.L. Collins of Bell Canada for permission to use the freezing rain data for Toronto, and to Mr. J. White of the Automotive Safety Engineering Branch of Transport Canada for permission to use information relating to tests on windshield de-icing.

## REFERENCES

Austin, J.M., and S.L. Hensel, 1956: Analysis of freezing precipitation along the eastern North American coastline. Massachusetts Institute of Technology, Lincoln Laboratory, Tech. Rept. 112, 46 pp.

Best, A.C., 1950: The size distribution of raindrops. Quart. J. Roy. Meteor. Soc., 76, 16-36.

Chainé, P.M., 1973: The variability of glaze ice in Quebec. Atmospheric Environment Service, Canada, Industrial Meteorology--Study I, 13 pp.

Chainé, P.M., Verge, R.W., Castonguay, G. and J. Gariépy, 1974: Wind and ice loading in Canada. Atmospheric Environment Service, Canada, Industrial Meteorology--Study II, 32 pp.

Collins, E.L., 1971: Private communication.

Gee, G.W., and D.N. Tozer, 1968: The January 1968 ice/snow storm in southern Ontario. Dept. of Transport, Canada, Meteorological Branch, Tech. Memorandum, TEC 685, 35 pp.

Harlin, B.W., 1952: The great southern glaze storm of 1951. Weatherwise, 5, 10-13.

Lewis, W., and P.J. Perkins, 1958: A flight evaluation and analysis of the effect of icing conditions on the ZPG-2 airship. National Advisory Committee for Aeronautics, Tech. Note TN 4220, 66 pp.

Marshall, J.S., and W. McK. Palmer, 1948: The distribution of raindrops with size. Jour. Meteor., 5, 165-166.

Mason, B.J., 1971: The physics of clouds. Clarendon Press, Oxford, 2nd Ed., p. 610.

Thomas, M.K., 1960: Glaze storm of December 26-28, 1959, in southern Ontario. Dept. of Transport, Canada, Meteorological Branch, Circular 3322, 11 pp.

Werner, J.B., 1975: The development of an advanced anti-icing/de-icing capability for U.S. Army helicopters. Volume 1--Design criteria and technology considerations. U.S. Army Air Mobility Research and Development Laboratory, Rept. No. USAAMRDL-TR-75-34A, 253 pp.

Wiesner, J., 1895: Beitrage zur kenntnis des tropischen regens. Sber. Akad. Wiss. Wien, 104, 1397.

# SESSION 2:
# DESIGN-ORIENTED RESEARCH

AD P001675

# ICE AS AN INFLUENCE ON COMPACT LINE PHASE SPACING

James R. Stewart Power Technologies, Inc.

## ABSTRACT

Vertical motion of power transmission line conductors caused by the release of accreted ice may limit the minimum vertical conductor separation. In the past, criteria based on static loadings have been used to determine the required clearance. Design based on the dynamics of ice shedding may allow smaller dimensions and additional line compaction. Experimentally tested physical models have produced conductor motion data for lines with and without in-span insulating spacers. Spacers increase the stiffness of the conductor system and reduce the motion to a greater degree than from an equivalent reduction in span length. Methods now exist for prediction and mitigation of ice-induced conductor motion on compact high voltage transmission lines.

## INTRODUCTION

Environmental and right of way constraints often pressure designers to specify the minimum possible phase spacing for high voltage power transmission lines. This minimum phase spacing may be limited by dynamic motions due to the release of ice accretions on the conductors. When conductors are vertically configured, sufficient clearance must be maintained to prevent flashover during all conditions of conductor motion. These phase spacing considerations are different from structure ice loading requirements but they do play an important part in the overall structure design since they impact the conductor location. EPRI projects RP 260-1 [1] and RP 260-2 [2] included in their scope an investigation of the effect of ice induced motion on minimum conductor spacing. This discussion summarizes the results of these projects.

## ICE LOADING AS A FACTOR IN PHASE SPACING

As power transmission voltages have increased, more sophisticated design approaches have been developed to allow phase spacings which are smaller multiples of the basic power frequency voltage flashover distance. The EPRI-sponsored compact transmission line work was a combination of an effort to apply the results of this research to line design in the 115-138 kV range and to develop new information where it was lacking in the existing literature. Of these areas of new research, ice shedding induced motion was one of the more significant.

As considered in this paper, compact lines are assumed to be constructed with post-type insulators or similar restraint to permit no significant movement of the conductor at the structure. This reduces the amount of conductor motion possible under conditions of ice release because each conductor is restrained not only by the structure but by all of the conductors of adjacent spans. This same feature increases the complexity of the analytical simulation because of the many mechanical parameters which affect the motion. A small error in the determination of the horizontal span due to structure deflection translates into a significant error in midspan sag, necessitating methods which are relatively insensitive to this variable. Since only the maximum conductor jump is of interest for phase spacing, energy formulations which predict only the peak jump rather than the entire motion are a possibility. This leads to the calculus of variations [3] where specific quantities can be predicted from stationary functions without a dynamic simulation.

Compact lines can be designed with horizontal, vertical, or delta phase configurations. Experimental results have shown that for post insulator lines without spacers, there is very little translation of vertical motion into horizontal motion. This means that the conductor arrangements sensitive to ice shedding are the vertical and delta configurations where a lower conductor rises to near proximity with the phase directly above it. Spacings greater than power frequency withstand must be maintained during this motion for flashover to be avoided.

## Static Criteria

Under static conditions the differential sag of two vertically adjacent conductors can be calculated by assuming one conductor has ice and the other has none. Normally, sufficient clearance is provided to accommodate this sag difference, including a factor for sag error and a margin for switching surge withstand.

Utility practice, based on historically satisfactory field performance, typically uses the following criteria for vertical phase-phase clearance due to ice.

1. A maximum sag error of 6 inches is assumed.
2. The upper conductor is assumed to be subject to maximum ice load, typically 1 inch for short ruling spans, 0.5 inch for unusually long spans.
3. The lower conductor is assumed to be completely free of ice.
4. Clearance sufficient to withstand the maximum switching surge is to be provided.

The calculation is performed using normal sag-tension procedures.

## Design Based on Dynamics of Ice Shedding

Vertical motion due to ice shedding is dependent on span length, tension, conductor size, ice thickness, and the amount of ice shed at any one time. The following is a possible set of criteria to use for dynamic ice shedding:

1. Assume a maximum sag error of 6 inches.
2. Assume the upper conductor has an ice load equal to 50 percent of the criterion for unequal static ice load (usually 0.50 X 1 inch, or 0.5 inch).
3. Assume that the lower conductor, previously with the same ice load as cited above, has already shed 25 percent.
4. Assume that the remaining 75 percent of the ice on the lower conductor is shed at one time.
5. Provide sufficient initial separation to ensure adequate clearance to withstand 60-Hz voltage during the subsequent jump.

On the basis of the observed tendency for shedding to occur in segments, an alternative criterion could be based on a fixed length of ice.

Figure 1 compares the results of the static ice loading criterion and the two jump criteria cited, all for an example of a 795 kcmil Drake conductor at

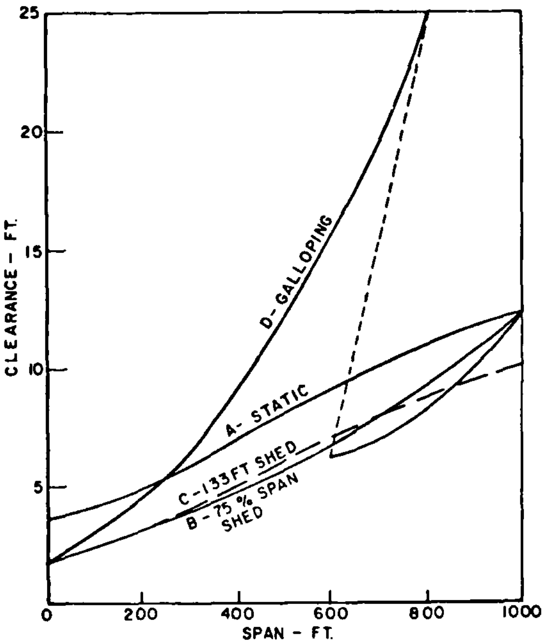

Figure 1. Example Comparison of Design Clearance For Ice Shedding.

a tension of 18 percent of ultimate at final (60°F) sag. The required vertical conductor separation is shown as a function of span length. Also shown are the limits which would be required by galloping if it were applicable as a criterion. The areas where maximum compaction is required, however, are usually congested and do not present the proper conditions for galloping. This allows galloping to be eliminated as a design factor in many compact line applications.

## EXPERIMENTAL PROCEDURE

The experimental configurations were subjected to artificial ice loading and subsequent shedding in order to define and record:

1. The most severe shock-induced conductor motions, both vertical and horizontal, for each line configuration.
2. Data to validate a calculation method.
3. Unanticipated phenomena which could affect compact line performance or design.

Ice loading was simulated with an equivalent weight rather than actual ice buildup to ensure repeatability and accuracy of tests. The technique for weight application and release is illustrated in Figure 2 and pictured in Figure 3. An actual test is shown in Figure 4.

A length of conductor serves as a distributed weight. The conductor is suspended from the test span by means of nylon cords spaced every ten feet. Inserted in each nylon cord is a pair of interlocking wire hooks. All of the hooks for the entire span are threaded with a length of low-energy blasting fuse which serves to simultaneously release the simulated ice load. This fuse burns at 4 miles per second, releasing the hooked wire hangers essentially simultaneously.

Tests were conducted using this technique on both the prototype compact lines themselves and a specially constructed ground level span. This latter span was used to study the effects of in-span insulating spacers by means of prototype insulators and the load cell

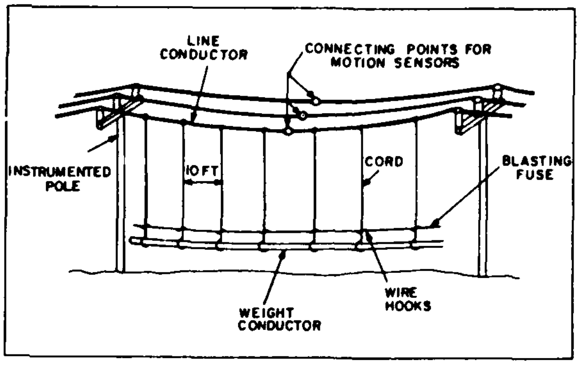

Figure 2. Artificial Ice Shedding Technique.

Figure 3. Set Up for Ice Shedding Test.

Figure 4. Ice Shedding Test in Progress.

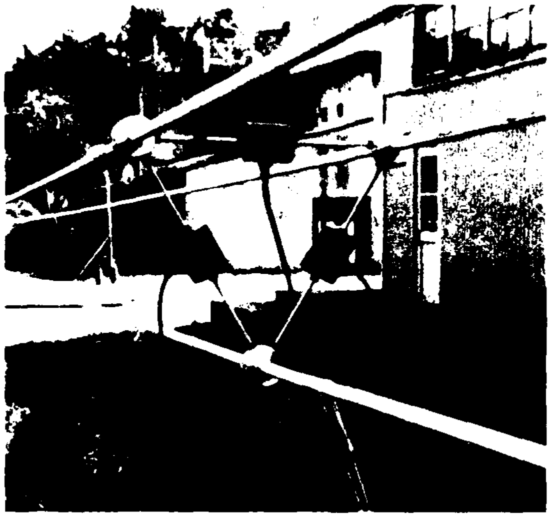

Figure 5. Load Cell Spacer Model on Ground Span.

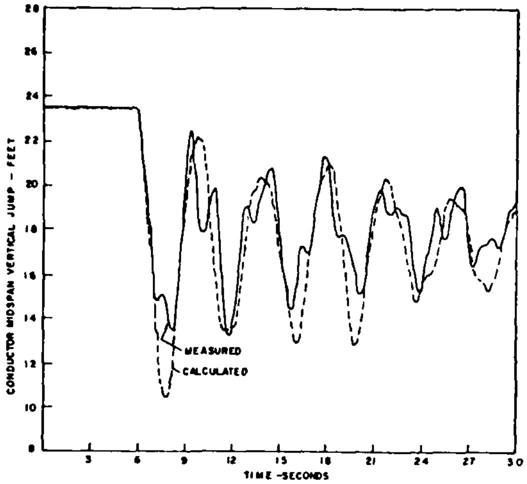

Figure 6. Record of Conductor Midspan Vertical Jump.

model of Figure 5 which was used for force measurements.

Conductor and structure motion were instrumented using various means:

1. Fine stainless steel stranded cable driving potentiometers giving an analog voltage proportional to deflection.

2. Optical tracking using a specially designed digital scanning of a photodiode array.

3. High-speed movie film recording against a calibrated backdrop.

Data was recorded both on a pen recorder and a digital data logger, the latter for transfer directly to a digital computer for processing and plotting.

## PHYSICAL PHENOMENA FOR POST INSULATOR LINES

When a single conductor of a span of transmission line is loaded by ice, there are a number of simultaneous effects. For a compact line using wood pole, crossarm, and post insulator construction, the pole deflects and twists in the ground; the pole itself deflects and twists; the crossarm/pole joint, having a certain degree of looseness, is deformed; the insulators rotate in a vertical plane by the twisting of the crossarm; and the conductor sags are changed (some increased and some decreased). This sag change is caused by the movement of the conductor attachment position with a resultant change in horizontal span, conductor tensions and elongations. Changed tensions on shield wires add to the forces on the structures and the stiffness of the poles themselves influence the total motion.

For a static loaded condition, all of the above reach equilibrium and the total energy stored in the system is increased. Upon release of the load, a dynamic condition ensues wherein conductors stretch, rise and fall; poles bend and twist; etc. The subsequent wave shape of the vertical motion is essentially sinusoidal, with a superimposed higher-frequency component, as illustrated by the measured response shown in Figure 6. These two frequencies are due to transverse and longitudinal oscillations in the conductor. The transverse oscillations are described by the wave equation for a vibrating string, and the longitudinal oscillations by a spring and mass equation. These two oscillations have different fundamental frequencies and neither can be neglected in the analysis.

Calculated motion at the midspan, assuming only fundamental frequency oscillations of an inextensible conductor and the measured endpoint positions, is shown by the response designated as "Calculated" in Figure 6. These correspond to the transverse wave equation motions and are those which would occur with a conductor of infinite elastic modulus. The primary difference between the calculated motion and observed motion is due to the longitudinal oscillation in the conductor. These occur at a higher frequency than the transverse oscillations causing the two to be out of phase at the peak of the initial conductor swing. There is a net reduction in the overall rise as compared with what would would occur if the conductor were inextensible. This reduction occurred in all ice dropping tests on the experimental lines.

The change in energy of the system is closely approximated by the sum of the decrease in elevation of the midspan of the loaded conductor and the increase in elevation of the midspan of the same conductor on the adjacent span. This difference in height is a very accurate approximation of the total jump of the loaded conductor, allowing a complex model to be reduced to a much simpler one that is relatively insensitive to small variations.

## PHYSICAL PHENOMENA WITH IN-SPAN INSULATING SPACERS

Insulating spacers in the spans alter the behavior of conductors under ice shedding from that without them. Delta conductor configurations with spacers incur bundle rotation during induced motion which increases the complexity of the problem. The spacers maintain phase separation at their locations and increase the total stiffness of the system. However, the motion coupling between phases increases the complexity of the motion since it is no longer only in the vertical plane.

The addition of spacers to the span results in a noticeable increase in span stiffness and damping. While the quantification of the increase depends on the specific spacer, motion damps out much more quickly with the spacers in place than without them. The physical mechanism is that an ice load on one conductor is transferred to the other conductors through the spacers. Thus there is less sag increase caused by the weight. Upon release of the weight, motions are immediately coupled to all the phase conductors. These usually have slightly different natural frequencies due to the sag error. As the available energy is divided into a larger number of oscillation modes, each mode has a smaller amplitude. The net result is that the overall conductor motion is significantly smaller than it would be without spacers and a span shortened to one-third of its original length.

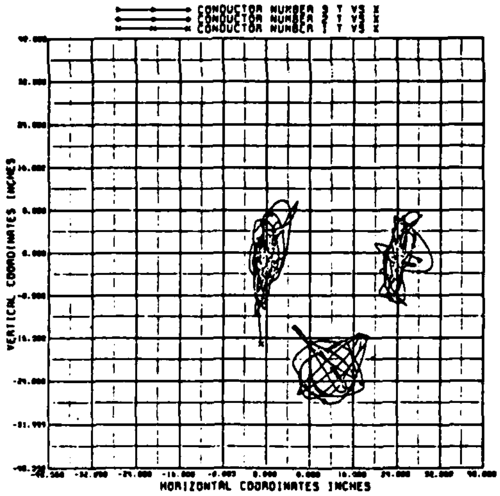

Figure 7. Measured Conductor Motion at Midspan With Spacing.

Figure 7 presents a cross section view at the midspan of the ground level span during a simulated ice release with spacers at the 1/3 and 2/3 locations along the span. A considerable decrease in magnitude of movement is apparent when compared with Figure 6.

## DESIGN CURVES FOR ICE SHEDDING

The results of these experimental studies are given in References [1] and [2]. Figure 8 from Reference [1] presents ice jump magnitude as a function of span length for compact lines without spacers for the conductor conditions of Figure 1. A full span of one-half inch ice is assumed shed at 32°F. Correction curves for other conductors and loading conditions are also included in Reference [1].

Figure 9 from Reference [2] presents minimum phase-phase spacing for delta configurations with spacers at the 1/3 and 2/3 points of the span. Because of the smaller but more complex motions with spacers, an ordinate of minimum phase-phase spacing is a more appropriate form for presentation. Correction curves for other conductors and loading conditions are also included in Reference [2].

For comparison, consider a 300 foot span without spacers. The jump magnitude of Figure 8 is about 22 inches. Adding 18.5 inches for withstand

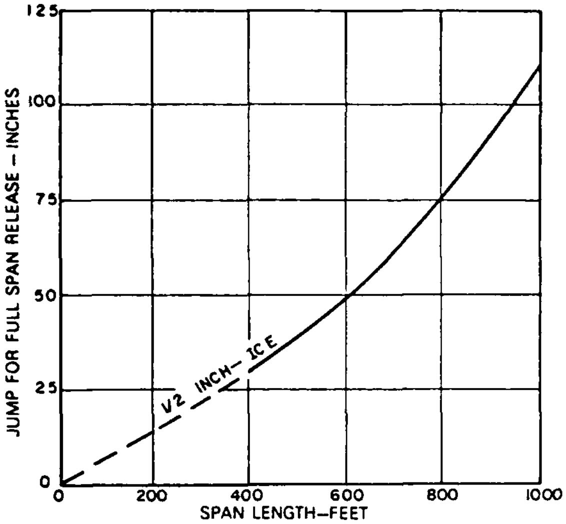

Figure 8. Ice Jump Vs. Design Curve Without Spacers.

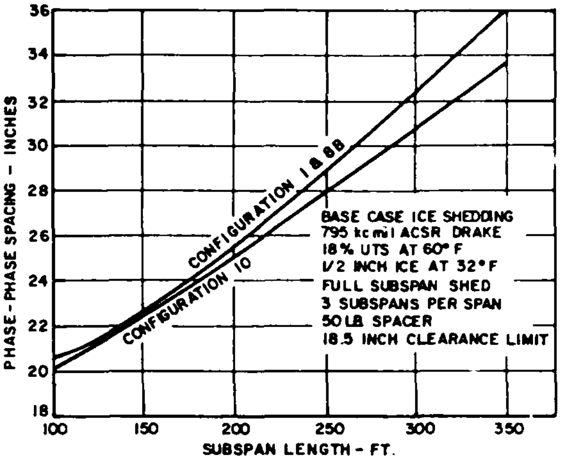

Figure 9. Spacer Application Base Case Subspan Length Vs. Phase Spacing For Ice Shedding.

clearance gives 40.5 inches minimum vertical separation without allowance for sag error or ice load on the upper conductor. A 900 foot span with spacers at the 1/3 and 2/3 points (300 foot subspan) has a minimum clearance requirement of 32.5 inches from Figure 9, again without any additional allowances. This demonstrates the reduction in ice shedding motion by use of in-span spacers. The ice motion is reduced a greater amount by the addition of spacers than by an equivalent span reduction.

## CONCLUSIONS

Analytical models have been developed to predict the dynamic behavior of transmission line conductors following ice shedding. These provide an additional method for calculating required vertical conductor spacing and form an alternative to the customary static analysis.

The dynamic calculations usually give reduced clearances as compared with static assumptions and thus allow greater line compaction.

Observations of actual ice conditions including the manner in which ice falls from lines are limited. This means that even for the dynamic calculations the assumptions are conservative in that long segments of ice are assumed to drop simultaneously. Additional information in this area may allow further compaction in the future. In the meantime the specified criteria are appropriate.

Conductor restraint at the structures using post-type insulators reduces the magnitude of the motion when compared to similar performance with suspension type insulators. In-span insulating spacers change the physics of motion such that their impact in reducing ice induced motion is greater than that caused by simply reducing the effective span length. Thus significant compaction of high voltage transmission lines is possible even in areas of heavy ice loading.

## ACKNOWLEDGEMENTS

The work reported in this paper was sponsored by EPRI Electrical Systems Division under contracts RP 260-1 and RP 260-2. Mr. Richard Kennon was the most recent Program Manager.

## REFERENCES

1. Transmission Line Reference Book, 115-138 kV Compact Line Design, EPRI Publication, 1978.
2. Bundled Circuit Design for 115-138 kV Compact Transmission Lines, EPRI report EL-1314, 2 volumes, 1980.
3. F. B. Hildebrand, Methods of Applied Mathematics, Second Edition, Prentice-Hall, Englewood Cliffs, N. J. , 1965.

AD P001676

# ADHESION OF ICE ON ALUMINUM CONDUCTOR AND CRYSTAL SIZE IN THE SURFACE LAYER

Jean-Louis Laforte Université du Québec à Chicoutimi
C. Luan Phan Université du Québec à Chicoutimi
Beatrice Felin Hydro-Québec
Richard Martin Hydro-Québec

## ABSTRACT

Ice accretions of various densities are formed in a wind tunnel on an aluminium cylinder of 3.15 cm diameter. Environmental growth conditions cover the range of icing intensity and ambient temperature which prevail normally in field situations with glaze and hard rime storms on actual power line conductors. Density, ice crystal dimensions and adhesive strength in brittle conditions of deformation are measured. From the experimental results obtained, it is found that the adhesion of atmospheric ice on a metallic surface depends on its internal structure, mainly the porosity which is related to the density of ice accretion. The adhesive strength depends also upon the mean crystal width in the boundary layer near the conductor surface.

## INTRODUCTION

The adhesion and accumulation of glaze and rime to conductors and structures of power lines is a subject of practical importance in cold regions such as northern areas of the United States and Canada. For example, in the province of Quebec only, during the last ten years, failures of transmission lines due to icing events account for the loss of many millions of dollars. Nevertheless the problem of adhesion of ice to solid is rather complex as is pointed out by the great number of studies on this subject. Therefore, an effective solution, economical and practical to this problem of transmission lines requires a better understanding of the fundamental factors that control bonding of aerodynamically formed ice on metallic surfaces.

Although there are many studies on the adhesion of cold box ice,[1-6] those related to the adhesion of aerodynamically formed ice from supercooled water droplets[7-11] are much less numerous. Moreover, most of them[8-10] concern icing on aircraft and helicopters, where droplet speeds are considerably higher than air speeds involved in ice accretion on transmission lines.

The factors influencing adhesive strength of atmospheric ice on conductors can be divided into two great categories. The first category groups the factors relating the surface properties of the materials to which the ice adheres. These are roughness, surface porosity, wettability and cleanness. The second includes factors pertaining to the mechanical properties of ice: these are the conditions of loading[12-13] and the kind of ice which are determined by the meteorological conditions under which the ice is built up. These latter control the rate of freezing of impacting droplets and are responsible principally for the internal structure of the ice, more precisely for the porosity and crystal texture on which ice strength is particularly dependent. In the authors' recent work,[11] the interdependence of the adhesive strength of glaze and rime with density and ice crystal dimension is mentioned. However, in almost all other studies on atmospheric ice, no particular attention is brought to porosity and microstructural features of ice, especially in the boundary layer near the material substrate. The purpose of present work is to study systematically adhesive strength of artificial deposits of glaze and hard rime grown under controlled conditions in relation with the mean bulk density of ice and the size of ice crystals in the boundary area near the conductor surface.

## EXPERIMENTAL SET-UP AND PROCEDURES

Ice accretion is grown on a smooth aluminium cylinder placed in the 23cm x 23cm working section of an open wind tunnel. The tunnel (Fig. 1) is horizontally installed in a 4.3x8.8x3.3m cold room where a minimum temperature of -40 ±5°C may be maintained. The diameter of the conductor is 3.15 cm, which is in the same order of magnitude as those used on actual power lines. In order to obtain a uniform ice thickness around the conductor, the latter is rotated at 1 rpm by a synchronous motor.

Water droplets of 38 ±3 μm and 96 ±5 μm mean volume diameter are produced by a painter's electric gun, model Wagner 300 with nozzle no. 8. A pneumatic nozzle is used for smaller droplets of 12 ±1 μm and 22 ±2 μm. Droplets spectra are determined at the position of the conductor using the silver colloid film method.[14] Tapwater of conductivity between 45 and 68 μS/cm is supplied to the nozzles from a large reservoir at room temperature. These values of conductivity are lightly smaller than those of rainwater collected in Quebec areas, which range from 20 to 100 μS/cm.[15]

The liquid water content W of the air is measured by the single cyli der method.[16] In most of the experiments, it is varied from 0,4 to 0,8 g/m$^3$. However, in one series of tests, W was extended to values of 1,2 and 2,4 g/m$^3$.

FIG. 1 WIND TUNNEL

Before each experiment, the conductor is carefully cleaned with hot water and commercial soap. It is then installed in the working section of the tunnel where it is kept for 2 hours before beginning the test. Ice is accreted on the conductor until a uniform thickness of 15 ±3 mm is reached. At the end of the run, which lasts from 30 minutes to 3 hours depending on the growth conditions, an ice sample of 3 cm long is cut from the central part of the ice accretion where the growing conditions are the most uniform. The conductor with the ice sample is then put in the apparatus used for adhesion measurement. This is done essentially by measuring adhesive strength by shear experiments which have been described in detail in previous papers,[11-12] by the authors. After the adhesive test, the ice sample is usually broken in three or four pieces. The measurements of density and preparation of thin sections for crystal texture observation are made with those ice pieces taken from the ice sample. All measurements are done in the cold room at the same temperature as that used in the accretion test. Thin sections are prepared with a sledge type microtome, model Leitz 401. They are then observed through a low power microscope which permits identification of structural features under ordinary and polarized light.

## EXPERIMENTAL RESULTS

### Nature of ice deposits grown in tunnel

As mentioned in the introductory section, inherent properties of ice adhesion depend on the internal structure (crystal size and porosity) which is controlled by meteorological environmental parameters. So, before presenting adhesion results, it is important to depict the nature of ice samples grown in the present series of tests.

Experiments of the present study are chosen to cover the range of intensity of accretion and air temperature prevailing normally during formation of glaze and hard rime. Distinction between the two types of ice can be obtained at first glance from visual inspection of the accretion.

Figure 2 shows appearance and surface finishes of ice accretion grown at different ambient temperatures and air velocities. In this series of tests, mean volumic diameter $d_V$ and water liquid content W are kept constant at 38μm and 0,8 g/m$^3$ respectively.

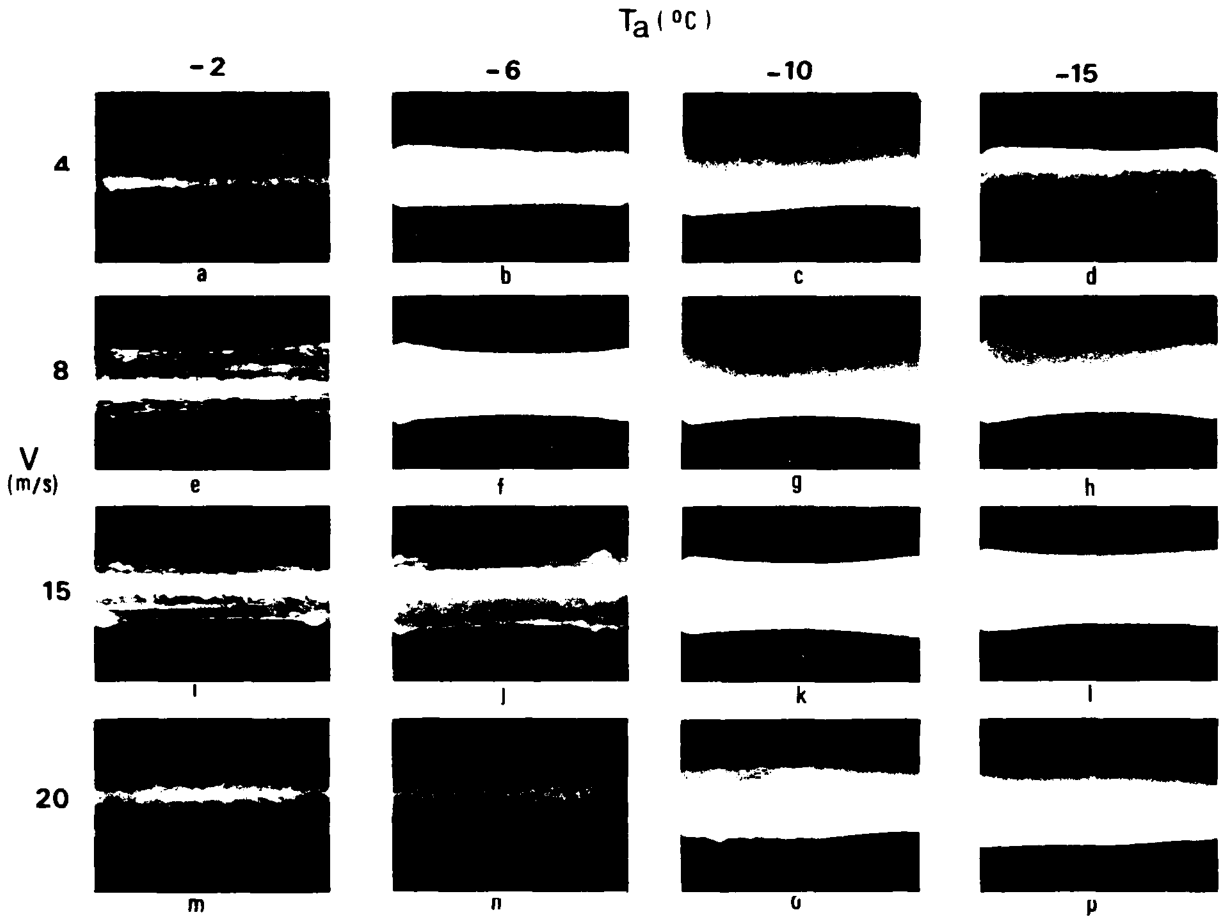

FIG. 2 VISUAL APPEARANCE OF ICE ACCR' N GROWN UNDER DIFFERENT AMBIENT TEMPERATURE AND AIR VELOCITIES

From these photographs (Fig. 2), it can be seen that at air temperature $T_a$ of -2°C and -6°C, the ice is glaze characterized by a smooth external surface and high degree of transparence.

At -10°C and -15°C, it is rime with a non-smooth surface finish and low transparence or high opacity. Incidentally, surface roughness and opacity tend to increase with decreasing ambient temperature $T_a$ wile they decrease at increasing air velocities V. Surface protuberances appearing on glaze samples formed at 20 m/s and -2°C and -6°C (Figs. 2m and 2n) may be attributed to the presence of a thin film of liquid water on the accretion surface. In fact, at these values of $T_a$ and V, the flux of water is rather high and then all impinging droplets on the conductor do not have time to freeze completely. This water film causes some turbulences which locally perturb the collection and freezing rate of the water droplets.

Figure 3 illustrates the effect of liquid water content upon the kind of ice built up from two different droplets spectra. In these tests, ambient temperature and air speed are kept constant at -6°C and 8 m/s respectively. It may be seen in Fig. 3 that ice samples obtained from 12-μm-diameter droplets are hard rime with a rather smooth external surface. Moreover, the opacity of these ice accretions decreases continuously with increasing values of W. Ice deposits obtained from 96-μm droplets, however, are glaze type ice and appear on the whole less opaque (or more transparent) than ice grown from 12-μm droplets within the same conditions. This change in degree of transparency may be attributed to the difference between mean values (0.21 and 0.94) of the collection efficiency of 12- and 96-μm droplets respectively. Furthermore, some protuberances of external surfaces of ice accretions as seen on Figs. 2m and 2n are also observed on Figs. 3g and 3h.

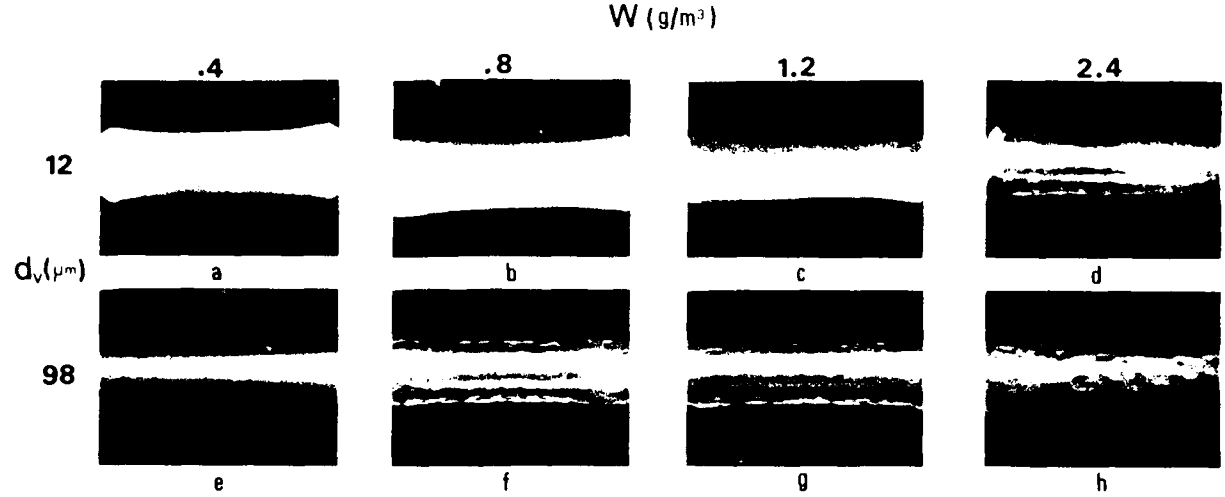

FIG. 3 VISUAL APPEARANCE OF ICE ACCRETED FROM TWO DROPLETS SPECTRA IN INCREASING LIQUID WATER CONTENT OF AIR

These may be explained as previously, by a thin film of liquid water formed on the conductor surface under high values of W. From these observations, it appears that the artificial ice accretions grown in the present series of tests are similar to natural ice accretions.

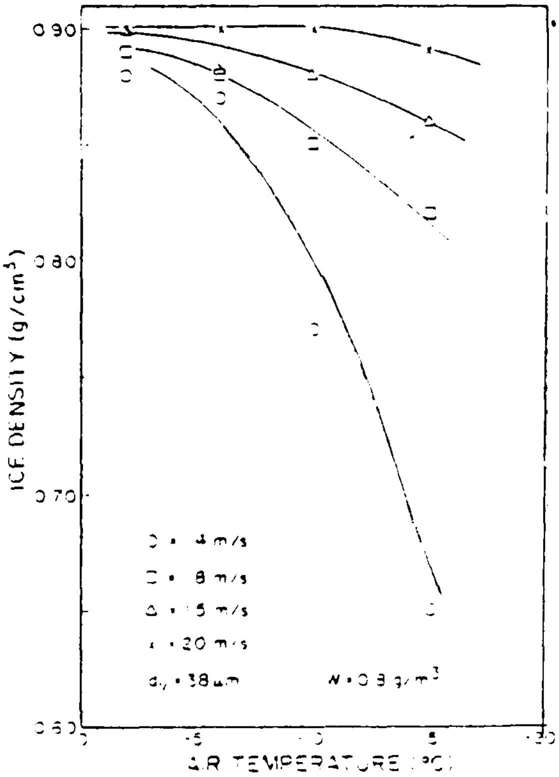

FIG. 4 DENSITY OF ICE AS A FUNCTION OF AMBIENT TEMPERATURE AND AIR VELOCITY.

Mean density of ice deposits

Figure 4 presents the mean density as a function of $T_a$ and V for ice accretions grown in the same conditions as those shown in Fig. 2. For glaze samples (at -2°C), the density is nearly equal to

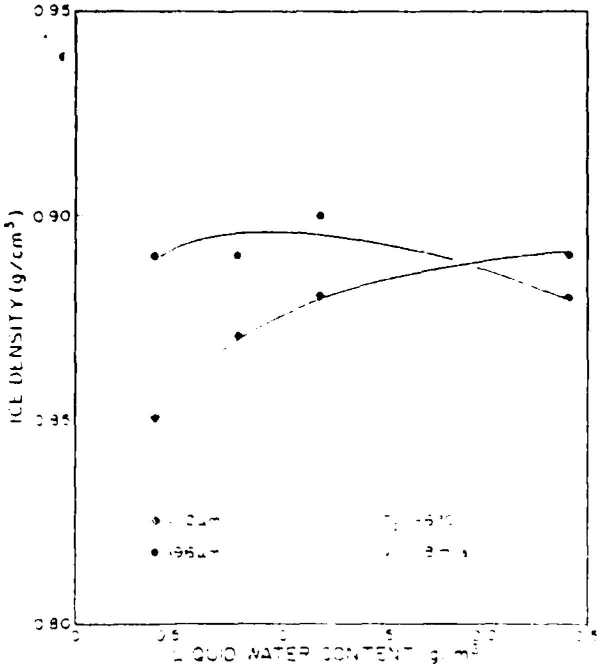

FIG. 5 DENSITY OF ICE ACCRETED FROM TWO DROPLETS SPECTRA AS A FUNCTION OF LIQUID WATER CONTENT

AD-A131 869 PROCEEDINGS OF INTERNATIONAL WORKSHOP ON ATMOSPHERIC 2/4
ICING OF STRUCTURES (..(U) COLD REGIONS RESEARCH AND
ENGINEERING LAB HANOVER NH L D MINSK JUN 83
UNCLASSIFIED CRREL-SR-83-17 F/G 8/12 NL

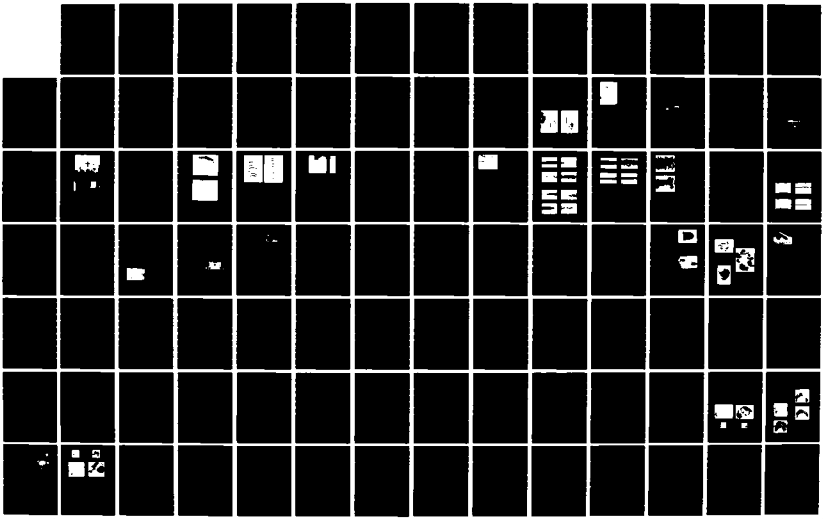

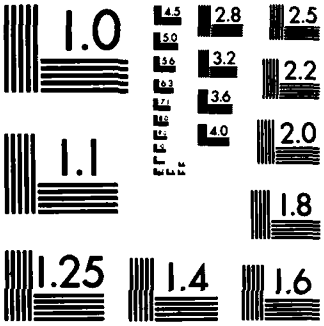
1.0
4.5
5.0
5.6
6.3
2.8
3.2
3.6
4.0
2.5
2.2
2.0
1.1
1.8
1.25
1.4
1.6

MICROCOPY RESOLUTION TEST CHART
NATIONAL BUREAU OF STANDARDS-1963-A

the maximum density of ice (0.916) independently of air speed. For hard rime samples, densities take on values under 0,90 and decrease continuously with decreasing values of $T_a$ and V. Figure 5 shows the variations in mean density observed for ice accretions grown at increasing values of W from two droplets spectra. For 12-μm droplet spectrum, ice is hard rime with increasing density until it becomes glaze at a value of W equal to 2,4 g/m$^3$. On the other hand, for 96-μm droplets, ice passes from hard rime at W = 0,4 g/m$^3$ to glaze for upper values of W. If we compare these results of ice density with the observations made in the above section on ice transparence, it is found that they show comparable dependencies upon meteorological parameters such as $T_a$, V, W and $d_v$. This resemblance may be understood if we consider that the relative degree of transparency or opacity of atmospheric ice is caused by the presence of ice of tiny air bubbles which determine its porosity. This latter is defined by the ratio of the volume of bubbles to the total volume of the ice sample.

Adhesive strength of ice deposits

Figure 6 gives the adhesive strength measured for glaze and hard rime samples shown previously in Fig. 2. Adhesion test was performed at a constant speed of deformation about 26 mm/min. and the temperature of the test was the same as that used during the growth of the accretion. For this relatively fast rate of loading, the mode of rupture is adhesive. In fact, in all tests it was observed that the conductor is free of ice after the removal of the test samples. At -2°C, where ice is glaze, within the accuracy of the measurements no significant effect of the air velocity is seen. For $T_a$ under -2°C, where ice is hard rime, the adhesive strength increases with increasing air speed. This increase may be explained by the effect of the velocity of air on the porosity of ice. If d is the density of ice, the porosity of ice, e, is expressed by

$$e = 1-d/0.916 \qquad (1)$$

Then, as the density of atmospheric ice is found to increase with air speed (Fig. 4), the porosity would decrease and the adhesive strength would be expected to increase. Concerning the effect of ambient temperature, it is seen on Fig. 6 that for the four values of V, the adhesive strengths present nearly identical trends. Starting from a common value at -2°C, it increases continuously to reach a peak and then it begins to decrease.

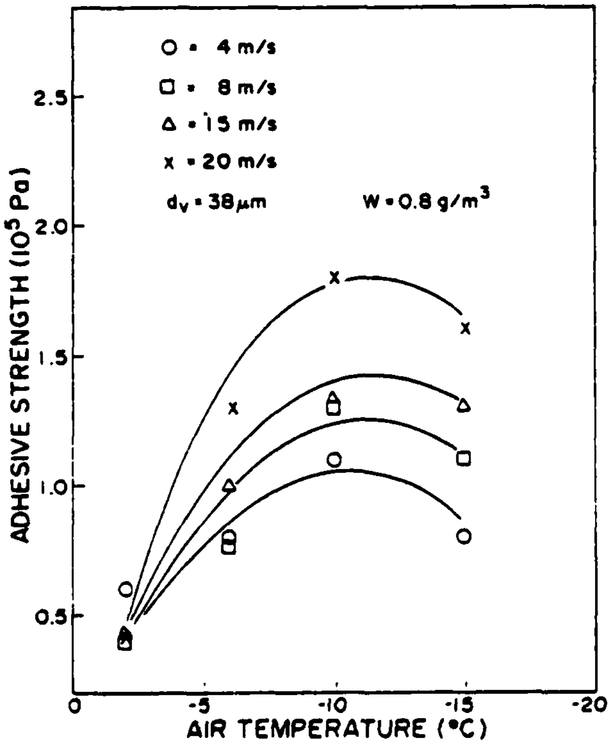

FIG. 6 ADHESIVE STRENGTH OF ICE ACCRETION GROWN AT DIFFERENT AMBIENT TEMPERATURE AND AIR VELOCITIES

This dependence of the adhesive strength of ice upon ambient temperature may be explained by the influence of two factors having counter effects: the porosity, which is dependent on density is responsible for the decrease in adhesion, while the temperature acting directly or indirectly is responsible for its increase. More details about these factors will be given in the discussion.

Concerning the effect of liquid water content and droplet size, Fig. 7 presents the results of adhesive tests, obtained for ice accretion grown in increasing liquid water content from two droplets spectra. As with Fig. 4, ambient temperature and air speed are kept constant at -6°C and 8 m/s respectively during the growth of the accretions. For hard rime obtained from 12-μm droplets it was observed that adhesion shows small increases with increasing W. For glaze accreted from 96-μm droplets, the adhesive strength decreases slightly with increasing values of W. The results obtained may be interpreted by the effects of W and $d_v$ upon the porosity of ice e. Effectively, in the growth conditions corresponding to Fig. 7, the porosity is the only factor that varies,

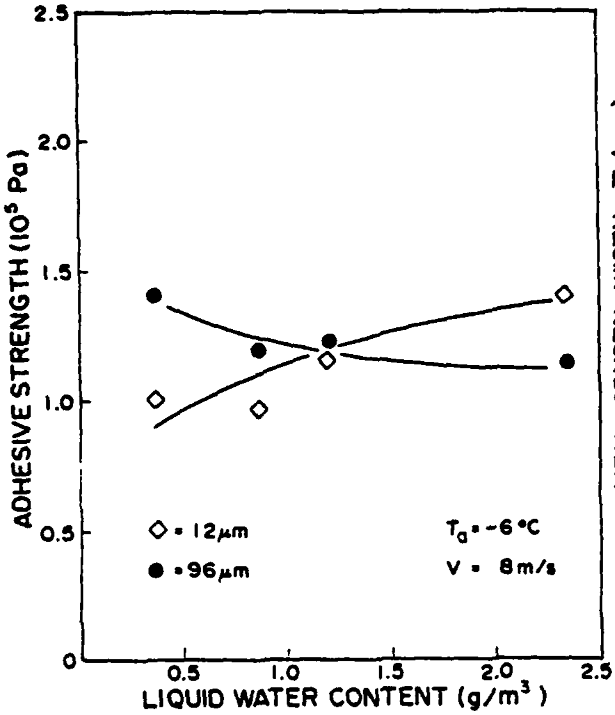

FIG. 7 EFFECT OF LIQUID WATER CONTENT UPON THE ADHESION OF ICE ACCRETED FROM TWO DROPLETS SPECTRA

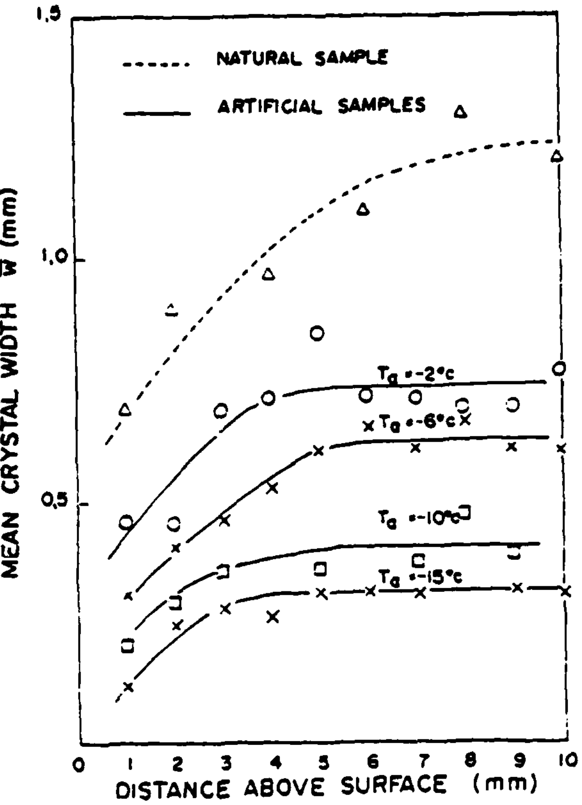

FIG. 8 VARIATION OF MEAN WIDTH OF ICE CRYSTAL WITH THE AMBIENT TEMPERATURE AND THE RADIAL DISTANCE ABOVE THE CONDUCTOR SURFACE

all other parameters being considered as constant.

Mean crystal width of ice deposits

As mentioned in the introduction, in addition to the porosity, the crystal dimension has been reported to be one of the factors which can influence greatly the mechanical properties of ice. Moreover, it is known from authors' recent microstructural study, that ice accretions grown in tunnels present generally columnar grains elongated in the radial direction of cylinder. Fig. 8 depicts mean crystal width measured at different positions above the surface of metallic conductor for ice accretions grown at four air temperatures. It can be observed on this figure that the mean width of ice crystals decreases with a decrease in ambient temperature. In fact the air temperature appears to be the main factor controlling the growth of ice crystals, the influence of all other factors being less important. It can be observed on Fig. 8 that the mean crystal width $\bar{w}$ increases with decreasing $T_a$.

In fact, in the growth conditions of glaze and hard rime used in the present series of experiments, it is the air temperature $T_a$ or the supercooling of impact droplets which is the main factor influencing the crystal dimensions, the influence of all other parameters is less important, and shows only secondary effects. On the other hand, for the four values of temperature used, the mean crystal width $\bar{w}$ increases rapidly with the radial distance in the first mm of ice accretion. The rate of increase is less for greater radial distances and $\bar{w}$ approaches a constant value for a radial distance equal or larger than 6 mm. The grain texture of glaze and hard rime grown in a tunnel may be compared to that of columnar grain ice commonly found in an ice cover of fresh water (lake). Meanwhile, atmospheric ice contains a greater number of air bubbles of different sizes and therefore its density may be considerably lower than 0.916. Atmospheric ice also shows smaller values of crystal width. For example, crystal widths of atmospheric ice range between 0.1 and 1.5 mm, while that of an ice cover of fresh water is between 2.5 and over 25 mm. These differences are mainly attributable to the faster freezing rate observed with ice accreted from droplets than the rate prevailing usually with bulk ice.

## DISCUSSION

As previously mentioned, the adhesive strength of atmospheric ice may be expected to depend largely upon the mechanical strength of the layer of ice near the conductor surface. On the other hand, it is also known that the mechanical strength of ice is influenced by the conditions of loading, the ambient temperature and the internal structure of ice, particularly its porosity and crystal structure. Fig. 9 presents a plot of adhesive strength of all glaze and rime samples obtained in present series of experiments, as a function of the mean density of ice accretion. In this figure, it may be noted that the experimental points corresponding to the four temperatures used in this work can be represented tentatively by a series of straight lines, which correspond to the decreasing pattern of adhesive strength with density. There is some scattering within the experimental points but the scattering observed at -2°C and -6°C is smaller than that seen at -10°C and -15°C. This is due to the relatively small number of tests performed at these low temperatures as mentioned above. The decrease of adhesion with density can be explained by the presence of air bubbles in ice, i.e. its porosity. On this aspect, atmospheric ice appears to behave as bulk ice whose strength is known to be considerably reduced by the presence of air bubbles. Brine pockets, like those observed in sea ice also show comparable effects. The reduction coefficient of strength for fresh water ice takes the form $(1-e/0.285)^{-\frac{1}{2}}$ due to the porosity effect as proposed by Michel,[13] while that suggested by Weeks and Assur[17] for sea ice is $1-(e/0.25)^{-\frac{1}{2}}$. It is not possible from the results obtained to precise which of both coefficients would be the best applied for atmospheric ice. This is partly due to the relatively small number of points corresponding to ice of density lower than 0.8. Therefore more experiments are needed to cover the whole range of densities before a better evaluation of the dependence of adhesive strength upon porosity can be made.

In addition to the porosity effect, Fig. 9 implies also the influence of grain dimensions upon the adhesive strength of atmospheric ice. In fact, it is the temperature prevailing during the formation of the glaze and rime samples which largely determines the width of crystals in the boundary layer and inside the bulk deposit. For example, mean crystal width of glaze and hard rime samples measured at 6 mm above the conductor surface decreases from 1-1.5 mm to 0.2-0.3 mm when the temperature of the accretion test is lowered from -2°C to -15°C. Mean crystal widths in the boundary layer are on average two times smaller than that measured at 6 mm above the surface conductor.

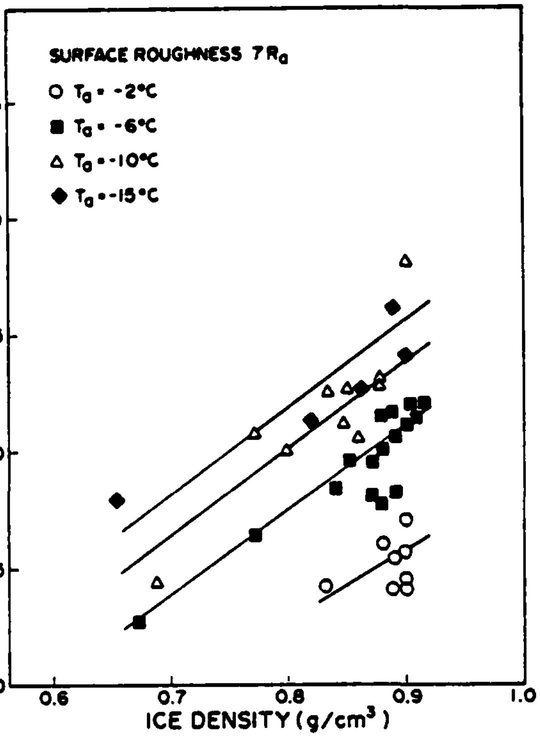

FIG. 9 ADHESIVE STRENGTH OF ICE VERSUS DENSITY AND AIR TEMPERATURE FOR ALL ACCRETION TESTS PERFORMED IN THE PRESENT SET OF THE EXPERIMENTS

The dependence of mechanical strength of ice on grain size is much more complicated than the dependence on porosity previously discussed. As the adhesive test performed in the present work is essentially a shear test at a rate of deformation of $10^{-2}$ $s^{-1}$, it may be assumed that the break at the interface (cohesive rupture is not considered in this work) is characteristic of the brittle mode of rupture. In fact, the mode of rupture in tensile or shear tests is brittle when the deformation rate exceeds $10^{-4}$ $s^{-1}$. For this mode of rupture the fracture strength of cold box ice samples increases mainly with decreasing grain size and to a lesser degree with increasing ambient temperature during the test. For columnar ice like that of fresh water ice, the grain diameter used is the smallest dimension of crystals in the ice samples. In the present work, this corresponds to the mean width in the boundary layer of ice near the conductor surface. The mechanical strength of cold box ice increases with decreasing crystal size $\bar{w}$ and the increase coefficient takes on the form $(\bar{w})^{-\frac{1}{2}}$. For example, for the observed variations of mean crystal widths changing on the whole from 0,1 to 1 mm in the temperature interval of -2 and -15°C, the increase coefficient can be evaluated to about $(1mm/0.1mm)^{-\frac{1}{2}}=3.2$. This means that the adhesive strength at -15°C would take on a value near 3.2 times that measured at -2°C. The actual ratio giving $1.7/0.5=3.4$ agrees within experimental accuracy to the ratio of 3.2 expected from the grain dimension effect. Meanwhile, before a firm conclusion may be drawn, additional work is needed. Even if it appears difficult to perform tensile tests with atmospheric ice due to the limited thickness of its deposits, it may be possible to verify the dependence of the adhesive strength on crystal size from compressive measurements.

## CONCLUSION

From the results obtained with glaze and hard rime samples adhering on metallic conductors, the following conclusions can be drawn:

1. The dependence of adhesion of atmospheric ice upon meteorological parameters can be reduced to two fundamental factors pertaining to its internal structure, i.e. porosity and crystal size.

2. If the lower density and smaller grain size of atmospheric ice is taken into account these dependences appear to be similar to those observed with box ice in comparable conditions of deformation.

## ACKNOWLEDGMENTS

The work reported here was supported by Hydro-Quebec and the Foundation of University of Quebec at Chicoutimi. The authors are indebted to Mr. L. Lemieux for the draft work and to Mr. D. Du Nguyen for growing ice accretions and numerous meticulous measurements.

## REFERENCES

1. Eskin, S.G., Fontaine, W.E. and Witzell, O.W., 1957. Strength characteristics of ice. Refrigerating Engineering, December, 33-38.
2. Raraty, L.E., Tabor, D., 1958. The adhesion and strength properties of ice. Proc. Roy. Soc. A 245, 184-201.
3. Jellinek, H.H.G., 1962. Ice adhesion. Canadian Journal of Physics, 40, 1294-1309.
4. Bascom, W.D., Cottington, R.L. and Singleterry, C.R., 1969, J. Adhesion, 1, 246-263.
5. Jones, J.R. and Gardos, M.N., 1972. Adhesive shear strength of ice to bonded solid lubrifiants. Lubrification Engineerings, 28, 464-471.
6. Landy, M., and Freiberger, A., 1967. Studies of ice adhesion 1, Adhesion of ice to plastics. Journal of Colloid and Interface Science, 256, 544-551.
7. Stallabrass, J.R. and Price, R.D., 1963. On the adhesion of ice to various materials. Can. Aero. and Space J., 9, 199-204.
8. Merkle, E.L., 1968. Icing tunnel tests of icephobic coatings. Proc. 8th Nat. Conf. on environmental effects of aircraft and propulsion systems, pp. 25-31.
9. Millar, D.M., 1970. Investigation of ice accretion characteristics of hydrophobics materials. Federal Aeration Administration. Rep. FAA-DS-70-11, p. 12.
10. Phan, C.L., McComber, P. and Mansiaux, A., 1976. Adhesion of rime and glaze on conductors protected by various materials. Trans. CSME, 4, 204-208.
11. Druez, J., Phan, C.L., Laforte, J.L. and Nguyen, D.D. 1978-1979. The adhesion of glaze and rime on aluminium electrical conductors. Trans. CSME, 5, 215-220.
12. Gold, L.W., 1970. Process of failure in ice. Canadian Geotechnical Journal, 7, 405-413.
13. Michel, B., 1978. The strength of polycrystalline ice. Can. Journ. of Civil Eng., 5, 285-300.
14. Godard, S., 1960. Mesure des gouttelettes de nuage avec un film de collargol. Bull. Obser. du Puy-de-Dôme, 2, 41-46.
15. Grimard, Y., 1981. Contribution à l'étude de la vulnérabilité des eaux lacustes québécoises face à l'acidité des précipitations. Service de la qualité des eaux, Ministère de l'Environnement, Québec, 38 p.
16. Rush, C.K. and Wardlaw, R.L., 1957. Icing measurements with a single rotating cylinder. N.A.E.C. Res. Rep., paper no. LR-206.
17. Weeks, W.F. and Assur, A., 1967. The mechanical properties of sea ice. USA CRREL Monograph II-C3.

## DISCUSSION

Olsen: I didn't quite understand how you are accreting the ice. Are you measuring your adhesive strength while the cloud is on - while it's accreting or, in fact, did you stop?

Laforte: We may prepare from the accretion test - after the accretion test is completed, and that lasts 30 minutes to 1 hour depending on conditions. We cut out the center portion of the ice accretion, a portion 3 cm long. We cut the ice with great care and put the cut piece firmly on the carriage. We apply a push on the ice center until the removal of the accretion [...] trend is the maximum force measured divided by the area of the press which is in contact with the accretion. We don't take account of the irregularity of the surface, we take the calculated surface [...]

Ackley: How thick were the samples and what was the range of crystal sizes that you saw?

Laforte: The thickness of our samples varied from 10-20 millimeters. The length of ice crystal varied over the length of crystals, so we have compared the mean width to the length, because the length was not practical to use. The variation of the range of mean crystal width was from 0.1-1.5 millimeters. Compared to grain, the width of ice crystal of Colbeck's fresh water ice is very smaller. Fresh water ice has a mean width of 2.5-25 millimeters with the length of about 2-4 times, depending on temperature.

AD P001677

# HOW EFFECTIVE ARE ICEPHOBIC COATINGS?

L.D. Minsk U.S. Army Cold Regions Research and Engineering Laboratory,
Hanover, New Hampshire 03755

## ABSTRACT

Much effort over many years has gone into the search for an effective, durable, easily applied and inexpensive material to eliminate the force of adhesion between ice and a substrate. The objective of zero ice adhesion on an unheated surface which would either prevent the formation of ice or ensure self-shedding of very thin accretions has not yet been achieved. Many commercially-available coatings do succeed in reducing the force of adhesion below 15 psi (103.4 kPa) and survive at least five freeze-release cycles, two arbitrarily established criteria. Exposure to rain erosion, however, increases the force of adhesion beyond this value for most materials. As part of a continuing project at CRREL, a test procedure for measuring the shear strength of ice at failure has been developed and a large number of candidate materials have been tested.

## INTRODUCTION

The principal objective of CRREL's ice adhesion research program is the protection of helicopter rotor blades from accreting ice sufficient to reduce lift beyond a safe level or to result in asymmetric shedding with the consequent probability of high, destructive vibrational forces. Though heated surfaces have been developed as a method of controlling ice accretion (Werner 1975), the weight penalty associated with this approach has spurred the search for a passive coating which will exhibit low adhesion to ice and which will survive surface erosion from impact of raindrops. Rain erosion tests have been carried out on specimens mounted in the rain erosion simulator at the US Air Force Materials Laboratory in Dayton, Ohio. Though the conditions of the test - 10 min. exposure to rain falling at the rate of 1 in./hr. and a velocity of 500 mph - are more extreme than those which surface structures can be expected to experience, they have stimulated the development of coatings which may have an interfacial shear stress of 15 psi (103 kPa) after rain erosion. This value is based on the mean of surface shear forces resulting from centrifugal and viscous drag forces acting on the ice accreting on a rotating blade.

## DESCRIPTION OF TEST

Apparatus. A number of laboratories have conducted tests to determine the strength of adhesion of ice to various surfaces. These tests generally apply a shear force to ice specimens frozen onto the test surface within a mold. Unless the specimen mold is constrained to move parallel to the test surface, tensile forces can develop that prevent a pure shear failure, affecting reproducibility of the test and contributing to wide scattering of the data. To ensure pure shear failure, a unique device developed at CRREL by Larry Gould of the Technical Services Division was used in the work reported here. It consists of a Lexan mold mounted on the underside of a plate attached to the

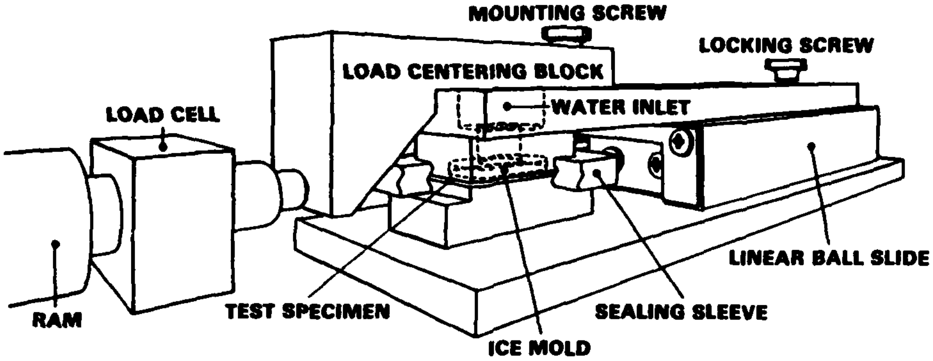

Shear test apparatus.

upper surface of a linear ball slide (Yankee ball slide model Y3-30, Design Components, Medfield, Massachusetts 02052). The mold is positioned directly above the 2-in.$^2$ (12.9-cm$^2$) test specimen, and separated from it by a gap of about 0.08 in. (2 mm) (see figure). The force applied to a load block along the ice/substrate interface is measured by a load cell (Interface SM-250 or SM-50) whose output is fed to a strip chart recorder.

Test specimen. The aluminum test block is dimensioned to meet the requirements for mounting on the whirling arm of the Air Force Materials Laboratory rain erosion simulator (Hurley and Schmitt 1970). Block dimensions are 2.44 in. (6.18 cm) base length, 1 in. (2.54 cm) width, and a test surface area of 2 in.$^2$ (12.9 cm$^2$). A hollow is milled in the base to reduce mass. The test surface is machine-finished with an end mill, and a uniform reproducible surface is obtained by sandblasting with an S.S. White Industrial Abrasive Unit Model C, using 50-μm aluminum oxide abrasive powder (White No. 3). The Lexan mold is milled to leave a 2-mm (0.08-in.) lip around the periphery, and a hole is provided in the upper surface for addition of water.

Sample preparation. The freshly abraded surface of an aluminum specimen is washed with detergent to remove the fine abrasive powder, wiped dry, and then wiped with toluene immediately prior to application of the test coating. Application can be accomplished by spray, wipe, or brush methods, depending on the form of the material; coatings too viscous for spraying are applied by brush in these tests. All specimens with the test coatings are placed in a dust-free enclosure until removed to the coldroom for mounting on the shear test apparatus.

Test procedure. The aluminum specimen block is mounted on the base plate of the shear test apparatus with two machine screws; the Lexan mold is also mounted on the top (sliding) plate with two machne screws. The mold is positioned directly above the specimen, and a silicone rubber gasket (pre-positioned on the mold) is slid over the opening between the two parts to prevent water leakage. The slider is locked with a set screw and the entire apparatus is allowed to stabilize at coldroom temperature (-10°C for all tests reported here). Following this, deaired, distilled water at room temperature is poured through the hole in both the top plate and the Lexan mold, and the apparatus is then tilted slightly in a rolling motion to dislodge any air trapped in the 1- to 2-mm gap between the specimen and the mold. Sufficient water is added to ensure complete coverage of the test surface, and, if necessary, additional water is added to bring th ice level to the top of the mold. Generally, specimens were prepared in the afternoon and tested the following morning. The frozen specimen in its slide support is carefully placed on the indexing pins of the shear test apparatus, a fixture mounted on the top plate to permit load application in line with the ice/substrate interface, and a hydraulic cylinder is actuated to drive the load cell against the slider. Output is read on a strip chart recorder. Cylinder travel speed is controlled by a flow-control valve (Sperry Vickers Model FCG) and is adjusted for a speed of 0.1 in./s (0.25 cm/s).

| Material | Fresh Surface | Rain Eroded |
|---|---|---|
| Silicone rubber | Excellent | Poor |
| Silicone grease | Excellent | Poor |
| Silcone compounds | Excellent | Poor to good |
| Teflon (sheet) | Good | Poor |
| Teflon (dispersion) | Poor | Poor |
| Polyimide | Poor | - |
| Urethane | Poor | Poor |
| Acrylic | Poor | - |
| Nylon | Poor | - |

Ratings (based on shear strength at release, psi):
Excellent, 5; Good 5-15; Poor, >15.

Rain erosion. Specimens in most tests were exposed for 10 minutes at a speed of 500 mph (805 km/hr) to rainfall at a rate of 1 in./hr (2.54 cm/hr), with a median droplet size of 1.8 mm (0.071 in.). Most coatings failed this severe condition.

## EXPERIMENTAL RESULTS

A minimum of two replicates of each test surface were run for both the pristine coating and for those that were selected for the rain erosion test. This small number does not permit any valid statistical measures of dispersion, but are justified on the grounds that a large number of candidate coatings needed to be screened. In many cases ice did not break cleanly from the test surface: these exhibited cohesional failure with a portion of the ice remaining on the surface.

Ice has a low strength of adhesion on many materials not subjected to rain erosion. Most of the satisfactory rain-eroded surfaces are silicone-based materials. The above table indicates the general classes of materials tested and their category of ice release strength at failure.

## LITERATURE CITED

Hurley, C.J. and G.F. Schmitt, Jr. (1970) Development and calibration of a Mach 1.2 rain erosion test apparatus. Technical Report AFML-TR-70-240, Air Force Materials Laboratory, Air Force Systems Command, Wright-Patterson Air Force Base, Ohio.

Werner, J.B. (1975) The development of an advanced anti-wing/deicing capability for US Army helicopters. Vol. II. Ice protection system application to the UH-1H helicopter. USAAMRDL-TR-75-34B. Eustis Directorate, US Army Air Mobility Research and Development Laboratory, Fort Eustis, Virginia. AD A019049.

AD P001678

# ABHESION OF ICE FROM HELICOPTER ROTOR BLADES
## Preliminary Work

H.H. G. Jellinek Department of Chemistry, Clarkson College of Technology,
I. Chodak Potsdam, New York 13676

Ice is one of the best adhesives in nature. Many of the general fundamental principles of surface science are applicable to ice but are often completely masked by other parameters such as rheological ones, porosity etc. A difficulty in this field is that often suitable coatings for ice abhesion can be found. However, after one or two abhesions they have disappeared or have become contaminated. For helicopter rotors, the coatings have also to be rain-resistant in addition to having excellent ice abhesion properties. It is not sufficient just to have a very hydrophobic coating; such coating must also have the proper rheological properties.

During a previous investigation where ice releasing coatings for lock walls were required, we found that one of the block-copolymers (LR5630) of Bis(-A-polycarbonate)polydimethyl-siloxane was superior to all the other co-polymers of this series. It had a polycarbonate content of 35%. Siloxane and carbonate chain lengths of 20 and 3 respectively and a glass-temperature $T_g$ of -60°C. Silicone oil (10% w/w of polymer) was added. This coating reduced the adhesive strength by 99.7% and lasted longer than one year.

## EXPERIMENTAL

The technique for this work was based on measuring the adhesive force at the moment when an ice coating came off the substrate due to centrifugal force.

### Apparatus

A double-walled cold box was constructed (1.0x1.0x0.8m; two walls of plywood filled with urethane foam, total wall thickness 5 cm, 3 thermopane windows). So far all experiments have been carried out at -10 ±0.6°C.

Shear forces were applied with a centrifuge (International Equipment Corp., Model HN-S), length of arm of the axle 0.13 m, max. speed ca. 2000 rpm. This centrifuge was placed in the middle of the box, a light beam was directed onto the ice-covered part. The beam was reflected into a photocell (NSL 3162) causing a signal on an oscilloscope screen (Tetronix, Model T921). Actually, there were two signals during one rotation as two specimens have to be used for balancing (Fig. 1a, b). The distance of the signals on the oscilloscope screen gives the time of one-half of a rotation. As soon as the ice is sheared off, the shape of the signal changes.

### Technique

Ice and polymer application. A schematic drawing of the Al-rotor section specimen (A), which we prepared, is shown in Figure 2. Its dimensions are on the average $a = 0.87$ cm, $\ell = 4.1$ cm (weight = 17.4 g). The specimen has a screw-thread where the connector to the centrifuge can be fixed (Fig. 3). The distance of the polymer coat/ice interface from the centrifuge axle is on the average 0.14 m.

The Al-surfaces of rotor specimens were thoroughly cleaned with "Alconox" (14 h), rinsed with tap water (1.5 h) with distilled water (0.5 h) and finally dried in an oven at 120°C for about 20 minutes. A soft camel hair brush was dipped into a

10% wt/vol. solution of the polymer in methylenedichloride; the brush was squeezed while immersed in the solution for removal of air bubbles. Usually several coats were applied to the Al-surface (coat thickness ranged from 25-40μ). The coats were dried in vacuum at 50°C.

The ice layer was applied as follows. A small container of Al-foil (ca. 0.3 mm thick foil, see Fig. 4) closed on both ends with PVC-foil, was filled with boiled-out distilled water. This was first cooled down to just below 0°C. The cooled rotor specimen (just above 0°C) was then inserted into the ice to the desired depth. The ice melted during this procedure (Fig. 5) but froze to the Al-surface soon afterwards. The whole assembly plus the Al-foil was fixed to the centrifuge. The weight of the Al-foil was so small that abhesion invariably took place at the Al/ice (blank) or coating/ice interface. For blank experiments a relatively large mass of ice had to be applied because of the appreciable adhesive strength. Its shape is shown in Figure 7 ($m = 2$ g, $A = 0.2$ cm$^2$); for abhesion from polymer coats less ice is needed ($m = 1.2$ g; $A = 0.7$ cm$^2$).

Numerical evaluation of test results. The centrifugal shearing force $F_C$ at the ice/polymer interface is at a maximum (see Fig. 8). All the forces beyond this layer up to the outer layer are smaller. The break should therefore be an adhesive one unless there are appreciable defects in the ice. The centrifugal shearing force in the interface is,

$$F_C = m_i \gamma = m_i r \omega^2 = \frac{m_i v^2}{r} \text{ Dyn}$$

$$v = \frac{\text{rpm} 2\pi r}{60} \text{ ms}^{-1}$$

Hence,

$$F_C = m_i \left(\frac{\text{rpm} 2\pi}{60}\right)^2 r \text{ kg} \qquad (1)$$

r ∿ distance of interface from axle (m), $m_i$ ∿ weight of ice plus Al-foil (kg); rpm ∿ revolutions per minute; $\gamma$ ∿ radial acceleration; $\omega$ ∿ angular velocity; v ∿ linear velocity (ms$^{-1}$). The rpm at the moment when the ice is sheared off is obtained from the oscilloscope-signal. The length of the arm to the interface is usually $r = 0.14$ m, $m_i$ is obtained by weighing (on the average $m_i \sim 1.2$ g).

The adhesive strength $F'_C = F_C/A$ (A is the interfacial area in m$^2$, i.e. of the curved area) is obtained as follows: the best fit to the contour of the specimen is a circle r' (a parabola does not fit as well, see Fig. 8). Hence,

$$ABC = 2r' \frac{\alpha}{180} m_i$$

and

$$\alpha = \alpha_1 + \alpha_2 = \cos^{-1} \frac{r' - a_1}{r'^2} + \cos^{-1} \frac{r' - a_2}{r'^2} .$$

The area is given by

$$A = \pi r' \frac{\alpha}{180} \cdot \ell \, (\text{m}^2)$$

$\ell$ ∿ length of ice-coat in meters. Finally,

$$F'_C = m_i \left(\frac{\text{rpm}}{60}\right) 4\pi \frac{180 r}{2r' \ell} \quad (\text{kg/cm}^2)$$

or if $n = 2\text{rpm}/60$, then

$$F'_C = \frac{m_i n^2 \pi 180 r}{\alpha 10^4 r \cdot \ell} \quad (\text{kg/cm}^2). \qquad (2)$$

### Results

Blank tests. There were very few mixed breaks. The average values of the adhesive breaks are given below. The arithmetic mean of all tests for the adhesive strengths for the blank test was found to be

$$F' = 4.90 \pm 1.22 \text{ kg/cm}^2$$

(standard deviation)

Polymer coatings. A large number of abhesion experiments was carried out with a polymer of the series which was not the most efficient one in this respect for perfecting the technique (LR3320: siloxane 43%, carbonate 57%, chain lengths: siloxane-carbonate 10-4, $T_F$-20°C). The results for this polymer will not be given here except for one series of experiments.

Abhesion results. -10°C.

1) LR3320,[1)] brush, squeezed out, dried in vacuo at 50°C, 4 h.

Mean (7 experiments)

$$F'_C = 0.31 \pm 0.14 \text{ kg/cm}^2$$

2) LR5630, brush squeezed out plus 10% by wt of polymer of Si-oil, dried in vacuo at 50°C, 4 h.

All were adhesive breaks.

Exp. - Nos. 6 and 7 (Table I) do not fit at all into this series and have been omitted for calculating the mean value.

Table I. Abhesion from Al-rotor specimens.
LR5630 coats, -10°C.

| Experiment no. | Al-rotor specimen no. | Length ($\ell$) of ice layer (cm) | Mass of ice (g) | Area of ice (cm$^2$) | Speed (rpm) | $F'_C$ (kg/cm$^2$) |
|---|---|---|---|---|---|---|
| 1 | 1 | 1.60 | 0.821 | 1.12 | 652 | 0.087 |
| 2 | 2 | 1.55 | 0.534 | 1.25 | 500 | 0.089 |
| 3 | 3 | 1.57 | 0.859 | 1.11 | 405 | 0.032 |
| 4 | 4 | 2.00 | 1.43 | 1.31 | 588 | 0.048 |
| 5 | 1 | 1.95 | 0.965 | 0.94 | 550 | 0.045 |
| 6 | 3 | 1.87 | 1.16 | 1.08 | 124 | 0.22 |
| 7 | 4 | 1.84 | 1.10 | 0.82 | 208 | 0.49 |
| 8 | 1 | 1.82 | 0.481 | 0.98 | 578 | 0.05 |

Mean (6 experiments)

$F'_C = 0.06 \pm 0.02$ kg/cm$^2$

FIGURE 1

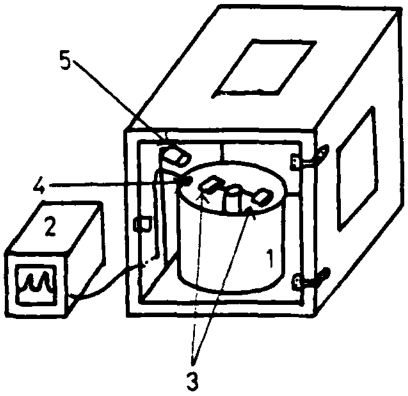

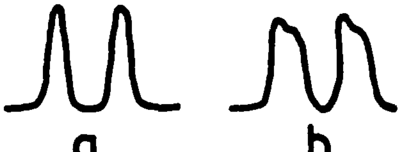

FIGURE 2

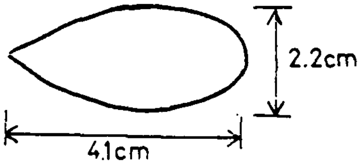

FIGURE 3

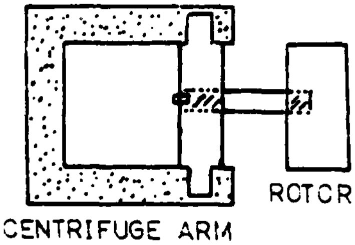

FIGURE 4

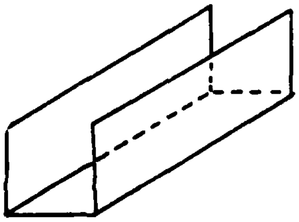

FIGURE 5

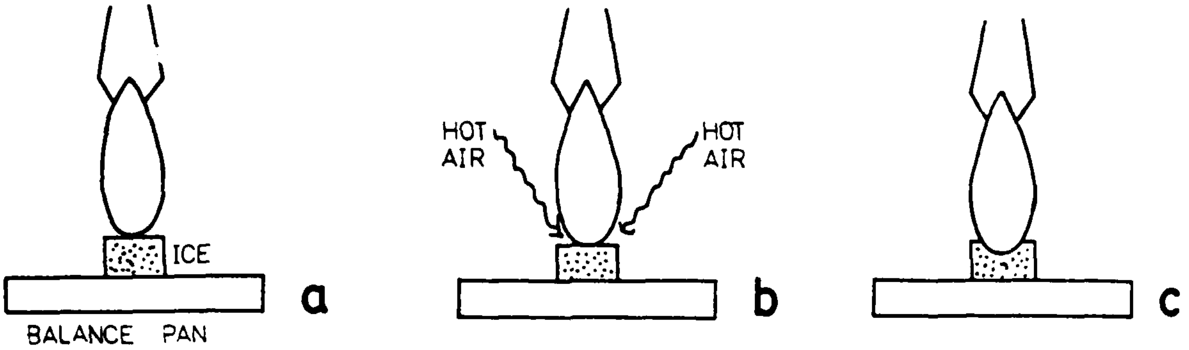

FIGURE 6

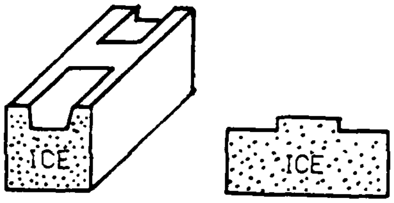

FIGURE 7

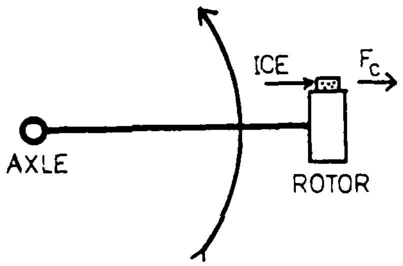

FIGURE 8

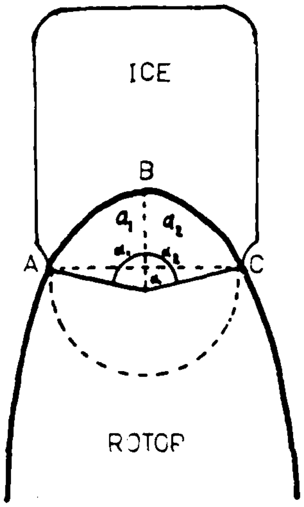

FIGURE 9

DISCUSSION

Question: (unintelligible)

Jellinek: No, I said the critical surface tension of a layer of methyl groups like this. You have a monolayer of methyl groups. It's about 80 dynes/cm. If you have fluorine groups, this goes down to six. That's the lowest you ever get so far.

Question: (unintelligible)

Jellinek: Teflon is no good for ice abhesion because of its pores and there's mechanical interaction. It's very easily contaminated. Everybody says, try Teflon first - it never works.

Question: (unintelligible)

Jellinek: You can't. The lowest is $CF_3$. If you have, instead of $CH_3$, $CF_3$ groups, for instance perfluoric acid, then you can go down to 6 dynes/centimeter. But that's the lowest which has been observed so far. That would be the best - if you can produce that. But probably you don't need to go that low an extreme. You can probably get away with three and three. For instance, if you put this coating on an air wing, and you put it in a wind tunnel, you get snow sticking to it. It's not enough to decrease the adhesion; you have to do something else. What else, we have to find out. If it's a higher velocity in a wind tunnel - we have tried it at NASA, and they tried it, I don't known how well they cleaned the coating, but they told me they get quite a thick snow layer on it, a sticky one. Of course, that can be pushed up, not so easily, but it can be pushed up but it's not sufficient to have this if you have any wind or any force against the substrate. Then it starts sticking, and it was found with the radar disks you have to heat it a little bit to get it off, but very little.

Nauman: Do you have any reason to suspect this might be effective in spray icing?

Jellinek: In what?

Nauman: For decreasing spray icing - superstructure icing on ships.

Jellinek: Yes.

Nauman: You do feel that there is some promise?

Jellinek: Yes, definitely. The ice will stick when there is very little force ...

Lozowski: I hope you don't think this is an impertinent question, but while we're on the subject of icephobic coatings, I was wondering if you or anyone else here could give me some idea of how birds manage to keep from icing up?

Jellinek: Birds? Well, the feathers are in a certain structure, you see, which decreases the ice accretion. I can't explain exactly what the geometrical structure of the feathers is so that you don't have any icing. You can imitate it to a certain extent with layers of feathers, and you can work it out theoretically. It's quite a different effect than these coatings.

Minsk: Birds are grounded under the conditions that the Army hopes to fly helicopters.

Thowless: To follow the previous question, I've often wondered why polar bears coming out of the Arctic water in subfreezing temperatures don't accrete ice?

Jellinek: I suppose the water doesn't penetrate the fur; it's greasy. I can't answer why there is no ice on it.

Thowless: I've been told that one cannot detect a polar bear with infrared - the insulation of their fur is that good.

AD P001679

# AIRCRAFT ICING RESEARCH AT NASA

J. J. Reinmann NASA Lewis Research Center, Cleveland, Ohio 44135
R. J. Shaw NASA Lewis Research Center, Cleveland, Ohio 44135
W. A. Olsen, Jr. NASA Lewis Research Center, Cleveland, Ohio 44135

## ABSTRACT

NASA is again actively involved in aircraft icing research. This paper briefly describes the new research activity in: ice protection systems, icing instrumentation, experimental methods, analytical modeling for the above, and in flight research. The renewed interest in aircraft icing has come about because of the new need for All-Weather Helicopters and General Aviation aircraft. Because of increased fuel costs, tomorrow's Commercial Transport aircraft will also require new types of ice protection systems and better estimates of the aeropenalties caused by ice on unprotected surfaces.

The physics of aircraft icing is very similar to the icing that occurs on ground structures and structures at sea; all involve droplets that freeze on the surfaces because of the cold air. Therefore all icing research groups will benefit greatly by sharing their research information.

## INTRODUCTION

If an aircraft is to fly safely through icing clouds, it requires protection on those surfaces that suffer unacceptable aerodegradation from ice accretion. During the 1940's and 1950's, both the NACA and industry helped solve the icing problems for those aircraft that flew IFR (instrument flight rules), which included mainly the commercial and military transports, a few general aviation aircraft, but no helicopters (Refs. 1 and 2).

Today, due to technological advances in avionics and flight controls, nearly all general aviation aircraft and helicopters can be equipped to fly IFR. Yet only a few military helicopters have icing clearances, and no civil helicopter has yet been certified by the FAA for flight into forecasted icing. Many of today's general aviation aircraft are certified for icing, but they rely on ice protection technology that is over 20 years old. The relatively small payload fraction and low power margins of these smaller aircraft mean that their ice protection systems must be light in weight and low in power consumption. Since small objects accrete ice faster than large objects, all the deleterious effects of icing happen faster and are more serious on an unprotected small aircraft: drag rise, torque rise, power loss, lift deterioration, stall angle decrease, and stall speed increase.

Because of high fuel costs, today's large commercial transports need lighter and more efficient ice protection systems. Tomorrow's aircraft will need alternatives to the hot-air ice protection system because bleed air will be scarce on the more efficient high-by-pass-ratio engines or high speed turboprop engines.

Thus, the helicopter, general aviation, light transport, and commercial transport aircraft now share common icing requirements: highly effective, lightweight, low-power-consuming deicing systems, and detailed knowledge of the aeropenalties due to ice on aircraft surfaces.

NASA has organized a new aircraft icing resarch program at the Lewis Research Center to help solve the icing problems for modern aircraft. This new program is concentrating on (1) new ice protection systems, (2) new icing instrumentation, (3) improved icing test facilities and testing techniques (especially for helicopters), and (4) widespread use of large high speed computers to lower development and certification time and cost. Our long-range plan is based on recommendations made in several studies of the icing needs for modern aircraft (Refs. 3 to 7). This report gives an overview of NASA's current efforts in this new icing research program.

## NASA AIRCRAFT ICING PROGRAM

Figure 1 shows on the left the main elements of NASA's current aircraft icing research program, and on the right the detailed efforts included in each element. We shall briefly describe the research efforts in each element.

### Ice Protection Systems

Pneumatic Deicers for Helicopters. Currently, helicopter rotor blades use electrothermal deicers. An alternative is the pneumatic boot deicer which offers the potential of lower weight, lower power consumption, simpler operating controls, and lower costs. In a joint research program, NASA Lewis and B. F. Goodrich Co. developed pneumatic deicer boots for UH-1H helicopter rotor blades (Ref. 8). The best deicer boots developed in the IRT (Lewis Icing Research Tunnel) tests (Fig. 2) were installed on a U.S. Army UH-1H helicopter at the U.S. Army Aviation Engineering Flight Activity at Edwards AFB, California. These boots will be tested on the UH-1H in icing next year under a joint program between the Army, NASA Ames, and B. F. Goodrich Co.

Electrothermal Deicers. Lewis is developing one- and two-dimensional transient heat conduction codes to analyze electrothermal deicer systems (Ref. 9). To obtain validation data for the codes, B. F. Goodrich Co. will install an electrothermal heater blanket on a UH-1H rotor blade section, and Lewis will instrument it with over 50 thermocouples between the various layers of the heater blanket. The UH-1H blade section will be tested on an oscillating blade rig in the IRT. These tests and the heat conduction codes may help determine proper heater power levels and on/off times as a function of outside air temperature and cloud liquid water content.

Glycol Fluid Systems. There is considerable interest in freezing-point-depressant systems. The University of Kansas, under a grant from Lewis, has tested (Ref. 10) the glycol system on two modern general aviation airfoils in the IRT (Fig. 3). The systems used the modern fluid distributor made of stainless steel mesh by TKS, Ltd., of Great Britain. We have also tested a fluid distributor made of a porous composite material that offers the potential advantages of lighter weight and lower costs than the stainless steel mesh. Further development of the composite distributor is needed before it can replace the stainless steel distributor. Another application for the leading edge fluid distributor is to keep bugs off laminar flow wings. In a joint program between NASA Langley and Lewis, a fluid distributor will be installed on a laminar flow wing and tested for bug and ice protection. Lewis is using all test data on the glycol system to develop a data base and design procedure for the modern porous leading edge fluid distributors, which are more efficient than the distributors tested in the 1940's and 1950's.

Electromagnetic Impulse Deicers. The electromagnetic impulse system offers potential savings in power over the conventional anti-icing systems (Ref. 6). The heart of this system consists of a flat spirally wound coil of copper wire (about number 10 gauge) mounted on a 2- to 3-in.-diameter disk made of an electrical insulator and installed inside the leading edge of the airfoil. The magnetic field of the coil induces eddy currents in the airfoil skin, causing it to deflect rapidly.

An electromagnetic impulse deicer system for commercial transports was recently tested in the IRT in a joint

Lewis/industry program. Data from that test are being analyzed. Lewis also has a new effort to develop the impulse system for general aviation aircraft and to test it in the IRT. This involves a grant to Wichita State University who will work with Beech Aircraft and Cessna Aircraft.

Icephobics. Icephobics is the generic name given to any material that, when applied to a surface, reduces the adhesive bond between the ice and the surface. Besides reducing the adhesive bond of ice, an icephobic suitable for aircraft also must resist erosion by rain and sand, must not be carried away with the shed ice, and must withstand exposure to weather including the sun's heat and ultraviolet rays.

As part of a joint program between NASA, the Air Force, and the Army, several icephobic coatings were tested in the IRT with the interfacial shear rig shown in Figure 4. However, no coating met all of the above criteria. Lewis currently has a grant with Clarkson College of Technology to develop an icephobic coating. Dr. H. Jellinek, the principal investigator for this grant, successfully developed an icephobic coating for the St. Lawrence Seaway locks while he was working for the Army Cold Regions Research and Engineering Laboratory.

A special need exists for designing experiments to measure ice adhesion and the various structural properties of ice while the IRT cloud is operating and at proper airspeed. While droplets are striking the test object and freezing, they release their heat of fusion which sometimes can result in a mushy water-ice mixture. The properties of this mixture could differ markedly from the ice that results after shutting off the spray cloud and lowering the airspeed, causing the mushy ice to freeze. This procedure could even induce stresses in the ice. These properties are needed in order to better understand and design mechanical ice removal systems such as pneumatic deicers and impulse deicers.

### Icing Instrumentation

Cloud Instrument Evaluation. In a joint program between Lewis and the Air Force Flight Test Center (Edwards AFB, Calif.) a number of modern and old style icing cloud instruments were compared in the IRT spray cloud to determine their relative accuracy and their limitations over a broad range of conditions. The instruments tested were primarily those used to determine drop size and liquid water content (LWC). All instruments were installed and checked out by the user (owner) or the manufacturer of the instrument to insure that it was operating properly. The IRT spray cloud proved to be adequately repeatable and spatially uniform for the needs of the program.

LWC Instruments. The LWC indicated by all of the instruments tested were compared with the LWC set according to the standard IRT calibration. Figure 5 shows that all instruments agree with each other and the old IRT calibration within about ±20 percent; the laser spectrometers generally exhibit a larger scatter in their LWC indications. The data shown were taken at a very low temperature to avoid any thermal error that causes water run-off.

Drop Size Instruments. Eight ASSP (Axial Scattering Spectrometer Probe) and three FSSP (Forward Scattering Spectrometer Probe) laser spectrometers were compared in the IRT spray cloud. Data from six of these were obtained; the others failed for various reasons. The ASSP data showed a scatter of about ±4 μm over the range of 10 to 25 μm. The FSSP data were about 4 μm higher than the ASSP data. Figure 6 shows what a ±4-μm variation in droplet size caused in ice shape and drag on a NACA 0012 airfoil (21-in. chord). The ice shape changed significantly and the resulting drag coefficient changed by a factor of five.

Ice Detectors. Lewis has funded Ideal Research, Inc., (Ref. 11) to develop an instrument to detect ice on the surface of an aircraft component and to measure the ice thickness and growth rate. The MIAMI (Microwave Ice Accretion Measurement Instrument) consists of a resonant surface waveguide with related electronics and a microprocessor. The wave guide, which mounts flush with the surface, is 0.2 in. wide by 1.41 in. long by 0.393 in. deep. It has a resonant frequency of 6.27 GHz. As ice builds up, the resonant frequency of the waveguide shifts. A plot of the experimental resonant frequency shift versus ice thickness is shown and compared to an empirical curve fit in Figure 7. This curve-fit is programmed into the microprocessor to calculate ice thickness and ice growth rate.

Ideal Research, Inc., has demonstrated that the MIAMI works in principle. But further development is required to demonstrate that it can distinguish between water and ice, because under glaze icing conditions both water and ice are present on the surface. This problem seems to be solvable.

## Experimental Methods

Icing Research Tunnel. The Lewis Icing Research Tunnel (IRT) is the largest icing wind tunnel in North America (Fig. 8). The IRT has a 6-ft high by 9 ft wide by 20 ft long test section; a top airspeed of 300 mph; a refrigeration plant which produces total air temperatures down to -30° F and which provides for year-round operation; and 77 air atomizing water nozzles which produce a simulated icing cloud with liquid water contents from 0.5 to over 2 $g/m^3$. The IRT test section operates from sea level (at 0 mph) to 3000 ft altitude (at 300 mph). The IRT was built in 1944; today it is in continual use and constantly has a 2-year backlog of test requests. The IRT can test selected full-scale components such as airfoils and engine inlets, and it has even tested propellers and aircraft engines in the diffuser leg downstream of the main test section.

Airfoil Performance in Icing. There is a universal need for data on the aerodynamic degradation of two-dimensional airfoils in icing. From tests in the IRT during the 1940's and 1950's empirical formulas were developed (Ref. 12) that predicted lift and drag increments while accounting for chord and thickness of the airfoil, liquid water content and temperature of the cloud, airspeed, and duration of the icing encounter. We recently tested in the IRT two airfoils currently used on general aviation aircraft. One of these airfoils has a blunter leading edge that gives higher maximum lift coefficientss and "softer" stall characteristics than the older airfoils that were tested to obtain the empirical formulas. Figure 9 shows the drag predicted from the empirical formula versus the measured drag for the two airfoils over a wide range of icing conditions. The data for the modern airfoils fall within the rather wide spread of results for the older airfoils. The results of the high LWC tests, which were only done for the modern airfoils, show that the empirical formula seriously overestimates the drag. These results point up the need for better analytical methods for predicting airfoil performance in icing.

Testing with Artificial Ice. High speed computers are now available and must be used to model the ice accretion process and to analyze the complex flow around airfoils having irregular shaped ice caps and rough surfaces that can cause flow separation and reattachment. To determine what physics must be included in the aerodynamic flow model, the surface static pressures must be measured around the airfoil including the ice cap. These surface pressures are extremely difficult to measure under icing conditions, so we have replaced the actual ice on the leading edge with a wooden replica and obtained static pressures and drag data in the IRT without the icing cloud (Ref. 13). Drag results are shown in Figure 10 for both the real ice and the wood replica (roughness was simulated with grit) for both rime and glaze ice. The drag for the artificial ice agrees satisfactorily with the real ice. Fixed-wing aircraft are often flown with artificial ice in order to determine the aeropenalties due to ice. Artificial ice may some day be applied to helicopter rotor blades to determine aeropenalties.

Helicopter Test Rigs. As mentioned earlier, no civil helicopter is yet certified by the FAA for flight into forecasted icing. A key reason for this lag in technology is the lack of adequate icing test facilities for helicopters and their components. Flight testing in natural icing clouds is extremely expensive because experience indicates that it would take several years of winter flying in natural icing conditions to prove that the helicopter meets icing certification criteria, and even longer to get research type of icing data.

Two icing simulators exist for testing complete helicopters: the Icing Spray Rig, a ground test facility at Ottawa, Canada; and the HISS (Helicopter Icing Spray System), the U.S. Army's inflight icing simulator. The Ottawa Spray Rig tests helicopters in hover or low-speed transition. The HISS tests helicopters in forward flight. Both operate only in the short winter season and are subject to the whims of the weather.

The Lewis IRT has tested full-scale engine inlets for nearly all U.S. helicopters that fly IFR. What the helicopter industry lacks is an icing tunnel that can test main rotor blades under simulated flight conditions. In an attempt to see if the IRT can be useful in testing rotor blades, we are building two rotorcraft test rigs (Fig. 11): an oscillating blade rig and a rotating blade rig. The oscillating blade rig will simulate variations in pitch angle during foward flight, thereby giving more realistic ice shape data on full-scale rotor airfoil sections. Lift and drag data can be obtained for these iced-up rotor blades. This aerodynamic data may be useful in predicting performance degradation of helicopters without ice protection. The oscillating rotor blade in the IRT may also prove useful for initial testing of deicer systems even though the oscillating rig does not simulate centrifugal forces and the air speed is less than Mach 0.4 in the IRT.

The rotating blade test rig will be used to test an OH-58 tail rotor (about 5 ft in diameter). For the OH-58 blade, rotating blade test results will be compared with oscillating blade test results to determine the importance of centrifugal force and Mach number on ice shape. The main usefulness of the rotating blade rig will be to study the ice formations and to measure the aerodynamic degradation caused by the ice. Model rotors could also be tested in the IRT, but the icing scaling laws must be verified and nozzles that produce water droplet volume median diameters less than 10 µm are required. We are working toward these goals.

Lewis has been advocating that their now dormant Altitude Wind Tunnel (AWT) be rehabilitated into an icing research (or extreme weather) and propulsion win tunnel (Fig. 12). The new AWT would have two test sections: a 20-ft diameter section with speeds up to Mach 1 and a 45-ft diameter section with speeds up to 50 knots. The high speed section would test deicers on oscillating, full-scale rotor blades up to blade-tip Mach numbers; it would test helicopter inlets with simulated rotor downwash; and it would do complete rotor tests on typical scale model rotors. The low-speed section would test complete helicopters (with truncated blades), and it would have a rotor whirl rig for testing full-scale rotor blade deicer systems.

Icing Scaling Laws. All icing simulation facilities have limited capabilities in the velocity, size, altitude, droplet size, liquid water content, and temperature they can generally attain. As a consequence they cannot duplicate all of the conditions necessary to test an aircraft component flying through an icing cloud. To get around these facility limitations, icing scaling laws were derived in the 1950's (Ref. 14); however, these relationships have never been properly verified. Proper experimental verification is extremely difficult because of serious facility and icing instrument limitations.

In an attempt to verify the icing scaling laws, Lewis and AEDC (Arnold Air Development Center, Tullahoma, Tenn.) have entered into a joint Research program. The experimental verification uses the complementary capabilities of the large low speed Lewis IRT and the AEDC small high-speed free jet. Lewis is performing research on the energy balance, the heat transfer coefficients, and the catch efficiency of airfoils to improve the existing icing scaling laws. AEDC is testing several spray nozzles to find one that produces the small droplets required for testing small scale models and also to improve all icing simulation facilities. Verification tests will consist of testing a series of airfoils under several sets of icing tunnel conditions that are predicted by the scaling laws to give equivalent drag and ice shape results.

Verified icing scaling laws would (1) permit accurate tests at actual facility conditions which duplicate results of conditions unattainable by that facility, and (2) permit tests of small-scale models of aircraft and rotors to determine the aeropenalties of icing.

## Analytical Methods

The NASA aircraft icing research effort includes extensive aircraft icing analysis. The long-term goal is to use computers to predict the details of an aircraft icing encounter. Computer codes will be developed to predict overall aircraft performance degradation due to ice accretions on unprotected surfaces and the resultant changes in aircraft handling characteristics. Other codes will be developed to design ice protection systems and analyze their performance.

Today's large, high-speed digital computers were not available to the NACA icing researchers in the 1940's and 1950's, and up until 1980 virtually no icing analysis codes were published in the open literature. With the increasing costs of conducting tests in icing wind tunnels and in icing flights there now is a strong motivation to develop an aircraft icing analysis methodology to hold test programs to the minimum.

Currently we are developing some of the required codes and verifying their accuracy with appropriate experiments. These codes are being developed through a combination of in-house efforts and various grants and contracts. Figure 13 indicates the large number of computer codes required. Also shown are some (but by no means all) of the required interfaces. The figure also shows areas of current research in NASA.

FWG Associates, Inc., is developing a particle trajectory code (Ref. 15) to calculate two-dimensional trajectories about single- and multi-element airfoils, two-dimensional inlets, and axisymmetric inlets at angle of attack (symmetry plane only). The flow fields are calculated using appropriate Douglas Aircraft potential flow codes.

Atmospheric Science Associates has developed a three-dimensional particle trajectory code which is capable of calculating trajectories about three-dimensional nonlifting (Ref. 16) and lifting bodies. The code can calculate water droplet trajectories about the complete aircraft. Again, appropriate potential flow field codes developed by Douglas Aircraft are used to predict the aircraft flow field.

The University of Dayton Research Institute is developing an ice accretion modeling code (Ref. 17) which will calculate two-dimensional ice accretion shapes on airfoils for rime through glaze icing conditions. The approach extends the work of Stallabrass and Lozowski (Ref. 18) and Ackley and Templeton (Ref. 19). The code is compatible with the water droplet trajectory code developed by FWG, and allows the airfoil flow field and resultant collection efficiency to be recomputed as the ice accretion changes the airfoil contour.

The University of Toledo is developing one- and two-dimensional transient heat conduction codes to model electrothermal deicers. A preliminary version of the one-dimensional code is given in Reference 9. These codes include a moving water-ice interface.

The Ohio State University is developing a capability for predicting aerodynamic performance degradation of airfoils due to ice accretions (Ref. 20). They start with existing aerodynamic analysis codes for airfoils, and modify them wherever needed to model the flow around airfoils with ice accretions. As a separate activity, Ohio State is developing a simplified method to predict overall aircraft performance that uses the results of the various other two-dimensional codes being developed.

Texas A&M University is using the fixed-wing methodology developed at Ohio State University and extending it to calculate the performance degradation of propellers and helicopter rotors, both in hover and in forward flight (Ref. 21).

As Figure 13 indicates, many additional computer codes remain to be developed. Before many of them can be developed, fundamental experiments must be conducted to gain a better understanding of the physics to guide the modeling efforts. Also of critical importance is accurate verification data to determine computer code capabilities and limitations. Unfortunately little verification data exist and getting it will require the development of new icing simulation facilities, test rigs, and instrumentation capabilities.

## Flight Research

Lewis has started an icing research flight program using NASA's Twin Otter airplane (Fig. 14). It will be flown out of Lewis during the icing season from November through April. The flight program is intended to insure that researchers conducting icing tests in the IRT or developing computer codes in support of icing have first-hand knowledge of how their results compare with flight test results in real icing conditions.

Validation Data for Icing Simulation Facilities. There does not seem to have been any systematic attempt to prove that icing simulators do a reasonable job of duplicating the natural icing conditions. Lewis plans to obtain during flights in natural icing conditions, ice shapes on standard cylinders and airfoils that any icing simulator can try to reproduce.

For example, the same airfoils and cylinders used in flight will be installed in the IRT where flight icing conditions (airspeed, LWC, drop size, and temperature) will be duplicated. Drag, ice shapes, and ice growth characteristics obtained in the IRT will be compared with those from natural icing. The flight and IRT data comparisons will measure the IRT's ability to simulate natural icing conditions.

Instrument Evaluation. This flight program affords an opportunity to compare several modern cloud instruments with one another and also with the rotating multicylinders and oil slide instruments that were used in the 1940's and 1950's. The Twin Otter will be equipped with all of the modern flightworthy cloud instruments.

Icing Cloud Data. On each icing flight NASA will collect icing cloud data and give it to the FAA who is collecting and correlating icing cloud data taken at lower altitudes with modern instrumentation.

Meteorology. NASA Langley has developed a numerical code (Ref. 22) to forecast the future state of the atmosphere at mesoscale. The code is entitled MASA (Mesoscale Atmosphere Simulation System). MASS uses a 50 km grid spacing over North America, with 14 levels in altitude and 51 sec computation time interval. After each icing flight, Lewis gives Langley the location and altitude where the Twin Otter encountered icing. Langley uses this data to validate MASS by backcasting the conditions at the specified location of the icing encounter.

Airplane Performance. NASA and the Ohio State University will conduct inflight icing experiments to measure lift and drag degradation of the Twin Otter's wings, and also overall performance loss. Ohio State will install a heated wake survey probe and a static pressure belt on one of the Twin Otter's wings. Thrust horsepower measurement techniques will be developed. Flight results will be compared with similar results of tests in the IRT on a Twin Otter wing section.

## CONCLUDING REMARKS

As you can see from this review of NASA's new icing research program, it is broadbased and covers both basic research and engineering applications. Undoubtedly you have seen areas in the NASA program to which some of your own research applies and vice versa. We would like to take the opportunity provided by this international meeting to explore possible ways that we could cooperate, such as, comparing computer code predictions, or providing experimental data for guiding and validating analytical methods, conducting joint experiments, comparing experiences with various icing instruments, or devising experimental techniques for measuring structural properties of ice under actual operating conditions in the IRT.

## REFERENCES

1. Reinmann, J. J.: Selected Bibliography of NACA-NASA Aircraft Icing Publications. NASA TM-81651, 1981.
2. Bowden, D. T.; Gensemer, A. E.; and Skeen, C. A.: Engineering Summary of Airframe Icing Technical Data. FAA-ADS-4, Federal Aviation Agency, 1963.

3. Peterson, A. A.; Dadone, L.; and Bevan, A.: Rotorcraft Aviation Icing Research Requirements. Research Review and Recommendations. (D210-11662-1, Boeing Vertol Co.; NASA Contract NAS3-22384.) NASA CR-165344, 1981.
4. Breeze, R. K.; and Clark, G. M.: Light Transport and General Aviation Aircraft Icing Research Requirements. (NA-81-110, Rockwell International Corp.; NASA Contract NAS3-22186.) NASA CR-165290, 1981.
5. Koegeboehn, L. P.: Commercial Aviation Icing Research Requirements. NASA CR-165336, 1981.
6. Rotorcraft Icing--Status and Prospects. AGARD AR-166, 1981.
7. Engineering and Development Program Plan--Helicopter Icing Technology Research. FAA-ED-18-8, Federal Aviation Administration, 1981.
8. Blaha, B. J.; and Evanich, P. L.: Pneumatic Boot for Helicopter Rotor Deicing. NASA CP-2170, 1980.
9. DeWitt, K. J.; and Baliga, G.: Numerical Simulation of One-Dimensional Heat Transfer in Composite Bodies with Phase Change. NASA CR-165607, 1982.
10. Kohlman, D. L.; Schweikhard, W. G.; and Albright, A. E.: Icing Tunnel Tests of a Glycol-Exuding Porous Leading Edge Ice Protection System on a General Aviation Airfoil. (KU-FRL-464-1, Kansas Univ. Center for Research, Inc.; NASA Contract NAG3-71.) NASA CR-165444, 1981.
11. Magenheim, B.; and Rocks, J. K.: Development and Test of a Microwave Ice Accretion Measurement Instrument (MIAMI). NASA CR-3598, 1982.
12. Gray, V. H.: Prediction of Aerodynamic Penalties Caused by Ice Formations on Various Airfoils. NASA TN D-2166, 1964.
13. Bragg, M. B.; Gregorek, G. M.; and Shaw, R. J.: Wind Tunnel Investigation of Airfoil Performance Degradation Due to Icing. AIAA-82-0582, 1982.
14. Dodson, E. D.: Scale Model Analogy for Icing Tunnel Testing. D6-7976, Boeing Airplane Company, 1966.
15. Frost, W. F.; Chang, H.; Shien, C.; and Kimble, K.: Two Dimensional Particle Trajectory Computer Program. NASA CR to be published.
16. Norment, H. G.: Calculation of Water Drop Trajectories to and about Arbitrary Three-Dimensional Bodies in Potential Airflow. NASA CR-3291, 1980.
17. MacArthur, C. D.; Keller, J. L.; and Luers, J. K.: Mathematical Modeling of Ice Accretion on Airfoils. AIAA Paper 82-0284, 1982.
18. Lozowski, E. P.; Stallabrass, J. R.; and Hearty, P. F.: The Icing of an Unheated Non Rotating Cylinder in Liquid Water Droplet-Ice Crystal Clouds. LTR-LT-96, Natural Research Council of Canada, 1979.
19. Ackley, S. F. and Templeton, M. K.: Computer Modeling of Atmospheric Ice Accretion. CRREL-79-4, Army Cold Regions Research and Engineering Lab., 1979.
20. Bragg, M. B.; Gregorek, G. M.; and Shaw, R. J.: An Analytical Approach to Airfoil Icing. AIAA 81-0403, 1981.
21. Korkan, K. D.; Dadone, L.; and Shaw, R. J.: Performance Degradation of Propeller/Rotor Systems Due to Rime Ice Accretion. AIAA-82-0286, 1982.
22. Kaplan, M. L.; et al.: A Mesoscale Eighth Order Numerical Modeling System and the "Red River" Tornado Outbreak of 1979, Parts I and II. Presented at the 12th AMS Conference on Severe Local Storms, (San Antonio, Texas), Jan. 11-15, 1982.

| | |
|---|---|
| ● ICE PROTECTION SYSTEMS | · PNEUMATIC DEICERS FOR HELICOPTERS<br>· ELECTROTHERMAL DEICERS<br>· GLYCOL FLUID SYSTEMS<br>· ELECTROMAGNETIC IMPULSE DEICERS<br>· ICEPHOBICS |
| ● ICING INSTRUMENTATION | · CLOUD INSTRUMENT EVALUATION<br>· ICE DETECTORS |
| ● EXPERIMENTAL METHODS | · ICING RESEARCH TUNNEL<br>· AIRFOIL PERFORMANCE IN ICING<br>· TESTING WITH ARTIFICIAL ICE<br>· HELICOPTER TEST RIGS<br>· ICING SCALING LAWS |
| ● ANALYTICAL METHODS | · COMPUTER CODES FOR:<br>● WATER DROPLET TRAJECTORIES<br>● ICE ACCRETION MODELING<br>● AERO PERFORMANCE PENALTIES<br>● TRANSIENT DEICER ANALYSIS |
| ● FLIGHT RESEARCH | · VALIDATION DATA FOR ICING SIMULATION FACILITIES<br>· INSTRUMENT EVALUATION<br>· ICING CLOUD DATA<br>· METEOROLOGY<br>· AIRPLANE PERFORMANCE |

CD-82-13130

Figure 1. Elements of NASA's Aircraft Icing Program.

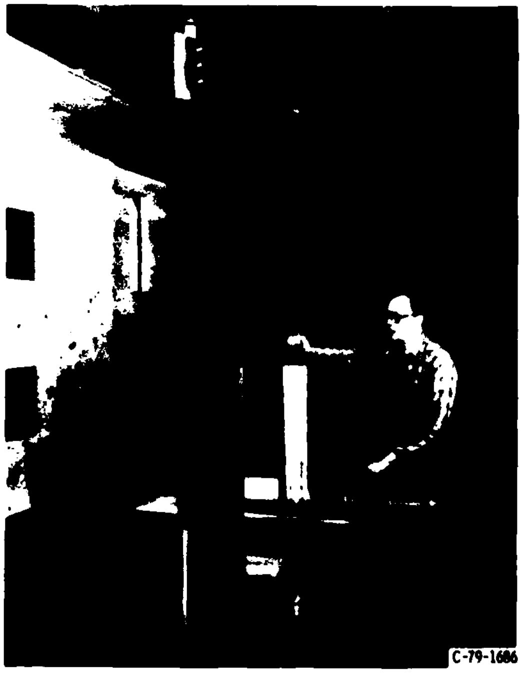

Figure 2. Pneumatic boot deicer on UH-1H rotor blade, and wake survey probe in the LeRC Icing Research Tunnel.

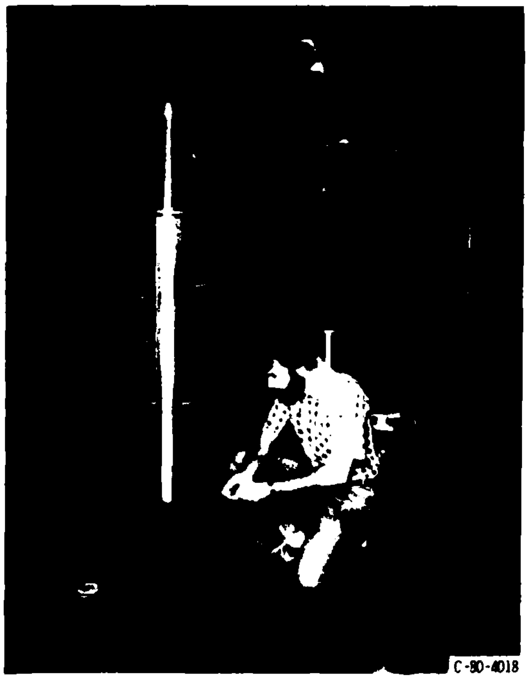

Figure 3. Glycol fluid distributor (porous stainless steel) on leading edge of wing in the LeRC Icing Research Tunnel.

Figure 4. Icephobics interfacial shear stress test rig in the LeRC Icing Research Tunnel.

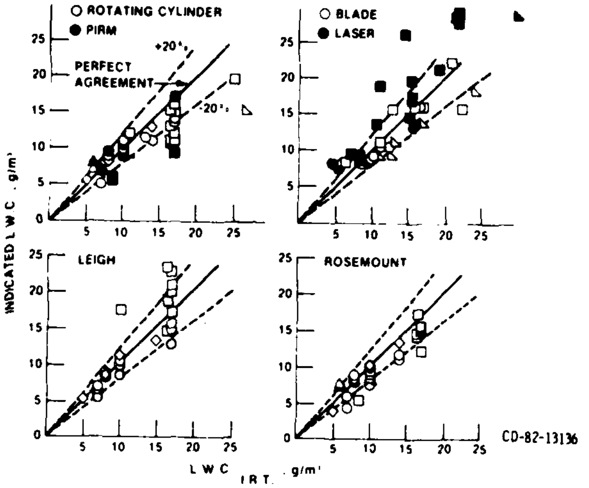

Figure 5. Results of tests comparing several liquid-water-content meters in the Lewis IRT.

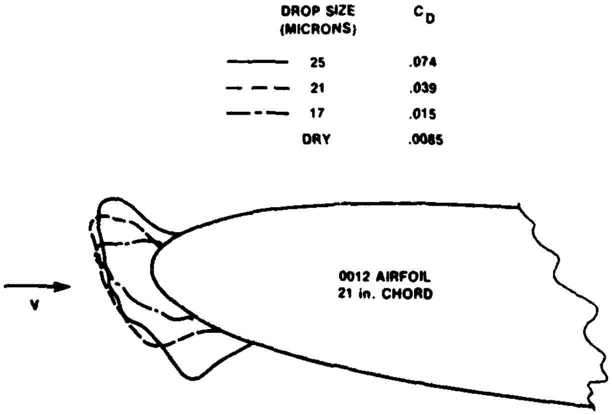
DROP SIZE (MICRONS)
$C_D$
25
.074
21
.039
17
.015
DRY
.0085
0012 AIRFOIL
21 in. CHORD
V

AIRSPEED, 130 mph; AIR TEMP, +18° F; LWC, 1.3 G/M³; TIME 8 min; ANGLE, 4°
CD-82-13131

Figure 6. Effect of cloud volume median droplet size on ice shape and drag, from measurements in the Lewis IRT.

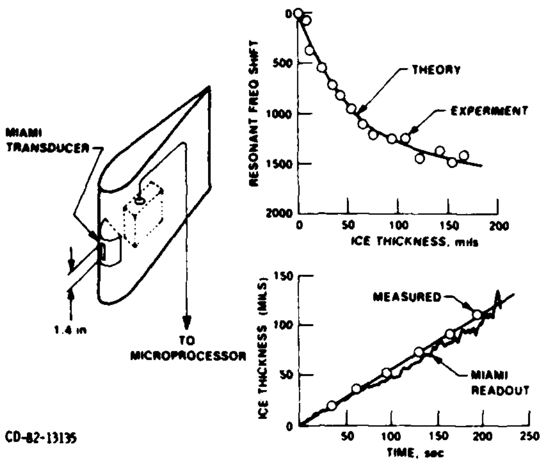

CD-82-13135

Figure 7. Relationship between resonant frequency shift and ice thickness for the Microwave Ice Accretion Measurement Instrument (MIAMI).

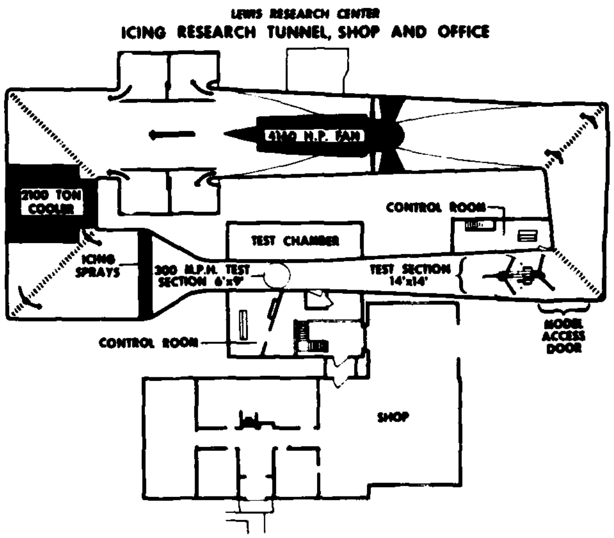
LEWIS RESEARCH CENTER
ICING RESEARCH TUNNEL, SHOP AND OFFICE
4160 H.P. FAN
2100 TON COOLER
CONTROL ROOM
TEST CHAMBER
ICING SPRAYS
300 M.P.H. TEST SECTION 6'x9'
TEST SECTION 14'x14'
MODEL ACCESS DOOR
CONTROL ROOM
SHOP

Figure 8. Loop schematic of the Lewis Icing Research Tunnel.

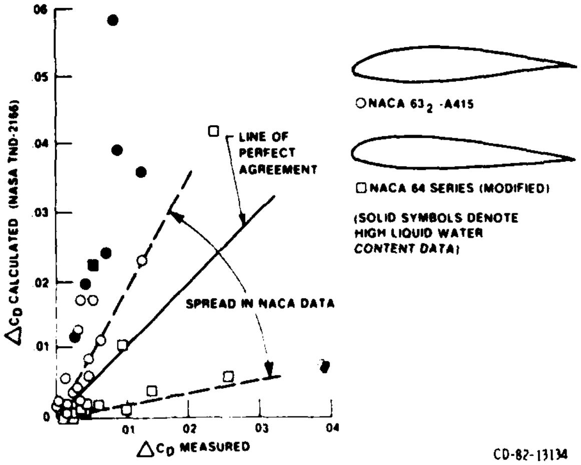

CD-82-13134

Figure 9. Predicted drag increments due to ice accretion (from NASA TN D-2166) versus drag increments measured in the Lewis IRT.

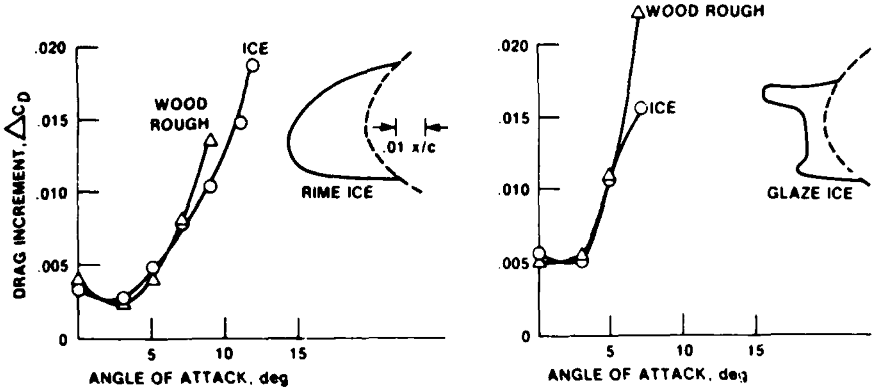

CD-82-13133

Figure 10. Drag increments from real ice compared with the drag increments from wooden replicas of the ice.

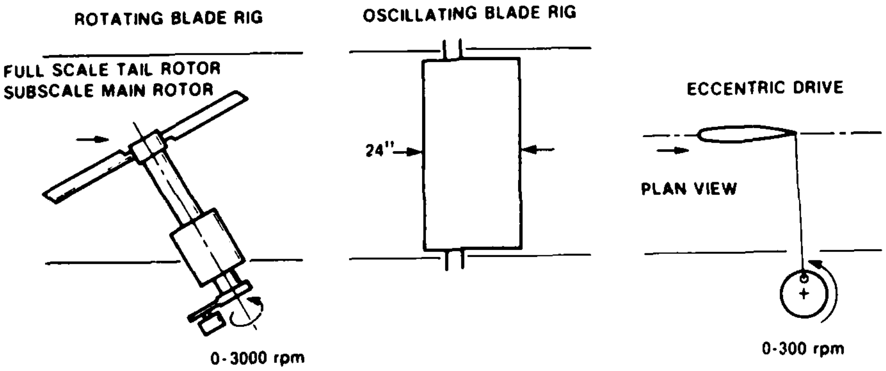

ROTATING BLADE RIG
FULL SCALE TAIL ROTOR
SUBSCALE MAIN ROTOR
0-3000 rpm
OSCILLATING BLADE RIG
24"
ECCENTRIC DRIVE
PLAN VIEW
0-300 rpm

CD-82-13132

Figure 11. Rotor blade test techniques being developed for the Lewis IRT.

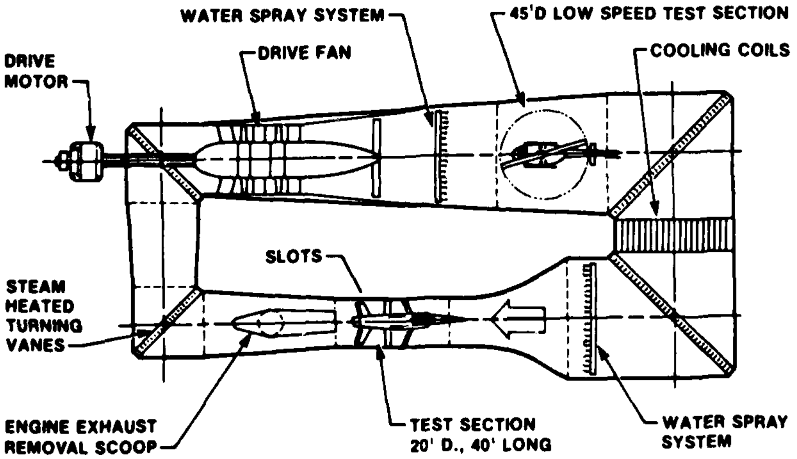

WATER SPRAY SYSTEM
45'D LOW SPEED TEST SECTION
DRIVE MOTOR
DRIVE FAN
COOLING COILS
SLOTS
STEAM HEATED TURNING VANES
ENGINE EXHAUST REMOVAL SCOOP
TEST SECTION 20' D., 40' LONG
WATER SPRAY SYSTEM

CD-82-13129

Figure 12. Flow circuit for proposed rehabilitation of the Lewis Altitude Wind Tunnel (AWT).

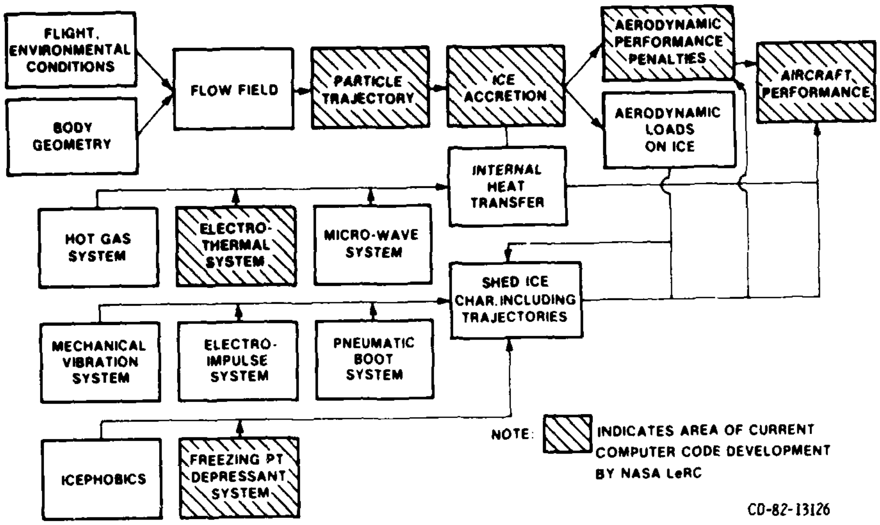
FLIGHT, ENVIRONMENTAL CONDITIONS
BODY GEOMETRY
FLOW FIELD
PARTICLE TRAJECTORY
ICE ACCRETION
AERODYNAMIC PERFORMANCE PENALTIES
AERODYNAMIC LOADS ON ICE
AIRCRAFT PERFORMANCE
INTERNAL HEAT TRANSFER
HOT GAS SYSTEM
ELECTRO-THERMAL SYSTEM
MICRO-WAVE SYSTEM
SHED ICE CHAR. INCLUDING TRAJECTORIES
MECHANICAL VIBRATION SYSTEM
ELECTRO-IMPULSE SYSTEM
PNEUMATIC BOOT SYSTEM
ICEPHOBICS
FREEZING PT DEPRESSANT SYSTEM
NOTE: ▨ INDICATES AREA OF CURRENT COMPUTER CODE DEVELOPMENT BY NASA LeRC

CD-82-13126

Figure 13. Flow chart showing NASA's methodology for aircraft icing analysis.

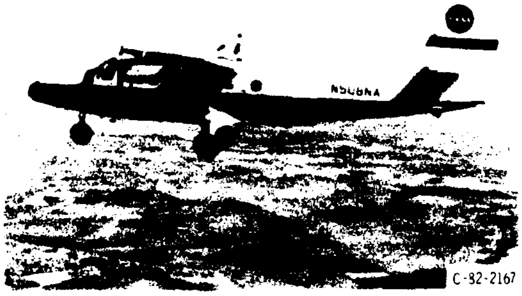

C-82-2167

Figure 14. The NASA icing flight research aircraft.

AD P001680

# STUDIES OF HIGH-SPEED ROTOR ICING UNDER NATURAL CONDITIONS

K. Itagaki USACRREL*
G.E. Lemieux USACRREL
H.W. Bosworth USACRREL
J. O'Keefe USACRREL
G. Hogan USACRREL

## ABSTRACT

Icing on high-speed rotors was studied under natural conditions on the summit of Mt. Washington. Differences in the growth conditions from those of laboratory tests, such as rapidly variable water supplies and abundant freezing nuclei, seem to have contributed to raising the temperature of the wet growth regime and producing finer crystals than in laboratory experiments.

## INTRODUCTION

The problem of icing on high-speed rotors is associated with the operation of helicopters and propeller-driven aircraft. Recent advances in wind energy technology have also introduced icing problems in regard to windmills and wind turbines.

Icing itself is a complicated process involving the supply of water droplets and the removal of heat generated by phase change from a liquid to a solid. Further complications arising with high-speed rotors include the effects of centrifugal force, distribution of air speed along the span of the rotor, radial air flow and vibration. Unlike stable laboratory conditions, field conditions affecting the icing never remain constant. Also factors unexpected or difficult to include in the laboratory experiments add more complexity in the natural condition.

The study of high-speed rotor icing described in this paper was conducted at Mt. Washington, New Hampshire, the highest peak in the Northeastern United States (1,917 m). On 12 April 1934, Mt. Washington Observatory at the summit recorded the world's highest surface windspeed, 103.2 m/s (231 mph). The mean annual temperature at the observatory is -2.8°C (26.9°F) and fog is observed on the average for more than 300 days/year, or 430 hr of fog/month. The combination of below-freezing temperatures and fog make the summit an excellent location for icing observations. The observatory provides standard meteorological data once every three hours and also more specific data on request. Although access to the summit during the snow season is limited to "snow cat" transportation, heavy equipment can be transported during snow-free periods over an auto road. Accommodations for personnel are available at the observatory and power can be obtained from a TV station next to the observatory.

### Equipment

Rotor assembly. The rotor assembly used in this study consisted of two pairs of rotors with different cross sections. One pair was a circular (3.81 cm in diameter) and the other was an airfoil having a chord of 15.2 cm and a pitch set at 1.1 m at the tip. Both pairs of blades were mounted

---

* U.S. Army Cold Regions Research and Engineering Laboratory, Hanover, N.H.

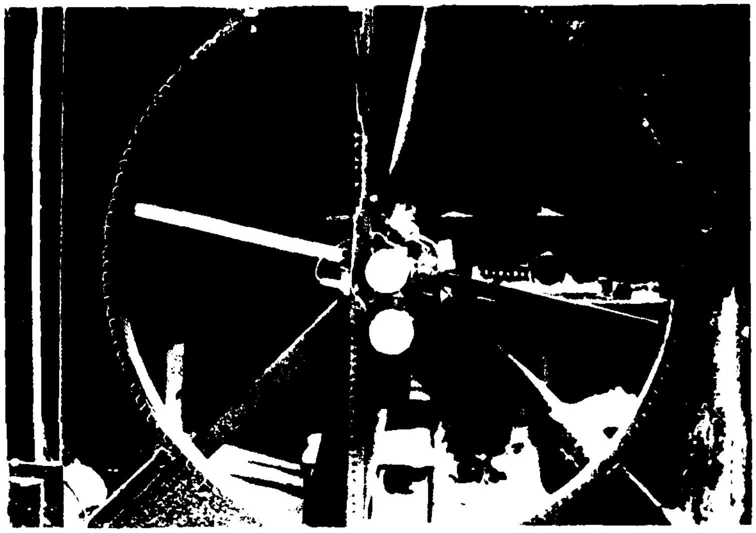

Figure 1. Rotor assembly showing ice accumulation on airfoil and cylindrical rotors.

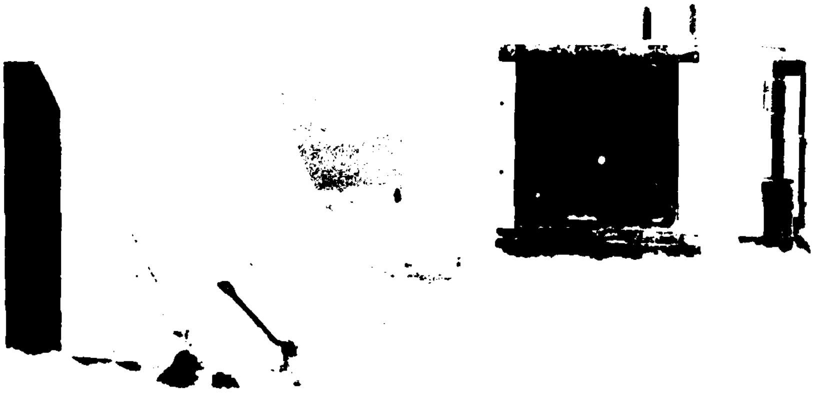

Figure 2. Overall view showing observation shack in foreground and rotor shelter in background. The front door of the rotor shelter is open, showing the rotor, but the side door is closed.

in symmetrical positions on the hub so that they were balanced and exposed to identical conditions (Fig. 1). One airfoil blade was instrumented with two rows of three thermistors each, with two thermistors located near the tip of the blade (66.75 cm), two at the middle (47.25 cm), and two near the hub (26.75 cm). All thermistors, together with the resistance strain gages, were connected to measuring circuits of a data logger through a slip ring system.

The rotor assembly was driven by a Ford V-8 industrial gasoline engine through a set of pulleys and V-belts. A plywood shelter with a large opening in front and on the side for free air flow around the rotor assembly protected the driving system and the rotors from the elements while not in use. A baffle prevented warm air circulating around the engine room from entering the rotor area. The speed of the engine and operation of a brake/clutch system to disengage the rotor to the engine could be controlled remotely from an observation shack located about 10 m away. The overall arrangement is shown in Figure 2.

The rotor system was operated at around 1800 RPM ±10%. Tip speed corresponding to 1800 RPM is 141 m/s or

Mach 0.43, about 1.5 times higher than in the earlier laboratory experiments (Ackley et al. 1979). The 2.54-cm-diam. cylindrical rotor used in laboratory experiments was 25 cm in radius from tip to center of rotation. At 3600 RPM the tip speed was 94 m/s or Mach 0.285 and the corresponding acceleration at the tip was 35,500 m/s$^2$ in contrast to the field observation of 26,650 m/s$^2$ for the rotor radius of 75 cm.

Data Logger. Blade temperatures, ambient temperature, wind speed, and engine and rotor speed were converted into electrical signals and recorded on magnetic tape with a Datel Model DL-2 digital cassette data logger. Data cassettes were then taken back to CRREL and processed.

Rotoscope. The rotor was monitored through a rotoscope, which enabled continuous observation of ice buildup on the rotor with a synchronized rotating Dove prism (Itagaki, 1978). Icing runs were continued until sufficient icing was built up on the rotor blades.

Liquid water content measurement. Two types of measurements were made to determine liquid water contents in the atmosphere. A rotating multicylinder was used to measure the average liquid water content while an impactor was able to supply instantaneous data. Both methods were used independently or concurrently. The highest liquid water content measured during the observation was 0.54 g/m$^3$ by the multicylinder method.

Laser profile camera. Cross sections of ice buildup were photographed with the laser profile camera shown in Figure 3 for every 5-cm interval after the icing run. This camera, which used a laser beam diverged by a cylindrical lens to illuminate a two-dimensional field, observed the illuminated area from a near-perpendicular direction. Examples of profiles obtained by the laser profile camera (shown in Fig. 4a and b) indicated that the cross section of the accumulated ice can be quite irregular under certain conditions.

Ice sample collection. Accumulated ice grown on blades was cut at 5-cm intervals and removed from the blade. Examples of thin sections made from the accumulated ice are shown in Figures 5a and b. These thin sections revealed that the grain size of the ice grown under natural conditions was considerably smaller than the grain size of ice grown in the laboratory.

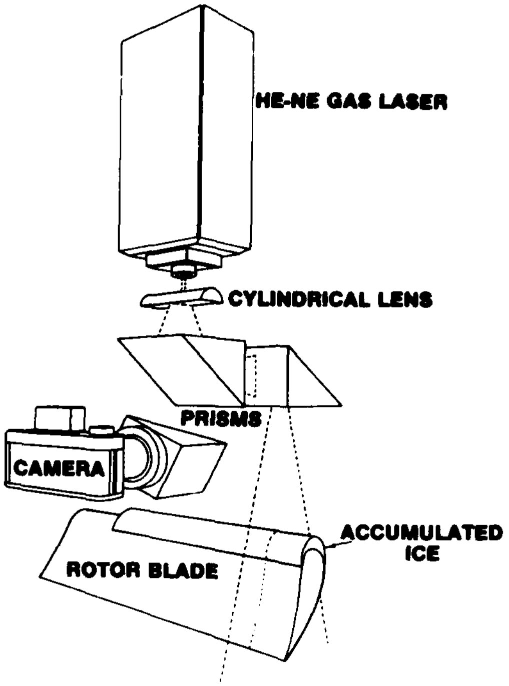

Figure 3. Schematic drawing of the laser profile camera. Laser beam is expanded by the cylindrical lens and illuminates the ice through a set of right-angle prisms. A camera having a narrow band-pass filter set for the wavelength of He-Ne laser (6328 Å) photographs the illuminated area through the third right-angle prism.

## Results

In Figure 6 an example of a time vs. temperature plot is shown for the thermistors along the blade. Combination of the effects of latent heat of freezing and aerodynamic heating is clearly shown in the curve marked Ch 1, which corresponds to the tip temperature. Lesser effects were seen for the temperatures inward of the tip. Such a temperature rise, when combined with other effects such as water supply and flow field, seems to result in a wide variety of crystallographic structures and shapes as shown in Figures 5a and b, taken at different distances from the rotor hub.

Fine, randomly oriented ice grains were found near the hub, where flow is slow and water supply is low due to lower relative air speed and collection efficiency. Little difference in ice structure was seen along the chord in this area. Further away from the hub, flow speed as well as aerodynamic and centrifugal force increased. Around

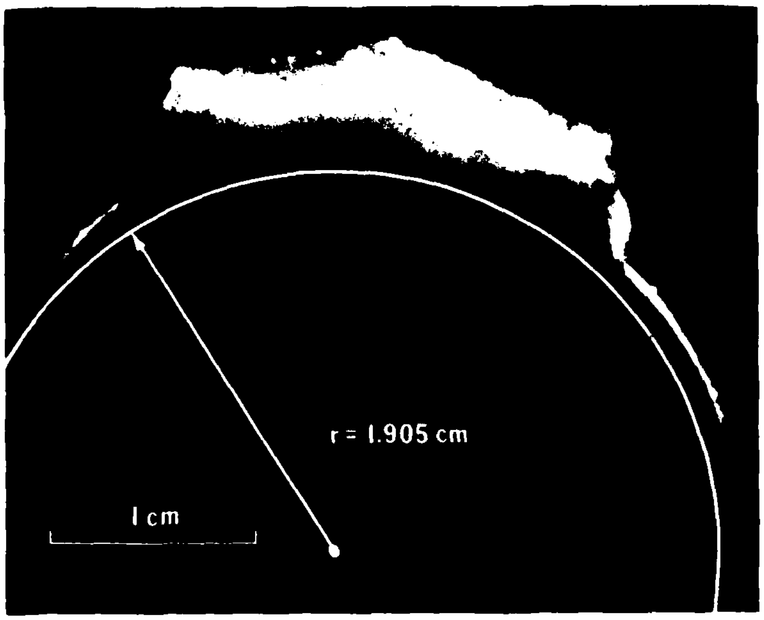

a. Laser profile of ice accreted on cylindrical rotor blade, indicating slightly asymmetrical growth of accretion.

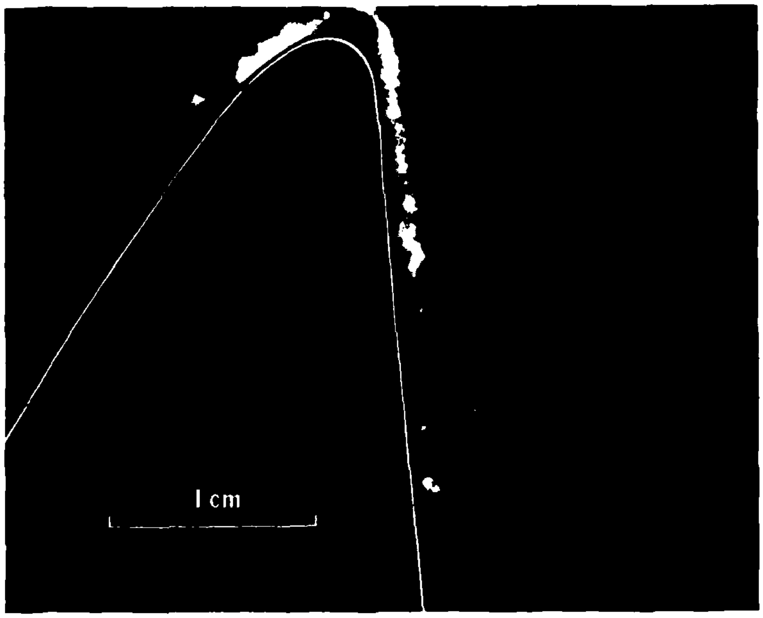

b. Laser profile of ice accreted on airfoil. Ice accretion on the positive pressure side (shown on the right) continues farther down towards the trailing edge of the blade while ice accretion on the negative pressure side stops just beyond the leading edge.

Figure 4. Laser profiles of ice accreted on cylindrical rotor blace and on airfoil.

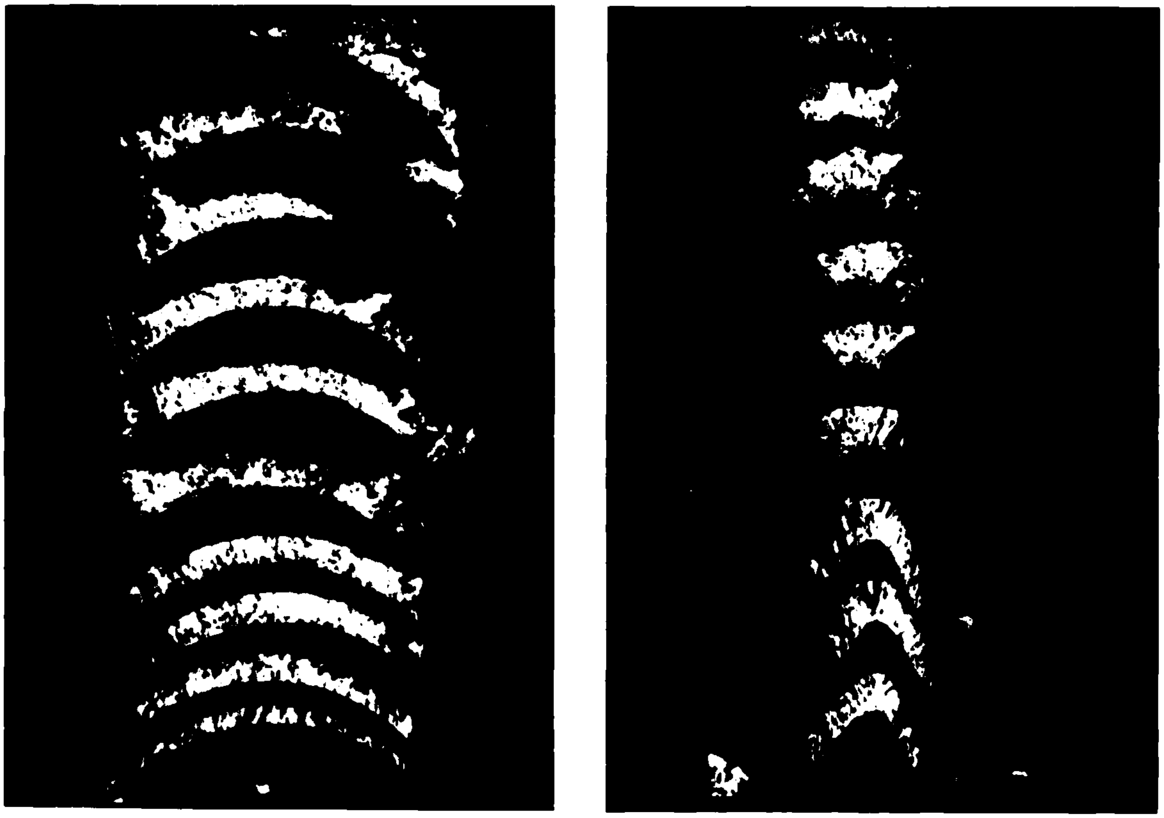

a. Thin sections of accreted ice grown on the cylindrical rotor blade and placed between a cross polarizer, showing different orientations and grain sizes.

b. Similar thin sections of accreted ice on airfoil blade under the same growth conditions, showing a more ragged outline.

Figure 5. Thin sections of accreted ice grown on cylindrical rotor blade and on airfoil blade.

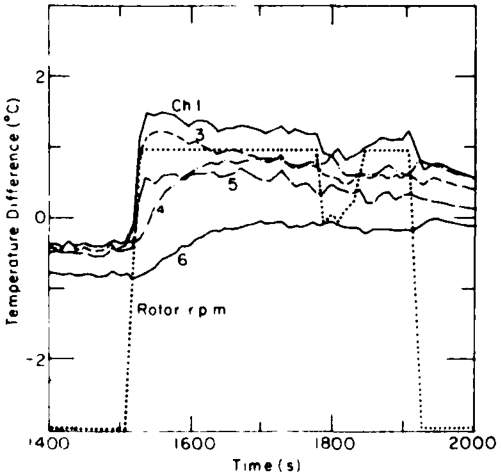

Figure 6. Variation of rotor surface temperature with time. Channels 1, 3 and 5 are at the leading edge and 4 and 6 are at the midpoint. Note that the thermistors at the leading edge register a quick response while those at the midpoint change slowly. Also the temperature at channel 1, located near the tip, rises the most and the innermost thermisters register the least rise.

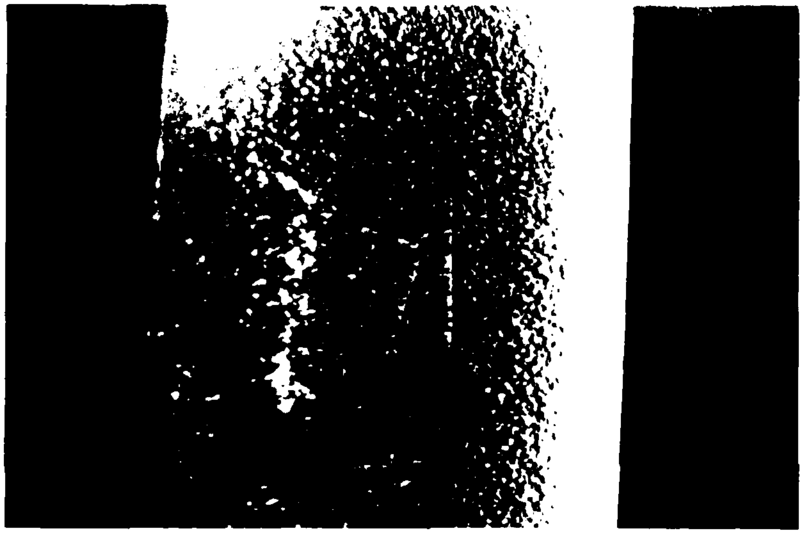

Figure 7. Individual granular cone-shaped accretion spread over the positive pressure side of an airfoil blade away from the main accretion.

the stagnation point, the grain size initially increased as ice grew with random orientations, and then larger grains were formed which tended to have a columnar structure. This increase in grain size indicates that the growth conditions changed from a dry growth regime (surface temperature below 0°C) to a wet growth regime (surface temperature at 0°C) as ice continued to accrete. The effect of air flow on the ice structure became pronounced away from the stagnation points. Frequently the accretions grew into the shape of acute cones having their axes parallel to the air flow. These cones were separated by cavities. Such cones protruded beyond the ice grown near the stagnation point, giving the appearance of humps at higher temperatures (-3°C) and high water supply conditions as shown in Figure 5a. Protrusions on the airfoil blades were more pronounced than those on the cylindrical shaft (Figure 5b), probably due to the higher water supply on the smaller radius of curvature.

Separate, more obtuse cones were found away from the main icing growth. Various sizes of these cones were distributed randomly on the lower surface (positive pressure side) almost all the way to the trailing edge (Fig. 7). No such cones were found on the upper surface or on either side of the cylindrical blade beyond the widest point. Only the main part of the icing extended to the high point of the chord. Outside the wet growth regime, icing began with the freezing of supercooled drops randomly captured on the surface. These frozen drops acted as nuclei of the cones. The size and shape of the cones were determined by the growth conditions. The acute cones found near the stagnation points may have had the same origin and growth mechanisms but may have been exposed to harsher conditions.

## SUMMARY AND CONCLUSIONS

In order to examine the applicability of the results of laboratory icing experiments to natural conditions, field observation of natural icing was made. Although the general trends agree with each other, several significant differences were noted:

1. Relevant conditions, especially the water supply, vary quickly and widely in the natural environment.

2. The existence of freezing nuclei may be especially important if snow crystals are blown up from the snow-covered ground and act as nuclei for ice formation. A smaller ice grain size observed under natural conditions than in the laboratory may have been caused by the effects of these nuclei.

3. The observed accretion rate in the natural case ($\approx 7\times10^{-4}$ cm/s) was less than 20% of the rate in laboratory tests ($\approx 4 \times 10^{-3}$ cm/s). The major

cause of this discrepancy may be the greater liquid water content used in the laboratory tests (1.2 $g/m^3$) as compared to the observed natural liquid water content (0.54 $g/m^3$) on the summit of Mt. Washington.

4. The temperature range of the wet growth regime during natural icing was almost 10°C higher than that observed during the laboratory tests. This difference probably is the result of the higher water supply due to the higher liquid water content in the laboratory experiments.

5. No large-scale self-shedding of ice was observed in the field case compared to the lab conditions. Three factors may contribute to this effect: a) centrifugal acceleration is lower (less than 75% that of laboratory experiments); b) accretion rate is lower so that the necessary ice thickness was not reached for self-shedding, and c) the grain size was smaller than found in the laboratory tests so that the strength of accreted ice might have been higher than that of larger grained ice.

These factors should be taken into account in applying laboratory icing results to those from natural situations.

## REFERENCES

Ackley, S.F., G.E. Lemieux, K. Itagaki and J. O'Keefe (1979) Laboratory experiments on icing of rotating blades. Proceedings of the Second International Symposium, Snow Removal and Ice Control Research, Transportation Research Board Special Report 185.

Itagaki, K. (1978) "Rotoscope" an Instrument to Observe Rotating Machines by Production of a Continuous Stationary Image. CRREL Technical Note.

## DISCUSSION

Power: I wasn't quite sure what you were getting at with these cone-shaped forms, these striations in the type of ice formation, but I'm wondering whether that isn't a reflection of some kind of a supercritical flow, either in a film of liquid water, or in some type of compressional wave that's flowing through the ice that's forming. These are very thin films, you could have a supercritical flow in such thin films which would, in effect, be what you would call "Mach lines" in the flow in the ice. That would give that type of a structure.

Itagaki: I have given thought to that kind of a prospect. I thought that, more or less, nucleation of icing and growth occurs at a particular point. Nucleation starts at one point [...]

Power: But the nucleation might be guided by some sort of "Mach line" in the ice.

Itagaki: I don't know if this really happens in this condition because this is a very sharp corner.

Jellinek: Do you have any idea what kind of nuclei these are? From the surface, or some dust ...?

Itagaki: That's a good possibility. I suspect that snow blown up from the ground can act as nuclei.

AD P001681

# ICE TREEING UNDER DC AND AC ELECTRIC FIELDS AT DIFFERENT INTENSITIES OF ACCRETION

Luan C. Phan Université du Québec à Chicoutimi
Jean-Louis Laforte Université du Québec à Chicoutimi
Du D. Nguyen Université du Québec à Chicoutimi

## ABSTRACT

Atmospheric ice is accreted on an aluminium conductor of 3.15cm diameter at different intensities of accretion. High voltage (ac and dc) is applied to the conductor to produce an electric field at the surface of the conductor in the same range as that existing on actual power lines. The visual aspect of ice accretion shows the formation of ice treeing with thick branches under ac and dc positive fields. The ice trees are small and their branches are very thin under negative field above -10kV/cm. From the study of corona pulses it is shown that corona streamers are responsible for the ice treeing. The results obtained show that for low and medium precipitation intensities, the amount of ice accreted under dc negative field above -10kV/cm is negligeable.

## INTRODUCTION

In northern countries, ice frequently accretes on conductors of transmission lines, whether they are deenergized or energized with alternating current (a.c.). Thus an a.c. electric field on actual power lines seems to have little effect upon atmospheric ice accretion. On the other hand, high voltage direct current (H.V.D.C.) power transmission is a recent addition to the field of electrical energy transmission systems, reasons being the cost advantages for long distance overhead transmission.

Concerning the effect of d.c. electric field upon the formation of atmospheric ice, it may be said that most of the studies known are for the purpose of investigating the influence of natural electric fields upon ice nucleation in atmospheric clouds. According to the published reports (1-7) on these topics, ice nucleation by an electric field (electro-freezing) can occur in natural clouds only under special conditions, i.e. when a d.c. electric field and hydrophobic substances or ice are present. In addition the mechanism by which an electric field influences the ice nucleation is not known.

The objective of the research project undertaken at the University of Quebec is to investigate systematically the effect of d.c. and a.c. electric fields upon ice accretions formed on power line conductors under different atmospheric conditions. Preliminary results published (8) in 1981 by the authors showed that the density as well as the adhesive strength of ice decreases with increasing applied d.c. field. However only one combination of atmospheric conditions was used and no systematic corona study was made in the previous work.

The aim of the present report is to extend the study to other atmospheric conditions and to investigate the corona pulses during the accretion of ice in order to bring us closer to a comprehensible mechanism of the influence of the electric field upon ice accretions on power line conductors.

## EXPERIMENTAL CONDITIONS AND PROCEDURE

Experiments are conducted in a 4.8x2.8x2.56m$^3$ cold chamber where a minimum temperature of -35°C±0.5°C can be maintained. Some elements of the experimental setup are shown in Fig. 1. A smooth aluminium conductor of 3.15cm in diameter is

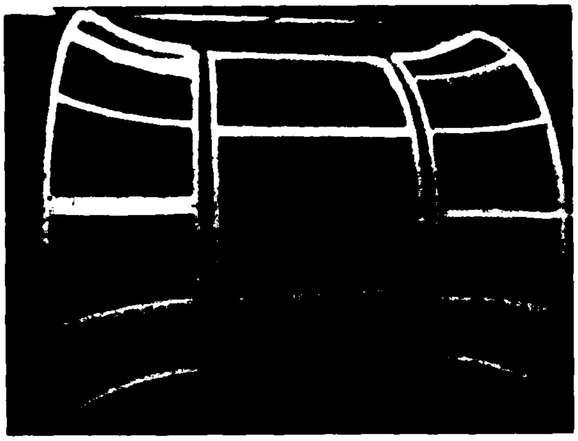

Fig. 1 Experimental arrangement

placed in the axis of a mesh cage of 1m in diameter. In order to obtain uniform accretion, the conductor is rotated at 1rpm, in some experiments a stationary conductor is also used. Supercooled droplets are produced by an electric gun model Wagner 300 nozzle no 5, behind which is placed a rectangular block of tubings and a fan used to produce a laminar wind. High voltage is supplied to the conductor from a Messwandler-Bau source of 200kV, a.c./d.c., 10kVA. Concerning the atmospheric parameters, mean droplet diameter (40μm), liquid water content (1.1g/m$^3$) and ambient temperature (-10°C) are kept constant. In order to vary the intensity of ice accretion I, (defined as the product of the collection efficiency of water droplets ε, the liquid water content W and the velocity of air V) the air velocity is varied from 2 to 8m/s. Table 1 gives the value of the atmospheric conditions used and the corresponding intensities of ice accretion $I_o$ obtained in the absence of an electric field.

TABLE 1

Intensity of ice accretion at different air velocities ($T=-15^\circ C$, $d_v=40\mu m$, $E=0kV/cm$)

| V(m/s) | ε | W(g/m$^3$) | $I_o$(g/m$^2$s) | |
|---|---|---|---|---|
| | | | εWV | exper. |
| 2 | 0.51 | 1.1 | 1.1 | 1 |
| 4 | 0.64 | 1.1 | 2.8 | 2 |
| 6 | 0.71 | 1.1 | 4.7 | 5 |
| 8 | 0.76 | 2.0 | 12.2 | 12 |

The liquid water content W is measured by the single cylinder method (9) while the experimental value of the intensity of accretion I is measured from the mass m of ice collected during a time t according to the following equation

$$I = \frac{m}{L}\,\frac{1}{t(D+e)} \qquad (1)$$

where L and e are respectively the length and the thickness of ice accretion and D is the diameter of the bare conductor. The difference between the desired value (product of εWV) and the experimental value of $I_o$ is due to the difference between the theoretical and the experimental values of ε, W and to a small degree the distribution of air speed along the axis of the ice accretion. For instance at V equal 4m/s, the actual velocity varies between 3 and 4m/s, the experimental value of ε and W are 0.64 and 1.1±0.1g/m$^3$ respectively. As a result the product of the experimental values of E, V and W is between 2.1 and 2.83, i.e. very close to the value of $I_{exp.}$ measured from the mass of ice collected.

The conductivity of tap water is between 45 and 68μS. The density of ice is obtained by weight and volume measurements as already described in the previous (8) paper. However for ice of very low density the graphical method is used: from the photograph of the shape of the ice accretion its volume is numerically evaluated from section to section by a computer program. Macklin (10) showed that a value of the density as low as 0.05 can be determined from this method.

At the surface of the conductors of actual H.V.A.C. power lines the electric field strength is about 15kVrms/cm or lower while the corresponding value of H.V.D.C. power lines is a little larger. Therefore in these experiments the strength of the electric field at the surface of the conductor does not exceed 15kV/cm and ±20kV/cm for a.c. and d.c. fields respectively. Corona current and corona pulses are measured with a microameter and a large band oscilloscope through a resitor of 1kΩ placed between the cage and the ground.

## RESULTS AND DISCUSSIONS

### Visual aspect of ice accretion

The appearance of the ice accretion depends upon the strength of the applied electric field and the intensity of ice accretion.

### Effect of increasing applied electric field at the surface of the conductor

The intensity of ice accretion in the absence of an electric field being kept constant, $I_o=2g/m^2s$, Fig. 2 shows the visual aspect of ice obtained under different a.c. and dc field strengths.

Under an a.c. applied field it may be seen that the aspect of ice formed at 5kVrms/cm is similar to that obtained in the absence of an electric field. Some ice trees

AC ( kVrms/cm )

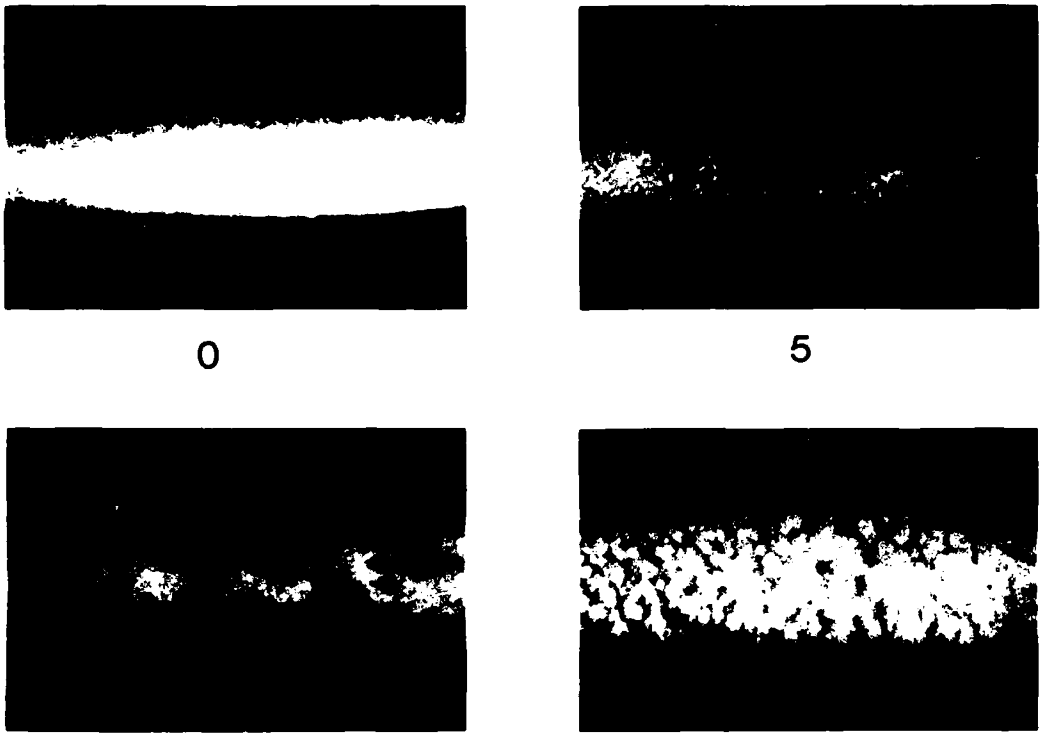

0

5

10

15

(a)

DC + ( kV/cm )

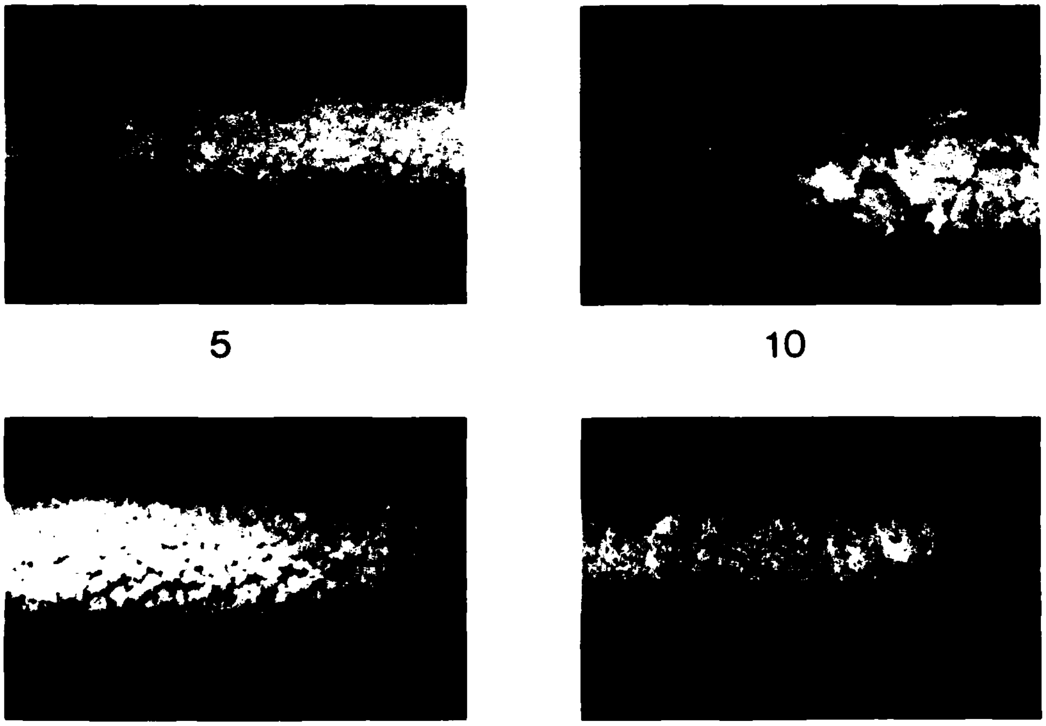

5

10

15

20

(b)

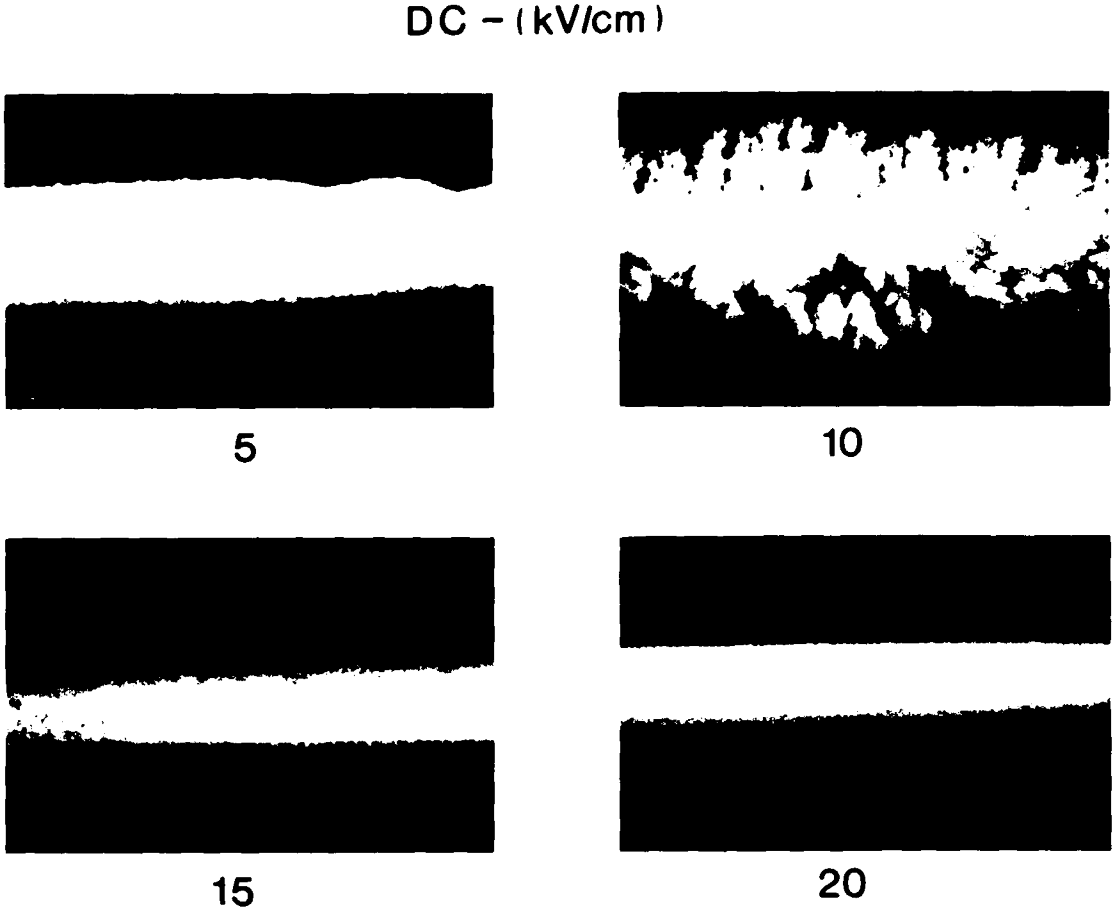

(c)

Fig. 2 Visual aspect of ice accretions under electric fields ($I_o$= $2g/m^2s$)

with thick branches are visible at a field of 10kVrms/cm but the number of trees increases considerably at 15kVrms/cm.

In Fig. 2b, it is seen that ice formed under positive dc applied field strength between +5 and +10kV/cm is similar to that observed under a.c. field of the same strength. However at a field strength equal to +15kV/cm, ice trees seem to be more numerous and ice branches are thinner compared to those observed under a.c. field of 15kVrms/cm. It is interesting to observe that at +20kV/cm ice branches are very thin and converging.

Under dc negative field, ice trees appear at -10kV/cm as observed with positive d.c. or a.c. applied voltage, however they become smaller at increasing negative dc applied field. In fact, it is clearly shown in Fig. 2c that the concentration of ice trees increases with increasing negative applied field. But the most important observation which can be made concerns the height and the trunk of ice tree which decrease considerably at negative applied field above -10kV/cm. In fact it is seen that the thickness of ice accreted is negligeable at negative field of -15kV/cm and above.

Effect of intensity of accretion upon the formation of ice treeing.

As shown in the table 1, if the velocity of air is reduced from 4 to 2m/s, $I_o$ is decreased from about 2 to $1g/m^2s$. It has been observed that for field strength above 10kV/cm the visual aspect of ice is similar to that corresponding to $I_o$=$2g/m^2s$ shown in Fig. 2. But the most significant difference is observed at low field strength. Fig. 3 shows that with an intensity of $1g/m^2s$ ice trees begin to be visible at a dc field strength as low as 5kV/cm. It may be recalled that at 5kV/cm (a.c. or d.c.), ice formed at $2g/m^2s$ has a similar aspect (Fig. 2a) to which forms in the absence of an electric field. With higher intensity of accretion the formation of ice treeing begins at higher electric field. At $I_o$= $5g/m^2s$ it is seen in Fig. 3b that in a d.c. positive field of +10kV/cm ice treeing is less important than that observed at a lower intensity of accretion. On the other hand an a.c. electric field in the same range as that existing at the surface of ac-

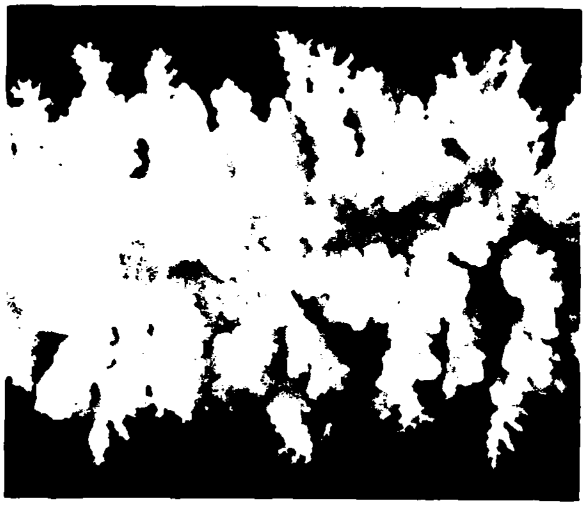

(a) $I_0$=1g/m$^2$s , E=+5kV/cm

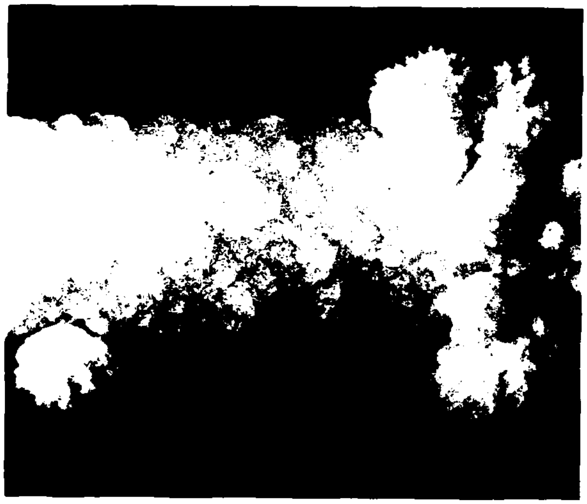

(b) $I_0$=5g/m$^2$s, E=+10kV/cm

Fig. 3 Visual aspect of ice at other intensities $I_0$ of accretion

tual power lines (between 10 and 15kVrms/cm) has little effect upon the visual aspect of ice.

Effect of the electric field upon the density of ice.

In Fig. 4, the density of ice is presented as a function of a.c. and d.c. electric fields for two values of $I_0$. It may be seen that at $I_0$=12g/m$^2$s ac electric field has practically no effect upon the density of ice. On the other hand negative electric field between -10 and -20kV/cm presents a strong effect upon the density of ice. In fact, ice obtained in the absence of an electric field presents a density of 0.88, which is almost the maximum density of atmospheric ice while in a field of -20kV/cm the type of ice obtained is almost soft rime with a density of 0.67. But 12g/m$^2$s is rather high as intensity of accretion compared to that observed under natural icing conditions. For a low intensity of accretion $I_0$=2g/m$^2$s, Fig. 4 shows that the density decreases rapidly for electric field strengths between 5 and 10kV/cm and again the density of ice is smallest under a dc negative field. In addition, at this low intensity of accretion the density of ice is also small under an ac field (0.3g/cm$^3$ at 18kVrms/cm). It is also observed that the density of ice obtained under a dc positive electric field is between that obtained under a.c. and dc negative fields.

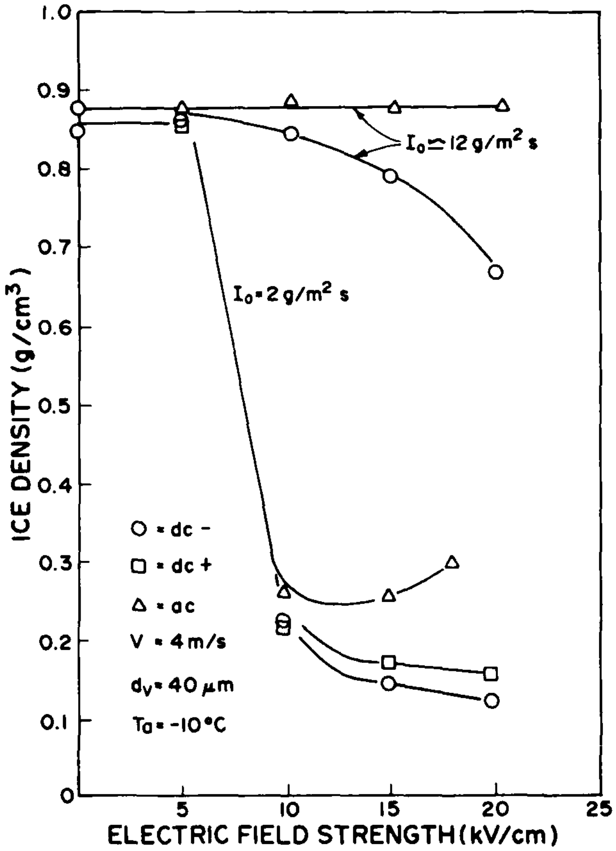

Fig. 4 Density of ice under ac and dc fields ($I_0$=2g/m$^2$s)

Ratio of $I/I_0$ versus applied electric field strength at the surface of the conductor.

As mentioned in the table 1 the intensity I of ice accretion is defined as the product of the collection efficiency ε of water droplets, the liquid water content W and the air velocity V. I represents the amount of impinging water per unit of surface of the conductor during one second. $I_0$ is the intensity of accretion in the absence of an electric field. Fig. 5 shows

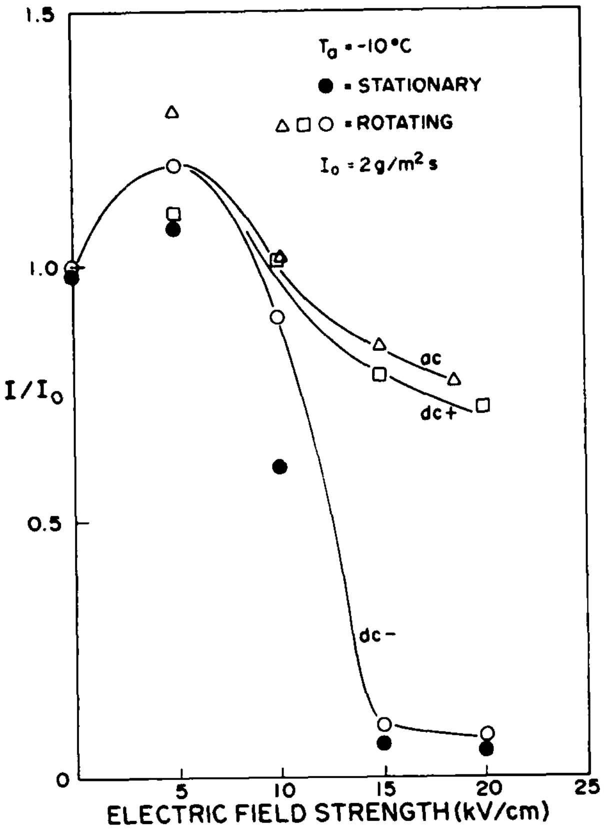

Fig. 5 $I/I_0$ as a function of applied electric field

the variation of the experimental value of the ratio $I/I_0$ as a function of the applied electric field. It is believed that the advantage of this method of presentation is that $I/I_0$ is less dependant on the size of the conductor than I. For $I_0$ equal to $2g/m^2s$, it is shown in fig. 5 that at a field strength of 5kV/cm, $I/I_0$ increases about 20% with respect to the field free value. This increase of $I/I_0$ may be attributed to the increase of the collection efficiency ε due to the dipole attraction of the electric field. The moment of the dielectric dipole is proportional to the square of the applied field strength, as a result the increase of the $I/I_0$ is observed under ac field and dc fields of both polarities. On the other hand ice treeing is not observed (Fig. 2) at a field strength of about 5kV/cm.

With $I_0=2g/m^2s$, the decrease of $I/I_0$ is similar between ac and dc positive field strengths between 5 and 20kV/cm, at the latter value of the electric field, the decrease of $I/I_0$ under dc negative field is very important. At a field strength between -15 and -20kV/cm, $I/I_0$ is about 8% of the field free value and the same result is obtained with a fixed conductor. It may be recalled that the ratio $I/I_0$ can be considered as proportional to the masses $m/m_0$ (c.f. eq. (1)) of ice collected in the presence and in the absence of a field. The results obtained show that at low intensity of ice accretion ($I_0$ small) the mass of ice collected under negative applied field is negligeable.

With $I_0$ equal to $5g/m^2s$, the decrease of $I/I_0$ under dc applied field is less important than that observed at $I_0=2g/m^2s$. In addition, an ac applied field has practically no effect upon the ratio $I/I_0$.

## Corona activities during ice accretion in relation to the visual aspect of ice

Corona current measured during ice accretion is shown in Fig. 6. For each value of applied electric field, i.e. for each experiment, the corresponding value of the corona current presented in Fig. 6 is the average current during an accretion. It is shown that the corona onset field is about 5kV/cm under both polarities. As the field strength increases, corona current under negative polarity increases more rapidly than does the current under positive polarity. The average value of the corona

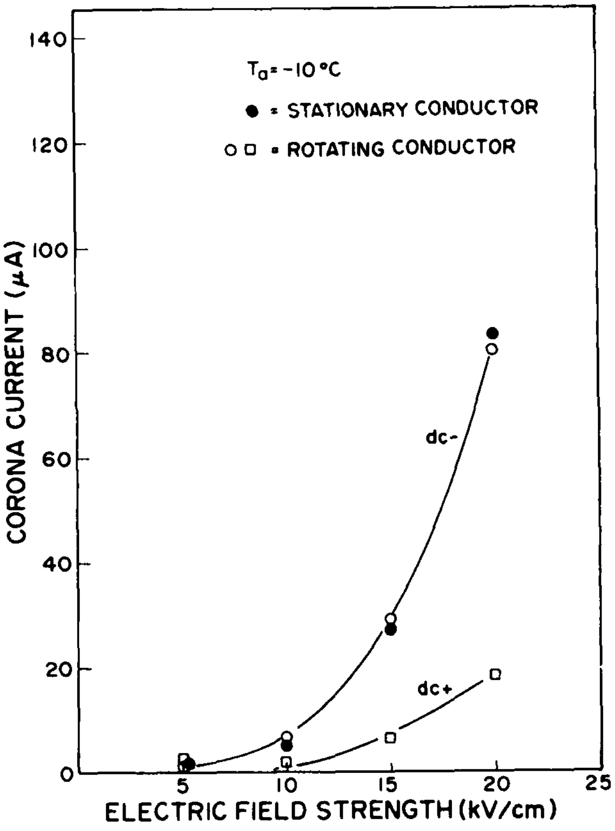

Fig. 6 Corona current versus applied dc field strength

current under negative applied voltage for a fixed conductor is nearly equal to that obtained with a rotating conductor.

These currents give birth to a corona wind, its intensity is proportional to the square root of the corona current.

According to Marco and Velkoff[11] the average heat transfer coefficient is proportional to one-quarter power of the corona discharge current. Thus it may be argued from the results shown in Fig. 6 that a dc negative electric field produces a cooling effect more efficient than a dc positive electric field.

This difference in the cooling effect may be responsible for the low density of ice (small ratio of $I/I_0$) observed under dc negative field compared to that obtained under dc positive field.

Due to the similarity between the shape of ice treeing and that of corona streamer, it is interesting to investigate the formation of corona streamer through the corona pulses. In fact when a corona streamer, which is an avalanche of ions, propagates radially into space for a few ten nanoseconds, then the discharge current is choked off by the space charge developed, as a result a corona pulse is produced. Because there are many thousands streamers per second, a train of pulses is usually observed on the oscilloscope screen. Although ice point yields the same forms of corona discharge as liquid point, the amplitude of corona pulses obtained from ice point is usually smaller than that corresponding to a water or metal point[12]. In fact, the peak of the ice point deteriorates easily due to melting by corona bombardment which limits therefore the discharge generation.

It was observed in the present experiments that, in dry growth regime corona pulses are too small to be clearly observed on the oscilloscope. As the growth regime tends toward the wet limit the amplitude of corona pulses increases. In other words it is easier to observe corona pulses at warmer ambient temperature or with higher liquid water content.

In Fig. 7, corona pulses were measured at -5°C, the other atmospheric conditions were the same as those used in Figs 2-6. Fig. 7b shows that under dc negative applied voltage, the amplitude of corona pulses is very small (20 times smaller)

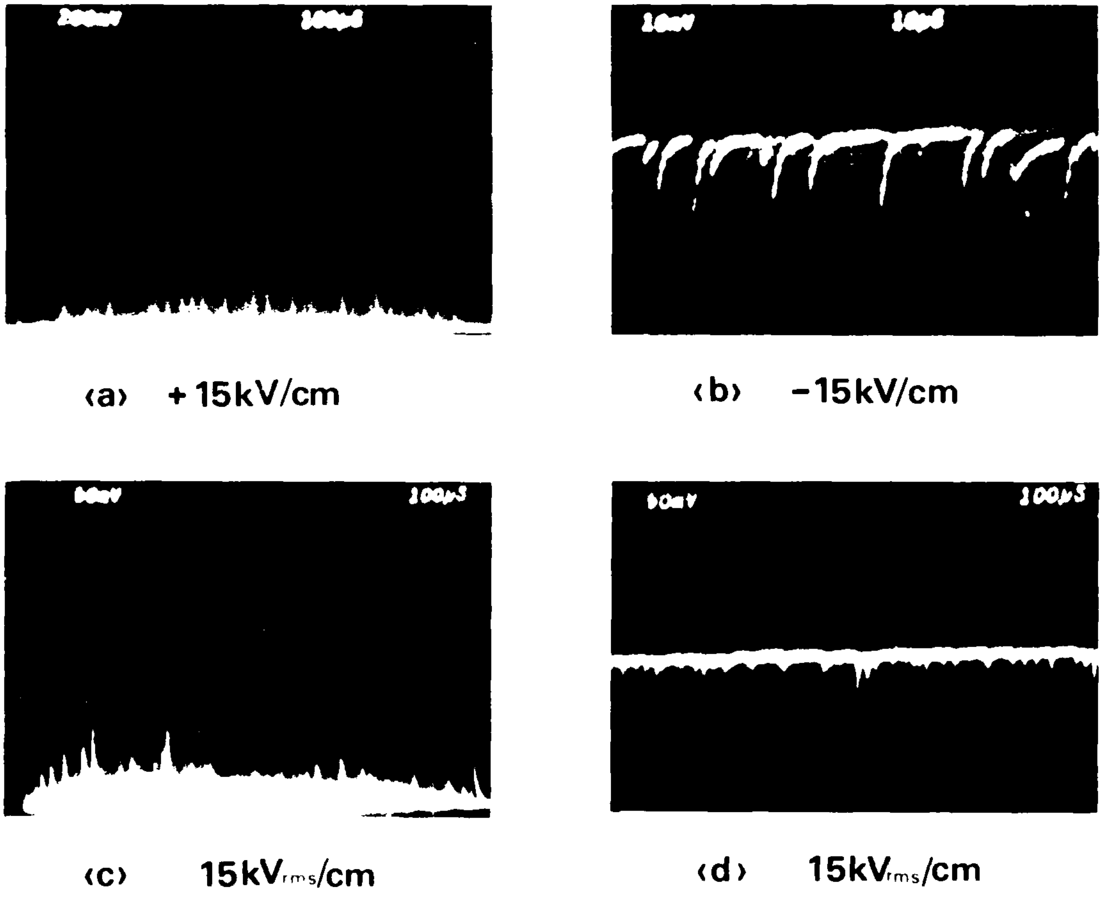

(a) + 15kV/cm

(b) -15kV/cm

(c) $15\text{kV}_{\text{rms}}$/cm

(d) $15\text{kV}_{\text{rms}}$/cm

Fig. 7 Corona pulses during ice accretion

compared to that observed under positive (Fig. 7a) applied voltage. Frequency of d.c. negative corona pulses, measured with a Hewlet-Packard 5315A pulse counter, varies from 9.5kHz at the start of the ice accretion to about 20kHz at the end of the accretion. The spectrum of the negative pulses is very narrow, it ranges from 10 to 60mV. On the other hand, the spectrum of dc positive pulses is very broad and flat, the amplitude of the positive pulses ranges from 10mV to 400mV while the frequency of these positive pulses varies from 4kHz at the start of the experiment to about 14kHz at the end. These results show a similarity between the ice trees and the corona pulses observed under the two polarities of the applied voltage: under dc negative applied voltage, there are numerous small ice trees (Fig. 2c) while ice trees obtained under dc positive applied field present thick trunk and thick branches. Concerning the ac applied voltage, it may be seen that corona pulses during the negative half-cycle (Fig. 7d) are also composed of small pulses. The frequency spectrum of corona pulses measured during the positive half-cycle is also very broad, the amplitude of these pulses is up to 500mV. This may explain the similarity of the visual aspect of ice formed under ac and positive dc fields (Fig. 2a and 2b).

## DISCUSSION

The influence of an electric field upon the ice accretion has been attributed to the corona wind and the freezing of the supercooled droplets along the corona streamers. However, there is no direct proof to confirm the above hypothesis. More work is needed to bring us closer to the actual mechanism.

The most interesting result shown in this report is the negligible amount of ice accreted under negative dc applied field. The enhancement of air convection due to corona wind was mentioned previously as one of the probable causes. Thus, the rapid freezing of droplets before they reach the conductor surface due to corona wind may be responsible of the sharp decrease in the mass of ice accreted (which is proportional to the ratio $I/I_0$ shown in Fig. 5) at negative electric field equal or larger than -15kV/cm. On the other hand, the very thin branches of numerous ice trees observed under dc negative field may be broken under the action of the wind. The spark between the droplets and the conductor may also contribute to the freezing of the droplets when they are approaching the surface of the conductor. It is hoped that the above mentioned phenomenon will be clarified in the next phase of this research program at the University of Quebec.

## CONCLUSIONS

Although a limited number of intensities of accretion have been investigated to date, the following conclusions may be drawn:

1. For low or medium intensities of accretion the amount of ice accreted is negligeable for negative applied field above -10kV/cm.
2. Alternating applied field has little effect upon ice accretion and ice treeing if the intensity of accretion is high.
3. The decrease of the density of ice under dc positive field are between those obtained under a.c. field and dc negative field.
4. From the study on the corona pulses, it is shown that the corona streamers may be responsible for the ice treeing, however more work is needed to verify this hypothesis.

## ACKNOWLEDGEMENT

This work is supported by the Natural Sciences and Engineering Research Council of Canada.

## REFERENCES

1. Prupracher, H.R. (1963). The effect of an external electric field on the supercooling of water drops, J. Geophys. Res., vol. 68, pp. 4463-4474.

2. Pruppracher, H.R. (1973). Electrofreezing of supercooled water, Pure Appl. Geophys., vol. 104, pp. 623-633.

3. Roulleau, M. (1968). The influence of an electric field on the freezing of water, Proc. Int. Symp. on Physics of Ice, Munich, Germany, pp. 631-640.

4. Roulleau, M., Evans, L.F. and Fukuta, N. (1971). The electrical nucleation of ice in supercooled clouds, J. Atmos. Sci., vol. 28, pp. 737-740.

5. Abbas, M.A. and Latham, J., (1969). The electrofreezing of supercooled

water drops, J. Meteor. Soc. Japan, vol. 47, pp. 65-74.

6. Smith, M.H., Griffiths, R.F. and Latham, J. (1971). The freezing of raindrops falling through strong electric fields, Q.J.R. Meteorol. Soc., vol. 97, pp. 494-505.

7. Evans, L.F. (1973). The growth and fragmentation of ice crystals in an electric field. J. Atmos. Sci., vol. 30, pp. 1657-1664.

8. Phan, C.L. and Laforte, J.L. (1981). The influence of electro-freezing on ice formation on high voltage DC transmission lines. Cold. Reg. Sc. & Tech., vol. 4, pp. 15-25,

9. Rush, C.K. and Wardlaw (1957). Icing measurements with a single rotating cylinder. National Aeraunotical Establishement, Canada, Report LT-16.

10. Macklin, W.C. (1962). The density and structure of ice formed by accretion. Quart. J. Roy. Met. Soc., vol. 88, pp. 30-50.

11. Marco, S.M. and Velkoff, H.R. (1963). Effect of electrostatic Fields of Free Convection Heat Transfer. ASME paper no 63-HT-9.

12. Phan, C.L., Pirotte, P., Brunelle, R. and Trinh, N.G. (1974). A Study of Corona Discharge at Water Drops over the Freezing Temperature Range. IEEE Trans. on Power App. & Syst.,vol.PAS-93, no 2, pp. 727-734.

---

DISCUSSION

Stewart: Did you do radio or audible-noise measurements at the same time as you measured the corona current on the iced conductor?

Phan: Not yet, but we have other ground effects and audible noise is the very bulk of it. ...

Lozowski: I'm wondering if you measured the charge on your droplets? I missed the first part of your talk - I'm sorry - and perhaps you mentioned that. Does the spraying process, in fact, charge the droplets, and does this have an effect on the ice accretion?

Phan: We did not measure the charge of droplets, but I think that in the presence of the corona all droplets are very highly charged, but no measurements were made.

Whapham: Has this ice treeing been seen in natural icing conditions on actual lines? Can this be seen in the ice formation or has it been observed?

Phan: We have not observed icing under [...] conditions. But [...] shows the amount of icing on a negative one is very, very small when compared to the amount of ice observed under the positive one on a d-c line.

AD P001682

# THE IMPACT OF FALLING ICE ON ELASTIC STRUCTURES

J.R. Murat, Asst. Prof.
L. Lainey, Res. Asst.
Ecole Polytechnique, P.O. Box 6079, Station "A",
Montréal, Québec, Canada H3C 3A7

A functional model is proposed to predict the deformations induced in an elastic structure by the impact of a free falling block of ice. The initial shock, assumed to be of plastic nature, causes extensive cracking in the ice block. The subsequent contact forces are then neglected and the motions become uncoupled.

The proposed analytical relationship is verified by experimental data involving 58 impact tests on two model structures of different rigidities.

## INTRODUCTION

Telecommunication towers consisting of a slender mast supported at different levels by flexible guy cables are especially prone to ice accumulation. Combination of wind and temperature variations can cause large fragments of ice weighing tens of kilograms to become free from the structure and fall from considerable heights - risking possible damage to any installations below. (figure 1).

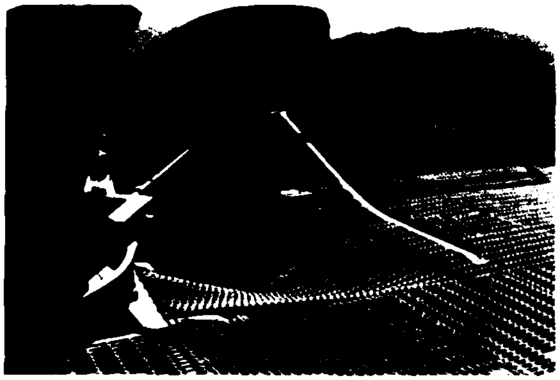

Figure 1 - Damages caused by the impact of falling ice.

It thus becomes important to conceive adequate protection devices for those structures housing costly electronic components. A proper knowledge of the impact mechanism is mandatory to establish reliable design criterion.

Knowing the falling height, the mass and shape of the ice fragment, the potential energy can be accurately estimated by taking into account the air drag. On the other hand, the transfer mechanism of this available energy to the structure is not fully understood.

We have thus attempted, based upon impact tests on an elastic model, to simulate the actual impact behaviour on the protective installation.

The protective structure considered here consists of a steel grating weighing 24 kg/m$^2$ supported by parallel W360x33 steel beams, 1,5 meter apart and spanning 10,9 meters. The resulting natural period of one beam is 0,35 second and its stiffness is 613 N.mm$^{-1}$ for a load applied at mid-span (Clough and Penzien, 1975).

The model structure used for the tests consists of a stiffened steel plate weighing 60 kg supported by four springs. Two spring stiffnesses (259 [illegible] 484 N.mm$^{-1}$) have been used, yielding natural periods of 0,10 and 0,07 second respectively.

The stiffnesses and periods of the model and of the actual structure are within the same range. Only the masses are different, this being a compromise between testing a full scale structure and testing a model that could be easily handled in the laboratory.

A total of fifty height blocks of ice, weighing from 14 to 72 kilograms were dropped on the model structure from heights varying between 2,75 and 12,2 meters, and maximum vertical displacements were measured.

After describing the test procedure, the results will be analysed and a theoretical model of impact will be presented and discussed.

## EXPERIMENTAL MEASUREMENTS

### Model structure

The model structure used in the tests consists of a very stiff mobile loading plate supported by four identical springs, resting on a massive steel base (figure 2). Deflections are recorded at each corner by means of markers attached to the loading plate (figure 3).

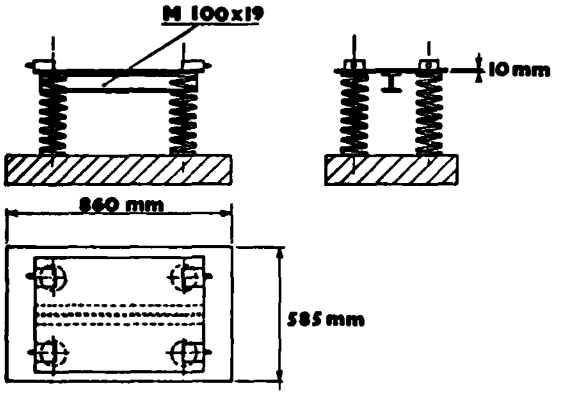

Figure 2 - Plan and elevation views of model structure

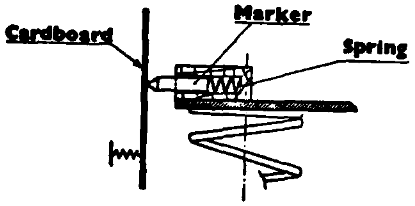

Figure 3 - Recording device

All the springs used were individually calibrated, and it was found that their behaviours were perfectly linear within the range of deformations experienced during the tests. Also, for each rigidity, the calibration curves of the four springs were for all practical purposes identical.

### Ice specimen

The ice used in the test was mechanically cut from commercially available ice-blocks measuring 250 x 550 x 1220 mm. The compressive strenght of the ice was evaluated by a series of tests performed at -10°C on 100 mm cubes loaded at a rate of 0,11 MPa.s$^{-1}$. The average strenght thus obtained was 1,87 MPa with a standard deviation of 0,22 MPa.

### Testing procedure

Prior to testing, the ice blocks were cut to the required dimensions and stored in a coldroom at -10°C. Just before testing, they were measured and weighed and then lifted to the desired height. The zeros of the deflection recorders were noted and the block was dropped onto the target. The release mechanism, which can be seen in figure 4 was designed to insure that the block stayed perfectly vertical during the free fall.

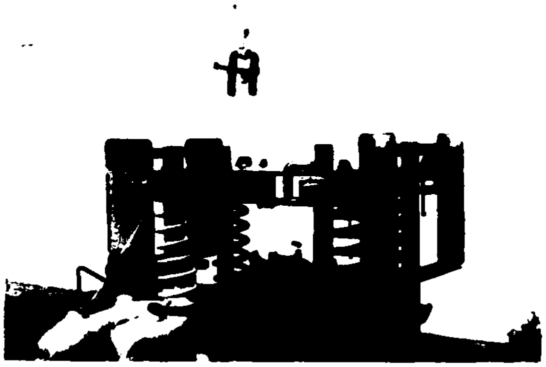

Figure 4 - General view of the model structure showing the release mechanism.

The impact invariably caused the destruction of at least half the block, scattering small chips of less than 20 mm in diameter in all directions (figure 5).

The maximum recorded deflections were then measured at each corner and only the average of the four was considered.

### Test results

The obtained results are given in

Tables 1 and 2 for the two tested structural rigidities. For each test, the following informations are tabulated:

h = free fall height (m)
$m_1$ = mass of the ice block (kg)
$\alpha$ = mass ratio of the ice block to the mobile loading plate
V = potential energy of the ice block just before impact (N.m)
z = average maximum vertical deflection of the target (mm).

In Tables 1 and 2, the tests are classified into three categories corresponding to similar values of $\alpha$(0,25; 0,6; 1,0) and within each group are placed in order of increasing values of potential energy.

Figure 5 - *Impact of ice block on the model structure.*

Table 1 - Experimental data for a structural rigidity of 259 $N.mm^{-1}$

| h (m) | $m_1$ (kg) | $\alpha$ | V (N.m) | z (mm) | h (m) | $m_1$ (kg) | $\alpha$ | V (N.m) | z (mm) | h (m) | $m_1$ (kg) | $\alpha$ | V (N.m) | z (mm) |
|---|---|---|---|---|---|---|---|---|---|---|---|---|---|---|
| 6.0 | 14 | 0.23 | 824 | 26 | 11.2 | 41 | 0.68 | 4430 | 69 | 5.1 | 66 | 1.09 | 3245 | 70 |
| 6.0 | 14 | 0.23 | 824 | 33 | 11.2 | 41 | 0.68 | 4483 | 63 | 5.1 | 66 | 1.10 | 3260 | 59 |
| 6.0 | 16 | 0.27 | 942 | 35 | 11.6 | 40 | 0.66 | 4495 | 74 | 5.1 | 69 | 1.14 | 3394 | 70 |
|  |  |  |  |  |  |  |  |  |  | 6.4 | 69 | 1.15 | 4313 | 63 |
| 5.6 | 28 | 0.47 | 1538 | 36 | 2.8 | 46 | 0.88 | 1252 | 51 | 11.5 | 54 | 0.89 | 6036 | 83 |
| 5.6 | 29 | 0.48 | 1593 | 39 | 5.4 | 43 | 0.81 | 2278 | 59 | 11.3 | 56 | 0.94 | 6202 | 98 |
| 5.6 | 29 | 0.48 | 1593 | 51 | 5.4 | 45 | 0.85 | 2384 | 58 | 11.5 | 57 | 0.95 | 6430 | 102 |
| 5.6 | 32 | 0.53 | 1758 | 43 | 5.4 | 45 | 0.85 | 2384 | 62 | 11.6 | 57 | 0.95 | 6486 | 98 |
| 5.6 | 33 | 0.55 | 1813 | 37 | 5.4 | 46 | 0.87 | 2437 | 59 | 11.5 | 58 | 0.96 | 6459 | 98 |
| 5.6 | 35 | 0.58 | 1923 | 42 | 5.4 | 47 | 0.89 | 2490 | 51 | 11.5 | 58 | 0.96 | 6487 | 100 |
| 11.8 | 37 | 0.62 | 4294 | 64 | 5.4 | 48 | 0.91 | 2543 | 61 | 11.6 | 58 | 0.96 | 6515 | 99 |
| 11.5 | 39 | 0.64 | 4355 | 75 | 5.1 | 65 | 1.08 | 3205 | 60 | 11.4 | 59 | 0.98 | 6598 | 88 |
|  |  |  |  |  |  |  |  |  |  | 11.3 | 69 | 1.15 | 7615 | 112 |

Table 2 - Experimental data for a structural rigidity of 484 $N.mm^{-1}$

| h (m) | $m_1$ (kg) | $\alpha$ | V (N.m) | z (mm) | h (m) | $m_1$ (kg) | $\alpha$ | V (N.m) | z (mm) | h (m) | $m_1$ (kg) | $\alpha$ | V (N.m) | z (mm) |
|---|---|---|---|---|---|---|---|---|---|---|---|---|---|---|
| 5.7 | 14 | 0.23 | 783 | 19 | 5.7 | 30 | 0.51 | 1700 | 31 | 5.3 | 67 | 1.12 | 3484 | 34 |
|  |  |  |  |  | 11.8 | 35 | 0.59 | 4080 | 49 | 5.3 | 71 | 1.19 | 3707 | 41 |
| 5.7 | 27 | 0.45 | 1510 | 30 | 11.8 | 37 | 0.62 | 4311 | 49 | 5.3 | 72 | 1.20 | 3738 | 39 |
| 5.7 | 27 | 0.45 | 1521 | 23 | 11.8 | 40 | 0.67 | 4657 | 48 | 11.6 | 59 | 0.98 | 6714 | 61 |
| 5.7 | 28 | 0.46 | 1549 | 20 | 11.7 | 43 | 0.72 | 4935 | 53 | 11.5 | 60 | 1.01 | 6773 | 62 |
| 5.7 | 28 | 0.47 | 1577 | 20 | 11.7 | 45 | 0.75 | 5153 | 58 | 11.5 | 64 | 1.07 | 7189 | 65 |
| 5.7 | 29 | 0.49 | 1622 | 23 |  |  |  |  |  | 11.4 | 67 | 1.12 | 7460 | 74 |
| 5.7 | 30 | 0.50 | 1666 | 27 | 5.3 | 67 | 1.11 | 3463 | 38 | 11.4 | 68 | 1.13 | 7560 | 66 |
|  |  |  |  |  |  |  |  |  |  | 11.5 | 68 | 1.14 | 7694 | 74 |

## IMPACT MODEL

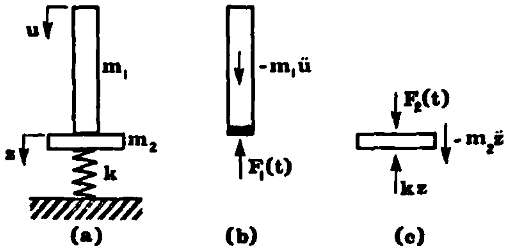

Figure 6 - Analysis of contact forces

For the purpose of this study, the ice block will be assumed to be a rigid body. Taking into account the experimental observations, we furthermore assumed the impact to be plastic (coefficient of restitution equal to zero). As shown in figure 6.a, the displacement of the ice block from its point of contact with the loading plate will be denoted by u and the displacement of the plate by z. The masses of the block of ice and of the plate are $m_1$ and $m_2$ respectively and the total stiffness of the springs is k.

The equilibirum of forces acting on the block of ice (figure 6.b) and on the plate (figure 6.c) during impact may be expressed by:

$$F_1(t) + m_1\ddot{u} = 0 \qquad (1)$$

and: $$F_2(t) + kz + m_2\ddot{z} = 0 \qquad (2)$$

Adding (1) to (2) and noting that $F_1(t) = -F_2(t)$ yields:

$$kz + m_1\ddot{u} + m_2\ddot{z} = 0 \qquad (3)$$

Also, the assumption of plastic impact requires that the movement of the ice block be equal to the displacement of the loading plate (Goldsmith, 1960), leading to the equation of motion:

$$\ddot{z}(m_1 + m_2) + kz = 0 \qquad (4)$$

The solution of this single degree of freedom damped free vibration equation is:

$$z = C_1 \sin \omega t + C_2 \cos \omega t \qquad (5)$$

where t represents the time (t=0 at impact) and ω is the natural frequency defined as:

$$\omega^2 = \frac{k}{m_1 + m_2} \qquad (6)$$

The constants $C_1$ and $C_2$ in equation (5) can be evaluated by consideration of the initial conditions. Just before impact, the block of ice has a velocity v given by the free fall relationship:

$$v = \sqrt{2\,g\,h} \qquad (7)$$

where g is the acceleration of gravity and h the height through which the block is dropped.

Conservation of momentum implies that:

$$m_1\,v = m_1\,\dot{u}_o + m_2\,\dot{z}_o \qquad (8)$$

where $\dot{u}_o$ and $\dot{z}_o$ are the initial velocity of the block and of the plate just after impact. Considering a plastic impact implies that $\dot{u}_o = \dot{z}_o$. Substituting (7) and (8) into (5), and noting that the initial displacement $z_o$ is zero yields:

$$z = \frac{m_1}{\omega(m_1 + m_2)} \sqrt{2\,g\,h}\,\sin \omega t \qquad (9)$$

If there would be no shattering of the ice during impact, the maximum displacement of the plate, $z_t$, would be as follows:

$$z_t = m_1 \sqrt{\frac{2gh}{k(m_1 + m_2)}} \qquad (10)$$

and the equations of motion for the plate will reduce to:

$$z = z_t \sin \omega t \qquad (11)$$

$$\dot{z} = z_t \sqrt{\frac{k}{m_1 + m_2}} \cos \omega t \qquad (12)$$

However, our experiments have shown that the ice invariably shatters. The driving force $F_1(t)$ may be expressed from equations (1) and (4) in term of the motion of the plate, i.e.:

$$F_1(t) = k\,\frac{m_1}{m_1 + m_2}\,z \qquad (13)$$

Rupture of the ice will begin at time $t_1$ when this force will reach the value:

$$F_1(t_1) = \sigma_c\,A \qquad (14)$$

where $\sigma_c$ is the dynamic crushing strength of the ice and A is the contact area.

Substituting this into (13) and using equations (11) and (12) gives the displacement $z_1$ and the velocity $\dot{z}_1$ of the plate at time $t_1$:

$$z_1 = u_1 = \sigma_c\,A\,\frac{m_1 + m_2}{k\,m_1} \qquad (15)$$

$$\dot{z}_1 = \dot{u}_1 = \sqrt{\frac{k}{m_1 + m_2}\,(z_t^2 - z_1^2)} \qquad (16)$$

where $z_t$ is defined by relation (10).

As long as the ice ruptures, the displacements u and z of the block and of the plate are different and the equations of motion become uncoupled. Substituting (14) into equations (1) and (2) yields:

$$m_1 \ddot{u} + \sigma_c A = 0 \qquad (17)$$

and

$$m_2 \ddot{z} + kz - \sigma_c A = 0 \qquad (18)$$

The solution of the equation of motion of the plate is of the form:

$$z = D_1 \sin \Omega\tau + D_2 \cos \Omega\tau + \frac{\sigma_c A}{k} \qquad (19)$$

when the time $\tau$ is defined as $t - t_1$ (thus $\tau = 0$ when the ice starts to crush) and $\Omega$ is the natural frequency of the structure alone:

$$\Omega^2 = \frac{k}{m_2} \qquad (20)$$

Now introducing the initial conditions of equations (15) and (16) into equation (19) leads to:

$$\text{At } \tau=0 \text{ , } z_1 = \sigma_c A \frac{m_1 + m_2}{k\ m_1} = D_2 + \frac{\sigma_c A}{k} \qquad (21)$$

$$\dot{z}_1 = \sqrt{\frac{k}{m_1 + m_2}(z_t^2 - z_1^2)} = \Omega\ D_1 \qquad (22)$$

Hence with these values substituted into equation (19), the final result for the plate displacement is:

$$z = \frac{\dot{z}_0}{\Omega} \sin \Omega\tau + \frac{\sigma_c A}{k} \frac{m_2}{m_1} \cos \Omega\tau + \frac{\sigma_c A}{k} \qquad (23)$$

from which the maximum displacement $z_{max}$ can be derived:

$$z_{max} = \frac{1}{\alpha+1} \sqrt{\frac{2V\alpha}{k} - \frac{\sigma_c^2 A^2}{k^2} (\alpha+1)^2} + \frac{\sigma_c A}{k} \qquad (24)$$

where $\alpha$ is the mass ratio of the block of ice to the mobile plate, and V is the potential energy of the falling block just before impact, given by:

$$V = m_1\ g\ h \qquad (25)$$

This solution is valid only if the ice keeps crushing until the loading plate reaches its maximum deflection.

## ANALYSIS OF RESULTS

From equation (24), the dynamic crushing strength of the ice can be expressed in term of the maximum displacement of the plate, that is:

$$\sigma_c = \frac{1}{2A} \left[ k z_{max} \pm \sqrt{\frac{4kV\alpha}{(1+\alpha)^2} - k^2\ z^2_{max}} \right] \qquad (26)$$

Substituting $z_{max}$ by the recorded maximum deflections yielded for $\sigma_c$ values ranging from 0 to -0,11 MPa for the structural rigidity of 259 N.mm$^{-1}$ and from -0,06 to -0,20 MPa for the structural rigidity of 484 N.mm$^{-1}$. These values are very small compared to the static crushing strength of the ice (2 MPa) and furthermore correspond to tensile stresses. This implies that during the motion of the plate, the contact forces are negligible and that the failure of the ice occurs only at the very beginning of the impact.

In order to evaluate the amplitude of the stresses developped in the block of ice at the time of impact, the elasticity of the ice must be taken into account.

A change $\Delta v$ of the velocity of one end of an elastic rod of constant cross-section gives rise to a maximum stress (Prescott, 1924) of amplitude:

$$\sigma = \Delta v \sqrt{\frac{\rho E}{g}} \qquad (27)$$

where $\rho$ is the weight density and E the elastic modulus of the rod.

The change of velocity at the contact face of the block can be expressed from equations (8) and (7):

$$\Delta\ v = v - \dot{u}_0 = \frac{1}{\alpha + 1} \sqrt{2\ g\ h} \qquad (28)$$

From our experimental conditions, the average value for $\Delta v$ was in the order of 8 m.s$^{-1}$ yielding a maximum stress of approximately 23 MPa. This will be more than sufficient to cause extensive crushing of the ice block.

Neglecting the contact forces during the subsequent motion of the plate leads to a simplified relationship for its maximum deflection:

$$z_{max} = \frac{1}{\alpha + 1} \sqrt{\frac{2\ V\ \alpha}{k}} \qquad (29)$$

In figures 7 and 8, the values of the maximum recorded deflections listed in Tables 1 and 2 are plotted against the potential energy, with ratio $\alpha$ as a parameter. The model predictions, computed from equation (27) are also plotted and are shown to be in good agreement with the experimental data.

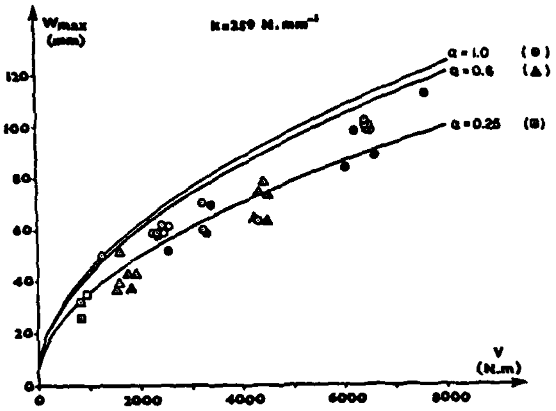

Figure 7 - Recorded deflections as a function of potential energy (eq. 29:-)

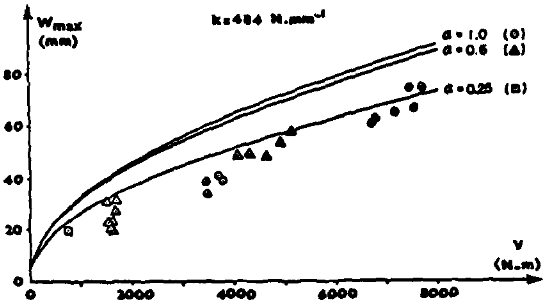

Figure 8 - Recorded deflections as a function of potential energy (eq. 29:-)

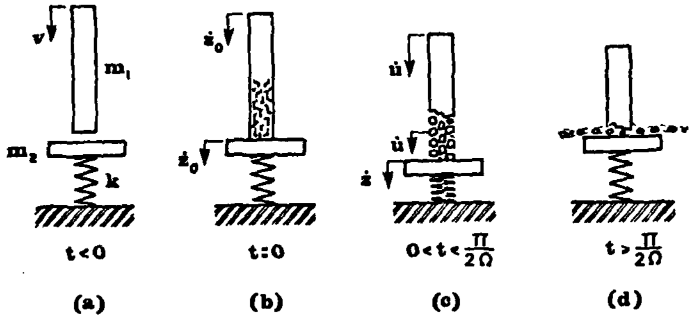

Figure 9 - Proposed impact model

## DISCUSSION AND CONCLUSIONS

The proposed model of impact is summarized in figure 9. The initial velocity of the structure is computed by assuming a perfectly plastic shock (figure 9.a). The impulsive force developped at the very time of impact causes an extensive rupturing of the ice (figure 9.b) which in turns cancels out any subsequent contact forces. The following movements of the block of ice and of the structure are then uncoupled (figure 9.c) until the structure reaches its maximum deflection. The applicability of the model ends at this point. The ensuing motions (figure 9.d) are associated with an horizontal scattering of the ice fragments (figure 5) and are not considered here.

From relation (29), the strain energy stored in the model structure may be expressed as:

$$U = \frac{1}{2} k z_{max}^2 = \frac{\alpha}{(\alpha + 1)^2} V \qquad (30)$$

The actual stored energy, deduced from the experimental measurements are plotted in figure 10, together with the straight lines representing equation (30) for typical values of α. Very good agreement is shown to exist between the experimental results and the analytical predictions. The difference between the actual and computed values of the strain energy may be related to the amount of energy required to deform and crush the ice.

In order to fully validate the proposed model, experimental recordings of the transient displacements and contact forces are currently underway.

## ACKNOWLEDGMENTS

This research has been partly sponsored by "La société de radio-télévision du Québec" (Radio-Québec) through the consulting office of Gascon, Vigneault, Dumais & Ass. and by the National Sciences and Engineering Research Council of Canada (grant no NRC A-1199).

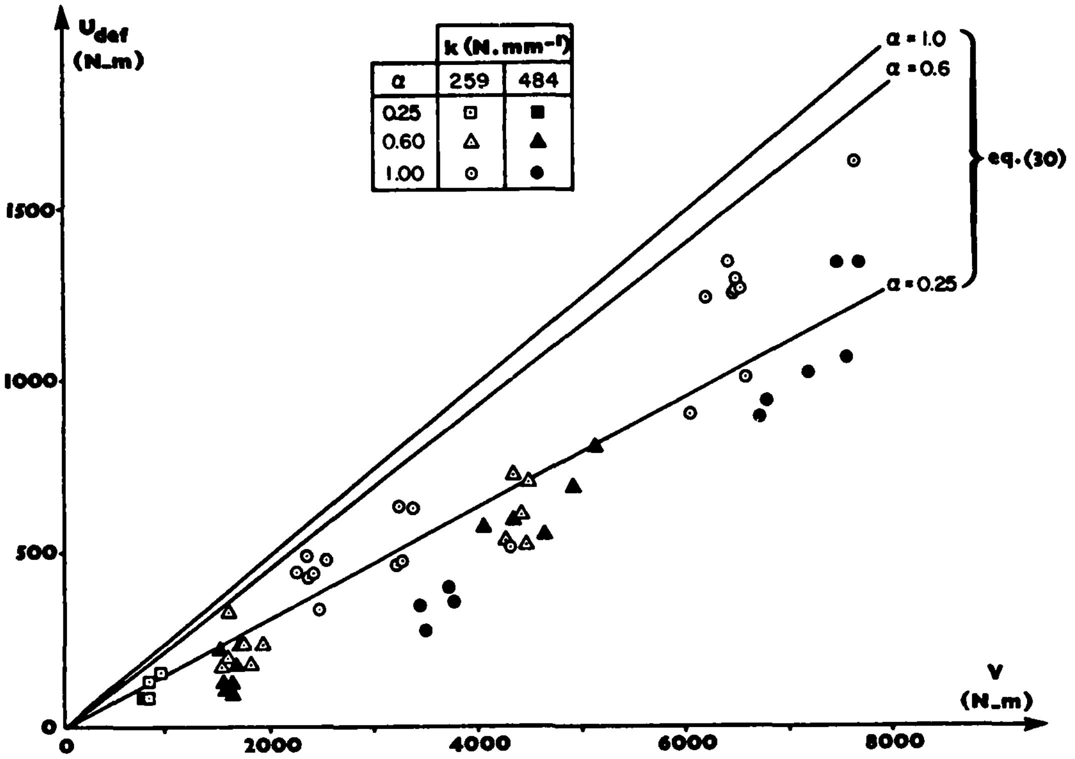

Figure 10 - Strain energy stored in the structure as a function of available potential energy. Experimental data and theoretical predictions.

REFERENCES

*CLOUGH, R.W.; PENZIEN, J. 1975. "Dynamic of Structures", McGraw-Hill Book Company.*

*GOLDSMITH, W. 1960. "Impact - The Theory and Physical Behaviour of Colliding Solids". Edward Arnold Publishers, London.*

*PRESCOTT, J. 1924. "Applied Elasticity". Longmans, Green and Co. London.*

DISCUSSION

Patnaik: The 1965 tower failure in Quebec - was that from ice falling?

Lainey: No, that was ice accumulation. It was not collapse due to the impact of ice.

Patnaik: On one slide you showed there was 10 cm accumulation of ice on the guys - was that the same tower?

Lainey: No.

Lozowski: I'm concerned about your use of fresh water ice as a model for accreted ice. Do you have any comments on that? My comment might be that one frequently observes hailstones, that are essentially accreted ice, bouncing off of hard surfaces, rather than actually crushing.

Lainey: We used fresh water ice because it was available and it's very easy to find. The density of ice is 0.9. I don't think it's a matter of the crushing strength because the impact is so high that in any case it crushes the ice. So I don't know if there is any problem in using fresh water ice - I don't think so.

AD P001683

# ESTIMATION OF COMBINED ICE AND WIND LOAD ON OVERHEAD TRANSMISSION LINES

Pierre McComber Université du Québec à Chicoutimi, Chicoutimi, Québec
Richard Martin Hydro-Québec, Montréal, Québec
Gilles Morin Université du Québec à Chicoutimi, Chicoutimi, Québec
Luong Vo Van Hydro-Québec, Montréal, Québec

## ABSTRACT

In recent years, the design of high voltage transmission lines has been increasingly optimized. In areas where ice accretion on conductors is possible, the load resulting from added weight or increased aerodynamic forces becomes an important design parameter. At the present, calculations for combined icewind loads do not take into account the effect of the accretion shape. Ice accretions are formed on a conductor in a wind tunnel for three types of ice: soft rime, hard rime and glaze. Aerodynamic vertical and horizontal forces are then measured for different wind velocities. It is shown that when the wind remains in the direction of the ice build-up, the aerodynamic force due to the asymmetrical shape is responsible for a significant increase in the total force and that the present combined ice-wind load calculations can dangerously underestimate the risk of an overload.

## INTRODUCTION

High voltage transmission lines are subjected like all structures to wind loading. Adequate meteorological data is available to evaluate this design factor in most regions. However in certain climatic area there is an added hazard of rime and glaze accretions on transmission lines (Bourgsdorf et al., 1968). In these areas glaze and rime has to be taken into account in the design (Ghannoum, 1980) eventhough at the moment, little or no statistical meteorological data is available on ice accretions in areas where the transmission lines are set up. Moreover ice and wind have a combined effect resulting in increased wind loading. In these cases not only the weight but the shape of the ice accretion has an important effect on the total load (Bassraskaya et al., 1981).

Most of the research that has been conducted on the combined effect of ice and wind has been related to wind induced vibrations (Blevins, 1979). Wind induced vibrations of the type referred to as galloping require an unsymmetrical shape which is obtained only on occasions where conductors are covered by an ice accretion. Since these vibrations start even for a thin layer of ice, these studies have not considered heavy loading due to ice.

For the calculations of the combined static load, the shape of the accretion is important, and there is practically no study existing to determine possible iceaccretion shape of a type large enough to create an overload.

In this paper the design criteria used by an hydro-electric power company (Hydro-Quebec) to predict wind and ice combined loading are compared with loads measured for wind tunnel accretions.

## PRESENT METHOD FOR THE CALCULATION OF WIND AND ICE LOADS

Recent Hydro-Quebec transmission lines are disigned to withstand some limit loads. The first one, wind load on bare cables consists of a wind speed of 136.8 km/hr (85 mph). A second load consists of a maximum radial ice thickness of 4.45 cm (1.75 in.) with no wind. Another load consists of combined wind and ice: 3.18 cm (1.25 in.) of ice with a wind speed of 72.4 km/hr (45 mph). These loads are all assumed to have a return period of at least 50 years. For these conditions, the forces are calculated as follows.

### Wind limit force

The limit horizontal or drag force due to the wind on a bare conductor is calculated by the following relation:

$$F_h = 0.6469\ D_o V^2 \qquad [1]$$

where $F_h$ is the horizontal force (N/m); $D_o$ the conductor diameter (m); V the wind velocity (m/s).

### Ice limit force

The ice on a conductor adds a weight. An increased vertical force (N/m) $F_V$ is calculated by adding the weight of ice to the weight of the conductor $W_c$:

$$F_V = W_c + W_i \qquad [2]$$

### Combined limit force

The calculation of the combined limit load is based on the assumption of a cylindrical shape for the ice accretion. This shape has no positive or negative aerodynamic lift forces, so that the vertical force is simply calculated by equation (2). The horizontal force is obtained from equation (1) but using a modified diameter to account for the ice. The volume and weight of the ice are related by the following expression:

$$\frac{\pi}{4}(D^2 - D_o^2) = \frac{W_i}{\rho_i g} \qquad [3]$$

in which $\rho_i$ is the ice density (0.92).

The horizontal and vertical force are the added vectorially to yield the total force:

$$F_T = (F_h^2 + F_V^2)^{\frac{1}{2}} \qquad [4]$$

## AVAILABLE DATA ON WIND AND ICING LOADS

In order to be able to evaluate combined wind and ice loads, statistical meteorological data on ice thicknesses as well as wind speeds during icing or immediately after must be considered. Unfortunately, there is no reliable data at the present on ice accretion thicknesses. Measurements for ice accretion thicknesses have just started being taken recently. Wind speeds have been measured for a much longer time. Table 1 for example shows the annual maximum wind speeds obtained during icing precipitations and the period during which temperature is below 0°C with a maximum of 72 hours for a few Canadian airports.

TABLE 1

| | Recurrence interval (years) | | | | | | |
|---|---|---|---|---|---|---|---|
| | 2 | 5 | 10 | 25 | 50 | 100 | 150 |
| Bagotville (24 years) | 14.8 | 17.0 | 18.3 | 20.1 | 21.5 | 22.8 | 23.7 |
| Dorval (24 years) | 14.3 | 17.0 | 18.8 | 21.0 | 22.8 | 24.6 | 25.0 |
| Goose (24 years) | 13.9 | 16.1 | 17.9 | 20.1 | 21.5 | 23.3 | 23.7 |
| Knoblake (24 years) | 15.2 | 17.9 | 20.1 | 22.8 | 24.6 | 26.8 | 27.3 |
| Mont-Joli (24 years) | 15.7 | 18.8 | 20.6 | 22.8 | 24.6 | 26.8 | 27.3 |
| Ottawa (24 years) | 13.4 | 16.1 | 17.9 | 20.1 | 21.5 | 23.3 | 23.7 |
| Sept-Iles (24 years) | 17.4 | 20.6 | 22.4 | 24.1 | 26.4 | 28.2 | 29.1 |
| Val d'Or (24 years) | 10.7 | 12.3 | 13.9 | 15.2 | 16.1 | 17.4 | 17.9 |

## COMPARISON OF WIND TUNNEL AND FIELDS SAMPLES

Ice accretion samples were obtained in a refrigerated wind tunnel having a test section of 0.61 x 0.61 m. Samples were formed on a BERSIMIS conductor: 3.5 cm in diameter, and a weight of 21.46 N/m.

### Supercooled droplets

Six nozzles were used in the wind tunnel to produce the supercooled droplets 3 m upstream of the test section before the contraction (air atomizing Nozzles #30, fluid cap #40100, air cap #120-6-35-60). The air and water pressures were adjusted in the nozzles to give the good combination of water content and droplet diameters required to produce either rime or glaze. A spectrum of droplet diameters was obtained for each nozzle setting using the silver colloid film method (Godard, 1960). For example a mean volume diameter of 24.3 mm was used to produce soft rime.

### Water content

The water content of the air was measured by the single cylinder method (Rush et al. 1957). From the weight of ice accumulated on a 3.15 mm radius cylinder during a short period of time (30 s to 1 min) the water content is evaluated by the following equation:

$$m = \frac{\pi}{V_i hVT} \left[ \left( \frac{V_i W}{\pi l} + r_l^2 \right)^{\frac{1}{2}} - r_i \right] \qquad [5]$$

where m is the water content (g/m$^3$); T the accumulation time (s); V the air speed (m/s); $v_i$ the specific volume of the rime (cm$^3$/g); w the mass of accumulated ice (g); $_i r$ , $\ell$ and h are the radius (cm) length (cm) and collection efficiency of the cylinder respectively.

### Ice accretion samples

For the wind tunnel ice accretion experiments, the conductor was supported at each end by ball bearings and a small metal rod was used as a torsion spring to control the rotation of the conductor during ice formation. A 1,9 mm steel rod 21,4 cm long was used as a spring. This simulates the torsional rigidity existing in the center of a 70 m sub-span. A sub-span is defined as the length of conductor between spacer-dampers on a four - conductor bundle.

### Comparison of different ice accretion shapes

Figure 1 shows an ice accretion obtained on a fixed cylinder in the wind tunnel.

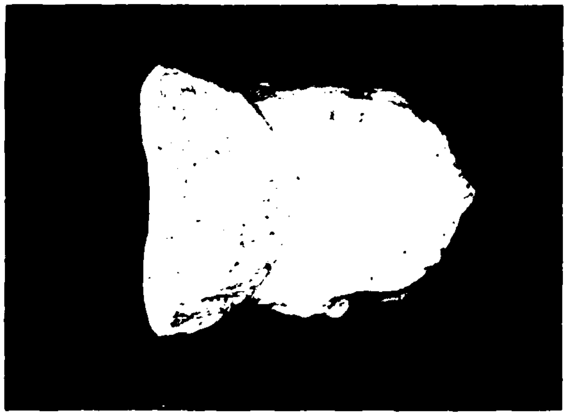

Fig. 1 Ice accretion obtained on a fixed cylinder in a wind tunnel.

On Figure 2, a two conductor bundle is shown (Kellow and Martin, 1976) which remained almost fixed during ice formation, the torsional rigidity being much greater. It is clear from the photograph that when the conductor is not permitted to rotate and the wind is steady in its direction, the ice forms on only one side of the conductor.

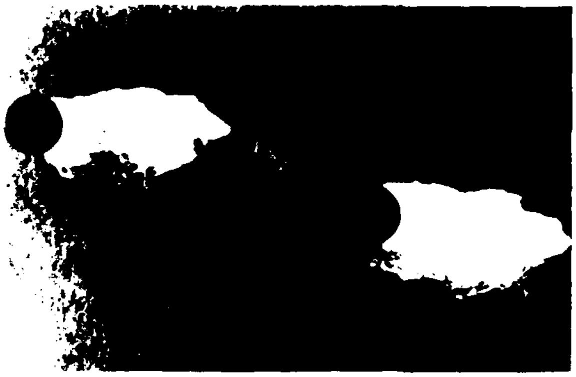

Fig. 2 Photograph of the cross-section of ice accretion on a two-conductor bundle after 15 3/4 hrs of icing in a wind tunnel.

This is explained by the fact that supercooled droplets hit the iced surface only on the front part of an exposed object (McComber, 1981).

Long conductors however can usually rotate somewhat around their axis under the weight of the ice formed. This can be verified on natural ice samples. Figure 3 is a photograph under polarized light of an accretion cross-section.

This sample was collected in the Baie-Comeau area after glaze was formed on transmission lines April 6th 1981 (Laforte, 1982). For a fixed cable, ice crystal would grow almost radially, the spiraled growth visible on Figure 3 is a result of a torsion of the cable while the ice was building up.

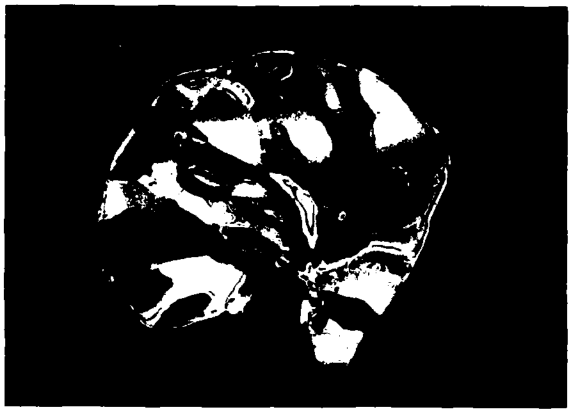

Fig. 3 Photograph under polarized light of a transmission line accretion formed in the Baie-Comeau area (6/4/81)

Figure 4 shows samples that were obtained in the wind tunnel with the torsion spring described above.

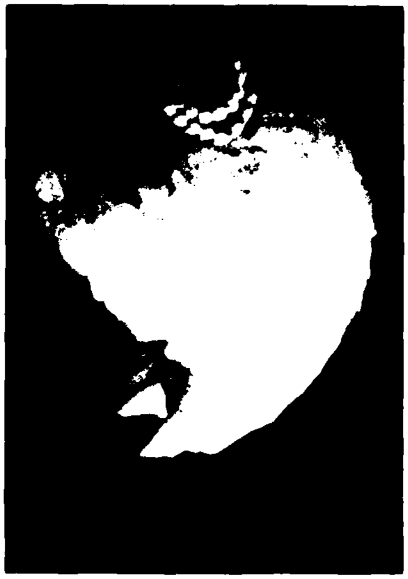

Fig.4 Photograph of ice accretion obtained on a cylinder permitted to rotate in a wind tunnel.

Figure 5 shows shapes of ice accretion obtained on a six conductor bundle, also in a wind tunnel, with an experimental set-up permitting a small rotation of the bundle under the weight of ice. Figure 6 is a photograph of sample actually collected in the field by Hydro-Quebec. On this occasion, a four-conductor bundle twisted on itself. The spacing between the conductors is 457 mm. Even if one considers the possibility of slight changes in the wind direction, such a shape is again best explained by the torsion of the conductor thus permitting ice build up on approximately 180° around the conductor.

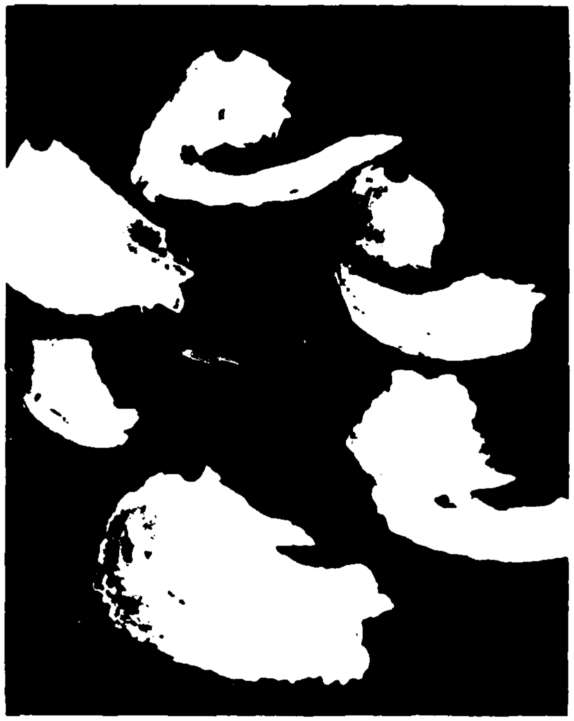

Fig. 5 Photograph of cross-section of ice accretion on a six-conductor mini-bundle after 20 1/4 hrs of icing in a wind tunnel.

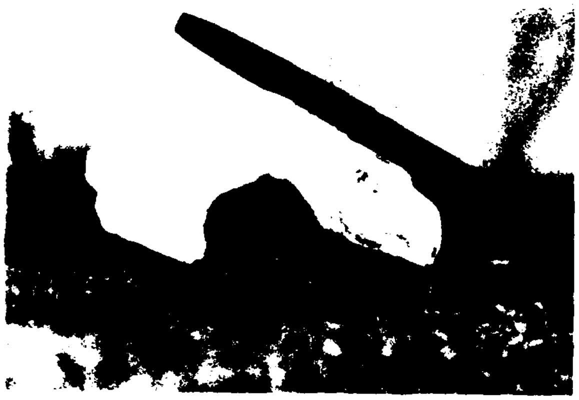

Fig. 6 Photograph of the ice accretion formed on an actual transmission line conductor (25/2/78), in the Quebec City area.

## INSTRUMENTATION AND CALIBRATION

### Temperature and wind speed measurements

Temperatures are measured in the wind tunnel with a thermometer (± 0.5°C). Wind speeds are measured with a Pitot tube (Dwyer No. 160, 7.9 mm diam.). The accuracy of the water manometer was 0.64 mm.

### Lift and drag forces measurements

Vertical forces on ice covered conductors are measured with a load cell Interface In. B50 while the drag force is measured by strain gauges (Intertechnology, EA-13 - 125AD - 12C E) monted on thin plates of metal. A set-up permits the uncoupling of the drag and lift forces by blocking the vertical deflection while the horizontal force is measured and vice-versa.

A resistance bridge and an amplifier (10 channel) is used to handle the signal (Intertechnology Ltd, Vishay No. 2100). The signals are then recorded on a graph by a pen recorder.

### End effects for the measurements of drag and lift forces on a short cylinder

Since the drag and lift forces are measured in a wind tunnel, one must consider end effect corrections, experi- mental length being relatively short. This correction varies with the wind speed equivalent to Reynolds number = $8.8 \times 10^4$. Goldstein (1965) gives a correction factor reproduced on Fig. 7. This correction factor was used to modify the wind tunnel measurements in order to obtain the results applicable for a large L/D ratio.

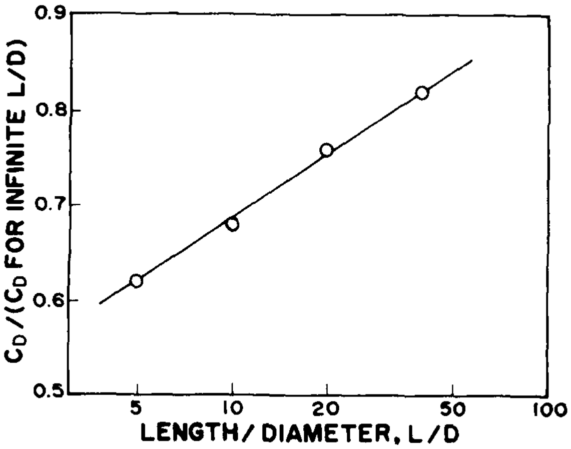

Fig. 7 Correction factor on the drag coefficient for finite length cylinder (Goldstein, 1965)

### Force measurements checking

A calibration check was made by measuring the drag coefficient of a 3.5 cm diameter cylinder. Fig. 8 compares the drag coefficient obtained with the wind tunnel set-up and results obtained by various authors and reported by Goldstein (1965). The experimental values of the drag force were first corrected for end effects. The comparison on Fig. 8 indicates that the instrumentation set-up to measure forces was adequate and could be applied to measurements on ice covered conductors.

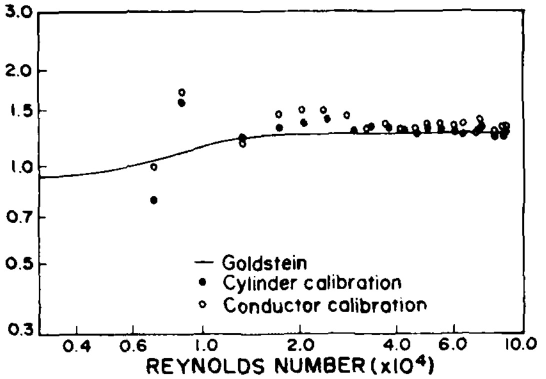

Fig. 8 Cylinder and conductor drag coefficient as a function of Reynolds number.

## Experimental procedure

The experiment was done in two steps: ice formation and measurement on the sample using wind only. Once the adjustements were made for the flow, the ice accretion samples were formed using the torsion spring set-up. The size of the ice accretion sample was controlled by the duration of icing period. Once the sample was formed, its dimensions and weight were recorded and a photograph was taken.

Then, it was reinstalled on the measurement support, and drag and lift forces were measured at different wind speeds for the different samples. The measurements were made for speeds up to 37 m/s or until the ice accretion shattered under the effect of high wind speeds.

## RESULTS

In order to obtain information on the behavior of different types of ice, conductors were covered in succession by soft rime, hard rime and glaze. Also, in order to verify how there results could be reproduced in the wind tunnel, the soft rime experiments were done three times for each thickness. Finally, for each type of ice, experiments were done for three sizes. The meteorological parameters for these experiments are summarized in Table 2. These conditions were chosen in order to simulate as closely as possible the natural conditions of icing.

TABLE 2

Wind tunnel conditions during conductors icing

| Type of ice | Sample no. | Temp. °C | L.W.C. $g/m^3$ | Wind speed m/s | Duration Hr : Min | Rotation Ang. (Deg) | Accretion Weight N/M | Equiv. Dia. (Calculated) |
|---|---|---|---|---|---|---|---|---|
| SOFT RIME | 1.0 | -15.0 | 2.9 | 5.58 | 1:00 | 20 | 7.65 | 48.0 |
| | 1.1 | -15.5 | 2.9 | 5.63 | 1:00 | 18 | 6.20 | 45.7 |
| | 1.2 | -15.5 | 2.9 | 5.63 | 1:00 | 18 | 4.38 | 42.9 |
| | 2.0 | -15.0 | 2.9 | 5.58 | 2:15 | 87 | 23.27 | 67.1 |
| | 2.1 | -15.0 | 2.9 | 5.63 | 2:15 | 85 | 19.43 | 63.0 |
| | 2.2 | -15.0 | 2.9 | 5.63 | 2:15 | 85 | 21.59 | 65.3 |
| | 3.0 | -15.0 | 2.9 | 5.58 | 4:00 | 127 | 47.35 | 88.9 |
| | 3.1 | -15.5 | 2.9 | 5.63 | 3:50 | 114 | 35.39 | 73.8 |
| | 3.2 | -15.5 | 2.9 | 5.63 | 3:50 | 114 | 34.36 | 77.9 |
| HARD RIME | 4 | -11.0 | 2.5 | 7.75 | 1.30 | 55 | 23.71 | 67.6 |
| | 5 | -11,0 | 2.5 | 7.75 | 2.30 | 100 | 30.57 | 74.4 |
| | 6 | -11.0 | 2.5 | 7.75 | 4:30 | 153 | 71.86 | 106.6 |
| GLAZE | 7 | - 6.0 | 1.9 | 12.55 | 1:00 | 30 | 25.97 | 69.9 |
| | 8 | - 6.0 | 1.9 | 12.55 | 1:35 | 55 | 44.28 | 86.5 |
| | 9 | - 6.0 | 1.9 | 12.55 | 2:45 | 110 | 95.93 | 121.5 |

- In all cases the calculated equivalent diameter was calculated assuming a 0.9 specific weight for ice, using a 35 mm conductor.

However, tests being made in a tunnel, certain conditions had to be adjusted to correspond to realistic parameters in the wind tunnel. The accretion had to take place somewhat faster, which is possible by using a higher water content and a lower temperature. As far as glaze is concerned, it had to be made at a velocity higher than the velocity usually encountered in natural conditions. The shape of glaze accretion is therefore less accurate than the rime accretion.

Figure 9, 10 and 11 show the drag and lift forces as a function of velocities for the three sizes of soft rime. The three curves appearing on each figure correspond to the three samples made for each size.

Figure 12 and 13 show the same type of results for rime and glaze respectively.

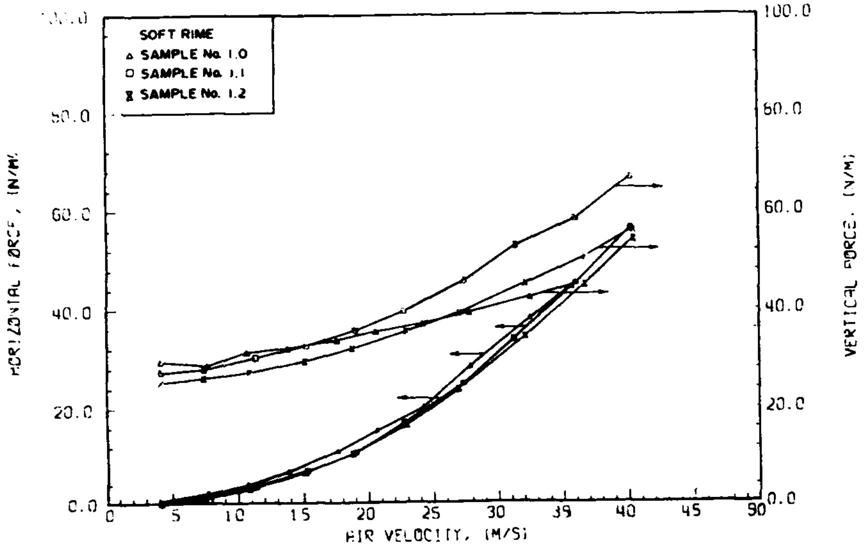

Fig. 9 Horizontal and vertical forces on soft rime accretion (D = 45 mm) as a function of air velocity

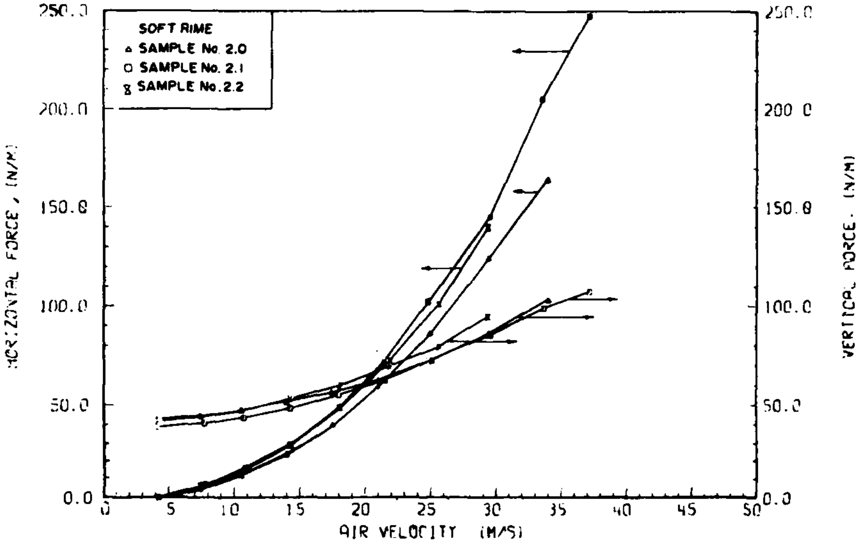

Fig. 10 Horizontal and vertical forces on soft rime accretion (D = 65 mm) as a function of air velocity.

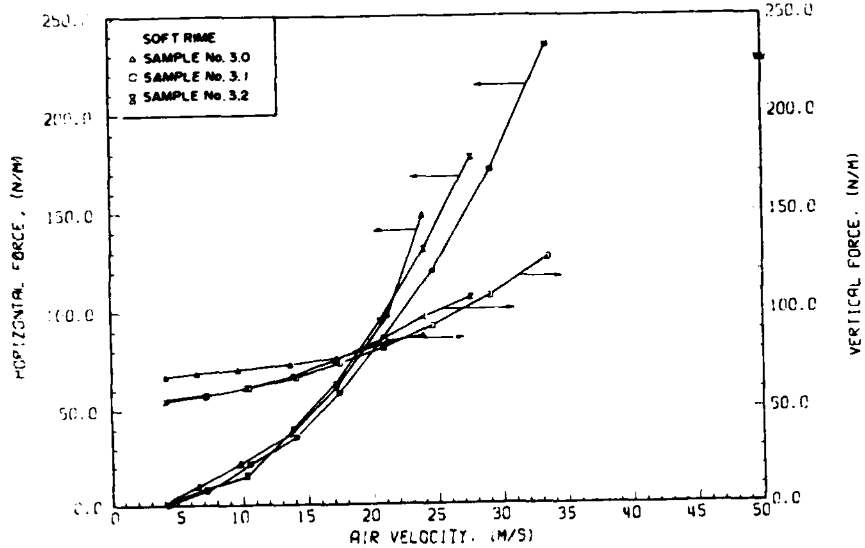

Fig. 11 Horizontal and vertical forces on soft rime accretion (D = 80 mm) as a function of air velocity

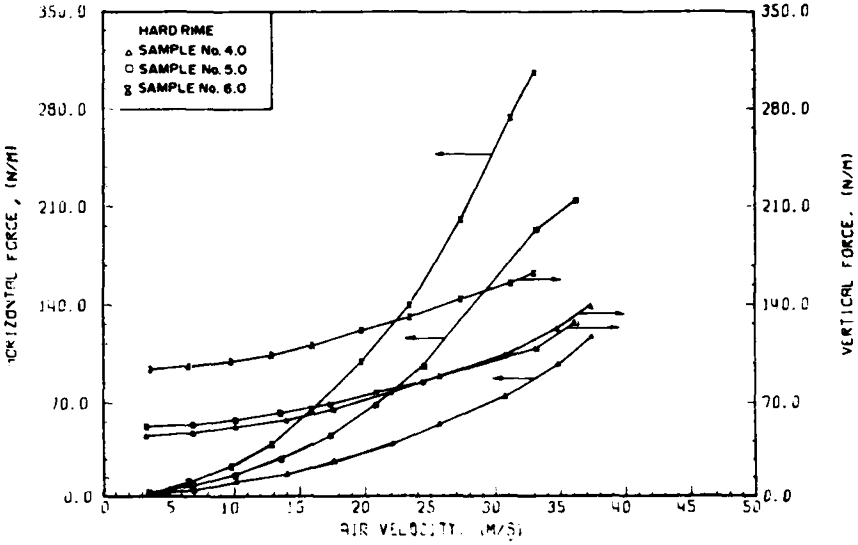

Fig. 12 Horizontal and vertical forces on hard rime accretion as a function of air velocity

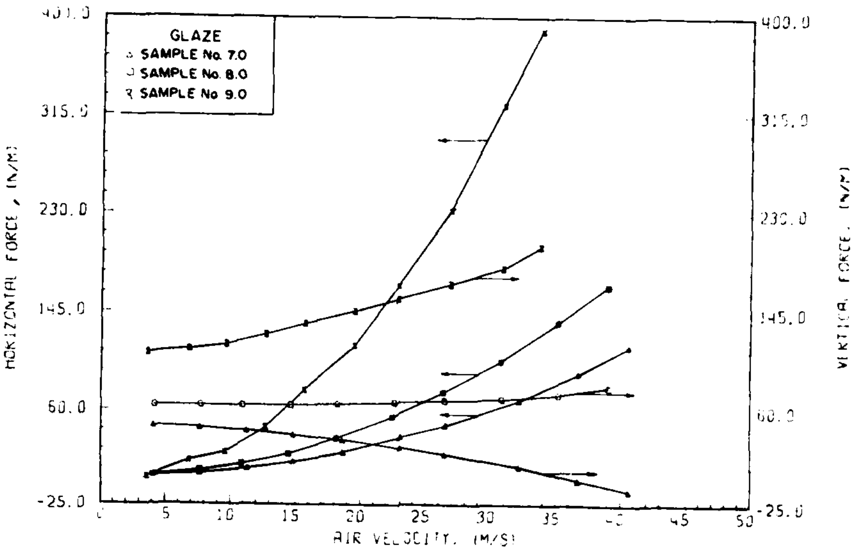

Fig. 13 Horizontal and vertical forces on glaze accretion as a function of velocity.

TABLE 3

Comparison of calculated and experimental ice-wind loads.

| Wind Speed m/s | 22.35 m/s (50 mph) | | | | | | | | |
|---|---|---|---|---|---|---|---|---|---|
| Forces | Calculated Forces Eqs. 1,2,4 | | | Measured Forces | | | Ratio | | |
| | $F_H$ | $F_V$ | $F_T$ | $F'_H$ | $F'_V$ | $F'_T$ | $F'_H/F_H$ | $F'_V/F_V$ | $F'_T/F_T$ |
| Sample #2 (soft rime) | 20.1 | 45.4 | 49.7 | 67.2 | 65.6 | 93.9 | 2.99 | 1.44 | 1.89 |
| Sample #4 (hard rime) | 20.3 | 45.8 | 50.1 | 39.6 | 84.6 | 92.9 | 1.95 | 1.83 | 1.85 |
| Sample #8 (glaze) | 26.0 | 65.7 | 70.7 | 54.3 | 67.1 | 86.3 | 2.09 | 1.02 | 1.22 |
| Wind Speed m/s | 26.37 m/s (59 mph) | | | | | | | | |
| Forces | Calculated Forces Eqs. 1,2,4 | | | Measured Forces | | | Ratio | | |
| | $F_H$ | $F_V$ | $F_T$ | $F'_H$ | $F'_V$ | $F'_T$ | $F'_H/F_H$ | $F'_V/F_V$ | $F'_T/F_T$ |
| Sample #2 (soft rime) | 28.0 | 45.4 | 53.3 | 98.4 | 76.8 | 124.8 | 3.51 | 1.69 | 2.34 |
| Sample #4 (hard rime) | 28.2 | 45.8 | 53.8 | 58.3 | 95.6 | 112.0 | 2.06 | 2.09 | 2.08 |
| Sample #8 (glaze) | 36.1 | 65.7 | 75.0 | 77.0 | 68.5 | 103.1 | 2.13 | 1.04 | 1.37 |

## COMPARISON OF CALCULATED AND EXPERIMENTAL WIND AND ICE LOAD

On Table 3, a comparison is made of the calculated drag and lift forces from Equations 1 and 2 with the wind tunnel measurements. This comparison is made for two wind speeds: 22.35 m/s (50 mph) and 26.82 m/s (60 mph) and for the medium size accretion (≈ 20 mm radial ice) of soft rime, hard rime and glaze. The resulting ratio of experimental to calculated forces is also shown.

From the results of Table 3, a comparison of the loads is made in Table 4 for a four-conductor bundle (conductors dia. 35 mm) with a span of 488.8 m (1600 ft). This example is calculated for hard rime (sample #4) with a wind speed of 22.35 m/s (50 mph). As an example, for a suspension assembly, a radial ice loading of 38 mm (1.5 in), with no wind, results in a load of 163 kN and has a return period of approximately 50 years. Table 4 indicates that much less icing (16.3 mm) combined with a 22.35 m/sec wind speed results in a 181.6 kN loading, and this thickness is reached for conditions much more frequent (10 years return period).

Table 4 compares also as an example the resulting tension force in the dead end horizontal position assembly. This force is calculated from the total combined force using a catenary equation. The force obtained is 132% of the limit load permitted on the conductor and 86% UTS (Ultimate Tensile Stress) of the conductor.

TABLE 4

Comparison of the combined loads for a four conductor bundle with a 488.8 m span 16.3 mm radial ice and 22.35 m/s wind.

| | Calculated force | Measured force |
|---|---|---|
| Suspension: | | |
| Horizontal force | 39.7 kN | 77.4 kN |
| Vertical force | 89.5 kN | 164.2 kN |
| Total force | 98.0 kN | 181.6 kN |
| Dead end assembly | | |
| *Tension force | 384.8 kN | 528 5 kN |
| % UTS of conductor | 63 % | 86 % |

* Calculated from the total force using a catenary.

## DISCUSSION

The comparison of Table 3 indicates the measured horizontal and vertical forces are larger than the calculated ones in all cases. Since an identical weight is used for the comparison, the difference is attributed to the aerodynamic forces.

The measured horizontal force is larger for two reasons. First a cross-section of the type shown in Figs. 3,4,5 and 6 offers an increased drag force when compared with the same weight distributed in a cylindrical shape. In all cases these shapes are the result of the fact that under the combined effects of weight and torsional rigidity of the conductor, ice accumulates mostly under the cylinder creating a shape which has a larger wind resistance.

The second reason for an underestimation of the calculated horizontal force is that for soft and hard rime the specific weight is lower than 0.9. For the same weight, natural ice accretion will therefore have a larger volume resulting in larger drag force.

The aerodynamic vertical or lift force is non-existant for a axisymmetrical shape. The calculated vertical force is obtained only the ice and conductor weights. The asymmetrical shape, however, creates a lift force.

In all the tests except one for glaze, the lift force obtained was negative and therefore equivalent to an added weight. The shapes responsible for this negative lift are again the result of ice weight and torsional rigidity of the conductor. As far as the exception (sample #7) is concerned it must be pointed out that the shape obtained for glaze are less realistic than those for soft and hard rime. To produce glaze samples, the wind speed had to be increased in order to prevent icicles from blocking the test section.

The torsional rigidity of the conductor is a determinant factor in the shape of the ice accretion. It can be verified that for a fixed conductor and steady wind, the accretion forms only on the front part (Figure 1). On the other hand if the rigidity constant were zero, the conductor would rotate as soon as a unbalanced weight is created, and the rotation would then rapidly exceed 360° and a spiraled shape, close to cylindrical shape would be formed.

The rigidity of real conductors is between these two extreme cases, and furthermore it varies along the span of a transmission line since the supports will increase the rigidity at certain locations.

The results presented were obtained for one value of the rigidity constant. Since the final shape of an ice accretion depends strongly on the time history of ice build up, it will remain difficult to predict the aerodynamic forces on a transmission line. The results presented above are an indication of the importance of aerodynamic forces due to the asymmetrical shape of the ice accretions. This importance is such that even if these forces are difficult to predict accurately, they should not be ignored in the calculations of combined ice-wind loads.

## CONCLUSIONS

Ice accretions are usually not uniformly distributed around conductors of transmission lines. This has been observed on real transmission lines, and verified in wind tunnels. The usual method of combined wind and ice load calculation has two disadvantages. When a symmetrical shape is assumed around the conductor, drag forces are underestimated while lift forces are not considered.

These forces are often very important. Secondly, the assumption that the density is 0.9 for all type of ice underestimates soft rime thicknesses and this results in lower overall loads as well.

In order to be able to make an accurate calculations of combined loads for ice covered conductor, a "shape factor" should be taken into consideration; if this is not done, the total load can be dangerously underestimated.

## ACKNOWLEDGEMENT

The present work was done by the UNIVERSITY OF QUEBEC IN CHICOUTIMI under a contract from HYDRO-QUEBEC.

## REFERENCES

1. Bassarskaya, T.A., Gohkova, T.N., Lomilina, L.F., Nikiforov, E.P., Toporkova, G.D. (1981), "Ice and Ice-wind Loads o Conductors of Overhead Transmission Lines", CIGRE S-22-81, 111-08, p.5.

2. Blevins, R.D. (1977), "Flow-Induced Vibrations", Van Nostrand Reinhold, New-York, pp. 55-88.

3. Bourgsdorf, V.V., Nikiforov, E.P., Zelitchenko, A.S. (1968), "Charge de givre sur les lignes aériennes", CIGRE, Vol. 2, pp. 1-8.

4. Ghannoum, E. (1980), "Une nouvelle approche de la conception des pylônes des lignes de transport", Canadian Engineering Conference, 37 p.

5. Godard, S. (1960), "Mesure de gouttelettes de nuage avec un film de collargol", Bull. Observ. du Puy-de-Dôme, 2, pp. 41-46.

6. Goldstein, S. ed. (1965), "Modern Developments in Fluid Dynamics", Dover Publications, New-York, pp. 401-440.

7. Kellow, M., Martin, R. (1976), "Characteristics of the Icing of Bundle Conductors", IEEE PES, Winter Meeting, paper A-76-088-5.

8. Laforte, J.L., Nguyen, D.D. (1982), "Examen des échantillons de givre et de verglas pour l'année 1981", Rapport soumis à Hydro-Québec.

9. McComber, P., Touzot, G. (1981), "Calculation of the Impingement of Cloud Droplets in a Cylinder by the Finite Element Method, J. Atmos. Sci. 38, pp. 1028-1036.

10. Rush, C.K., Wardlaw, R.L. (1957), "Icing Measurements with a Single Rotating Cylinder MAEC., Res. Rept No. LR-206.

## DISCUSSION

Krishnasamy: Did you see any different types of ice?

Martin: The way we worked it, since the shapes are so uneven, we worked on total force because to go back to a Cd, a drag coefficient, you need to know shapes, you need to known cross sections. And this was too difficult to obtain. On the practical side, what we did was to measure the forces. We could eventually take the shapes and get a cross section, but it was very difficult for us to do so. Since this was not a theoretical paper we wanted to tell what to expect, so we did it that way. We went by the actual horizontal and vertical forces.

Krishnasamy: Of course you had a ratio between the calculated and measured forces.

Martin: It's easy to see there's a big difference because the calculated just took the weight, divided, and give a cylindrical shape, an equivalent shape of 0.92.

Krishnasamy: Why I'm asking is that the ratio that you're getting when you measure and then calculate forces is partly due to the different [shape] that you use.

Martin: We know this, we expected it. It's a different shape, it's a different everything, but I'm sure the drag coefficient changes with the shape. But it's lost in the measurements. The measurements were not so refined as to discriminate between the variation of the pure $C_d$ and then bend the shape of it, the cross section.

Krishnasamy: Going back to my first question, you did calculate the drag coefficient of an iced conductor and ... radial ice was very, very small, a millimeter or so, but the increase in drag coefficient of the iced conductor was 60-70%.

Martin: But this is not included for the project engineer. The project engineer just sees a cylindrical shape of equivalent ice - we did the work sort of for them, to make sure that they eventually look at this point.

Mozer: How many different occurrences did you have of these measurements where you can actually observe this ratio of 1.8 or 1.9 between measured and calculated - do these represent several cases?

Martin: What you saw here is purely wind tunnel testing. The shapes of ice that were shown were examples of ice that were similar to the wind tunnel testing.

Lozowski: When you put your accretions into the wind tunnel to measure the drag, how did you determine what orientation to use?

Martin: We just noted the angle at the end of the accretion and put the accretion at exactly the same angle ... Seven years ago, people thought that if you made a 6-conductor or 8-conductor bundle, ice would build up on this side. Let's say the wind came from this way [slide projected], ice would build up this way and eventually close the little holes here, and act as a huge conductor - a large diameter conductor, and eventually you would have less accretion - that was the whole idea. We tried it in the wind tunnel - it was not perfect - the minimum wind tunnel speed was 30 mph, and that was quite high. There were a lot of vibrations during the experiment. The conductor oscillated a good deal. And it was funny, because ice just flew here like in a funnel, and accreted this way. And the best case was the one previous, was this one. But the idea was good, I suppose, at the beginning, but we proved it wrong in the laboratory.

AD P001684

# APPLICATION OF A BLOCK COPOLYMER SOLUTION TO ICE-PRONE STRUCTURES

B. Hanamoto USACRREL*

## INTRODUCTION

The formation of ice on structures causes both operational and structural problems, and much effort must be expended in keeping the systems comprising these structures functional. Preventing ice formation is the ideal solution, but this is usually impossible or cost-prohibitive. An alternative is to make it easier to remove the ice once it forms. Providing a surface that will cause the adhesive bond between the ice and the surface to be weak is a passive means of doing this. Heat or mechanical systems would be active means.

A problem arose some years back when thought was being given to extending the navigation season on the inland waterways of the northern United States later into the winter season, or even making it year-round. Mid- to late-December is the usual cut-off time for shipping on the Great Lakes and St. Lawrence Seaway. After this, navigation channels start icing up and the connecting locks on these waterways start encountering ice-related problems. One of these problems at the locks was ice build-up on the walls. The build-up occurs as an ice collar growing out as much as 2 to 3 ft (0.6 to 0.9 m) at the high pool level and extending vertically 6 to 8 ft (1.8 to 2.4 m).

When this happens at the lock at Sault Ste. Marie, Michigan, which connects Lakes Superior and Huron by way of the St. Marys River, the large, bulk cargo carriers experience problems passing through the lock. Ships of the *Roger Blough* and *Presque Isle* class are 1000 ft (305 m) long and 105 ft (32 m) wide. The Poe Lock at the Soo is 110 ft (33.5 m) wide. Similar passage problems occur on the upper Mississippi, Ohio and Illinois Rivers with the tow and barge traffic. Here a reduction in tow width is possible from three barges abreast to two, but this cuts down on traffic volume. A solution to the interference problem was sought so that lockage delays and volume reductions could be minimized for winter traffic.

The U.S. Army Cold Regions Research and Engineering Laboratory, together with H.H.G. Jellinek of Clarkson College, worked on developing a coating with reduced adhesive strength properties between the ice and the coated surface so that ice removal could be facilitated. A long chain, block copolymer was selected after many compounds with the desired properties had been tested. The compound, a poly(dimethylsiloxane)-bisphenol-A-polycarbonate, drastically reduced the force needed to break the ice/coating bond (Jellinek et al. 1978). After being sprayed onto a surface, the resulting coating is a pliable, thin (4 to 5 mils), non-wearing clear film.

The copolymer coating was applied to the Poe Lock walls at the high pool level (from just above to 10 ft (3.1 m) below). The Poe Lock is operated so that all traffic ties off on the north wall during lockage. This wall remains rub-free. This was fortunate since the coating cannot with stand abrasion and rubbing. Equipment to clean the wall and spray-coat the copolymer was placed on a barge moved by a small tug. The walls were cleaned of algae, oil scum and dirt using a steam cleaner with detergent added to the cleaning water and allowed to dry thoroughly. The copolymer solution can be applied either by brush or as a spray. On the lock walls, a high-pressure airless spray system was used. Three coats were applied. Spraying a monolith section 22 ft (6.7 m) long down to the 10-ft (3.1 m) depth, the curing time was such that by the time the sprayers finished the third monolith with a single coat, the second coat could be applied, starting with the first monolith. A half-hour curing time is sufficient.

---

* U.S. Army Cold Regions Research and Engineering Laboratory, Hanover, N.H.

The coating does not prevent the formation of ice--it just makes it easier to remove. High pressure water jets and large ice-cutting saws for removing ice collars were also tried at this time. At one time, while the collar was being cut with the saw, the vibration from the cutting operation was enough to remove a section extending about 40 ft (12.4 m) or nearly two monoliths ahead of the cutter. Steam was also available along the wall. Steam spreader bars placed on top of the collar removed sections of ice within 15 to 20 minutes. In uncoated areas, the steam bar just melted through the collar, taking hours.

An active heat source in conjuction with the coating is an efficient way to remove the ice build-up. This was demonstrated in another application of the copolmer coating.

The U.S. Army Satellite Communications Agency is responsible for tracking systems located at many sites throughout the world. Some of these tracking stations are in areas where icing of the antenna dish occurs causing signal degradation problems. Ice forms on the parabolic dish during particular weather conditions--temperatures in the -3° to +3°C range and with wet snow, sleet and freezing rain. Temperatures lower than -3°C usually result in drier snow, which does not accumulate.

CRREL was asked to conduct tests to determine the merits of the copolymer coating in relieving the icing problem. Comparative tests were conducted in the coldroom of the Ice Engineering Facility at CRREL. Panel sections of antenna dishes from operational units in the field were used. The standard panel was compared to a coated panel. Heat cables were placed in back of each panel. Heat was used to remove the ice cover since ice will form on the coating. Determining the ease of ice removal was the aim of the tests. Each test panel was coated with 0.25 in. (0.6 cm) of ice using an air spray gun. Problems were encountered in forming the ice cover on the coated panel until the room temperature was dropped to 15°F (-9°C). Water would roll off the panel in droplets before freezing until the temperature was lowered. Water near freezing was used in the spray canister. After an ice sheet had been formed on each panel, the heat cables were turned on. Room temperature was raised to -3°C. The time required for ice removal was the measure of effectiveness. Ice melted near the heat cables first, with a water film visible beneath the ice cover. This zone gradually expanded. The first indication of a water film appeared after 5 minutes on both panels. The entire sheet of ice on the coated panel slid off in about 20 minutes. On the uncoated panel, strips along the cables melted through the ice with little or no sliding. After about 2 hours this panel was free of ice. Heat cable spacing was about 4 inches (10 cm) and output was 23 W/m. The attitude of the panel was about 30° from the vertical, close to the operating angle of the units in the field. Tests were also conducted to ensure that the coating did not affect the R-F characteristics of the antenna in the frequency range of interest, 7.2 to 8.6 GHz. No effects were noted.

A request to coat the dish of an operating unit in Omaha, Nebraska, was received in the fall of 1979 following a favorable review of the laboratory results. The 60-ft (18.3-m) dish was first washed with a detergent solution and water-rinsed thoroughly. When it was completely dry, an airless high-pressure spray system was used to apply the copolymer solution. Three coats were applied. Starting from the periphery, a band about 4 ft (1.2 m) wide was sprayed around the dish. The coating at the starting point was dry by the time the band was completed. Two more turns over the same strip completed this section. The next-lower 1.2-m strip was then coated. The coating procedure was completed in two 6-hour sessions on two successive days. The antenna was operational between these sessions.

No down-time due to ice build-up was encountered during the winter seasons of 1979-80 and 1980-81. In December of 1980, a severe ice storm occurred, with build-up over an inch (2.54 cm) at ground level. Some ice accumulated on the lower lip of the dish, but the unit remained operational throughout the storm. In December of 1981, another storm hit the Omaha area, with near-surface air temperatures close to 25°F (-4°C) and a temperature inversion in the upper layer. Rain and freezing rain occurred at 1000 hours. By 1400 hours the temperature dropped to 15°F (-9.5°C) at the surface, with wet snow. A cover of ice and snow formed on the dish and the signal started to degrade. At this time, the warm glycol deicing unit was removed with no interruption in operations.

Other operational antennas in the field have been coated subsequently. Units similar to the one in Omaha have been coated in Europe, the Far East, and Alaska. Problems of ice build-up on the coated unit in Germany were reported, but particulars as to the nature of the problem and the conditions have not been clarified. A 33-m antenna dish located in the Shenandoah Mountains has been coated for the National Security Agency. The unique feature of this system is the active heating blankets on the backside of the dish panels. On Thanksgiving weekend of 1981, a wet snow condition at 30°F (-1.1°C) caused a 4-inch (10-cm) build-up to occur on the dish. The deicing blanket was turned on, and within 2 minutes the entire sheet slid off. Dry snow conditions at -1°C were also reported but no build-up occurred.

The above has been a description of a means to reduce ice build-up problems on different structures. Some results have been favorable, others not. The method for surface preparation is simple, and the application is speedy and uses readily available equipment. The life of the coating is not known, but after three winters the coating on one system is still intact and functional. The merits of the copolymer coating to facilitate ice build-up removal have been shown by both laboratory and field applications. When the coated surface is augmented by an active heating system, the two combine effectively to remove the ice before problems can occur.

## LITERATURE CITED

Jellinek, H.H.G., H. Kachi, S. Kittaka, M. Lee and R. Yokota (1979) Ice-releasing block-copolymer coatings. Colloid and Polymer Science, 256, 544-51.

## DISCUSSION

Smith: I have several questions for you. Do you have any applications on any vessels?

Frankenstein (in author's absence): No.

Smith: We have been in touch with you concerning this particular coating, and also we have a study here at CRREL looking at the assessment of the technology of marine icing. On this type of coating - are you saying that you have to have an extremely clean surface, something that would be extraordinary on a rig in the Arctic?

Frankenstein: No. Have you ever seen a lock wall up close? It's pretty grimy. There's not much that would adhere to it, and we tried putting it on there without cleaning it. The antennas, by the way, are pretty high, and you get a lot of dirt, especially in industrial areas. In Europe, it's very industrialized, as you know, but the one in Omaha, we did not clean, we sprayed right on there. I don't think there is a coating around that will prevent ice from adhering to. What we're saying is that in a couple of cases on the antennas, the ice did not adhere to the dish of the antenna. In other words, the antenna was never full. They never had to go up and get the ice away. Even last year, with that combination of snow and freezing rain, the stuff which is the worst case, they were able, with a very small effort, to get rid of all that, and not have to shut down the antenna at all.

Smith: Why hasn't the Navy tried this out?

Frankenstein: I have no idea. Is there a Navy man here? I'm not so sure, to be honest with you. I'm not so sure, and I think Hans [Jellinek] will go along with me, that the abrasion that's involved with the ship ice, in other words, with getting rid of it - you know normally with sea ice, they use baseball bats. On the Great Lakes, I guess they don't do much of anything, they just use chisels and things like that. I'm not so sure that it would withstand that. I think there's more work needed on the vessel deicing problem, for coatings for vessels.

Jellinek: It would be very useful to spray Navy ships with this process, and the ice would come off very easily, with much less energy.

Frankenstein: I think we should really be spending some research dollars to look at a coating for that purpose.

Smith: I see you've applied the coating to dish antennas, but there are also towers and maybe that's another problem.

Frankenstein: The dish antennas have been very successful, that happens to be a feather in our cap.

Nauman: Have you ever had to recoat? Do you have any idea how long the coating lasts?

Frankenstein: Its's been four years since the coating was applied to the lock walls, and we did the first antenna three years ago and there we had to repair only a very small section, maybe as big as that blackboard there, is all, because they damaged it somehow. We went back and explained to them how to repair it and they did, and it's been very successful.

Question: What was the orange coating that you used on the lock wall?

Frankenstein: That was just an undercoating.

Question: What kind was that - an epoxy coating?

Frankenstein: I think it was an epoxy; it was something they had there. It was a problem at first because there was ammonia in it.

Question: You steam cleaned that. I was interested to find out whether the block copolymer worked better on the coated surface, or ...?

Frankenstein: Well, on our first test it didn't make any difference. It wasn't an epoxy that we put on as the second coat. We just wanted something to fill up all the pores in the concrete.

Question: What kind of cost are you talking about? Can you give a rough idea?

Frankenstein: I think it was $35/gal.

Thowless: Has this coating been tried on any radomes that cover antennas?

Frankenstein: No, because the story we get, they don't need anything on radomes. I'm just quoting people when I say that. And the reason they use the coating on one of these big satellite antennas is that the cost of putting a cover on there is extremely high. So therefore they wanted to try this. And like I say, it's worked in all the places we've put it on. They have not had any downtime except that one in Germany. And once that guy went up there and vibrated it then the downtime went to something like five minutes compared to hours the year before.

Question: Does it also act as a protective coating against corrosion, or something like that? In case of steel?

Frankenstein: I don't know, I would say that any coating would - even a paint would. But I think one thing it will do is pick up the dirt in the atmosphere. Any material like that will, up to a point. That can be washed off. By the way - someone talked about durability - the antenna in New Jersey is exposed to a lot of industrial smoke there. We recommended they try scrubbing it off, and they did. We examined it, and the coating was all intact. Of course, you don't use real hard scrub brushes.

AD P001685

# "ICE-PHOBIC" COATINGS APPLIED TO SALINE-ICE-COVERED WHIP-TYPE ANTENNAS

Eric A. Thowless Naval Ocean Systems Center, San Diego, California 92152

## ABSTRACT

Three types of silicone products were selected for testing as "ice-phobic" coatings on antennas because of the very low adhesion forces previously measured by planar shear tests conducted at CRREL. These wipe-on coatings were not helpful in either decreasing the rate of ice accretion or facilitating the removal of ice from saline-ice-coated whip-type radio antennas.

## BACKGROUND

An engineering effort at Naval Ocean Systems Center was conducted to determine to what extent sea spray ice on communications antennas can disrupt radio communications, and what can be done to solve or alleviate the problem. The cold weather icing tests were performed at CRREL.

The antennas are typically used aboard small military craft and mounted not far above the sea surface and, hence, subject to sea spray icing during windy, sub-freezing weather conditions. Space, energy (power) and economic limitations are factors that make it impractical to employ bulky, exotic, or complex methods to discourage ice accretion and enhance ice shedding - methods such as heating, shock/vibration, inflation/deflation boot technique, or even redesign of the antenna's cylindrical form factor. An easy-to-use and inexpensive solution is being sought.

## INITIAL ELECTRICAL TESTS

For electrical tests, the primary purpose of the icing study, six antennas (mostly whip-type) were sprayed with cold saline water (of sea water salinity) at sub-freezing temperatures to produce a coating of ice. Quantitative measurements were made of changes in the electrical impedances of the antennas, and of the magnitude of signal loss through the antennas.

The results of the electrical tests are succinctly summarized. A coating of saline ice on all of these antennas tends to decrease the normal range of impedance variations as a function of radio frequency. Also, the impedance characteristics are altered in a manner that provides little or no indication to the radio operator of incipient communications failure, in that the transmitter continues to function perfectly yet the radiated signal level from the antenna is decreasing. Not surprising, the thicker the ice the greater the signal loss. The perception of loss of a received signal will generally be slow enough to deceive the radio operator. When the received signal-to-noise ratio becomes sufficiently low, poor enough to alert the radio operator, the antenna will already be well coated with ice.

During the numerous ice coatings of these antennas for the electronic measurements (without "ice-phobic" coatings), several mechanical manifestations of ice behavior were qualitatively observed. It had been believed that extreme flexibility of a whip antenna might be an answer to help shed ice. Not so. When an ice-coated whip-type antenna flexes, the ice cracks transversely, but not longitudinally. The result is a series of stacked cylinders of ice encircling the antenna most of which, if not all, still adhere to the antenna. In other words, by bending the whip, tension and compressive forces crack the ice crosswise only. No mechanical force exists to crack the ice longitudinally and no force exists from the self-motion of the antenna to overcome the cohesive strength within the cylinders of ice - even when a whip antenna is bent tip to base and then let loose, or when a whip antenna is shaken as vigorously as possible. A glazed ceramic insulator (supporting the VHF Receive-Only Antenna) was the only material from which ice would readily shed, once the ice was well cracked, seemly shedding easier than from any other surface. Bending of any flexible base (e.g., spring) cause the ice to easily crack with some, but not complete, shedding.

## "ICE-PHOBIC" COATINGS

A silicone oil, a silicone grease, and silicone rubber all exhibiting very low ice adhesion forces were selected to coat five antennas to test for decreased adhesion between ice and antenna and to test for decreased rate of ice accretion. The selection was based upon test data of these products measured by Mr. David Minsk of CRREL. Table 1 lists the antennas and their respective "ice-phobic" coatings.

The results were discouraging. No improvement in ice shedding was observed. The ice shedding behavior for the oil and rubber did not differ appreciably from that of non-coated antennas. The silicone grease was worse than nothing in that ice still adhered to the antenna even after the ice had been well shattered by repeated strikes with a wooden stick. The grease behaved in a very sticky and adhesive manner, like sticky jam. The silicone rubber on the glazed ceramic insulator kept the ice from dropping off after the ice had been cracked. On the rigid cylindrical antennas coated with grease, difficulty was experienced in cracking the ice by striking it with a wooden stick, almost as though the very thin coating of grease was acting as a cushion.

The rate of ice accretion on coatings of "ice-phobic" materials may have been slowed slightly, but not appreciably. The initail ice formation on grease and rubber was by widely scattered beads of ice. Once the ice beads formed, the rate of ice accretion seemed about the same as with no coating. Ice formation on the silicone oil was rather even and without appreciable beading.

In view of the discouraging results of the three coatings used for anti-icing tests, coatings which at first seem suitable based upon results of one type of ice adhesion test directed toward a specific application may not be suitable for a different application. Certainly, initial tests, such as the planar shear tests, are required to select those materials with inherently low ice adhesion. It is now obvious that following the initial selection process subsequent series of ice adhesion tests should be developed that are specifically tailored for the mechanical problem, material and form-factor of interest---in this case, small diameter (0.5 - 4.0 cm) cylindrical whip-type shape, oriented vertically, and rigid to very flexible.

## CONCLUSIONS

It seems reasonable to assume that ice-phobic coatings, such as these low ice adhesion products of silicone oil, grease, and rubber will not, by themselves, provide a solution to this antenna icing problem. A likely approach to a solution may be in using ice-phobic coatings in a synergistic relationship with some other mechanism.

## REFERENCES

Thowless, E. A. 1980. Study of Sea-Spray Icing of Communications Antennas--Exploratory. Naval Ocean Systems Center, NOSC TN 904.

Table 1. Antennas and Ice-Phobic Coatings

| Antenna | Flexibility/Stiffness | Exterior Surface | Ice-Phobic Coatings |
|---|---|---|---|
| AS-1729/VRC | Rather rigid. Spring at base. | *Base:* GE LEXAN, a polycarbonate resin. Whip section: alkyd enamel. | Silicone oil, Dow Corning, E-2460-40-1 |
| Developmental whip, NOSC | Very flexible, *(no spring)*. | Polyurethane paint. | Silicone oil, Dow Corning, E-2460-40-1 |
| Receive-only whip | Moderately flexible. Flexible rubber above ceramic insulator. | Alkyd enamel. | Silicone "rubber" GE RTV158. |
| Broadband whip, Marconi/Cincinnati Electronics Corp. | Moderately rigid. Spring at base. | (Paint). | Silicone grease, GE G661. |
| AS-1404/PRC-41 | Rigid cylinder. | Alkyd enamel. | Silicone grease, GE G661. |

# A REVIEW OF THE EFFECT OF ICE STORMS ON THE POWER INDUSTRY

William B. Bendel Environmental Research & Technology, Inc., Concord, Mass.
Dawna Paton Environmental Research & Technology, Inc., Concord, Mass.

## ABSTRACT

The relationship between ice storms (glaze) and their impact on the utility industry is examined. An investigation of the climatology of ice storms resulted in an assessment of the cost of ice damage to utilities and a determination of the number of utility customers affected by the major storms in the midwest and northeast regions of the country. An extreme icing episode which occurred in 1976 in Wisconsin is examined and specific cost damage is developed.

Probabilities of occurrence of ice storms of particular thickness in a given area and time period are reported.

It is suggested that a standardized classification scheme for identifying relationships between ice storm characteristics be developed. Such a scheme would allow more concise assessment of the impact of ice storms on the utility industry and assist in establishing cost to benefit relationships for storm-related cost-preventive measures.

## DISCUSSION

Franklin: Have you done much work in the field of extreme value distributions?

Bendel: Like Gumbel distributions, and things like that?

Franklin: No,going beyond that - like flood predictions.

Bendel: We are doing a lot of risk assessments, but not necessarily extreme. Years ago I used to do some extreme surge studies, and things like that, but in the last 5-6 years I have not been involved in that.

Franklin: We're thinking of applying that towards ice storms. What's your opinion on that?

Bendel: Well, I had in this paper, but I guess I missed saying that, but Paul Tattelman, in reference to his work, had some estimates of recurrence intervals. In other words, what is the possibility - what is the recurrence interval - for a specific intensity storm in a particular area. That is, will you get a 2 in. or 10-cm storm once in 100 years? Once in 50 years? That sort of recurrence interval storm. But the problem is that since there's no real characterization of storms. A storm, measured only by the amount of ice fall, is not necessarily the most intense storm. You have to combine that with wind loadings and possibly duration to come up with a characterization of what an intense storm is.

Franklin: The reason I asked is that we have a lot of areas where we have no information.

---

*This paper was presented, but was previously published in Journal of Applied Meteorology, vol. 20, no. 12, December 1981.

Bendel: Your holes.

Franklin: Right. We're thinking of the shortest period of time we can use to acquire the data.

Bendel: Of course, one way of doing it is statistically. But you have to be very careful, because if you have no data and you're extrapolating, the error function can take over your statistics very quickly.

Assur: Bilello at CRREL once made an analysis of when icing occurs depending upon certain standard climatological observations, and that could be used because the normal observational data like temperature, and snowfall, and so forth, are available in published data.

Bendel: There has to be a professional [...] before you get into any of the statistical approaches.

Assur: Well, you have to do statistics, and you have to define the conditions under which icing can occur.

Nauman: Is it possible, as they do for the 100-year forecast, to hind cast icing events? Is that a possibility?

Bendel: I think one of the reasons that this has not been done is that there is so little basic data on classification of ice storms and the intensity of those particular ice storms. Any extreme event should lend itself towards that sort of approach.

Nauman: The reason I'm bringing it up, though, is that in Alaska we have the same problem - we have very little or no data, and they use this process a lot.

# SESSION 3: METEOROLOGICAL MEASUREMENTS AND DAMAGE OBSERVATION

AD P001686

# THE EFFECT OF METEOROLOGICAL PARAMETERS ON RIME FORMATION IN FINLAND

Lasse Makkonen Institute of Marine Research, Finland
Kari Ahti Finnish Meteorological Institute

## Abstract

The dependence of the growth rate of rime on routinely measured meteorological parameters in northern Finland is examined. The rate of rime formation I (in g cm$^{-2}$h$^{-1}$) on a vertically situated 5 cm diameter measurement cylinder is found to be significantly correlated with the wind speed v (in ms$^{-1}$), the regression equation being $I=11\cdot10^{-3}v$. The wind speed multiplied by the time during which the cloud base observed in the valley area is at a lower elevation than the rime observation point seems to give a fair index of the ice load. No dependence of the rate of rime formation on air temperature is found, but the occurence of glaze instead of rime is affected by air temperature as well as by wind speed. There is no correlation between the intensity of ice accretion and precipitation measured with a rain gauge.

Connections of the results with observations from other localities and with theoretical considerations are discussed.

## 1. INTRODUCTION

In cold regions the optimum structural design and positioning of power lines, for example, require information on the probability of occurence and on the expected intensity of ice accretion in different atmospheric conditions. Therefore data on the frequency of different types of ice deposits (soft rime, hard rime, glaze, wet snow) in different air temperatures, wind speeds and intensities of precipitation have been collected in many localities. However, there is rather little quantitative information on the dependence of the ice formation intensity on these meteorological parameters. Also, theoretical results cannot easily be applied to practical problems since the cross-correlations of the parameters affecting the ice growth are not well known. Hence the possibilities of estimating or predicting the growth of ice loads are very limited - the present methods giving differences of one order of magnitude after 100 hours of deposition (Anon, 1979).

In order to develop at least a rough estimation method based on empirical results, measurements of ice accretion together with registration of meteorological conditions were made in different localities in Finland during 1970's. The results related to the quantitative estimation of ice loads are limited to the cases of rime formation only, since heavy deposition of clear ice was too rare for making a corresponding analysis for glaze. The results are further limited to low wind speed range, since rime formation in Finland usually occurs when the wind speed is lower than ~10 ms$^{-1}$.

## 2. THE MEASUREMENTS

The data of the study comes from three separate series of measurements. The first experiment aimed at revealing the possible connection between precipitation and the amount of accreted ice, and the second experiment at studying the dependence of the rime formation rate on air temperature and wind speed. In the third experiment the conditions in which rime formation changes to glaze formation were examined.

The measurements of the daily ice accumulation and the daily amount of precipitation were made at the Värriö Subarctic Research Station (67°45'N, 29°37'E, altitude above sea level=h=390m, see fig. 1) during the winter 1972-73. The instrument for collecting rime consisted of a vertical sheet made of steel (20 cm x 10 cm). The amount of accreted ice was measured by determining its volume after melting. Precipitation was measured with a standard Finnish precipitation gauge (catchment area 500 cm$^2$).

The experiment for studying the dependence of rime formation intensity on air temperature and wind speed was made at Pyhätunturi (67°01'N, 27°13'E, h=477 m) during the winter 1976-77. In this experiment a 5 cm diameter aluminium cylinder was used to collect the ice deposit. The wind speed was recorded with an integrating cup-anemometer . The ice accumulation and the average wind speed were observed once a day, and the time of accumulation was determined as the time at which the cloud base observed at the Rovaniemi airport (66°31'N, 25°50'E, h=197 m) and Sodankylä Geophysical Observatory (67°22'N, 26°39'E, h=197 m) was lower than the elevation of the observation point. There were no temperature measurements at Pyhätunturi but air temperature was determined from the temperature soundings at Rovaniemi and Sodankylä. The error introduced by this prodedure presumably did not exceed ±2°C because of the relatively uniform structure of the temperature profiles in the observed icing situations.

In addition to the measurements directly related to the rate of rime formation, measurements were made to determine the meteorological conditions in which the change from the formation of rime to the formation of clear ice i.e., glaze, occurs. The data (1976-77) is from three localities where ice accretion is quite common but where the intensity of accretion is too small for studying its connections with meteorological conditions. In these locations (Rovaniemi, Sodankylä and Jyväskylä airport, 60°24'N, 25°40'E, h=143 m) wind speed and air temperature were measured in the vicinity of the measurement cylinder. The structure of the ice deposit was determined visually.

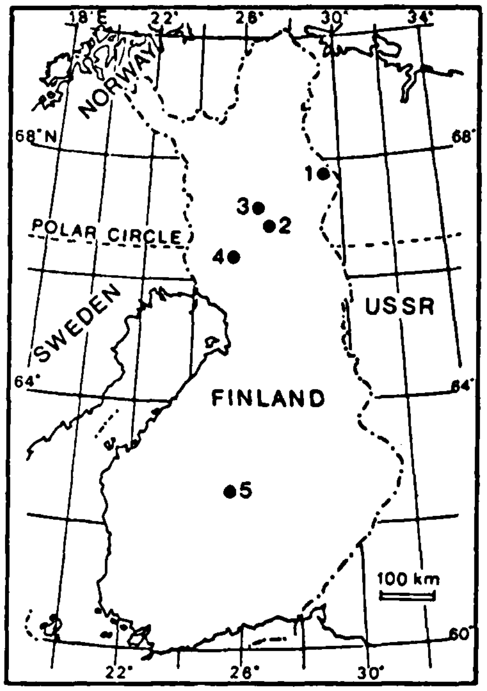

Fig. 1. The observation points: Värriö (1), Pyhätunturi (2), Sodankylä (3), Rovaniemi (4) and Jyväskylä (5).

## 3. CONNECTION BETWEEN THE RATE OF RIME FORMATION AND METEOROLOGICAL PARAMETERS

### 3.1 Precipitation and air temperature

The amount of precipitation measured with a rain gauge has often been used in examining the intensity of ice accretion (Lenhard,1955, Grunow and Tollner, 1969, McKay and Thompson,1969, Chainé, 1973, McLeod,1981). Following this approach the correlation coefficient

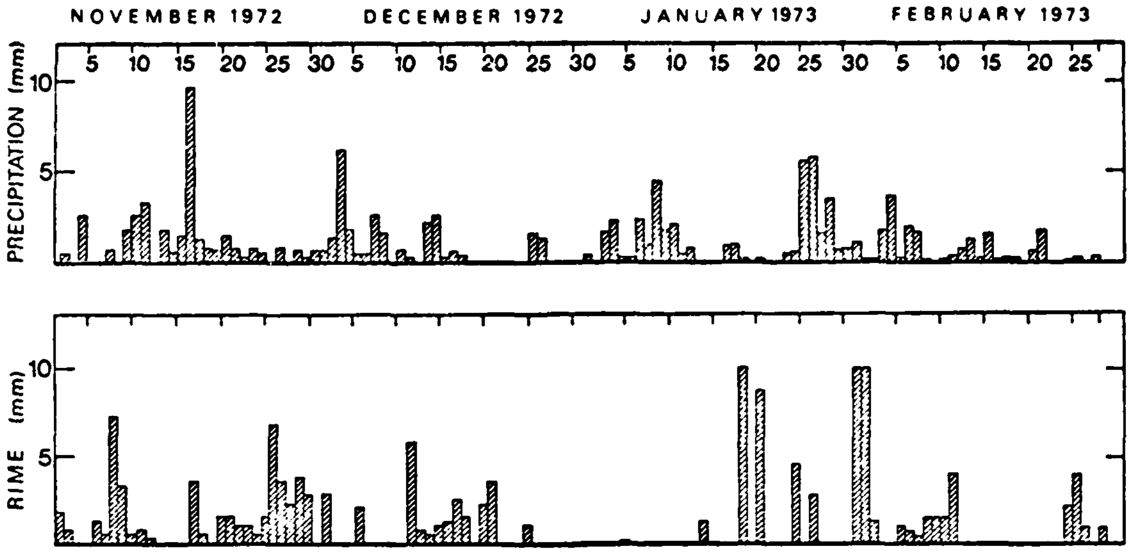

Fig. 2. The daily amounts of rime and precipitation at Värriö (Ahti, 1976).

between the daily amount of precipitation and the measured ice deposit was calculated for the data from Värriö. No correlation was found (r=-0.08). Ice deposit and precipitation data is given in fig.2.

One might suppose that air temperature $t_a$ has an effect on the rate of rime formation I, because of the possible connection between air temperature and liquid water content of air, for example. In order to test this assumption the correlation coefficient between I and $t_a$ was calculated for the data from Pyhätunturi. No correlation was found (r=0.08). This was not due to the compensating effect of wind speed v, since there was no correlation in the data between $t_a$ and v.

### 3.2 Wind speed

Ice is accreted on a vertical surface when supercooled water droplets moving with the wind strike the surface (snow accretion is not considered here and was not observed in our data). Obviously the vertical component of the motion of these droplets is very small, since precipitation does not correlate with the rate of ice formation. In the case of rime (dry growth) all the droplets striking the surface actually freeze and there is no direct connection with the icing intensity and air temperature as in the case of glaze (wet growth). Therefore, the intensity of rime formation I on a measurement cylinder can be calculated according to eq. (1).

$$I = E w v \qquad (1)$$

where E is the collection efficiency, i.e., the ratio of the mass flow of droplets striking the cylinder to the mass flow of droplets that would strike it if the droplets were not deflected following the air stream around the object, w is the liquid water content in air and v is the wind speed. The collection efficiency E is dependent mainly on wind speed, droplet size distribution and the dimensions of the icing object (see e.g., McComber and Touzot, 1981).

The liquid water content of air and the droplet size spectrum are extremely difficult to measure or to predict. These parameters are probably related to e.g., the direction of the wind, but the dependence of I on wind direction could not be examined in our data due to the predominance of southwesterly winds during ice accretion. However, it is interesting to test with observational data if an estimation method for I, based on eq. (1), could be constructed by simply neglecting the variation of liquid water content and droplet size and finding out if I and v covary. This was attempted using the data from Pyhätunturi, rejecting the few cases of glaze for which eq. (1) is not expected to be valid (Makkonen, 1981). The correlation coefficient 0.58 was obtained between I and v. This is significant at the 0.5 %-level (t-test). The data is given in fig. 3.

In fig. 3 also the linear regression line for the data is presented. The regression line is forced through the origin, since the results of Sadowski (1965) and Volobueva (1975) (see also fig. 5) show that rime is formed down to the wind speed values as small as the starting speed of the anemometer and since, on the other hand, the rate of accretion in zero wind speed (sublimation) is negligible in the fog conditions which prevailed during the deposition. The linear regression equation obtained for I is

$$I = 11.0 \cdot 10^{-3} \, v \quad , \qquad (2)$$

where I is in g $cm^{-2} h^{-1}$ and v in $ms^{-1}$. The standard deviation of the proportionality factor in eq. (2) is $0.9 \cdot 10^{-3}$.

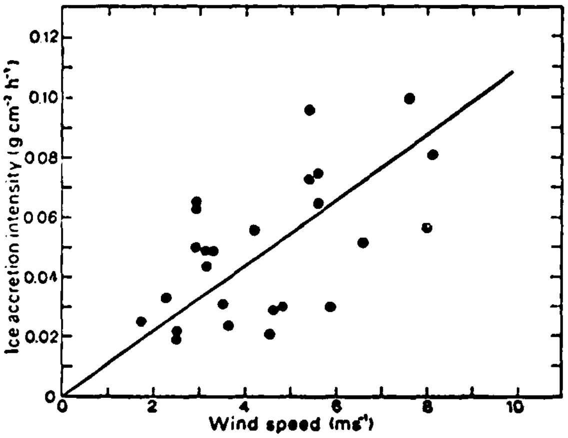

Fig. 3. The intensity of rime formation versus wind speed at Pyhätunturi.

## 4. AN ESTIMATION METHOD

For practical purposes the weight of ice after some time of accumulation is most important. Because of the lack of information of the effects of meteorological conditions on ice accretion intensity the duration of deposition has sometimes been used as the only predictor when estimating the formation of ice loads (e.g., Diem, 1956). In our data, too, the ice load correlated more strongly with the duration of icing $\tau$ ($r = 0.70$) than with any of the meteorological predictors, although $\tau$ was not directly observed but was determined from cloud height observations.

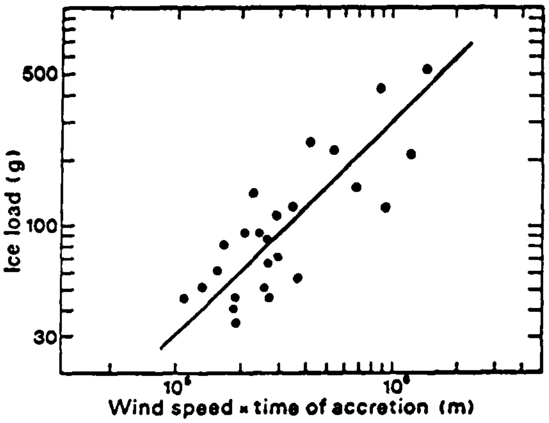

Fig. 4. The ice load versus wind speed multiplied by the time of ice accretion at Pyhätunturi. The time of accretion is estimated from cloud height observations in the valley area.

Since wind speed explains a noticeable part of the variation of the intensity of rime formation and since I seems to be approximately proportional to v, it is to be expected that $\tau$ multiplied by v is a better index for the ice load L than $\tau$ alone. Therefore the correlation coefficient between L and $v\tau$ was calculated, yielding $r = 0.81$. The data and the linear regression line are presented in fig. 4 in the logarithmic coordinates. The correlation coefficient between log(L) and log($v\tau$) was 0.86.

## 5. RIME OR GLAZE ?

The empirical relationship between the rate of ice accretion and wind speed in our data could be examined for rime only. Theoretically it is to be expected that this connection is weaker for glaze due to the temperature dependence of glaze accretion intensity (Makkonen, 1981).

Therefore, it is important for the application of the presented estimation method to know the conditions in which the resulting ice deposit is glaze instead of rime. These critical conditions were studied simply by plotting the data of glaze, hard rime and soft rime on the v versus $t_a$ diagram (fig. 5). There were no noticeable differences between the data from different localities.

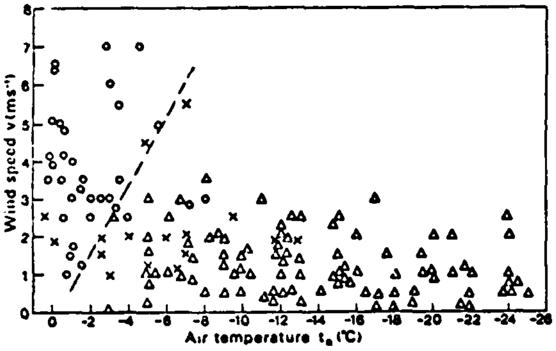

Fig. 5. Obsrevations of soft rime (Δ), hard rime (x) and glaze (o) in different air temperatures and wind speeds at Rovaniemi, Sodankylä and Jyväskylä.

## 6. DISCUSSION

The results concerning the effect of precipitation on icing intensity may be affected by local factors which play an important role in determining the frequency of precipitaion during ice accretion (Lomilina, 1977). However, it should be pointed out that actual data from other localities, too, do not support the usefulness of precipitation in estimating the rate of formation of ice loads: Waibel (1956) found no connection between precipitation and icing intensity in Feldberg, West Germany and the correlation coefficient obtained by Lenhard (1955) was not more than 0.41 for the data from Pennsylvania, USA. It has also been shown by Rink (1938), Sadowski (1965) and Lomilina (1977) that the majority of cases of rime formation occurs during days with no precipitation.

That there seems to be no correlation between the rime formation intensity and the air temperature is in agreement with the conclusion of Waibel (1956). Also, Rink's (1938) data coincides with the present result in the temperature regime of rime formation. Baranowski and Liebersbach (1977) have found a slight dependence on air temperature for hard rime and soft rime separately, but as a whole their data does not indicate a connection either. In the light of theoretical considerations (see Makkonen, 1981). these results indicate that the connection between liquid water content and air temperature is not very strong in the conditions where rime is formed.

Although there is a significant linear correlation between the intensity of rime formation and the mean wind speed, the scatter of the points in fig. 3 is considerable. This is probably mainly because there are large variations in the liquid water content, the droplet size distribution and the duration of icing. When comparing the obtained connecttion between I and v with other observations it is interesting to note that also the data of Rink (1938) from Germany and of Baranowski and Liebersbach (1977) from the Sudety Mountains show a linear relationship within a much larger range of wind speed values. The linear regression equation between I and v for a 10 cm diameter cylinder was calculated by Baranowski and Liebersbach (1977) separately for soft rime and hard rime and yielded $I = 7.5 \cdot 10^{-3}$ v for soft rime and $I = 15 \cdot 10^{-3}$ v for hard rime, the correlation coefficients being r = 0.60 and r = 0.50 respectively. Also the data of Waibel (1956) and Leavengood and Smith (1968) support the near-linear relationship indicating further that wind speed is a useful index of the rate of rime formation, although the hourly values of ice load and wind speed may not be strongly correlated (see Paoni and Tavano, 1981). A linear relationship between I and v would mean that - if liquid water content is not connected to wind speed - the collection efficiency E in eq. (1) could, as a first approximation, be considered independent of the wind speed on average. This would not be in agreement with the theoretical prediction that E increases with wind speed, other conditions being unchanged. However, the amount of data is too small to reveal a slightly nonlinear relationship, and there are several reasons which make it possible for the linear relationship to be valid in spite of the variable nature of E. These are for example the compensating effects of changes in average liquid water content and droplet size with changing wind speed, the more rapid increase of deposit dimensions in higher wind speeds and turbulent motion of the droplets. These are all factors which should be examined in future studies.

From fig. 4, it can be seen that the quantity $v\tau$, i.e., the wind speed multiplied by the time during which the cloud base is at a lower elevation than the rime observation point, seems to be a useful predictor of the ice load. The importance of cloud height on the ice formation makes it easy to see why the severity of icing is clearly dependent on elevation (Piehl, 1973, Glukhov, 1974, Lomilina, 1977). Due to the large variation of the ice load a much larger data set would be required in order to find out if the exponents $\alpha$ and $\beta$ different from unity should be used in the ice load predictor $v^{\alpha}\tau^{\beta}$ as suggested by Diem (1956) and Anon (1979). However, the results can be seen encouraging since they indicate that at least rough estimates of the ice load can be made using the wind speed and cloud height data.

According to fig. 5 the change from rime to glaze seems to occur approximately when $-t_a$ (in °C) is equal to v (in $ms^{-1}$), the overlap of the points being, however, considerable. This is comparable with the results of Volobueva (1975), but shows glaze formation in much lower values of air temperature than observed by Kuroiwa (1965). It is suggested by the theory that the increase of liquid water content makes it possible for glaze to occur in lower air temperatures (Makkonen, 1981). Hence, it is probable that differences in the critical air temperature in various data are mainly due to the different frequency of precipitation (i.e., very large liquid water content) in different localities in the icing conditions. This assumption is supported by the fact that also Sadowski (1965) and Glukhov (1974) have made observations of glaze in air temperatures as low as -10 °C, whereas according to Gaponov (1939) glaze is formed only in the temperature range from 0 °C to -2.2 °C when the observations with simultanious precipitation are excluded.

To summarize the results, it can be stated that of the routinely observed meteorological parameters only wind speed seems to be useful in predicting the intensity of rime formation. Air temperature, however, can be used in determining the conditions where glaze is formed instead of rime. The mean wind speed multiplied by the duration of in-cloud conditions seems to be the best available predictor of the ice load. This parameter should be useful in estimating the ice loads on power lines, masts, trees etc., using, say, climatological data. The accuracy of this method is, however, limited by the large variations in the liquid water content of air and droplet size distribution. Estimation methods of these factors should be developed in order to improve the reliability of ice load calculations.

## REFERENCES

Ahti, K., 1976: On the formation and measurement of rime in Finland. Värriö Subarctic Research Station of the University of Helsinki, Rep., 61, 8 pp.

Anon, 1979: Ice load. Elektrisitetsforsyningens Forskningsinstitutt. Teknisk Rapport TR 2458, Trondheim, 71 pp. (in Norwegian).

Baranowski, S. and J. Liebersbach, 1977: The intensity of different kinds of rime on the upper tree line in the Sudety Mountains. J. Glaciol., 19, 489-497.

Chaîné, P. M., 1973: The variability of glaze ice in Quebec. Environment Canada, Industrial Meteorology - Study I, 13 pp.

Diem, M., 1956: Over loads of rime deposits on high voltage electrical lines in the mountains. Arch. Met. Geoph. Biokl., Ser. B, 7, 84-95 (in German with English summary).

Gaponov, B, S., 1939: Temperature limits for glaze and rime formation from supercooled fog. Akademiya Nauk, SSSR, Izvestiya, Ser. Geogr. i. Geofiz., 3: 205-216 (in Russian).

Glukhov, V. G., 1974: Distribution of glaze-rime deposits in the lower 300-meter layer of the atmosphere. Glavnaya Geofiz. Observ., Leningrad, Trudy, No. 246: 63-72 (in Russian).

Grunow, J. and H. Tollner, 1969: Fog deposition in high mountains. Arch. Met. Geoph. Biokl., Ser. B, 17: 201-228 (in German with English summary).

Kuroiwa, D., 1965: Icing and snow accretion on electric wires. Cold Regions Res. Eng. Lab., 123, 10 pp.

Leavengood, D. C. and T. B. Smith, 1968: Studies of transmission line icing. Meteorology Research Inc., Final report, MRI63 FR-801., 42 pp.

Lenhard, R. W., 1955: An indirect method for estimating the weight of glaze on wires. Bull. Amer. Meteor. Soc., 36: 1-5.

Lomilina, L. E., 1977: The effect of relief on glaze-ice and rime deposition. Sov. Meteor. Hydrol., 2: 39-43.

McComber, P. and G. Touzot, 1981: Calculation of the impingement of cloud droplets in a cylinder by the finite-element method. J. Atmos. Sci., 38: 1027-1036.

McKay, G. A. and H. A Thompson, 1969: Estimating the hazard of ice accretion in Canada from climatological data. J. Appl. Meteor., 8: 927-935.

McLeod. W. R., 1981: Atmospheric superstructure ice accumulation measurements. Proc. 6th Conference on Port and Ocean Engineering in Arctic Conditions: 1067-1093.

Makkonen, L., 1981: Estimating intensity of atmospheric ice accretion on stationary structures. J. Appl. Meteor., 20: 595-600.

Paoni, P. and F. Tavano, 1981: Ice accretions on conductors of overhead electrical lines - results of years of research. Proc. CIGRÉ Symposium S 22-81, Paper 111-13, 6 pp.

Piehl, H.-D., 1973: On the effect of orography on the risk of rime desposition. Adhandl. Meteor. Dienst. DDR, Nr. 107: 20-25 (in German).

Rink, J., 1938: The melt water amount of rime deposits. Reichsamt für Wetterdienst, Wissenschaftliche Abhandlungen, 5. Nr. 7, 26 pp. (in German).

Sadowski, M., 1965: Ice accretion on electric wires in Poland. Prace Pańastwowego Instytutu Hydr.- Meteor., 87: 65-79 (in Polish with English summary).

Waibel, K., 1956: The meteorological conditions of rime deposition on high voltage electrical lines in the mountains. Arch. Met. Geoph. Biokl., Ser. B, 7: 74-83. (in German with English summary).

Volobueva, G. V., 1975: Classification of glaze-rime deposits according to their weight. Meteorologisteskie nagruzki na razlistnye sooruchenija: 34-40. Trudy 303, Gidrometeoizdat, Leningrad (in Russian).

## DISCUSSION

Félin: Do you have extensive data in Finland on (...) icing events?

Makkonen: Well, not extensive, but it's all there.

Félin: How many years of data?

Makkonen: Seventy-five...

Lozowski: The last graph you showed is very interesting. It suggests that perhaps the other parameters that go into the equation, like liquid water content and collection efficiency, are not strong.... Do you have any idea how much of that residual scatter is due to errors in the wind speed and how much is due to this unknown liquid water content and collection efficiency?

Makkonen: I don't have a good idea because... (unintelligible)

Minsk: Are you doing any work on the development of improved icing sensors--icing measurement devices?

Makkonen: No, except for an expendable one in an icing wind tunnel.

Minsk: Are you satisfied with present icing intensity measurement devices?

Makkonen: That's not a big problem.

AD P001687

# DETERMINING ATMOSPHERIC PARAMETERS DURING ICE ACCRETION FROM THE MICROSTRUCTURE OF NATURAL ICE SAMPLES

Jean-Louis Laforte Université du Québec à Chicoutimi
C. Luan Phan Université du Québec à Chicoutimi
Du D. Nguyen Université du Québec à Chicoutimi
Beatrice Félin Hydro-Québec

## ABSTRACT

Atmospheric ice accretion is controlled by four environmental parameters (temperature, wind speed, liquid water content and droplet size) as well as by the size and shape of the collector. Unfortunately, neither liquid water content nor droplet size are among the standard measurements such as those taken at first-order synoptic stations, and moreover, icing events will generally occur at some distance from the stations making it necessary to extrapolate wind and temperature as well. Any realistic attempt to model atmospheric ice accretion occuring in the field must be supported by realiable input estimates.

Based on earlier laboratory experiments which correlated the micro-structure of ice samples formed under dry and wet growth conditions to the four parameters listed above, several natural ice samples were collected on transmission lines after storms and were analysed to determine atmospheric conditions prevailing during the storms. The temperature is determined from microstructure analysis. When it is possible to get some information about the duration of storm, fairly good estimates of wind speed, liquid water content and droplet sizes may be obtained. Several interesting case studies are presented in this report.

## INTRODUCTION

Ice accretion per se and its combination with wind are a major hazard to transmission lines causing extensive damage and disrupting service, both of which entail very high financial and social costs. Establishing reliable design loads for ice loadings is in the best interest of utilities. Unfortunately, very little is known about the long term distribution of ice loads and of combined ice and wind loads. In Canada only two provinces, Quebec and Newfoundland, have a long term and standardized field program to measure ice deposits on passive collectors. However these programs were initiated only in the mid-seventies for Quebec and in the late seventies for Newfoundland, and have not yet been operational long enough to give a good data base on which statistical analyses could be done.

One approach to establishing design ice and combined ice and wind loads is to simulate ice accretion from current meteorological data using a theoretical model. This method takes advantage of the 20 years or so of existing meteorological records on which to build the distribution of the two afore-mentioned phenomena. However one of the principal drawbacks of this method is that the theoretical simulation of ice accretion using a physical model relies on input data which is not a standard meteorological measurement, namely liquid water content and droplet diameter. Moreover, since severe ice accretion usually occurs in remote and mountainous areas not as well represented as valley or shore-line first order weather stations, even the two other parameters which control ice accretion, namely temperature and wind speed are not necessarily well represented by the data measured at the weather stations.

In view of these difficulties and in

order to gain some knowledge of existing weather conditions during an ice storm it was surmised that a postfactum analysis of the physical and micro-physical properties of natural ice samples can be useful to estimate their growth conditions.

## PROPERTIES OF ARTIFICIAL ICE DEPOSITS

Previous work done by Université du Québec à Chicoutimi (UQAC) on artificial ice accretions formed in an icing tunnel (1) established the relation between different physical (density, transmittance, adhesiveness) and micro-physical properties (air bubbles and crystal texture) and prevailing conditions during ice growth. The results obtained (listed below) are generally in agreement with the results reported by others authors (2-4).

1. From the visual appearance observation ice can be classified into two main types: glazes which have a smooth and shiny surface and hard rimes which have a sealy or granular surface. Within broad limits, the type of ice depends on the mean surface temperature of the deposit $T_S$ and the product rV where r is the mean volume radius of droplet ($r = d_V/2$) and V the air velocity. This product rV is related to the momentum of the droplets which controls their spreading and freezing rate as they hit the conductor. Figure 1 illustrates this dependance with the experimental values obtained for the whole series of tests at the UQAC facilities. This particular mode of representation has been proposed by Macklin (2). However, in Macklin's original representation, impact droplet velocity was used instead of velocity of air as used in fig. 1. This may produce a slight difference in the product rV.

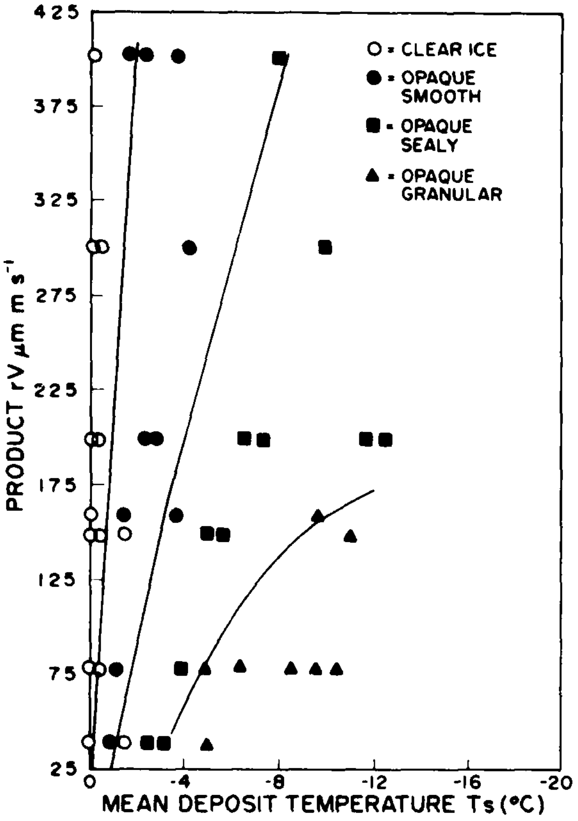

FIG. 1 THE APPEARANCE OF THE ICE DEPOSITS AS A FUNCTION OF THE PARAMETER rV AND THE MEAN SURFACE TEMPERATURE $T_S$

2. The density of hard rime increases with increasing air speed, liquid water content, mean volume diameter of droplets and air temperature, but decreases with increasing cylinder diameter. In figure 2, the density of ice for the whole series of tests is given as a function of the ratio $rV/T_S$, which are defined above. This mode of representation has been proposed also by Macklin (2) to express the dependance of the density of artificial rime upon the environmental growth parameters. As in figure 1, air velocity rather than impact droplet velocity was used. For the purpose of comparison, Macklin's results (dotted line) are shown also in fig. 2. It is obvious that the density measurements obtained in the present series of experiments

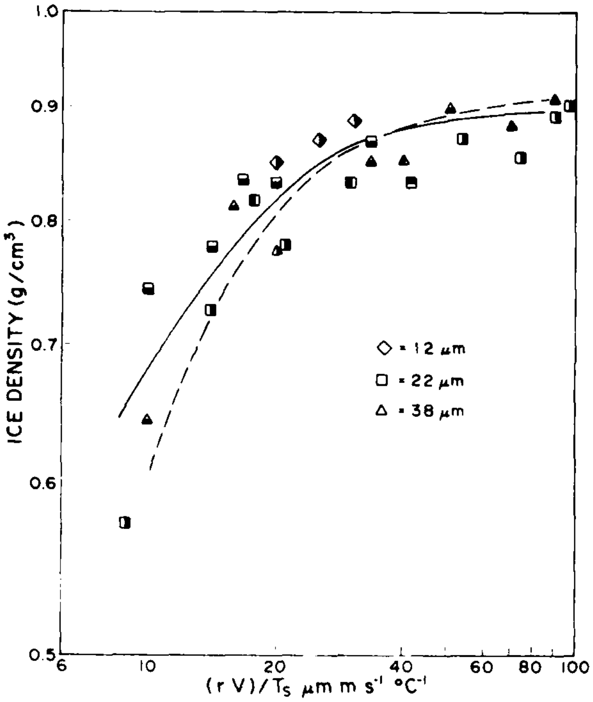

FIG. 2 THE MEAN DENSITY VALUES OF THE ICE DEPOSITS AS A FUNCTION OF THE RATIO $rV/T_S$

agree with those reported by this author.

3. Opacity of ice accretion, which is the inverse of transmittance, shows a similar trend to that of the density. Figure 3 gives the transmittance of ice deposits grown at different velocities V and air temperatures $T_a$. In the region where ice is glaze of constant density approaching the maximum density of ice ($T_a = -2°C$), transmittance of ice deposits is relatively high (> 0,90) with no great dependance on air speed. In the region where ice is hard rime of density lower than 0,90, the transmittance of ice decreases continuously with decreasing values of $T_a$ and V. From these results, it appears that ice density depends largely on the ambient temperature $T_a$ and the amount of collected water which is related to the intensity of accretion $I = \varepsilon WV$, where $\varepsilon$ is the collection efficiency of water droplets.

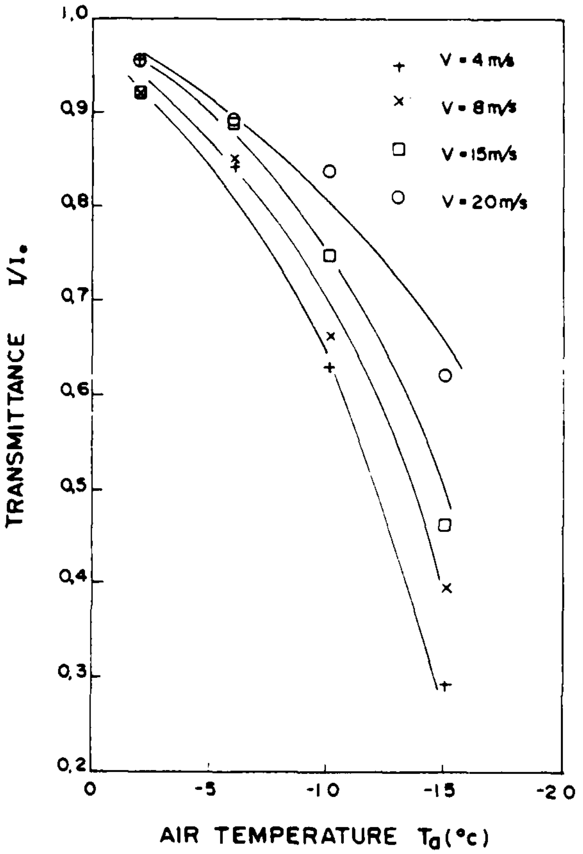

FIG. 3 TRANSMITTANCE OF ICE AT DIFFERENT AIR TEMPERATURES AND VELOCITIES

4. In the interval of air temperatures between -2 and -15°C, the dimensions of ice crystals of artificial glaze and rime samples depends mainly upon the ambient temperature and to a lesser degree on the wind velocity, especially at low wind velocities (4 m/s). Fig. 4 shows the variation of the mean crystal width $\overline{w}$ of ice crystals as a function of $T_a$ measured at two radial distances (1 mm and 6 mm) above the conductor surface. It is also clear in this figure that $\overline{w}$ at 6 mm is generally larger than $\overline{w}$ at 1 mm, i.e. in the boundary layer near the conductor surface. Moreover, this surface effect is more important at low temperature (1). About the effects of the droplet spectrum and water liquid content, it has been observed that these two parameters present negligeable influence upon mean crystal width of artificial glaze and rime when W is under 1.2 g/m$^3$. This is illustrated in fig. 5 where the mean width $\overline{w}$ corresponding to ice deposits grown from different droplets spectra are plotted as a function of the liquid water content W.

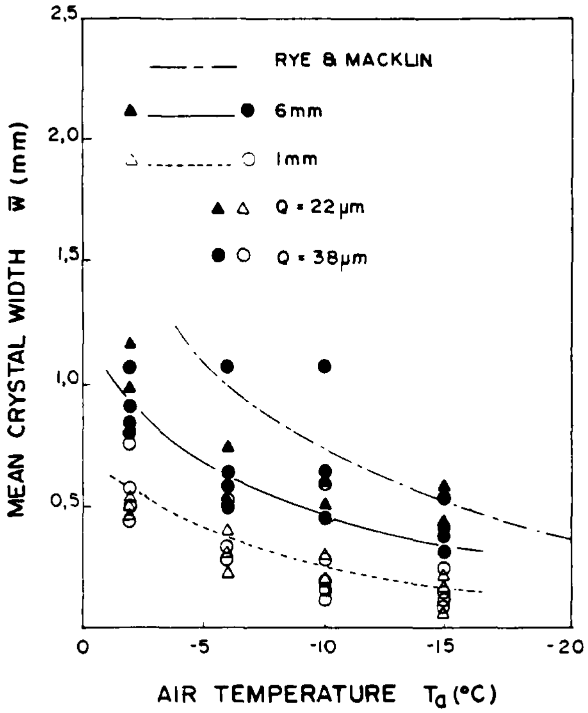

FIG. 4 MEAN WIDTH OF ICE CRYSTALS AS A FUNCTION OF THE AMBIENT TEMPERATURE

## COLLECTION OF NATURAL ICE DEPOSITS

Several natural ice samples were taken from transmission lines of the Hydro-Quebec network after significant ice storms. Samples collected in the field were put in an insulated cold box during the transportation to the author's laboratory. 7 kg of dry ice was placed in the box in order to keep the inside temperature at -15°C during the transportation. Upon reception, the ice deposits were photographed; then small pieces of ice were used to determine density and transmittance. Thin slices of ice

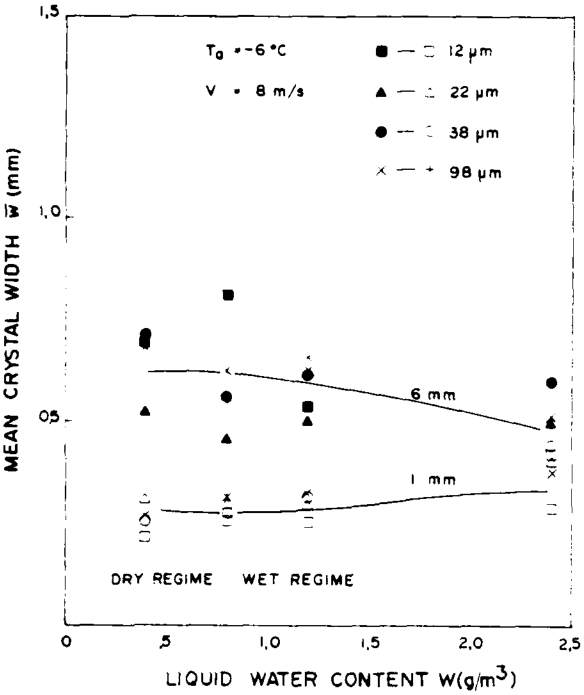

FIG. 5 MEAN WIDTH OF ICE CRYSTALS AS A FUNCTION OF THE LIQUID WATER CONTENT

are mounted on microscope slides and examined with low power microscope under both ordinary and polarized light. With proper handling and rapid delivery, the natural ice deposits arrived in a good state, so that no appreciable modification of the microstructure of ice were suspected to occur during the transportation. However, it was not possible to verify if any change occurred during the period of time preceeding the collection of the ice samples.

Among twenty and more ice samples collected from actual power lines during the winter seasons '79 to '81 only the most typical are presented in this report. Figure 6 shows the thin sections of two ice samples collected from power line conductor under ordinary light and polarized light. It can be seen on this figure that sample 1 is kidney shaped while sample 2 has rather the form of a half-ellipse. The ice of these deposits is transparent with a smooth external surface; both being characteristics of glazes. Ice of samples 1 and 2 is free of hyperfine air bubbles (fig. 6a), but sample 1 includes many large air inclusions (fig. 6a). According to

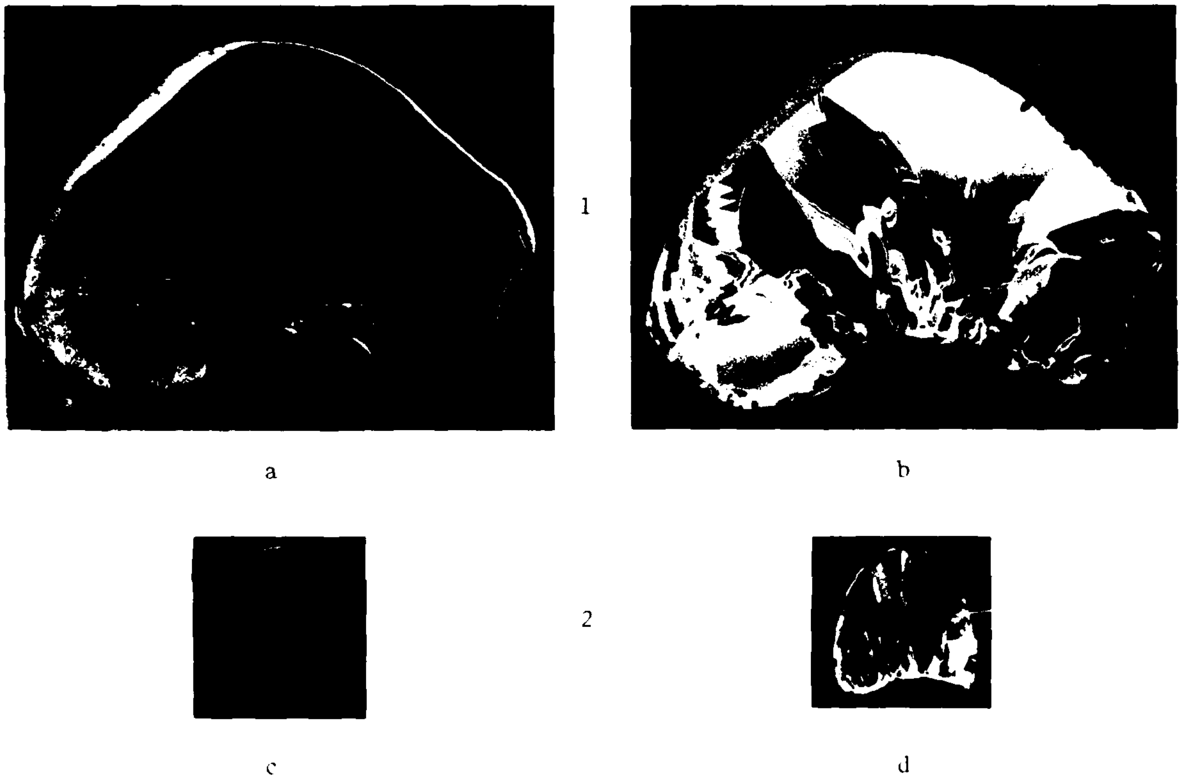

FIG. 6 NATURAL GLAZE DEPOSITS

1) wet growth condition
2) dry growth condition

the afore-mentioned study of artificial ice accretions, ice in sample 1 has been formed in wet growth regime, and sample 2 in the warm limit of the dry growth regime, i.e. the mean deposit temperature is about or near the melting point of ice 0°C. Figures 6b and 6d show that the crystal length is nearly equal to the thickness of ice accretion so the mean width must be used to characterise crystal dimensions of these samples. It has also been observed that the mean crystal width $\overline{w}$ increases with the radial distance from the surface of the conductor (1).

The accretion shown in figure 7 cover more than a half of the circumference of the conductor. This shape of ice is typical of wet snow accretion which twists usually around the conductor. This sample was effectively collected after a strong wet snow storm on the North Shore on the 4th and 5th December '80. Other samples of wet snow collected during the same storm have a density as low as 0,47. It may be seen that wet snow is opaque and that the size of its crystals is much smaller than that of the previously shown glaze samples.

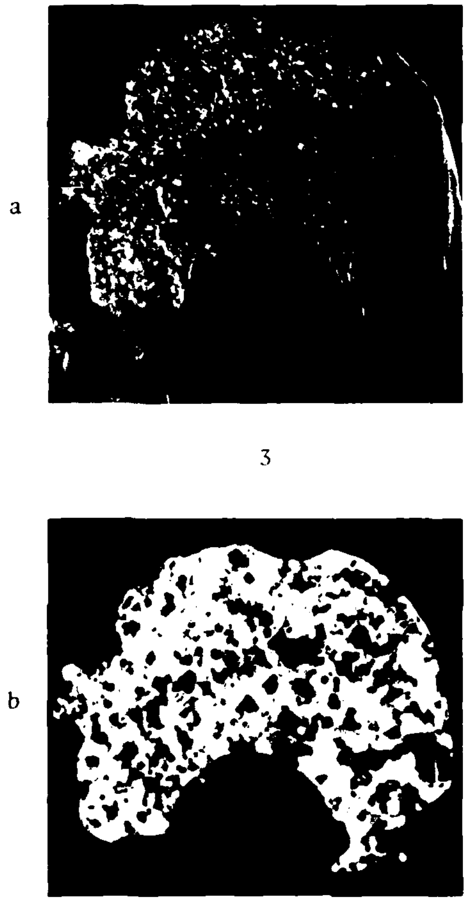

FIG. 7 WET SNOW DEPOSITS

In figure 8, thin sections of ice deposits formed from freezing rain on power line conductor are shown. This accretion has a hemicylindrical shape and was collected from a conductor of about 34 mm in diameter. Transparency of this deposit is less than that observed in glaze samples (fig. 6). In fact, this relatively greater opacity is due to large cavities located near grain boundaries (see fig. 9) which affect also density and other interrelated properties.

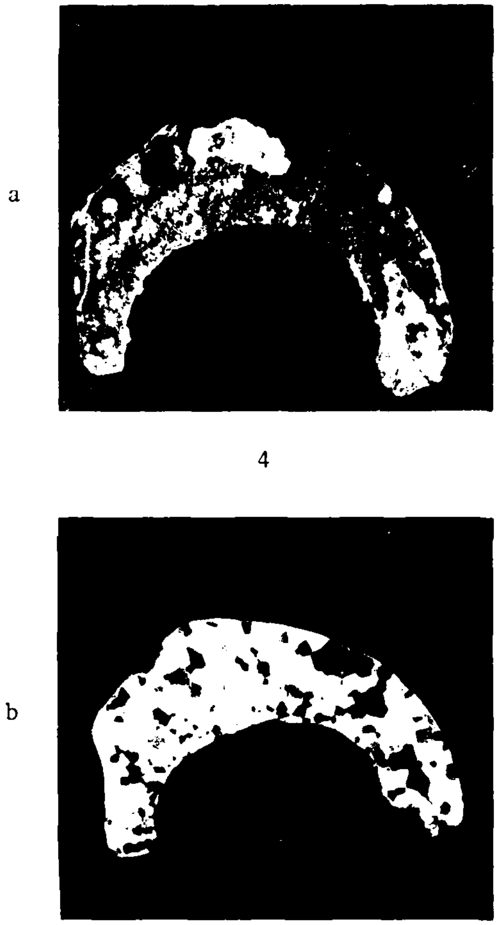

FIG. 8 ICE ACCRETION GROWN FROM FREEZING RAIN

It may be observed that the width and the length of ice crystals obtained from wet snow or freezing rain (figs 7b and 8b) are comparable in order of magnitude, while with glaze ice (figs 6b and d) the ice crystals are elongated in the growth direction. This may be explained by the fact that the processes involved in the crystal formation (nucleation and growth) of wet snow and freezing rain are different than those in glaze and rime icing. In fact wet snow is formed from partially melted snow flakes at a temperature near 0°C. Thus, it may be argued that the shape and the dimensions of wet snow ice crystals should correspond to those of the individual snow flakes. Concerning the freezing rain, crystal structure appears to result from the freezing of large supercooled rain drops. Depending on the temperature, individual rain drops may be solidified into a single crystal or into several crystals. With the deposit shown on fig. 9, it is the first mode of crystallization which has occurred. Both modes of crystallization (monocrystal and polycrystal formation) have been observed with the freezing rain samples analysed in the study (1) and have been interpretated by the variations observed in the ambient temperature during the accretion. These results are in agreement with Hallet (5) who showed that the number of crystals nucleated from large (up to 2 mm in diameter) drops increases with decreasing air temperature. This phenomena was also observed by Levi and al. (6) when singular drops of diameter in the 75-135 μm range collided into substrate in the absence of ventilation. Due to the difficulty to produce in laboratory this particular kind of glaze formed with very large drops it is of interest to collect other samples of ice formed from natural freezing rain.

Results obtained from laboratory analysis of these natural samples of ice are shown in table 1.

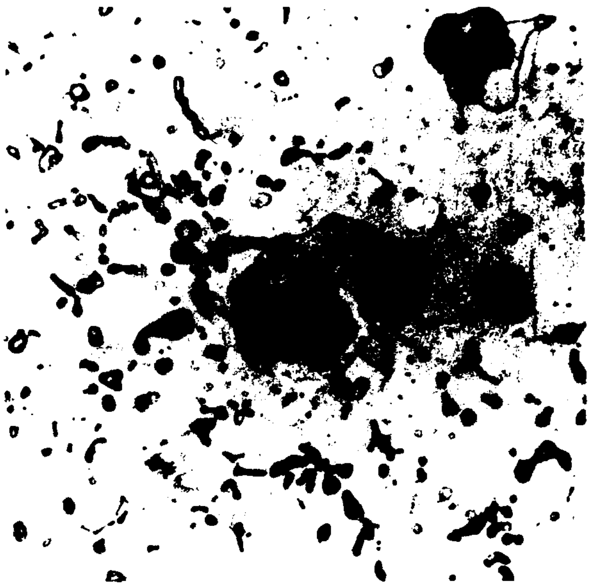

FIG. 9 PORES AS SEEN AT GRAIN BOUNDARIES INSIDE ACCRETION GROWN FROM FREEZING RAIN.

TABLE 1 CHARACTERISTICS OF NATURAL ICE DEPOSITS

| SAMPLE | ICING STORM | VISUAL APPEARANCE | $i/i_0$ | DENSITY $g/cm^3$ | $\overline{w}_1$* | $\overline{w}_6$* | $\ell_{max}$** mm | A ** $cm^2$ |
|---|---|---|---|---|---|---|---|---|
| 1 | Baie Comeau December '79 | Transparent | 0.92 | 0.88 | 1.5 | 2.9 | 44 | 38 |
| 2 | Baie de James<br>- | Transparent | 0.93 | 0.88 | 0.83 | 1.1 | 19 | 4 |
| 3 | Baie Comeau December '80 | Opaque | 0.20 | 0.86 | 0.67 | 0.81 | 32 | 25 |
| 4 | Saguenay November '81 | Semi-Transparent | - | 0.84 | 1.0 | 1.9 | 16 | 10 |
| 5 | Quebec April '80 | Transparent | - | 0.87 | 1.6 | 2.2 | 21 | 5 |
| 6 | Sept-Iles December '81 | Transparent | - | 0.89 | 2.6 | 3.4 | 55 | 30 |

* $\overline{w}_1$ and $\overline{w}_6$ are mean crystal width (in mm) measured at 1 mm and 6 mm respectively above the conductor surface.

** $\ell_{max}$: maximum thickness of accretion; A: area of the cross section.

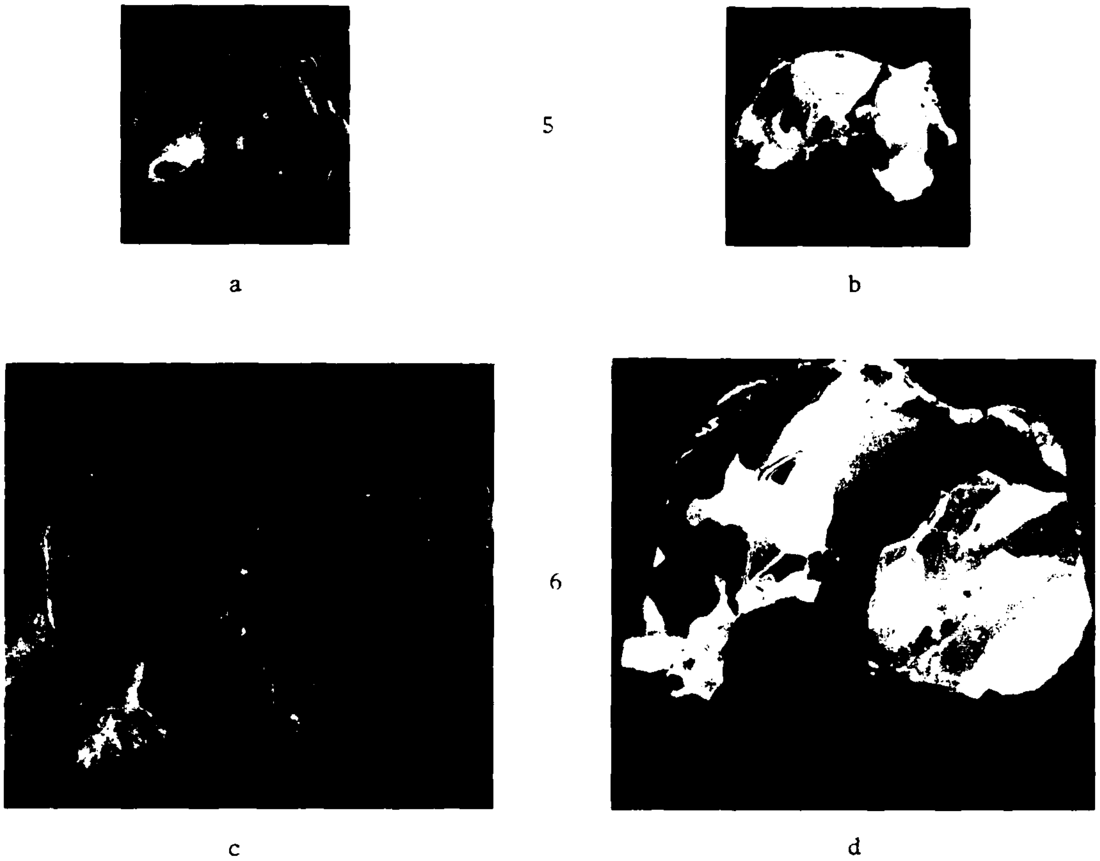

FIG. 10 NATURAL ICE ACCRETIONS ON ACTUAL POWER LINES

5) April '80 storm
6) December '81 storm

The sample corresponding to the first storm was collected from a 13 mm wire while the other comes from a 23 mm conductor. Environmental data such as ambient temperature, air velocity and duration for the two icing precipitation are given on table 2; these were measured at the meteorological station nearest to where the sample was collected.

On the other hand, results obtained from laboratory analyses of these two ice samples are depicted in table 1 (samples 5 and 6). The density of both samples approaches the maximum density of ice (0,916); the ice is transparent and contains large air bubbles (figs 10a and c). All these are characteristics of a wet growth regime ($T_s \simeq 0°C$). Concerning the crystal texture, it may be seen on figs 10b and d that the length of some crystals is equal to the thickness of the ice accretion. Moreover, the crystal texture of ice sample number 6 (fig. 10d) shows evidence of the partial twisting of the iced conductor. The mean crystal width of sample 6 is larger than that of sample 5, due to the higher ambient temperature of its formation. Let us mention that along with this latter factor, the duration of precipitation also may favorise grain growth (8). Table 3 presents values of $T_a$, $T_s$ and effective water content $\varepsilon W$ estimated from laboratory analyses and meteorological data using the procedure described previously. It can be observed in table 3 that the value of $T_a$ estimated from crystal size agrees well with the value measured at the meteorological station. Meanwhile, in the evaluation of effective liquid water content $\varepsilon W$, it is assumed that all impinging water has time to freeze on the conductor, so that actual values of $\varepsilon W$ may be higher. In addition, because the ice accretions were formed at a temperature near 0°C, it is more difficult to evaluate the mean droplet diameter prevailing during these storms. However this parameter may be obtained indirectly, from the dependence between the liquid water content and the mean volume droplet diameter. This dependence was suggested by Mason (9) from field data collected at Mount Washington.

## ESTIMATION PROCEDURE OF ENVIRONMENTAL GROWTH PARAMETERS OF NATURAL ICE DEPOSITS

The procedure used to establish environmental conditions prevailing during ice growth is based partly on the quantitative scheme developed by atmospheric searchers for deducing the growth parameters of hailstone trajectories from hailstone structure. This scheme involves utilizing the crystal sizes to deduce ambient temperatures ($T_a$) encountered by ice deposits during the accretion process. Other environmental parameters such as the effective liquid water content and the air velocity can be determined from $T_a$, density, growth duration and size of deposits with appropriate approximations and assumptions.

Let us mention here that this scheme was developed from many studies on artificial and natural hailstones; however these studies did not provide unique interpretations of growth conditions from the properties of the accretions. However, as mentioned by one of the recent reports (7) on this topic, relatively crude but useful deductions of growth temperature can be made with confidence. At the present state of knowledge, detailed deductions would have to be verified by others methods.

1. The growth of the accretion on structure can be dry or wet depending on whether the surface deposit temperature is lower or near the melting point of ice (0°C). In order to determinate the real mode of growth, crystal orientations must be measured with respect to the bulk growing direction (which is along the radius of the ice accretion). The determination of the mode of growth can also be made from the size of air bubbles. Generally, ice grown in a dry regime presents hyperfine bubble layers disposed in concentric shells while ice accreted in a wet regime contains large spherical air cavities.

2. Ambient temperature is determined from the mean width of ice crystals at 6 mm and 1 mm above the conductor surface. The ratio of $\overline{w}_6/\overline{w}_1$ can also be used for this estimation. The deposit temperature $T_s$ depends on the air temperature and the amount of water which is collected by the conductor. In a wet growth regime, $T_s$ is assumed to be 0°C. In a dry growth regime it can be estimated from transmittance measurements $i/i_0$.

3. The icing intensity or the product $\varepsilon WV$ defined previously, can be evaluated from the mass of ice collected per unit of length of conductor M/L and from the knowledge of either the average duration of precipitation t or the air velocity V assumed to be the droplet speed. These two parameters t and V are globaly interdependent and expressed by the following relation:

$$M/L = dA = \varepsilon WVtD \qquad (1)$$

where d represents the mean density of the ice accretion. This relation which is valid for cylindrical ice accretions grown on a rotating cylinder is assumed to be applicable to the deposits formed on a stationary conductor. On this basis, A refers directly to the cross section of natural ice deposit and D to the diameter of conductor. In case of the partial rotation of the iced conductor, D may take some larger values.

## CASE STUDIES

Since only environmental conditions characteristic of in-cloud icing can be simulated in an icing wind tunnel, this particular type of analysis is for the moment limited and does not apply to deposits formed under freezing rain or in wet snow. Moreover because of the difficulty of transporting light rime deposits (density less than 0.5 g/cm$^3$) which are very fragile, all samples analyzed were of the hard rime or glaze type with densities in the range of 0.86 - 0.90 g/cm$^3$.

Two cases are presented in this report to illustrate the afore-mentioned procedure. Figure 10 shows microphotographs of thin sections of two natural deposits obtained during two different icing storms. The first one (figs 10a and b) occurred in April '80 at 65 km north-east of Quebec City (Lac Lavoie) in an area quite often subjected to icing; and the second, in December '81 near Fermont, 150 km north of Sept-Iles and close to Labrador border.

TABLE 2 METEOROLOGICAL DATA MEASURED DURING THE ICING STORM

| SAMPLE NO | $T_a$ °C | V m/s | t h |
|---|---|---|---|
| 5* | +1 | 4 | 24 |
| 6 | -0.5 | 5-8 | 60 |

* Data recorded at station located at 400 m below the site of sample collection.

TABLE 3 ATMOSPHERIC PARAMETERS ESTIMATED FROM NATURAL ICE DEPOSIT ANALYSES

| SAMPLE NO | GROWTH REGIME | $T_a$ °C | $T_s$ °C | Effective water content εW g/m$^3$ |
|---|---|---|---|---|
| 5 | Wet | -1-2 | ≃0 | 0.05 (0.07)* |
| 6 | Wet | 0-1 | ≃0 | 0.10 |

* Value of W evaluated from rain collected at station located at 400 m below the site of sample collection (average rain precipitation rate: 1.15 mm/h).

## CONCLUSION

From the characteristics observed with artificial ice accretions, the following conclusions can be drawn about natural ice deposits collected from power line conductors.

1. Visual appearance, opacity and the crystal texture of natural glaze deposits are similar to those observed with ice grown in tunnel.
2. Ice crystals of freezing rain deposits seem to be formed from the solidification of individual drops.
3. The mean crystal width and the degree of transparence of wet snow are much smaller than those of glaze.
4. The mode of growth and ambient temperature during accretion may be deduced from air bubble and crystal size measurements.
5. Additional field studies and analyses are needed to determine with a better accuracy other environmental growth parameters such as air velocity and droplet size.

## ACKNOWLEDGEMENTS

This study presented in this report was supported by Hydro-Quebec (contract no: PLT-EN-79-011).

## REFERENCES

1. Laforte, J.L. & Phan, C.L., 1981. "Détermination des caractéristiques physiques et mécaniques des dépôts de givre et de verglas". Rapport PLT-EN-79-011, Hydro-Québec, 165 pages, unpublished. Some results of this report were submitted in March '82 for publication in Journal of Applied Meteorology.
2. Macklin, W.C., 1962. "The density and structure of ice formed by accretion". Quart. J. Roy. Met. Soc., 88, 30-50.
3. Carras, J.N., and Macklin, W.C., 1975. "The opacity of accreted ice". Quart. J. Roy. Met. Soc., 101, 203-206.
4. Rye, P.J., and Macklin, W.C., 1975. "Crystal size in accreted ice". Quart. J. Roy. Met. Soc., 101, 207-215.
5. Hallet, J., 1964. "Experimental studies of the crystallization of supercooled water". J. Atmos. Sci., 21, 671-682.
6. Levi, L., Nosello, D.B., and de Achaval, E.M., 1980. "Crystal structure of droplets frozen on an ice substrate after low speed collision". Journal of Crystal Growth, 48, 121-130.
7. Ashworth, E., and Ashworth, T., 1980. "Cylindrical ice accretions as simulation of hail growth 3. Analysis techniques and application to trajectory determination". J. Atmos. Sci., 37, 846-854.
8. Prodi, F., and Levi, L., 1980. "Aging of accreted ice". J. Atmos. Sci., 37, 1375-1384.
9. Mason, B.J., and Ludlam, F.H., 1951. "The microphysics of clouds". Rep. Proc. Phys. London Physical Society, Vol. 14, 147-195.

## DISCUSSION

Lozowski: One of the things that meteorologists who study hail have been interested in for a long time, as you know, is the interpretation of hailstone crystalline and bubble structure in an attempt to deduce the trajectories of hailstones through storms. And it hasn't been notably successful. One of the things that I wondered if you'd attempted to do to test you model for deducing air temperature and other parameters from the structure of ice, is to run a double-blind experiment in which one of your colleagues grows some ice in the wind tunnel and then you take a look at it and say, well, these were the conditions. Have you tried to do that?

Laforte: I know that many experiments were done with artificial [crystals], some of the conditions of simulation of hailstone are similar to natural glaze and rime deposits. Essentially, the difference between hailstones and [bulk] is the absence of [...] that can affect the [...] of ice crystal. When velocities are low, in the case of glaze and hard rime, some larger droplets can be expected, with precipitation near the ground. All those conditions were the tested in the tunnel to help us in the study of sample microstructure.

AD P001688

# ICING CLOUD MICROSTRUCTURE FROM IN SITU MEASUREMENTS

J.F. Gayet
M. Bain
University of Clermont II, Laboratoire Associé de Météorologie Physique
B.P. 45, 63170 Aubière, France.

## ABSTRACT

During several experiments carried out in France, Ivory Coast and Spain, many icing cloud penetrations were performed at different levels with instrumented research aircraft. The paper describes the range and the frequencies of occurrence of the relevant icing parameters computed on the cloud scale and for different cloud types.

Comparisons between microphysical parameters and meteorological radar signatures show the limitations of these radars when used as a means of locating icing clouds.

## I - INTRODUCTION

Existing weather statistics demonstrate some significant operational limitations due to icing for aircraft and helicopters. Unfortunately, the existing meteorological data base is insufficient to describe the operating environment in which aircraft and helicopters must conduct flights. In addition to the inadequacies of existing atmospheric icing models, a great deal of improvement is needed regarding nowcasting and forecasting capability.

Since 1972, the "Laboratoire Associé de Météorologie Physique" has been involved with studies on meteorological problems concerning the icing of aircraft and helicopters. During this period the atmospheric and cloud physics instrumentation has been extended and improved, and mounted on a DC 7*research aircraft up to 1979 and on a Piper Aztec** in 1981.

Several experiments were carried out in France during the winter and summer months (1975-1977), Ivory Coast (october 1977) and during the winter-spring months in Spain (1979 and 1981).

This paper describes the range of the relevant icing meteorological parameters measured during the first exploratory experiments in France and Ivory Coast, and a statistical analysis of the icing cloud microstructure in Spain where the data were better documented. Some comparisons between microphysical parameters and radar echo signatures are also described to give the limitation of meteorological radar used as a means of locating icing clouds.

## II - CLOUD PHYSICS INSTRUMENTATION

The available instrumentation on the two aircraft was as given in Table 1.

The spatial resolution of the tape recorded data was about 100 m for all the parameters and for both aircraft. A detailed description of the aircraft instrumentation and the measurement accuracies and limitations has been discussed in previous papers (Gayet and Friedlander, 1979 ; Gayet, 1981 ; Personne et al., 1982).

---

* The DC 7 aircraft was sponsored and operated by the "Direction des Recherches Etudes et Techniques" and by the "Centre d'Essais en Vol" in Brétigny.

**The Piper Aztec aircraft is sponsored and operated by the "Météorologie Nationale".

| Instrumentation | DC7 before 1979 | DC7 1979 | Piper Aztec 1981 |
|---|---|---|---|
| PMS* ASSP-100 $3 \leq D \leq 45$ µm | x | | x |
| PMS FSSP-100 $3 \leq D \leq 45$ µm | | x | |
| PMS 1D-C $20 \leq D \leq 300$ µm | x | x | |
| PMS 1D-P $300 \leq D \leq 4500$ µm | x | x | |
| PMS 2D-C $25 \leq D \leq 800$ µm | | x | x |
| PMS 2D-P $250 \leq D \leq 6000$ µm | | x | |
| Johnson-Williams meter ($D < 30$ µm) | | x | x |
| Total Water Content Probe | x | x | |
| Icing Probe | x | x | |
| Rosemount Temperature Probe | x | x | x |
| Reverse Flow Temperature Probe | | | x |
| Dew-Point | x | x | x |
| Pressures (static and dynamic) | x | x | x |
| 3 cm PPI radar | x | x | |
| Doppler radar | x | x | |
| Inertial Plateform | | x | |
| Radio-Beacon | x | x | x |
| Sideslip (Attack and Yawl angles) | x | x | x |
| Cameras | x | x | |

Table 1

* PMS : Particle Measuring Systems, Inc., Boulder, Co.

## III - AN ATTEMPT TO QUANTIFY ICING SEVERITY

The icing intensity can be related to the rate of ice accretion on an ice collector as a function of several parameters : the air temperature, supercooled liquid water content, ice content, collection efficiency, speed and flight duration in the cloud.

- Qualitative observations made from the aircraft show that the icing generally occurred in most of the clouds encountered for temperatures colder than - 2 / - 3°C with the DC 7 (100 m $s^{-1}$ cruise speed). With the Piper Aztec (60 m $s^{-1}$ cruise speed), a higher temperature was observed (- 1°C) due to the dynamic heating of the icing probe.

- Quantitative measurements of the ice profiles on a fixed cylinder (Bain and Gayet, 1982) show that increasing liquid water content is generally accompanied by increasing icing intensity. Figure 1-a displays the icing rate (R) measured from an icing probe versus the liquid water content (LWC) for several penetrations of stratiform and cumuliform clouds containing few ice particles (IPC < 5 $l^{-1}$) (Spring 1979 experiment, Spain).

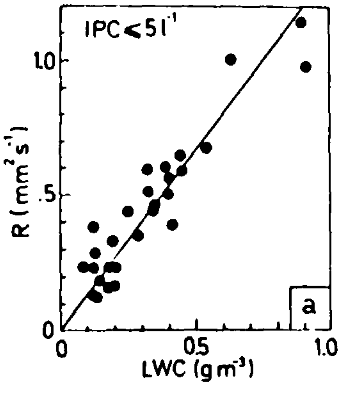

Figure 1-a

- The effect of the ice particles on the icing intensity is not clearly accounted for. Helicopters flying in natural icing conditions have occasionally experienced a sudden rise in the severity of icing (Lake and Bradley, 1976). This effect has been explained by the presence of ice crystals in the supercooled clouds. On the contrary, Bain and Gayet (1982) have shown a reduction of the icing rate in cumuliform clouds (near - 20°C) containing noticeable ice particle concentration (IPC > 5 $l^{-1}$) as displayed on Figure 1-b. This figure shows a measured icing rate (R) lower than case (a) possibly because of the erosion caused by the ice particles impinging on the ice deposit.

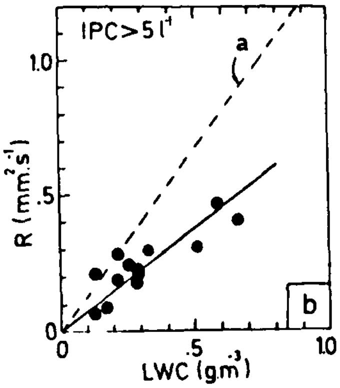

Figure 1-b

- The overall collection efficiency depends upon several parameters : those related to the air (temperature, density, viscosity), those related to the ice collector (shape and stream velocity) and those related to the cloud (concentration of water / ice, droplet spectrum). Therefore, it is expected that a given helicopter or aircraft type will be sensitive to a range of hazards created by icing on the airframe, rotor blades, air intakes, etc.) and that different helicopter or aircraft types will experience problems to various degrees in these areas.

These previous statements lead to present our results in term of meteorological parameters rather than in terms of icing severities.

## IV - SOME RESULTS OF THE EXPLORATORY EXPERIMENTS CARRIED OUT IN FRANCE AND IVORY COAST

Figure 2-a shows the mean values of the liquid water content versus the temperature at the penetration level for each traverse of icing clouds performed in France. Two symbols are used to distinguish the cumuliform clouds (▲) and the stratiform clouds (●) ; solid and open symbols correspond to winter and summer clouds respectively. Figure 2-b relates to the tropical cumuliform clouds experienced in Ivory Coast.

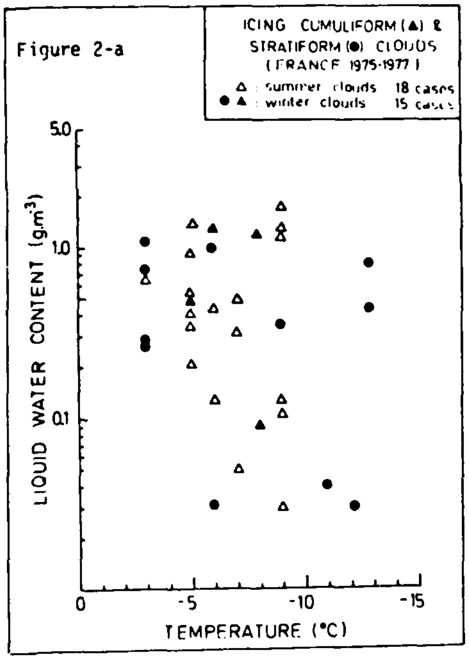

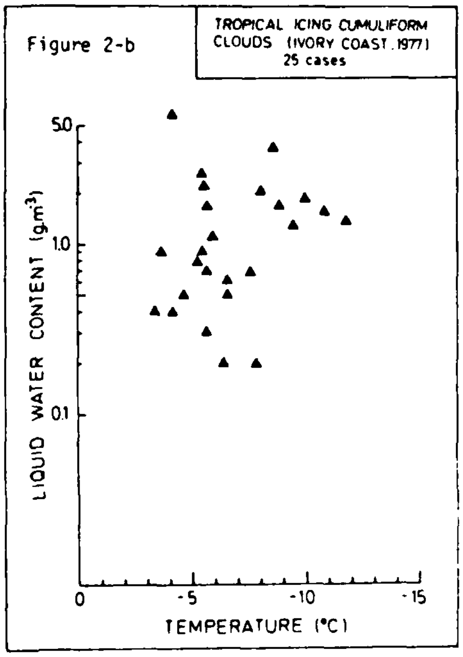

These two figures show scattered values of the liquid water content whatever the temperature between - 3 and - 15°C.

In France, for all the cases studied, the values of LWC range from 0.03 to 1.8 g $m^{-3}$ and 40 % of the clouds have a LWC greater than 0.5 g $m^{-3}$ (mean value about 0.5 g $m^{-3}$). The maximum frequency of occurrence of icing clouds is found between - 5 and - 7°C which corresponds to levels of 2700 m MSL in winter and 4300 m MSL in summer.

Tropical cumuliform clouds are characterized by larger LWC : from 0.2 to 5.8 g $m^{-3}$ (mean value of 1.3 g $m^{-3}$) and 80 % of the clouds have a LWC greater than 0.5 g $m^{-3}$.

The maximum frequency of occurrence of icing clouds is also found near - 6°C which corresponds to a level of 5800 m MSL.

The scattered values of LWC are due to the cloud microphysical structure which is variable both in space and time depending on the stage of the cloud life-time.

Local values of liquid water content much greater than the values displayed on Figures 2-a and 2-b were observed, particularly in tropical clouds where 20 g $m^{-3}$ was measured in an accumulation zone associated with strong updrafts up to 23 m $s^{-1}$ (Gayet et al., 1978).

Qualitative observations of the icing probe made during these cloud penetrations have shown that the icing rate is lower than that expected due to a loss of water by shedding. Indeed, when the liquid water content is much larger than the critical water content (limit of Ludlam, 1951) all the supercooled drops are not completely frozen during the impact, the ice grows wet and run-off of water occurs.

We have also noted that the ice deposit can be partially eroded due to the presence of large particles (graupel or hail).

## V - STATISTICAL STUDY OF THE MICROSTRUCTURE OF THE CLOUDS SAMPLED IN SPAIN (1979 - 1981 experiments).

The results presented in this chapter have been obtained from the data collected in an area in the north-west of Spain during the SSP 3 of the W.M.O. Precipitation Enhancement Project (PEP) in 1979 (from March 27th to April 4th) and in 1981 (from March 27th to May 16th).

Approximately 650 cloud penetrations at negative temperatures were performed on 33 different days ; this represents a total "in-cloud" length of about 3000 km.

Despite the fact that these data are geographically restricted and concern a short period (three months), they give a representative cloud sample including several synoptic situations and are presented as a statistical analysis.

This analysis concerns microphysical and thermodynamical parameters averaged over the cloud penetration. We call penetration a flight in a cloud with a length greater than ∿ 1000 m (10 discrete measurements) in which the liquid water content is greater than 0.05 g $m^{-3}$ or the ice particle concentration is greater than 0.1 $l^{-1}$. Under these criteria, the median penetration length was 4500 m and 80 % of the penetration lengths were between 1000 and 6000 m.

The mean value of the temperature at the penetration level is about - 8°C and 13 % of penetrations were carried out at a temperature less than - 14°C.

Three icing cloud types are considered : the cumuliform clouds including cumulus mediocris, winter cumulus congestus and cumulonimbus, the low stratiform clouds including stratocumulus, nimbostratus and the medium stratiform clouds (altocumulus, altostratus).

The mean levels of penetration of the different cloud types described above were : 2.8, 2.4 and 3.2 km MSL respectively. Due to the sampling period (winter/spring) the cumulus clouds were not very well-developed vertically (mean thickness of about 2.1 km) and were found in most cases in complex cloudy situations (embedded convection). The low and medium stratiform clouds had a similar thickness : 1.1 km.

1 - General characteristics of each cloud category

Figures 3 to 5 display the histograms of the cloud liquid water content (LWC), the median volume diameter (DV) and the ice particle concentration (IPC) for the cumuliform, low and medium stratiform cloud categories respectively.

Fig 3 : CUMULIFORM CLOUDS (393 penetrations)

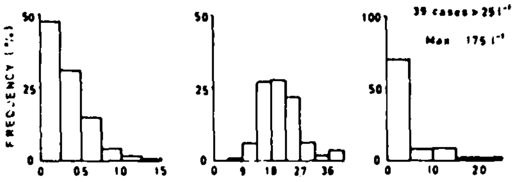

Fig 4 : LOW STRATIFORM CLOUDS (204 penetrations)

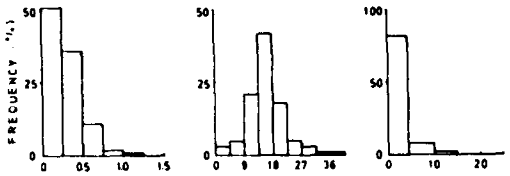

Fig 5 : MEDIUM STRATIFORM CLOUDS (55 penetrations)

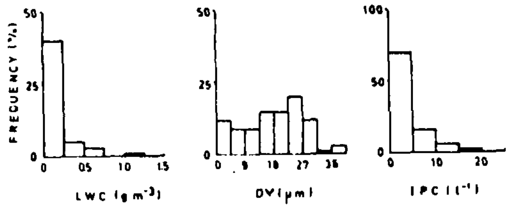

Table 2 summarizes the mean values (M.V.)and the standard deviations (S.D.) of the above mentioned parameters together with the horizontal cloud length (HCL).

Figures 3 to 5 and Table 2 show that liquid water content are similar (0.3 g $m^{-3}$) in cumuliform and low stratiform clouds, but lower (0.18 g $m^{-3}$) in medium stratiform clouds. Noticeable differences appear between the cumuliform and the low stratiform clouds for the median volume diameter (20.8 against 16.1 μm) and for the ice particle concentration (10.1 and

|  | LWC ($g\ m^{-3}$) |  | DV (μm) |  | IPC ($l^{-1}$) |  | HCL (km) |  |
|---|---|---|---|---|---|---|---|---|
|  | M.V. | S.D. | M.V. | S.D. | M.V. | S.D. | M.V. | S.D. |
| Cumuliform | 0.33 | 0.25 | 20.8 | 6.9 | 10.1 | 21.9 | 4.5 | 4.9 |
| Low Stratiform | 0.29 | 0.19 | 16.1 | 5.7 | 2.9 | 5.7 | 3.9 | 4.6 |
| Medium Stratif. | 0.18 | 0.27 | 18.9 | 9.7 | 7.2 | 13.8 | 6.8 | 9.3 |

Table 2

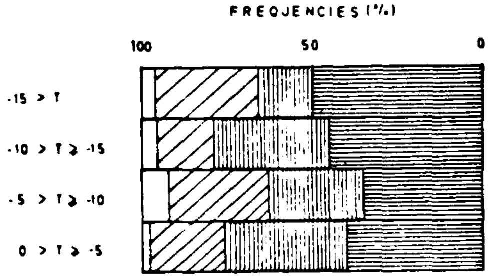

Figure 6

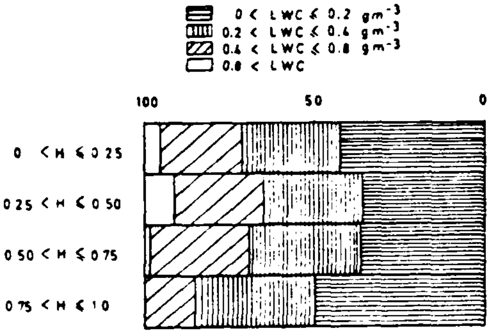

Figure 7

| Mean LWC $g\ m^3$ | | | |
|---|---|---|---|
| All categories | Cum | Low strat | Med strat |
| .30 | .30 | — | .36 |
| .27 | .27 | .31 | .21 |
| .36 | .41 | .31 | .11 |
| .29 | .33 | .26 | .12 |

Table 3

| All categories | | Cum | | Low strat | | Med strat | |
|---|---|---|---|---|---|---|---|
| LWC | DV | LWC | DV | LWC | DV | LWC | DV |
| .31 | 19.8 | .32 | 23.0 | .29 | 14.8 | .22 | 20.1 |
| .35 | 20.0 | .37 | 21.0 | .32 | 17.2 | .30 | 26.6 |
| .30 | 18.7 | .32 | 19.8 | .28 | 16.6 | .18 | 15.7 |
| .23 | 17.3 | .30 | 17.8 | .22 | 16.2 | .11 | 18.4 |

Table 4

2.9 $l^{-1}$). Intermediate values are found in the medium stratiform clouds (DV = 18.1 µm and IPC = 7.2 $l^{-1}$). The horizontal cloud length is found to be larger in the medium stratiform clouds (9.3 km), but this parameter does not represent the horizontal cloud extent on account of the flight procedures and the data processing method. Sometimes, stratiform cloud decks exhibit "holes" which are not taken into account in the evaluation of the microphysical parameters.

2 - Stratification of the microstructure versus the temperature and the level of penetrations

Figure 6 displays the frequency distributions of the liquid water content versus four ranges of the penetration temperature for all the cloud categories. Table 3 shows the mean values of the LWC in the same ranges of temperature for the sum of all cloud categories and for each cloud category individually. It appears that the largest LWC are found between - 5 and - 10°C, particularly for cumuliform clouds (0.41 $g\ m^{-3}$). This trend is not observed in medium stratiform clouds (maximum values observed for T < - 15°C) because most of these clouds occur below - 10°C.

Figure 7 with the same representation as Figure 6 shows the LWC frequencies for the four ranges of the penetration level (H) relative to the cloud depth (H = 0 corresponds to the cloud top, and H = 1 to the cloud base). Table 4 shows the mean values of LWC and DV in the corresponding relative altitude ranges.

For each cloud category, the greatest values of LWC are found at three quarters of the way up from the cloud base (maximum value in cumuliform : 0.37 $g\ m^{-3}$) and the median volume diameter increases from the base to the top for cumuliform clouds (17.8 to 23 µm).

3 - Stratification of the microstructure versus the horizontal cloud length and versus the ice particle concentration.

The relation between the cloud horizontal extent and the icing zone extent of a cloud is an important meteorological parameter for the quantification of the icing severity.

Figure 8 displays the frequency distributions of the liquid water content versus four ranges of the fractional cloud length (L) which contains a liquid water content greater than 0.05 $g\ m^{-3}$, for all the cloud categories. (For example : L = 0.25 corresponds to 25 % of the cloud penetration length characterized by a LWC > 0.05 $g\ m^{-3}$ and the other 75 % of the cloud only contains an ice particle concentration greater than 0.1 $l^{-1}$). Table 5 summarizes the mean values of the horizontal cloud length (HCL) and the liquid water content (mean values) in the same ranges as defined in Figure 8 for each

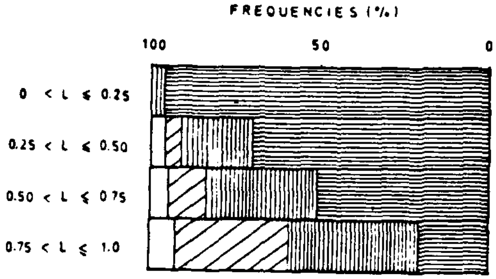

Figure 8

| All categories | | Cum. | L strat | M strat |
|---|---|---|---|---|
| HCL km | LWC | LWC | LWC | LWC |
| 6.2 | 0.08 | 0.09 | 0.07 | 0.05 |
| 4.1 | 0.19 | 0.21 | 0.20 | 0.08 |
| 4.4 | 0.25 | 0.28 | 0.21 | 0.26 |
| 4.2 | 0.40 | 0.42 | 0.36 | 0.32 |

Table 5

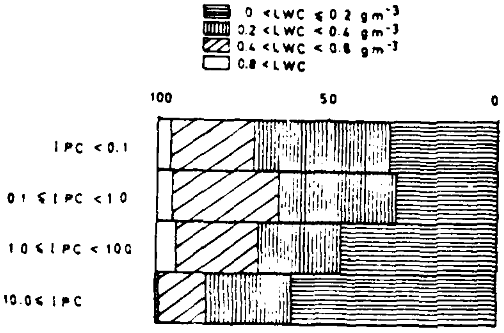

Figure 9

| Mean LWC g m$^{-3}$ | | | |
|---|---|---|---|
| All categ | Cum. | L strat | M strat |
| 0.32 | 0.37 | 0.26 | 0.10 |
| 0.36 | 0.36 | 0.34 | 0.45 |
| 0.30 | 0.33 | 0.31 | 0.14 |
| 0.23 | 0.25 | 0.16 | 0.09 |

Table 6

cloud category. Figure 8 and Table 5 show that the mean value of the liquid water content increases with the proportion of cloud containing a liquid water content greater than 0.05 g m$^{-3}$ for all cloud categories. The lowest values of LWC were found during the longest cloud penetrations (6.2 km) which correspond to the most glaciated clouds. This trend is confirmed in Figure 9 and Table 6 where the liquid water content frequency distributions are given versus four ranges of the ice particle concentration. The largest values of LWC were found in clouds containing low ice particle concentration (IPC < 0.1 l$^{-1}$).

## VI - DETECTION OF THE ICING ZONES FROM CONVENTIONAL METEOROLOGICAL RADARS

The objective of this section is to link meteorological radar information with the microphysical parameters and to indicate the limitations of these radars when used as a means of locating icing clouds.

To illustrate our purpose, we discuss the results of two successive penetrations carried out with the DC 7 in a growing cumulus congestus cloud at the level 4300 m MSL, - 5°C (summer 1976 experiment).

During the first traverse, the cloud is a single cell (labelled A) in the growing stage. The variations of the vertical velocity (WA) and the microphysical parameters are displayed in Figure 10.

An updraft of 7 m s$^{-1}$ is found in the cloud core and the LWC reaches 1 g m$^{-3}$. The median volume diameter (DV) of the cloud droplet spectrum is about 15 μm and

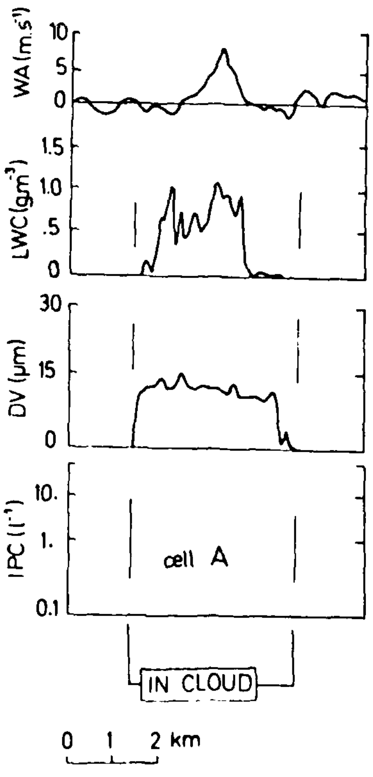

Figure 10

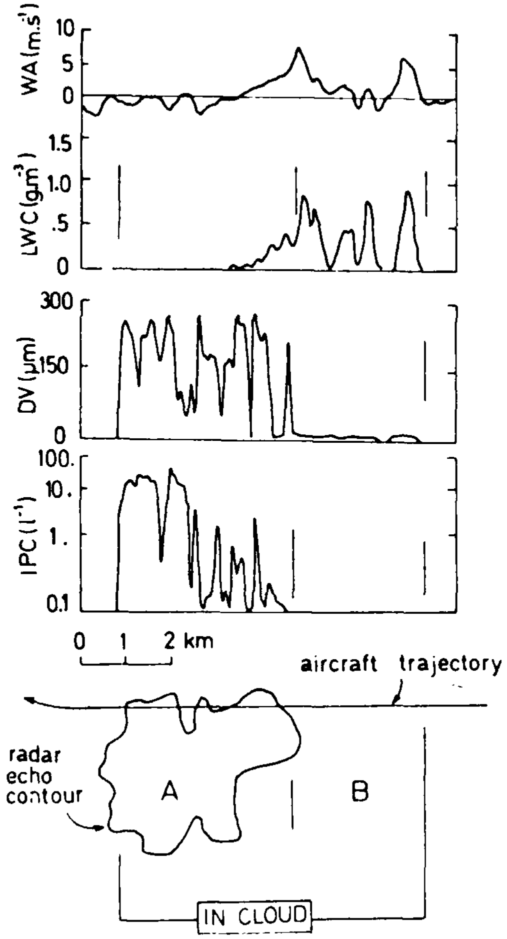

Figure 11

no particles greater than 200 μm (IPC) are measured. During this penetration no echo was detected by the airborne meteorological radar ($\lambda$ =   cm, Power = 220 km and range scale : 220 NM). However a light icing was observed due to a short penetration time duration (40 s).

Figure 11 represents the evolution of the parameters (described above) measured during the second penetration of the same cloud 1[illegible] mn later and the corresponding radar echo contour.

This figure reveals sharp discontinuities in the microphysical and dynamical features of the cloud and two cells can be identified :

- the cell B, which is mainly composed of supercooled droplets (LWC $\sim$ 1 g $m^{-3}$, DV $\sim$ 1[illegible] μm) ;
- the cell A (previously sampled) which presents no dynamical activity (WA $\sim$ 0), low values of LWC, noticeable concentration of particles greater than 200 μm (IPC) (up to 5[illegible] $l^{-1}$), median volume diameter (calculated on the A[illegible]-1D C range $3 \leqslant D \leqslant 300$ μm) of about 200 μm. Only the cell A is correlated with the radar echo contour, however the icing was judged more severe in cell B than in cell A.

These two examples show that the radar echo signature is a consequence of precipitation particles and that all the icing zones are not related to the radar echo.

The detection threshold depends on the concentration, size and also the nature of these particles (drops or ice crystals). From other investigations and considering the statistically significant minimum concentration of particles measured by the probes (1D-C or 2D-C), a concentration greater than 0.1 $l^{-1}$ of particles larger than 200 μm (diameter) seems to indicate the lowest limit of detectability with this radar. In the PEP data described in section V, about 27 % of the total sampled clouds are characterized by very low particle (D > 200 μm) concentration (< 0.1 $l^{-1}$ : non precipitating clouds).

This leads to the suggestion that such a percentage of icing clouds which contain a noticeable liquid water content (mean value : 0.3 g $m^{-3}$, see Table 6) are not detectable by conventional meteorological radars.

## VII - CONCLUSIONS

From the data collected during several experiments in France, Ivory Coast and Spain, the range of the relevant icing parameters are given. Scattered values of liquid water content are found whatever the temperature between - 3 and - 15°C due to the space and time variabilities of the cloud microstructure. Extreme values of liquid water content, up to 20 g $m^{-3}$ were found in tropical cumulonimbus cloud.

In Spain, the icing zones associated with the greatest values of liquid water content were found in a range of temperature between - 5 and - 10°C and were situated in the upper third quarter of the cloud depth.

The most horizontally extensive clouds and the most glaciated clouds present the lowest mean liquid water content and consequently the lowest icing occurrence. These observations are found to be generally true for the three suggested cloud categories.

The detection of icing zones by conventional meteorological radars seems to be ineffective for 27 % of the sampled clouds. Allowance must therefore be made for this inadequacy when radars are used for now casting or other methods must be relied upon.

## ACKNOWLEDGEMENTS

The authors would like to express their appreciation to Professor Soulage for his guidance during this study, Professor Coulman for his comments on the manuscript and Doctor Pointin for helpful discussions.

Thanks are due to the L.A.M.P.'s technical staff, DC 7 CEV and "Météorologie Nationale/EERM"'s crews.

This research was supported by the "Direction des Recherches Etudes et Techniques" under the contrats 79.34.183 and 80.34.294.

## REFERENCES

Bain M. and J.F. Gayet, 1982 : "Aircraft measurements of icing in supercooled and water droplets / ice crystals clouds", J. Appl. Met., 21, 11-21.

Gayet J.F., M. Jarmuzynski and R.G. Soulage, 1978 : "Microstructure of an accumulation zone in a tropical Cb cloud", Preprint of the Conf. on Cloud Physic and Atmos. Elec., July 31 - August 4, Issaquah, Wash., 318-323.

Gayet J.F. and Friedlander M., 1979 : "The DC 7 research aircraft of the Centre d'Essais en Vol de Brétigny", W.M.O., PEP report n° 13.

Gayet J.F., 1981 : Participation du L.A.M.P. à l'expérience PAP 81", Rapport scientifique du L.A.M.P. n° 39.

Lake H.B. and J. Bradley, 1976 : "The problem of certifying helicopters for flight in icing conditions", Aeronautical J., October 1976, 419-433.

Ludlam S.H., 1951 : "The heat economy of a rimed cylinder", Quart. J. Roy. Met. Soc., 77, 663-666.

Personne P., J.L. Brenguier, J.P. Pinty, Y. Pointin, 1982 : "Comparative study and calibration of sensors for the measurement of the liquid water content of clouds with small droplets", J. Appl. Met., 21, 73-80.

## DISCUSSION

Olsen: What altitude range did you fly at?

Gayet: It depended on the season. In France the mean level of penetration was about 2 km. In the Ivory Coast the mean level of penetration was about 6 km. To reach -5°C we must fly at an altitude of about 6 km on the Ivory Coast.

Olsen: So you made no attempt to get a correlation with altitude.

Gayet: No.

Lozowski: Your results about meteorological radar's ineffectiveness in detecting icing situations is disappointing, to say the least. Do you think there's a possibility that with some more imaginative research one might find an early warning system, so to speak, with meteorological radar for ice storms? I have another question - that is to do with your observation that when there are large ice particles, or at least a large concentration of ice particles around, that the icing intensity is diminished. Do you think there might be any applicability of cloud seeding upwind of fixed, stationary structures on the ground that might help to reduce the icing intensity? But what about the possibility of seeding clouds upwind of sensitive structures such as broadcasting antennas, or whatever, to increase the ice particle content and possibly diminish the icing intensity? Do you think that's worth thinking about?

Gayet: I think that the icing rate can be reduced but temperature is also an important [parameter]. The ice must be very dry because at warmer temperatures ice crystal ... can stick on surface of the ice deposit. It is only in very cold clouds that we observe [reduction in icing rate].

Olsen: Do you plan to share your data with the FAA [Federal Aviation Administration] which is putting together a large data bank?

Gayet: Yes, we have a lot of data now and we are participating in changing the parameterization to the new definition of icing norms.

Bilello: Your observations incorporated a large variety of types of clouds, running from the cumulonimbus which are very unstable to the very stable low stratus and middle clouds. I have a series of questions that you might answer by yes or no to. First, is your sampling of the ice physical characteristics only in the clouds, or is any of it taken off the ground? (G: In the cloud.) In the cloud only? (G: Yes.) In the cumulonimbus, you have a lot of updrafts, so I imagine that goes through the atmosphere several times - there have been instances where they go through upwards of five or six transmissions through the cloud, and down, and up again. Were you able to take this into account? Or do you think it would have any effect on the characteristics of your ice crystals or icings? (G: No.) No? Of course, the cloud itself goes through a series of water content, density, what have you, and I would imagine that would have a difference if you took a cross section of your cloud so you have some idea of the entire history of the icing taking place. And this was certainly different than the icing that you would get in a stable cloud where it might fall right through without going up again on the updraft. I just wondered if you take this updraft and downdraft into account. (G: Yes).

AD-A131 869   PROCEEDINGS OF INTERNATIONAL WORKSHOP ON ATMOSPHERIC   3/4
ICING OF STRUCTURES (..(U) COLD REGIONS RESEARCH AND
ENGINEERING LAB HANOVER NH  L D MINSK JUN 83
UNCLASSIFIED   CRREL-SR-83-17   F/G 8/12   NL

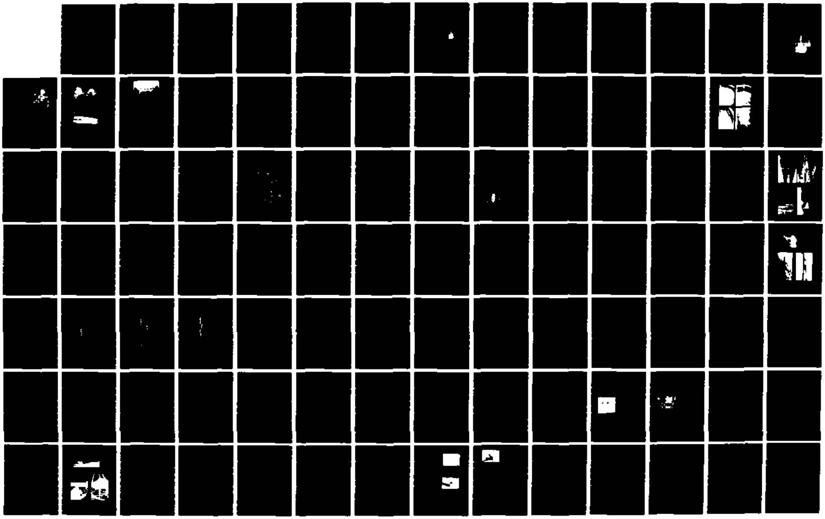

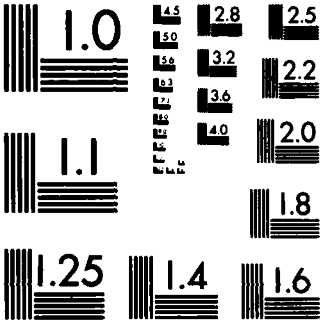
1.0
4.5
5.0
5.6
6.3
7.1
8.0
2.8
3.2
3.6
4.0
2.5
2.2
2.0
1.1
1.8
1.25
1.4
1.6

MICROCOPY RESOLUTION TEST CHART
NATIONAL BUREAU OF STANDARDS-1963-A

AD P001689

# SURFACE ICING RESEARCH AT AFGL

Paul Tattelman   Air Force Geophysics Laboratory, Hanscom AFB, Mass. 01731

## ABSTRACT

There is a lack of objective measurements of ice accumulations on surface structures. Such observations are needed by the Air Force to develop a climatology of surface icing amounts for use in determining design criteria for exposed structures. Over the past several years, the AF Geophysics Laboratory has conducted tests of an ice detector, in a climatic chamber and in the field, to develop an objective method for estimating the amount of ice accumulating on cylinders. The results of the tests, and the relationships of ice accretion characteristics on cylinders 3, 13, 25, and 50 mm in diameter for differing synoptic conditions are presented.

## THE ROSEMOUNT ICE DETECTOR

Sophisticated ice detectors have been developed for specific uses such as detecting icing on highways, runways, and on aircraft. Tests of some of these are discussed by Ackley et al (1973) and Hill (1973). Hill concluded that a detector manufactured by Rosemount, Inc., Minneapolis, Minnesota had the greatest potential as a meteorological instrument for the detection of icing.

Rosemount markets a line of ice detectors used primarily to detect ice formation in the intake portion of turbomachinery. These detectors are aerodynamically designed for use on aircraft, but they have been used to detect icing on towers. The ice detector works by the magnetostriction principle. An oscillator forces a small closed cylinder (the sensing probe) to vibrate longitudinally, parallel to its axis. It is driven at its resonant frequency when dry, but accretion of ice will cause a shift in resonance corresponding to the increase in mass adhering to the probe. After a small preset thickness of ice has accumulated, the sensor is deiced.

The advantages of using a Rosemount ice detector for observation of ice accretion are: convenient size, durability, and operation with limited human involvement. These advantages are quite attractive when compared to other methods and devices that have been tried. It was decided to test Rosemount detectors under controlled conditions in a climatic chamber in order to evaluate its ability to measure ice accretion. Accordingly, four model 872DC ice detectors, a newer model than those tested previously, were purchased from Rosemount. The main reason for the choice of this model is the long strut to keep accumulations on the mounting plate from influencing the flow past the sensor (Figure 1). It was also necessary to purchase a model 524H controller, kept remote from the detectors, to actuate the deicing system. A multi-channel event recorder was used to count deicing cycles.

The ice detectors were calibrated at the factory to emit an icing signal when 0.5 mm of ice has accumulated on the sensing probe; however, detectors with trip points up to 5 mm are available. The sensor is cylindrical with a hemispheric top and has a diameter of 6 mm and a length of 27 mm. Because of its geometry, it is a very efficient collector. Although the detectors were calibrated to deice at 0.5 mm, the actual amount of ice required to trip the deice signal varies slightly, depending on the density and distribution of ice on the sensor. After the trip point has been reached, the sensing probe and top 76 mm of the strut are deiced by an internal heater. Seven seconds after the start of the deicing cycle, the unit is ready to begin the next sensing cycle.

Although we obtained an event recorder to use the discrete output (that is, count the number of deicing cycles), a dc voltage recorder can be used to obtain an analog voltage output that will show the change in current as ice builds up on the sensor. It should be noted that light coatings of oil, dust, water, or other materials do not significantly affect operation of the ice detector.

## THE CLIMATIC CHAMBER TESTS

Testing of the Rosemount ice detectors was conducted in May 1977 and January 1978 at the McKinley Climatic Laboratory of the Armament Development and Test Center (ADTC), Eglin AFB, Florida. Because of initial problems with the model 872DC detectors, model 871FA detectors, which differ only in configuration and strut length (5 cm), were used for the first test period. Therefore, this article concentrates on the second test period, although Tattelman (1979) gives detailed information on all aspects of both test periods.

Two model 872DC detectors and one model 871FA detector were mounted on a stand. Measurements of ice thickness and mass were made on four horizontal cylinders, 3, 13, 25, and 50 mm in diameter located 30.5 cm behind and 15.2 cm above the sensors on the ice detectors. The cylinders were removable so that the mass of accreted ice could be determined. Room was not available to include vertically oriented cylinders, but previous icing tests by Stallabrass and Hearty (1967) indicate that, in spite of small differences in the shape of the ice accretion as a result of gravity affecting the run-off on a vertical cylinder, no difference in collection efficiency is apparent.

A total of 42 one hour tests were run in the main chamber, which has floor dimensions of 61 x 77 m. Half of the tests simulated freezing rainfall rates of approximately 1.27 and 2.54 mm $hr^{-1}$, at temperatures from -1° to -7°C, and wind speeds of 5 to 35 knots. The other tests simulated in-cloud icing with approximately 0.1, and 0.2 g $m^{-3}$ water content, temperatures of -1° to 10°C, and wind speeds of 15 to 35 knots. Additional longer-duration tests, some with varying conditions, were also run.

## ANALYSIS OF TEST RESULTS

At the conclusion of each test, measurements were made of the maximum radial ice thickness (the maximum ice thickness on the cylinder regardless of orientation), the vertical ice thickness (the total thickness of ice in the vertical, both above and below the cylinder, excluding icicles), and the mass of ice on each of the four cylinders. The color and shape of the ice formation was also noted. Measurements of ice density were not made because of problems in obtaining accurate measurements with the rotating cylinder that was tried during the original tests. The number of detector deicing cycles was also recorded for each test.

### a. Mass of Ice

The regression lines and scatter of the individual test points for the mass of ice on the 25-mm diameter cylinder versus the number of cycles for detector 1 (one of the model 872DC detectors) are shown for all forty-two 1-hr tests (Figure 2), for the 21 freezing rain tests (Figure 3), and for the twenty-one in-cloud icing tests (Figure 4). There is little difference in scatter diagrams for the other two detectors. The results of the linear regression analysis for the mass of ice on the 3-, 13-, and the 50-mm diameter cylinders (not presented) were very similar. The marked improvement in correlation and Standard Error of Estimate (SEE) that results from separating the in-cloud icing and freezing rain data is obvious.

For a specific number of detector cycles, a much greater mass of ice would accumulate on the cylinder during freezing rain than during in-cloud icing. This can be seen in Figure 5, which shows the regression lines of the mass of ice on the 3- and 25-mm diameter cylinders versus the number of detector cycles for detector 1. The difference in the regression lines can be best explained by considering the freezing fraction, that is, the ratio of the amount of ice that actually freezes on the collector to that amount which would accumulate if all the drops impinging on the collector freeze. During in-cloud icing, drops freeze quickly to the collector since the heat loss, especially the transfer of latent heat from the freezing of these small drops, is relatively rapid. The larger drops, during freezing rain, freeze more slowly. This allows part of the water to run off or be blown off the surface. Stallabrass and Hearty (1967) found that the freezing fraction is influenced by the ambient temperature and the water concentration. With these factors being equal, a larger surface area will allow a greater proportion of the impinging drops to freeze. This is primarily due to the increased time the drops remain on the surface, and the larger ice surface to which heat can be imparted. It seems likely that, during freezing rain, many of the drops impinging on the sensor will splatter, run off, or be blown off due to its smaller 6-mm diameter, whereas they are retained on the 25-mm diameter cylinder. The rapidly expanding ice surface on the 3-mm cylinder will gradually allow a larger percentage of these drops to freeze.

### b. Maximum Radial Ice Thickness

Linear least-squares regression lines of the maximum radial ice thickness (MRIT) on the 25-mm diameter cylinder versus the number of instrument cycles and scatter of the individual points, for all tests, for the 21 freezing rain tests, and for the 21 in-cloud icing tests for detector 1 are shown in Figure 6. They indicate that the fit of the regression line is improved by separating the freezing rain and in-cloud icing tests. However, the improvement is not as obvious as for the mass of ice. Figure 7 shows a comparison of the least-squares regression lines of the 3- and 25-mm diameter cylinders for the MRIT versus the number of instrument cycles. During in-cloud icing, the ice thickness is greater for the 3-mm cylinder as to be expected from icing theory. During freezing rain, however, the ice thickness is slightly greater on the 25-mm cylinder. The implication here is that the theoretical relationship of the collection efficiency of objects of different sizes is limited by the drop size; that is, once drops reach a certain volume, or mass, their inertia is great enough so that the drag effect is not sufficient to deflect a significant number of these large drops.

### c. Vertical Ice Thickness

Figure 8 shows the least squares linear regression lines of the vertical ice thickness (VIT) versus the number of instrument cycles for detector 1. The results were very similar for the other two detectors. Figure 8 indicates that during freezing rain the accreted ice adds to the vertical dimension on all four cylinders. Also, the smaller cylinder diameters generally favor more vertical growth. During in-cloud icing the same trend is evident. However, both the 25-mm and 50-mm cylinders experience negligible vertical growth. These results indicate that, during freezing rain, the large drops are not easily deflected, even by the 50-mm diameter cylinder. During in-cloud icing, the small droplets are deflected much more with increasing cylinder diameter. Consequently, vertical growth of the ice is less important during in-cloud than during freezing rain.

### d. Long-Duration Tests

In order to study more completely the performance of the ice detectors, six climatic chamber tests were run with durations from 2 to 17 hours, some with varying conditions. Figure 9 shows the least squares linear regression lines for the mass of ice on the 25-mm diameter cylinder versus the number of instrument cycles, from the climatic chamber 1-hour tests, for each detector. The values for the mass of ice on the 25-mm diameter cylinder versus the number of cycles for each detector in the long-duration tests are plotted. Test numbers 1-3 in the figure are in-cloud icing tests with durations of 2, 6, and 6 hours respectively. Tests 4-6 are freezing rain tests with durations of 5, 15, and 17 hours respectively.

As a result of these longer tests, a major problem area was uncovered. During the 15- and 17-hour freezing rain tests (test numbers 5 and 6), the detectors cycled erratically even though synoptic conditions remained unchanged. This was caused by melt water from the sensor accumulating on the flat surface area on the top of the strut, and held in place by surface tension. During test 6, with the temperature at -4$^{\circ}$C, the puddle froze rapidly. The sensor, which was partially submerged in the puddle, responded by returning to the deice mode. This accounted for a large number of cycles for Detectors 1 and 3 in this test. Because of the narrow strut on Detector 2 (Model 871FA), melt water drained more readily and no puddle formed.

During test 5, with the temperature at -1°C, the puddle was slow to freeze. It is not apparent what physical effect this had on the cycling of the detector. Although deicing intervals were irregular, excessive cycling did not occur as in test 6. Since the number of cycles for detectors 1 and 3 in test number 6 are not representative, they have not been plotted. Note that the regression lines for freezing rain underestimated the mass of ice in six of the seven cases. One explanation for this is the greater growth in the size of the cylinder plus ice, especially in the vertical plane, during freezing rain. As indicated previously, the larger the cylinder, the greater the mass of accumulated ice. Evidently, using the regression lines based on the 1-hour tests can lead to significant underestimates of the mass of ice during prolonged severe icing such as our long duration tests. This is not a serious problem during in-cloud icing because vertical growth on the cylinder is small and the frontal projection remains effectively unchanged.

## FIELD TESTS

### a. Data Collection

Rosemount Model 872DC ice detectors were mounted on a stand and installed at Hanscom AFB, MA in February 1979, and at Westford, MA, Blue Hill Observatory, Milton, MA, and the summit of Loon Mt., Lincoln, N.H. in November 1979. The elevation at the Bedford and Westford sites is less than 70 m, 190 m at the summit of Blue Hill, and 915 m at the summit of Loon Mt. A cylinder 25 mm in diameter, and 30.5 cm in length, selected as the standard for our observations, was mounted on a wind vane colocated on the stand with the ice detector. The cylinder is kept normal to the wind flow by the vane to standardize thickness measurement; it can be removed to determine the mass of the ice. The distance between the vane and the ice detector is approximately 1 m.

At the conclusion of each icing event, the MRIT, and VIT, the mass of the ice, the appearance of the ice, and information on icicles was recorded. Synoptic weather conditions for the period of icing were also noted. At the completion of data collection, the cylinder was cleared of ice and placed back on the vane. For each event, the analog output of the ice detectors was recorded in addition to the number of heating cycles. This was done to observe the detector response to ice on the sensor between the no-ice condition and the trip point, when the heater activates.

Data for all three detectors used in the chamber tests were pooled to smooth out the differences in their response before developing linear least-squares regression lines of the number of deicing cycles versus the mass of ice on a 25-mm diameter cylinder per 30.5 cm length. The resulting equations are:

$$\hat{M}_r = 9.1 + 5.8N, \text{ and} \tag{1}$$

$$\hat{M}_c = 9.4 + 2.0N \tag{2}$$

where $\hat{M}_r$ and $\hat{M}_c$ are estimates of the mass of ice for freezing rain, and in-cloud icing, respectively, and N is the number of detector deicing cycles. The correlations and SEE's are 0.98 and 13.3g for Eq. (1), and 0.92 and 9.0g for Eq. (2).

Estimates of ice thickness were based on the mass of the ice from Eqs. (1) and (2). For these estimates, the ice was considered to have a uniform thickness everywhere on the cylinder. For a cylinder radius of 12.7 mm, a length of 304.8 mm, and using an ice density of 0.8 for ice formed by freezing rain, and a density of 0.6 for in-cloud icing.

$$\hat{T}_r = 2\left(\frac{M_I}{76.6} + 1.61\right)^{1/2} - 2.54, \tag{3}$$

and

$$\hat{T}_c = 2\left(\frac{M_I}{57.4} + 1.61\right)^{1/2} - 2.54, \tag{4}$$

where $\hat{T}_r$, the estimated thickness due to freezing rain, and $\hat{T}_c$, the estimated thickness due to in-cloud icing, are in cm, and the mass of ice, $M_I$, is in grams. See Tattelman (1982) for derivation of Eqs. (3) and (4).

### b. Analysis

Figure 10 shows the regression lines for $\hat{M}_r$ and $\hat{M}_c$; also shown are circled points for the measured mass of ice on the cylinder for 11 icing events. For most events, a variety of conditions combined to produce icing. The optimum result would be to have the measured mass of ice on the cylinder, for the mixed icing or freezing drizzle icing events, fall between the freezing rain and in-cloud icing estimates.

Six of the 11 points in Figure 10 fall between the regression lines. Two of the five events not within the regression lines (numbers 1 and 2) were the result of wet snow. Two other events, numbers 3 and 9, had some snow mixed in. Although the ice detector response to wet snow is not known, this small sample indicates that the mass build-up of ice on the cylinder per instrument cycle may be less than that for in-cloud icing. Although an effort was made to measure icing amounts at the conclusion of an event, it was not always possible to tell if icing had ceased, and on some occasions the observer could not be present at the conclusion of icing. Events 3, 8, and 9 were the only instances where more than 1 hour elapsed before the observation was made. Even though temperatures remained at or below freezing during this period, some loss of ice on the cylinder, due to melting or evaporation, was likely. Therefore, all of the points below the in-cloud icing regression line in Figure 10 represent icing events which either involved snow and/or a substantial period before observation, allowing for potential ice loss.

The icing events included some other interesting aspects. For instance, icicles did not form during any of the events. Also, the two heaviest icing periods (events 4 and 5) occurred with only 0.8 mm (0.03 in) and 0.5 mm (0.02 in) of melted precipitation, respectively. Both events were part of a static synoptic situation with drizzle, separated by a period of time with no precipitation. Unfortunately, no in-cloud icing occurred, except at Blue Hill (events 1 and 2) when the bulk of resulting ice was caused by wet snow which formed a slush that froze.

To get an appreciation of our method for determining the ice thickness, Figure 11 compares the theoretical ice thickness curves from Eqs. (3) and (4) along with the plotted values of the actual mass of ice versus the average of the VIT and the MRIT for each icing event. Most of the icing events were the result of a mixture of conditions that could not be strictly categorized as either in-cloud icing or freezing rain. Ideally the points would lie on, or between, the two lines. Since only one event (number 7) is not close to, or between the curves, these results indicate that our ice thickness approach will provide reasonable estimates of ice thickness based on the mass of ice.

Examination of the information in Figures 10 and 11 leads one to support the potential of the Rosemount 872DC ice detection system as a network instrument for making objective observations of ice accretion. Additional data need to be collected, perhaps in a climatic chamber, to establish regression lines, for freezing drizzle or mixed icing, that would fall between those for freezing rain and in-cloud icing.

### c. Equipment Problems

The optimism expressed in the preceding section is tempered by two problems, water retention on the flat surface between the ice detector strut and the sensor, and instrument calibration. The problem of water retention on the strut was originally noted at the time of the chamber tests. During the heating cycle, melt water from the sensor flow down to the flat surface of the top of the strut. Surface tension keeps the liquid in place and it freezes. With subsequent deicing cycles, the melt water can eventually surround the sensor in a puddle deep enough to automatically trip the deice mode, even though the actual icing may have stopped. The most practical way to eliminate this problem would be to taper the top of the strut to facilitate drainage. Representatives at Rosemount indicated that this could be accomplished, but with additional cost.

The ice detectors were returned to Rosemount for evaluation at the conclusion of the winter field tests. Two of the four detectors were substantially out of calibration (by 24% and 14%). Rosemount was unable to determine cause, but noted that the sensors on these two detectors were discolored. They thought that this was probably caused by overheating, causing a material stress which affected the calibration. The discoloration was not present at the conclusion of the climatic chamber tests, but it did become apparent at the beginning of the field tests. It might have been caused by an extended period with the heater on while testing the initial installation in the field. The obvious change in color would at least signal the need for recalibration if this happened during actual use of the detector for icing observations. The events shown in Figure 10 were corrected for excessive cycling and calibration error.

## CONCLUSIONS

Based on the analyses of the climatic chamber test data, and subsequent field tests, the Rosemount Model 872DC ice detection system has proved to be an effective tool for determining the mass and thickness of ice accretion on cylinders. Further field testing, especially at locations that favor in-cloud (rime) icing, is necessary to refine the relationships between the number of detector deicing cycles and the mass and thickness of ice for different types and combinations of icing conditions.

The major hindrance to utilization of the detector "off-the-shelf" for making icing observations is the problem of retention of melt water on the flat surface area on top of the strut on which the sensor is located. This retained water can cause erroneous cycling upon refreezing. This situation occurs during light winds (<15 knots). Since stronger winds blow the melt water off, it is not a problem during in-cloud icing which requires fairly strong winds to blow supercooled droplets past a stationary surface to form ice. The problem could be eliminated by tapering the top of the strut to facilitate drainage.

Although the main emphasis in this report has been on observing the quantity of ice resulting from a period of ice accretion, it is also important in engineering design to know the distribution of concurrent observations of wind and ice. Since strong windspeeds could occur subsequent to a period of icing, especially in cold locations, an observation program should include a method for determining the quantity of residual ice remaining on structures after the icing has ceased.

## REFERENCES

Ackley, S. F., K. Itagaki, and M. Frank (1973) An Evaluation of Passive Deicing, Mechanical Deicing and Ice Detection, Department of Transportation, FAA-RD-74-50, Wash, D.C.

Hill, A. N. (1973) An Objective Observation Technique for Freezing Precipitation, Sterling Research and Development Center, Laboratory Report No. 7-73, Sterling, Virginia

Stallabrass, J. R., and P. F. Hearty (1967) The Icing of Cylinders in Conditions of Simulated Freezing Sea Spray, National Research Council of Canada, Ottawa, Canada

Tattelman, P. (1979) Climatic Chamber Tests of a Surface Ice Accretion Measurement System, Air Force Geophysics Laboratory, AFGL-TR-79-0079, AD A077022, Hanscom AFB, Massachusetts

Tattelman, P. (1982) An Objective Method for Measuring Surface Ice Accretion, Jour. of Appl. Meteorol., Vol. 21, Apr, pp 153-166

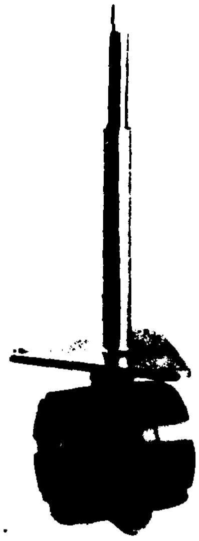

Figure 1. Rosemount Model 872DC

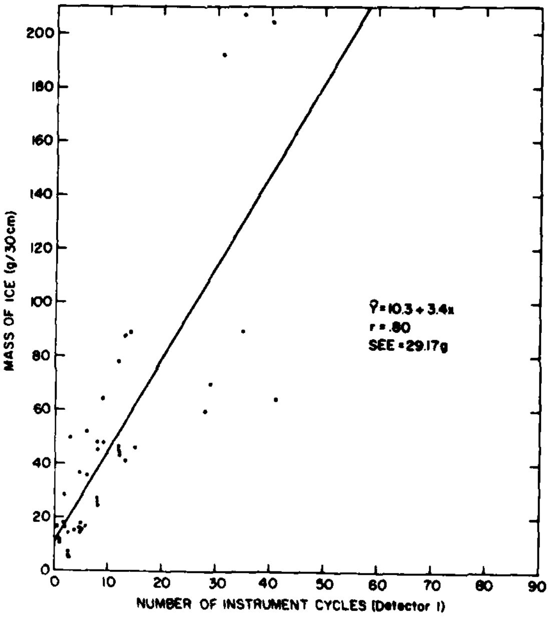

Figure 2. Mass vs cycles, All tests

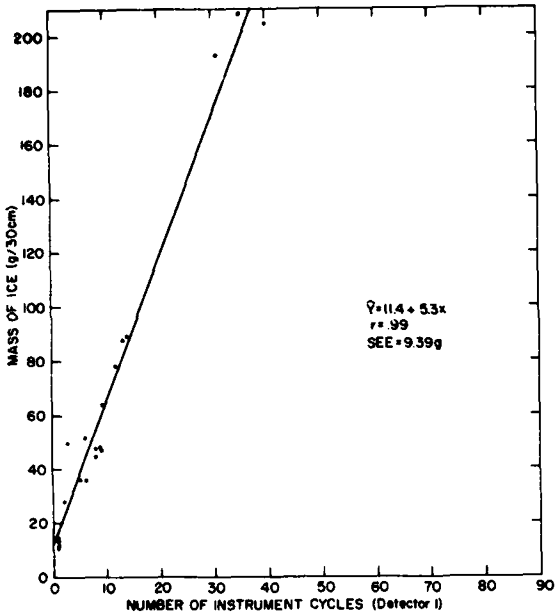

Figure 3. Mass vs cycles, Fzg rain

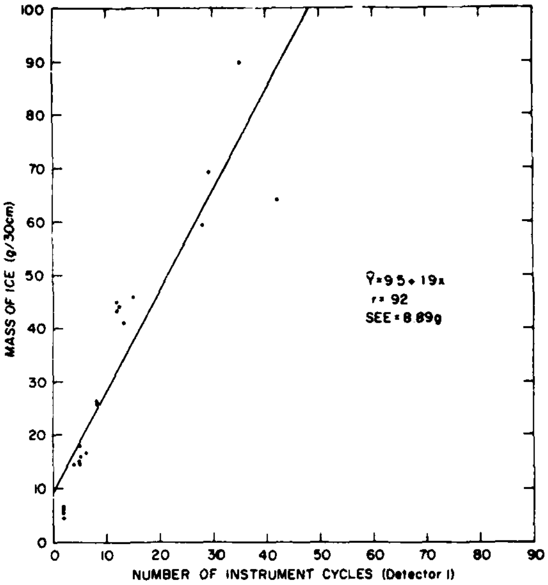

Figure 4. Mass vs cycles, In-cloud

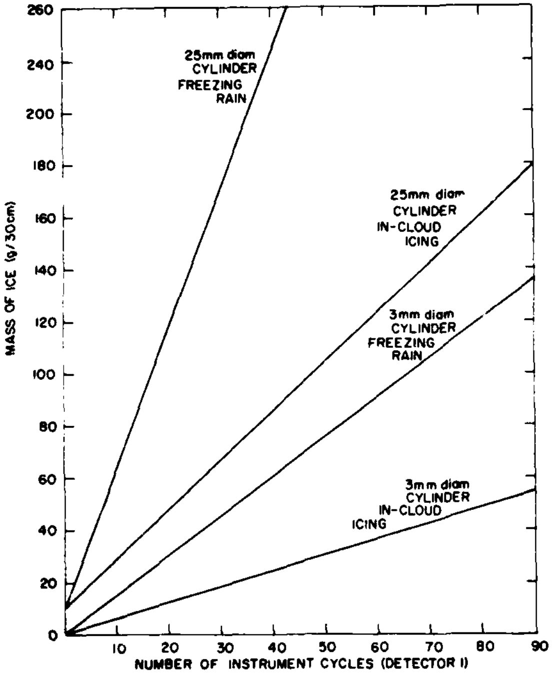

Figure 5. Mass vs cycles

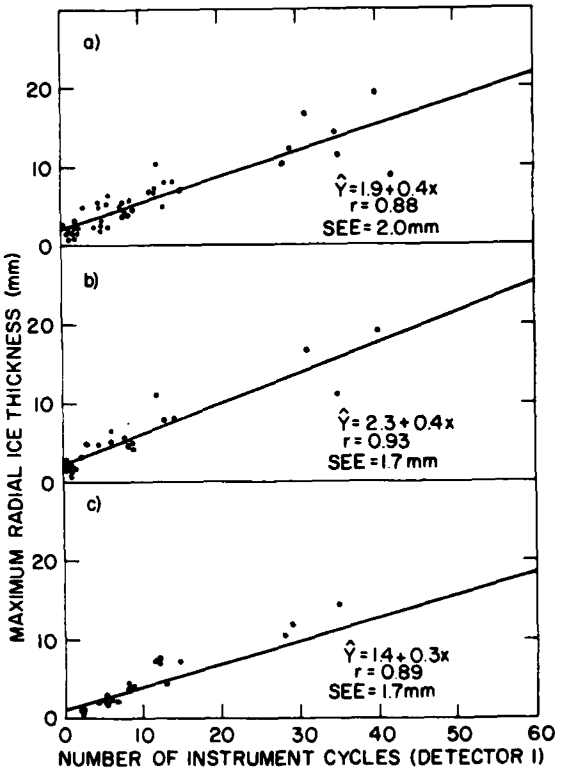

Figure 6. MRIT vs cycles for (a) All tests, (b) Fzg rain tests, (c) In-cloud icing tests

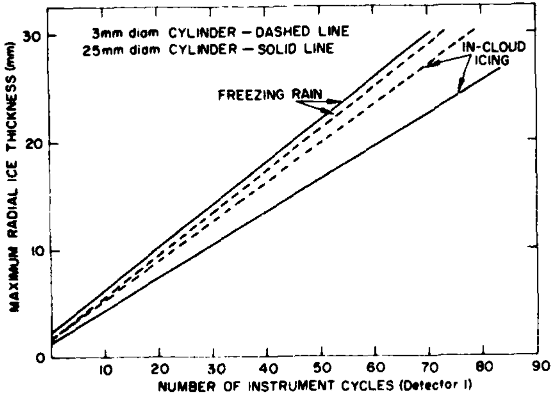

Figure 7. MRIT vs cycles

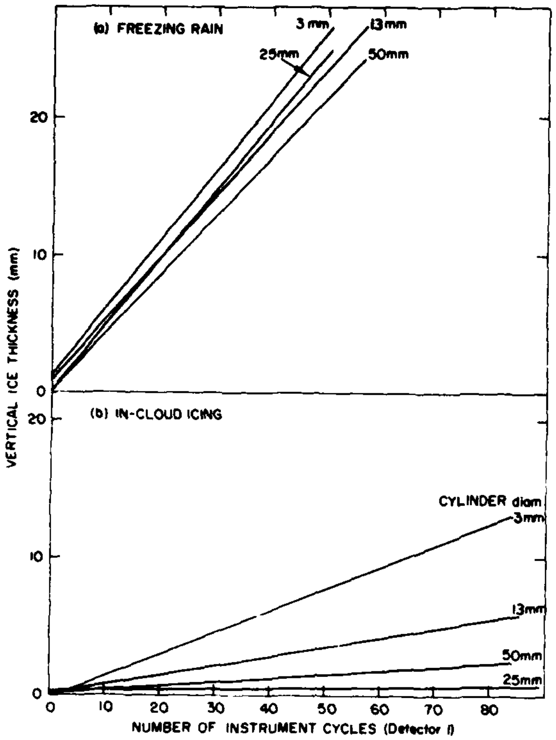

Figure 8. VIT vs cycles for: (a) Fzg rain, (b) In-cloud icing

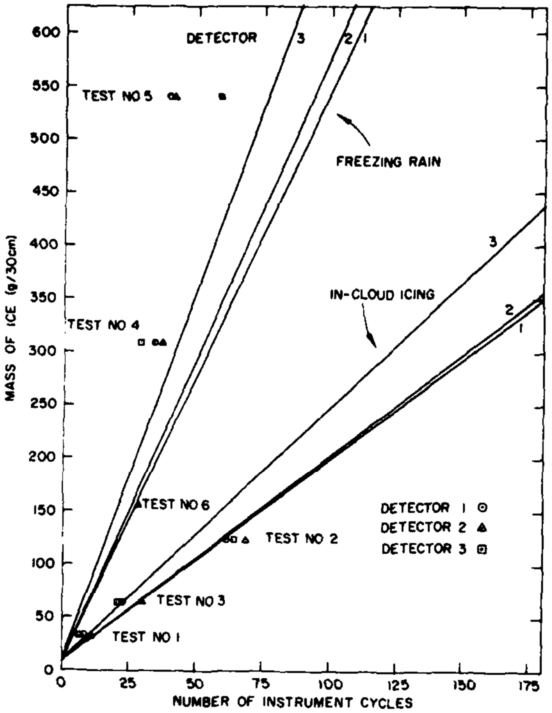

Figure 9. Mass vs cycles for each detector. Values for long duration tests are outlined

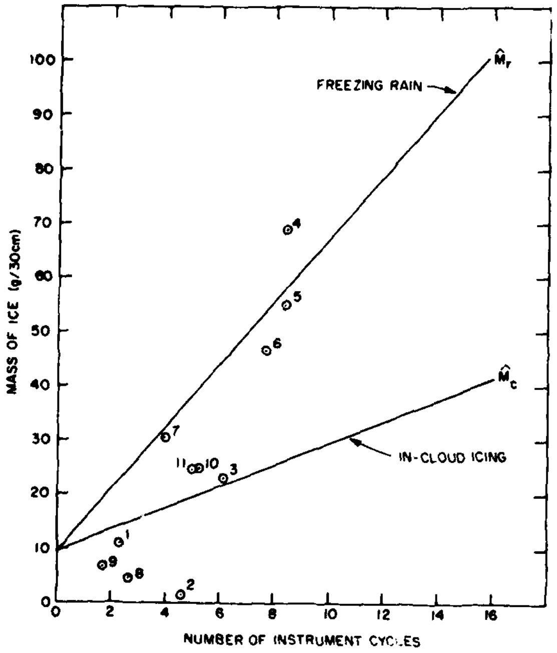

Figure 10. Mass vs cycles for fzg rain, $\hat{M}_r$, and in-cloud icing $\hat{M}_c$. Circled points represent field test measurements.

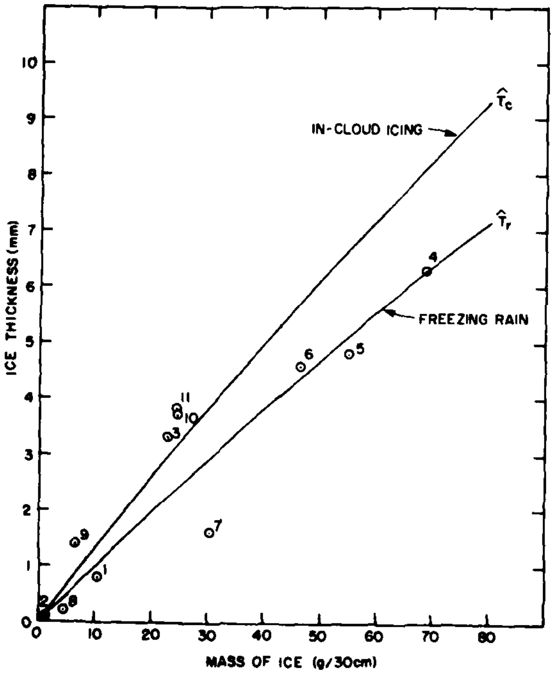

Figure 11. Thickness curves for in-cloud icing, $\hat{T}_c$, and fzg rain, $\hat{T}_r$, vs mass of ice. Circled points represent field test measurements.

DISCUSSION

Pohlman: Does the detector have to be hung in a vertical position? Couldn't you orient it horizontally or some other way, and eliminate your frozen puddle problem?

Tattelman: If you put the detector in a horizontal position, then it becomes sensitive to wind direction. Look at this over here [demonstrates]. If you orient the cylinder this way, then you have the problem of the mounting bracket obscuring one of the views. We tried tilting the ice detector to see at what angle the melt water would run off - we found that to be greater than 60°. Apparently the surface tension right at the the sensor, here, was such that it would accumulate around the sensor. If this sensor [probe] was not there, if it was just a flat surface area, the water would drain off.

Pohlman: Has Rosemount shown an interest in modifying the design?

Tattelman: No, they have not; they said that they would, and they sent me an estimate of the engineering costs and other aspects of modifying the instruments. So they would do it for a price. I don't doubt that you could have it done. My recollection is that each detector would cost about 25 or 50% more, and the engineering cost would be between $25,000 and $50,000.

Ervik: We have used the Rosemount ice detector on a mountain 1400 m MSL. As long as the icing was moderate it seemed to work fine and compared well to the icing test observations. But when icing was heavier, it stopped working because it was covered - the body of the instrument was covered with ice. Have you had this problem? Do you think something can be done to prevent the entire instrument from icing so that it doesn't work?

Tattelman: Did you have the same instrument that we used - the model 872, with the long strut?

Ervik: I think it was number [model] 572.

Tattelman: The reason we show this particular model is the long strut. There are a lot of other models available - even this particular model is available with a much shorter strut length. But this whole area is heated and, at least for our tests, we found that there's no problem with the detector keeping up with the icing. But we didn't look at anything that was truly severe by mountain top standards. I don't know if you have this exact same model, or if you have as much of a heated portion as this one has, and you've had that problem, but I would like to take a look at your results to complement my own.

Minsk: Do you feel comfortable in your observation that freezing rain accretes to a greater extent on a large cylinder? If you were to construct confidence limits on those two very close curves, I wonder if there would be no statistically significant difference?

Tattelman: No, I think that it's still safe to say that during freezing rain, the larger object will collect more ice. There's just too much consistency there, and I also found it to be true that - you have more of a problem with water loss due to splattering, or a low freezing fraction during freezing rain, than you have a problem with collection efficiency because the droplets, I guess, once they get greater than about 25 micrometers, seem to be very difficult to deflect. From what I have seen, and from the curves that I've got, I think that that's a safe assumption, that freezing rain will accumulate faster and to a greater extent on larger surfaces.

Howe: I think that's probably safe. The collection efficiency for raindrops for all these observations at normal wind speeds is so close to unity as to make no difference. What happens with a bigger object is that, as you said, the build-up itself grows faster, because the object is bigger and is collecting rain. You start getting icicles, in some cases, which then add an additional collecting surface. So, I think it's true that bigger objects will collect more freezing rain per unit volume.

Minsk: Do you have data to back that up?

Howe: Well, it's up here [pointing to head]. And another comment on the Rosemount: you have to be careful of them since some models are sensitive to radio frequency interference. That may be a big problem in some locations, particularly near radio antennas. They do make models which are insensitive to RFI but they are quite different configurations than we have on the mountain now. In some ways they're better than the long strut ones. It's obvious that for an icing episode that will last long enough, anything you have out there eventually is going to get obstructed by ice, no matter what you do.

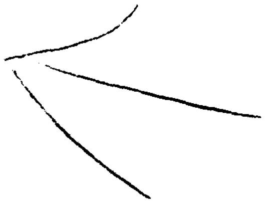

AD P001690

# FIELD MEASUREMENTS OF COMBINED ICING AND WIND LOADS ON WIRES

John W. Govoni USACRREL*
Stephen F. Ackley USACRREL

## ABSTRACT

Four winter field seasons of simulated power line icing data were obtained during the years 1977-1981. Measurements were obtained of the icing characteristics, loads on the wire, and wind conditions simultaneously. Loads were measured using a single-axis load cell in line with the wire during the first three seasons, and a tri-axial load cell (resolving three perpendicular force components) in the 1980-81 winter season. Winds were measured using a vaned pitot-static tube located near one end of the wire. Asymmetric ice accretions were sometimes observed if icing conditions were not of sufficient duration to develop cylindrical forms. Load analyses differentiated wind and gravity loading of the iced wire in winds up to 50 m/s. Load records indicated maximum loads in the 400- to 600-kg range (>50 kg/m) occurred from combined wind and ice loads. Correlations are made with wind speed records to establish drag coefficients for the various ice accretion types observed.

## INTRODUCTION

Power lines and poles are basically designed to take the load in compression imposed by the weight of the line and any accreted ice. Current design criteria assume all ice formations to [illegible]f cylindrical shape and uniform dens[illegible] [illegible]hus the design is essentially bas[illegible] maximum weight. While consideration is given to the effect of shear forces on the structures caused by the drag force of wind on the ice accretion, all accretions of the same weight are considered to have the same drag.

Another concern is wind-induced vibration (Blevins 1977, McComber et al. 1982). This vibration, referred to as "galloping," results from asymmetrical icing of wires (McComber et al. 1982). McComber et al. (1982), working with accretions formed in wind tunnels, found both increased drag and increased weight (negative lift) due to ice formation.

For the past four winters, 1977 to 1981, we have been obtaining simulated power line icing data near the summit of Mt. Washington, New Hampshire, at approximately 2000 m elevation (Howe 1978, 1979, 1982). This site was chosen because of its extreme icing conditions and winds, and also because personnel at the Mt. Washington Observatory, located at the summit, could monitor the experiment and collect the necessary data. Measurements were obtained of the icing characteristics, loads on the wire, and wind forces simultaneously.

In this paper we describe some results of loads, both drag and gravity, obtained during the formation of natural ice accretions on wires.

---

*U.S. Army Cold Regions Research and Engineering Laboratory, Hanover, N.H. 03755.

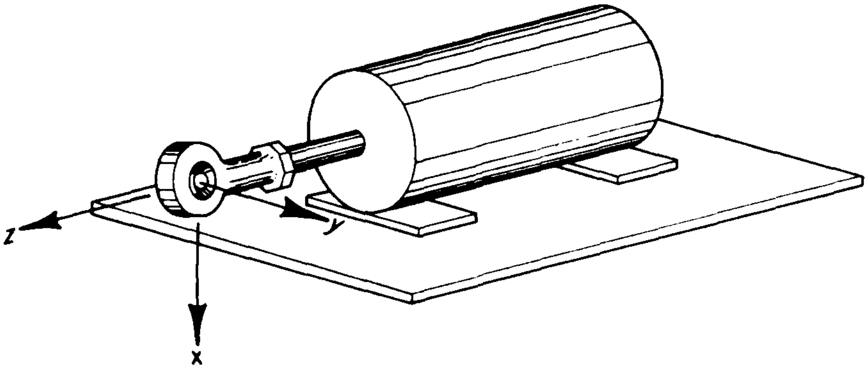

Figure 1. Triaxial load cell showing the three mutually perpendicular force components.

METHODOLOGY

The instrumentation for the study consisted of a triaxial load cell manufactured by A. L. Design, Inc., Tonawanda, N.Y. It is designed to measure three mutually perpendicular components of the cable tension load: X, the vertical component; Y, the horizontal component; and Z, the axial component (Fig. 1). It has a capacity of 500 lb in the X and Y coordinate directions and 2,000 lb in the Z coordinate direction.

The basic construction consists of three strain gauge bridge circuits, each with a sensitivity of 2.6 millivolts per volt. The gauges were placed so that the axial and bending moment loads did not influence one another. From these three measured components, the resultant load and the catenary angle can be calculated. A Baldwin Lima Hamilton (BLH), Type V-1, 2000-lb capacity load cell was placed in line with the cable to read cable tension. This load cell served as a check on the resultant force obtained from the triaxial load cell. Both cells were mounted to a set of steel cribs that were filled with stones to keep the system from being blown away (Fig. 2).

About 100 meters of shielded signal cable ran from the load cells to the recording system. Each load cell signal, including that from the single axis cell, was amplified with a Vishay Amplifier prior to recording. All load data were recorded on Esterline-Angus Model AW strip chart recorders. Although the response of this type of re-

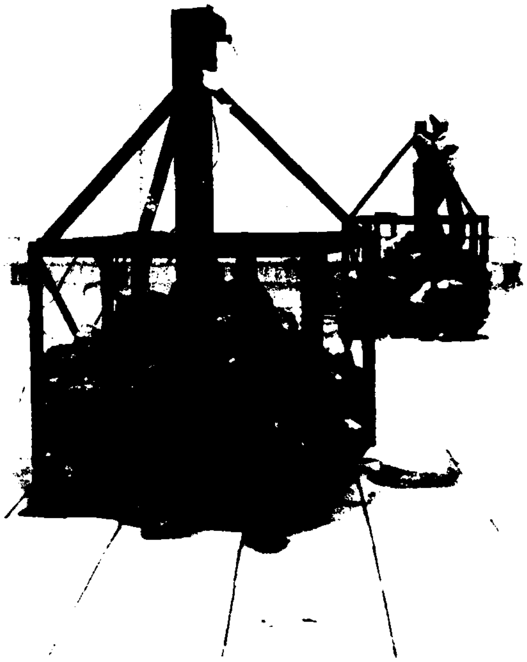

Figure 2. Instrumented cable experiment on the Mt. Washington Observatory roof. The load cells are rigidly attached to the cribs. The cribs are filled with stones to prevent the system from blowing away. The signal cable is tie-wrapped to prevent damage from wind.

corder is very slow, it offered the only feasible means of circumventing the severe RF noise common to the site due to the proximity of TV transmitting equipment. The system was calibrated so that 1 millivolt corresponded to 1 lb (0.45 kg) of load. The conductor between the load cells was 1/4-in. (0.6-cm) cable 27.5 ft (8.5 m) long. The cable was preset to a 15° catenary angle. A standard Air Force/Navy heated pitot static tube was installed near the experiment to measure the wind speed and direction.

## PROPERTIES OF ICE ACCRETIONS

In general, ice accretions in mountainous regions are formed when supercooled water droplets (fog or cloud) hit a cold object and freeze on contact. Thus the formation usually grows into the wind. On Mt. Washington the majority of the ice accretions were formed in this manner.

However, in some cases, if the temperature is just below freezing, water droplets hitting a cold object will not freeze on contact, but rather will be blown around to the leeward side and freeze in the shape of icicles. This process usually results in high density (900 kg/m$^3$) clear ice accretions.

We discovered three types of ice accretions at this location. Rime ice was most commonly observed, with density between 400 and 600 kg/m$^3$, depending on the conditions (temperature usually well below freezing). This type of ice has by far the roughest surface. Milky ice is smoother than rime ice but rougher than clear ice, and has a density of about 880 kg/m$^3$. Clear ice has the smoothest surface of all and has a density of 910 kg/m$^3$. It forms with ice surface temperatures at 0°C (Ackley and Templeton 1979).

We found that as rime ice formed on the windward side of the wire its weight and the wind pulled the accretion down, twisting the wire. This happened primarily in the center two-thirds of the span, where it could twist and oscillate freely (Fig. 3). We found that the wire and accretion gradually twisted about 180° as a whole unit in the same direction as more and more ice accreted on its windward side (Fig. 4). As a result, the cross section of the ice formation had a spiral shape. The ice remained firmly

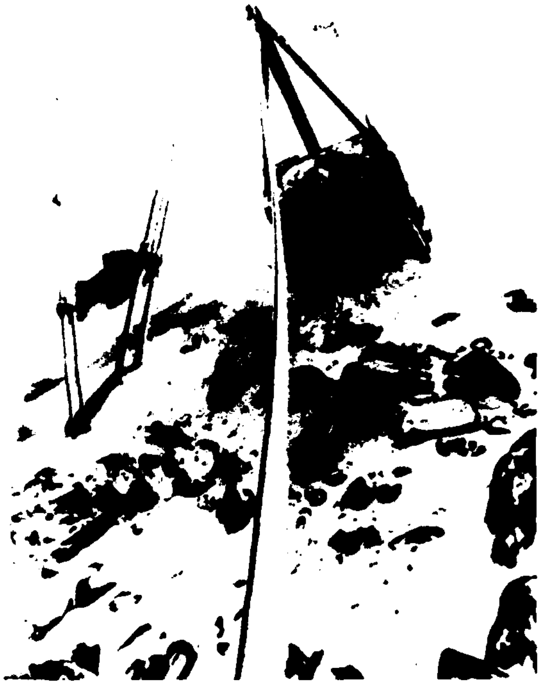

Figure 3. Photograph taken from one mount looking down the cable, showing how the effects of ice weight and wind pull down the center two-thirds of the span and twist the cable. Ice then continues to accrete on the wire.

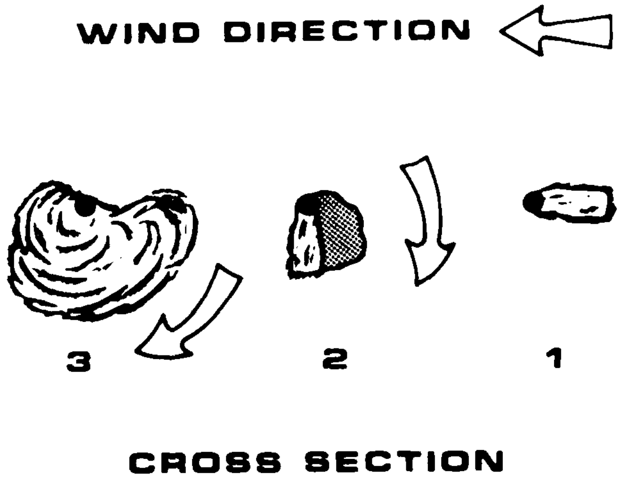

Figure 4. Rime ice accretion processes. 1) Initially the accretion grows into the wind. 2) Weight and wind pull the wire and the accretion down while the accretion is still growing. 3) Final shape of the accretion after 180° twisting of the wire and ice formation while it grows.

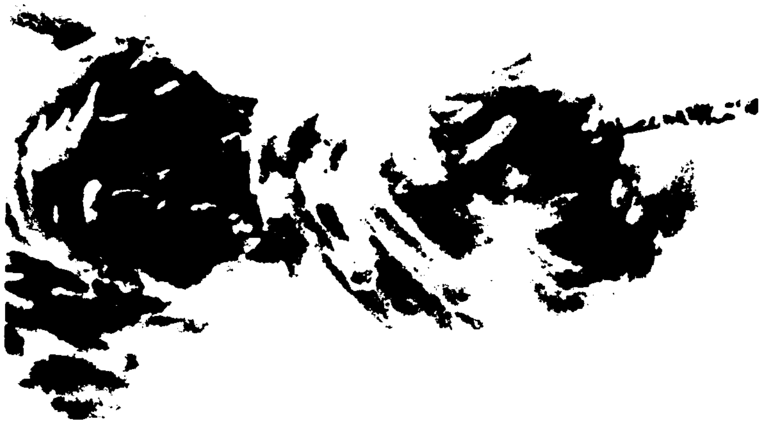

Figure 5. Final cross section of a large rime ice accretion. The spiral shape is formed from the 180° oscillation.

Figure 6. Breaking and cracking of uniform ice sections as they twist differentially and then independently oscillate. As shown, sections of ice are blown off during this process.

attached to the wire at all times (Fig. 5). These growth modes are different from those of wet snow accretions on wires, where the accretion can rotate independently of the wire (Wakahama 1979).

As the ice builds up, differential drag forces occur along the cable. As a result, sections of the original uniform ice formation attempt to oscillate independently of each other, causing cracking and breaking of the formation (Fig. 6). The remaining large sections of the ice then oscillate independently of each other, yet continue to grow as long as icing conditions persist (Fig. 7).

Figure 7. Several large sections of ice that have continued to grow to approximately 0.5 m diameter after some sections have broken off.

RESULTS

The load cell output could be resolved into three components, which allowed us to differentiate wind effects from the total load by looking at the horizontal channel (Y). Our analysis attempts to identify some relationship between the horizontal drag force $F_y$, ice roughness, and size characteristics identified by the drag coefficient $C_D$ and the diameter D of the accretion.

The total drag force $F_y$ is given by (Streeter and Wylie 1975)

$$F_y = C_D \, \rho_{air} \frac{D \ell V^2}{2}$$

where $C_D$ = drag coefficient (dimensionless, a function of surface roughness, shape and Reynolds number)
D = cross section of the accretion normal to the wind
$\ell$ = length of the wire
$\rho_{air}$ = air density
V = wind velocity normal to the wire.

For these computations, we correlated the wind velocity normal to the wire ($V_{normal}$) with the horizontal force normalized to the diameter of the accretion ($F_y/D$), since D is changing as ice accretes. Both the forces and wind velocity were averaged over 15-minute periods. On log-log paper $F_y/D$ vs $V_{normal}$ should give a slope 2 line for constant $C_D$, a point we address later in the paper. Figure 8 shows this plot for a milky ice (high density, intermediate roughness) accretion event which occurred on 28-29 November 1980. As shown here the best fit linear regression line has a slope of 2.19 with a correlation coefficient r = 0.96. The slope 2 line (corresponding to the equation above) is also shown. This plot indicates good correlation between the normalized drag force and wind velocity throughout the icing event, implying a relatively constant $C_D$ throughout the icing period.

Figure 9 shows the data from Figure 8 as well as two additional runs, a rime icing event (low density, rough) and a clear icing event (high density, smooth). During the last portion of the clear icing event, rough rime ice accumulated over the clear ice. The meteorological and load information for this experiment is presented in Table 1. Figure 9 indicates that the total data set for the normalized force does not show the level of correlation that the milky ice alone had, as indicated by the best fit line (for milky ice only). As well, the rime ice and clear ice alone both indicate relatively weak correlations ($r < 0.6$), with best fit slopes greatly different from the theoretical value (2). A number of factors can contribute to this behavior. These include changes in the drag coefficient

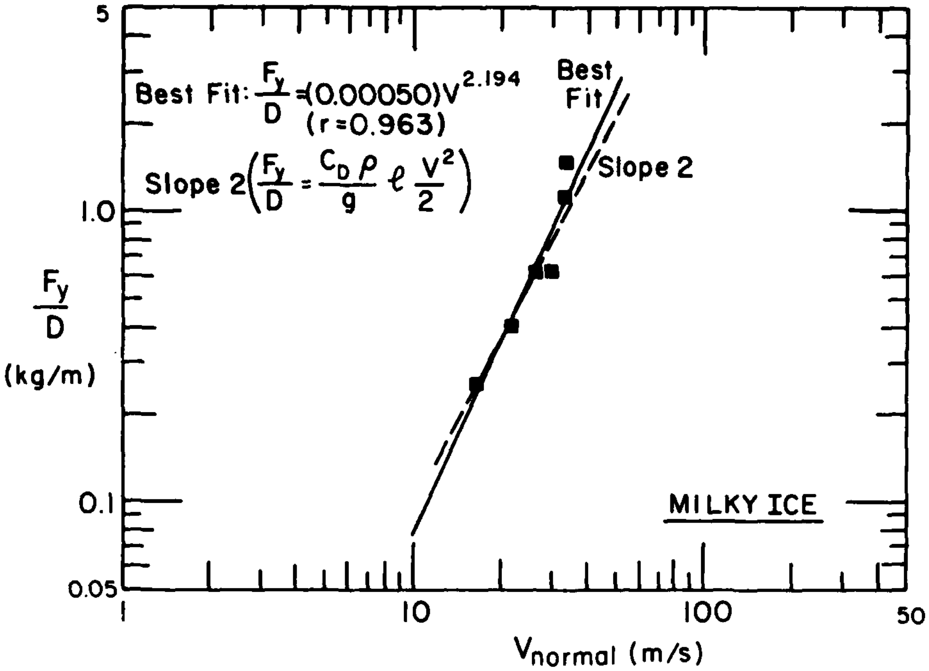

Figure 8. Horizontal or drag force $F_y$ normalized to the accretion diameter D versus the wind velocity normal to the wire ($V_{normal}$) for a milky ice run. As shown, the slope on this log-log plot of the best fit line is in agreement with the theoretical value (2).

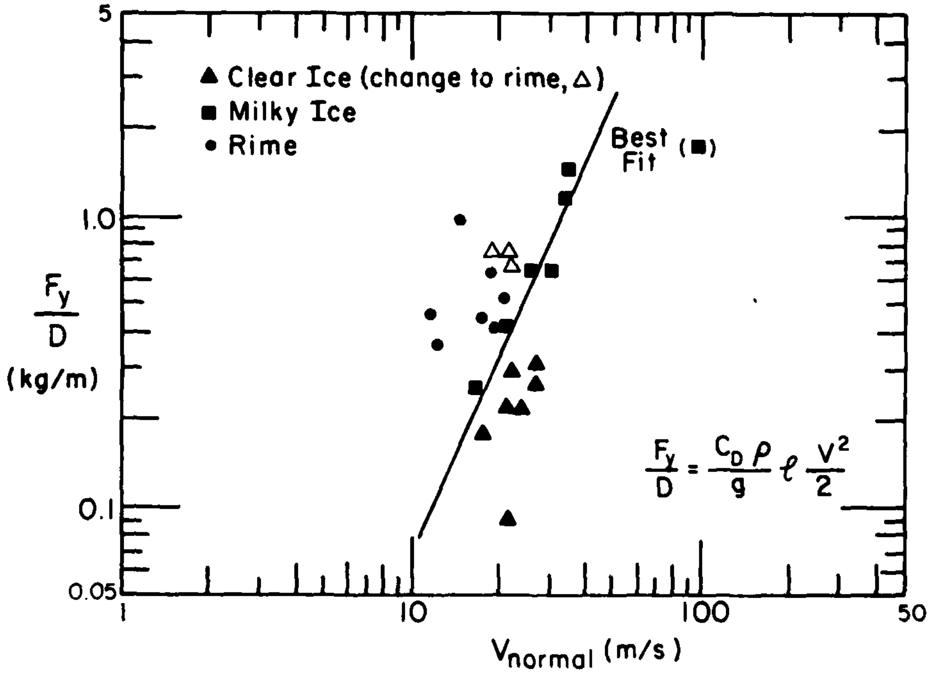

Figure 9. Horizontal or drag force $F_y$ normalized to the accretion diameter D versus the wind velocity normal to the wire ($V_{normal}$) for rime ice, milky ice (Fig. 8) and clear or glaze ice accretion. The best fit line for the milky ice run only is shown, as in Figure 8.

Table 1.

## MT. WASHINGTON ICING LOADS
### 23 – 25 February 1981

| Date | Time | Tri-axis load cell (kg) | | | |
|---|---|---|---|---|---|
| | | X | Y | Z | Total |
| 23 Feb | 2100 | 1.89 | 0 | 1.99 | 2.74 |
| 23 | 2200 | 3.79 | 0.46 | 3.49 | 5.17 |
| 24 | 0000 | 8.83 | 0.47 | 22.92 | 24.57 |
| 24 | 0300 | 22.72 | 1.86 | 73.76 | 77.20 |
| 24 | 0600 | 41.66 | 2.81 | 135.56 | 141.85 |
| 24 | 0720 | 51.76 | 2.81 | 175.43 | 182.93 |
| 24 | 0900 | 75.75 | 2.81 | 271.13 | 281.53 |
| 24 | 1120 | 116.16 | 5.63 | 430.62 | 446.05 |
| 24 | 1415 | 156.56 | 15.22 | 558.21 | 579.95 |
| 24 | 2215 | 186.86 | 18.78 | 653.90 | 680.34 |
| 25 | 0120 | 191.91 | 18.78 | 669.85 | 695.87 |

## CLIMATOLOGICAL DATA
### 23 – 25 February 1981

| Date | Time | Ice thickness (main body) (cm) | Wind direction and speed (m/s) | Air temp (°C) | Ice type | Weather conditions |
|---|---|---|---|---|---|---|
| 23 Feb | 2100 | 0.63 | 150°/20.6 | – 1.1° | Clear | R |
| 23 | 2200 | 2.54 | 140°/20.1 | – 1.1° | Clear | R |
| 24 | 0000 | 5.08 | 120°/21.5 | – 1.6° | Clear | ZR |
| 24 | 0300 | 6.98 | 120°/26.8 | – 1.6° | Clear | ZR F |
| 24 | 0600 | 8.89 | 130°/28.2 | – 1.1° | Clear | ZR F |
| 24 | 0720 | 12.70 | 130°/27.7 | – 2.2° | Clear | ZR F |
| 24 | 0900 | 12.70 | 130°/26.4 | – 3.3° | Clear | ZR F |
| 24 | 1120 | 20.32 | 130°/23.2 | – 3.3° | Clear | IP F |
| 24 | 1415 | 22.86 | 130°/23.2 | – 3.8° | Rime | IP ZR F |
| 24 | 2215 | 24.30 | 120°/19.2 | – 7.2° | Rime | BS S F |
| 25 | 0120 | 25.40 | 100°/21.5 | – 7.8° | Rime | BS S F |

R – rain; ZR – freezing rain; F – fog; IP – light ice pellets;
BS – blowing snow; S – light snow.
Density taken at 0500 hr was 654 kg/m³.

due to the changing shape of the accretion and possible Reynolds number variability (discussed later). At any given velocity, however, it is clearly evident that there is progressively higher normalized drag force for clear, milky and rime ice, i.e. for increasing roughness.

This behavior is also demonstrated by the clear ice event (black triangles), during the later part of which rime ice accreted (open triangles). In this case, the normalized drag force increased from the relatively low clear ice values to higher values, similar to another rime accretion run for similar wind velocity. The horizontal load increased by nearly three-fold for the small addition of ice (Table 1, Y-axis load cell data, 24 Feb, 1120 to 1415) for essentially the same wind velocity. While the wind force data indicate this three-fold change as the surface roughness increases, we still note that the primary loading is in the vertical direction due to the weight of the accumulated ice, as shown in the X column of the table. We still feel, however, that the horizontal forces are significant since the design of poles and lines does not usually take into account for the differences in force level that can result from different ice roughnesses. The salient point is that the failure of lines and poles may be horizontal shear failure, and the horizontal forces can have significantly different levels, depending on ice type.

## DISCUSSION AND CONCLUSIONS

As mentioned earlier, the variation of drag coefficients with wind velocity, ice type or surface roughness apparently is quite pronounced. In Figure 10 are plotted, in standard fluid mechanics terms, the computed drag coefficient $C_D$ versus Reynolds number (Re = VD/ν where, as before, V and D are velocity and cross-sectional diameter and ν is the kinematic viscosity of air). Much of the interpretation of this information is speculative, since we are probably comparing a moving three-dimensional system in a nonidealized configuration with interpretations based on relatively controlled and basically two-dimensional laboratory experiments in fluid mechanics. With this caution, we note the following features from this plot.

We apparently are computing low absolute levels of $C_D$ (≈ 0.1 to 0.3) for both clear and milky ice. Aside from the complex experimental configurations, two additional physical features may explain this behavior. Measurements were taken during the ice accretion runs, and for both clear and milky ice, surface temperatures are such that some liquid water is present and runs back, where it refreezes. Two possibilities for reducing drag are the presence of liquid water on the surface and some streamlining of the object into the shape of an airfoil through icicle formation on the leeward side of the accretion.

For the rime ice accretion (closed circles in Fig. 10) there is an apparent lowering of drag coefficient with Reynolds number. For a non-accreting body this apparent dropoff in $C_D$ might be expected as we transition from laminar to turbulent flow. This transition was quoted as roughly

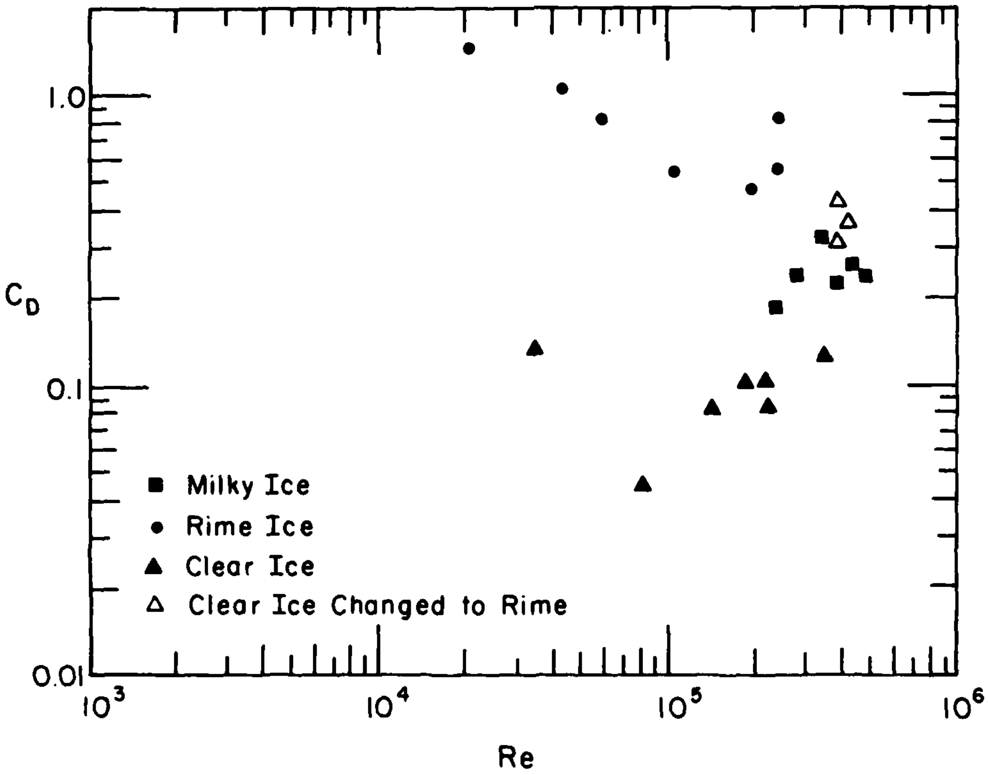

Figure 10. Drag coefficient $C_D$ versus Reynolds number (Re = VD/ν) for the rime, milky and clear ice experiments shown in Figure 9.

$1.5 \cdot 10^4$ for bare wires during discussions at the workshop. A possibility is that the extremely rough surface of the rime accretion trips the turbulence at these reduced Reynolds numbers. As we noted earlier, however, the shape of the rime ice accretion undergoes large changes as it grows. Examining Figure 10 more closely, we find that the higher $C_D$ values occur at low Re, where the shapes are more irregular during the early stages of the accretion, while the lower $C_D$ values (occurring at high Re) are generally associated with more nearly cylindrical shapes.

While a full explanation of the drag coefficient behavior with Reynolds number remains somewhat elusive, we feel that for practical applications the reported experiments have the advantage of dealing with "real" forces and wires in severe conditions and, as such, provide useful information for a freely twisting wire for extrapolation to various design situations.

## ACKNOWLEDGMENTS

The authors thank the following people for their help and support in this study: John Howe and the Mt. Washington Observatory staff for monitoring the experiment and collecting the data; Mike Ferrick and George Ashton for their interpretation of fluid mechanics; Herb Ueda and Terry Tucker for their instrumentation and mathematical advice, respectively; and Sandy Smith and Sandie Lukash for their data reduction and clerical help.

## BIBLIOGRAPHY

Ackley, S. and M. Templeton (1979) Computer modeling of atmospheric ice accretion. U.S. Army Cold Regions Research and Engineering Laboratory, CRREL Report 79-4, 36 p.

Blevins, R.D. (1977) Flow-induced Vibrations. New York: Van Nostrand Reinhold, p. 55-88.

Howe, J. (1978) Measurements and analysis of icing and wind loads on wires. Final data report to USACRREL, Mt. Washington Observatory, 9 pp.(unpublished).

Howe, J. (1979) Measurements and analysis of icing and wind loads on wires. Final data report to USACRREL, Mt. Washington Observatory, 9 pp. (unpublished).

Howe, J. (1982) Measurements and analysis of icing and wind loads on wires. Final report to USACRREL, Mt. Washington Observatory, 8 pp.(unpublished).

McComber, P., G. Morin, R. Martin and V.V. Luong (1982) Estimation of combined ice and wind load on overhead transmission lines. First International Workshop on Atmospheric Icing of Structures.

Streeter, V. and E. Wylie (1975) Fluid Mechanics. New York: McGraw-Hill, p. 278-282.

Wakahama, G. (1979) Experimental studies of snow accretion on electrical lines developed in a strong wind. Journal of Natural Disaster Science, vol. 1, no. 1, p. 21-33.

## DISCUSSION

Rawlins: What was the frequency of those oscillations?

Govoni: That's dependent on wind speed and ice type.

Rawlins: What range? Once per hour? Once per second?

Govoni: It could happen 3-4 times per second.

Rawlins: I might remark that the transition for stranded conductors, which are rough cylinders, begins around 15,000..., so it's not surprising that you got the transition that you did.

Yen: How do you define "D", the areal diameter?

Govoni: That's the ice thickness, the cross section normal to the wire, to the normal wind direction.

Yen: But that's changing all the time, right?

Govoni: As ice accretes, yes.

Yen: Do you measure continuous data or at a different time?

Govoni: Yes, different observations. Each data point has a different value of D and a different value of velocity.

Pohlman: Would it be possible for you to make a casting, or mold, of this ice shape where you have data, and then repeat the test in a wind tunnel so you can correlate between the real world and the wind tunnel test of those shapes?

Govoni: Yes, it's possible.

Pohlman: The technique of making castings has been done by Ontario Hydro.

Richmond: I noticed on your last pictorial slide, where you have the symmetrical rime the entire length of the line, that the support structure appeared to be glazed. You could see through it - the support structure through the ice. Is that right?

Govoni: That was a clear ice accretion that was originally formed, and then a rime accretion formed over it.

Richmond: Why would a rime accretion form only on the conductor, and not on the support structure?

Howe: The wind shifted ... the lee side

Richmond: Oh, okay. That answers it.

Martin: Could you go back two slides [Table 1]. You had x and y forces; the load cell x, for instance 116.16 - that's the weight of the ice?

Govoni: Over the total length, right. So if you wanted to get it per meter, just divide by 8.5.

Martin: Now, is there a contribution of the wind to that? Like a negative lift?

Govoni: That's something we are looking at.

Ackley: Yes, we're looking at it. We're having a little trouble with the lift right now in terms of establishing a correlation. I think in the first analysis it's only acting as an airfoil, the way the numbers look right now, but we're a little bewildered by that at the moment.

Martin: But if the wind stopped, did the amount of ice - number 116 for example, stay there? Or change?

Ackley: The wind never stops (laughter). These force values and the wind data are averaged over about a 15 minute period.

Martin: How do you prevent your load cell from clogging up?

Govoni: You don't really - that ices up. But we've had problems with seals leaking and had a lot of electrical connections leaking, and shorting. What solved the problem was - we filled the seal with oil.

Martin: The ice can build up over a rod and just plug everything and you wouldn't measure the right amount.

Howe: That happens, but then we deice it.

Rawlins: Where was the anemometer relative to this whole test set-up? Was the wind the same? Or was it [anemometer] off to one side?

Govoni: It was mounted [nearby] ... a pitotstatic tube.

Krishnasamy: You said you saw some galloping motion or oscillation at a certain speed. Do you know what speed?

Govoni: That would happen periodically for any wind speed at all. It was dependent mainly on ice type.

Howe: I don't think it goes faster then 2 or 3 per second - it was noticeably dependent on mass accumulation but I never meaured it, I just estimated it. But with a larger mass of accumulation it would be as small as one cycle per second or 2 seconds. The way it happens is that first, as it begins to accumulate, it slowly, very slowly rotates to form that spiral at the beginning. But then when it gets around 180° approximately, it can't twist any more and so it starts to oscillate in such a way that it builds up...

Martin: Since you brought that slide up, how do you measure the diameter?

Govoni: Very carefully [laughter]. We measured it periodically with a ruler. Sometimes it would have to be estimated from the observatory because the wind and the elements prevented us from getting out there.

Martin: I didn't mean the measuring instruments - I meant where do you start from? Is it a mean diameter?

Govoni: Yes. We take periodic measurements through the ice accretion.

Yen: From your data shown on the slide [...] you have only a few [wind speeds], 10 or 20 m/s, and you also have a conclusive conclusion. I would prefer to make a wider range of wind velocities and it will depend on what velocity at which the ice will not form. Maybe you should do some experiments in that way.

Govoni: I agree.

AD P001691

# AN APPLICATION OF DENDROCHRONOLOGY TO THE DETERMINATION OF THE RECURRENCE OF SEVERE ICE STORMS

Beatrice Félin    Hydro-Québec, Montreal
Julien Rivest    Rivest et Associés, Québec

## ABSTRACT

Major ice storms will cause extensive damage to vegetation. The combined effect of wind and ice loads will break off tree branches with the consequence that growth will be retarded for several years. In 1973 a very severe storm hit the North Shore of Québec and up to 75 per cent of the dominant tree crowns of the conifers were broken by the combined action of ice and wind. Closer analysis showed that older breaks were still visible and the hypothesis was formulated that such breaks had also been the consequence of an ice storm and that the growth ring pattern would reflect these growth retarding events.

A preliminary analysis of 90 tree samples was made to establish the feasability of a technique which could aid in determining the recurrence of severe ice storms. Encouraging results in this first study led to a more complete validation of the method which is presented herein. Five different sites and two species of trees [black spruce (Picea mariana) and balsam fir (Albies balsamea)] were considered. Other causes which could influence growth (in particular entomological factors) along with field procedures and inventory techniques are also discussed briefly.

## WHAT IS DENDROCHRONOLOGY?

It is a well known fact that the age of trees can be determined by counting the growth rings in the stem. However, interesting information can also be obtained from the **pattern** of the rings, the width of which will vary with changing climatic conditions. In areas where climatological records are sparse or unavailable, trees are an exceptionnally valuable source of information since they hold a continuous record of climatic events during their lifetime. Just how this can be of any aid in establishing the recurrence of severe icing storms will be described below.

## INTRODUCTION

In April 1973 a very severe icing storm hit the Rivière-Pentecôte area on the North Shore region of Québec province (Figure 1) and caused extensive damage to two of three 735 kV transmission lines crossing the area. Altogether 30 towers on the first two lines collapsed (the third line suffered little damage because it was under construction). Shortly after the storm, it was noticed that the area worse hit by the storm could easily be identified by the broken tree tops of the most common trees in the area [black spruce(Picea mariana) and balsam fir (Albies balsamea)]. A survey showed that up to 95% of the dominant tree tips were broken and that a high percentage (73%) of the fractures were fresh. This led to the hypothesis that earlier ice storms would have left similar traces, and that any significant breakage of the tree branches would cause a retardation of the growth process and would be visible in the growth ring pattern.

A feasability study conducted in 1973 showed promising results and was useful in orienting a large scale study with the objective of validating the dendrochronological method based on a larger number of tree samples taken over different geographical areas known to be exposed to severe icing and applying it to more than one tree species.

In 1981 Hydro-Québec commissioned a private forestry engineering firm, Rivest et Associés, which had already been involved in this type of work in 1973, to develop a dendrochronoligical method (1) which would be useful in determining the recurrence of severe ice storms in an area.

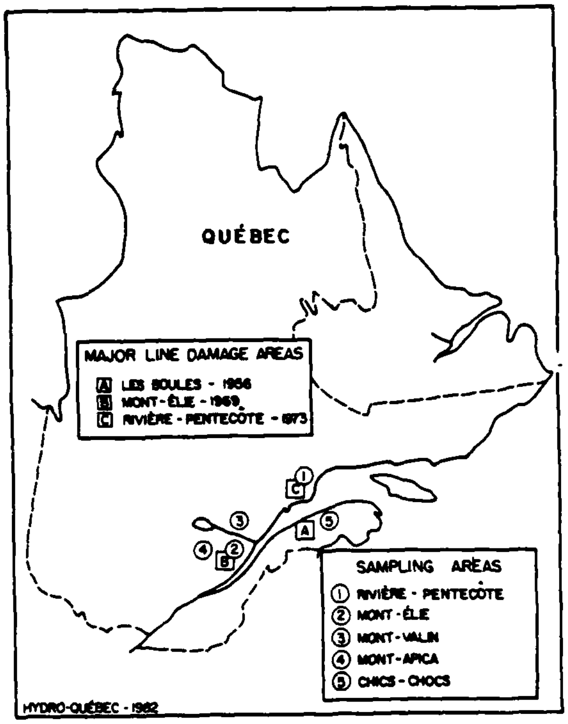

FIGURE 1 - Localization map.

## GENERAL CONSTRAINTS ON TREE GROWTH

The growth rate of trees is affected by several factors. These can be classified according to the characteristics of the tree itself (species, age, etc.) or to the environment in which it stands (soil, climate, etc.). Complex interactions exist between external factors, internal physiological processes and growth.

Figure 2 represents a typical time series of ring widths plotted as a function of the dated year.

Under normal conditions, it is possible to fit an exponential curve to the time series of the ring widths. A trend of declining growth with increasing tree age is apparent from the figure. Much of the variance observed can be explained by the variety of changes that occur throughout the life of the tree. For example stand disturbance, a changing forest environment, climatic variations, attack by disease or insect pest, fire, lightning... could become at some time growth limiting factors. Among all these factors only the entolomological factor could cause a large scale reduction of growth similar to the one that can be observed in the years following a severe ice storm which has damaged a tree.

## Entomological factors

In the study area two insects are liable to cause extensive damage to trees: the spruce budworm (Choristoneura fumiferana, Clem.) and the hemlock looper (Lambdina fiscellaria, Guess.).

Contrary to its name the spruce budworm does not attack only spruce but also fir trees. A severe infestation will last from 6 to 8 years. Over such a long period it is most probable that the balsam fir trees will be killed by the insects while the black spruce trees, since they are usually shunned by these insects, will usually survive. The effect of a spruce budworm attack on trees will appear only 2 to 4 years after its beginning on the growth ring pattern and is more visible at the top of the tree than near the stump. Normal growth will resume several years after the end of an infestation.

On the other hand, the hemlock looper will attack principally the balsam fir and will neglect the black spruce. Growth reduction is visible on the first year of infestation and will resume two years after its termination.

In Québec, insect epidemics are fairly well documented, and the duration, localization and type of each significant outbreak can be obtained from the appropriate organisms.

It is interesting to compare the dates where growth retardation was observed with the dates infestations were reported.

For example, at Site 1 (Rivière-Pentecôte) in 1939 a "break" in the growth ring pattern is visible. However no infestation was reported during that period. From 1948 to 1953 a light spruce budworm outbreak is reported, and the trees in that area show a marked break in the growth-ring pattern starting in 1949 and ending three years after the end of the infestation in 1956. In 1973 another "break" is evident from the growth-ring pattern (this event is certainly correlated to a severe ice storm which occured in the area and caused extensive damage to Hydro-Québec's 735 kV lines; observers after the storm actually saw and heard the trees snap due to the excessive weight of ice). The following year a severe infestation of spruce budworm errupted once again in the area and contributed to the growth retardation. Photographs of different trees showing these events are presented in Figure 3.

## DATA COLLECTION AND MEASUREMENT

Five areas were chosen throughout Québec from which tree samples were to be collected. The selection of the areas was governed by: 1- the frequent occurence of icing storms in the given area, and 2- its accessibility. All these areas were in the mountainous zone which borders on the Saint-Lawrence valley and which is frequently affected by in-cloud icing (icing due to super-cooled water droplets within the clouds).

For each area, four sites were chosen in exposed and mature stands which were most likely to have been affected by icing. At each site two strips of 4 x 500 m each were sampled. One hundred tree samples were taken for each one of the five areas that were studied. The maximum amount of useful information on trees, stand, soil, pathology, topography was collected for each strip from which samples were taken. Specimens 10 cm thick were cut out from

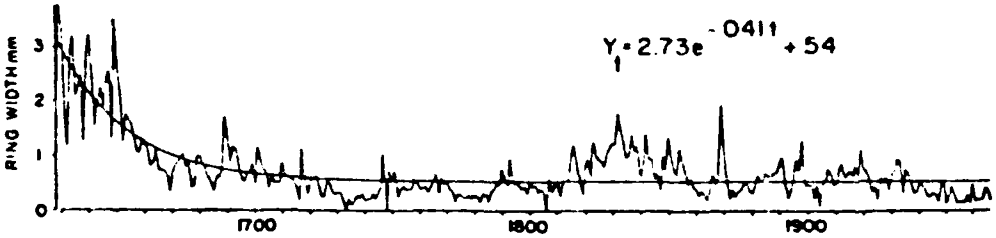

FIGURE 2 - Typical time series of ring widths plotted as a function of dated year along with the exponential curve that was fitted to the date [after Fritts, 1976].

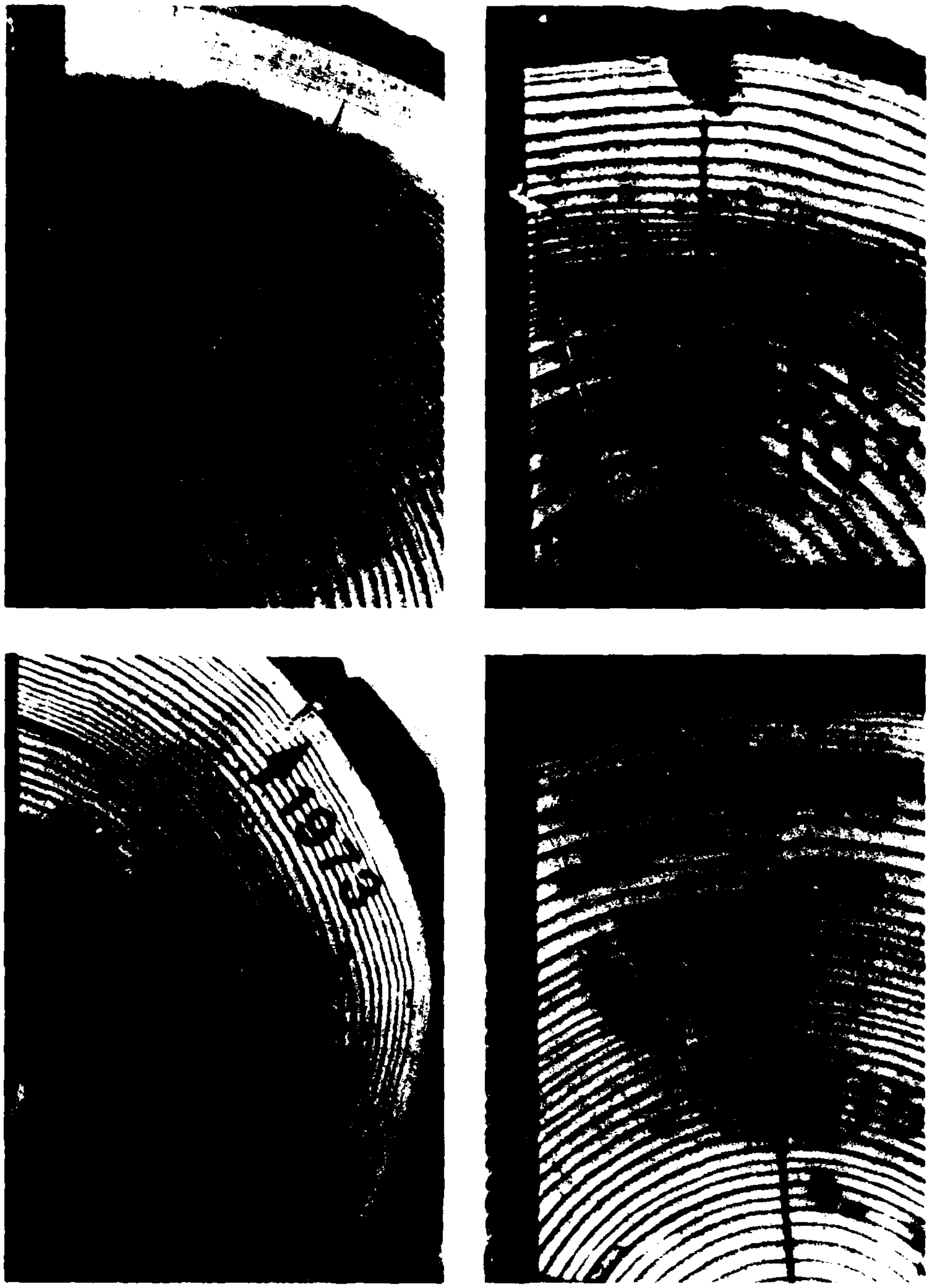

FIGURE 3. Four illustrations of sudden decrease in growth ring pattern dated 1939, 1956 and 1973 at Rivière-Pentecôte.

the stem below the break since growth retardation was more evident at this point than lower down on the stem.

When the properly identified specimens were received at the laboratory they were mounted and sanded to bring out the rings. Then the ring widths were carefully measured using a micrometer connected to an encoder which reduced the risk of introducing human errors.

## DATA ANALYSIS

All the information available was coded and put in a Hewlett-Packard minicomputer to facilitate data analysis. Each reduction in growth which was measured was classified into three categories according to its duration (5 years or more, 3 or 4 years and 1 or 2 years). Figure 4 illustrates the frequency of occurence of periods of slow growth lasting more than five years against the year of occurence at the Rivière-Pentecôte site.

Several years stand out from Figure 4: 1877-1878, 1939, 1956 and 1973-1974.

The episode 1877-1878 stands out clearly on the older trees that were analysed. However we do not hold any information at the present time which could confirm the occurence of a severe icing storm at that time.

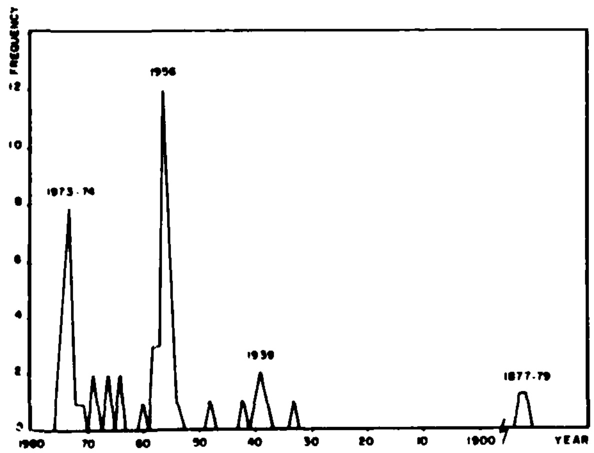

FIGURE 4 - Frequency of occurence of significant growth retardation (lasting 5 years or more) against dated year.

The following interesting event occured in 1939. As was discussed earlier no insect infestation was reported in that area and we have assumed that this growth retardation event was due to a severe icing storm.

The next year that stands out is 1956. As was noted earlier the area was under a light spruce budworm infestation from 1948 to 1953. Trees which broke in 1956 were certainly weaker than under normal conditions and it is difficult to establish from the tree ring data alone what is the real cause of this event. Nevertheless, it is a well established fact that a very severe storm caused extensive damage in 1956 on the northern shores of the Gaspé Peninsula (Figure 1). It could be surmised that the same storm, even though it may not have been very severe in the Rivière-Pentecôte area, could have caused extensive damage to the vegetation because of its weakened state.

Finally the two years 1973 and 1974 stand out from Figure 4. 1973 can certainly be correlated to the storm which caused thirty 735 kV towers to collapse. On the other hand, 1974 is the first year of a spruce budworm outbreak which would also have caused growth retardation and combine itself with the 1973 event on the tree-ring growth pattern.

### Discussion

In the course of this study, dating has been done in a rather straightforward manner by simply counting the rings from the outside to the center of the stem. The chronology resulting from this study can contain errors due to counting, mistaken identification of ring features, or ring absence. Indeed, sometimes during years of extreme climate, a tree may not form a ring on all portions of its stem. The ring is then said to be missing. At other times, a stress period occuring in the middle of the growing season may cause two rings to form within a particular year. Such a feature is then called a false ring. Some of the dispersion around the dated year of an event noticeable in Figure 4 could be explained by such considerations. To place correctly in time each growth layer and eliminate this variance, it would be necessary to crossdate the specimens to arrive at a correct regional chronology with agreement among the growth sequences of different trees.

However, crossdating is a very time consuming process which requires tedious examination of the specimens by eye and computer analysis. For the purpose of this study, crossdating was not deemed indispensable, since our purpose was only to obtain some idea of the recurrence of severe icing storms, and moreover, that any significant event could be correlated to historical data for verification.

## CONCLUSION

The Rivière-Pentecôte area is well known for its high vulnerability to icing storms, and serves well to illustrate the dendrochronological method with which it is possible to establish the recurrence of severe icing storms. In this particular example growth retardation could be correlated three times to an icing event: 1939, 1956 and 1973.

When used in conjunction with available historical data and when insect or disease attack are filtered out this method turns out to be a very useful tool especially when it is applied in remote areas where no meteorological data is available.

## REFERENCES

1- Julien F. Rivest et Associés, 1981. Étude dendrochronologique pour déterminer l'occurence et la récurrence des tempêtes majeures de givre. [Unpublished]

2- Fritts, H.C., 1976. Tree Rings and Climate, Academic Press, 567 pp.

## DISCUSSION

Laforte: Can you estimate the intensity of icing accretion from the diameter of the broken tree?

Félin: We haven't tried to do that. I don't know if you could do that because not all of the trees have the same resistance to breakage. Some are weaker than others, some are older, and it's very hard to obtain a reliable figure.

Power: You have the 1956 data. It's interesting that Mr. Howe's slides from yesterday showed a tremendous ice storm atop Mt. Washington in 1956. We did a study of prolonged easterly flow conditions which went back about 40 years. In our trying to determine the return periods of severe icing storms, we found that the 1956 storm was the worst storm in the Gaspé and in eastern Quebec over a 42-year period. So I think that what you're seeing from tree tops in 1956 relates to the Mt. Washington severe ice storm throughout.

Berry: Did you see any evidence in your tree surveys of multiple [breaking]. In other words, did you track down two or more severe events by having [...]

Félin: Yes, there was one tree which had more than one. It's hard to get more than one in one tree. A tree, once it's broken, is not a dominant tree anymore. It has to be the highest tree in the area in order to be broken. Once it's lower than the other trees it is much less effective [...] icing wind loads. But one tree did show this. We had one event going back to 1877-1879. It was evident there had been growth reduction but it's hard to say if it was icing or insects.

Richmond: Can you tell by the tree rings the effect of forest fire on stunting growth of a tree without killing it?

Félin: I don't think that a fire in northeastern America is like fire in the Southwest. The trees were all burned. You won't have any information once there's a forest fire.

Haugen: You can find evidence of forest fires in two ways. One is indirect in that a fire burns only part of the trees or changes somehow the competition among them so that this changes the growth rate. Occasionally there are flash fires which cause charring of trees, but don't actually kill them. In that case, you can find charcoal in a cross section of a tree, and date the fire by counting rings. Usually there is external evidence of the past fire. I've seen many cases of this.

Félin: From trees that were taken from this type of area?

Haugen: Well, my experience is in Alaska, which is a somewhat more severe climate.

Félin: A 150-year old tree here may have a 6-in. diameter.

Laflamme: You did mention that - this technique ... to get information on the extent ... Did you check this?

Félin: Yes one part of the study that we were hoping to do and we just couldn't manage was - I can show you on the last slide [slide]. This is a set-up we were hoping to use last year. It's a stereometric chamber - two Hasselblad cameras are mounted on the boom here - on the helicopter which flies at low altitude and low speed. Pictures are taken, and with this method, you can have a resolution of ±1 inch on the ground. We were hoping that by flying over an area, and taking pictures with this system, we could count the number of trees that were damaged by icing. You could actually see the bayonets, you could see the top part of the stem which was broken, by this method. Unfortunately the team wasn't available when we were doing the study. They did some work for us, but the helicopter was flying too fast and the pictures were not overlapping, so we couldn't get the stereometric effect, and we couldn't make any useful readings with the pictures we had. But this method hopefully will help us count number of trees that were damaged by icing over quite a large area. It gives you some indication, at least, whether one area is prone or not to icing. And also if there are no trees. We've done surveys for the James Bay project where we looked around and tried to find trees that were broken by icing, and we found none. James Bay is just not an area which is very prone to any kind of icing. This [survey] simply confirmed the fact that there is no severe icing.

Fikke: How do you think the tree rings are correlated with snow accretion on the lines? Could it be possible that you have a heavy snowfall that is caught by the trees but not by the transmission lines, for instance?

Félin: Sometimes the trees will look very much loaded. Once the wind starts blowing it just starts going off. I don't think that covered trees can be damaged by excessive [snowfall]. Not the trees we've seen, at least. The snow just blows off and falls through the trees.

Bilello: In your survey of a number of trees that were broken, were you able to separate the height of the crowns so that you might see a combination of wind and the weight of the snow or the ice that would crack it?

Félin: All the trees that are broken are by definition trees that are above the average height of the other trees. As a result we have no idea at all of the icing or wind loads ... This is just an indication of the trends of severe icing.

Laflamme: I was there in the 1973 storm when tree tops broke. They broke by weight - just from the weight. They were frozen, and when some melting [occurred] under the tree top, the weight was unbalanced, and they broke. But there was no wind.

Félin: One of the pictures I showed was a general view of the forest and some of the tree tops were bent, a *lot simply* bent. You can have a lot of snow before they break - it takes quite a bit of load, and the snow has quite a low density so it wouldn't be heavy enough to cause the breakage.

Olsen: The question I'm asking is whether that area has a history of not icing. Or whether it just happened you were flying after one particular storm and noted there was nothing broken in that particular area.

Félin: No, no. We were flying through the area during the summer. All the trees looked perfectly mature and perfectly formed - there were no bayonet trees. So there was no reason to start doing a tree ring analysis - any growth reduction was probably due to insect infestation.

[At request of session chairman, Haugen gives brief description of CRREL dendrochronology work.]

Haugen: In the past, I've been working in Alaska, and have been primarily concerned with attempting to reconstruct past climates by means of tree ring analysis. In this particular approach, we use timber line trees, which are sensitive to air temperature during the growing season, and by developing tree ring records we have a relative indicator of the past. We've also done some work on dating of events.

Power: Are there any indications of icing in Alaska?

Haugen: Well, we've had similar situations, but we haven't attempted to date that.

Thowless: I know there's been a lot of dendrochronology in recent decades. Is this information being compiled into an atlas for the North American continent?

Haugen: The Laboratory of Tree-Ring Research in Tucson has done a lot of that.

Richmond: Was your work in Alaska done in this manner - cutting the tree down and counting the rings, or is that done by core samples?

Haugen: Mostly with cores.

Minsk: Is it really necessary to cut a tree for core analysis?

Haugen: It depends on what you're looking for. If a tree is undamaged, and regular in its growth, usually a core will do the trick. But with something like fire damage, where it might have affected only part of the tree, and you're trying to date, then it requires a cross section.

Thowless: As indicated by the previous speaker, their sampling as I recall is done close to the damaged area of the tree - the fractured area. Now, in routine analyses of trees, how much variation is there as a function of, say, height, when you examine the cores.

Haugen: If you can imagine it in a living tree, tree rings are like a series of cones which are just piled on top of each other. So, generally if there's an effect on the ring of one part of the tree, it shows up in the entire tree. So really, if there is an effect on a particular ring, it's just a matter of establishing the date of that ring, to determine what you need to know. Generally speaking, the whole basis for the science of dendrochronology is cross dating the rings, showing that a pattern exists from tree to tree, the same pattern of wide and narrow rings. Once this is done, it's fairly easy to date a particular event that affected that ring.

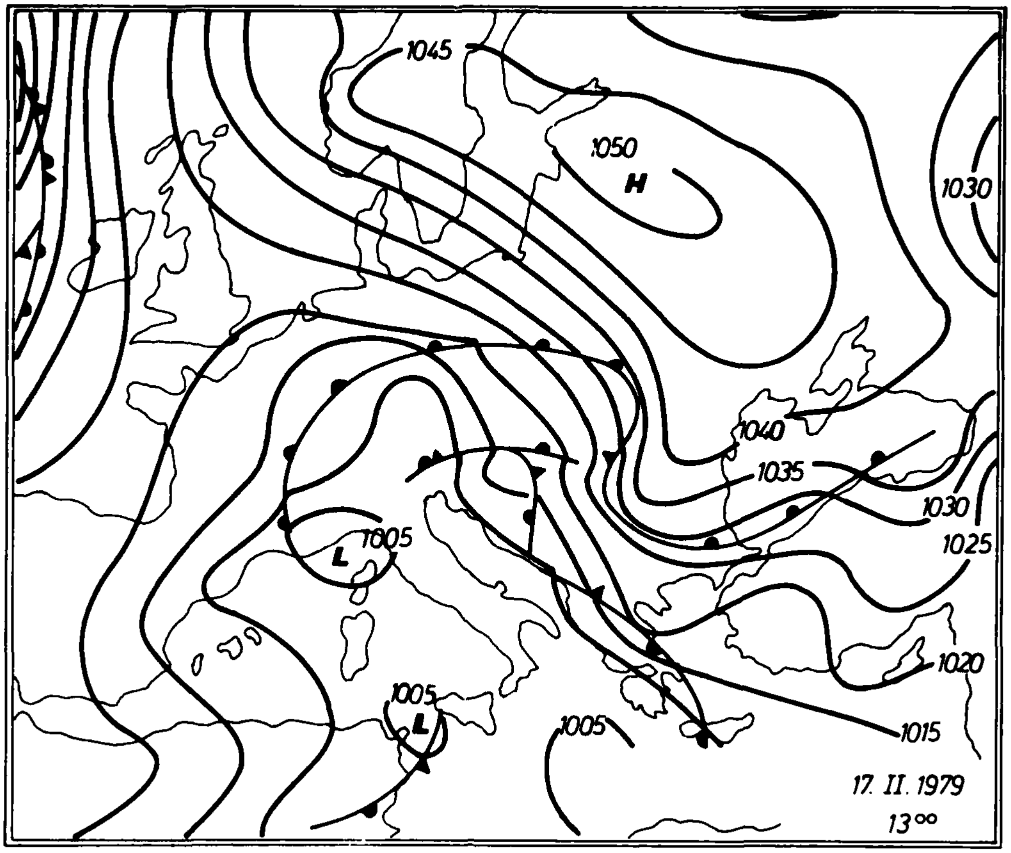

Fig.1. Daily Weather Map.surface chart, 1300 GMT, Feb.17.1979.

lone circulation having a cyclone center over the Genoese gulf. At the same time, over the Adriatic sea, Bakans and Pannonian depression there was a prevailing strong south upper wind that caused the spreading of warm air masses coming from the north Africa (figure 3).

The cold air penetration over the territory of the USSR in the direction of Charpatians and Black sea and the existing of anticyclone over Baltik and east Europe caused a noticeable temperature decrease for 5 to $10^{\circ}C$ in the east part of Yugoslavia and even more in hilly-mountainous regions, with periodical rainfall, frozen rain drops or snow.

The Kosava gusts had the velocity of 70 to 110 km/h and in the plains north from the damaged place, even to 160 km/h. These were the strongest gusts in the period of the last decade.

In the regions where the damages occurred, at the temperature of about $0^{\circ}C$, the gusts were associated with the rainfall, frozen rain drops and snow, i.e. favorable conditions for ice accretion on overhead lines.

According to the radio-sounding measurement data a strong southeast wind Kosava blew in a relatively narrow level up to the height of 900 meters above sea level (figure 4). Above this level, there was a prevailing strong south and west wind. Due to the cold air penetration in narrow level and wind shear (dynamic turbulence) at the temperature of about $0^{\circ}C$, there is a strong upper air inversion being 300 m thick, with a base at the altitude of 650 m above surface. The temperature lapse rate was $\gamma = -2.6^{\circ}C/100m$. This temperature and air humidity distribution in the upper layer show that in winter period when there is Kosava blowing, there are favourable conditions for the frozen rain drop occurrence.

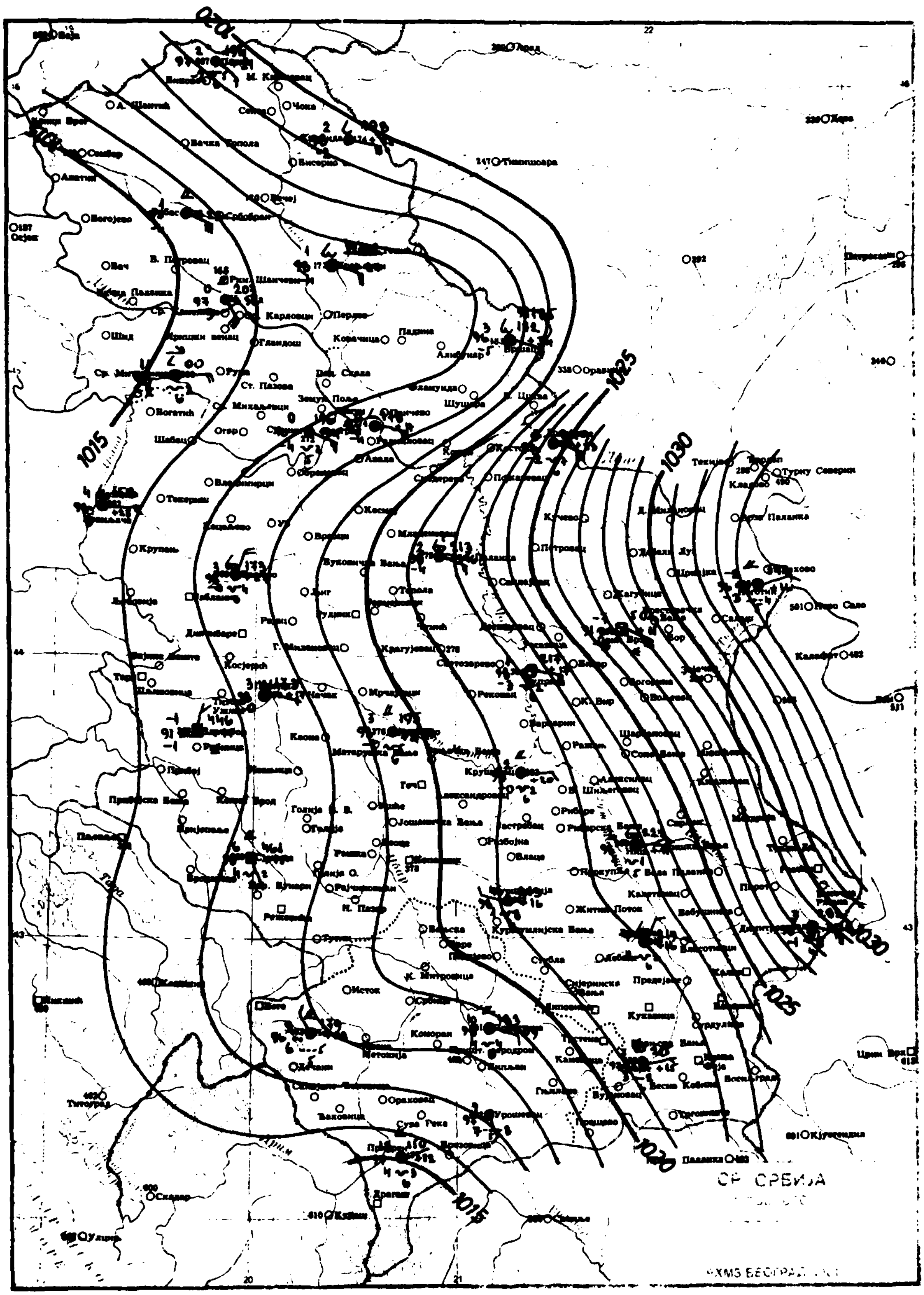
1015
1020
1025
1030
СР СРБИЈА
РХМЗ БЕОГРАД

Fig.2. Distribution of pressure (isobars) over East SFR Yugouslavia (SR Serbia), 0700 GMT, Feb.17.1979.

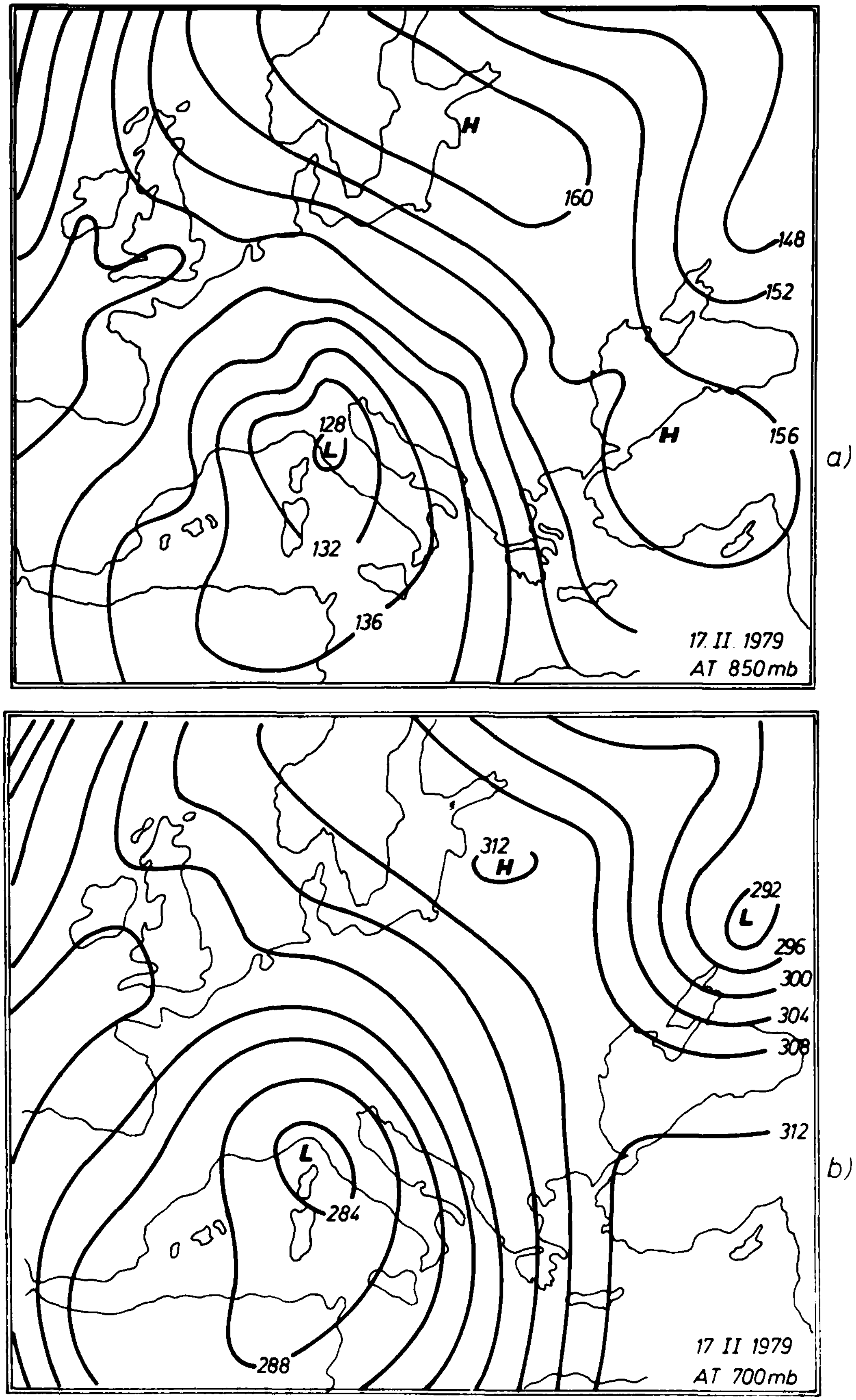
H
160
148
152
128
L
H
156
a)
132
136
17.II. 1979
AT 850mb
312
H
292
L
296
300
304
308
312
b)
L
284
288
17 II 1979
AT 700mb

Fig.3. Upper air charts, contours 850 mbara
(a) and 700 mbara (b) 0100 GMT,Feb.17.1979.

## 2. SURFACE METEOROLOGICAL OBSERVATION DATA

In a vaste region where the damage occured there are several meteorological stations of various kinds (main meteorological stations, climatological stations and precipitation stations), showind the following changes of the meteorological elements and phenomena during the day of February 17.

Djerdap: During the day there was a rain, then granular snow and snow. East wind velocity 11 to 14m/s. Maximum wind velocity at 1600 was 19 m/s. The temperature at 0100 was 6°C, at 1500 it was -1.7°C, after that increased to the value of -0.4°C. The soil covered with snow.

Tekija: Cloudy with frozen raindrops, rain and sleet. Daily temperature about 0°C to -2.8°C. North wind, velocity 19 m/s. Glaze on the overhead objects.

Brza Palanka: Cloudy with snow. Temperature decreasing, between -1 and -1.8°C.

Donji Milanovac: Cloudy with snow and sleet. Temperature about -2°C.

Negotin: Cloudy with precipitation during the whole day. Snow

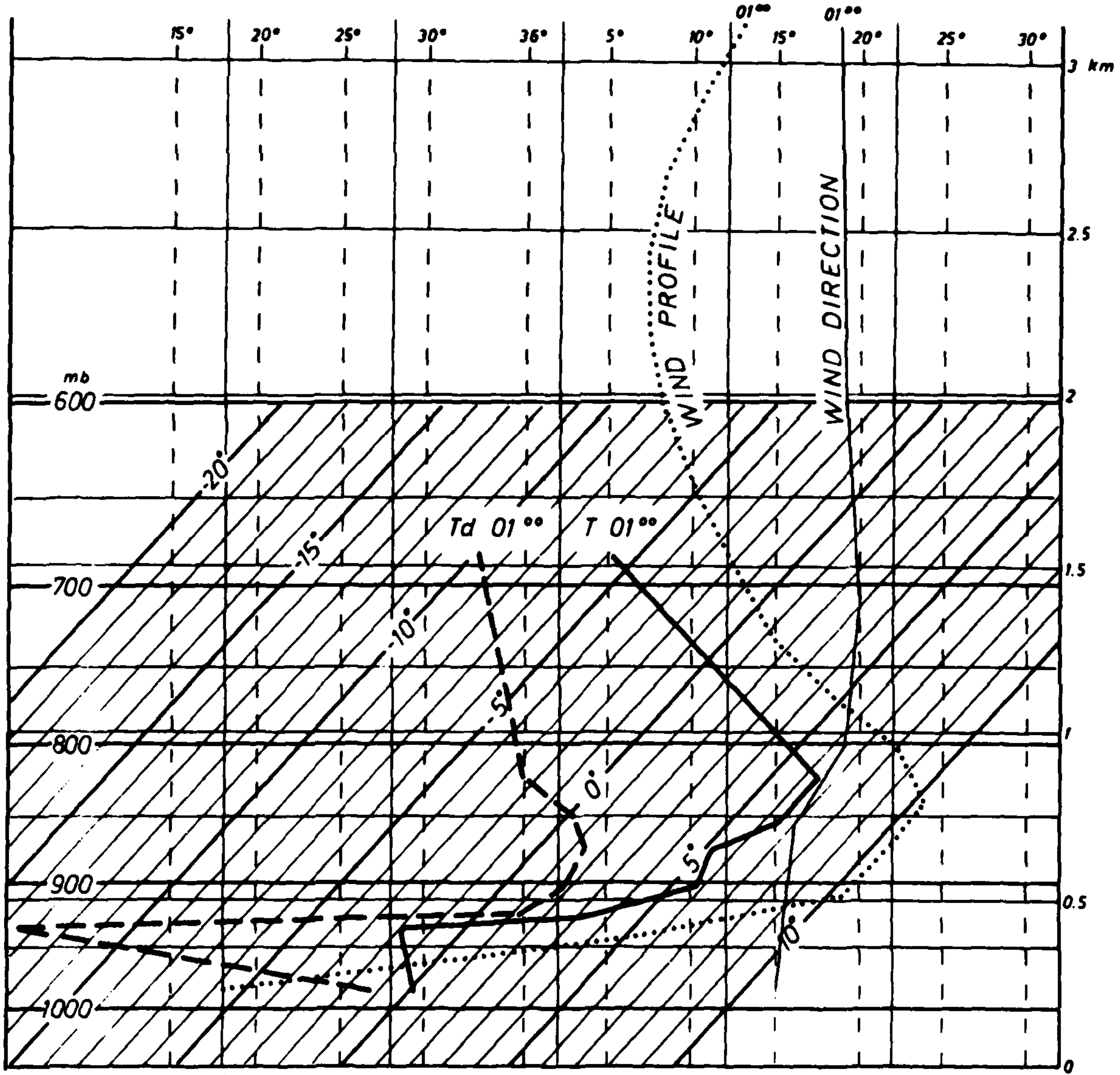

Fig.4. Rawinsonde data, the vertikal distribution of temperature, dew point, wind speed and direction, 0100 GMT, Feb.17.1979.

from midnight to 0300, then frozen rain to 0845, granular snow to 1000, and then snow to 1530. Again the frozen rain till the end of the day. Wind from the east direction, variable in velocity, from 14.6 m/s at 0100 to 6.8 m/s at 1500. Then wind velocity increased again to the value of 10 m/s at the end of the day. Snow cover with a glaze layer, the same on all overhead objects. The air temperature varied from -0.4 to -3.1°C.

Zaječar: Drizzling during the night. Glaze at the soil. Snow started at 0855. Northeast wind, velocity about 15 m/s. Temperature from -9.5 to -4.1°C.

Minićevo: Cloudy without any precipitation. Wind east and northeast, velocity 8-14 m/s. Air temperature from 2.0 to -3.0°C.

Crni Vrh: This is the only mountain station (860 meters above sea level). During the day the temperature fell from -5.4°C at 0100 to the value of -9.0°C at 1200. In the afternoon, it had the value of about -7.4°C. Very strong wind blew from the east direction continuously, changing the velocity from 25 to 28 m/s. The icing of the overhead objects very intensive with thick layers of granular hoar frost. At the beginning of the day there was a frozen rain and in the afternoon (from 1500 to 2400) snow and snowstorm.

The surface observation data from meteorological stations next to the region where the damages occurred, show the occurrence of frozen rain having a duration of several days with periodical snow or sleet. The air temperature had a value of about 0°C, or bellow. The wind blew from the east quadrant, having the velocity of about 15 to 20 m/s. A glaze might be noticed on the surface and overhead objects.

## 3. DATA ON CONDUCTOR ICING AND WIND

In accordance with the methodology that has been using in our country (S.Plazinić, 1964), our network of the main meteorological stations make continuous and sistematic measurements and observations of all kinds of ice accretions and wet snow accumulated on the instrument for the conducter ice measurement (SPAN). There is a continuous recording of all types of accretions, their diameter, thickness and weight using the instrument conductor 0.5 cm, as well as the accompanying meteorological phenomena and elements.

At the time of the structure damage, the maximum measured accretion weights were as follows:

At the meteorological station Djerdap maximum accretion weight was 0.5 kg/m. This station is fairly far from the damage location. At the meteorological station Negotin, during the night between February 16 and 17, there was a glaze layer on the instrument conductors due to the continous frozen rain. The air temperature was -0.4 to -2.5°C, wind velocity from the east directions was 5-7 m/s. Glaze accretion of the holster type was accumulated on all conductors but the dimensions were much bigger on the lines having north-south direction. On February 17, during the night, the glaze accretion increased and had the following dimens.: P(diameter)= = 44mm; D(thickness)=22; $\gamma$ (density) =830 kg/$m^3$ and the accretion weight (G) was 0.6 kg/m. In this case the air temperature was -1.4°C and wind velocity 4 m/s.

The glaze accretion dimensions were not significantly big at the meteorological station Zaječar. Maximum value was 0.5 kg/m. At the same time, at the meteorological station Crni Vrh (860 meters above sea level) on the accumulated layer of glaze and granular hoar frost, there was the accretion of wet snow that later was frozen. This accretion remained even at the wind velocity of 19.3 m/s. Maximum dimensions at the instrument were as follows: diameter 116 mm, thickness 46, density 430 kg/$m^3$, accretion weight 1.6 kg/m. Using the data on icing measured at the stations as well as the method for the calculation of the accretion weight for various types of conductors of transmission power lines and their heights, we have obtained the following weight values: 2,6 kg/m for the 110 kV transmission lines, 3.4 kg/m for the 380 kV transmission lines for the location around Negotin and Zaječar. However, the weights were about 3.5 kg/m for the lines at Crni Vrh.
It should be noted that these stations are at various altitude above sea level and 20km far from the

damage location.

## 4. FIELD INVESTIGATIONS AND MEASUREMENTS OF ICING AT THE LOCATION OF STRUCTURE DAMAGES

In order to estimate the type of ice accretions, their dimensions and weights causing the damage of various structures and all overhead objects and to establish the spatial distribution of icing, we visited the region of east Serbia on February 20,21 and 22, i.e.two days after the damage.

Field investigations have shown the accumulation of the glaze and granular hoar frost occurred in the whole territory of east Serbia.Bigger dimensions were noticed in various regions so it was difficult to see the distribution refering to the physical-geographical conditions.

Bigger accretion dimensions that caused the damages have been noticed in the region of the river Danube to the line Majdanpek - Bor, 45 km long and 30 km wide.The figure 5 shows a vaste region of east Serbia being influenced by the maximum icing.

At the territory of damaged area,in vicinity of Bor, there was a glaze accretion, oval and bolster type, on all overhead objects,with the dimensions of 20 to 30 mm. The accretion was a homogeneous layer of hard glassy ice with a smooth surface. It has been accumulated in the leeward side of the construction. The accretions were not of big dimensions so the damages were not reported. However, moving toward the mountain Deli Jovan where the prevailing wind blew from the east in a big angle, there were glaze accretions of oval shape causing noticeable damages to the trees and overhead post-telegraph lines and 35 kV electrical power lines. The accretions of big dimensions have also been found in the regions beyound 300 meters above sea level. Thick glaze accretions were especially noticed on the damaged electrical power lines and trees along the line across the mountain sides normal to the direction of the prevailing east wind, at the altitudes of 350 to 450 meters above sea level, at the open and unprotected terrains (Metriš-Brestovac-Trnjani

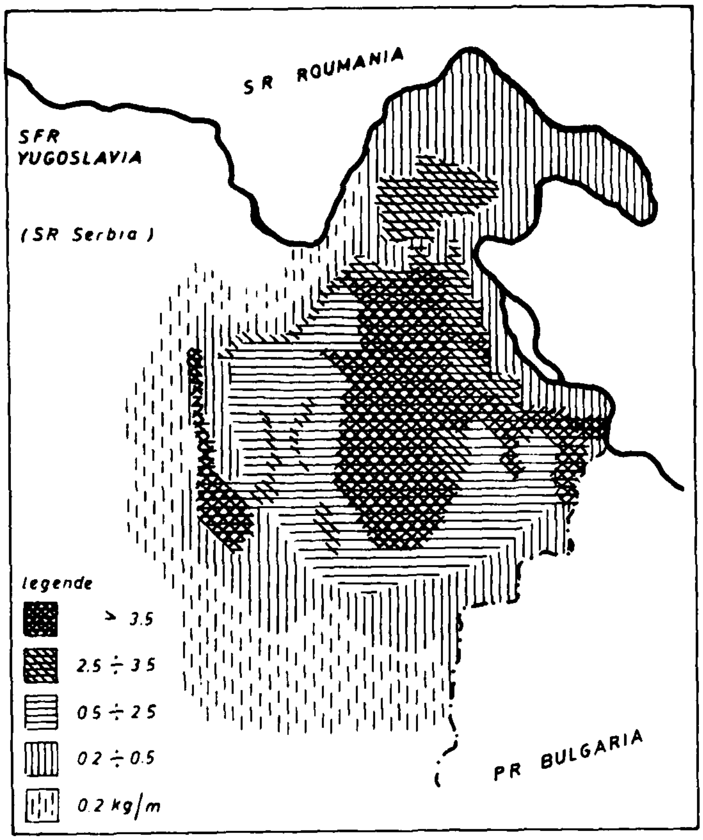

Fig.5. Distribution of ice accretion (kg/m) resulting from field investigations.

-Korbulovo-Jesenice-Štubik). The trees flattened or were broken, power line poles fell down or were damaged (380,220 and 110 kV), post-telegraph lines have been blown down along the distances sometimes overpassing 10 km. Two days after the damage, the measurements were performed at this locations.

The method of V.J.Bučinski(1960) was used in calculations of accretion weights for the height and diameter electrical power conductors and construction elements. This method includes the following parameters: accretion diameter P(in mm) or the big axias since it had elliptical shape, thickness D(in mm) or the small axis; wall thickness of the elliptical accretion b(in cm), density $\gamma$ (in kg/m$^3$) weight G(in kg/m). The average conductor heights are 10, 15 and 20 m above the surface and the diameters 1.7, 2.6 and 3.2 cm.

Salaš region. In this region, the following accretion dimensions have been measured: P=85, D=45, $\gamma$=770, B=24 and G=2.0 kg/m. The converted weights for 380 kV, 220 kV and 110 kV

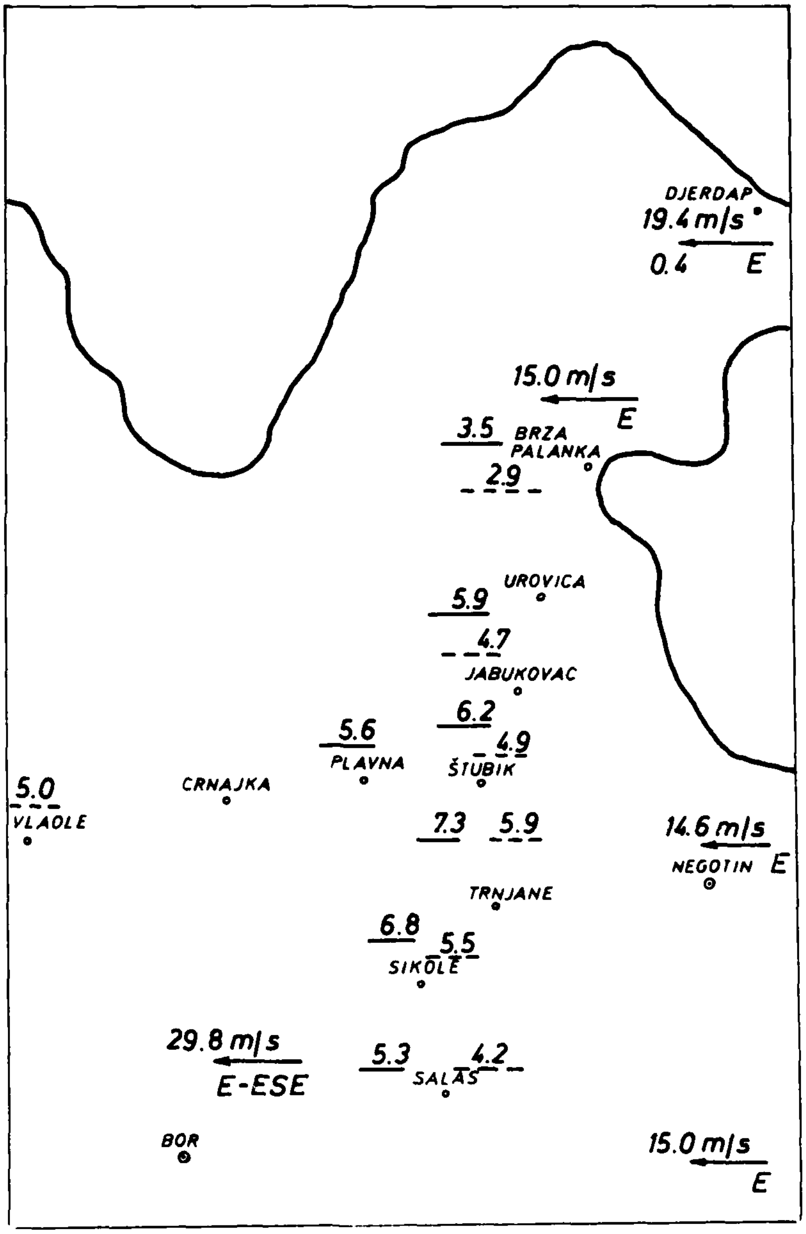
DJERDAP
19.4 m/s
0.4
E
15.0 m/s
E
3.5
BRZA PALANKA
2.9
UROVICA
5.9
4.7
JABUKOVAC
6.2
4.9
5.6
PLAVNA
ŠTUBIK
5.0
VLAOLE
CRNAJKA
7.3
5.9
14.6 m/s
NEGOTIN
E
TRNJANE
6.8
5.5
SIKOLE
29.8 m/s
E-ESE
5.3
4.2
SALAŠ
BOR
15.0 m/s
E

Fig.6. Distribution of ice loading on transmission lines 110 kV (---) and 380 kV (——), and wind direction and velocity on February 17.1979.

electric power line heights and diameters were G=2.8-3.7 kg/m. The measured accretion weight on one meter construction element was about 2.6 kg/m.

Sikol region. The measured accretion parameters at one meter conductors were:P=137,D=56, b=3.5, $\gamma$=770 and G=3.9 kg/m. The converted values G=5.5-6.8 kg/m.

Dubrava region. This was the region with biggest damages. The following values were measured:P=130--154, D=61,$\gamma$ =830 and G=3.6 kg/m. Converted values for the construction height and diameter:G=4.6 to 7.3 kg/m. In convertion, we have used the gradient measurement data from the research station Crni Vrh (Plazinić, 1971).

Mali Krš region. This is a mountainous terrain having the altitude of 700 meters above sea level where we found very serious damages on 110 kV electrical power lines. The ice accretion weight on the power line pole element G=4.5 to 6.2 kg/m.

It is necessary to mention that together with the accretion forming there was a very strong wind but the damage degree depended on the structure position, terrain configuration and the construction height and type. In the region of Mali Krš, at the location that was exposed to the strong wind, the poles were distroyed from the bottom and fell to the opposite side. This might not be stated for the lower locations where we had 380 and 220 kV power lines. However, in the lowest region, the 35 kV poles were broken in the middle and had the position opposite to the wind direction (we enclose the photos showing the characteristical structure and tree damages in the above said regions). Figure 6 shows the distribution of ice accretion weghts and wind direction and velocity on February 17, 1979.

## 5. LONG-TERM METEOROLOGICAL ICING DATA MEASURED BEFORE THE DAMAGE

The long-term meteorological icing data measured before the damage the field investigations before the damage occurred. These data were the meteorological base for the construction design and building in this region. In brief, this analysis includes the following:

- Air circulations are influenced by the mountain complexes,so during a year, the prevailing circulations come from the northwest and west direction, having a phön character. Due to the hold up zone in the region of the river Danube and cold air lake forming in winter, the prevailing winds can come from the other directions as well (east, northeast and north).
- The region from Djerdap to Bor in winter has a very high relative air humidity so in some meteorological situations the ice accretions are formed.
- The weights refering to the conductor icing, measured at the meteorological stations and used for the construction design were 0.2 to 0.8 kg/m and for the power lines 1.3 kg/m but not bellow $1.0 \times \sqrt{d}$ , where d=conductor diameter in mm.
- The probability of the maximum wind pressure was calculated on the basis of the wind data obtained from the main meteorological stations that did not have any longer observation periods. So the values of 60 and 75 daN/m2 were obtained.
- Microclimatological studies in this part of Serbia have shown that there was no damage of surrounding objects, forest complexes atc. due to icing or wind destructive effect. Further, according to the information obtained from the post--telegraph services responsible for the line connection maintenance,the companies maintaining the power lines and the population, there was no serious damage in the last twenty or more years due to icing and strong wind, except in the before said mountain sides (saddles).
- In the period 1968-1970, we have established a few additional measuring points for the purpose of ice measuring. So, using these data, the maximum accretion loads were calculated for the purpose of power lines design and construction. These values did not exceed 1.0 kg/m.
- In order to establish the probability of icing occurrence in this region, the data on icing for the period 1964-1978 were processed. The table 1 presents the ice occurrence frequences in types: crystal hoar frost (V), granular hoar frost(▼), glaze (~), wet snow ($\dot{*}$), frozen wet snow ($\boxed{\dot{*}}$) and compound accretion (~ ▼).

Tbl 1

| station | period year | t y p e s |  |  |  |  |  | summary |
|---|---|---|---|---|---|---|---|---|
|  |  | V | **V** | ∼ | –✱– | [–✱–] | ∼**V** |  |
| CRNI VRH | 14 | 12 | 226 | 70 | 30 | 8 | 159 | 505 |
|  | % | 2 | 45 | 14 | 6 | 2 | 31 | 100 |
| NEGOTIN | 12 | 36 | 17 | 22 | 32 | 6 | 3 | 116 |
|  | % | 31 | 15 | 19 | 27 | 5 | 3 | 100 |
| ZAJEČAR | 12 | 19 | 1 | 17 | 27 | 1 | · | 65 |
|  | % | 29 | 1.5 | 26 | 42 | 1.5 | · | 100 |

On the basis of the long-term icing measurement and investigation data before the damage, there was no meteorological reason for using the additional big loads due to ice accretion and wind in order to prevent the damage of constructions.

## 6. OCCURRENCE PROBABILITY OF ICE ACCRETIONS

The question may be raised whether it is correct and economically justified to take the values measured after the damage for the future desing and building of power lines and constructions.

In order to answer this question to a certain degree, it has been tried to find the probabilities of additional loads due to ice accretions since lately for this purpose the methods of probability theory has been used. For the statistical analysis, the method of Fisher and Tippet of maximum values distribution (M.V. Zavarina, 1972) has been used. Figure 7 shows the distribution probability of the ice accretion wall thickness (b) for Negotin.

Maximum weights of the ice accretions were calculated using the obtained probability for the wall thickness (b) of the accretion in a

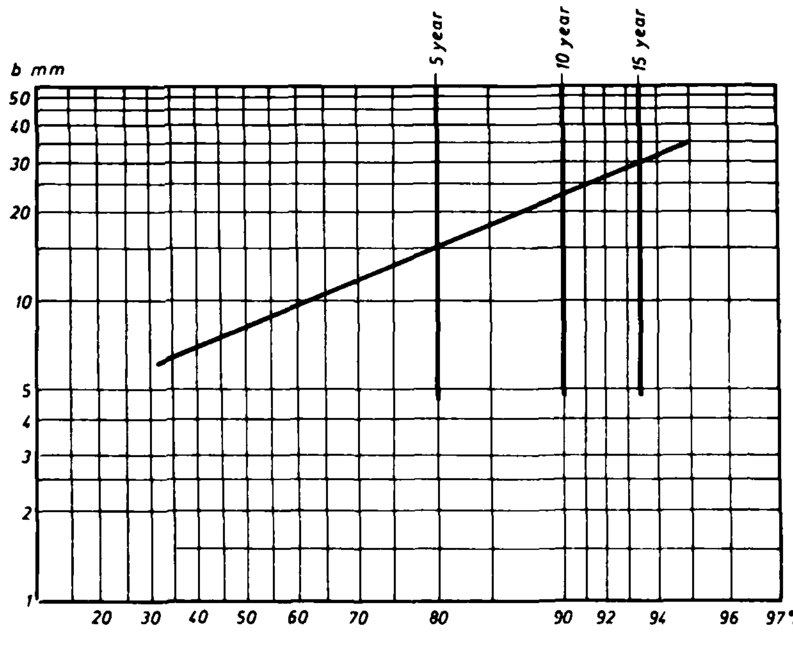

Fig.7. Distribution of probability of the ice accretion wall thickness (b) for Negotin.

form:

$$G = \pi \gamma b (b + d)\ kg/m$$

$$b = \frac{1}{2}\sqrt{(ac - d^2)\frac{\gamma'}{\gamma} + d^2} - d$$

a,c,=accretion dimensions; $\gamma'$=density; d=conductor diameter.

Negotin:occurrence probability for
5 years G=0.8kg/m
10 years G=1.6kg/m
15 years G=2.2kg/m

CONCLUSION

On the basis of the experience after a serious damage of various structures, mainly electrical power lines, we came to the conclusion it is necessary to begin a detailed study of the icing and simultaneous wind effect, either for the purpose of design and building of the structures or for the purpose of their maintenance. For the purpose of making the preventive safety measures, it is necessary to make the following:

1.to organize the weather condition information and the prediction for the successive days refering to the icing, wind and other meteorological parameters (weather forecast and radar observations);

2.to organize the systematic studies of icing according to the following program:

2.1. ice measurements and measurements of accompanying meteorological elements and phenomena at the meteorologica stations and economical objects network relevant to the structures.

2.2. To make the special ice measurements at the research-experimental stations (icing changes depending on the structure kind and type. laboratory investigations of icing, ice and wind influence to the construction vibrations, icing in exposed conductors, etc.).

2.3. To collect and study the data on damages of the electrical power lines, post-telegraph lines, building objects and constructions, forest complexes etc. (data, descriptions, photos, drawings, etc.).

2.4. To make the comparative damage and ice analysis and make the maps of spatial and time distribution of the ice parameters. To study the ice and wind effects.

3. To improve the methods of measuring, processing and analysis of the meteorological data necessary for the design, building, operation and maintenance of the structures and especially electrical transmission systems. To make the advanced training of the personnel,instrument and equipment modernization, exchange of the experts and experience,application of the recommandations of CIGRE, WMO etc.

LITERATURA:

1. Plazinić S.:
Uputstva za osmatranje i merenje zaledjivanja,Republički hidrometeorološki Zavod,Beograd,1965.
2. Organisation météorologique mondiale:
Guide des pratiques climatologiques,Suppl.No.5/VII,19661.Genéve, Suisse
3. Plazinić S.i Miljković N.:
Zaledjivanja provodnika nadzemnih vodova na teritoriji SR Srbije, RHMZ SRS, 1969.
4. Zavarina,M.V.:
Stroiteljnaja klimatologija,Gidrometizdat,Lenjingrad,1972.
5. Bučinski,V.J.:
Gololed i borba s njim, Gidrometizdat, Lenjingrad, 1960.
6. Burgsdorf,V.V.:
Obledenie provodov elektroperedači Vniie, Moskva, 1968.
7. Djukanović,D.i Plazinić,S.:
O proučavanju zaledjivanja dalekovoda u Srbiji, Referat na VIII stručnom savetovanju Jugoslovenskog nacionalnog komiteta CIGRE, Mostar, 1966.
8. Nikiforov,J.P.:
Uticaj konstrukcije vazdušnih vodovova elektroprenosa na izračunavanje dodatnog opterećenja usled zaledjivanja,Gosenergoizdat, 1964.(prevod D.Vukmirović).
9. Elaborat o analizi havarija dalekovoda 380 kV, 220 kV i 110 kV u istočnoj Srbiji, za 17.02 1979 RHMZ SRS,Beograd, 1979.
10. Plazinić,S.
Gradijentna merenja zaledjivanja provodnika na Crnom Vrhu,izdanje RHMZ SRS, Beograd, 1971.

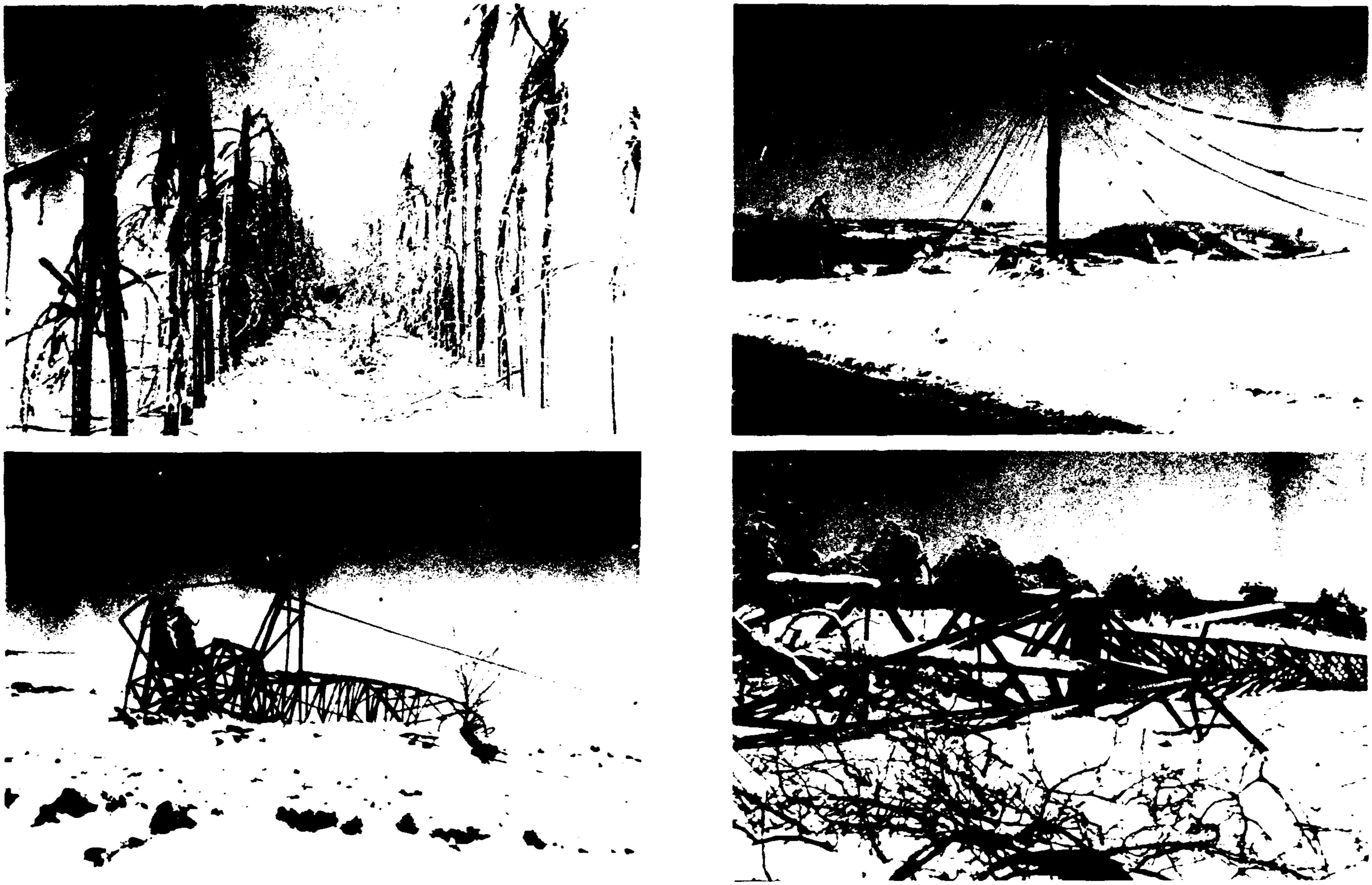

Characteristical structure and tree damages in East Serbia

THE ENCLOSED I

AD P001693

# ICING RELATED PROBLEMS, EFFECT OF LINE DESIGN AND ICE LOAD MAPPING

Eu.P. Nikiforov All-Union Research Institute of Energetics, USSR

## Abstract

The paper deals with the estimation of ice loads on overhead transmission lines in the USSR.

The correlation is given between ice thickness on OH line conductors and on conductor at weather station, which allows to account for the effect of line design on ice load.

The problems of choice of the standard return period and ice thickness intervals for design ice loads are considered.

## Report

In the Soviet Union evaluation of ice loads on OH lines is based on the data from observations at weather stations, where measurements are taken of the ice forming on a rigidly clamped horizontal lendth of conductor, 5 mm in diameter, arranged 2 metres above the ground. At each weather station there are two conductors, one running North-to-South, and the other East-to-West. The wind velocity is taken to be the average for the two minute interval.

The ice loads on the conductors of OH lines differ appreciably from those recrded at weather stations, since a weather station conductor may be screened by buildings bushes and the like. Overhead line conductors are higher above the ground and have larger diameters. Furthermore, conductors on an OH line are strung in long spans and are "live".

In order to permit more accurate use of ice load measurements from weather stations in determining the mechanical loads for OH lines, field and laboratory tests have been conducted into the effect of conductor screening at weather stations on the ice deposits on the conductors and into the influence of the design characteristics of OH lines on ice and/or wind loads.

The theoretical analysis which has been carried out permits a sound interpretation of the experimental data obtained.

1. Droplet size during ice formation can vary over a wide range. When ice is formed from fine droplets at low temperatures, the result is a friable white deposit; hoar-frost. If the size of the drops becomes larger or the temperature increases, the number of air occlusions is reduced through droplet fusion, making the deposit denser. With large drops of highly cooled rain, what is formed transparent (pure) ice. When temperature and the dominant size of drops vary, it is possible to have one form of deposit superimposed on another, resulting in a "mixture".

In the following the term "icing" or "ice" will be used to cover all forms of ice deposits.

The expression for droplet travel in a stream of air may be written in the form:

$$\bar{F}_g + \bar{F}_i + \bar{F}_{fr} = 0 \qquad (1)$$

where

$\bar{F}_g = m_{dr}\bar{g}$ is gravity ($m_{dr}$ being the mass of the droplet, and $\bar{g}$ the acceleration due to gravity);

$F_i = -m_{dr}\bar{a}$ is the inertia ($\bar{a} = \frac{dV_{dr}}{dt}$ being the acceleration of the droplet, wherein $V_{dr}$ is the droplet velocity.

$F_{fr} = 6\pi\mu r_{dr}(V - V_{dr})$ is the friction between air and droplet (Stokes' law), $V$ being the air velocity, $r_{dr}$ the droplet radius and $\mu$ the coefficient of air viscosity.

For the more common case of ice formation from fine water droplets in fog or drizzle, it can be assumed that, in the main, they travel horizontally in the air stream which accounts for the deposition of droplets on the windward side of conductors. Referring to Fig.1, near a cylinder (the conductor), the lines of flow are deflected, and the relationship between the air/droplet friction ($F_{fr}$), the inertia of the droplet ($F_i$) and its weight ($F_g$) results in the width of the strip $2\lambda$, in which the water droplets strike the conductor, being less than its diameter d.

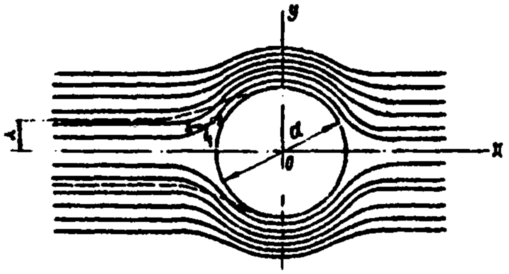

Fig.1. Flow of air past a conductor, and droplet travel in the air flow.

1 - $F_g$, 2 - $F_i$, 3 - $F_{fr}$

——— lines of flow

------ critical droplet path

The rate of increase of the ice load for droplets with a radius $r_{dr}$ at the beginning of ice formation can be defined by the formula:

$$dP_{dr} = 2\lambda_{dr} W_{dr} V_{dr}\, dt \qquad (2)$$

where $dP_{dr}$ is the rate of increase of the weight of the ice load produced by drops of a given size;

$2\lambda_{dr}$ is the width of the strip from which drops of a given size are deposited on the conductor;

$W_{dr}$ is the mean moisture content in the air, brought about by drops of a given size;

$V_{dr0}$ is the steady velocity of drops of a given size in the air flow.

The relationship of $2\lambda_{dr}$ to the conductor diameter and droplet size can be determined by solving the equation for the travel of a droplet which has ceased moving at the point $x = 0$, $y - d/2$, for which we determine $y = \lambda$ - the initial ordinate of the droplet concerned. In so doing, we assume, that: 1) $F_g = 0$, 2) all the air particles moving along the flow lines within the limits $\lambda < d/2$ are subject to one generalized dependance $V = f(t)$, t being time.

Under these assumptions we obtain

$$2\lambda_{dr} = d\left\{1 - \frac{1}{\frac{m_{dr}}{k\frac{d}{2}}(V_{e.dr} - V_0)^2 + 1}\right\} \qquad (3)$$

where $V_0$ is the wind velocity;

$V_{e.dr}$ is the velocity of an extreme droplet immediately before it strikes the conductor;

$m_{dr}$ is the mass of the droplet

$d$ is the conductor diameter;

$k = 6\pi\mu r_{dr}$.

According to equation (3), the relatioship $2\lambda_{dr} = f(d)$ has a maximum. The smaller the size of the droplet, the smaller will be the diameter corresponding to the maximum of $2\lambda_{dr}$.

Droplet size can vary greatly; the rate of increase of the weight of the ice load, taking account of droplets of all sizes, can be defined as:

$$\sum_{k=0}^{k=k_0} dP_{dr} = \sum_{k=0}^{k=k_0} 2\lambda_{dr} W_{dr} V_{dr}\, dt \qquad (4)$$

Equations (3) and (4) permit qualitative evaluation of the factors causing the difference between the ice loads on weather station conductors and OH line conductors.

2. Screening of weather station conductors by buildings, fences, trees or bushes affects the histogram of droplet sizes, the wind velocity and direction at the location of the conductor and finally results in a reduction of the ice load. Field tests on screening by buildings, fences, belts of trees etc., have been conducted.

3. Design characteristics of overhead lines favour the increase of ice loads compared with loads on weather station conductors.

3.1. The diameter of OH line conductors is always greater than 5 mm. Since the value $2\lambda_{dr}$ in eq.(4) increases appreciably with d, at conductor diameters used in practice, their increase will lead to a higher rate of ice load growth.

The increase in the weight of ice is also favoured by the very process of ice forming, since an increase in the dimension of ice increases $2\lambda_{dr}$. Consequently, the relationship of the weights of ice $P_d$ on conductors of two different diameters is non-linear.

In view of the fact that $2\lambda_{dr}$ (eq.4) os appreciably affected by the mass of the droplets of moisture from which ice is formed, the relationship $P_{d1} = f(P_{d2})$ will, quantitatively speaking, be different for ice, hoar-frost and mixtures.

3.2. The height of suspension of OH line conductors is always greater than the height of weather station conductors. A greater wind speed, accompanied by an increased height above the ground, tends to increase droplet velocity and the rate of increase of the ice load (eq.4).

In a number of cases there is also an increase in the humidity content as the height above the ground level is increased. All this tends to increase the growth rate of the ice load with height.

An increase in the weight of ice is accompanied by an increase in its dimension, thus affecting the value of $2\lambda_{dr}$. As a result, the ice weight $P_h$ at different heights is not closely related to conductor diameter.

The mathematical treatment of the data of observations on rigidly fixed conductor lengths has resulted in the following equations of regression:

$$P'_h=0.046h+(0.7+0.84h)P_2 \qquad (5)$$

for $P_2 = 0 \div 2.94$ N

$h = 8 \div 25$ m

$$P''_h=(-0.9+0.243h)+(0.95+0.212h)P_2 \qquad (6)$$

for $P_2 = 2.9 \div 9.8$ N

$h = 8 \div 25$ m,

Where h - conductor height, m

$P_2$ - ice weight at 2 m above the ground, N.

Owing to the variation of conductor height along the span, the ice weight on a 1 m conductor section and ice dimensions increase with progression from the middle of a span to towers. Variation in the ice weight along the span causes the shape of curve for conductor sag to deviate from the catenary. Practically this leads to a decrease in sag as compared with calculated one on assumption of uniform ice density on the conductor, especially with severe icing when conductor clearances are greatly decreased.

3.3. One-sided build-up of the ice on a conductor produces a moment.

3.3.1. On single-conductor OH lines under the influence of a moment M =pl conductor twisting occurs. As a result, the ice shape varies along the span. In the middle of the span, even with the small ice weight, the shape of ice closely resembles a round cylinder in whose axis the conductor is situated. In the vicinity of towers ice builds up mainly on one side, its shape closely resembling an elliptical cylinder, the conductor being located in one of the foci of its cross section.

3.3.2. On the lines with bundled conductors and with spacers permitting conductor twisting (hinged joint spacers), the ice shape differs only slightly from that in the case of single conductors.

With rigid spacers the ice shape along the entire conductor length closely resembles an elliptical cylinder, the conductor being located in one of the foci of its cross section.

Asymmetrical location of ice with respect to the axis of the bundled phase produces a moment twisting the phase during ice build-up. The angle of twisting is influenced by spacer design (rigid or hinged joint type), number of bundled conductors N, phase configuration, distance from the clamp and the weight of ice on conductors.

The ice weight being equal, with hinged joint spacers the twisting angle is smaller as compared to that with rigid spacers ( the studies were carried out for the symmetrical triangle $N = 3$ and for $N = 2$ with horizontal conductor arrangement). With rigid spacers and $N = 2$ (horizontal arrangement) the twisting angle drastically increases at ice weights of 10 - 15 N/m.

Special studies of twisting angles in the conditions of ice build-up are desirable for the bundles with $N > 3$.

3.4. Horizontal travel of droplets tends to screen one of the bundled conductors and , as a result, causes a decrease in the ice weight on the screened conductor.

Measurements showd that screening of one conductor located in a horizontal plane, reduces the ice weight on it by 10 and 25%, respectively in the middle of the span and near the towers.

3.5. The electric field of the conductor turns neutral drops of water into dipoles. The interaction between the electric field and a dipole is defined by the following expression:

$$F_e = \frac{1}{3} r_{dr}^{3} \, \mathrm{grad} \bar{E}^{2} \qquad (7)$$

where $\bar{E}$ is electric field strength of the conductor at a given point.

Laboratory and field investigations have shown that with field gradients at the conductor surface of $E = 15$ to 25 $\mathrm{kV}_{max}$/cm the effect of the force $F_e$ is considerable with small droplets ($r_{dr} = 2.5 \mu m$), so that the capture zone $2\lambda_{e.dr}$ for such droplets increases and, as a result, the weight of ice and its dimensions increase, too.

The increased capture of small droplets by the electric field, compared with large drops, is manifested in a 20 to 40% reduction of the ice deposit density and a corresponding increase of the dimension.

3.6. For practical purposes it is of relevance to determine the resultant relationship of the OH line conductor ice load to the weather-station conductor ice load.

A great number of simultaneous ice-load measurements on conductors of experimental OH line spans (from 6 to 500 kV) and on nearby weather-station conductors have shown that the equivalent ice thicknesses (ice cylindrical in shape with a density of 0.9 g/cm$^3$) can be characterized, over a wide range of loads, by the relationship:

$$b_L = 1.05 + 1.325 \, b_{WS} \qquad (8)$$

where

$b_L$ is the equivalent ice thickness on OH line conductor, mm

$b_{WS}$ is the same for weather station conductor, mm.

Satisfactory correlation between $b_L$ and $b_{WS}$ for OH lines of various designs ( 6, 35 and 500 kV ) confirms the validity of the method of calculation based upon the same equivalent ice thickness for lines of different configurations.

The introduction of correction factors for possible weather-station conductor screening and for the effect of line design permits reasonably accurate evaluation of the ice load on OH line conductors on the basis of weather station data, provided the line and the weather station are in identical condition to the ice-bearing flow.

4. The absolute altitude of the site and its exposure to the ice-bearing flow have an appreciable influence on the magnitude of ice loads. On the summits of hills, on windward slopes, and in valleys open to the air flow the wind velocity increases, stepping up the growth rate of the ice load. When there is a rise in the absolute altitude, there is a certain increase in the moisture content of the air flow, which also increases the ice-load growth rate.

The loads measured on a WS conductor are therefore characteristic of OH lines located not only at identical absolute site altitudes but also similarly exposed to the ice-bearing flow.

If the weather station network is sufficiently dense, it is possible to find a correlation between ice loads (b) and the altitude of weather stations (H) situated in analogous terrain conditions. From the lines of regression $b = f(H)$ the loads under macro-terrain conditions characteristic of the transmission line route can be determined.

5. The standard ice thickness $b_d$ corresponding to a $T_d$ years return period is determined by a statistical probability method on the basis of the maximum annual loads observed over a period of ten years or more.

As the distribution function we take the second limiting distribution:

$$F(b) = e^{-\left(\frac{b}{\beta}\right)^{-\gamma}} \qquad (9)$$

where b is the equivalent ice thickness;

F(b) is the probability of a given ice thickness not being exceeded;

$\beta, \gamma$ are distribution parameters.

Provided the density of the meteorological stations measuring icing is sufficient, maps of standard ice loads can be produced.

In this case the maximum loads measured on a weather station conductor during a year will be corrected for screening and the influence of OH line design. The data obtained undergo statistical processing and the relationship $b = f\ F(b)$ is constructed, together with its lines of regression on probability paper for the second limiting distribution. From the graf for F(b) we can determine b for the standard return period of $T_d$ years.

$$T_d = \frac{1}{1 - F_d(b_d)} \qquad (10)$$

The next step is to construct the relationship of the ice thickness b for $F_d(b)$ to the absolute site elevation H for meteorological stations iv a given region, which are located on an identical type and sub-type of terrain, followed by the lines of regression.

The climatic-zone boundaries are drawn on a hypsometric map (scale 1 : 500000), following the isohypses, in accordance with the relationship $b = f(H)$, for a given terrain sub-type.

6. The most important point is the choice of the design return period for a given ice thickness (in other words $F_d(b)$7, and the value of ice thickness intervals $\Delta b_d$.

The following factors should be taken into account: 1) reliability of the data for maximum annual ice thickness; 2) probability of realisation of the design load during line operation; 3) operational reliability, economical and social aspects.

6.1. Wind velocity, ice size and weight at a weather station (WS), effect of WS conductor screening, effect of line design and terrain on ice thickness - all these factors are measured with an error, which can be estimated only approximately. It is due to these errors that the measurements of ice weight on OH line conductors often don't agree with the data obtained at WS. In these cases we have to rely upon the results of line measurements, and to make a correction of WS statistical series by the value $\Delta b = b_{L'} - b_d$, where $b_{L'}$ is equivalent ice thickness calculated on the basis of ice weight measurements on OH line, distribution parameter $\gamma$ being unchanged. The correlation between $b_{L'}$ and $b_d$ should be found when possible.

6.2. To improve the reliability of ice load predictions, the maximal values in the load interval are taken as design values. Then the adopted standard return period $T_d$ for $b_d$ would correspond presisely only to a part of lines and weather stations.

6.2.1. Application of ice thickness intervals for design ice loads with the limited value of $F_d(b_d)$, reduces the range of possible $T_d$ for the weather stations in the given load interval.

Figure 2 shows an example of the statistical treatment of the data obtained from 375 weather stations, located throughout the USSR territiry. The distribution function for the design load return periods is given for $b_d = 15$ mm with interval $\Delta b_d = 5$mm (for $b_d = 15$mm $F_d(b_d) = 0.96$). As can be seen from Fig. 2, in this case there is no OH lines (or WS) with $T_d$ less than 25 years. Only for 14% of lines (53 WS) in the given load interval the value of $b_d$ corresponds to 25 year return period, whereas for all remaining lines (WS) this period is more than 25 years. For 25% of lines (94 WS) $T_d > 49$ years, and for 7.7% of lines $T_d > 100$ years (the curve for $T_d > 50$ years is not shown on Fig. 2). Therefore, in this case (with $\Delta b = 5$ mm) the probability $p_{b_d}$ of realisation of ice load corresponding to $b_d = 15$ mm throughout the USSR territory is equal to 0.14.

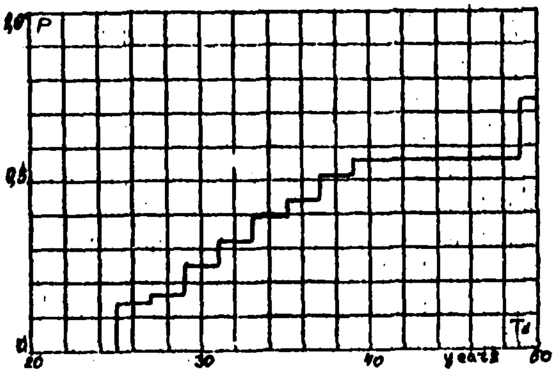

Fig.2. Distribution function for the design return periods of ice load. $T_{d\,min} = 25$ years.

Reducing the interval of ice thickness ($\Delta b = 4$ mm) results in decreasing the number of WS with $T_d > 49$ years to 4% (10 WS). Then the probability of realisation of $b_d = 15$ mm would increase to $p_{b_d} = 0.2$, though the number of WS with $b_d = 15$ mm and $F(b_d) = F_d(b_d)$ would remain unchanged.

6.2.2. In the regions where $b_d$ corresponds to the standard return period (according to WS data) the probability of combinations of $b_d$ and $F_d(b_d)$ is less than 1. It can be explained by the fact that the combination of $b_d$ and $F_d(b_d)$ in a given region corresponds to a certain orientation of ice-carrying flow. Only for the lines which are perpendicular to the dangerous ice-carrying flow, there is a relation between $b_d$ and $F_d(b_d)$. If the angle $\varphi$ between the line and ice-carrying flow is less than 90°, the ice coating on conductors will have smaller sizes and weight, and wind pressure on conductors will decrease. Therefore, in this case $F(b_d) > F_d(b_d)$ for a given value of $b_d$.

The results of the field measurements of ice load on test lines have shown that the relation between ice weight and angle $\varphi$ can be approximated by the following equation:

$$P = P_{90}\left[0.1 + 0.9\cos^3(90 - \varphi)\right] \qquad (11)$$

As can be seen from (11) when $\varphi = \pm 45°$ ice load on conductors becomes 30% less comparing with $\varphi = 90°$.

In a sufficiently large region all the values of $\varphi$ are equally probable. For the purpose of rough estimate in the range of $\varphi = 90° \pm 30°$ it may be assumed that $b_{d\varphi} \approx b_d$. Then, within a large region only 30% of lines will have ice load corresponding to equivalent thickness $b_d$ with the return period $T_d$, i.e. $F(b_d) = F_d(b_d)$, and for all other lines $F(b_d) > F_d(b_d)$. Therfore, probability of realisation of $b_d$ will be $p_\varphi \leq 0.3$, due to variations of line direction.

6.3. When estimating the value of $F_d(b_d)$ it is necessary to compare construction capital costs and the costs of failures.

6.4. When choosing the design load return period $T_d$ and the corresponding $F_d(b_d)$, one should consider the probability of occurence of the loads $b_m > b_d$ with $T_m > T_d$.

It is known that the probability of exceeding the design load, related to 1 year, is equal to $1 - F_d(b_d)$. However, the value of the excess is not known.

In theory, $b_m$ could correspond to very long return periods (even more than 1000 years). In practice, meteorological phenomena with the return periods above 100 years, have not been observed. Therefore, the value of $1 - F(b_d) = 0.99$ ($T_d = 100$ years) should be considered the possible upper limit.

However, small overloads ($\Delta b_{md} \leq 3$ mm) should be accounted for when choosing strength and deformation safety factors.

The probability of practically real dangerous overloads in the regions with $F_1(b_d) = F_d(b_d)$ can be estimated by the equation:

$$p_{1m_d} = 0.99 - F_1(b_d + 3) \qquad (12)$$

The probability of realisation of dangerous loads on OH lines, oriented with equal probability in different directions will be $p_\varphi \, p_{1m_d} = 0.3 \, p_{1m_d}$. In a sufficiently large area, consisting of n regions each with its $F_n(b_d) \geqslant F_d(b_d)$, probability of realisation of $F_{d1}(b_d)$ is equal to $p_{1b_d}$, therefore annual probability of occurence of dangerous line loads in this area, where $F_1(b_d) = F_d(b_d)$ will be:

$$p_1 = 1 - (1 - 0.3p_{1m_d})^{np_{1b_d}} \qquad (13)$$

For some n-th region within this large area probability of dangerous loads occurence, $p_{nm_d}$, is defined by equation similar to (12). Annual probability $p_n$ of occurence of dangerous loads in the n-th region, where $F(b_d) > F_d(b_d)$ will be determined by equation similar to (13). It is clear, that $p_n < p_1$. For the purpose of an approximate analysis it is more convenient to consider the value of $p_1$.

It follows from (13) that the more is $p_{b_d}$ (probability of realization ) the more will be p ( probability of occurence ). As it was shown above, $p_{bd}$ grows with the reduced design load intervals.

From the relationship $p = f(\Delta b_d)$, obtained from eq.(13) for $T_d = 25$ years and $n = 30$ (there is usually about this number of weather stations within the area of a large electric system) it can be seen that with $\Delta b_d > 5$ mm variations of p are relatively small. For example, the increase of $\Delta b_d$ from 5 mm to 10 mm corresponds to the decrease of p from 0.016 to 0.008.

Thus the value of $\Delta b_d \approx 5$ mm is close to optimum from the point of view of its influence on p. This value may be recommended as a standard interval for the design ice loads. It should be noted, that with $\Delta b_d = 1$ mm (i.e. practically without intervals), to obtain $p = 0.016$ ( as with $T_d = 25$ years and $\Delta b_d = 5$ mm ) we should take $T_d = 75 - 80$ years.

What is the influence of $T_d$ on p ? From the relation $p = f(T_d)$ according to (13), with $n = 30$, $p_{bd} = 0.14$ ($\Delta b_d = 5$). It can be seen that variations of p are very small when $T_d > 25$ years. When $T_d$ decreases from 25 years to 20 years the value of p is increased by $\Delta p = 0.026 - 0.016 = 0.01$ To obtain the corresponding decrease in the p value, $T_d$ should be increased from 25 to 50 years.

## Conclusions

1. In the USSR there is a wide network of weather stations at which regular measurements of ice weight are carried out on a 5 mm diameter conductor arranged at 2 metres above the ground.

2. As a result of investigations a correlation has been found between ice thickness on weather station conductors and line conductors. The technique has been developed for spatial interpolation of ice loads, with account for ice weight variations due to terrain altitude.

3. Ice load is estimated using the statistics of extreme values, distribution function being the second limiting distribution.

4. In the process of ice load mapping it should be taken into account that the value of design load intervals and standard return period are interrelated, and they should be estimated basing upon the probability of their realisation in operation and upon the reliability of OH line.

# SESSION 4: ICELOAD MEASUREMENTS AND DESIGN PRACTICES

AD P001694

# ICE ACCUMULATION ON TALL RADIO AND TV TOWERS IN FINLAND

Y. Jaakkola	Finnish Broadcasting Co. Ltd., Mast & Antenna Dept.,
J. Laiho	Helsinki, Finland
M. Vuorenvirta

## ABSTRACT

The Gulf Stream helps to keep the climate fairly mild in Finland, except for a few cold winter months. During the autumn period, from September to December, the average 24-hour temperature remains around 0°C. This, together with the humid south-western air current, creates favorable circumstances for icing.

Finland's topography is very flat. To get a good coverage, about 30 radio and TV towers have been built. They are normally guyed lattice towers, the heigths varying between 210 and 325 meters.

It was supposed that the towers will not accumulate much ice. However, a 75-meter high tower collapsed in 1962, and another one, 212 meters high, in 1970. The reason was very heavy icing and oscillations caused by it. Based on the statement of the Board of Inquiry, a special working group for guyed towers was founded in 1972. This group has also made icing observations from various towers for the past 12 years. Recommendations for the design and analyzing of towers were completed in 1980. No recommendation can, however, eliminate atmospheric icing of structures.

Especially asymmetrical ice loads of guy ropes cause great static deflections and overloading of the structures. The profilization of the guy ropes and also of the tower body, caused by ice, often leads to oscillations.

Designed according to the new instructions, the newest towers in Finland are about three times heavier than the old ones, bearing now the static ice loads. Deicing has been tried by heating. On a large scale this method is too expensive, and structurally easily damaged. Protection of the structures has been tried with fibre glass radomes and cylinders; this has again caused severe oscillations. At the end of 1981, a simple mechanical ice removing method of the guy ropes has been structurally tested.

Oscillation control instruments have been installed on several towers. The first ice load control instrumentation will be installed on a tower which is built this year and which is known to accumulate heavy ice loads.

## INTRODUCTION

Systematic observation regarding the icing of radio and TV towers has been carried out in Finland for the past ten years. Observation results have been collected from about 40 different districts, from towers the heights of which vary from 60 to 320 meters. The geographical location of the towers, as well as the altitudes of their locations, cover very well the topography of entire Finland. The observation has been empiric estimation of the quantity and quality of ice. Because most of the points of observation have been at distant automatic stations, the observation has not been completely continuous. Together with other studies carried out during the past ten years it has, however, helped to create a very good idea of the ice loads which have to be taken into account when building high towers. At the same time it has been possible to develop new calculation methods for towers, and to experiment with deicing methods, and to improve the control of the loadings by installing special control systems on towers.

## CLIMATE AND TOPOGRAPHY OF FINLAND

Finland is a northern country in Europe, located as far North as Alaska, between the 60th and 70th latitudes. The climate in Finland is not, however, arctic, but belongs to the temperate zone. The mildness of the climate is mainly due to the Gulf Stream, directed toward the North off the coast of Norway.

Finland´s area is approximately 340000 km$^2$, and the topography is rather flat, the highest hills rising about 1300 meters above the sea level. The terrain is rising from the coast toward the North, and additionally there are some sporadic ridge areas and areas of upland in southern and central Finland. In northern Finland there are some hill areas which are clearly distinguishable from the surrounding terrain. See the map, figure 1. The locations of some broadcasting stations have also been marked on the map. The corresponding altitudes and the heights of the towers are presented in appendix 1.

During the winter months there is frequent snowfall in the entire country, and additionally freezing fog in certain areas. In southern and central Finland long cold periods are not common, but the temperature often rises above 0$^o$C, whereas in northern and eastern Finland the winter is rather cold: from September to December the average 24-hour temperature remains around 0$^o$C, and from January to March clearly below 0$^o$C.

In the early winter the prevailing winds blow from the South-West, and that is when the climate is rather humid and the circumstances for icing are very favorable. The worst periods as for the development of rime is the period from October to March, when the wind blows from the South/West sector 40-50% of the time. /1/

## FM AND TV NETWORKS IN FINLAND

Due to the evenness of the country and some radiotechnical factors, the Finnish Broadcasting Company has in its time decided upon a network which consists of about 30 towers, the heights varying between 200 and 300 meters. When the building began in the late 50´s, there was not very much knowledge about ice loads, nor was it presumed that big simultaneous wind and ice loads could occur. This idea had obviously been adopted during the AM-radio period in the 40´s and 50´s, when the towers were not higher than 160 meters and were located in rather low places. There was hardly any knowledge about the oscillation problems caused by ice accreted on the towers and on their guy ropes. The general recommendations for the design of steel structures, and the loading standard of structures, which were used as guidelines in the design of towers, did not require that ice loads should be taken into account, nor did they mention anything of the wind conditions in hill areas.

## ICE ACCUMULATION ON TOWERS

According to observations, ice accretion in Finland is worst on the southern/south-western sides of towers, when the wind is blowing from these directions. The ice thus created is either glaze, clear ice, or rime. Most commonly, however, appears rime. The ice which has accumulated during the long freezingly cold period, or in northern Finland during the entire autumn-winter period, is usually a mixture of all ice types. The density of the ice has been measured to be 300-400 kg/m$^3$ on the shaft, and 400-600 kg/m$^3$ on the guy ropes. The greater density of the ice on guy ropes is considered to be due to its way of formation./2/ Softer ice with a smaller density does not stay fast on the rope, as the rope turns because of the weight of the ice, while the wind blows directly toward the edge of the ice.

In Finland the towers are without exception lattice constructions. Inside the tower there are stairs, a cable ladder, cables, and an elevator rail. During the long cold period the entire structure is easily covered by ice (app. 1). A short period of milder temperature does not remove the ice. Hard winds have not been observed to remove ice, either, by other methods than erosion. In three different areas, Yllästunturi, Pyhätunturi, and Koli (app. 1), the monthly ice accretion has been observed to follow the values given below:

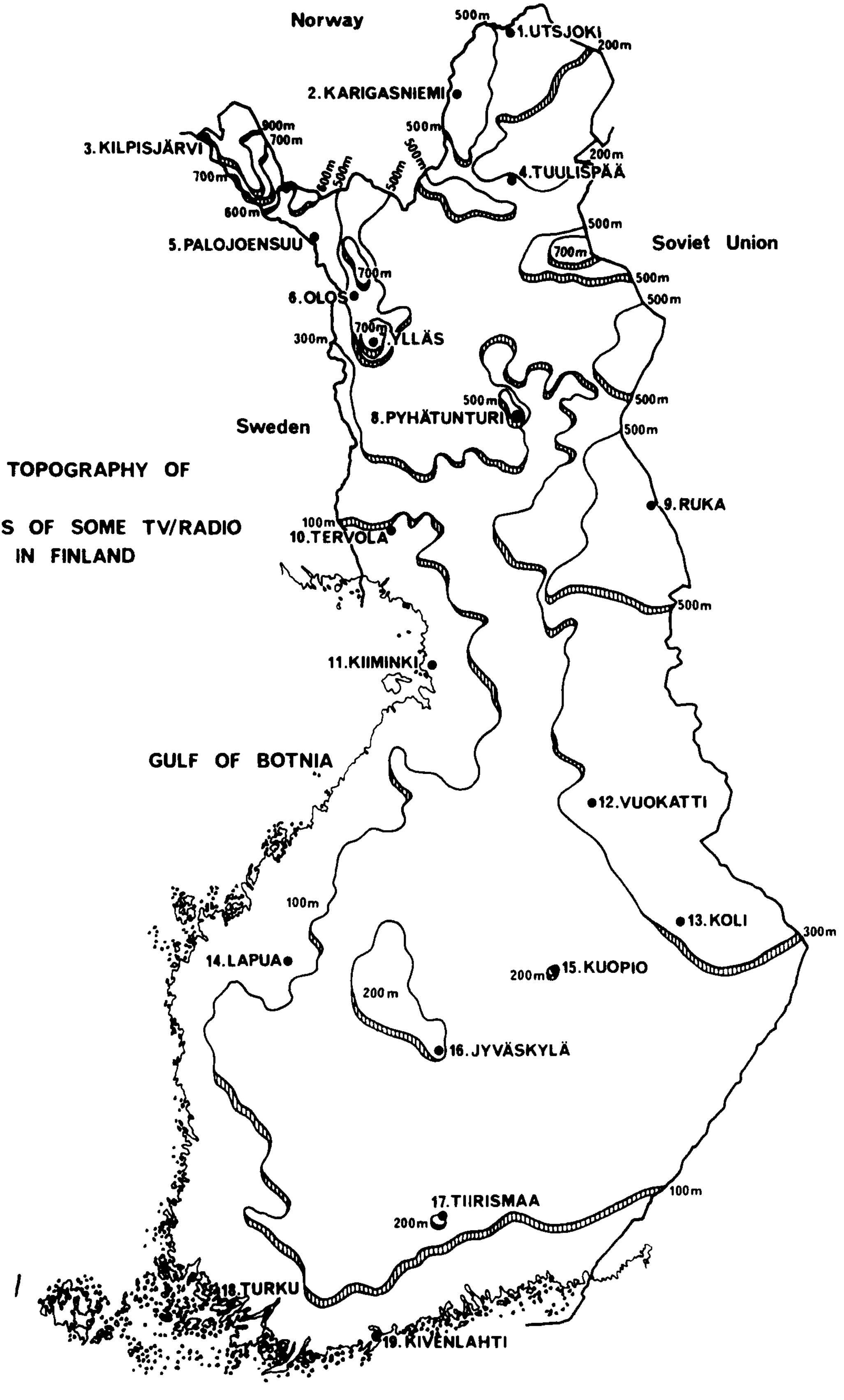

GENERAL TOPOGRAPHY OF FINLAND
LOCATIONS OF SOME TV/RADIO STATIONS IN FINLAND

Norway
500m
1.UTSJOKI
200m
2.KARIGASNIEMI
900m
700m
3.KILPISJÄRVI
700m
600m
600m
500m
500m
500m
500m
200m
4.TUULISPÄÄ
500m
Soviet Union
700m
5.PALOJOENSUU
700m
500m
500m
6.OLOS
700m
300m
7.YLLÄS
500m
8.PYHÄTUNTURI
500m
500m
Sweden
9.RUKA
100m
10.TERVOLA
500m
11.KIIMINKI
GULF OF BOTNIA
12.VUOKATTI
100m
13.KOLI
300m
14.LAPUA
200m
15.KUOPIO
200m
16.JYVÄSKYLÄ
17.TIIRISMAA
200m
100m
18.TURKU
19.KIVENLAHTI
GULF OF FINLAND

Fig. 1

| Area | Type of Terrain | Altit. | Monthly Accretion |
|---|---|---|---|
| Ylläst. | Open hill | 700 m | 500-1000 mm |
| Pyhät. | " " | 500 m | 100- 200 mm |
| Koli | Forest on hill | 300 m | 10- 20 mm |

The low value in the last area, Koli, is quite obviously due to the shielding effect of the forest in the measuring area. The tower of Koli, however, has been observed to freeze just as much as the tower of Pyhätunturi, for instance. The lower edge of a cloud is mostly 300 meters or below during a freezingly cold period. /3, 4/

## DAMAGES CAUSED BY ICE

During the beginning of the building of the FM/TV network, a 75-meter high tower collapsed in Pyhätunturi in 1962. The collapse was found out to be due to a heavy ice load. Serious attention had obviously not been paid to the accreted ice, as the tower was structurally "very light" compared to the towers of 200-300 meters of height, which were under construction at the same time and which were believed to bear such ice loads. A new, 320-meter high tower was built in place of the collapsed one. The new tower has been shortened twice afterwards (present height is 260 meters) because of ice loads.

In 1970 another tower, height 212 meters, collapsed in Yllästunturi. A Board of Inquiry was set up to study the reasons of this collapse. According to the statement /5/ given by the Board, the tower collapsed in mild wind after a long, freezingly cold period, due to the combined effect of an ice load and oscillation.

Based on the recommendation given by the Board, a special working group on tower branch was founded in Finland. The cooperative committee has prepared a Recommendation for guyed masts, which was published in 1980 /6/. The preliminary work of the recommendation has been done simultaneously with the corresponding international recommendation. The international recommendation was published in 1982 /7/.

## PROBLEMS CAUSED TO TOWERS BY ICE

Accreted, asymmetrical ice loads of long duration cause the following problems:

- static overloading of structures
- dynamic problems caused by the ice-profilized shaft and/or guy ropes, such as oscillation
- deterioration of the radiation characteristics of the antennas, or changes in the position of the antenna (also symmetrical ice)
- difficulties in service in wintertime

To illustrate the static effect of ice loads, figures 2-5 show the effect of a symmetrical and of an asymmetrical ice load on the tensions of the leg members of the tower and on the deflection curve of the tower, as well as the situation without ice, or when the ice has been removed from the guy ropes. The tower of Koli is used as a sample tower with real ice loads. The tower will be shortened in 1983. The tower was designed in the late 50´s, without taking into consideration the effect of ice loads. Nor has the difference in altitudes between the actual location of the tower and the surrounding terrain been taken into account.

## EXPERIMENTS IN DEICING

Because the formation of ice cannot be prevented at present without detrimental side effects, the design of tower structures has since 1975 strived for taking the local plausible ice loads into account. Consequentially, the weight of the tower structures has approximately doubled, and the structures have correspondingly become more expensive. The antenna structures have also been chosen mechanically strongly built, and very weatherproof. The trouble caused to the transmission characteristics of the antennas by ice or oscillations cannot, however, be removed by these methods.

Removing ice from guy ropes was successfully tried at the tower of Koli in the winter of 1981/82. A common concrete vibrator was used in the experiments; it was attached to the guy rope. The frequency fed to the rope was about 20-30 Hz, and the ice loosened already after a few minutes of vibration. The method seems worth developing, and it will be tested next winter after the icing of towers has taken place.

Deicing of the tower shaft and of the guy ropes has been tried by heating in 1974, by heating the parts in question with a heating cable, the heating powers being 50-120 W/m. In difficult circumstances the required heating power was calculated to be over 120 W/m, and

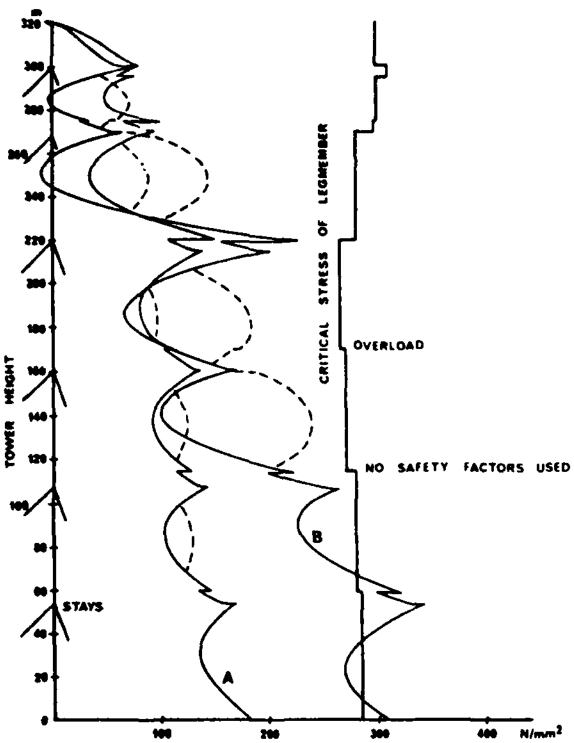

Fig.2 Legmember stresses
A:Compressionstress due to windload. Windpressure coeff. 1,0
B:Compressionstress due to symmetric iceload on the tower body. No iceload on the guys. Windpressure coeff. 0,7
(Dotted curves:Max stress has changed on other legmember.)

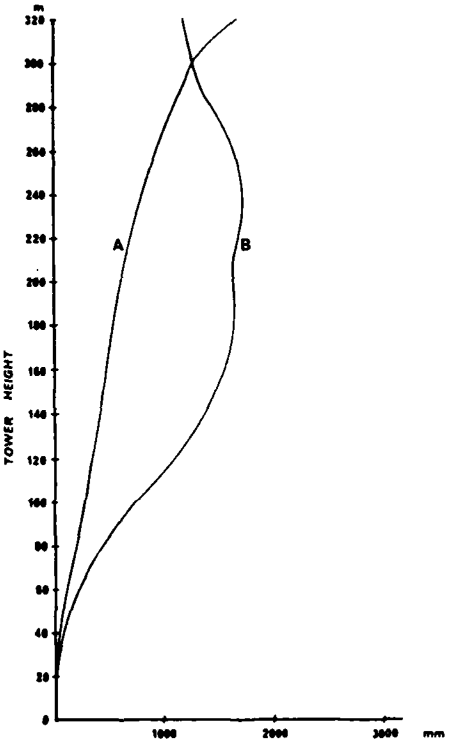

Fig.3 Tower deflection
A:Windload
B:Symmetric iceload on the tower body. No iceload on the guys.

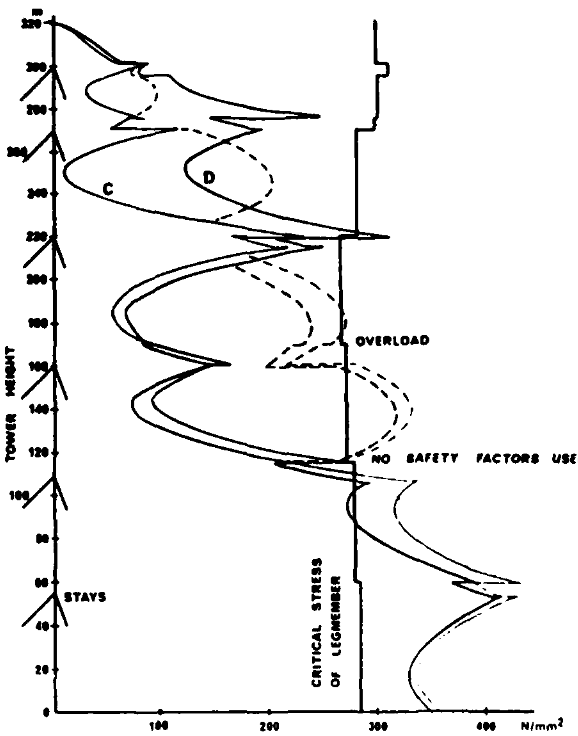

Fig.4 Legmember stresses
C:Compressionstress due to symmetric iceload on the tower body and guys. Windpressure coeff. 0,7
D:Compressionstress due to asymmetric iceload on the uppermost guys. No iceload on two leeward side guys. Symmetric iceload on the tower body. Windpressure coeff. 0,7
(Dotted curves as on fig.2)

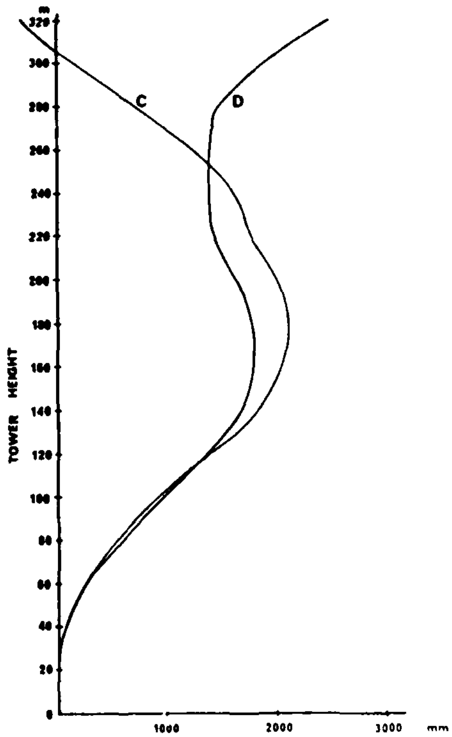

Fig.5 Tower deflection
C:Symmetric iceload on the tower body and guys.
D:Asymmetric iceload on the uppermost guys. Symmetric iceload on the tower body

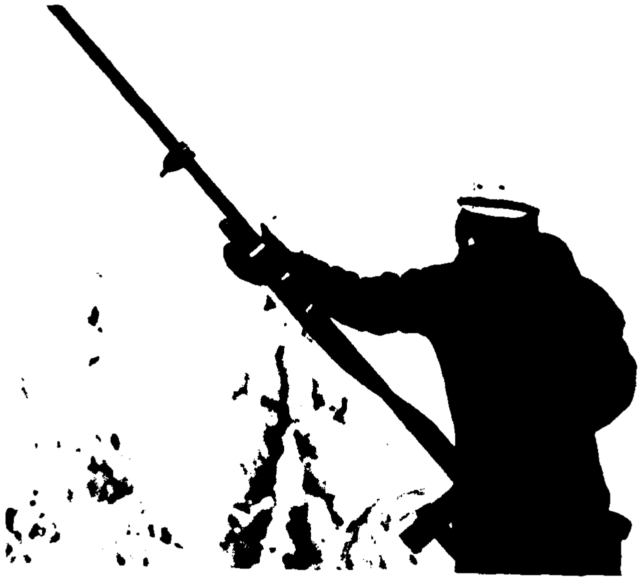

Fig. 6.

A concretevibrator
attached on the
guyrope.

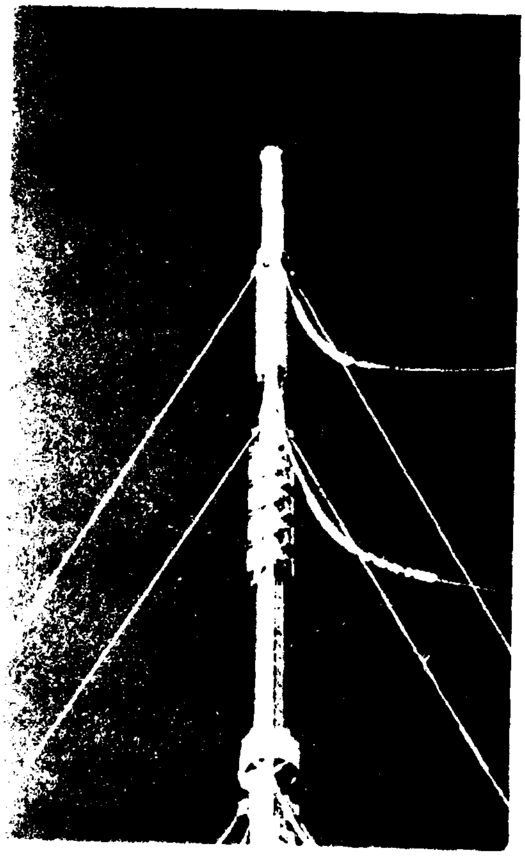

Fig. 7.

Ice on the guys before
removing it.

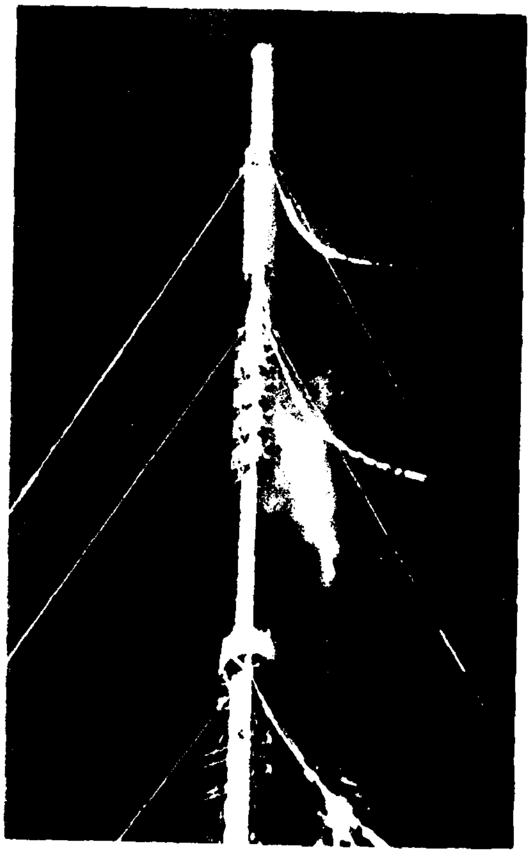

Fig. 8.

Ice removing using
the concretevibrator.

the time of deicing about 8 hours. The power required of the heating system for a 100-meter high tower would have been over 300 kW, which in a faraway area is unreasonable, compared with the other power requirements of the station. The system was not considered to be able even mechanically to endure the strains on the tower structure.

Experiments were made with cylinder structures in three places in all. The oscillation caused by the cylinders was the reason for dismounting these structures. Combined with effective damping systems, the use of cylinders can be considered in high towers.

## SUMMARY

The icing of towers causes both great mechanical and electrical difficulties for the radio and TV antenna equipment in Finland. To obtain real loading information, part of the problematic towers will be equipped with microprocessor controlled instruments to measure the loadings and to collect weather information. Calculation methods will also be tested by comparing the measuring results with theoretical values. Because the mere reinforcement of the structures eliminates only a part of the problems, also the development of *more effective deicing methods* is strived for.

References:

/1/ Climatological Tables in Finland, 1961-1975, by Reino Heino, The Finnish Meteorological Institute.

/2/ D. Kuroiwa, Icing and Snow Accretion on Electric Wires. U.S. Army Material Command Cold Regions & Engineering Laboratory, Research Report 129.

/3/ Kari Ahti, On the Factors Affecting Formation and Amount of Rime in Finland. The Meteorological Institute of the University of Helsinki, Pro Gradu Study, Jan. 20, 1978.

/4/ Heikki Miettinen, An Ice Load Research of Masts in Finland, Administration of Posts and Telegraphs, Radio Division, Sept. 18, 1973.

/5/ The Collapse of the Yllas Mast, The Statement of the Board of Inquiry and the Results of the Study.

/6/ Recommendation for the Design, Analysis, Manufacturing, Building, and Service of Masts, 1980. Cooperative Committee on Mast Branch in Finland, Oct. 21, 1982.

/7/ Recommendations for Guyed Masts. International Association for Shell and Spatial Structures, Working Group No. 4, 1981.

App. 1

## ICING STATISTICS OF SOME TV/RADIO TOWERS IN FINLAND

Worst cases between 1973 - 1981.
Ice quantities based on observations

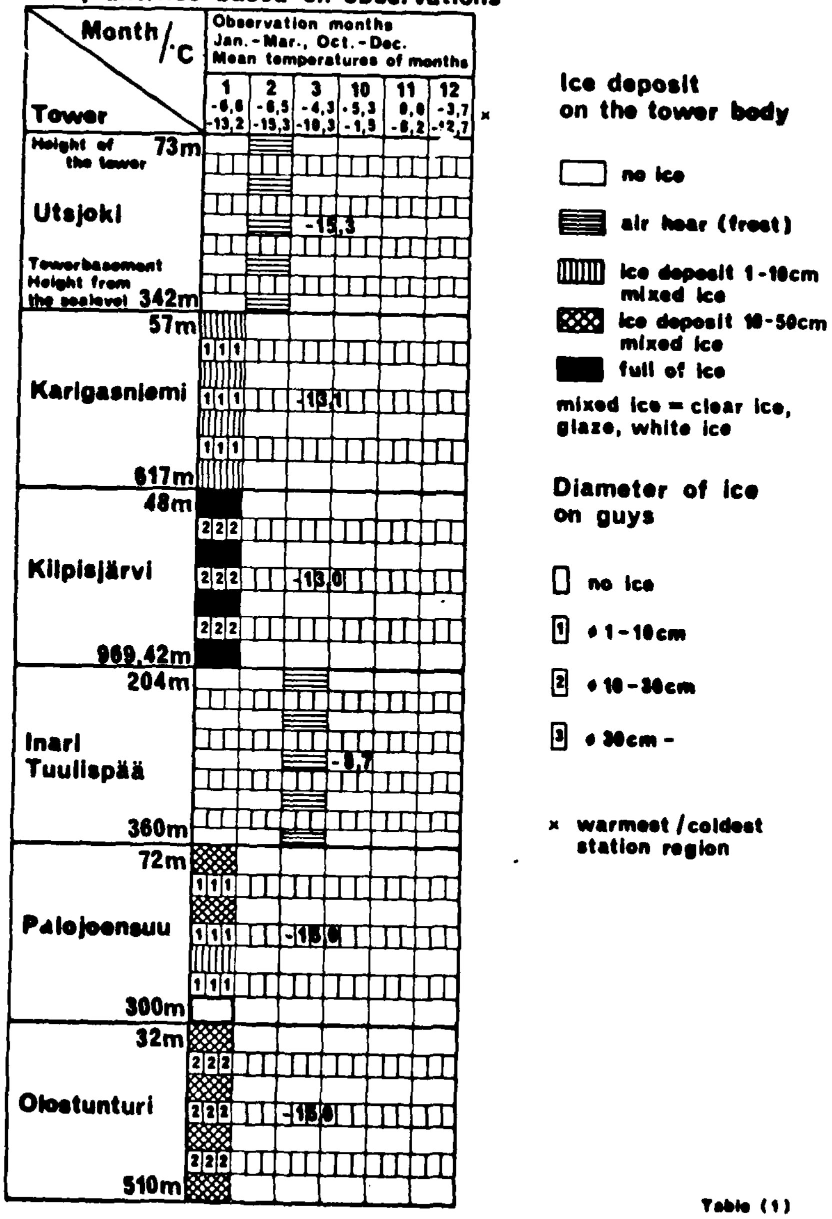

Table (1)

## ICING STATISTICS OF SOME TV/RADIO TOWERS IN FINLAND

**Worst cases between 1973 - 1981.**
**Ice quantities based on observations**

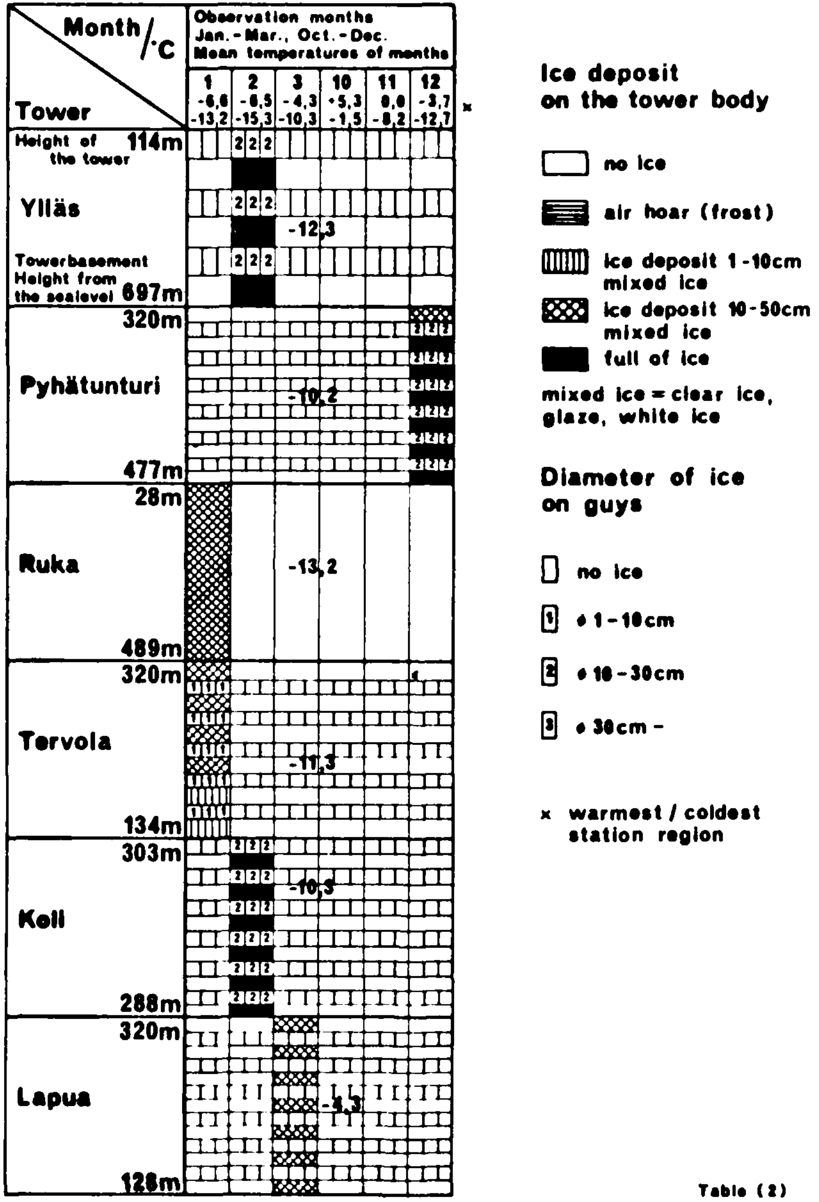

Table (2)

# ICING STATISTICS OF SOME TV/RADIO TOWERS IN FINLAND

**Worst cases between 1973 - 1981.**
**Ice quantities based on observations**

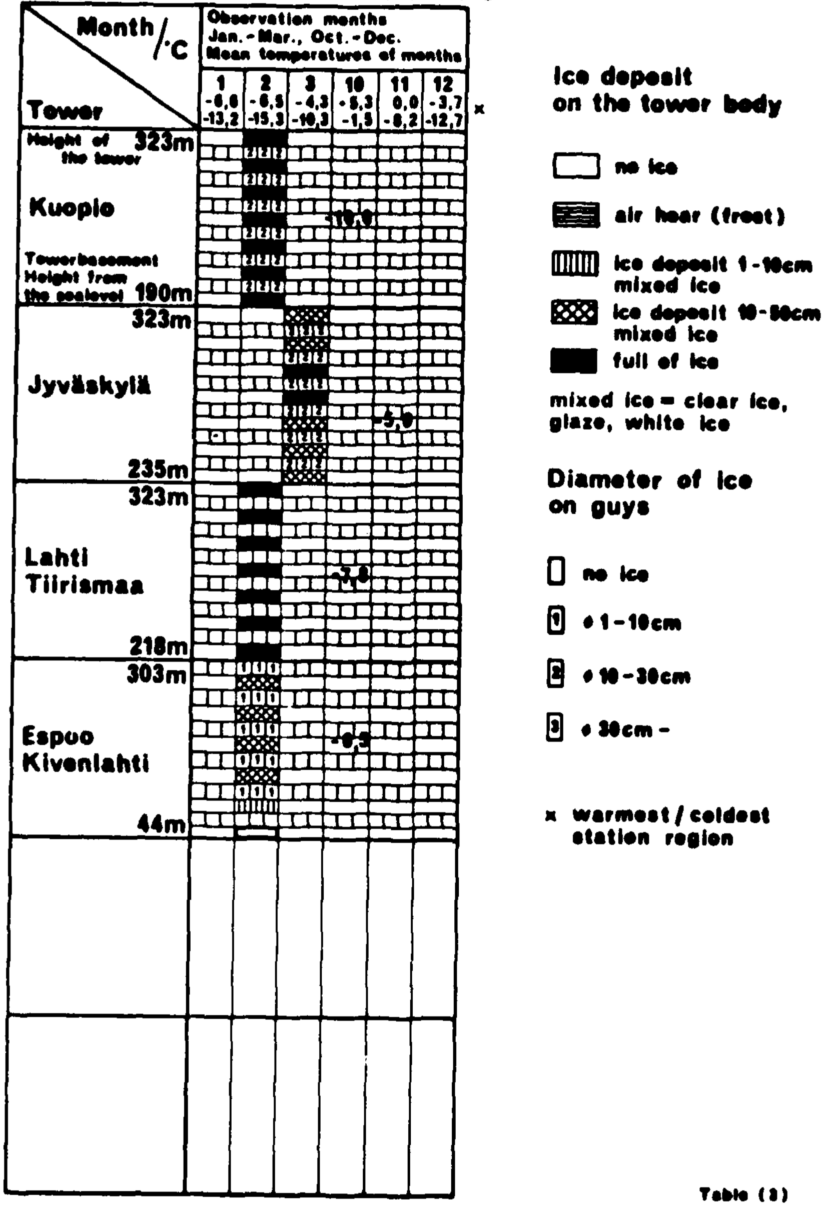

Table (3)

DISCUSSION

Patnaik: Did you increase your design loads after you had the Koli tower and the Ylläs(tunturi) tower failures?

Jaakkola: No we didn't, but this tower - I mean the Koli tower - is an old design, a very old Swedish design.

Patnaik: In the 60's?

Jaakkola: Late 50's, I think. You can see the tower - gets smaller and smaller upwards. Nowadays, when we are constructing our new towers, they are a 2.4 m from down to up - a constant width.

Patnaik: But what about the wind and ice load designs?

Jaakkola: They are the same, but we now make stronger towers because of this accident.

Martin: Do you put a coating on your cables? Or is it just a bare cable?

Jaakkola: Just a bare cable.

Martin: Do you think that using Dr. Jellinek's coating is better?

Jaakkola: That's what we thought also - and also on the cylinders which we have up there. It could be useful.

Fikke: You said the Ylläs tower was situated on a mountain and you got wind from south and west (J: Yes). I always thought that Norway [acted as shelter] for this kind of icing.

Jaakkola: There is the Gulf of Bothnia you saw on the map. I think Norway shelters from the west. Maybe [we get winds] - from southwest. Maybe not so far from the west.

Fikke: On your last picture, you had wind measurements (Yes). Are they automatically recorded? (J: Yes, they are.) How do you make sure that you really are recording the wind speed? I mean, if there's icing on the anemometer cups.

Jaakkola: Yes, that has been a problem, and we have tried to solve it by a heater which was above the measuring system.

Fikke: A heater above?

Jaakkola: Yes, so it heats all the time, and keeps [the ice] away.

Fikke: Has it worked OK?

Jaakkola: Not 100% of the time.

Patnaik: These concrete vibrators that you used to vibrate ice off the guy wires - were they suitable for long guys, like 1200-1400 feet?

Jaakkola: The guy wires which you saw in these pictures are over 300 meters - that's about 1000 feet.

Patnaik: And you only utilized this at the base of the tower? (J: Yes). When do these spots experience such a heavy ice load?

Jaakkola: One, there is hard ice. It doesn't come up at once. It's slow - when we experienced it, it was about 1-3 minutes. It doesn't come up suddenly.

Patnaik: In other words, you have to catch it during the thick ice period or something like that - you shake the ice. You said that when you got to the place it was towards the tail end of winter? After the season was over?

Jaakkola: Yes, it was spring.

Patnaik: So it's really not a permanent solution. You have to be available at the site.

Jaakkola: Yes, that's right, when there's heavy icing they have to be permanent [vibrators] or you have to get there.

Patnaik: Are you looking into some other methods now, or in the future?

Jaakkola: We haven't decided yet.

Smith: Do you plan on trying this vibrating technique on the shaft?

Jaakkola: We tried vibrating on the shaft of the mast, on the leg members.

Ackley: Are the ice formations that you see derived from in-cloud icing or wet snow? Do you have any idea of the source of the icing?

Jaakkola: A lot of rime and also

in-cloud. The Ylläs mast which collapsed was in a cloud about two weeks and you couldn't see it - you couldn't see what was happening.

Franklin: A two part question: the first part is, do you take into consideration in your design the dynamics of the tower, including if the cable snaps? The second part of the question is: do you think there's enough ice on a cable which if it falls onto another cable would snap that guy wire?

Jaakkola: In the design, there is one computer analysis which considers a system of one guy wire totally [failing] - any one of them.

Minsk: Was your vibrator oscillating at a fixed frequency?

Jaakkola: Yes, it was. We measured it quite near 106 Hz.

Minsk: You would get maximum energy transfer if the length of the line was cut to its natural frequency and the vibrator was placed at a particular node.

Jaakkola: We tried to figure out where was the best place to put it. There's some thought about the pulling force of the guy, and that affects the frequency.

Makkonen: I'd just like to make a general comment on icing in Finland related to these figures. You may have noticed that on some of the figures [slides] that there were no trees or no tree tops. [The climate] is not that severe [with regard to temperature] so we should have trees there. It is believed that the reason why there are no trees [...] is because they have been destroyed by the ice loads, and this of course makes a dendrochronology study [impossible].

AD P001695

# ICING AND COMBINED WIND AND ICE DESIGN LOADINGS FOR TRANSMISSION LINES IN REMOTE AREAS

M. C. Richmond Meteorology Research, Inc.
Altadena, California 91001

## ABSTRACT

The decision of what meteorological loadings should be used in the design of overhead transmission lines has been a major cause of loss of sleep for design engineers throughout many parts of the world. When the line is to be constructed through remote areas where no prior lines exist, the decision becomes even more agonizing. Codes and minimum loading requirements are of little help when the reliability of the line and the extreme difficulty of maintenance or repair may be the most important factors.

Unfortunately, some of these remote transmission line routes are through extensive areas of extreme loadings. In the balancing of excessive line costs against line reliability or risk of line failure the need for accurate, defendable loading predictions is obvious. How to develop these accurate, defendable predictions is the real problem.

This paper reviews some of the methodologies which have been used for developing design loadings in remote areas of eastern Canada and the northwestern United States. How loadings are expressed in terms of return period probabilities and the possible impact of the very long lines crossing two or more independent weather regimes are discussed. Finally, the importance of early involvement of meteorological evaluations and on-going observation programs are stressed.

## BACKGROUND

The decision of what meteorological loadings should be used in the design of overhead transmission lines has been a major cause of loss of sleep for design engineers throughout many parts of the world. When the line is to be constructed through remote areas where no prior lines exist, the decision becomes even more agonizing. Codes and minimum loading requirements are of little help when the reliability of the line and the extreme difficulty of maintenance or repair may be the most important factors.

Unfortunately, some of these remote transmission line routes are through extensive areas of extreme loadings. In the balancing of excessive line costs against line reliability or risk of line failure the need for accurate, defendable loading predictions is obvious. How to develop these accurate, defendable predictions is the real problem.

Meteorology Research, Inc. (MRI) has been actively engaged in furnishing meteorological loading predictions for the design of transmission lines since 1968. During the ensuing years we have learned a great deal about what affects the accretion of icing, how much and what type can be expected to form from a given storm, how the ice falls off the conductors, and how this information can be expressed in a manner useful to design engineers.

We know the elements that go into the formation of icing and the type of ice which will result from the various combinations of these elements. Several papers such as Tedesco, et al. [1] have described the theory and conditions of ice formation on structures and conductors. In general, the type of ice formed is determined by the particular combination of air temperature, wind speed, drop size, and liquid water content of the cloud or rainfall intensity. In the case of wet snow, snowfall rate, air temperature, and wind speed are the principal elements involved.

Unfortunately, we do not routinely know much about some of these elements such as drop size, liquid water content, and snowfall rate even in our populated areas. As a result, in many calculations some assumed values are used for these elements. Obviously, this must be done for remote areas as well. These assumptions may simply be mean values or they may be based on what impact the geographic location, elevation, and local topography is expected to have. Since these elements are likely to be assumed values wherever icing loads are being calculated, the real elements of concern for the remote areas are the frequency of occurrence of combinations of air temperature, wind speed, rainfall, snowfall, and cloud at the proposed line level and location and the magnitudes of these elements during each occurrence. If these elements were known, the frequency and magnitude of icing conditions could be calculated. Quite obviously, for remote areas the the long term climatological records from which these data could be extracted are not going to be available since no routine weather observations have been taken there. New observation sites could and should be established at representative locations in the remote area, but in most cases preliminary loading values for planning or feasibility purposes will be required long before sufficient new data can be collected. These loading values must be generated based on best estimates. Time permitting before final design, they will later be verified or refined as on-site data becomes available.

The "best estimate" values will in most cases be developed by extrapolating either predicted ice accumulations from a station or stations with available climatology or the various meteorological elements observed at that station during potential icing conditions. In either case, this extrapolation should be performed by an experienced meteorologist who understands the physical processes involved and the impact that elevation, latitude, terrain, moisture sources, distance, and typical storm patterns have on these elements.

In North America in recent years long transmission lines have been constructed or at least planned in several remote areas. In the United States locating large coal-fired power plants at the mine sites and transporting the power rather than the coal to population centers has resulted in the need for UHV transmission over new areas of mountains and deserts, far from any recorded climatological data. In Canada the increasing need for power has resulted in tapping the vast potential for hydroelectric power in the unpopulated far north and transporting that power over great distances to the population centers along the southern fringes of the country. While structural icing is not a significant concern in the desert regions of southwestern United States, it is a major concern for the areas where mountain ranges must be crossed. In the northwestern United States, where major lines have been constructed in the Rocky Mountains of Montana, Wyoming and Idaho, structural icing loads have been critical factors in the designs. The line routes through the mountainous terrain rarely pass near any established meteorological station. In northern Quebec and Labrador, in most cases, the proposed routes were far from any previous lines or recorded climatological data. In the few cases where they passed within a few miles of existing stations, the exposures and elevations were nearly always different from the stations.

New meteorological measurement sites have been established in critical areas along the remote stretches of each of these major line routes during the planning phase of the routes; however, in each case preliminary loading values had to be estimated early in the project, even before locations for the new meteorological sites were chosen.

## CASE HISTORY

The proposed transmission line connecting a hydro-electric generating site on the Churchill River in northwestern Labrador with the population centers in eastern Newfoundland is a classical example of a very long line route traversing unpopulated sections of a region known to experience some of the most severe wind and icing conditions in North America. The proposed route was over 900 kilometers long with only the eastern 300 kilometers of Newfoundland being in an area with climatological records. As might be expected, there were also some existing transmission lines in that area. During the previous fifteen years several extensive and costly glaze storms had damaged those transmission lines and there was general agreement that the area experienced the greatest accumulation of glaze icing reported in Canada.

The feasibility study for this route was initiated in late summer of 1973 and Meteorology Research, Inc. was commissioned to conduct a meteorological evaluation of the proposed routes. The initial three-month study consisted of three phases: a field survey; a climatological study; and, the analysis of data and application to route segments.

The field survey consisted of an on-site route familiarization and information gathering visit to Newfoundland and Labrador. This included a three-day helicopter trip along the entire length of the proposed route in company with engineers from both the utility and the engineering company responsible for the preliminary design. During this trip, the terrain and exposure of possible routes were studied and evaluated. Where trees existed, evidence of wind or ice storm damage was looked for, as well as flagging due to persistent strong winds from one direction. Obvious problem areas from a meteorological viewpoint were discussed with the engineers during the trip and, where possible, these areas were avoided in the line route which resulted from that trip. Also included in the field survey phase of the study were personal interviews with both professional meteorologists in the area and with engineers and maintenance personnel who lived and worked in Newfoundland and were familiar with the damaging storms which had occurred there in recent years. Detailed damage reports were acquired for several storms and meteorological data not available through the Atmospheric Environmental Service (AES) were located and copied.

The climatology study phase consisted of a review of all available published materials for the region as well as a large volume of summarized data prepared by the AES. Standard climatological summaries of hourly observations do not present the data in forms useable for ice accretion prediction. Special summaries which allowed identification of potential periods of glaze ice or wet snow accretion at the surface, and rime ice accretion at the surface and selected levels above the surface, as well as computation of probable accretion amounts were acquired from the AES. Summaries were supplied for twelve stations in Newfoundland, Labrador, and Quebec. Few of these stations were close enough to be considered representative of the proposed route; however, they did define somewhat the range of expected icing and the apparent effects of local terrain, elevation, latitude and distance from open water.

In the analysis and application phase, accretion amounts were calculated for each probable icing case at each station and the maximum accretions of each type, for each year of record, were used to develop 25-, 50-, and 75-year return period values using extreme probability statistics. The proposed route was divided into 23 various sized segments based on elevation and exposure and loading values were assigned to each segment based on extrapolation from the station or stations most representative of that segment. The extrapolation was accomplished as objectively as possible; however, the effect of many of the variables involved was not always quantifiable. Such extrapolation is always impacted by differences in elevation, sheltering by terrain or forest cover, terrain roughness, distances from open water and possible funneling, channeling, or streaming of local winds. Evaluation of these impacts becomes a subjective forecast based on the experience of the meteorologist.

Of extreme importance on this route was the effect of combined wind and icing loads, the effect on towers and conductors resulting from the combined loadings of the weight of the ice plus the pressure of the wind on the increased surface area. In 1973 prediction of these combined loadings was a controversial subject and it still is today. The accretion rate is a function of wind speed. The faster the wind the more rapidly ice will build up. To determine the maximum combination, it was necessary to know when during the storm the strongest wind occurred and how much ice had accumulated at that time. If the strongest wind occurred early in the storm, the greatest combined effect may have occurred later with a lesser wind speed and a greater surface area and weight of ice. Superimposed on this was the effect of wind direction both on accretion rate and transverse and longitudinal wind loadings. Going beyond this, we had the problem of how long the ice could be expected to stay on the conductors. The longer the ice stayed on, the greater the vulnerability to high winds not associated with the storm which caused the ice.

A review of both the glaze and rime producing storm periods at the reporting stations revealed no pattern to the time within the storm period that the maximum wind occurred. The peak wind time appeared to have occurred randomly throughout the icing period and up to at least six hours subsequent to the termination of icing conditions. Because of the manner in which the case histories were extracted from the climatological records, no more than six hours of records past the icing termination point were available in most cases. How long the ice might stay on the conductors varied with each storm. In some cases, the temperature rose immediately and the melting and cracking process started. At the other extreme, a prolonged cold period could result in the ice remaining for several days or in some locations perhaps weeks.

The possibility that ice might stay on the conductors for several days resulted in the possibility that the maximum wind speeds experienced by the ice loaded lines occurred with a subsequent storm system and the winds and ice loading then become independent variables. The maximum wind speeds throughout the area occurred in the winter months. Considering the possibility that those maximum winds might have occurred with ice on the conductors we simply used the combined probabilities to develop the combined wind and ice values in that preliminary study.

The following summer a study was conducted to determine the effect of computing the combined loadings using only winds which had occurred during or within six hours following icing episodes. The resulting combined loadings were somewhat lower for sustained winds with the loadings for gusts being approximately equal to the original predictions.

In the fall of 1974 four remote meteorological measurement sites were established at potential heavy loading points along the route. One site was located in Labrador approximately 42 km north of the Strait of Belle Isle crossing point, at an elevation of 545 meters. One site was on the west side of the Great Northern Peninsula of Newfoundland at an elevation of 455 meters. One was located on the ridge near the high point of the proposed route at 606 meters. This site was on the west coast of Newfoundland near the base of the Great Northern Peninsula. The fourth site was on the top of a hill in northern Newfoundland at an elevation of 455 meters.

Instrumentation was the same at each of the sites consisting of two 10-meter towers 16.5 meters apart, spanned by a conductor 3.4 cm in diameter. An ice rate meter (IRM) which measured increased tension due to ice loading was connected in series with the conductor. At the top of each tower was a Mechanical Weather Station (MWS) that recorded wind direction, wind run, temperature, and relative humidity. The four sites were operated during the winter of 1974-1975 and deactivated in the summer of 1975. The purpose of this measurement program was to validate and refine the loading values predicted in the original study.

Data collected at the sites were correlated with those recorded at the standard weather stations and some changes in the extrapolation factors resulted. No revisions to the ice loading estimates resulted from the new data; however, wind speed estimates at the ridge level on the Great Northern Peninsula were increased by forty percent. Fortunately by that time the proposed route had been moved to a somewhat less exposed crossing of the ridge.

The number of hours of freezing precipitation was a little below normal at the standard reporting stations during the 1974-1975 measurement period. No significant amount of icing was measured at the hill site in northern Newfoundland during the period. Several minor icing accumulations were recorded at the site on the northwest side of the Great Northern Peninsula and on one occasion approximately 63.5 kilos of ice (4 kg/m) were recorded. This occurred between site visits and was not observed visually. Weather conditions indicated that it would have been rime ice. At the ridge site and the Labrador site very severe conditions were quite frequent.

At the ridge site there were 12 periods when ice accumulations exceeded 9 kilos per meter with a maximum loading near 22 kilos per meter occurring at the end of a seven-day icing period. Wind speeds exceeding 160 km/hr were recorded during the winter. Unfortunately, wind speeds during most periods of maximum ice loads were not recorded due to ice buildup on the instrumentation. On one occasion an ice load equivalent to 18.6 cm in diameter of hard rime occurred with 112 km/hr winds before the cups blew off the anemometer and the IRM failed due to vibration.

The climate at the Labrador site proved to be more continental with the December to February period being too cold and dry for major icing. Heavy loadings with high wind speeds occurred early and late in the season.

The instrumentation was removed from the sites in early summer 1975; however, the 10-meter guyed towers were left standing at each of the four sites. No further measurements were made until early winter 1976 when utility personnel started monthly visits to the sites to observe, measure and record by photography and narrative description the ice which had accumulated on the towers and guys. This proved to be a very worthwhile, informative program. They have continued the monthly visits through the past six years during which time they have added numerous new towers as passive collectors throughout the Great Northern Peninsula and southeastern Labrador. In addition they have installed an extensive network of Hydro-Quebec Passive Ice Meters at the populated points in the region. As a result, a great deal of documentation now exists of ice storms which have occurred in the last few years.

All of the early studies had assumed that the proposed transmission line would be located along the western half of the Great Northern Peninsula. There is a coastal plain and highway along that side. In the spring of 1977 it became necessary to consider crossing the peninsula farther north and bringing the line route down the eastern side. MRI conducted an evaluation of the probable meteorological loadings which would be encountered along that route. With no existing weather stations nor structures of any kind other than a couple of small fishing villages on the shore, the only answer was once again extrapolation and predictions based on forecaster experience. Subsequently, the passive towers erected in the area have verified that frequent heavy glaze storms occur along the entire eastern half of the peninsula. The rugged terrain with long stretches of heavy ice loadings ruled out the eastern side as as a viable option.

By late 1979 four alternative routes over the ridge had been identified. Each of these routes had been carefully selected to take advantage of all the possible sheltering from the surrounding terrain. MRI conducted a detailed evaluation of each of those routes presenting the predicted loading values for many short line segments. The extreme loadings still exist - they cannot be avoided. However, the maximum exposure area has been refined down to a few kilometers. The proposed line is still considered to be in the preliminary design phase having been delayed by a variety of financial and political reasons. If ultimately the decision is to build the line, further detailed meteorological evaluations will probably be required prior to final design.

## NEED FOR STANDARD APPROACH

As referred to earlier, meteorological loadings are frequently expressed in terms of return period probabilities. That is, those maximum loads which can be expected to occur once in 25 years, once in 50 years, etc. Obviously the 50-year storm may occur anytime during a given 50-year period. The 200-year storm may occur next year. Assigning 50-year return values to each segment of a proposed line route is quite straightforward and generally an accepted practice. How the user applies this information in terms of overall line reliability is not uniform among the utilities or engineering companies. The subject becomes increasingly debatable if the line is long enough to cross through two or more independent weather regimes or storm tracks. I believe this is a subject that needs joint consideration by knowledgeable meteorologists, engineers, and statisticians.

Meteorologists, knowledgeable in the many variables which can affect ice accretion and in the needs of design engineers can make important contributions to the design of large transmission lines. The importance of early involvement before the route and structure design are fixed beyond economical variation cannot be stressed too much.

## REFERENCES

[1] Tedesco, P.A., et al., 1977: Loading and Strength of Transmission Line Systems, Part III Icing and Combined Ice and Wind Loads, IEEE PES Winter Meeting, New York, NY, January 1977, 1-7.

AD P001696

# PREDICTING ICE AND SNOW LOADS FOR TRANSMISSION LINE DESIGN

E.J. Goodwin, III Pennsylvania Power and Light Company
J.D. Mozer GAI Consultants, Inc.
A.M. DiGioia, Jr. GAI Consultants, Inc.
B.A. Power Weather Engineering Corporation of Canada, Ltd.

## ABSTRACT

A methodology is proposed to transform standard meteorological data into probability-based transmission structure loads at any location within the Pennsylvania Power and Light Company's service area. Proposed accretion models are presented for estimating ice and snow accumulation on transmission line conductors using standard weather station data. The results are synthesized and subjected to extreme value analysis to yield return period versus ice or snow loading relationships. A methodology for combining wind and snow events to predict peak transverse loads is described.

The paper focuses on the application of icing models and describes the techniques and assumptions required to institute a probability-based ice and snow load criteria.

## HISTORICAL BACKGROUND

The National Electrical Safety Code (NESC) has been used throughout the United States as a minimum design loading standard [1]*. The NESC stipulates combinations of minimum load levels for three general climatic loading districts throughout the United States. These specified combinations of ice thickness and wind pressure on the lines are used to calculate structure loads which are multiplied by overload capacity factors (load factors) to achieve structure safety. The NESC, however, does not provide requirements or guidelines for the modification of loads and overload capacity factors to represent an individual utility's unique climatic or terrain requirements nor does it provide the opportunity to design by a probability-based approach.

An IEEE guide on transmission structure design loadings published in 1964[2] recommended the use of "realistic ultimate" loads in the design of towers. In recent years, working subgroups within the IEEE have been refining the 1964 proposal. During the 1977 Winter Meeting of the IEEE Power Engineering Society, a series of papers was presented which recommend the application of probability-based climatic loads for preparing structure loading agendas [3].

In 1971 and 1974, the American Society of Civil Engineers (ASCE) published two guides [4,5] for the design of steel towers and steel pole structures. These guides used the NESC Sixth Edition as their load basis. Probability-based climatic loads are recommended for application in areas of known abnormal climatic events.

Neither of these guides nor NESC provide specific recommendations on procedures for determining climatic loads, and for this reason, current practice among the different electric utility companies and agencies is quite varied. This variability in practice is clearly evident from the results of a utility practice questionnaire recently compiled by ASCE [6]. In the case of ice loads, the questionnaire responses were summarized by an equivalent radial glaze ice thickness map. On the basis of these responses, Pohlman and Landers [7] have observed that "...present practice for specifying ice loads is intuitively based and generally more conservative than legislated controls". Since there is little available data in the United States on ice accretion on transmission lines, some utilities, such as the Pennsylvania Power and Light Company (PP&L), have developed their own data base and procedures for predicting ice loadings.

---

*Numbers in brackets denote references cited at the end of the paper.

Up to the present time, PP&L has used NESC loads as a minimum requirement and imposed higher loads where deemed necessary to reflect specific climatic characteristics of its service area. In 1977, PP&L management established a task force consisting of PP&L personnel and outside consultants to research and document present PP&L design philosophies and design criteria. In addition to documenting present practice, the task force was also charged with the responsibility of modifying and improving present PP&L design practices through an evaluation of recent advances in the state-of-the-art of meteorological load prediction and probability-based design approaches. These approaches were documented in a Structure Loading Guide for the design of transmission line structures in the PP&L service region. This paper summarizes the loading guide procedures and recommendations for ice and snow loads and the statistical combinations of wind, ice and snow loads.

## ICE AND SNOW ACCRETION MODELS

No data exists in the United States which are based on direct measurements of icing on transmission lines due to various atmospheric conditions. Therefore, it was necessary to select appropriate mathematical models from the literature that can be used to compute ice accretion based on meteorological data that are readily available from the National Climatic Center (NCC) or other sources.

Three types of icing were considered by the PP&L task force: glaze ice, rime ice (or cloud ice) and wet snow. Since the physical mechanism and mathematical models that govern the three types are different, they are discussed separately in the following subsections of the paper.

### Glaze Ice

Glaze icing is a clear transparent ice having a typical density of 0.9 gram per cubic centimeter (g/cc). Glaze icing occurs during conditions of freezing rain or freezing drizzle. The following accretion equation for glaze on transmission line conductors was formulated by Imai [8] and Kuroiwa [9]:

$$\frac{dM}{dt} = 2EwVR \qquad (1)$$

where, M is the mass of ice per unit length of cable in grams per centimeter (g/cm), t is the storm duration in seconds (sec), w is the liquid water content of air in grams per cubic centimeter (g/cc), V is the wind speed in centimeters/second (cm/sec), R is the radius of the collector in centimeters (cm) and E is the collection efficiency. The collection efficiency is assumed to be 1 for glaze, that is, it is assumed that every water drop which strikes the collector (in this case the conductor) adheres and freezes to it.

Intergrating Equation 1 gives:

$$t = \frac{\rho\pi}{Vw} \int_{R_1}^{R_2} \frac{dR}{E} \qquad (2)$$

in which $\rho$ is the ice density in g/cc.

Imai and Kuriowa's formula depends on the horizontal velocity of the droplets associated with the wind. It is assumed, however, that the droplets actually have a resultant velocity, V, which is due to both the wind velocity, $V_w$, and the falling speed of the droplets, $V_t$. Thus,

$$V = \sqrt{V_w^2 + V_t^2} \qquad (3a)$$

In the case of freezing rain, the liquid water content, w, can be estimated from the rain gauge precipitation depth, $H_g$, as

$$w = \frac{H_g}{V_t t} \qquad (3b)$$

The accretion formula resulting from substituting Equations 3 and E=1 into Equation 2 and integrating is:

$$\Delta R = \frac{H_g}{\rho\pi}\sqrt{1 + (V_w/V_t)^2} \qquad (4)$$

where $H_g$ is in cm, and $\Delta R$ is the radial increment of glaze ice, in cm, accreted over the time interval in which Hg is measured during conditions of freezing precipitation.

### Rime Ice

Rime icing occurs at higher elevations by deposition of supercooled liquid cloud droplets on the cables. The density of the rime varies from "soft" rime (0.3 to 0.6 g/cc) to "hard" rime (0.2 to 0.8 g/cc) depending on the size and speed with which the water droplets freeze. In the case of rime icing, the use of Equation 2 is appropriate except that the terminal fall velocity is negligible and the collection efficiency, E, is less than unity, decreasing to near zero as the diameter of the conductor plus ice increases. In effect, the small water droplets in the cloud are blown around and past the conductor by the wind airstream thus preventing them from adhering to the conductor. Langmuir and Blodgett [10] have developed tables and charts for the collection efficiency as functions of dimensionless parameters K and Φ, where

$$K = \frac{2\rho_s V_w r^2}{9\eta R} \qquad (5)$$

$$\Phi = \frac{18\rho_a^2 R V_w}{\eta \rho_s} \qquad (6)$$

in which $\rho_s$ is the density of the water droplets in g/cc, r is the average radius of the water droplets in cm, η is the viscosity of air in g/cm-sec, R is the combined radius of conductor and ice in cm, $\rho_a$ is the density of air in g/cc, and $V_w$ is the velocity of the wind in cm/sec. Because E varies with R, the accretion rate is dependent on the initial conductor diameter. Analytical solutions of the above equation are not possible; however, it can be solved by iteration. Rime icing is particularly sensitive to elevation because the cloud water content, which increases from zero at the cloud base to a maximum at the cloud top.

WET SNOW

Wet snow loadings occur when falling snow is wet enough to be adhesive to the conductors, structures, and other snow-[illegible] snow occurs most frequently and is most severe between 0°C and 3°C with a density range of 0.1 to 0.8 g/cc. Conventionally, it was thought that wet snow [illegible] accumulates at low wind speeds. However, it has been determined that wet snow [illegible] accumulate at wind speeds up to [illegible] meters per second (m/s) as well as at [illegible] wind speeds [8].

[illegible] WEAN [11] studied a series of [illegible] events for Saskatchewan Power Corp [illegible] adapted Equation 2 to wet snow [illegible] for the first time. A good agreement between observed and calculated snow accretions was obtained provided a density of 0.4 g/cc and a collection efficiency of unity were used. When this model was reviewed with a 1958 storm in the PP&L territory, it was determined that E may not be unity but may be diameter and velocity dependent for wet snow. It is not possible to solve for E, since, $V_t$ and $\rho_s$ are not known for wet snow. However, sufficient data were available from the 1958 storm to derive an empirical approximation for wet snow accretion. By varying E with diameter and testing several densities, a good correlation with the actual storm related data was found. On this basis, a density of 0.1 g/cc seemed reasonable for wet snow in the PP&L region.

ANALYSIS OF ICING EVENTS

Using the accretion models described above and hourly climatic data tapes from the NCC for four first order weather stations in the PP&L service region, predicted ice and snow thicknesses were computed for all potential ice and snow events over approximately 23 years of record. The results were used to develop a series of annual extreme ice and snow events for each weather station.

A Gumbel or Type I extreme value distribution was used to transform these populations of annual extreme ice and snow events into return period versus magnitude relationships [12]. The Type I exceedence probability function is given as:

$$P(>X) = 1-e^{-e^{-a(X-u)}} \qquad (7)$$

in which P(>X) is the annual probability of exceeding a given thickness X of the icing event, u is the mode or position parameter of the distribution and a is the dispersion parameter. These parameters were determined from the series of annual extreme data for each station using least-square relationships for the Type I distribution given by Gumbel. The return period, T (in years), associated with the magnitude of X is simply given as

$$T = \frac{1}{P(>X)} \qquad (8)$$

The Type I distribution has been found to fit the distribution of extreme meteorological events well and is widely used to permit extrapolation to return periods longer than those in the historical period of observations.

## VERTICAL LOADINGS DUE TO ICE OR SNOW

### Total Probability for Ice or Snow

Since vertical loads are generated by glaze, rime or snow and their respective densities differ, it is necessary to work with the vertical weight as a variable rather than the ice or snow thickness. Therefore, for each weather station, the series of annual extreme ice and snow thicknesses were converted to vertical loadings using the appropriate densities. Since the ice and snow events are mutually exclusive, the annaul probability P(>X) of exceeding a vertical load X on the conductor due to either ice or snow is given by

$$P(>X) = P_I(>X) + P_S(>X) \qquad (9)$$

where $P_I(>X)$ is the annual probability of an ice load exceeding X and $P_S(>X)$ is the annual probability of a snow load exceeding X. Using Equation 8, the above equation may be expressed in terms of the respective return periods as follows:

$$\frac{1}{T} = \frac{1}{T_I} + \frac{1}{T_s} \qquad (10)$$

### Weight Equations

The results from the extreme value analysis for the predicted ice and snow events at each of the four weather stations were substituted into Equation 10 to obtain return period versus loading relationships for ice and snow. These relationships were used to develop design equations for vertical loadings as functions of return period for various conductor diameters, elevations and terrain roughnesses. The latter three parameters enter into the equations because the vertical loadings due to cloud ice are functions of collection efficiency (diameter dependent), cloud water content (elevation dependent) and relative wind velocity (terrain roughness dependent). With these design equations, vertical loadings due to ice or snow can be predicted for any location in the PP&L service region. Typical results for 50-year vertical loadings are shown in Table 1.

Table 1

Extreme Vertical Loadings
Due to Ice or Snow
50-year Return Period
Conductor Diameter = 25 mm (1 inch)

| | Vertical Loading* N/m (lb/ft) | | |
|---|---|---|---|
| Elevation (m) | Flat Open Terrain | Broken Farmland | Woods, Suburban Areas |
| 120 | 47 (3.2) | 43 (3.0) | 36 (2.4) |
| 430 | 62 (4.2) | 56 (3.9) | 47 (3.2) |
| 730 | 77 (5.3) | 71 (4.8) | 59 (4.1) |

---

*Loading due to weight of the conductor is not included.

From this table, it is evident that the vertical load reduces as terrain surface roughness increases due to the reduction in wind speed in a rougher surface terrain. Also, note the increase in load with elevation as more water is available in the clouds for rime accretion at higher elevations.

### Comparison with Field Observations

Calibration of the accretion models was obtained through comparison of estimated radial ice thicknesses based on meteorological records with observed ice thicknesses on transmission lines in the PP&L service territory. Three specific observations were compared to the glaze and rime ice accretion models described previously. The three comparisons tabulated in Table 2 indicate that the accretion models give calculated results that

Table 2

Comparison of Accretion Model Estimates
with Observed Ice Thicknesses

| | Radial Ice Thickness in mm (inches) | | |
|---|---|---|---|
| | Cetronia Village January 1953 | Shenandoah Borough December 1962 | Vulcan Mountain January 1953 |
| Type Ice | Glaze | Glaze | Glaze & Rime |
| Observed thickness | 25 (1.00) | 5 (0.2) | 64 (2.5) |
| Calculated thickness | 24 (0.9) | 5 (0.2) | 65 (2.6) |

compare quite well with observed ice thicknesses.

When the Vulcan Mountain storm was studied, the effects of cloud icing became very apparent. Based on recorded precipitation at three weather stations, the glaze ice accretion model predicted only 24 mm radial thickness, whereas the observed accretion at Vulcan Mountain was 64 mm as noted in Table 2. The topography at the Vulcan Mountain site and the climatic conditions during the storm indicated a high potential for in-cloud icing. Using cloud physics and the Kuroiwa rime accretion model, a 41 mm rime accretion was predicted, which when added to calculated glaze accretion gives a total calculated radial ice thickness of 65 mm. This compares very well with the observed thickness at Vulcan Mountain as shown in Table 2.

During two very severe snow storms, total snow accretion diameters (conductor diameter plus snow) were measured at two locations in the PP&L service region. Calculated diameters based on the snow model and climatic data from nearby weather stations compare reasonably well with these measurements as shown in Table 3.

Table 3

Wet Snow Accretion Comparisons of the Accretion Model and Observed Snow Diameters

| Location | Total Diameter in mm (inches) Observed | Total Diameter in mm (inches) Calculated |
|---|---|---|
| Sterret's Gap March 1950 | 203 (8.0) | 186 (7.33) |
| Mt. Nebo March 1958 | 178 (7.0) | 163 (6.4) |

From these comparisons with observed data, it can be concluded that the proposed accretion models provide accurate representations of the expected ice and snow loadings on overhead lines in the PP&L service area.

## TRANSVERSE LOADINGS DUE TO WIND AND SNOW

In this study it was found that the maximum transverse loadings for the PP&L service area were governed by the combination of wind and snow. Therefore, glaze ice and rime ice accretions, which were considerably smaller than the snow thicknesses, were not considered in the transverse load analysis.

The transverse load, F, due to wind acting on a snow-covered conductor is given as

$$F = \frac{1}{2} \rho_a V^2 C_D (d_c + 2S) \qquad (11)$$

where $\rho_a$ is the air density, V is the horizontal wind velocity component normal to the conductor, $C_D$ is the conductor drag coefficient, $d_c$ is the conductor diameter and S is the radial snow thickness. Two methods, described below, were used to determine the expected lifetime maximum values for F.

### Historical Storms Method

The first method involves an extreme value analysis of combined snow and wind transverse load events from all historical storms. For each storm on record, the peak transverse load is calculated by determining the snow accretion and the peak wind during or soon after the snowfall and substituting these quantities into Equation 11. It was observed that the peak wind always occurred within two days of the snow storm which coincides with the passing of a cold front following a storm. Results from this method using the historical data recorded at the Allentown, Pennsylvania weather station are shown in Table 4.

### Combined Probability Method

The second method combines snow and wind assuming they are statistically independent events. With this assumption, the annual probability P(>F) of exceeding a transverse load F (calculated by Equation 11) is given as

$$P(>F) = P_s(>S) \times P_w(V|S) \qquad (12)$$

where $P_s(>S)$ is the annual probability of exceeding a specified snow thickness S and $P_w(V|S)$ is the probability of a specific wind velocity V being exceeded during residence of the snow on the line. If it is further assumed that the average snow residence time is m-days, then

$$P_w(V|S) = 1 - \left[ 1 - P_d(>V) \right]^m \qquad (13)$$

in which $P_d(>V)$ is the probability of exceeding a specified wind velocity V in a one-day period. Substituting Equation 13 into Equation 12 and using the general return period- exceedence probability relationship of Equation 8, the following return period equation for the combined event is obtained:

$$T = \frac{T_s}{1 - \left(1 - \frac{1}{T_{wd}}\right)^m} \qquad (14)$$

where T is the design return period (i.e. the return period, in years, of the combined event), $T_s$ is the return period of the specified snow thickness in years and $T_{wd}$ is the return period of the specified wind velocity in days. Therefore, the combination of a wind velocity with a $T_{wd}$-day return period and a snow thickness with a $T_s$-year return period will yield, by means of Equation 14, a T-year design return period for the combined event. The transverse load corresponding to each combined event is calculated by Equation 11.

Since there are numerous combinations of snow thickness and wind velocity that will correspond to a given combined event return period T, the combination giving the maximum transverse load calculated by Equation 11 is used in design. This is determined by a trial and error procedure. Typical results are given in Table 4.

Comparison of Methods

In Table 4 transverse loading results from the historical storms and combined probability methods are compared. Note that the historical method gives loadings that are about 68 percent of those determined by the combined probability method. The wind data used to generate the combined probability loads are the daily extremes for 23 years of record. These data will provide higher predicted wind speeds than the actual winds of record following icing or snow events. The proper statistical combination, therefore, would involve annual extreme snow thicknesses combined with daily extreme wind velocities measured during and immediately following the snow events. Additional analysis would be required to obtain these distributions of selected winds and the results would be applicable only to the weather station locations. Since procedures were developed for predicting daily extreme winds over the entire service region, these values are used in the combined probability method and the results are multiplied by a 0.68 reduction factor to give design transverse loadings that are comparable to historical storm predictions.

Table 4

Extreme Transverse Loadings Due to
Wind on Snow-Covered Conductor

Allentown, Pennsylvania
Conductor Diameter = 25 mm (1 inch)

| | Transverse Loading in N/m (lb/ft) | |
|---|---|---|
| Return Period in Years | Historical Storms Methods | Combined Probability Method |
| 25 | 19 (1.3) | 28 (1.9) |
| 50 | 22 (1.5) | 32 (2.2) |
| 75 | 24 (1.6) | 35 (2.4) |
| 100 | 25 (1.7) | 37 (2.5) |

SUMMARY AND CONCLUSIONS

Mathematical accretion models have been developed to predict ice and snow loadings on transmission lines using recorded meteorological data. These models along with extreme value analysis procedures were used to derive vertical loading equations for any location in the PP&L service region. Results from these equations and recorded weather data give 50-year return period loadings that are considerably more conservative than the NESC ice loading for this region. However, for individual storms, the accretion model predictions compare well with field observations.

A combined probability procedure was used to predict maximum transverse loads due to combined wind and snow events. The procedure gives results that are somewhat more conservative than those given by the historical storms method using data measured at weather station locations. However, the combined probability method is more suitable for predicting transverse loadings for other locations in the PP&L territory.

Electric utility companies are concerned primarily with ice and snow thicknesses for two loading conditions, extreme vertical loads and extreme transverse loads due to wind on snow or ice-covered conductors. Accurate predictions of maximum expected loads can be very beneficial in designing economical and reliable structures. The development of easily applied accretion models is, therefore, a vital concern of the utilities.

Since most utilities in the United States do not have existing ice accretion monitoring facilities, the utility engineer must rely on historical climatic data accumulated over many years at specific weather bureau monitoring sites. The engineer must use these data to develop by means of accretion models and statistical analysis the most probable extreme loadings over the lifetime of the transmission line. Further transposition of these loadings to transmission line locations (based on conductor height and diameter, terrain roughness, topography and elevation) is then required.

To provide models which are flexible and adaptable for transmission line applications, additional research and documentation should be performed in the following areas:

- Develop simple accretion models that use climatic data readily available to the utility engineer, i.e., FAA or National Weather Service Facilities.
- Develop correction factors to adjust ice accretion data for various terrain conditions.
- Further the research in wet snow accretion since wet snow combined with wind plays a more important role in transverse loading analysis than does ice and wind for many service areas.
- Develop an improved statistical procedure for determining extreme transverse loadings due to combined wind and snow.
- Establish a continuing line of communication between the utilities and researchers so that the utilities' needs are addressed and represented in future research.

## ACKNOWLEDGMENTS

This paper contains, in part, the results of a study on transmission line structure loading conducted by a task force sponsored by the Pennsylvania Power and Light Company (PP&L) of Allentown, Pennsylvania. The members of the task force are: Mr. E. J. Goodwin, III of PP&L; Drs. A. M. DiGioia, H. L. Davidson and J. D. Mozer of GAI Consultants, Inc.; Mr. B. A. Power of Weather Engineering Corporation of Canada, Ltd.; and Dr. A. G. Davenport of the University of Western Ontario. The work of the task force was performed under the general management of Mr. M. A. Valastiak of PP&L.

## REFERENCES

1. ANSI C2-1981, National Electrical Safety Code, 1981 Edition, Institute of Electrical and Electronics Engineers, New York, New York.

2. Farr, F. W., McMurtrie, H. J., White, H. B., Ferguson, C. M., Steiner, J. R. and Zobel, G. S. "A Guide to Transmission Tower Design Loadings", IEEE, TP 64-92, November 1964.

3. "Loading and Strength of Transmission Line Systems", IEEE/PES Winter Meeting, New York, February 1979.

4. "Guide for Design of Steel Transmission Towers", ASCE, Manual No. 52, 1971.

5. "Guide for Design of Steel Transmission Pole Structures", ASCE, 1974.

6. Wilhoit, G M., "Loadings for Electrical Transmission Structures," Committee on Electrical Transmission Structures of the Committee on Analysis and Design of Structures of the Structural Division, J. Struct. Div., ASCE, Vol. 108, No. ST5, May 1982, pp. 1088-1105.

7. Pohlman, J. C., and Landers, P., "Present State-of-the-Art of Transmission Line Icing," IEEE/PES T&D Conference and Exposition, Minneapolis, Minnesota, September 1981 Preprint No. 81 TD 717-8.

8. Imai, I. "Studies on Ice Accretion" Researches on Snow and Ice, No. 1, 1953, pp 35-44.

9. Kuroiwa, D. "Icing and Snow Accretion on Electric Wires" Research Paper 123, U.S. Army Material Command, CRREL, January 1965.

10. Langmuir, I. and Blodgett K. "A Mathematical Investigation of Water Droplet Tragectories", Army Air Force Technical Report No. 5418, 1946.

11. "Final Report-Vertical and Transverse Loading Study - Saskatchewan Power Corporation" Weather Engineering Corporatin of Canada, Ltd., July 1972.

12. Gumbel E. J., "Statistical Theory of Extreme Values and Some Practical Applications", National Bureau of Standards, Applied Mathematics Series No. 33, February 12, 1954.

## DISCUSSION

Franklin: ... you figured that two days was sufficient period of time to get extreme value separation?

Goodwin: We looked at 80 events over 22 years, and the peak transverse event occurred within two days of the snow stopping. So, we're looking at whatever length of time it takes for the snow to accrete, and then two days after that we're saying a front will pass through, and within that period we'll have our peak transverse forces.

Franklin: That's different than saying two days would be a minimum amount of time for two storms going through.

Goodwin: No, no - you have your icing or snow event, and within two days after that event stops, we feel the front will come through, and that's when we'll have our peak transverse. You don't have everything in two days.

Franklin: What would you consider a minimum period of time for two mutually independent occurrences, such as storms greater than four days? For ice storms.

Power: I can answer that. I think I would say that it would depend upon the area. Most of the ice and snow storms were 24 hours or less.

Goodwin: So four days would be enough for our particular service area, probably.

Assur: The speaker addressed himself to the potential of overdesign, and I think we should be concerned with that. One possibility of overdesign, which you share in your paper with many others, is the assumption that the ice accretion is proportional to the wind speed, which is of course a classical assumption. However, there are two pieces of evidence that this is not so, and there is also reasoning that this should not be so. One piece of evidence is a laboratory experiment conducted at CRREL with a rotating blade where in one experiment you get every single velocity up to extremely high velocities. At extremely high velocities, where conventional design would assume heavy ice accretion, we observe very little ice accretion. The other piece of evidence, which is probably more palatable to an engineer, was direct observations of the TV tower in Moscow, which I mentioned. And Dave Minsk published that evidence in one of his reports, where there is a clear indication that the ice accretion is proportional to the wind speed, reaches a maximum, and then decreases. The reason is, of course, that contrary to classical assumptions, a droplet which impinges does not necessarily freeze - it's blown off by high wind. So if we are working in an area which is relatively flat, with the assumption of modest wind speed, then this assumption may be all right. It exaggerates a little bit, but if we wanted to design things for high mountains, and the Germans did this, they made fantastic assumptions and obviously ovedesigned. Now another consideration could be - there should be - a difference between rime and just ice accretion, but that's still an open question. The proportionality of ice accretion to wind speed ought to be examined. Most of the speakers here still make that drastic assumption. There's some evidence in some of these papers on the maximum speed reached.

Mozer: I'd like to make just one comment. One of the things that is inherent in the assumptions that were used in this particular approach for the combined wind and ice condition or wind and snow condition was the assumption of statistical independence between the wind and snow amount, and that was essentially based on some observations where it was observed there is a weak correlation in this particular area. However, I've also noticed in the comments, both by Dave Leavengood and Ritch Richmond, that there are situations where that is not the case, and obviously that's going to have a very significant effect on what we had done in this situation. I guess my question instead of being for Ed is for the other two gentlemen - would they have any comments on what sort of weather systems would you expect where that might be the case, and areas where that might not be the case?

Bilello: I think what we're missing here, in many cases, is how these things are really formed. What's really at the surface may be a frontal system, but the entire characteristics of the atmosphere from the ground up to where the frozen particles are being formed must be considered. For instance it could be pure raindrops at a certain level, then they go through another area where they freeze, or they might bounce up again and form another layer, or it might be water when it hits a cold surface and form what is called freezing rain. You're really looking at the atmosphere, and that gets back to what he said earlier - it depends on where you are, and the characteristics of the system that's passing through your area, whether it's a wet snow, a dry snow, or a freezing rain situation. It could be ice pellets, ice crystals -- you have some 87 different categories - it's listed by National Weather Service in "present weather." And each of these is dependent on what kind of atmosphere these things are formed through and what passes through your region.

Mozer: I guess the question I have is - can you identify how strongly correlated the maximum transverse loads are between ice and the ice accretion in the wind. The observation we made in this case was that they are weakly correlated, and also working with Samy [Krishnasamy] with support from Ontario Hydro, we also observed that.

Power: I think there is one more distinction to be made - that the correlation for glaze is entirely different than it is for rime. On high mountains, the transverse forces are highly correlated with wind during the rime formation. So each case is different - it depends on the loading, it depends on the location. There is an important point to remember here that, as Ed pointed out - if you use the probability method which is desirable plus flexible, you've got an ice accretion series and a wind series. You can play around with these and be able to transpose into different parts of a complicated surface area. But, on the other hand, if you check this against the historical method you'll find you're high--above 68%. Well, use the flexible method and then apply a correction factor and then meanwhile let us address this, put our minds to it, and perhaps in a year or two we'll come up with a better method.

Makkonen: Did I understand correctly that in your model for the rate of glaze [formation] you did not consider air temperature?

Mozer: Oh yes, the assumption is it is decreasing - there is no wet growth. It's assumed that there is complete accretion - there's no runoff or drip-off assumed.

AD P001697

# ICELOAD MEASUREMENTS AND DESIGN PRACTICE

S.M. Fikke Norwegian Research Institute of Electricity Supply
K. Schjetne Norwegian Water Resources and State Power System,
B.D. Evensen Transmission Lines Division

## ABSTRACT

This paper gives a brief description of the following:

- The geographical and meteorological conditions favourable for the formation of atmospheric icing.
- The history of iceload measurements.
- The procedure for determining iceloads on transmission lines.
- The cost consequences for the transmission line as a function of design iceloads.
- Experience from maintenance.
- Field stations in operation. Their construction, methods of iceload measurements, instrumentation and problems concerning instrumentation.
- How the iceloads are treated in the tower design procedure.
- Future works.

## GEOGRAPHICAL AND METEOROLOGICAL BACKGROUND

Norway is ranging from $58^{\circ}$ to $71^{\circ}$ N on the Scandinavian peninsula, and is facing the North-Atlantic ocean and the Norwegian Sea up to arctic waters. The coastline is approximately 2650 km long. Going eastwards from the coast in southern Norway, mountains are raising up to more than 2000 m a.s.l. The south-eastern basin of the country is sheltered by mountains towards west and north. In the northern part of the country the mountains are raising to 1000-2000 m a.s.l. near the Swedish boarder. Glaciers are found in most of the mountain ranges.

In spite of the fact that the latitudes are comparable with Alaska's, the climate is rather mild. This is due to the general circulation of the atmosphere, which on the average is south-westerly across to the north-western part of Europe. The south-western winds also give energy to the North-Atlantic current which transports the warm water towards our western coastline. These warm coastal waters also regulate the winter temperatures in the country.

Another feature characterizing the weather in Norway is the waves on the Polar front. The Polar front divides subtropical airmasses from the cold polar air, and the frontal waves develop as they move eastwards across the Atlantic. Often they are at the most well developed stage when reaching the Norwegian coast, giving high wind speeds, extensive cloud covers and precipitation. The average precipitation varies from 3000-5000 mm/year in the coastal mountains in western Norway, to below 300 mm/year in the precipitation shadow.

## ICING CONDITIONS

The atmospheric processes described above are favourable for the formation of atmospheric ice in great parts of the country. Due to the distribution of mountains and the north-south extension, the icing conditions are different in different parts of the country.

In south-west, the mild and moist air from the ocean is lifted by the mountains. The air is cooled adiabatically which causes the cloud droplets to grow, and the initiation of more droplets. The south-westerly stream is generally too mild to give icing below 800-1000 m a.s.l. But winds from south and north-west can give severe icing from the 400-600 m level on in terrain exposed to those directions.

The highest iceload ever registered on a transmission line in the country was 3050 N/m at 1400 m altitude in these regions.

In the south-eastern part of Norway icing occurs with winds from around south-east.

South-westerly winds reaching Northern Norway have lower temperatures than in the south. Thus winds between south-west and north-west may cause icing from the 200-300 m level onwards. Iceloads of 500-1000 N/m are observed.

The above description is valid for high level terrain where both incloud icing and precipitation icing (wet snow) can occur. At levels below we are likely to have accumulation of wet snow. Transmission lines are built for 40-80 N ice/m for this purpose. Supercooled rain (or drizzle) is not an important process in Norway as it is e.g. in Canada and USA.

## EXPOSURE AND TOPOGRAPHICAL SHELTERING

Especially in terrain where incloud icing is expected, it is the practice, if possible, to find sheltered routes for transmission lines when crossing a high level plateau. This is especially important, since only a few metres difference in line height can mean totally different icing climates, meaning at least a factor of 2-5 of the ice loads. When planning a new route, it is therefore important to examine the local terrain as well as the general pattern of the landscape, and also the exposure to ice-leading winds.

However, the expected iceloads at specific places have traditionally been based on meteorological judgement of all the factors involved and of experience. There has therefore been a strong need for direct measurements of ice since many of the parameters in the theoretical accumulation models are not sufficiently well known.

## ICE MEASUREMENTS

### History

The work with icing problems has been cooperated and organized by two succeeding committees since 1953. Several test stations have been operated, and information is gathered from the electricity companies about their experiences with their power lines (especially lines of 66 kV or more). Different public and private electricity companies, consulting engineers and engineers from research institutes were represented in the committees. In the latter, the Norwegian Meteorological Institute was represented as well.

The comittees were sponsored by the Norwegian Research Institute of Electricity Supply, and the Norwegian Water Resources and Electricity Board, State Power System.

### Test stations

Most of the test stations were situated along actual routes for future power lines in high level terrain, the highest at 1750 m a.s.l. They have been equipped with test spans and tube constructions of different designs. The test spans were instrumented with dynamometers, some showing maximum loads only, other gave registration sheets. The tubes were inspected manually, and geometry and density of the ice cover were measured. Some of the stations were inspected daily, the others mostly at weekly intervals.

In addition to observing the general icing conditions at representative places, the instalments should also show variations with height within the area, height above ground, different wire diameters and differences in the longitudial and transversal directions of the valley. Finally, differences in behaviour between cold wires and electrified wires were tested, as well as spacers for bundle conductors.

## Meteorological observations

Two stations were placed close to regular meteorological stations. Two manned stations were equipped with thermometers, thermographs, hygrographs, and anemographs. Additionally, there were regular meteorological stations not too far away.

## Results

The instrumentations and results are published in [1] and [2]. The stations were more or less in operation for 5-10 years and valuable information was gathered. Iceloads up to about 1000 N/m are measured. The most useful data are probably from the most exposed places, where incloud icing occur regularly. In sheltered areas icing will happen more seldom, often with intervals of several years. The latter case naturally demands series of measurements over a longer period of time.

The following conclusions are among the most important ones from the earliest test stations:

- heights of 50 m above lineheight in the upwind terrain give almost complete protection aganist incloud icing,
- glaze is very rare in the mountains,
- ice cover is much less in forests than in open terrain,
- tube constructions are fairly representative for the study of the local conditions,
- it is probably not possible to feed mountain peaks by thin conductors and high current to avoid icing.

No definite conclusions were drawn with attention to the variation of iceload with height above ground or with the diameter of the conductors.

## Icing model

The data from the two most recent stations were used additionally for developing an icing model based on regular meteorological data. (See companion paper: Attempts Toward Estimating Ice Loadings Based on General Climatological Data.) These two stations were more conveniently situated and instrumented for comparisons between the local weather and the general conditions of the atmosphere. The greatest difficulties with these stations have been connected with the density measurements and the inspection frequency.

## TODAYS PRACTICE

When a transmission line has to be built in areas with severe in-cloud icing, it is of great importance that the different people responsible for line routing, survey, meteorological investigations, tower spotting, and the design of structures work in close cooperation. It must be realized that the amount of ice on conductors may vary to a large extent from one span to another. Experience shows that severe iceloads can occur in one or a few spans, whilst adjacent spans are almost free of ice.

This phenomenon is introducing severe longitudinal forces on suspension towers, and may result in tower collapse if not taken into account. Such local iceloads are also dramatically increasing the sag, and the conductor to ground clearance may become critical.

Design iceload cases are dealt with more detailed in a later chapter.

A more frequent observation is that large longitudinal loads cause the earth wires to slide in the clamps and sag down between the conductors. Resulting flashovers have caused burning off of the earth wires. In such spans the earth wires have to be removed from towers and placed in the ground.

In areas with iceloads higher than 250 N/m twin bundles have been replaced by a large single conductor with a diameter up to 57 mm.

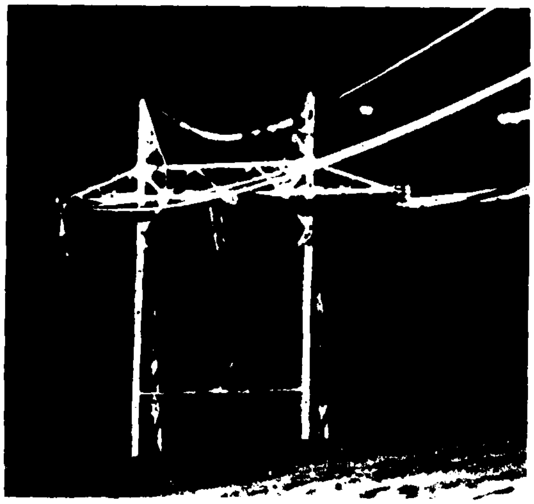

Tower and conductors after icing period.

COSTS

In later years attempts have been made to try to correlate the magnitude of iceloads, steel assumption and the overall cost of a transmission line. When analysing alternative routes for a transmission line, it is of great value if the cost can be obtained as a function of the design iceload. Calculations have shown that there is a good correlation between the weight of towers per kilometre and the overall cost per kilometre.

In Norway the overall cost for 420 kV lines are varying between US$ 6000 and 8000 per metric ton of steeltowers that are used.

The variation is mainly dependent on construction factors such as accessibility of line route, type of foundation etc. Two transmission line projects completed in 1979 and 1981 have been analysed, and the steel weight per kilometre for sections with the same iceloads have been calculated. Both lines have twin bundles of Parrot conductor (ACSR 766/97 (54/19)), and are connecting the western and eastern parts of Norway. The line lengths are 101 and 191 kilometres respectively.

Fig. 1 shows the correlation between tower weight per kilometre and the iceloads in Newtons per metre.

The fig. shows a dramatic increase in tower weight with increasing iceload. This can be explained as a result partly of increasing tower loadings, partly as a reduction of span lengths to keep within the limit of the conductor strength, and partly due to an increasing number of angle (tension) towers. The reason for the extensive use of angle towers is that we make the line routes follow small valleys and depressions in the terrain to obtain sheltering effects avoiding even higher iceloads.

Fig 2 shows the relation between iceloads and span lengths.

From the cost point of view one can conclude that the iceloads have a considerable influence on the overall cost of a project, and that an analysis of the route alternatives with regard to ice loading may give good indications on what alternative should be recommended.

The approach used in our cost calculations is that an estimate of the steel consumption for a certain section is worked out, based on the magnitude of iceloads (given in a detailed meteorological report).

The cost per ton of steel is then estimated, based on an evaluation of topography, accessability, and other relevant construction factors.

## EXPERIENCE FROM MAINTENANCE

On transmission lines owned by the Norwegian State Power System serious damages caused by icing on conductors and earth wires have been registered on thirty towers in the period from 1965 to 1982.

Twelve of the towers collapsed completely. The others were either damaged in the upper part of the tower body or had damaged crossarms.

The damaged towers were registered in all parts of the country.

Resulting outages lasted three weeks on average. Loss of revenue in connection with outages is said to be in the range of US$ 3000-8000 per hour for 300 kV lines.

A more frequent cause of outages is, as previously mentioned, the sagging of earth wires down between the conductors.

It should also be mentioned that far more towers are damaged by avalanches than by icing.

To study the effects of avalanches, we will during this summer (82) establish a test station for measuring forces on constructions in avalanche paths and avalanche wind forces on conductors spanning across avalanche paths. Avalanches will be initiated serveral times during the winter.

## FIELD STATIONS IN OPERATION

At present the Norwegian State Power System has 11 test stations in operation for measuring iceloads on conductors. Nine of the stations are located in the vicinity of 420 kV lines to be built or under construction. Meteorologists have made an evaluation of probable iceloads for the routes. The iceloads registered at the stations will be used to verify or adjust the assumptions made by the meteorologists.

Five of the stations are located in Northern Norway at altitudes ranging from 720 to 930 metres and at varying distances from the coastline. We have four stations in Southern Norway. Three of them are located on ths same mountain plateau at altitudes from 1100 to 1200 metres, the fourth on a mountain top of an altitude of 1400 metres.

The remaining two are at test stations used for developing the icing model.

This chapter will deal with the construction of the stations, methods of iceload measurements, instrumentation, problems concerning instrumentation, and evaluation of measurements made.

The test stations were erected in 1978 and 79. A station consists of two towers and a horizontal tube with a diametre of 55 mm and a length of 10,5 metres, suspended at two points 7 metres apart. Height above ground approx. 5 metres.

Fig. 3 shows the arrangement.

The damper is installed to absorb sideways horisontal vibrations due to wind on the tube.

Icing on a horisontal tube is assumed to give a good simulation of icing on conductors.

The reaction at one of the suspension points are to be measured.

At the outset two important requirements had to be fulfilled:

- The load recording instruments had to be reliable and free of maintenance due to the very limited accessibility of the stations (only by helicopter).
- To provide contineous load recordings during the winter season.

Originally the stations were equipped with Prewitt scratch gauges to give continuous readings of iceloads on the tube. The load history was to be recorded by making a scratch on a circular disc rotated by variations in loading on the tube. However, unforeseen vibrations in the suspension system gave a continuous rotation of the disc and a resulting carving out of a deep groove in the disc. Hence no loading history was recorded.

As a result the scratch gauges were rejected and a study to find a more reliable method of load registration was carried out.

It was decided to continue with the type of test stations previously described, but to replace the scratch gauges with strain gauges. The strain gauge was placed on a rod in the suspension system.

The strain gauges require electric power, amplifier, and plotter units.

Conventional batteries were chosen for power supply.

Problems at low surrounding temperatures were foreseen and the batteries were placed in an insulated box. The box will either have to be artificially heated or dug down in the snow or in the ground.

Experience from other fields suggested logging of data on tape to be the most reliable method. This type of equipment requires small amounts of power and has few moving parts. A 12 channel Data logger made by Aanderaa of Norway was chosen and placed in the same insulated box as the batteries. The manufacturer guarantees the logger down to -4 C. If placed sufficiently deep in snow the temperature will be kept above this level.

Strain gauges with data loggers were installed at three stations. In addition all eleven stations were equipped with dynamometers with "max. value reading".

The strain gauges and data loggers were in operation during the winters 79/80 and 80/81. Load recordings were made every third hour. Recordings on tapes were compared to the max. value readings on dynamometers. The results were disappointing. Two of the stations (in Northern Norway) showed parallell loading histories during the first season, but only one of the two showed good correlation between dynamometer reading and the tape (winter 79/80). The third was considered useless. A probable explanation is "sliding" of the strain gauges an faults in the cable connections. After the winter 80/81 we started looking for a new type of strain gauge or load cell. We hope to have load cells installed for the winter 82/83.

The max. ice loads registered by the dynamometres during the winters 79/80 and 80/81, have for Northern Norway ranged from 30N to 690N per metre of the tube.

In Southern Norway from 50N/m to 170N/m.

The loads are, with the exception of the undated reading of 690N/m, less than the expected maximums.

The general meteorological conditions in this period have not been favourable for icing.

## DESIGN PRACTICE

When the process of line routing, necessary surveying and evaluation of iceloads and wind speeds are completed, the individual towers of the line are designed.

The iceloads are treated as follows:

The suspension towers are designed for vertical loads and differential longitudinal loads due to max. ice in all spans. In addition the towers are designed to withstand longitudinal loads due to local ice either on one earth wire or one conductor (phase).

For 420 kV horisontal formation single circuit lines the range of longitudinal loads on suspension towers are:

1) Local ice on one conductor (one phase)

See fig. 4.

QLF is the resultant longitudinal load at the top of the tower leg.

QLF from 25 KN (lower limit) to 78 KN. In this case the lower and upper limits of longitudinal load from earth wire (LE) are:

$10KN \lesssim LE \lesssim 30KN + 0.7 \times$ (vertical load due to max. ice on earth wire)

2) Local ice on one earth wire

See fig. 5.

LE from 20 KN (lower limit) to 56 KN
The upper limit of LE = 30KN + 0.7 x (vertical load due to local ice)
In this case the lower limit of $QLF \gtrsim 10KN$

If the upper limit of the longitudinal load from the earth wire is exceeded, the earthwire will slide in the clamp.

Tension towers are designed for the same iceload cases, but local ice is replaced by the broken conductor case. See fig. 6.

Experience suggests that the ability of the suspension towers to withstand longitudinal loads are sufficient to prevent cascading.

## FUTURE WORKS

We have at present no plans for the establishment of more field stations, but we intend for as long as possible, to continue operating those already established. Work will also be carried out to improve measurement techniques.

Another project of some interest are the test spans on "Gaustadtoppen" mountain. "Gaustadtoppen", altitude 1800 metres a.s.l., is situated in south-eastern Norway and has severe climatic conditions.

Heavy icing and strong winds occur several times during a normal winter.

Test spans put up during the period 1960-65 showed that expected iceloads on a single conductor of approx. 250N per metre were far exceeded and led to the collapse of the spans.

Design iceloads on a single conductor for the new test spans are assumed to be 500N per metre.

The main purpose of the test spans are to study and test accessories such as dampers, phase to phase spacers, and spacers.

Further to study the behaviour of twin-0and triple bundle conductors under heavy iceloads and strong winds.

The test spans will be equipped with load cells to measure the conductor tension at the terminal towers. A video camera will be installed to record the movement of conductors and the ice accretion on conductors. Wind speed, temperature, and humidity will also be recorded.

Instrument panels will be placed indoors and electric power for instruments is also available.

[1] Norwegian Research Institute of Electricity Supply.
Technical Report, Part I, Dec. 1959 (in Norwegian).

[2] Norwegian Research Institute of Electricity Supply.
Technical Report, Part II, 1968 (in Norwegian).

4371mAMW

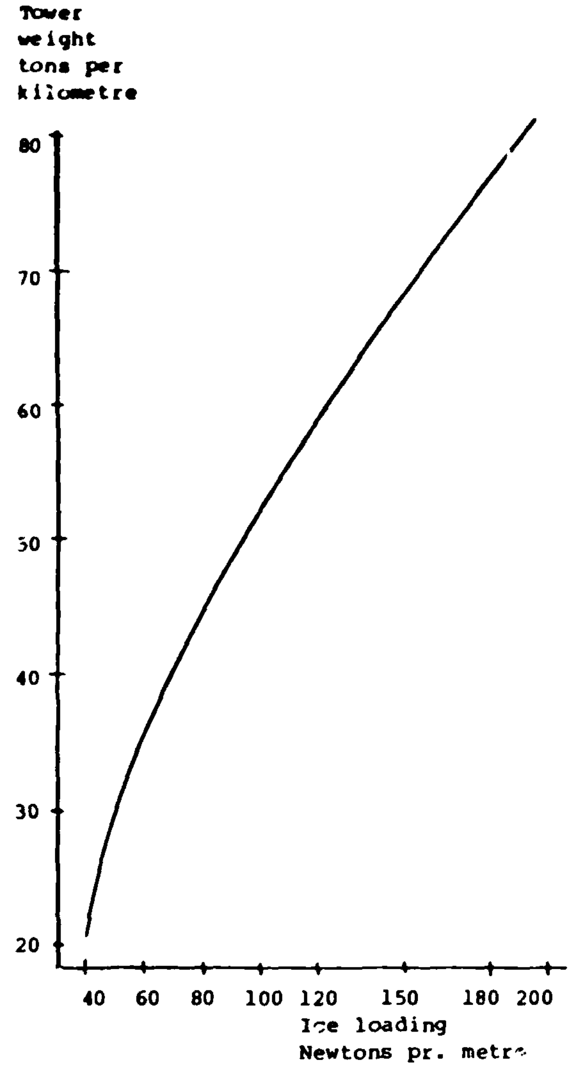

Figure 1.

Correlation between iceload on conductors and tower weight per kilometre.

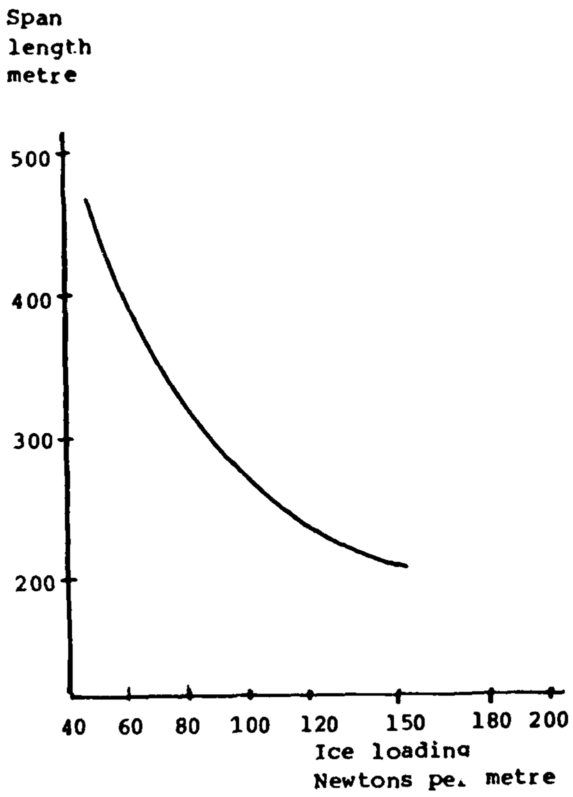

Figure 2.
Relation between ice loading and span length.

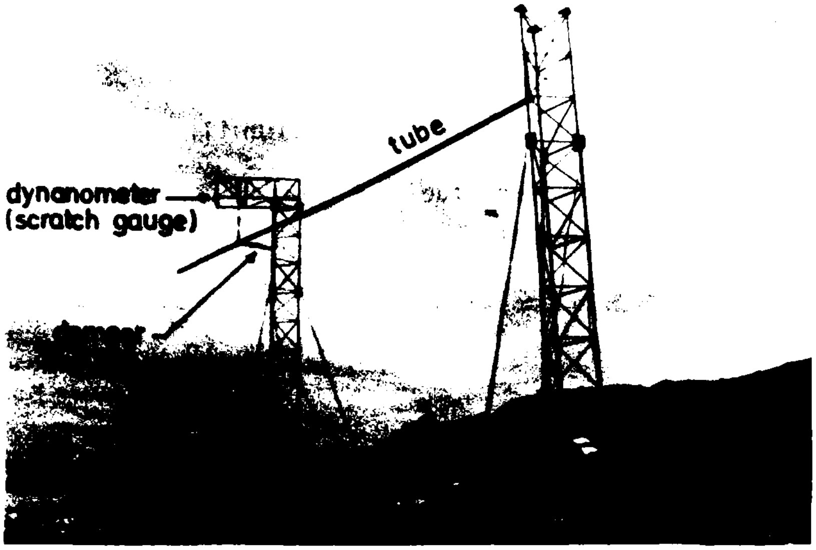
tube
dynanometer
(scratch gauge)
damper

Test station

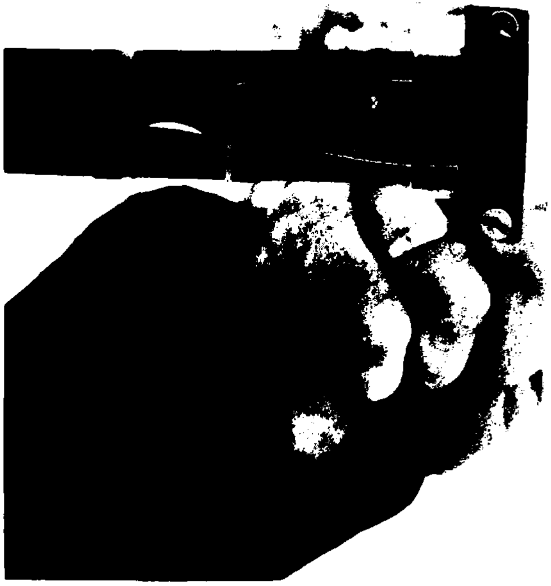

Prewitt scratch gauge

Dynanometer

Fig. 3

Range of longitudinal loads:
QLF from 25 kN (lower limit) to 78 kN

Limits of longitudinal loads from earth wires (LE):

$10\ \mathrm{kN} \leq LE \leq 30\ \mathrm{kN} + 0{,}7 \times$ (vertical load due to max ice on earth wire)

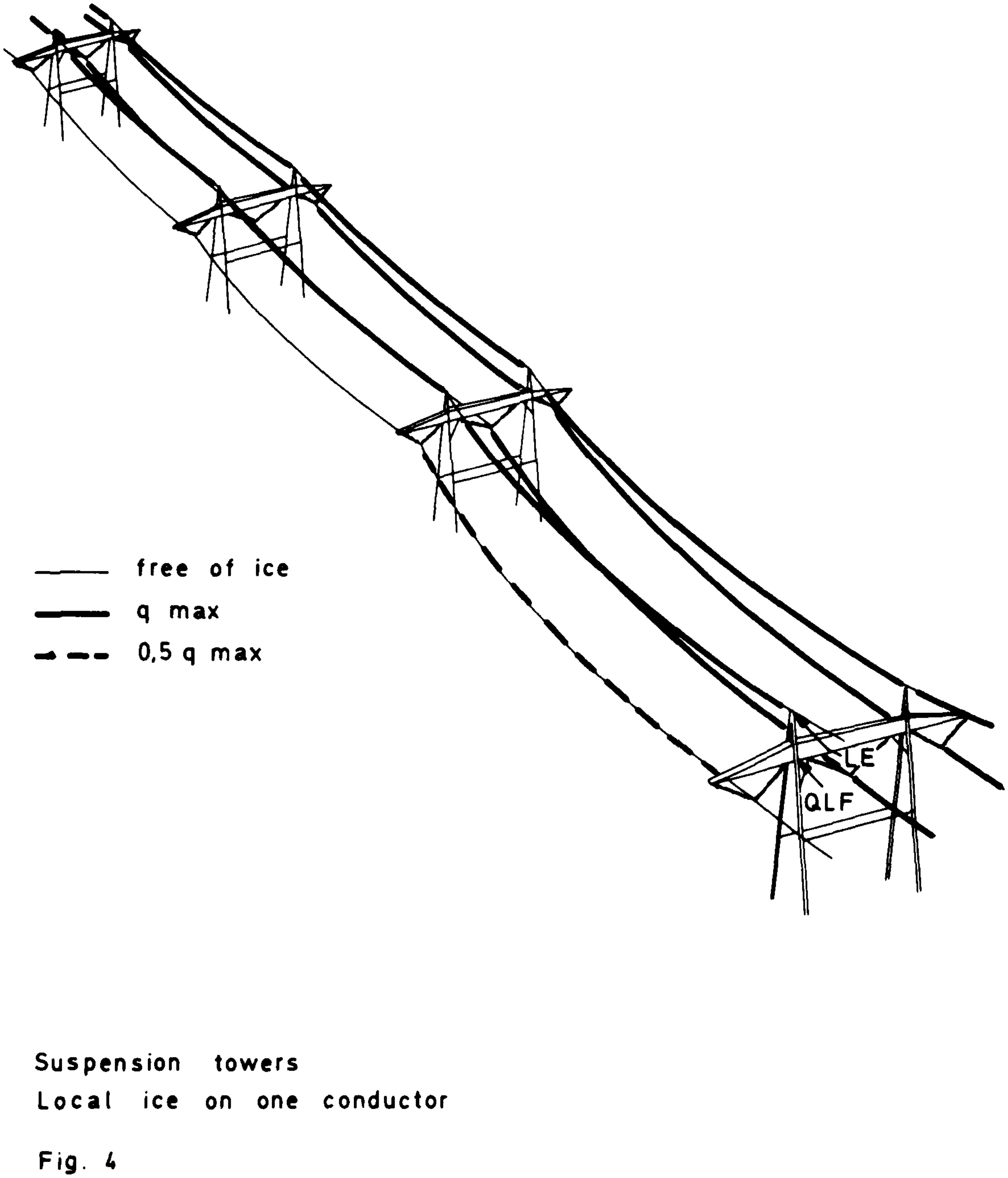
free of ice
q max
0,5 q max
LE
QLF

Suspension towers
Local ice on one conductor

Fig. 4

Range of longitudinal loads :
LE from 20 kN (lower limit) to 56 kN

Upper limit for longitudinal loads from earth wire :
LE ≤ 30 kN + 0,7 × (vertical load due to local ice)

Lower limit of QLF ≥ 10 kN

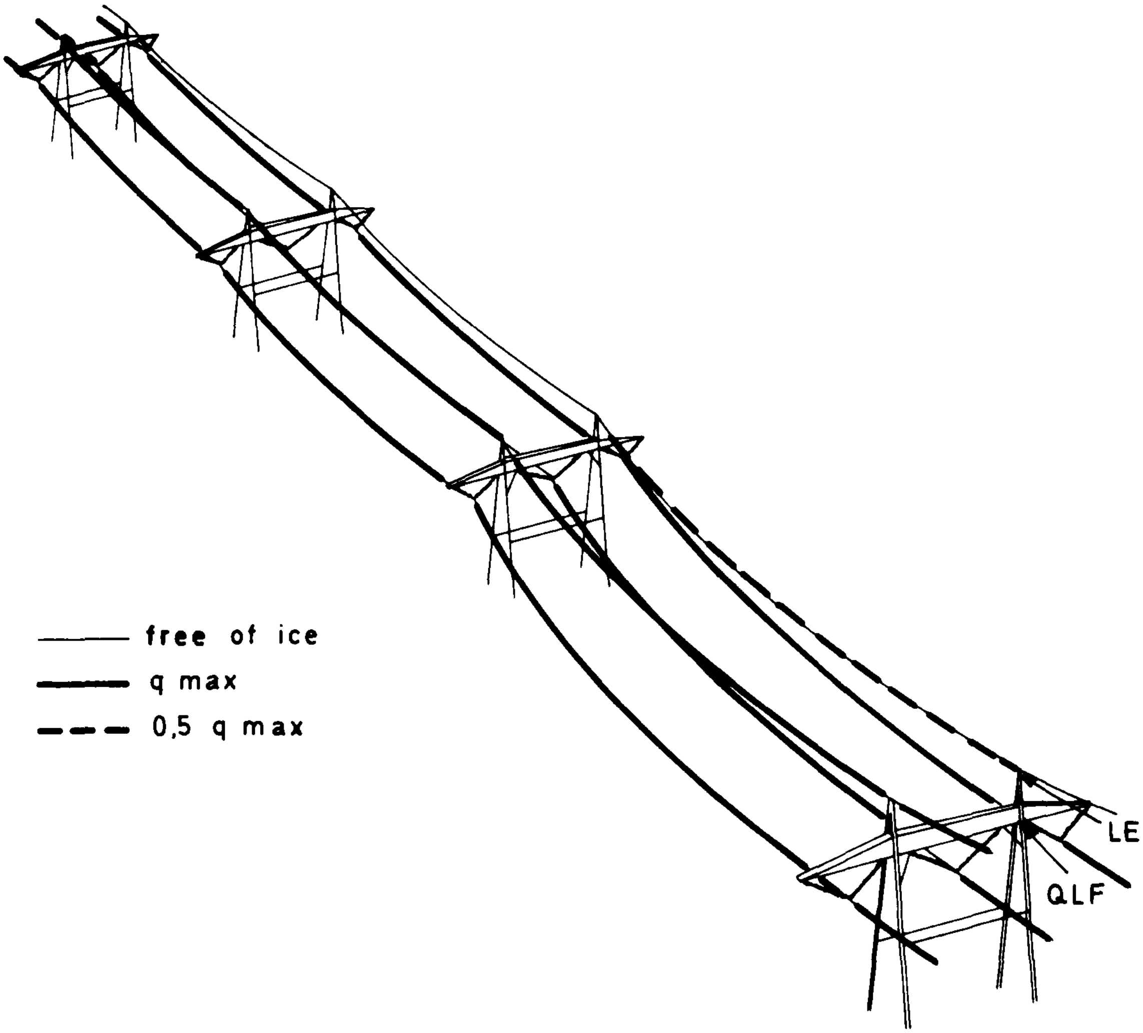
LE
QLF
free of ice
q max
0,5 q max

Suspension towers
Local ice on earthwire

Fig. 5

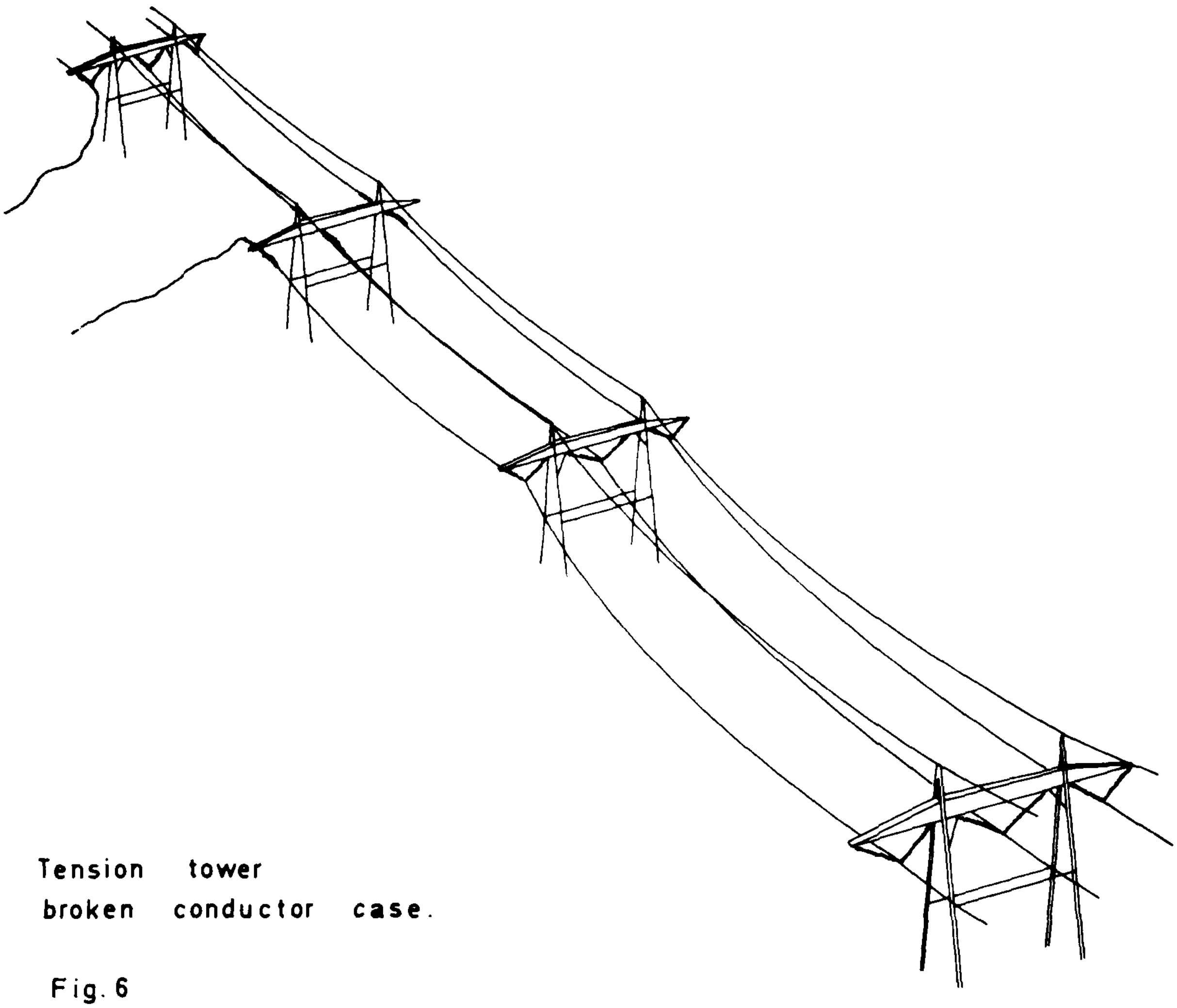

Tension tower broken conductor case.

Fig. 6

DISCUSSION

Laflamme: In your cost analysis you relate the ice loading to the cost of the towers. Are you planning to go a bit further, instead of just taking the weight, but look at the overall cost and try to use another type of tower? There are many types of tower which are less expensive and use less steel.

Evensen: Yes, I know. Oh yes. We have done some work on that. We are working on development of a [V-type] of tower ... something similar to what you have in Canada. It has a cross-arm. We considered that and we also tried to introduce it in Norway but it has met stiff opposition... So it hasn't got anywhere yet.

Mozer: Have you had any failures on your line system due to broken conductor associated with heavy ice? Secondly, is this part of the reason why your cost curves, your weight per kilometer as a function of ice load, goes up so high because of your combination of broken conductor and heavy ice?

Evensen: Yes, certainly. But I don't know if I can say with any certainty that we have experienced failure because of broken conductor. But what I forgot to mention early on - we have had quite a lot of outages caused by the sagging of the earth [ground] wires. As far as I know we haven't had any broken conductor causing any damage.

Pohlman: Your cost curves, where you're plotting against increasing ice loads - that is only based on the cost of the structure? It doesn't include erection and foundation?

Evensen: No, but as I said it's modified by a construction factor [...] taking into consideration soil conditions, the method of erection, accessability, and so on. It seems to be quite a good indication of what it's all about.

Patnaik: These tower weights you have given - are they for a particular type of steel?

Evensen: Yes, what we call 37 steel.

Phan: Do you have an added factor for the type of ice accreted on the conductor and not on the [ground] wire?

Fikke: On this transmission line there are big line diameters, the conductors are not heated. We have to [...] with cold conductors . There is no significant difference. There can be a difference between the ground wire and the conductor.

AD P001698

# MEASUREMENT OF ICE ACCRETION ON OVERHEAD TRANSMISSION LINE CONDUCTORS

S.G. Krishnasamy  Ontario Hydro, Toronto, Ontario, Canada

## ABSTRACT

The information gathered on ice storms between 1975 and 1982 at Ontario Hydro's five tower load monitoring stations have been analyzed to study ice accretion on transmission line conductors and its consequences. The data show that the drag forces of lightly ice covered conductors are significantly higher than that of ice free conductors and confirm that conductor galloping occurs only under certain wind and icing conditions.

## INTRODUCTION

For the past several years Ontario Hydro, through a network of four transmission line load monitoring sites (Table 1), has been involved in the measurement of weather related loads on transmission structures. As a part of this long range program a complete instrumentation package/1/ has been developed to measure wind and ice loads on conductors, insulator swing angles, dynamic loads due to conductor oscillation, wind speed and direction, air temperature and selected structural responses.

*In this paper, data on several ice* storms are analyzed to study the process of ice build-up, conductor oscillation and the resulting loads on transmission structures. The effect of ice accretion on conductor drag force is also discussed.

TABLE I

DETAILS OF TRANSMISSION LINES AT TOWER LOAD MEASUREMENT SITES

| TOWER LOCATION AND IN-SERVICE YEAR | | APPROXIMATE LINE ORIENTATION* | AVG SPAN LENGTH (m) | TOWER HEIGHT (m) | CONDUCTOR SIZE (mm) | LOAD CELL HEIGHT (m) | WIND SENSOR HEIGHT (m) | SITE DESCRIPTION |
|---|---|---|---|---|---|---|---|---|
| ORANGEVILLE<br>1975 | | 115 | 459 | 46 | 34** | 35 | 48 | SLIGHTLY ROLLING FARMLAND WITH SCATTERED TREES AND BUSHES |
| LONDON<br>1976 | | 0 | 418 | 43 | 28** | 38 | 45 | FARMLAND WITH DENSE BUSHES, BORDERED ONE SIDE BY HOUSES |
| BRANTFORD<br>1978 | | 60 | 328 | | 34** | 21 | 28 | FLAT FARMLAND WITH SCATTERED TREES AND HOUSES |
| NANTICOKE<br>1976 | 230 kV | 165 | 216 | 40 | 41** | 34 | 42 | |
| 1981 | 500 kV | 165 | 216 | 37 | 24*** | 36 | 39 | |

* DEGREES CLOCKWISE FROM NORTH
** SINGLE STEEL REINFORCED ALUMINUM CONDUCTOR
*** STEEL REINFORCED ALUMINUM 4-CONDUCTOR BUNDLE

## TOWER LOAD MEASURING AND DATA ACQUISITION (TOLDA) SYSTEM

The conductor load measuring system/1/ consists of a commercial load cell and two rotary transducers attached through a universal joint to the tower arm in series with the insulator string. The insulator swing angles in two orthogonal directions are measured by the two rotary transducers mounted on the load cell frame. From the measured insulator string load and swing angles, the vertical, longitudinal and transverse components of conductor load can be calculated. Strain gauges and linear-displacement transducers are also used to measure the response of tower legs and foundation movements respectively. The instruments are effectively protected against snow, ice and rain. A propeller-type anemometer located at the top of the tower is used to measure wind speed and direction.

The data acquisition in the TOLDA System consists of a micro-processor-based data analyzer and a digital tape recorder. It is capable of providing statistical information on conductor loads and wind, and switching to a faster recording mode for collecting data on ice storms and conductor galloping.

The TOLDA System, which is designed to operate from a storage battery, has a low power requirement and is suitable for remote applications. The battery can be kept charged by a solar panel or some other low-power source. A view of the TOLDA System and a schematic of the measuring and data acquisition system installed on a 500 kV line at Nanticoke are shown in Figures 1,2 and 3.

## TRANSVERSE PRESSURE ON TRANSMISSION LINE CONDUCTOR

The transverse horizontal mean wind pressure on a transmission conductor can be calculated by the following relationship:

$$p = \frac{1}{2} \rho_a U^2_o C_{DC}$$

where p = wind pressure on conductor

$\rho_a$ = air density

$U_o$ = mean wind speed normal to conductor, and

$C_{DC}$ = conductor drag coefficient

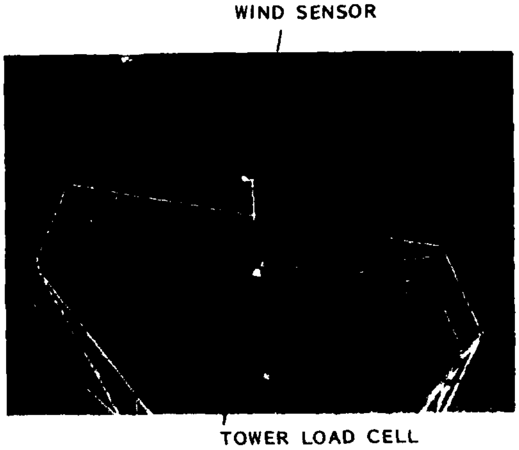

FIGURE 1(A)

TOWER LOAD CELL AND WIND SENSOR AT NANTICOKE (500 kV)

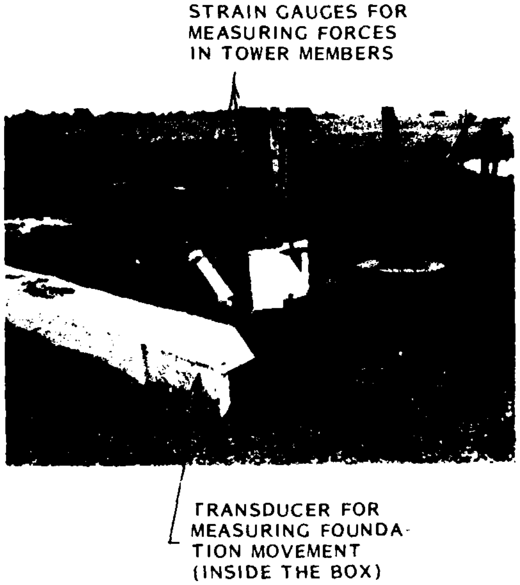
STRAIN GAUGES FOR MEASURING FORCES IN TOWER MEMBERS
TRANSDUCER FOR MEASURING FOUNDATION MOVEMENT (INSIDE THE BOX)

FIGURE 1(B)

INSTRUMENTS FOR MEASURING TOWER MEMBER FORCES AND FOUNDATION MOVEMENT

The use of an appropriate value for the conductor drag coefficient is critical in calculating realistic conductor loads. A value of unity is commonly used in design for both ice free and ice covered conductors. As seen later in the paper the value of unity for $C_{DC}$ could lead to excessive loads at certain conditions.

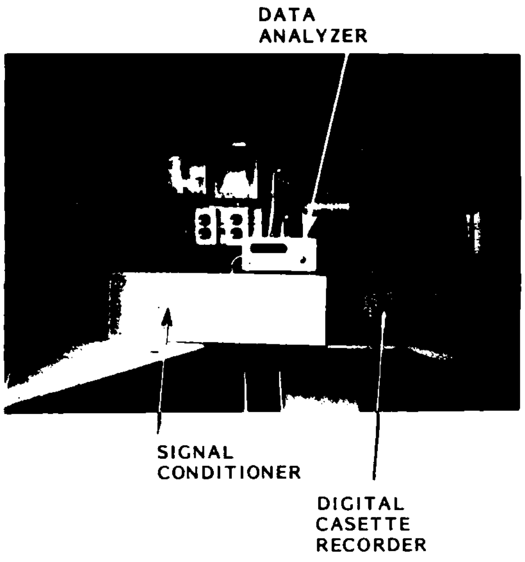
DATA ANALYZER
SIGNAL CONDITIONER
DIGITAL CASETTE RECORDER

FIGURE 2

DATA LOGGING INSTRUMENTATION AT NANTICOKE (500 kV)

In this section, the conductor drag coefficients calculated from wind and conductor load data at one of the Ontario Hydro's tower load monitoring sites are correlated with those determined from wind tunnel investigations on similar conductors. The effect of ice accretion on conductor drag forces is also discussed.

For a given terrain the drag coefficient is a function of wind speed and conductor load as explained in /2/.

### Drag Coefficient of Ice Free Conductors

In Figure 4, the values of conductor drag coefficient calculated from the measured data for the Nanticoke (230 kV) test site are compared with values obtained from wind tunnel studies/3,4/. Even though the shape of the $C_{DC}$ curves obtained from the wind tunnel and long-span measurements is similar, the latter values are significantly lower. The reasons for the lack of good correlation between two sets of $C_{DC}$ data are currently under investigation. The influence of end conditions used and the absence of turbulence in the wind tunnel modelling could be the cause for the observed discrepancies.

### Drag Coefficient of Ice Covered Conductors

In calculating the transverse wind pressure on ice covered conductors, the value of $C_{DC}$ normally used is the same as that of ice free conductors. A number of storms from the Nanticoke (230 kV) test site, during which the conductor was covered with a thin coat of ice, were analyzed to study the effect of ice accretion on conductor drag coefficient. The maximum measured equivalent radial ice on the conductor during the storms did not exceed 3 mm, which decreased the roughness of the conductor.

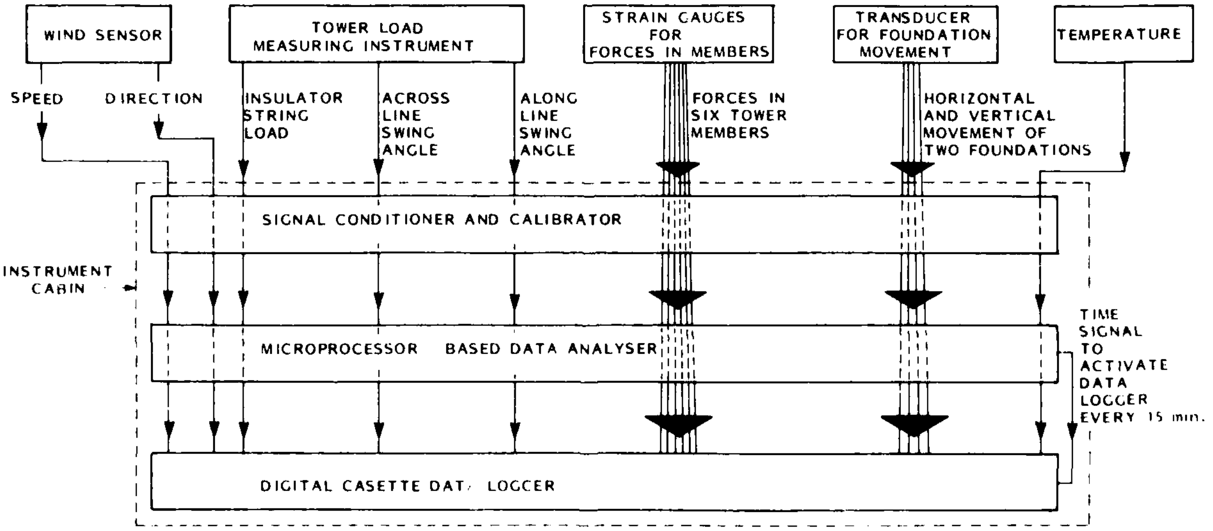
WIND SENSOR
TOWER LOAD MEASURING INSTRUMENT
STRAIN GAUGES FOR FORCES IN MEMBERS
TRANSDUCER FOR FOUNDATION MOVEMENT
TEMPERATURE
SPEED
DIRECTION
INSULATOR STRING LOAD
ACROSS LINE SWING ANGLE
ALONG LINE SWING ANGLE
FORCES IN SIX TOWER MEMBERS
HORIZONTAL AND VERTICAL MOVEMENT OF TWO FOUNDATIONS
SIGNAL CONDITIONER AND CALIBRATOR
INSTRUMENT CABIN
MICROPROCESSOR BASED DATA ANALYSER
TIME SIGNAL TO ACTIVATE DATA LOGGER EVERY 15 min.
DIGITAL CASETTE DATA LOGGER

FIGURE 3

A SCHEMATIC OF TOWER LOAD MEASURING AND DATA ACQUISITION SYSTEM AT NANTICOKE (500 kv)

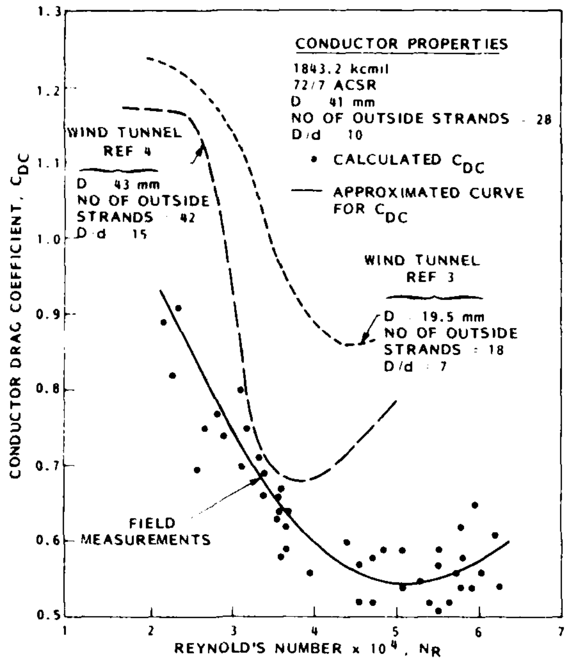

FIGURE 4

MEASURED CONDUCTOR DRAG COEFFICIENTS FOR ICE FREE CONDUCTOR AT THE NANTICOKE TOWER LOAD MEASUREMENT SITE

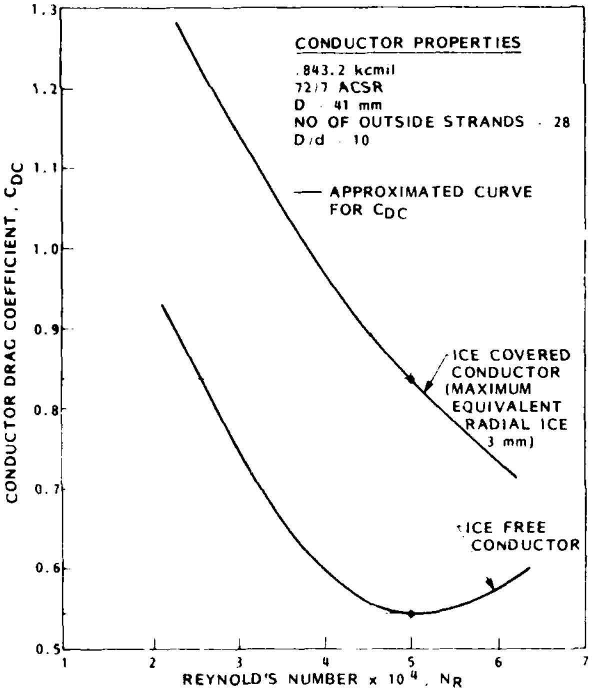

RATIO OF $C_{DC}$ CORRESPONDING TO $N_R$, $5 \times 10^4$ ,

$\frac{0.84}{0.55}$ 1.5

FIGURE 5

CONDUCTOR DRAG COEFFICIENTS FOR ICE FREE AND ICE-COVERED CONDUCTORS AT THE NANTICOKE TOWER LOAD MEASUREMENT SITE

The conductor drag coefficients of ice covered conductors are plotted in Figure 5 along with $C_{DC}$ for ice free conductors for comparison. The drag coefficient of the ice covered conductor corresponding to a Reynold's number of $5\text{x}10^4$, is about 50 per cent higher than that of the ice free conductor. The difference between the two drag coefficient curves is qualitatively similar to that observed in wind tunnel studies of rough and smooth cylinders/5/ shown here in Figure 6. The lightly ice covered conductor in this instance would be considered as a slightly rough cylinder and the ice free conductor as a rough cylinder.

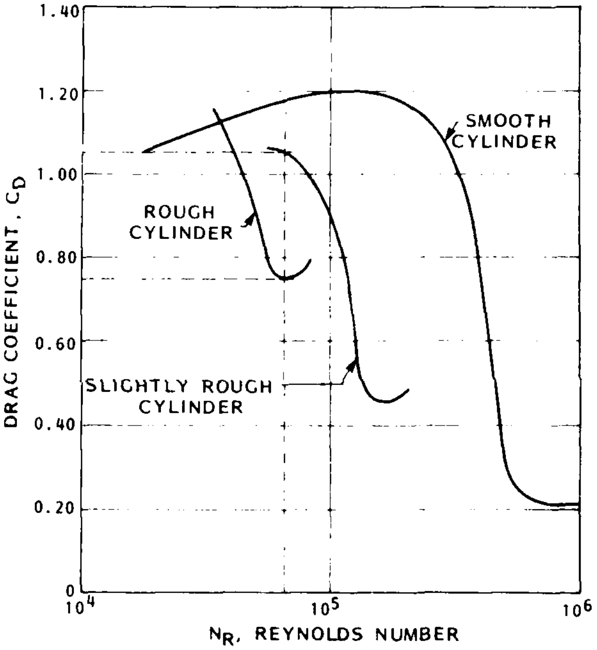

RATIO OF $C_D$ CORRESPONDING TO $N_R$, $8 \times 10^4$

$\frac{1.05 \text{ (FOR SLIGHTLY ROUGH CLYINDER)}}{0.75 \text{ (FOR ROUGH CYLINDER)}}$ 1.4

FIGURE 6

VARIATION OF DRAG COEFFICIENT FOR CIRCULAR CYLINDER 5

## ICE ACCRETION ON TRANSMISSION LINE CONDUCTORS AND ITS CONSEQUENCES

Since 1976 data have been gathered on a total of 26 ice storms from the Orangeville, London and Nanticoke (230 kV) tower load monitoring sites. In this section the data have been analyzed to study ice accretion on conductor and conductor galloping.

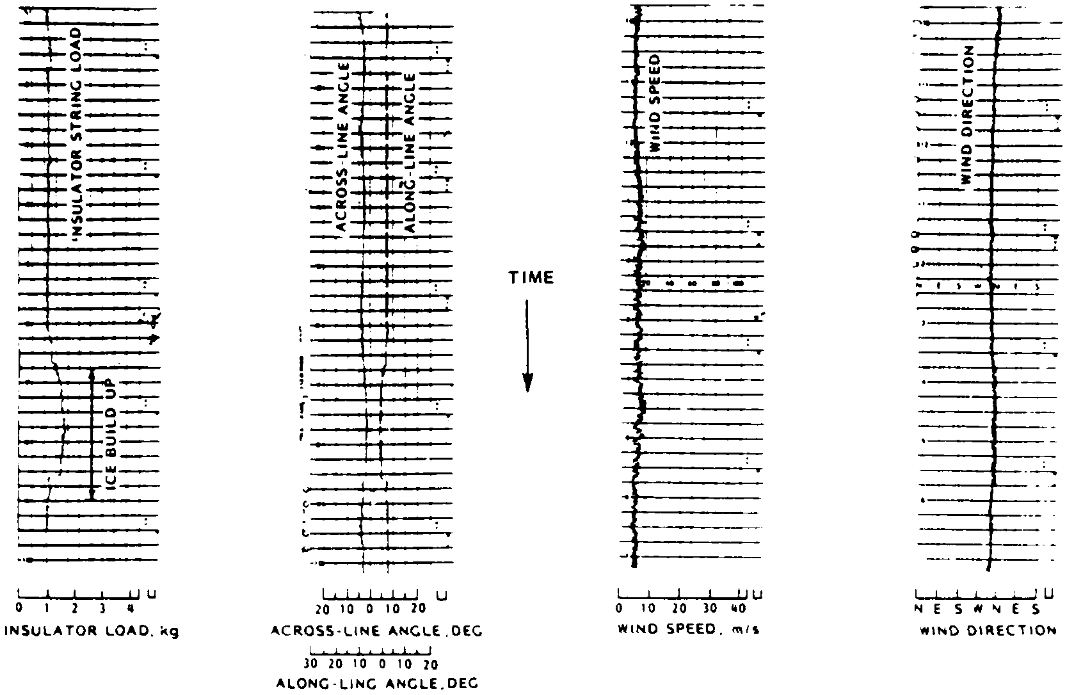

FIGURE 7

WIND AND CONDUCTOR LOAD DATA FROM ORANGEVILLE TEST SITE SHOWING ICE BUILD-UP

## A Typical Record of Ice Accretion on Conductor

A typical record showing ice load on a conductor obtained in the early hours of January 25, 1979, from the Orangeville test site is shown in Figure 7. The gradual ice build-up started several hours before reaching 12 mm maximum equivalent radial ice at about 0800 hours. During that period, the one-minute mean and peak wind speeds were about 7 m/s, and 10 m/s, respectively, with an approximately 90 degrees incidence angle to the line axis. The force along the line axis was about 0.9 kN. Several such records have been analyzed for ice accretion and some typical results are summarized in Table 2.

TABLE 2

TYPICAL ICE STORMS

| DATE TIME PLACE | TIME OF MAXIMUM ICING | WIND SPEED DURING ICING (m/s) | | PREVAILING WIND DIRECTION | AMOUNT OF EQUIV RADIAL ICING (mm) | ACROSS THE LINE ANGLE (DEG) | ALONG THE LINE ANGLE (DEG) | COMMENTS |
|---|---|---|---|---|---|---|---|---|
| | | MEAN | MAX | | | | | |
| DEC 17, 1976 1200 h TO DEC 18, 1976 1200 h ORANGEVILLE | ABOUT 1200 h DEC 17, 1976 | 3.6 | 4.4 | APPROX 70 DEGREES TO LINE | 6.6 | 1.0 | 0.0 | APPROX SYMMETRICAL ICING AS SEEN FROM THE ABSENCE OF LONGITUDINAL SWING |
| MAY 6, 1978 0000 2000 h ORANGEVILLE | ABOUT 1300 h | 4.2 | 5.8 | APPROX 45 DEGREES TO LINE | 13.7 | 1.0 | 5.0 | NONSYMMETRICAL ICING AS SEEN FROM THE LARGE SWING |
| DEC 3, 1976 0000 2000 h LONDON | ABOUT 1200 h | 8.9 | 14.5 | APPROX NORMAL TO LINE | 14.5 | 2.0 | 0.5 | |
| MAR 25, 1978 2200 h TO MAR 26 1978 2400 h NANTICOKE | ABOUT 0700 h MAR 26, 1978 | | | | 11.7 | 4.0 | 4.0 | NO WIND DATA AVAILABLE |

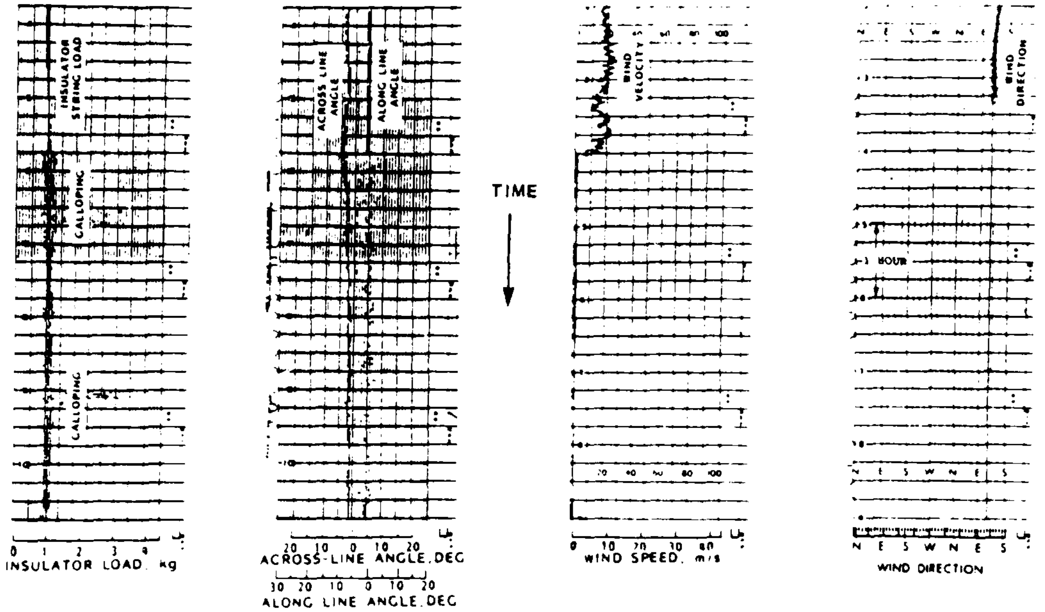

FIGURE 8

WIND AND CONDUCTOR LOAD DATA FROM NANTICOKE TEST SITE SHOWING CONDUCTOR GALLOPING

## A Typical Example of Conductor Galloping

A typical galloping occurrence at the Nanticoke (230 kV) site was analyzed to determine the dynamic forces involved. The data shown in Figure 8 were recorded on December 3, 1978, between 0500 and 1100 hours during which period the maximum vertical dynamic load (including conductor weight) was approximately 1.6 times the conductor weight. The dynamic force along the line axis was about 1.2 kN. The ice load on the conductor did not exceed 1 kg/m, which is equivalent to approximately 8 mm of radial ice. The one-minue mean and peak wind speeds recorded about 1-1/2 hours before the galloping started were about 8 m/s and 12 m/s, respectively, with a 30 degree incidence angle to the line axis. Since the anemometer became iced, no wind data were available during the galloping period.

Several other galloping records have been analyzed and some typical examples are summarized in Table 3 for the Orangeville, London and Nanticoke sites. The maximum measured vertical dynamic load on conductors is approximately two times the conductor weight. The measured dynamic force along the line axis was about 2.[illegible] kN.

## Consequences of Ice Accumulation on Conductors

Conductor galloping was observed in 15 out of the 26 recorded ice storms almost every time the equivalent radial ice was approximately 10 mm or less and the wind speed was favourable, with the incidence angle about 90 degrees to the line axis. In all the galloping records the one-minute mean wind speed did not exceed 10 m/s. Even when the equivalent radial ice was approximately 10 mm or less, if either the wind incidence angle to the line axis was significantly less than 90 degrees or the wind speed was considerably higher than 10 m/s, usually galloping did not occur. If the equivalent radial ice exceeded 10 mm, even wind normal to the line axis usually did not result in conductor galloping. In most galloping events the along-line swing angle either exceeded the corresponding across-line swing angle or was about the same, suggesting a two dimensional conductor motion.

The measured ambient temperature during various conductor galloping events ranged from [illegible]°C to -18°C. Favourable wind conditions and ice on the conductor from an earlier storm

TABLE 3

TYPICAL GALLOPING EVENTS

| NO. | DATE TIME PLACE | TIME OF ICING | MEAN WIND SPEED DURING ICING (m/s) | PREVAILING WIND DIRECTION | AMOUNT OF EQUIV RADIAL ICING (mm) | MAX WIND SPEED DURING ICING (m/s) | ACROSS-THE-LINE ANGLE (DEG) | ALONG-THE-LINE ANGLE (DEG) | COMMENTS |
|---|---|---|---|---|---|---|---|---|---|
| 1 | FEB 26, 1977<br>1600 h TO<br>FEB 27, 1977<br>1600 h<br>NANTICOKE | MAX ICING<br>AT 0400 h<br>FEB 27, 1977 | 1.4 | ABOUT NORMAL TO LINE | 5 | 2.2 | 4.5 | 0.0 | ANOMOMETER FROZE AFTER THIS READING.<br>GALLOPING LASTED 2.5 h<br>VERTICAL DYNAMIC LOAD 1.2 X CONDUCTOR WEIGHT. NO APPRECIABLE ALONG-THE-LINE DYNAMIC FORCE. |
| 2 | DEC 3, 1978<br>0300 - 1300 h<br>NANTICOKE | MAX ICING<br>AT 0600 h | 7.5 | ABOUT 30° TO LINE | 8 | 11.7 | 4.5 | 6.0 | ANOMOMETER FROZE.<br>WIND DATA ESTIMATED FROM IMMEDIATE RECORDS. VERTICAL DYNAMIC LOAD 1.6 X CONDUCTOR WEIGHT. ALONG-THE-LINE DYNAMIC FORCE 1.2 kN. GALLOPING LASTED 5 h. |
| 3 | APR 8, 1979<br>APR 9, 1979<br>1100 h<br>NANTICOKE | UNIFORM COATING THROUGHOUT PERIOD | 9 | ABOUT NORMAL TO LINE | 8 | - | 11 | 15 | GALLOPING LASTED 11.5 h, ALMOST CONTINUOUSLY. VERTICAL DYNAMIC LOAD 2 X CONDUCTOR WEIGHT.<br>ALONG-THE-LINE DYNAMIC FORCE 4 kN.<br>ANEMOMETER MALFUNCTION. DATA FROM METEOROLOGICAL SITE 2 km AWAY. |
| 4 | APR 3, 1978<br>0,400 2400 h<br>LONDON | MAX ICING OCCURRED DURING<br>1200 - 1500 h | 7.2 | ABOUT NORMAL TO LINE | 3.4 | 7.5 | 2.5 | 1.5 | GALLOPING OCCURRED.<br>NO SIGNIFICANT ALONG-THE-LINE DYNAMIC FORCE. VERTICAL DYNAMIC LOAD 1.2 X CONDUCTOR WEIGHT. |
| 5 | NOV 24, 1978<br>0000 - 0400 h<br>LONDON | VERY LIGHT UNIFORM COATING THROUGHOUT PERIOD | 8.9 | ABOUT NORMAL TO LINE | - | 12.5 | 0.0 | 2.0 | GALLOPING OCCURRED.<br>ICE COATING TOO THIN FOR QUANTATIVE MEASUREMENT.<br>NO SIGNIFICANT DYNAMIC LOAD. |
| 6 | MAR 26, 1978<br>0000 h TO<br>MAR 27, 1978<br>1800 h<br>ORANGEVILLE | MAX ICING<br>AT 1200 h | | | 3.0 | - | 0.5 | 1.0 | GALLOPING OCCURRED.<br>NO WIND DATA AVAILABLE. NO SIGINIFICANT ALONG-THE-LINE DYNAMIC FORCE. VERTICAL DYNAMIC LOAD 1.8 X CONDUCTOR WEIGHT. |

resulted in galloping at significantly below freezing temperatures. In situations where the temperature was around freezing at the time of galloping normally the ice shedding led to the end of galloping. When the galloping occurred at a temperature significantly lower than 0°C it was the absence of appropriate wind conditions that halted the conductor motion.

## CONCLUSIONS

Since 1975 Ontario Hydro has been gathering data on conductor wind and ice loads at five test sites in Southern Ontario. The analysis of data collected from three test sites between 1975 and 1982 leads to the following conclusions:

- The conductor drag coefficient of ice free conductors obtained from wind tunnel studies are significantly higher than those obtained from actual field measurements. The influence of end conditions used and the absence of turbulence in the wind tunnel could be the cause for the observed discrepancies.
- The field data on conductor loading indicate that the conductor drag coefficients of lightly ice covered conductors are significantly higher than that of ice free conductors.
- Conductor galloping occurred almost every time the equivalent radial ice was approximately 10 mm or less and the wind speed was favourable, with wind incidence angle about 90 degrees to the line axis. In all the galloping events recorded the one-minute mean wind speed ranged from 1.5 m/s to 10 m/s.
- Even when the equivalent radial ice was approximately 10 mm or less, if the wind incidence angle to the line axis was significantly less than 90 degrees, usually galloping did not occur.
- If the equivalent radial ice exceeded 10 mm, even wind normal to the line axis usually did not result in conductor galloping.
- In most of the galloping events the longitudinal insulator swing angle either exceeded the corresponding transverse swing angle or was about the same suggesting a two-dimensional conductor-motion.

## REFERENCES

1. S.G. Krishnasamy, "Wind and Ice Loading on Overhead Transmission Lines", Proceedings of the Fourth US National Conference on Wind Engineering Research, University of Washington, Seattle, Washington, USA, July 27-29, 1981.

2. "Transmission Line Wind Loading Research", EPRI Project RP-1277, Interim Report, Palo Alto, California, April 1980.

3. J. Counihan, "Lift and Drag Measurements on Stranded Cables", Report No 117. Imperial College of Science and Technology, Aeronautics Department, August 1963.

4. D.A. Davis, D.J.W. Richards, and R.A. Scriven, "Investigation of Conductor Oscillation on the 275 1V Crossing Over the Rivers Severn and Wye, Proceedings of IEE, Volume 110, No 1, January 1963, pp 205-219.

5. J.A. Chadha, "Galloping Mechanism-Based on the Flow of Air in the Critical Range of Reynold's Number", Ontario Hydro Research Division Report No 72-219-K, June 1, 1972.

## DISCUSSION

Krishnasamy: [...] as much as two times the conductor tension, in several places. The tension was estimated at two because we don't have any way of measuring it. The one galloping we had, two years ago, lasted continuously about seven hours.

Ackley: How did you estimate the thickness of the accretion for your $C_d$ vs R?

Krishnasamy: Well, we just used the weight and calculated the equilibrium radius.

Ackley: So you just [reduce] everything to an equivalent?

Krishnasamy: Yes, we considered it glaze ice because the area where we are measuring this is just glaze ice.

AD-A131 869 PROCEEDINGS OF INTERNATIONAL WORKSHOP ON ATMOSPHERIC ICING OF STRUCTURES (..(U) COLD REGIONS RESEARCH AND ENGINEERING LAB HANOVER NH L D MINSK JUN 83 4/4

UNCLASSIFIED CRREL-SR-83-17 F/G 8/12 NL

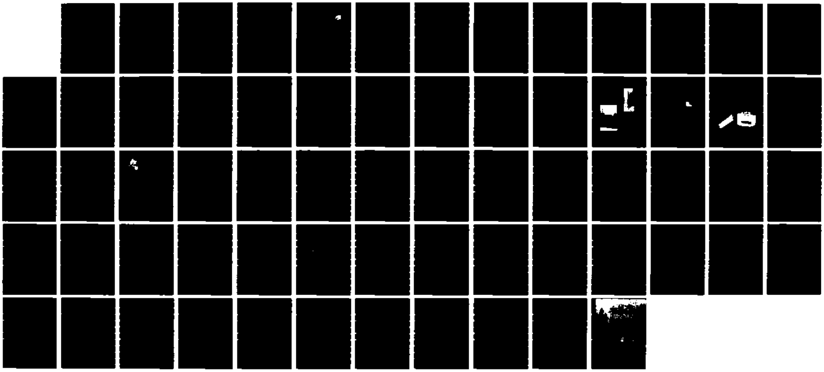

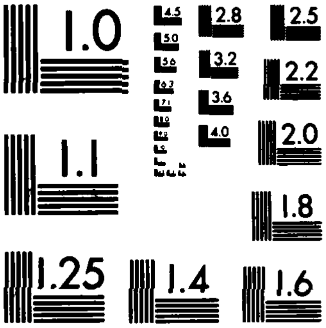
1.0
4.5
5.0
5.6
6.3
7.1
8.0
9.0
2.8
3.2
3.6
4.0
2.5
2.2
2.0
1.1
1.8
1.25
1.4
1.6

MICROCOPY RESOLUTION TEST CHART
NATIONAL BUREAU OF STANDARDS-1963-A

AD P001699

# EXTREME GLAZE AND RIME ICE LOADS IN SOUTHERN CALIFORNIA
## Part I: Rime

Joel H. Mallory    Southern California Edison Company
David C. Leavengood    Leavengood & Associates

Two 500 kV transmission lines of the Southern California Edison Company (SCE) originally crossed over the Anaverde Summit area, southwest of Palmdale, at an elevation of approximately 1,524 meters (5,000 feet). The design of these lines was based on California Public Utility Commission (CPUC) G.O. 95-Heavy Loading, 1.229 Kg/m$^2$ (6 lb/ft$^2$) wind on 1.27 cm (1/2 inch) radial ice. Because of the 1,524 meters (5,000 foot) elevation and wind problems that occurred in this area prior to operation of the line, winds of 193 Km/hr. (120 mph) without ice were also accounted for in the design criteria.

In the first years of operating experience, 1967-68, it soon became apparent that the lines were underdesigned for the severe snow, rime ice and wind loads that would occur in the Anaverde Summit area. SCE hired a meteorological consultant, Meteorology Research, Inc. (MRI), who, with the use of a mechanical weather station and previously recorded data in the region, was able to predict storm loadings, including frequencies for the Anaverde Summit area.

The lines were analyzed in terms of withstanding separate predicted ice and wind loads for different return periods. It was finally concluded that due to the severity of ice storms that may occur in the Anaverde Summit area, the lines should be relocated to a lower elevation on the leeward side.

Based on transmission line operating experience at Anaverde Summit, SCE adopted the criteria of requiring meteorological studies to be made on all future transmission line routes.

## ANAVERDE SUMMIT AREA

Southern California Edison Company's No. 1 and No. 2 Midway-Vincent 500 kV Transmission Lines originally crossed over the Anaverde Summit area at an elevation just over 1,524 meters (5,000 feet). The summit area is located approximately 8 miles west of Palmdale, California.

These lines were designed based on California Public Utility Commission (CPUC) G.O. 95-Heavy Loading, 1.229 Kg/m$^2$ (6 lb./ft.$^2$) wind on 1.27 cm (1/2 inch) radial ice. Because of the high elevation, local topography and wind problems that occurred prior to the operation of the line, winds of 193 Km/hr. (120 mph) without ice were also accounted for in the design criteria.

Heavy ice accumulated on the transmission lines during the first operating years of the lines, twice in April 1967, once in December 1967, and January 1968. It soon became very apparent that the line design could not withstand vertical loads caused by extremely heavy ice that may form in this area.

Meteorology Research, Inc. (MRI) was contracted by SCE to investigate the possible occurrences and magnitude of icing in the Anaverde Summit area.

## Meteorological Study

Because of those problems which occurred prior to the completion of construction and during the first operating years of the lines, a meteorological study of the Anaverde Saddle Area was conducted for SCE by the meteorological consulting firm. The study consisted of a literature search of reported icing research and icing occurrences on transmission lines, a field measurement study and the analysis and conclusion of the program.

The literature search indicated that little research had been conducted on the icing of transmission lines and the available icing models were not adequate to describe the accumulation of rime ice on a conductor in a real world situation.

The field studies included the installations of wind-speed, wind-direction, and temperature measurement equipment at three locations. A mechanical weather station, which measured wind-speed, wind-direction and temperature, was installed at the highest point of the Summit, and another one was installed along the transmission right-of-way. The third unit, that measured wind-speed, horizontal wind direction and vertical wind direction, was installed at 24.4-m (80 ft.) above the surface on the bridge of one of the transmission towers. Data were collected from these instruments from early January through the end of April 1968. Measurements were made of the drop size of the cloud particles during the winter storm conditions at the top of Anaverde Summit. Daily observations of sky conditions, visibility, wind-speed and wind direction were taken along the transmission line on the Summit. In addition, a detailed onsite evaluation was made of a severe ice storm that occurred during the measurement period.

The preliminary evaluation of the line location along the Anaverde Summit by the meteorologist revealed the following:

1. The location of the line was along the southwest slope of the Anaverde Summit which placed it on the upslope side of the mountain during the occurrence of the most frequent icing condition in Southern California (southwesterly wind flow, prefrontal, during winter storms).

2. The wind speeds during the storm conditions would be much greater than for a typical 1524 meter (5000 ft.) location in Southern California because of the extreme topographical channeling upwind (southwest) of the Anaverde Summit.

3. The transmission lines were oriented 45° to 75° to the prefrontal winds.

4. The transmission lines were oriented about parallel to the post-frontal (northwest to northerly) wind directions.

5. Ice could occur with post-frontal winds.

6. The strongest wind speeds normally occurred with post-frontal wind directions or with northeasterly winds (known as Santa Ana winds).

7. Topographical channeling did not exist to the northwest or northeast of the summit area; therefore, the typical winds would not have been increased in magnitude.

8. The winds from 160° through 250 had an upward component as they crossed the Summit area. The winds from 315° through 90° had a downward component as they passed the transmission lines. A downward component would tend to dampen conductor motion, whereas an upward component would tend to increase conductor motion.

During the analysis phase of the study, the data from the Anaverde Summit on the frequency of occurrence and severity of rime ice and wind velocities was "calibrated" with respect to a nearby National Weather Service station (Sandberg) with a long period of record. Criteria were developed that related icing occurrences at Anaverde Summit to icing occurrences at Sandberg. These criteria permitted a search of icing occurrences over a ten-year period of past weather data at Sandberg. From that data an emperical rime ice model was developed.

During the analysis phase of the study, the data from the Anaverde Summit, on the frequency of occurrence and severity of rime ice and wind velocities, were "calibrated" with respect to a nearby National Weather Service station (Sandberg) with a long period of record. Criteria were developed that related icing occurrences at Anaverde Summit to icing occurrences at Sandberg. These criteria permitted a search of icing occurrences over a ten year period of past weather data at Sandberg. From those data an empirical rime ice model was developed.

In order to develop a knowledge of icing and winds at the Anaverde Summit, it was necessary to relate the summit area to an area with a long period of weather data. Fortunately, a National Weather Service Station (Sandberg) with a long period of data existed within thirty miles of the summit. The two stations were in the same mountain range with Sandberg at 1370m (4500 feet) elevation compared to the 1524m (5000 feet) at Anaverde Summit. The severe topographical channeling to the south-southwest of Anaverde Summit was the major difference between the two locations.

The data was analyzed to determine:

1. Maximum winds, no ice
2. Maximum ice, no winds
3. Combined maximum winds and ice

### Winds

Wind speeds measured at Anaverde Summit were compared to simultaneous wind speeds at Sandberg. The analysis was divided into two ranges of directions, winds affected by the channeling upwind of the summit and wind directions that were not affected by the channeling. Two winters of data are represented in Figures 1 and 2. Figure 1 indicates that similar terrain subjected to similar meteorological conditions, produces essentially the same wind speeds.

Figure 2 relates the effect of the upwind channeling at Anaverde Summit to the nonchanneled air flow at Sandberg. At wind speeds of 7 mps (15 mph) or less the channeling effect increases the wind speeds by a factor of 2.25. However, the increased friction associated with the channeling and ridge speed-up effect will not permit such a large factor at higher wind speeds. A detailed analysis of hourly winds over the two years measurement period showed the wind directions at the Anaverde Summit during storms and/or icing conditions were from the S to SSW 95 percent of the time.

After the comparisons were developed, a long term wind history was constructed for the Anaverde Summit by utilizing Sandberg data and the above comparisons for specific meteorological conditions.

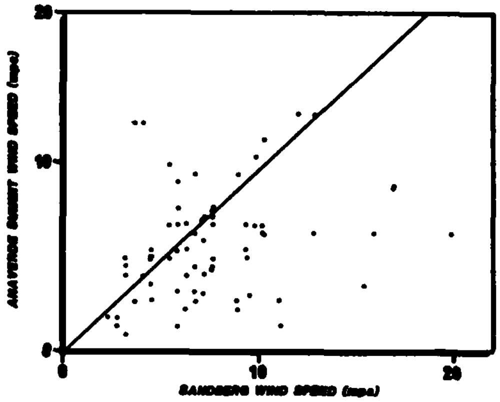

Fig. 1 SANDBERG AND ANAVERDE SUMMIT WIND SPEED COMPARISON FOR WNW TO NNE WIND DIRECTIONS

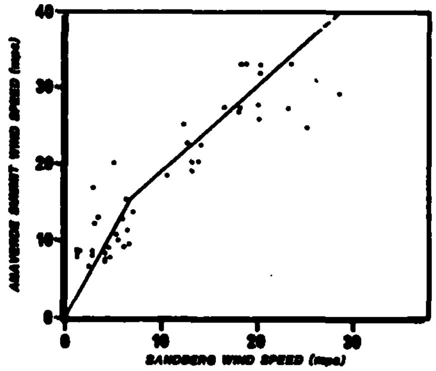

Fig. 2 SANDBERG AND ANAVERDE SUMMIT WIND SPEED COMPARISON FOR ICING CONDITIONS WITH SSE TO WSW WIND DIRECTIONS

### Icing

In order to develop an icing climatology for the Anaverde Summit, it was necessary to determine the weather conditons at Sandberg during the occurrence of icing at Anaverde Summit. The four known storm periods of ice at Anaverde were used to develop criteria for Sandberg that indicated ice was occurring at Anaverde. The criteria were developed for the two basic wind sectors at Anaverde: SSE to WSW and WNW to NNE.

The Sandberg criteria used to indicate that rime was occurring at Anaverde were:

1. Temperature 0°C

2. Visibility (horizontal) 400 m (1/4 miles)

3. Ceiling or sky conditions: 60 m (200 ft.)

4. Precipitation: light precipitation may occur, primarily light snow; however, the ceiling and visibility requirements must be met.

The ten years of Sandberg data were analyzed to determine the number of occurrences, the durations and the average wind speeds during the icing conditions. Thirty-five percent of the riming conditions with SSE to WSW wind directions were ten hours or longer. However, riming conditions associated with WNW to NNE wind directions did not exceed 11 hours during the ten years period of record.

Possible cases of wet snow and glaze were reviewed. Both those types of icing occurrences and durations were so small that loading conditions did not equal or exceed loads associated with the rime conditions.

The ice accumulations were estimated by two methods, from the theory developed by Langmuir and Blodgett (1945) and empirically from measurements of ice accumulations taken by the Japanese, Germans and at Anaverde. The theory was compared to the available observed rates of icing accumulations during specific icing conditions. Neither the rate of accumulation nor the maximum amount were predicted reasonably well. A comparison of the various data indicated that the drop size of the storms, the liquid water content and the temperature for Southern California and Japan were essentially the same. Therefore these data were used to construct an empirical model that related duration of icing conditions, average wind speed during the icing conditions and diameter of ice. The completed model is shown in Figure 3.

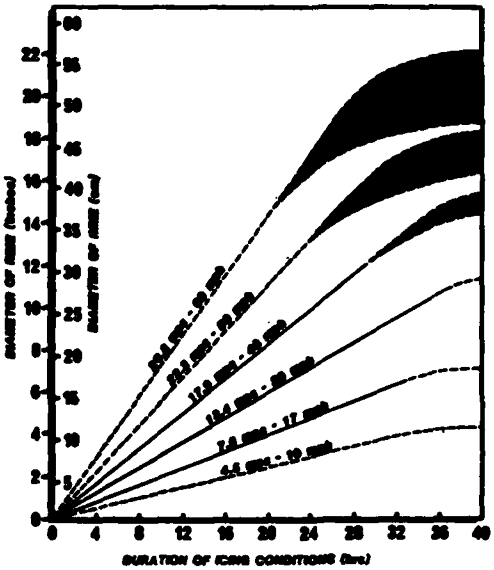

Fig. 3 GROWTH OF RIME FOR VARIOUS WIND SPEEDS AND DURATIONS OF ICING CONDITIONS

It was determined that rime ice on conductors formed either in a triangular or pennant shape or in a circular shape. The rime ice forms on the windward side of the conductor. The two shapes of rime formed because of constraints or the lack of constraints on the conductors. The circular shaped ice formed as the weight of the ice on the conductor was heavy enough to cause it to rotate. Bundled conductors will not rotate; therefore, shield wires and unbundled conductors will form circular deposits. Bundled conductors do not rotate; therefore, the ice deposit accumulates on the windward side of the conductor. The ice builds into the wind and accumulates in a pennant or elliptical shape. The circular shape contains a greater weight per unit length of conductor for the same diameter of ice than the pennant shape. If the mass of ice and wind loading are great enough to break the spacers, the conductors would accumulate rime in a circular manner and could increase the loading over initial estimates.

## Winds and Ice

The analysis of the winds during the icing conditions over the ten year period of data indicated three important findings.

1. The maximum wind speed is equally likely to occur at any time during the icing conditions.

2. The maximum wind speed during icing conditions averaged 1.5 times greater than the average wind speed.

3. The maximum wind speed, bearing on the ice loaded conductors, occurred during the icing conditions not after the icing ceased.

Based on the analysis of the ten years of data, the "calibration" of the NWS station data to represent the Anaverde Summit area, the empirical icing model and the wind speed relationships from above return periods were developed for simultaneous combinations of rime ice and wind speeds. Tables 1 and 2 show the 105 and 45 year return periods for simultaneous combinations of icing and wind along the transmission route on the Anaverde Summit. Table 3 summarizes the ranges of wind and ice loadings to be expected on the Summit area for return periods of 1.5 to 105 years.

TABLE 1

105-Year Return Period
for Simultaneous Occurrence
of 90 MPH and 20 Inches
of Rime at Anaverde Summit

| Location Construction # M-V Line 1 | Diameter of Rime (inches) | Max. 5-Min. Avg. Speed (mph) |
|---|---|---|
| 471-473 | 8 | 50 |
| 473-474 | 15 | 70 |
| 474-477 | 20 | 90 |
| 477-478 | 15 | 70 |
| 478-479 | 12 | 60 |
| 479-482 | 8 | 50 |
| 482-483 | 12 | 60 |
| 483-484 | 15 | 70 |
| 484-487 | 18 | 80 |
| 487-488 | 6 | 40 |

TABLE 2

45-Year Return Period
for Simultaneous Occurrence
of 80 MPH and 16.5 Inches
of Rime at Anaverde Summit

| Location Construction # M-V Line 1 | Diameter of Rime (inches) | Max. 5-Min. Avg. Speed (mph) |
|---|---|---|
| 471-473 | 7.0 | 45 |
| 473-474 | 13.0 | 62 |
| 474-477 | 16.5 | 80 |
| 477-478 | 13.0 | 62 |
| 478-479 | 10.0 | 53 |
| 479-482 | 7.0 | 45 |
| 482-483 | 10.0 | 53 |
| 483-484 | 13.0 | 62 |
| 484-487 | 15.0 | 71 |
| 487-488 | 5.0 | 36 |

TABLE 3

Simultaneous Occurrence
of Storm Loadings
at Anaverde Summit

| Return Period (years) | Range of Rime Ice (inches) | Maximum 5 Minute Average Wind Speed (mph) |
|---|---|---|
| 105 | 6.0-20.0 | 40-90 |
| 45 | 5.0-16.5 | 36-80 |
| 21* | 6.0-20.0 | 27-60 |
| 9* | 5.0-16.5 | 25-53 |
| 3 | 3.0-10.0 | 27-60 |
| 2 | 2.4-8.0 | 27-60 |
| 1.5 | 1.8-6.0 | 27-60 |

The conclusions of the study were as follows:

1. The ice that occurred on the Anaverde Summit was principally rime.

2. Drop size measurements made during storm passages compared favorably to other cloud drop size measurements taken in Southern California and confirmed that it was reasonable to assume an average drop size for the duration of the icing conditions.

3. Ninety-five percent of all winds that occurred during icing conditions at Anaverde Summit were from 180° to 210° (south to about south-southwest).

4. The maximum wind speed during storm conditions occurred with equal probability at any time during the storm.

5. The channeling effect of the terrain to the southwest of the Anaverde Summit increased the wind speeds at the Summit to a much greater value than at Sandberg. For example, an 18 m/s (40 mph) windspeed at Sandberg was a 32 m/s (72 mph) windspeed at Anaverde Summit.

6. Rime ice accumulated in a circular form on conductors free to rotate.

7. Rime ice accumulated on the bundled conductors in a pennant or elliptical form with the major axis pointed into the wind.

8. Windspeed and storm duration were found to be the principal factors that determined the magnitude of the rime ice formations at Anaverde Summit.

9. The 45-year return period for combined ice and wind loading was estimated to be 36 m/s (80 mph) windspeed and 41.9 cm (16.5 inches) of rime ice.

10. The 105-year return period for combined ice and wind loading was estimated to be 40 m/s (90 mph) windspeed and 50.8 cm (20 inches) of rime ice.

It is noted that heavy loading as defined by California Code GO-95 is more severe for transverse and vertical tower loads on some of the towers in the summit area than the storm loadings listed in Table I, but less severe for longitudinal tower loads.

## TRANSMISSION LINE ANALYSES

The originally constructed lines were analyzed to determine the maximum storm loadings that they could withstand without modification. The conductor, tower, insulator-hardware and footing systems were then investigated to determine what modifications would be required to withstand loadings that would occur during storms with the probability of occurring once every 105 years, 45 years, and 21 years.

### A. Assumptions and Conditions

1. Unit Weight of Rime Ice. The unit weight of rime ice was derived from expected densities. Since the densities vary from storm to storm, calculations were made to determine the average unit weight of rime ice for 105 year and 45 year return period storms. The maximum differential between the average unit weights of the rime deposits for these two storms was only 0.002 pounds per square inch of rime per foot of conductor. It was, therefore, decided to use the same average unit weight of ice for all calculations, regardless of storm duration or diameter of rime deposited.

2. Conductor Loading Calculations. Tower loads were determined for wind and ice loading for the two conductor Bluebird bundle. This approach was used so that complete loading information was available for each tower location.

3. Study Limitations and Factors of Safety. Maximum conductor tensions under fully loaded conditions were limited to 70% of the ultimate tensile strength of the conductor. The minimum factor of safety used for towers under fully loaded conditions was 1.0, while the minimum factor of safety for insulator-hardware assemblies was maintained at 2.0. The minimum conductor to ground clearance was kept at 35 feet in all instances.

4. Rime Ice and Wind on Tower Members. It was found that the dead weight of a suspension tower was increased by approximately 6 kips due to the buildup of rime on the tower members. Since this increase is within the 50% overload to which the tower was designed, it was decided that rime on the tower members would not be a significant factor and could be neglected for purposes of the studies.

The Anaverde Summit area was originally designed for 120 mph wind without ice and the calculations indicate that the bending stresses in the tower members are governed by 120 mph wind without ice rather than 90 mph wind on rime covered members. Where tower replacement was recommended, the new towers were checked for 120 mph wind loading capability.

5. Rime Ice on Insulator Strings. Calculations were made to determine the increase in vertical load due to the buildup of rime on the insulator strings. It was decided that this loading could be neglected on suspension towers since it was not significant when compared to the total vertical loads being considered. However, the increase in vertical load was included in calculations of deadend tower loading since this loading is a significant part of the tower loading.

6. Footing System. No modification of the footing system will be required for towers that would remain in place since the footings in this area were originally designed to support the design loads of the towers with a factor of safety of 1.65. However, where towers were recommended for replacement, the footing system should be designed to be compatible with expected tower loadings.

## 105 YEAR RETURN PERIOD STORM

1. General. The 105 year return period storm represents the worst probable storm that could be expected in the Anaverde Summit area. The lines would have to withstand a maximum 5 minute average wind of 90 mph blowing on a 20-inch diameter rime covered conductor.

2. Conductor System. Maximum conductor tensions were calculated for a two conductor bundle of Bluebird conductor across the entire Anaverde Summit section. Where conductor tensions exceeded 70% of the ultimate tensile strength of Bluebird, calculations were made to determine the maximum conductor tensions for a single 2.7 inch diameter conductor. It was found that the conductor in the entire Anaverde Summit section would have to be replaced with a single 2.7 inch diameter conductor per phase.

3. Tower System. The maximum transverse, vertical and longitudinal loads were determined for each tower, and tower replacements were recommended where these loading combinations exceeded the tower capability as determined by computer. In addition, tower replacements were also recommended if ground clearances were reduced below 35 feet or if it were necessary to install a deadend tower to effect the change in the conductor system to a single conductor. It was found that suspension towers and light deadend towers would have to be replaced with medium deadend towers and heavy running angle towers.

4. Insulator-Hardware System. The insulator-hardware system would have to be redesigned to support the single 2.7 inch conductor and new suspension assemblies would have to be developed using either 66,000 pound rated insulators or double 40,000 pound units. New four string deadend assemblies using 66,000 pound insulators would have to be developed for use on some of the deadends.

## 45 YEAR RETURN PERIOD STORM

1. General. The maximum loadings of a 45 year return period storm at the higher elevations are expected to be 80 mph winds on a 16.5 inch rime covered conductor.

2. Conductor System. Even with the reduction in loading it was still found necessary to replace the existing bundled Bluebird conductor with single 2.7 inch diameter conductor for a number of the spans. It should be noted, however, that the amount of conductor replacement required to withstand the loadings of a 45 year return period storm is less than that required to withstand a 21 year return period storm. The reason for this is that the 21 year return period storm has a larger diameter of rime ice under maximum loading conditions and the vertical weight is

the governing factor as far as conductor tensions are concerned. Therefore, the amount of conductor replaced should at least include the requirements for a 21 year return period storm since two such storms are likely to occur in a given 45 year period.

3. Tower System. To withstand the 45 year return period storm the tower system of both lines requires considerable modification. This involves changing suspension towers with deadend towers or heavy running angle towers.

4. Insulator-Hardware System. The insulator-hardware system would have to be modified to support a single 2.7 inch conductor and the suspension assemblies would have to be redesigned for either 66,000 pound insulator units or twin 40,000 pound units. Four string deadend assemblies using 50,000 pound insulator units would be adequate for the expected loadings on all deadends except one where 66,000 pound units should be used.

## 21 YEAR RETURN PERIOD STORM

1. General. The 21 year return period storm is a storm which could be expected to deposit a 20 inch diameter of rime ice on the conductors, but in which the maximum five minute average wind would occur at some period during the storm other than at the maximum rime conditon. It was assumed, therefore, that the average wind of the storm, two-thirds of the maximum five minute average, would be blowing on the conductors at the time of maximum rime. For purposes of this study a 60 mph wind and 20 inch diameter of rime were used as the maximum loading conditions.

2. Conductor System. The same analyses as were used in the 105 year storm study were applied to the study of the conductor system for this storm.

3. Tower System. After the maximum vertical, transverse and longitudinal loads were calculated for each tower location, it was determined that it would be necessary to replace suspension with deadend and heavy running angle towers.

4. Insulator-Hardware System. In general, the insulator-hardware system will have to be redesigned to support a single 2.7 inch conductor and a suspension assembly of single 66,000 pound insulator units or twin 40,000 pound units will have to be developed. Four string assemblies using 50,000 pound insulators will be required for the deadend assemblies.

## MAXIMUM STORM WITHOUT LINE MODIFICATION

1. General. The lines on Anaverde Summit were also analyzed to determine the maximum storm that they could withstand without modification.

It was found the lines could not withstand the three year return period storm loading without modification. Therefore, a lesser storm with a return period of two years was investigated for these lines. The maximum five minute average wind for this storm is 60 mph with a rime deposit of 8 inches.

It was found that all components could withstand the loadings of a two year return period storm, but that one suspension would still fail even under these loadings. A new study was made reducing the rime ice deposit to 6 inches, maintaining the wind at 60 mph maximum five minute average. This represents the maximum storm that the lines can withstand without modification and this storm can be expected two years out of three.

2. Conductor System. The maximum tensions developed in the conductor system due to the loadings of a three year return period storm are less than 70% of the ultimate tensile strength of the conductor.

3. Tower System. The towers were found to be capable of withstanding the loads imposed by a three year return period storm with the exceptions of one suspension tower. Either major modification of members of this tower or complete tower replacement would be required to insure its capability to withstand the loads of this storm. Therefore, the maximum storm withstand capability of the lines is equivalent to that of a 1.5 year return period storm.

4. Insulator-Hardware System. The deadend strain assemblies for both lines are capable of withstanding the loads without modification with factors of safety in excess of 2.0.

## CONCLUSIONS

### A. Anaverde Summit Area

The ice and wind loadings in the Anaverde Summit area are such that for a given winter season there is one chance in two that a storm will develop that will exceed the capability of the line as originally constructed. If reliable operation was to continue in the area, the lines had to be modified to withstand more severe ice and wind loadings. The modifications required for each storm considered in this report are summarized below.

It was concluded that the lines should be relocated to the leeward side of the Anaverde Summit area at a lower elevation.

## GENERAL CONCLUSIONS

1. SCE's present design practice for transmission lines requires that meteorological studies be conducted for new routes which include instrumentation for questionable areas.
2. Elevations of 1,524 meters (5,000 feet) or more are to be avoided wherever possible in routing transmission lines.

## REFERENCES

1. K. L. Griffing and D. P. McMillan, "Experiences with Meteorological Liabilities Encountered on an EHV Transmission Line," paper 70 CP 622-PWR presented at the IEEE Summer Power Meeting and EHV Conference, July 1970, Los Angeles, California.
2. David C. Leavengood, "Meteorology Can It Be Useful?" paper presented to the Canadian Electrical Association, Transmission Section, October 1972, Edmonton, Alberta.
3. A. G. Davenport, "Rationale for Determining Design Wind Velocities," Journal of the Structural Division, ASCE, Vol. 86, No. ST4. Proc. Paper 2475, April 1960. pp. 49-68.
4. C. W. Thornthwaite and M. Halstead, "Note on the Variation of Wind with Height in the Layer Near the Ground," Transactions American Geophysical Union, Vol. 23, 1942. pg. 249-255.
5. Bourgsdorf, V. V., Nikiphorov, E. P. and Zelitchenko, A. S., 1968. "Ice Loads on Overhead Transmission Lines," International Conference on Large High Tension Electric Systems, Paris, P. 23-05.

TABLE IV

SUMMARY OF MAJOR MODIFICATIONS REQUIRED FOR VARIOUS STORMS

| Storm Return Period | Add Deadend Tower | Add Heavy Running Angle Tower | Add 2.7" Cond. (Ckt. Ft.) | Remove Suspension Tower | Remove Light Deadend Tower | Remove Bluebird Cond. (Ckt. Ft.) |
|---|---|---|---|---|---|---|
| 105 | 14 | 6 | 28,526 | 15 | 3 | 28,526 |
| 45 | 7 | 13 | 25,775 | 15 | 3 | 25,775 |
| 21 | 4 | 15 | 25,775 | 15 | 3 | 25,775 |

## REFERENCES (Cont'd)

6. Court, A. "1953 Wind Extremes as Design Factors." J. Franklin, Inst., 256, 39, 40-56.

7. Fisher, R. A., and L. H. C. Tippett, 1928: "Limiting Forms of the Frequency Distribution of the Largest or Smallest Member of a Sample" Proc. Cambridge Phil. Soc., 24, pt 2, 180-190.

8. Kuroiwa, D., 1965. "Icing and Snow Accretion on Electric Wires." U.S. Army Material Command, Research Rpt. 123.

9. Leavengood, D. C., and T. B. Smith, 1969: "Studies of Transmission Line Icing. Rpt. by MRI to Southern California Edison Company, Los Angeles, California, Cont. No. L-2127, MRI68 FR-801.

10. Langmuir, I. and K. B. Blodgett, 1945: "Mathematical Investigation of Water Droplet Trajectories." General Electric Research Laboratory, Report RL-225.

11. Leibfried, W., and H. Mors, 1964: "The Bundled Conductor." Experimental Station at Hormisgrinde, Germany.

12. Weiss, L. L., 1955: "A Nomogram Based on the Theory of Extreme Values for Determining Values for Various Return Periods. Mon. Wea. Rev., 83, 69-71.

13. Boyd, D. W., 1965: Climatic Information for Building Design in Canada, Supplement No. 1 to the National Building Code of Canada. National Research Council NRC No. 8329, Ottawa.

## REFERENCES (Cont'd)

14. DeMarris, G. A., 1959: Wind Speed Profiles at Brookhaven National Laboratory, J. Meteorol., 16 (No. 2): 181-190.

15. Johnson, O., 1959: An Examination of Vertical Wind Profile in the Lowest Layers of the Atmosphere, J. Meteorol., 16 (No. 9): 144-148.

16. Shellard, H. C., 1965: The Estimation of Design Wind Speeds. Wind Effects on Buildings and Structures, National Physics Laboratory Symposium (No. 16): Pg. 30-51.

## DISCUSSION

Mozer: The wind increases [...] on the top [...]. Do you figure that was only due to channelization, or also to some speed-up effects over it as well? Were you able to distinguish the differences between these two?

Leavengood: No, we didn't. We weren't able to distinguish the difference, but there certainly could be some speed-up effect. Probably where you could see the difference is at the knee in the graph, that the speed-up effect at lower speed is a little greater, than it is at higher speed due to channeling, which made it much greater, at the same time.

AD P001700

# EXTREME GLAZE AND RIME ICE LOADS IN SOUTHERN CALIFORNIA
## Part II: Glaze

Joel H. Mallory Southern California Edison Company
David C. Leavengood Leavengood & Associates

## ABSTRACT

During 1975, an ice storm in the Tejon Ranch Summit area caused damage to Southern California Edison Company's 500 kV and 220 kV lines. This area is located about 45.1 Km (28 miles) north of the Anaverde Summit area. (Leavengood/Mallory Part 1).

The design for the 500 kV line through the Tejon Ranch Summit area was based on soft rime ice and wind loads that were predicted by a meteorological consultant, Meteorology Research, Inc. (MRI) in 1971.

The consultant was requested to analyze the 1975 ice storm. This specific storm's meteorological characteristics were determined. Long term climatological surface weather records, weather maps, and upper air measurements were reviewed for occurrences of similar conditions. In addition to the meteorological analysis of the storm, a dendrochronology study was conducted of the oak forest on the Tejon Summit. The meteorological study concluded that glaze ice formed on the conductor and towers rather than the predicted soft rime ice. The combined results of the meteorological survey and the forestry survey, estimated that the return period of the heavier ice and wind loads is 25 years, but not greater than 50 years.

The 500 kV line was modified to withstand these heavier predicted loads.

Much greater damage would have occurred in the Tejon Ranch Summit area if the line design had been based only on CPUC-G095-Heavy Loading and not on the rime ice loads originally predicted by the meteorological consultant.

## TEJON RANCH SUMMIT AREA

On January 9 and 10, 1975, an ice storm occurred in the Tejon Ranch Summit area. This area is located southeast of Bakersfield, northwest of Lancaster, and is located about 45.1 Km (28 miles) north of the Anaverde Summit area. It is the highest elevation, 1646 meters (5,400 feet), reached by the No. 3 Midway-Vincent 500 kV line as it crosses the Tehachapi Mountain Range between the San Joaquin Valley and the Antelope Valley.

Based on transmision line operating experience at Anaverde Summit, SCE had adopted the criteria of requiring meteorological studies to be made on all future transmission line routes. The 500 kV line through the Tejon Ranch Summit area was designed on a span basis, for soft rime ice loads of 1.19 to 5.51 Kg/M (0.8 to 3.7 pounds per foot) of conductor with 18.8 mps (42 mph) wind normal to the conductor. These values were predicted by the meteorological consultant in their study that was completed during the design stages of the line.

The consultant analyzed the January 1975 ice storm to determine if the predicted ice and wind loads and probability of occurrence needed to be revised.

## ICING AT TEJON RANCH SUMMIT

Ice occurred on the conductors, structures and vegetation from 1494 meters (4,900 feet) elevation on the northwest (windward) side of the ridge to 1555 meters (5,100 feet) on the southeast (leeward) side of the ridge. The magnitude of ice on the trees and towers increased with increasing elevation up to the Tejon Ranch Summit at 1646 meters (5,400 feet). The ice appeared to be all wind-driven. Only the north-northwest side of trees, bushes, and towers were covered with ice. This configuration of ice indicated the wind was almost parallel to the conductors during the storm. The amount of ice built into the wind from the members of the towers on the ridge ranged from about 25 cm (1 foot) at the base of the towers to 75 cm (3 feet) at the top. The graduation of ice diameter was caused by the increase in wind speed with height.

At a glance, the ice appeared to be white, opaque rime ice; however, closer inspection revealed a thin rime coating over solid glaze ice. The amount of ice on the conductors varied, but maximum accumulations on the bundled 500 kV conductors were observed to be as much as 13 to 15 cm (five to six radial inches). At first, it appeared the ice on the conductors of the 500 kV line had formed in a circular shape. Chunks of ice that had fallen from the conductor and pictures of the ice on the conductors showed the ice was in the shape of an ellipse with the conductor passing through the upper third portion of the ellipse. The density of the ice ranged from 0.7 g/cc (44 lbs/ft$^3$) to 0.8 g/cc (50 lbs/ft$^3$) with an average density of 0.75 g/cc (47 lbs/ft$^3$). The schematic representation of the ice is shown in Figure 1.

Average weight and dimensions of the ice, on a span-by-span basis with an average density of 0.75 g/cc were used to calculate actual loads that resulted from the ice storm on the transmission towers, conductors and hardware-insulator assemblies.

The maximum observed glaze ice on the conductors of each tower and the average wind speed required to create that amount of ice were determined from the meteorological analyses of the storm.

## 500 KV LINE DAMAGE

The ice storm caused the groundwire to pull out of deadend connectors or through suspension clamps. The hardware of a four barrel deadend assembly failed thus dropping the two bundle phase conductor. Some of the tower redundant members were bent from the dynamic loading caused by dropping the conductor.

## ANALYSIS OF THE WEATHER CONDITIONS IN THE TEJON SUMMIT AREA

The ice that occurred during the January 9-11, 1975, ice storm was glaze ice and not the usual rime ice.

Glaze ice is normally associated with freezing rain or drizzle, which occurs when warm, moist air overrides cold, subfreezing air at the surface. Precipitation that begins as rain freezes upon contact with the cold surfaces. The upper air soundings from Southern California showed the overriding situation did not exist. A substantial inversion occurred - at Edwards AFB at 0300 PST on January 9. However, the temperatures were entirely below freezing and very dry above the base of the inversion. This condition was due to mountain waves triggered by northwesterly winds flowing over the Tehachapis.

The icing at the Tejon Ranch Summit occurred in conjunction with post-frontal activity. Freezing rain or drizzle during those weather situations seldom, if ever, occur.

Moisture did exist at lower elevations, however. It is likely that rain was falling in the lower elevations of the Tehachapis as early as the night of January 8. Cold, dense clouds were observed flowing through the passes of the Tehachapis on January 10. The cloud droplets were probably quite large with a high number density. Strong winds blowing through the mountain passes could carry moisture in the form of large cloud droplets, drizzle, and small raindrops from the warmer air at lower elevations into the subfreezing air of the Tejon Ranch Summit, thus freezing upon contact with towers and conductors. If the time required for a supercooled droplet to freeze exceeds the impingement time interval, glaze ice results (Kuroiwa, 1965).

Adding to these already strong winds is the potential funneling effect of the Tejon Canyon. Winds would have funneled through Tejon Canyon with few obstructions, increasing in speed as the pass narrows. It is probable that winds in excess of 31.3 mps (70 mph) were experienced along the transmission line route.

During previous icing studies of the Tejon Canyon (Leavengood and Smith, 1970; Leavengood and Mirabella, 1971) and Anaverde Summit (Leavengood and Smith, 1968), only rime ice had been observed in the mountains of Southern California.
Measurements of various meteorological parameters during those earlier ice storms made it possible to compare the January 1975 ice storm with them in order to determine what factor or factors led to the unusual occurrence of severe glaze ice.

A major factor in ice accumulation is wind speed. Although wind speeds in the Tejon Canyon were quite high, Anaverde Summit also experienced very high winds during rime ice accumulation. The duration of the storm was not exceptionally long; the majority of the icing had accumulated within 24 hours.
Measurable precipitation during the icing period was light; the ground at the ridge was covered with only about one-half inch of snow. The key factor appears to be the size of the cloud droplets in the Tejon Ranch Summit area. Measurements made during the 1968 Anaverde Summit icing study indicated an average cloud drop diameter of 20 to 30 microns. Those drops, coupled with the high winds at the Anaverde Summit, still produced primarily soft rime. A wind of 22.35 to 31.3 mps (50 to 70 mph) blowing up the northwest slope of the Tejon Ranch Summit is capable of carrying with it droplets of a size in excess of 30 microns in diameter.

Note: The weight of the ice as determined by the meteorological consultant has previously been discussed. See Table I on page 8.

## RETURN PERIOD PROBABILITY OF SEVERE ICE STORMS ON THE TEJON RANCH SUMMIT

The ice accumulation of this storm is close to the 25 year icing value given in the 1971 report. The maximum vertical load on a section of conductor within a span at maximum ice accumulation, is approximately the same in both cases.

Historical icing damage was also recorded in the growth characteristics of the trees in the area. The services of a consulting forester were utilized to determine the effects of the local climate on the oak forests of the Tejon Ranch Summit. The general survey indicated the trees along the ridge were stunted in growth as a result of adapting themselves since seedling stage to severe icing every winter. The stunted growth area exists for 800 meters (one-half mile) down the northwest side of the crest, but disappears in a short distance down the southeast side. These growth patterns indicated most of the severe icing in the Tejon Ranch Summit was associated with post-frontal activity with its corresponding northwesterly winds.

In order to obtain an estimate of the frequency of severe icing storms in this area, dendrochronology sampling was performed by the consulting forester. This technique utilized the fact that when some force has caused severe tree damage, growth is slowed for several years thereafter, resulting in compressed tree rings. Four types of force would cause compressed growth rings, these are:

1. Drought
2. Insect Infestation
3. Fire
4. Severe Ice Accumulation

The main force acting on the trees in the Tejon Ranch Summit was concluded to be due to severe icing.

The core bore samples showed the growth rings were compressed for several years. Since insect infestation or drought results in compressed rings of two years or less, these were eliminated as possible causes. If fires had caused the compressions, carbon would have been present in the core bores, but that was not the case. Therefore, the remaining possibility of severe long periods of growth retardation was heavy ice accumulation.

The stands of trees along the crest of the Tejon Ranch Summit and for a short distance down the western side resemble similar trees found at much higher altitudes. The stunted character is more variable and less pronounced along the crest to the southwest and disappears entirely to the northeast.

The crest zone of white oaks and canyon live oaks is characterized by dense stagnated stands which appear as deciduous chaparral from a distance. Exposure to summer heating and prevailing insufficient rainfall has discouraged coniferous forest in the crest zone. The crest zone tree characteristics show evidence of considerably greater consistent mechanical loading than would be developed under severe rime icing.

In order to describe the relative severity of the icing along the crest, a comparison was made to a forest area that has been documented as a heavy frequent rime area. The Western San Bernardino Range of Southern California is known as "Rim of the World." Relatively heavy snowfall (254 cm) along with approximately 30.48 cm (12 inches) of fog interception, occuring as significant proportions of rime, has caused flattened crowns and the building of compression wood. On the Rim of the World, the rime develops as far as 18 cm into the wind very frequently and is accompanied by a subsequent snowfall. This sequence of snow accumulating on rime-iced trees result in very heavy loading. Even under these circumstances, the trees on the Rim of the World retain their arboreal (tree-like) stance instead of the dwarf growth as exhibited on the Tejon Ranch Summit.

The analysis of the various conditions eliminated the local snowfall, (unloaded) wind velocity, a moisture or soil nutrient deficiency, or plant species difference as the deforming agent of the Tejon Canyon Summit trees.

Occasionally, particularly severe variations of the icing problem will occur as was exhibited in the January 8-10 ice storm. Considerable new breakage over the crest on the east side showed the affect of unusually heavy loading on "unprepared" trees. The crest dwarf forest reaches maturity at 1.5 to 4.5 meters (5 to 15 feet) whereas the same species of trees only a short distance away to the northeast or southwest reach a mature height of 28 meters (90 feet).

Due to uncertainties and complications inherent in the sampling and analysis techniques, specific years of major icing damage cannot be pinpointed. However, general periods of major damage can be determined from the results of the study. Widespread damage to trees occurred 20 to 25 years prior to the 1975 storm. This was probably due to an icing storm in 1953 that damaged the 220 kV transmission lines on the ridge. Other periods of heavier than normal tree damage occurred approximately 55, 75 to 85, 105, and 130 to 135 years prior to 1975. Thus, a period of 20 to 30 years elapses between major icing storms. Heavy damage to trees on the southeast side of the ridge was an additional indication of severe icing. This type of damage was particularly evident in 1953 and 1920. Severe icing damage to trees on the southeast side of the ridge, due to the January 1975 storm, was also observed.

This evidence suggests that the ice storm of January 8 and 10, 1975, was at least a 25 year storm, but no more than a 50 year storm.

## CONCLUSIONS OF THE 1975 METEOROLOGICAL STUDY

1. The icing storm of January 8 and 10, 1975, was very localized and not readily apparent from weather observations at reporting stations in Southern California.

2. All of the icing occurred after passage of the cold front which passed through Southern California on the evening of January 8, 1975. Icing

continued no later than the morning of January 10, however, the majority of the severe icing occurred on January 9, 1975.

3. The glaze ice was caused by air, heavily ladened with moisture, channelled through the Tejon Canyon which cooled as it ascended toward the Tejon Ranch Summit. The amount of moisture in the air was too great for all of the water to freeze upon contact with the towers and conductors. The excess water froze in a solid mass with few or no air bubbles between the water molecules. The icing was confined to elevations greater than 1494 meters (4,900 feet).

4. The wind speed at the ridge averaged at least 22.3 mps (50 mph) throughout most of the icing storm with periods of wind in excess of 31.3 mps (70 mph).

5. The 1971 study indicated only rime to be a major problem throughout the Tejon Canyon Summit area. Meteorological and vegetative data indicated glaze ice occurs more frequently in the Tehachapi Mountains than previously believed.

6. Studies by a consulting forester indicated severe icing storms occur every 20 to 30 years. The data indicated the January 1975 storm was at least a 25 year storm, but not greater than a 50 year storm.

7. Table I below lists is the estimated average weight and dimensions of the ice which may be used in load calculations.

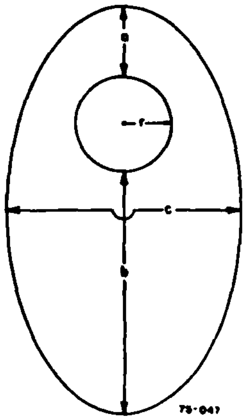

Figure 1. Assumed shape of the ice on the 400-kV conductors. Conductor of radius r passes through upper portion of ice. Letters a, b and c refer to dimensions presented in Table I.

TABLE I. AVERAGE OBSERVED DIMENSIONS OF ICE AND VERTICAL LOAD, BY SPAN

| | Average Ice Dimensions on Conductor* (inches) | | | | |
|---|---|---|---|---|---|
| Span | (a) | (b) | (c) | Equivalent Radius | Vertical# load (lb/ft) |
| 53 - 54 | 0.75 | 2.00 | 2.75 | 0.88 | 4.815 |
| 54 - 55 | 0.75 | 3.00 | 3.25 | 1.24 | 6.221 |
| 55 - 55A | 1.00 | 4.25 | 3.25 | 1.51 | 7.466 |
| 55A - 56 | 1.00 | 4.50 | 3.25 | 1.55 | 7.673 |
| 56 - 57 | 2.00 | 7.00 | 5.00 | 2.79 | 15.387 |
| 57 - 58 | 2.00 | 7.00 | 5.00 | 2.79 | 15.387 |
| 58 - 59 | 1.50 | 5.00 | 4.00 | 1.99 | 10.085 |
| 59 - 60 | 0.75 | 2.00 | 2.75 | 0.88 | 4.815 |
| 60 - 61 | 0.50 | 0.75 | 2.25 | 0.42 | 3.377 |

*See Figure 1 for description of parameters.

#Ice plus conductor, assuming a conductor weight of 2.439 lbs/ft and a density of ice of 0.75 g/cm$^3$.

## TRANSMISSION LINE ANALYSES

The No. 3 Midway-Vincent 500 kV line through the Tejon Ranch Summit area is designed based on the wind and ice loading that was determined from the MRI weather study completed in 1971.

The towers in the most severe area were located to provide a safety factor of 1.5 for vertical, transverse and longitudinal loads. The weight of the ice, including the conductor was 9.1 kgs/meter (6.1 pounds per foot). The density of the ice was 0.48 g/cc (30 pounds per cubic foot). The length of the longest axis of the pendant shaped formation was 25.4 cm (10 inches). The five minute average wind during the ice condition was considered to be 60 mph and 45° to the line. This results in wind pressure of 36.1 kg/sq. meter (7.4 pounds per square foot) when based on a flat surface. As previously mentioned, the probability of simultaneous occurrence of a 26.8 mps (60 mph) wind and 25.4 cm (10 inches) of ice was about one in 50 years.

The conductor and groundwire maximum working tension is designed so as not to exceed 33-1/3% of the ultimate tensile strength when based on G.O. 95 Heavy Loading Conditions.

The insulator and hardware systems will provide a safety factor of 3.0 when G.O. 95 Heavy Loading Conditions are applied.

### Resultant January 1975 Ice Storm Loads on the Present Line Design

The approximate loadings on the No. 3 Midway-Vincent 500 kV line have been calculated based on the average ice load per span as estimated by the meteorological analysis of the January 1975 ice storm. The wind speed used in their loading calculations was assumed to be 70 mph and varied between 6° and 20° to the line. This results in a wind force of 0.98 to 7.81 kgs/sq. meter (0.2 to 1.6 pounds per square foot).

The results of the transmission loading calculations are listed in the following tables under three separate areas: Towers, Conductor and Insulator-Hardware Assemblies.

In each of the above categories, the results are presented as a ratio of the calculated ice storm loads to the design load. The design load used in these calculations provide safety factors of 1.5 for towers, 3.0 for the conductor and 3.0 for the insulator-hardware assemblies.

### Alternatives

Alternate methods to improve the Midway-Vincent No. 3 500 kV line design through the Tejon Ranch Summit area were investigated. These alternatives included such modifications as: upgrading insulator-hardware assemblies, redesigning the line with a lesser

TABLE II

RATIO OF ICE STORM LOADS TO DESIGN LOADS

TOWERS

| Mile & Tower | 62/2 | 62/3 | 62/4 | 62/5 | 62/6 | 63/1 | 63/2 | 63/3 |
|---|---|---|---|---|---|---|---|---|
| Const. No. | 54 | 55 | 55A | 56 | 57 | 58 | 59 | 60 |
| Tower Type | EMT | ELD-T | ELD-T | ELD-T | ELD | ELD-T | ELD-T | ELD-S |
| Vertical Load | 1.108 | 0.676 | 0.164 | 1.206 | 0.806 | 0.923 | 0.656 | 0.951 |
| Transverse Load | 0.424 | 0.392 | 0.698 | 0.547 | 0.183 | 0.146 | 0.293 | 0.256 |
| Longitudinal Load: | | | | | | | | |
| Ahead | N/A | 1.228 | 1.777 | 0.288 | 0.602 | 1.994 | 1.030 | N/A |
| Back | 1.341 | 1.260 | 1.228 | 1.777 | 0.281 | 0.617 | 1.993 | N/A |
| Difference | 1.341 | 0.032 | 0.549 | 1.489 | 0.321 | 1.377 | 0.963 | 1.351 |

NOTE 1: Design loads per phase (pounds) for different tower types are as follows:

| | EMT | EHT-S | ELD | ELD-T |
|---|---|---|---|---|
| Vertical | 16,800 | 16,800 | 19,200 | 35,400 |
| Transverse | 7,800 | 8,700 | 50,600 | 12,600 |
| Longitudinal | 7,800 | 7,500 | 42,200 | 42,200 |

NOTE 2: The above design load values provide a safety factor of 1.5.

CONDUCTOR

| Mile & Tower | 62/2 | 62/3 | 62/4 | 62/5 | 62/6 | 63/1 | 63/2 | 63/3 |
|---|---|---|---|---|---|---|---|---|
| Const. No. | 54 | 55 | 55A | 56 | 57 | 58 | 59 | 60 |
| Tower Type | EMT | ELD-T | ELD-T | ELD-T | ELD | ELD-T | ELD-T | ELD-S |
| Wire Tension: | | | | | | | | |
| Ahead | 1.353 | 1.358 | 1.910 | 0.304 | 0.641 | 2.105 | 1.078 | 0.806 |
| Back | 1.119 | 1.358 | 1.319 | 2.102 | 0.307 | 0.622 | 2.017 | 1.047 |

NOTE: Ultimate tensile strength of 2156 mcm, ACSR/AW, Bluebird, 64,250 pounds; the designed maximum working tension is 33% of the ultimate tensile strength or 21,000 pounds.

INSULATOR-HARDWARE ASSEMBLIES

| Mile & Tower | 62/2 | 62/3 | 62/4 | 62/5 | 62/6 | 63/1 | 63/2 | 63/3 |
|---|---|---|---|---|---|---|---|---|
| Const. No. | 54 | 55 | 55A | 56 | 57 | 58 | 59 | 60 |
| Tower Type | EMT | ELD-T | ELD-T | ELD-T | ELD | ELD-T | ELD-T | ELD-S |
| Insulator Tension: | | | | | | | | |
| Ahead | N/A | 1.426 | 2.006 | 0.319 | 0.673 | 2.210 | 1.132 | N/A |
| Back | N/A | 1.425 | 1.384 | 2.207 | 0.322 | 0.653 | 2.118 | N/A |

NOTE: The M&E rating of the insulator is 40,000 pounds.

safety factor, redesigning the line for one 2,859 mcm ACSR conductor with a lesser safety factor, or removing the groundwire in the most critically loaded spans.

Description of the Alternatives

The following is a brief description and summary of the results of each alternative. Both glaze and rime ice quantities that would accumulate for a 25 year ice storm were used in these investigations.

a) Upgrading Insulator-Hardware Assemblies

The initial design could be improved when considering a 25 year glaze or rime ice storm, by changing out hardware and/or insulator-hardware assemblies on several towers.

The insulator tensions that resulted from the January 1975 ice storm at one tower location reduced the safety factor for the assemblies to 1.8.

The safety factor for the most severely loaded deadend assemblies could be improved to 2.3.

To raise the safety factor of the assemblies to 3.0, the existing insulators and hardware would need to be replaced with 66,000 pound insulator-hardware units.

b) Redesign with Lesser Safety Factor

The tower and conductor loading could be improved when considering a 25 year glaze or rime ice storm, by intersetting new towers and replacing existing suspension towers with deadend towers.

Three different safety factors were considered for maximum tower loading that would result from a 25 year ice storm.

The line was analyzed to provide safety factors of 1.1, 1.25 or 1.5 for vertical, transverse and longitudinal (one, two or three phases up one side only) tower loads. The maximum conductor ruling span tension for these three cases is 33-1/3% of the ultimate tensile strength. The insulator-hardware assemblies will have a minimum safety factor of 3.

### c) Replacing Two Bundle Conductor with One Large Conductor

The amount of glaze ice that forms on each subconductor is independent of the bundle configuration. The water droplets strike the conductor, slide down and then freeze forming an elliptical cross section.

This is not the case during rime icing conditions. The amount of rime ice that will form on a single conductor is considerably greater than the amount that will form on a subconductor of the bundle configuration. A single conductor has a better collection efficiency than a bundle conductor since it is free to rotate. The cross section distance of the pendant shaped ice that forms on the bundle configuration is equal to the diameter of the cylinderical shaped ice that will form on the single conductor.

The maximum tension on a single conductor during a 25 year rime ice storm at the summit would be 125% of the ultimate tensile strength of 2156 mcm ACSR/AW (Bluebird/AW) conductor. This figure could be lowered to 100% of the ultimate tensile strength if 2859 mcm AEACSR conductor was used.

Therefore, the single conductor per phase alternate for the initial line design was not be pursued due to the extremely high tensions resulting from a 25 year rime ice storm. The high tension could have been reduced by intersetting and changing out towers.

### d) Removing the Groundwire in Critical Loaded Spans

The problem of loading the groundwire beyond its ultimate tensile strength or the groundwire loading capabilities of the 500 kV deadend towers during a 25 year ice storm could be eliminated by removing the groundwire in critically loaded spans. The expected loads on the groundwire in the other spans during a 25 year ice storm would be within acceptable limits.

If the groundwire had not been removed from the above critically loaded spans, initial designed deadend towers would have been required approximately every 120 meters (400 feet).

The probability of outages due to direct lightning strokes with the groundwire removed from the three spans was calculated to be 0.0942 or 1 in 11 years. It was noted the groundwire for the two spans at the very top of the summit would not be removed. The following assumptions were made for the calculation:

1. The line length with the groundwire removed was 1.36 km (0.848 mile).

2. The longest span length was approximately 610 meters (2000 feet).

3. The footing resistance was 20 ohms or less.

4. The number of insulators per deadend insulator string was 34.

5. The isokeraunic level was 5 thunderstorms per year.

6. The probability of outage was equal to the sum of 85% of the total probability of flashovers plus 67% of the probabilty of direct strokes experienced by a 160 km (100 mile) section of tower line in an area having an isokeraunic level of 30 thunderstorm days per year.

7. The total probability of flashovers was equal to the sum of midspan flashovers, total flashovers and shielding failures.

8. Without the groundwire, midspan flashovers and shielding failures did exist.

9. The probability of outage was directly proportional to the line length and isokeraunic level.

## CONCLUSIONS

1. The following was concluded from the analysis of the January 8-10, 1975 ice storm at the Tejon Ranch Summit.

   a. The ice storm was localized.

   b. The ice that formed on the conductors and towers was glaze ice.

   c. The estimated average density of the ice was 0.75 grams per cubic centimeter. (46.8 pounds per cubic foot.)

   d. The maximum concentration of ice for the storm occurred on two spans, at the very top of the summit.
   The maximum weight of the ice for those spans was 56.8 Kgs/M (38.2 pounds per foot) with the average being 19.2 Kgs/M (12.9 pounds per foot) of conductor.

   e. The average wind speed during the icing condition was 31.3 mps (70 mph). The wind was essentially parallel to the line. The resulting component of the wind was 0.73 to 8.1 Kgs/sq. meter (0.15 to 1.65 pounds per square foot).

   f. This ice storm is classified as a 25 year storm but not greater than a 50 year storm.

2. The predicted frequency of 25 years for this type storm was also substantiated by work required over the years on the 220 kV lines through this area.

3. The initial line design provided the following safety factors when the above average ice and wind loads were applied to the line:

Towers -- 1.01 (both sides up)
Conductor -- 1.43 (68.8% of ultimate tensile strength)
Insulator/Hardware Assemblies -- 1.81

4. The number of additional towers required to provide safety factors of 1.1, 1.25 and 1.5 were as follows:

| Safety Factors | Additional Towers |
|---|---|
| 1.1 | Interset two deadend towers, replace one tower with deadend tower |
| 1.25 | Interset two deadend towers, replace two towers with deadend towers |
| 1.5 | Interset two deadend towers, replace two towers with deadend towers |

NOTE: The above safety factors are related to the vertical, transverse and longitudinal loadings (one side up only) imposed on the towers.

5. The maximum ruling span tension of the conductor under conditions described in the above item was 33 percent of the ultimate strength.

6. The insulator hardware assemblies had to be upgraded so as not to be overloaded in any of the three cases described in the above item.

7. The possibility of removing one subconductor per phase to reduce the ice loading on the towers was feasible for the glaze ice condition, but was not feasible for the rime ice condition.

   a. Considerably more rime ice will accumulate on a single conductor than one subconductor in a bundle arrangement.

   b. The resulting tension for a 25 year rime ice storm on a single phase conductor will exceed the ultime tensile strength of the conductor.

c. Rime ice storms are more likely to occur than glaze ice storms in this area.

8. The cost of redesigning the line to acceptable safety factors for one conductor per phase was more expensive than redesigning the line for the two-bundle phase conductor arrangement.

9. It was feasible to remove the groundwire from the most critically loaded spans. The probability of outages due to direct strokes was 0.0942 or 1 in 11 years.

The line design was improved by upgrading the hardware-insulator assemblies and by removing the groundwire in the three most critically loaded spans.

## GENERAL CONCLUSIONS

1. SCE's present design practice for transmission lines requires that meteorological studies be conducted for new routes and which includes instrumentation for questionable areas.

2. Elevations of 1,524 meters (5,000 feet) or more are to be avoided wherever possible in routing transmission lines.

## REFERENCES

1. K. L. Griffing and D. P. McMillan, "Experiences with Meteorological Liabilities Encountered on an EHV Transmission Line," paper 70 CP 622-PWR presented at the IEEE Summer Power Meeting and EHV Conference, July 1970, Los Angeles, California.
2. Kuroiwa, D., 1965. "Icing and Snow Accretion on Electric Wires." U.S. Army Material Command, Research Rpt. 123.
3. Leavengood, D. C., and T. B. Smith, 1969: "Studies of Transmission Line Icing. Rpt. by MRI to Southern California Edison Company, Los Angeles, California, Cont. No. L-2127, MRI68 FR-801.
4. Leavengood, D.C., and T. B. Smith, 1970: "Meteorological Studies For The Number Three Midway-Vincent 500 kV Transmission Line." Rpt. by MRI to Southern California Edison Company, Los Angeles, California, Cont. No. T2139902, MRI70 FR-896.
5. Leavengood, D.C., and V. A. Mirabella, 1971: "Addendum to the Final Report, Meteorological Studies for the Number Three Midway-Vincent 500 kV Transmission Line." Rpt. by MRI to Southern California Edison Company, Los Angeles, California, Cont. No. T3350924, MRI71 R-985.
6. Boomer, R. J., and M. C. Richmond, 1975: "The Meteorological Study of the January 1975 Ice Storm Along the Number Three Midway-Vincent 500 kV Transmission Line Route at The Tejon Ranch Summit." Rpt. by MRI to Southern California Edison Company, Los Angeles, California, Cont. No. U703901, MRI75 R-1313.
7. Mallory, Joe H., and D. C. Leavengood, 1982: "Extreme Glaze and Rime Ice Loads in Southern California - Part I Rime." Paper presented at the First International Workshop on Atmospheric Icing of Structures June 1-3, 1982, Hanover, N.H.

AD P001701

# FIELD RESEARCH ON THE GALLOPING OF ICED CONDUCTORS
## A Status Report

Joe C. Pohlman, P.E. Consultant
David Havard Ontario Hydro

## ABSTRACT

Galloping conductors have been a problem for designers and operators of overhead power lines for many decades. Despite extensive and continuous research into the problem, a complete understanding of the basic mechanism that causes galloping still eludes us and, without such understanding, development of effective control methods progresses slowly.

The paper discusses the many approaches to control that have been considered or are under appraisal at the present time. It also includes recommendations for the research and development, particularly in the instrumentation field, necessary to produce positive solutions to this problem within a reasonable time frame.

## BACKGROUND

A cable supported in a generally horizontal configuration has four degrees of freedom. It can move vertically, transversally, torsionally and axially. For a given supported span, each of these motions has its own natural frequencies, any two or more of which can couple. If such couplings occur at the fundamental or lower harmonic frequencies, total conductor movements that result can be extensive causing mechanical damage to line components and/or line trip outs and power outages.

Most galloping intiation is thought to require, as a minimum, an asymetrical ice shape on the conductor plus a wind of a sympathetic magnitude and direction. The wind on the bluff cross section will cause positive or negative lift forces depending upon the angle of attack between wind and ice shape. If some mechanism exists which changes the angle of attack at a frequency at or near a natural vibrating frequency of the conductor, the motion can build up until an energy balance condition is struck and will continue so long as the essential relationship among influencing parameters exists.

## APPROACHES TO STUDYING GALLOPING

The question logically arises, why don't we know more about the phenomenon after so much research effort has been expended over so many years? There are many reasons. Some of the more significant are discussed in the sections that follow.

### Wind Tunnel Tests

Since two of the most important factors are ice shape on conductor and wind, it would be obvious to turn to wind tunnel testing and certainly, over the years, valuable information has evolved from such tests. The difficulty arises in modeling real world conditions in the wind tunnel.

A major problem is modeling the stiffness of the conductor. In a real line, the conductor is rigidly held torsionally by a clamp on the end of the insulator support. At this point, the conductor has high torsional stiffness. In the center of the span, however, the conductor is quite free to rotate and does so as ice accretes on it. Thus, the ice shape itself, as well as, its orientation on the conductor vary along the span length.

A test sample conductor with one degree of freedom of movement can be mounted rather routinely in a tunnel. A test sample conductor with two degrees of freedom of movement can be mounted in a tunnel with great difficulty. A real conductor in a real line has four degrees of freedom of movement as mentioned before.

Wind along a conductor sample in a wind tunnel is uniform in characteristics and constant in velocity and direction. Wind blowing on a real conductor in a real world environment is neither of these.

While the results from wind tunnel testing are of interest, they can not really provide much verification of the total galloping phenomenon.

### Simulated Ice Shapes On Real Conductors

The technique of securing artificial ice shapes to full scale conductors exposed to natural winds has provided valuable insight into the understanding of the galloping mechanism. This technique was used by Ontario Hydro(2) to verify the theory of "detuning" a conductor as an approach to interfering with the galloping initiation, as well as, developing an empirically based approach for applying hardware to the conductor to accomplish the "detuning". Despite the fact that the technique provides a safe and convenient way to obtain and observe galloping conductors, it still does not provide all the answers required since the man-made ice shapes can not properly simulate the non-symetrical and wide variety of shapes actually known to exist in the real world. In addition, the cost of attaching simulated ice shapes to enough lines of different physical characteristics to demonstrate the influence line parameters have on the galloping event is a deterrent.

### Field Installed Instrumentation

Attempts have been made to record galloping events in the field on operating lines. Such attempts have enjoyed limited success for many reasons. First of all, instrumentation that will operate trouble-free in winter weather conditions is expensive in first cost and expensive to maintain. Second, such instrumentation has to be securely mounted. This can usually be accomplished only at a structure location. This means the instruments can only sense what is going on near the ends of the two supported spans and not generally in an area. It is very difficult to explain what the actual activity going on out in the mid span really is from the small relative movements recorded at the conductor support points on the structure. Since galloping is a random event, it is a lucky coincidence to have an actual galloping event occur at a site where the instrumentation is mounted.

### Personal Observations

Recognizing the need for descriptive information on galloping events, the Edison Electric Institute has, for a number of years, encouraged their member utilities to report on any galloping events occurring on their lines that were personally observed. An analysis(3) of these reports provided some additional useful information; but, hard and fast conclusions are difficult to draw in recognition of the subjective nature and generally unpleasant conditions under which the observations were made.

### Total Data Bank

While each of the specific activities described briefly above has produced useful data, each has one or more serious shortcomings or limitation that prevent the assembly of the data into a complete explanation or understanding of the galloping phenomenon. These voids in understanding impede the development and/or verification of effective control measures.

## APPROACHES TO CONTROL GALLOPING

Over the past several decades, a wide variety of approaches have been proposed to mitigate the disruptive problems connected with galloping. These approaches fall into two general categories:

o minimizing consequences if galloping occurs

- o preventing galloping from initiating

## Minimizing Consequences

Consequential damage to a power line consists of: mechanical damage to the mechanical support system caused by the beat frequency loads from the conductors; mechanical damage to the conductors, themselves, caused by their clashing together; unnecessary wear and tear to electrical interrupting devices; and lost revenues from power outages. Damage to the mechanical support system can normally be held to a tolerable value by proper design practice. The other contingencies are minimized by increasing clearances between conductors. When this is accomplished at the structure, it greatly increases the height and breadth of the structure and hence, its cost. A visual impression of this relationship can be seen in the two 230 kV lines shown in Figure 1. The line to the left has additional clearances incorporated to prevent conductor contacts as in normal design practice. Though admittedly expensive, increasing clearances at the structure is the only control that currently enjoys universal support.

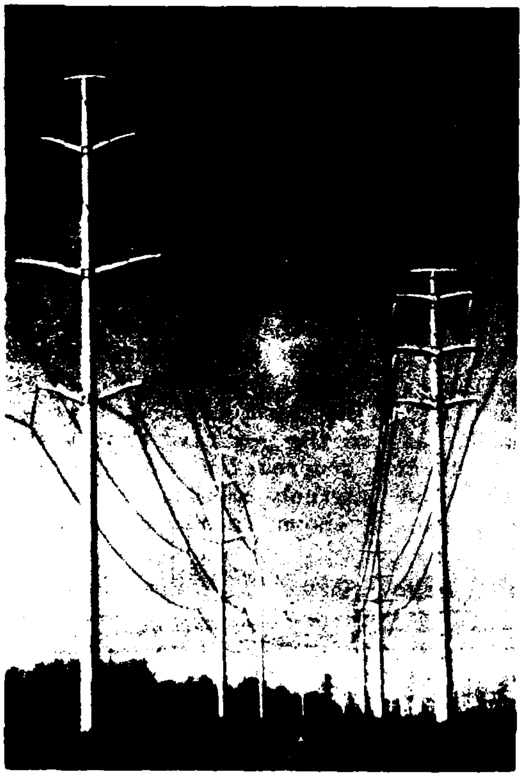

Figure 1: Conventional Design vs Design w/o Galloping Clearances

Separation of the conductors can also be accomplished by using insulating spacers(4) to hold the phases apart at strategic points within the span. This is shown in Figure 2. In addition to separating the phases, these spacers will change the galloping mode of the conductors reducing the maximum amplitude of travel. See Figure 3. The conductor motions are usually synchronized when they do gallop with such spacers and cyclic mechanical laodings may be significant.

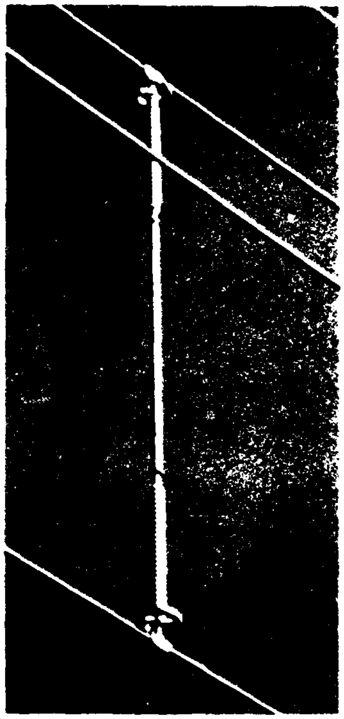

Figure 2: Interphase Spacer

## Preventing Galloping Initiation

The impelling cost incentive of potential reduction in structure dimensions has encouraged serious research on many approaches toward interfering with the galloping mechanism as a means to prevent its initiation. These approaches are as novel as they are numerous.

Using electric current in the line to heat the conductor to prevent ice from accreting or to melt it after formation is a positive but not often practical approach. The amount of

Figure 3: Lines With Interphase Spacers Galloping

current needed is excessive (many time normal) and there are few systems where the concerned circuit can be isolated and such high current supply is available.

The concept of applying a coating to the conductor to prevent ice from adhering has received an extraordinary amount of thought and attention, but, to date, no promising coating system has materialized.

Mechanical means, such as abrading off the ice coating using chains thrown over the conductors, have been resorted to under certain serious and long duration conditions, but they are not in general use because of possible damage to the conductor.

Another intriguing approach is to absorb the energy, much in the way aeolian vibration is suppressed. Drums of sand, dash pots and other energy absorbers have been configured to attach to the conductor at the structure support point. The most violent activity occurs out in the center of the span, of course. It is somewhat questionable, therefore, how much suppression can actually be accomplished by devices, located close to the attachment point at the structure, whose function is to prevent energy transfer between spans along the conductor. This approach has not gained significant support.

A concept that appears to have merit is to change the conductor profile continuously over the length of the span.(5,6) The idea is that this will counterbalance the positive and negative lift forces suppressing vertical movement. Two current embodiments of this approach are shown in Figures 4 and 5.

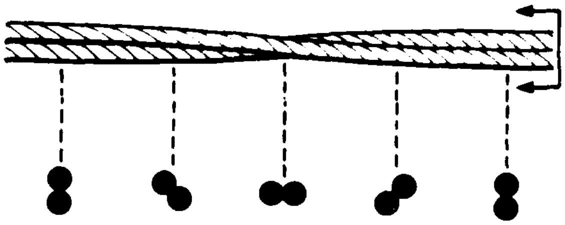

Figure 4: Twisted Conductor

In Figure 4, the conductor is constructed by twisting two smaller conductors together. In Figure 5 a similar sit-

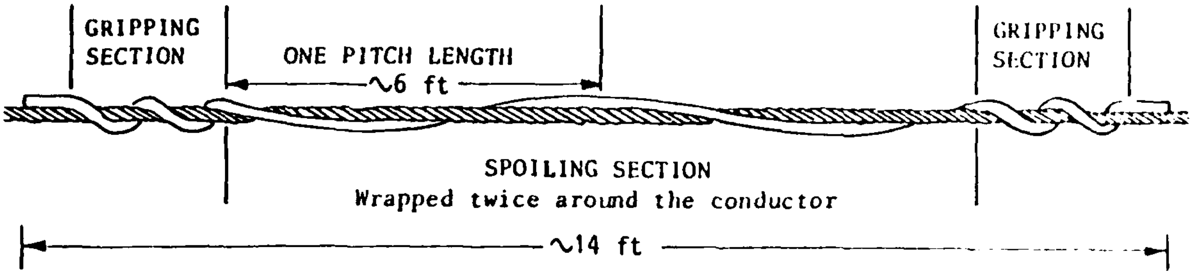

Figure 5: Air Flow Spoiler

tion is approached by adding a coiled "spoiler" to the conductor at periodic intervals.

Im most articulated explanations of galloping,(7) it is stated that the relative relationship between the drag and lift of the iced conductor is of fundamental importance. It follows that if means are applied that increase the drag of the conductor, the probability is raised that the critical relationship between lift and drag is positive and the incidence of galloping initiation lowered. Figure 6 shows an embodiment of an add-on device under current appraisal, designed to increase conductor drag.(8)

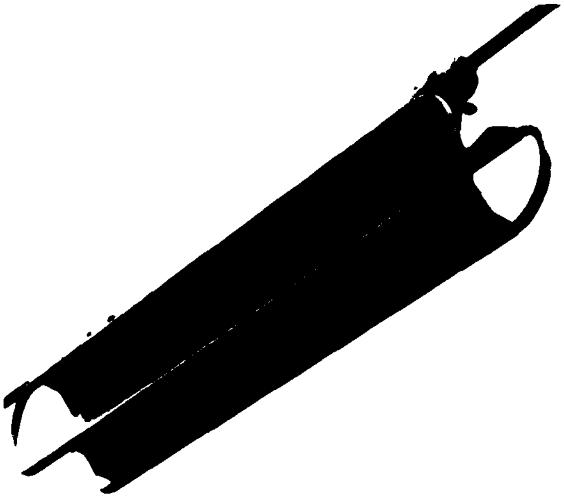

Figure 6: Aerodynamic Drag Damper

The add-on device with the most documented evidence of control to date is the detuning pendulum(2,9) which evolved from the simulated-ice-on-real-conductor experimental work conducted by Ontario Hydro. Observations of the artifically iced conductors led to the discovery that coupling of the vertical and torsional frequencies occurs during the galloping event development. It is believed that the torsional oscillation of the asymetrically iced conductor causes alternating change in wind attack angle, thus modulating the positive and negative lift forces needed for galloping initiation. Control is achieved by adding pendulums, Figure 7, to the conductor to maintain a proper separation between the vertical and torsional natural frequency of the iced-conductor plus pendulum system.

Figure 7: Detuning Pendulum

While the devices described above are discussed and illustrated in terms of single conductor applications, most approaches are also under evaluation for controlling galloping on bundle conductor lines as well. The impact of galloping is even more severe on bundle lines because of their greater capacity and importance as the main corridors of the bulk power distribution system. Galloping is also perceived to occur more frequently on bundle lines than on single conductor line systems. While the economic impact is greater, development and evaluation of control systems is slower. This is due to the greater complexity of the aerodynamics and the addition of the effects due to the mechanical coupling between the subconductors. There are also fewer field trial sites on bundle conductors, perhaps because the first bundle conductor lines were arranged in horizontal configurations and galloping seldom caused flashovers. Recently, more utilities have installed double circuit bundle conductor lines which are more susceptible to galloping caused flashovers. The need for significant effort to develop and verify performance of control devices for galloping of bundle conductors has now been recognized and about 25 percent of the field tests sites in the US, Canada and Europe(9) are on bundle conductor lines.

## PRESENT RESEARCH PROGRAM

Many of the devices described briefly above are undergoing disciplined field testing in the US, Canada and Europe at the present time. Controlled tests of detuning pendulums, aerodynamic drag dampers, interphase spacers, T-2 conductors and line spoilers are being conducted on approximately 175 sites. At each site, the control device is applied to one or two phases of a three phase line.(10,11) When climatic conditions are sympathetic, observers who have been specially trained are dispatched to the site and, finding galloping there, progress through a disciplined routine for reporting the relative motions of controlled vs uncontrolled phases at periodic intervals during the storm.

Because of the randomness of the event, results are accumulating at a slow rate. In addition, the data likely contains subjective bias caused by the emotional nature of the event itself plus the personal discomfort brought on by the weather conditions at the time. Nevertheless, the current data bank represents the best definitive information concerning galloping that has ever been assembled.

## RECOMMENDATIONS FOR FUTURE RESEARCH

There is reason to believe that some results are lost because the trained observers do not get to their assigned test site while galloping is going on. The proper storm conditions required to cause galloping can be micro-scale in proportion and many test sites are in isolated locations, out of sight of neighbors and passerbys. It would be very helpful, therefore, to have a durable/ positive/low cost alarm system which could sense when climatic conditions are conducive and alert the observers to deploy. There would also be a significant benefit from an automatic recording device, such as a self triggering movie camera, providing the cost can be kept low and an adequate level of reliability can be assured.

The four parameters that personal observers have the most difficulty quantifying are also the four parameters that are probably the most significant:

o wind speed at conductor height

o wind direction at conductor eight

o ice shape on conductor

o ice shape orientation on conductor

It would be highly desirable, therefore, to have the following sensors:

+ an ice free anomometer

+ a sensor to detect ice shape along the conductor

+ a sensor to detect the orientation of the ice shape along the conductor

## CONCLUSIONS

Present international research activities will eventually produce sufficient data to develop predictable and cost effective(12) control of the problems caused by galloping conductors on overhead lines. Because of the randomness of the event, however, it is likely to take a continuous and significant investment of money and effort over a long period of time to produce verified solutions with a high confidence level. This time frame could be drastically shortened and confidence levels greatly improved by the availability of a practical alarm system, a reliable ice free anemometer, sensors to record ice shape and orientation and an automatic movie camera system.

It is hoped that concepts for producing these needed equipments will evolve from discussions that occur during this First International Conference on Atmospheric Icing of Structures.

## REFERENCES

1. Rawlins, C.B., "Galloping Conductors", Chapter 4 of Transmission Line Reference Book, EPRI, 1979
2. Nigol, O. and Harvard, D.G., "Control of Torsionally Induced Conductor Galloping with Detuning Pendulums", IEEE Paper A 78 125-7, 1978
3. Rawlins, C.B., "Analysis of Conductor Galloping Field Observations - Single Conductors", IEEE Paper 81 WM 038-9, 1981
4. Edwards, A.T. and Ko, R.G., "Interphase Spacers for Controlling Galloping of Overhead Conductors", IEEE Symposium on Mechanical Oscillations of Overhead Conductors, 79TH0064-6-PWR
5. Douglas, D.A. and Roche, J.B., "Anti-Galloping Potential of a New Twisted Conductor Design", Canadian Electrical Association International Symposium on Overhead Conductor Dynamics, Toronto, 1981
6. Whapham, R., "Field Research for Control of Galloping with Air Flow Spoilers", Missouri Valley Electric Association Conference, Kansas City, Missouri, 1982
7. Den Hartog, J.P., "Transmission Line Vibration Due to Sleet", AIEE Transaction, Vol. 51, 1932
8. Richardson, A.S., "Design and Performance of an Aerodynamic Anti-Galloping Device", CIGRE Study Paper CSC -6-68-8, 1982
9. Havard, D.G. and Pohlman, J.C., "Control of Torsionally Induced Conductor Galloping with Detuning Pendulums", IEEE Paper A 78 125-7, 1978
10. Pohlman, J.C. and Rawlins, C.B., "Field Testing an Anti-Galloping Concept on Overhead Lines", IEEE/PES Overhead and Underground Conference and Exposition, Atlanta, Georgia, 1979
11. Havard, D.G., "EPRI Research Program RP-1095, Galloping Control by Detuning", Progress Report No. 4, May 1982
12. Havard, D.G., Paulson, A.S. and Pohlman, J.C., "The Economic Benefits of Controls for Conductor Galloping", CIGRE General Conference, Paris, 1982

AD P001702

# DEVELOPMENT OF AN ICE AND SNOW LOAD TRANSDUCER TO SIMULATE TRANSMISSION LINE LOADING

N.W. Brodie PEng, B.C. Hydro Research and Development
D.E. Franklin PEng, B.C. Hydro Research and Development

Transmission line planning and design engineers require detailed knowledge of atmospheric conditions along proposed routes. Specific details are required for local conditions in valleys and mountain passes as well for the general area. B. C. Hydro researchers have developed a relatively simple strain gauge based transducer which monitors snow and ice accretion on a simulated transmission line sample. The transducer has a dual range output, providing both high sensitivity under light icing conditions and low sensitivity under heavy icing conditions. Laboratory and field testing of the transducer has been done to eliminate structural problems found in the first prototype. The modified transducer has been in service for one year and has provided continuous analogue data. Plans to compare this device with other methods of ice accretion measurement are discussed.

## INTRODUCTION

B. C. Hydro has gathered ice and wind loading data by instrumenting existing transmission lines and by building instrumented test spans. The data has then been used to evaluate existing transmission line design and to form the basis for designing new lines.

Instrumenting existing lines or test spans is a sound method of generating transmission line loading data, however it is expensive. A relatively simple low cost device has therefore been developed for monitoring ice and snow loads on a simulated transmission line sample.

Initial field testing of the device resulted in fatigue failures in several components. A subsequent model was provided with mechanical vibration damping and a helical strake to discourage aeolian vibration. Wind tunnel and field tests of the modified device have been completed satisfactorily.

## TRANSDUCER DESIGN

The transducer consists of a one metre long tube which is supported horizontally in cantilever configuration by two strain gauged webs. The weight of ice or snow accumulated on the tube produces high levels of shear strain in the webs. The structural arrangement is shown in Figures I and II.

The body of the transducer, shown in Figure III was designed so that it could be easily milled from 25 mm thick 6061-T6 aluminum plate.

The tube can pivot freely on the webs and record normal ice and snow loads. An independent tapered steel rod has been fitted concentrically into the base of the tube. If the loads become excessive, the tube contacts the steel rod. The tube and rod then move together providing a lower sensitivity range to record high loads.

This dual range feature allows a sensitive measurement of a light icing condition while at the same time allowing accurate recording of heavy loads.

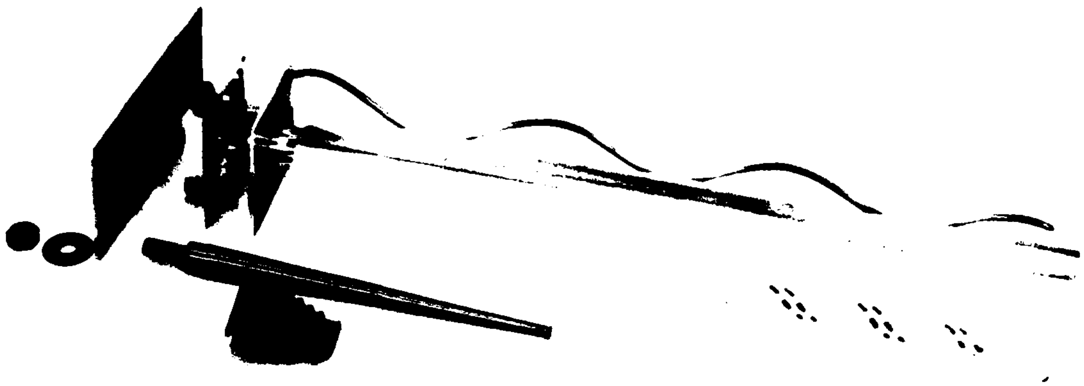

Figure I Photograph illustrating the components of the prototype.

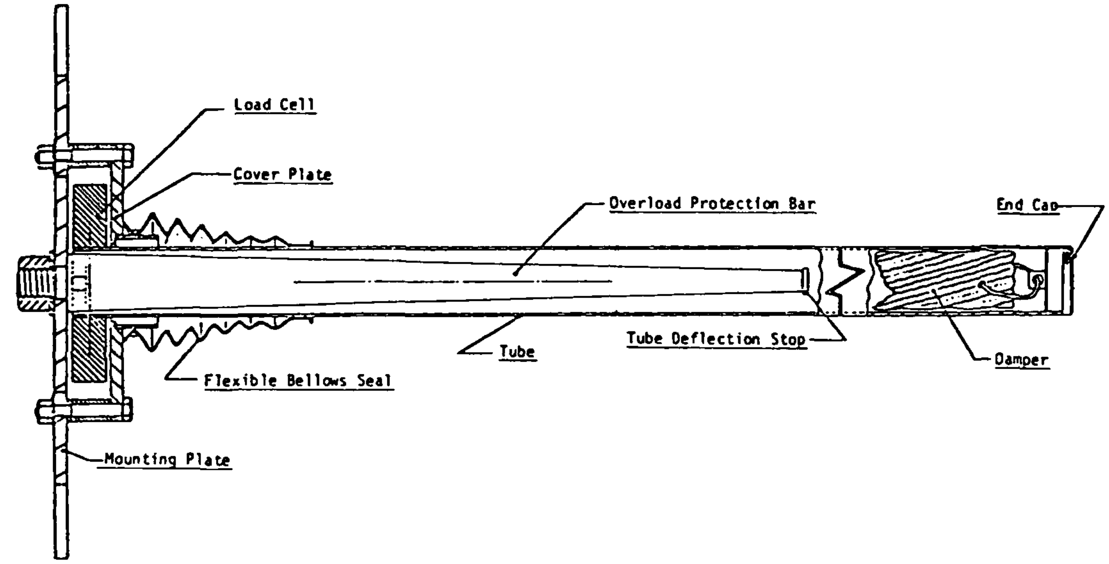
Load Cell
Cover Plate
Overload Protection Bar
End Cap
Tube
Tube Deflection Stop
Damper
Flexible Bellows Seal
Mounting Plate

Figure II Sectional view illustrating major features of the transducer.

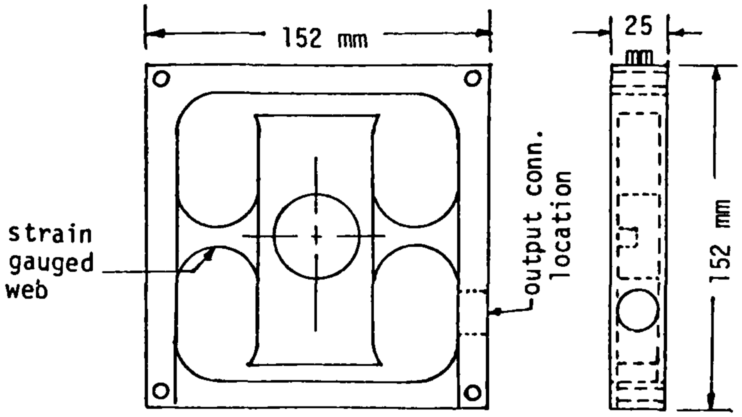
152 mm
25 mm
strain gauged web
output conn. location
152 mm

Figure III Details of the shear-strain sensitive body of the transducer.

It also protects the load sensing portions of the cell from plastic overload if workers use the device as a climbing aid or if there are very heavy ice loads. The device has been designed to be insensitive to horizontal wind forces.

During early field trials, the first prototype unit suffered fatigue failures in the measuring webs and in the tube. A mechanical vibration damper and a helical aerodynamic vortex spoiler were subsequently incorporated into the transducer design. The helical strake was produced by wrapping one strand of 6 mm diameter armour rod around the full length of the tube.

Several types of mechancial vibration dampers were examined. The final choice was to place a 250 to 300 mm length of 25 mm diameter rope into the free end of the tube and tether it to the tube cap. This rope consisted of a braided nylon jacket over a braided polypropylene core. The construction is probably not too important as long as the rope is flexible and easily deformed. For moderate to high vibration amplitudes the log decrement (which is proportional to damping factor) for the free tube was about 0.03 and improved to about 0.60 with the rope impact damper. The damper system proved satisfactory in both wind tunnel testing and subsequent field evaluations. It is simple, inexpensive, durable and effective. In order to fully control vibration, however, one must also ensure that the structure on which the transducer is mounted is stiff enough or sufficiently well damped that it does not introduce high levels of vibration into the unit.

## TESTING AND EVALUATION

### Calibration

The prototype transducers were calibrated using dead weights. The assumption was made that the ice distribution would be uniform over the length of the transducer so that the output calibration was expressed as kilograms of ice per metre. Figure IV illustrates the calibration of the transducer as a function of ice/snow weight per metre.

### Damper Evaluation

The logarithmic decrement evaluation of the damping system was accomplished by displacing the end of the tube then releasing it and allowing the unit to vibrate freely. The amplitude of vibration was recorded from the normal transducer strain gauge output. Impact type dampers are ineffective at low amplitudes of vibration, however, the components operate below the fatigue limit of the metal under these conditions. This has not presented any problem.

Wind tunnel tests to velocities of approximately 25 metres per second were carried out on the modified prototype transducer. The helical spoiler proved effective in attenuating the formation of vortices and the mechanical damper proved effective in controlling vibration amplitudes excited.

### Recording

The signal output from the transducer is normally recorded as a one minute average on a data logger, however, the signal may be recorded in real time or as an average or peak over any period designated.

### Field Trials

Field trials have been successfully conducted since the summer of 1981. Icing has been recorded on every monthly record from October until the time of writing this paper in April 1982.

From late November until March icing has been virtually continuous. It has varied from a high of over 20 Kg/m to almost no ice at all and has built up and dissipated many times. Examples of the output data are illustrated in Figures V and VI.

The field trials have been conducted at our Mission Ridge instrumentation test site. This site is located at a microwave repeater station which is about 1900 metres above sea level. The site is on a ridge in the coast mountains. Because of the topography of the region, the wind normally blows across the ridge and it is frequently subjected to adiabatic cooling. As a result of these factors, high winds and structural icing are quite common in the area. Any instrument which functions well at this site should be adequate for monitoring most proposed transmission line routes.

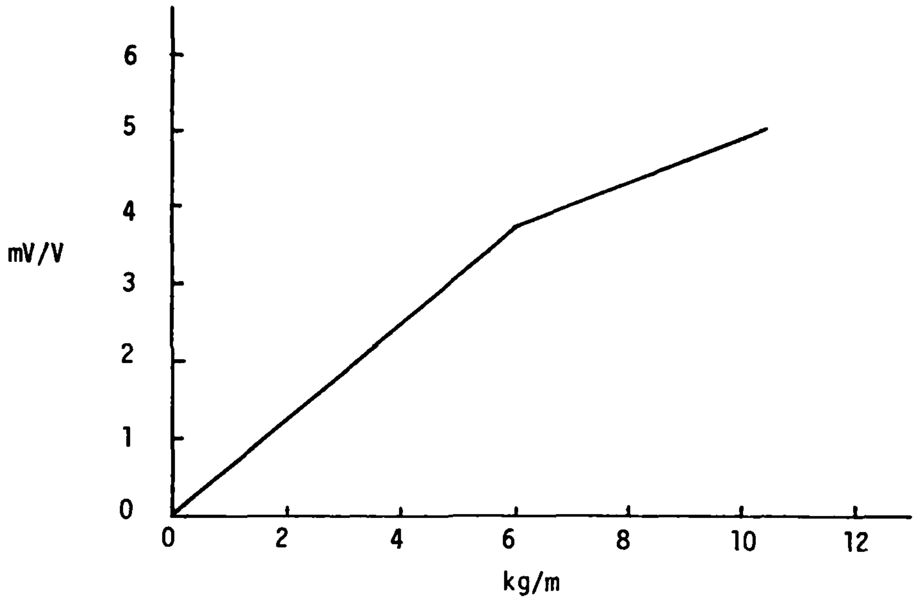

**Figure IV** Calibration chart for the transducer expressed in millivolts per volt as a function of the ice/snow load per metre.

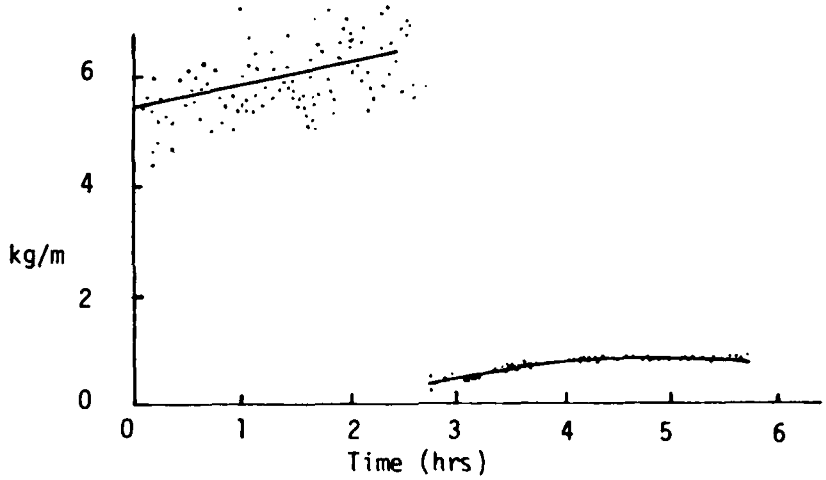

**Figure V** Sample output from transducer illustrating build-up of ice and sudden drop-off.

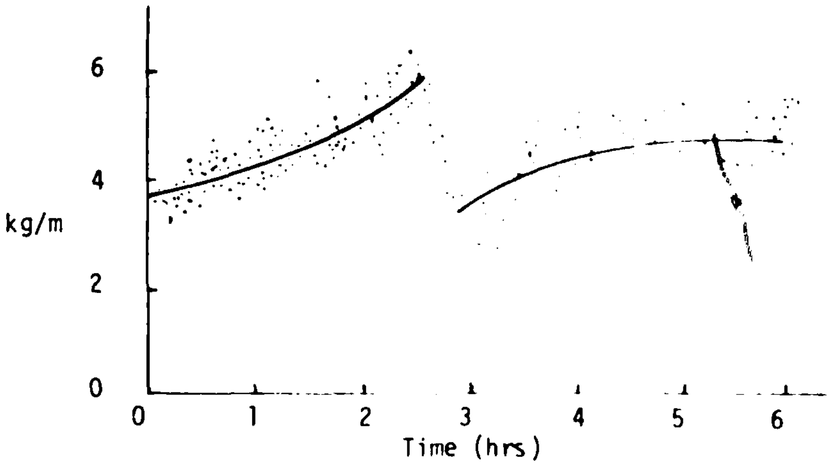

**Figure VI** Sample output from transducer illustrating build-up of snow/ice with partial drop-off during sampling period.

### Future Developments

This year, correlation studies will begin to compare the output from the transducers with the loads measured on adjacent instrumented transmission line spans.

Additional consideration is also being given to modifying the surface texture of the cantilevered tube to better approximate the actual surface of a proposed conductor. The thermal mass of a conductor is also under investigation to see if changes in this parameter would be required to simulate actual conductor loading.

Work has begun to develop a modified version of the transducer with a very simple mechanical load recorder. The objective will be to produce a low cost unit which could be placed in remote areas with no mains power supply or electrical batteries. Such a unit would record either the maximum load or else the magnitude of various loads without a record of the time of occurrence. Even the simplest of such devices would provide additional data to help produce a predictive model of icing conditions in proposed transmission line corridors.

## DISCUSSION

Active and passive techniques are used by others to monitor ice accretion on either transmission line samples or on actual transmission lines. Passive devices have included the use of a set of mechanical fuses which break under progressively higher loads and visual observations of ice accretion. Active devices include load cells to weigh a test span or an existing transmission line and vibrating reed devices which monitor the rate of ice accumulation.

The most accurate way to monitor ice accretion and dissipation is to weigh a transmission line. This is not always possible however since new routes will not have existing lines and a test span may be too expensive to install.

## CONCLUSION

A simple and reliable transducer has been developed to measure and record ice and snow accumulation as it will occur on electrical transmission lines. Field studies are underway to compare the output from this device with loads measured on adjacent instrumented transmission lines. Plans have been made to develop a mechanical recording version of the transducer which would record maximum ice loads without the need of an electrical power supply.

AD P001703

# EXPERIENCE CONCERNING ICE LOADS ON OVERHEAD LINES IN AUSTRIA

H. Schauer Österr. Elektrizitätswirtschaft AG, Vienna, Austria
W. Hammerschmid Osterr. Elektrizitätswirtschaft AG, Vienna, Austria

## Abstract.

After a description of the climatic and topographic conditions, a short outline is given of design rules practised by Austria´s overhead line engineers with respect to ice loadings. This is followed by a summary of actual experience gained in line operation.

## Climatic and topographic conditions.

Austria is an Alpine country situated not only in the heart of Europe but also in an area where three major climatic regions meet and overlap. The westerly winds bring Atlantic depressions, normally accompanied by precipitation, and penetrate to the eastern parts of the country, which in addition are frequently affected by the continental cold air masses from the east. Finally, the areas situated on the southern slope of the Alps are greatly influenced by the climate of the adriatic region.

Apart from the overall meteorological situation, which is often complex and may vary considerably over the country as a whole, secondary conditions may develop along individual transmission lines, resulting in a variety of greatly different local situations. These in turn may lead to extreme span-to-span differences in ice loadings. Such striking inconsistencies tend to occur mainly in the north-south passes in the Alps when strong southerly winds bringing moist and warm air masses from the Adriatic region blow up the steep southern slopes of the Tauern massif and reach the freezing limit at the mountain passes, many of which narrow like nozzles. This results in substantial ice loads, which often occur in form of rime. (Incloud icing. The maximum ice weight measured so far was 18 kg/m).

Similar phenomena are encountered on the northern foothills of the Alps irrespective of the altitude, mainly on the west and northwest slopes in the Danube valley and in the northern and western parts of the Vienna Woods. The valleys and lowlands, finally, also receive heavy rainfalls, chiefly brought by westerly winds, and at falling temperatures wet snow starts to stick on the conductors and may also cause considerable additional loads if wind is acting simultaineously.

Neither the altitude of the areas concerned nor the map of local snow loads given by Austrian standards committee, may be regarded as a sufficiently valid criterion of the magnitude of expected ice loadings.

On the other hand, however, consideration of topographic details, observation of climatic facts in the field and, in some cases, application of geobotanic knowledge combined with personal judgment may yield hints concerning potential rime and ice areas. But Austria´s line construction engineers have largely had to depend, from the very beginning, on the instructive but thorny path of personal experience and exchange of experience.

## Icing observations and design ice loading assumptions.

The need for a more detailed knowledge of local icing has given rise, in Austria as in other countries, to attempts at experimental forecasts. However, apart from some minor test stations, it took a long time for the first systematically run ice load measuring station to be installed. This is probably due to the very large local icing variety mentioned before and to the distribution of zones of increased icing situations over the whole country, as well as to the fact that not only the Verbund Combine but a number of regional electricity companies are in charge of energy generation and distribution. It was not before the foundation of a study association for "Ice Load Measurement", comprising all major Austrian Electricity Companies, that a mobile measuring station was provided, which was used first in winter 1963/1964. Apart from recorders for wind direction and velocity (cup anemometer), air temperature and humidity (thermohygrograph), the station essentially consists of a mechanical conductor pull measuring device (dynamometer). It may be installed both on existing lines and on test spans, and it automatically records all quantitative pullvariations by means of an electric resistance meter.

However, as there is much demand for these installations on the part of the electricity companies, they are passed on frequently, and it is not suprising, that no sensational results have so far been obtained. But the measurements made have confirmed that the assumptions regarding the annual normal ice deposits are essentially correct. Recording the occurrence of exceptional ice loadings of course needs longer periods but is essential for the statement of design loadings. It may be interesting to note in this context that the earlier Austrian regulations on overhead lines did not contain any differentiation of ice loadings, neither regarding the type of icing nor the probability of occurence.Especially the latter is of essential importance for the design which in Austria is done by calculation only.

Icing with high probability of occurence (say "normal ice load") needs a higher degree of withstand capacity of towers and other line elements, while icing with low probability of occurence (say "exceptional ice load") may allow a reduced degree of safety depending on the needed line reliability.

When preparing the ÖVE-L1/1°5o regulation the term "exceptional ice load" was introduced and defined as a "multiple of the normal ice load" but, following earlier practices, its application was confined on the conductor and their "fastening on the towers".

Only when the ÖVE-L1 regulation was revised in 1956, the consideration of an exceptional loading case in the design of the towers and their foundations was made a binding requirement for "lines of special importance with a rated voltage from 6o kV". However, as the revised regulation only covered the consideration of increased angle pulls due to exceptional ice load and did not cover longitudinal pulls resulting from unbalanced ice loads, this provision remained likewise unsatisfactory.

In view of the tower failures caused by extreme ice loads on the networks of several electricity companies in the years 1954 to 1958, the line construction engineers of Verbundgesellschaft and of several other electricity companies found an internal solution to the problem by adopting their own "special loadings cases". These consider, in addition to the angle pulls, longitudinal pulls (50 percent reduction of the pull of all the conductors in one span) and torsional loading cases due to unbalanced ice loading.

Initiated by this trend, a new revision of the regulations on overhead lines was undertaken. The result was the ÖVE-L11/1967 regulation, which is still in force. This revision of the regulations concerning the "construction of high voltage overhead lines of more than 1 kV", which was carried out with much conscientiousness and on a large scale in the technical committees, not only did away with the inconsistency resulting from the discrepancies in the mechanical safety coefficients applied to the individual elements of overhead lines, but introduced a redeterminination of the minimum "exceptional ice loads" in the form of fixed values independent on conductor diameters:

| | |
|---|---|
| 2.5 kg/m | for overhead lines with a rated voltage of not more than 45 kV, |
| 3.5 kg/m | for overhead lines with a rated voltage from 45 to 110 kV, |

| | |
|---|---|
| 4.0 kg/m | for overhead lines with a rated voltage from 110 to 220 kV, |
| 5.0 kg/m | for overhead lines with a rated voltage of 380 kV. |

The reason for choosing this differentiation based on the rated voltage was the desire to weigh the contradictory requirements of reliability on the one hand and economy on the other hand, regarding the voltage level as approximative criterion.

It should finally be mentioned for the sake of clearness that all the figures given above refer to minimum values and must be applied to all conductors resp. subconductors. The new overhead line structures of Verbundgesellschaft normally are designed to withstand 50% increased loadings for areas of high icing probability, or even twice the above given minimum ice loads in extreme situations (mainly in the high mountains). This results in exceptional ice loads up to 10 kg/m, causing enormous mechanical loads, especially in the case of bundle conductors and multicircuit lines. Extra high tension lines thus become imposing structures of great constructional interest representative of our modern technology.

## Conductor spacing and arrangement.

The magnitude of the ice deposits has a bearing not only on the mechanical design of overhead line elements, but also on the choice of conductor spacing and, consequently, the arrangement of the conductors on the towers. So the Austrian line construction engineers have found, that the generally known spacing formula

$$A = K.\sqrt{f + l} + Z$$

where A ... spacing

K ... factor dependent on shape of conductor arrangement

f ... sag

l ... string length

Z ... addition dependent on rated voltage

by no means ensures adequate security against conductor clashing due to unbalanced or dropping off ice resp. wet snow deposits, even where conductors of same material and same cross-section are used. This experience mainly applies to the so-called "barrel" configuration, which is very much in use for double circuit lines in Austria (vertical arrangement of the phases of each system with horizontal stagger).

On the other hand, a method developed by H. Krautt using as a criterion the rebounding of conductors when ice is dropping off, combined with simultaneous deflection due to wind action, has proved successful and is generally used in Austria. But it may, and must, be stressed in this context that the attainment of absolutely disaster-proof reliability by the don´t-dare-otherwise approach is not only unworthy of a modern engineer but is simply presposterous from the economic point of view.

## Practical Experience gained during line operation.

When in 1947 Verbundgesellschaft was founded to succeed the former Alpen-Elektrowerke, it took over a stock of 826 km 110 kV lines, 184 km completed and 159 km 220 kV lines under construction. In the years which followed many more lines were built, which - according to the date of design- meet modern experience and design rules to a greater or lesser degree.

Nowadays the grid system, reaching up to altitudes of 25oo m above sea level, has spread out to:

573 km 38o kV lines (at present operated at 220 kV), with bundle conductors,
1786 km 220 kV lines, most of them equipped with bundle conductors,
11o8 km 11o kV lines, (all lengths are actual route lengths, most lines are double circuit ones).

The failure statistics of the grid system of Verbundgesellschaft, of which an abstract is given in the Annex convey a true idea of the practical experience gained with ice and wet snow loadings. These failures may be summarized and interpreted as follows:

Towers damaged or collapsed by excessive mechanical loads resulting from extremely thick ice or wet snow loadings on conductors: Serious failures of this type only occurred on old lines which were designed for normal ice loadings only. An especially unfavourable factor in the major break-down near Lienz (November 1958) was the rectangular cross-section of the suspension tower bodies then widely in use. After the deadend tower had failed, the resulting longitudinal pulls tore down the following suspension towers like houses of cards. For the rest, heavy failures were confined to the 110 kV network. This is easily explained by the fact that most of 220 kV lines were constructed later on. So, in consequence of the revisions of the design regulations, the discrepancy between the design ice load and the actual ice loadings is smaller for newer lines. In addition, the increased length of insulator strings for suspension towers is producing a welcome reduction of conductor pulls due to unbalanced ice deposits. Up to now, no failures on 38o kV towers occured.

Damage caused to insulator strings and conductor clamps in very steep spans by pieces of ice crusts sliding down the conductors has led to the conclusion that a water film forms in the spehre between conductor and surrounding ice coating at the time the ice starts to melt, causing the ice crust to glide down with great speed. Ice splitting clamps especially designed for this purpose were then mounted in front of insulator strings subjected to such risks and have proved successful.

Conductor breakage due to ice load is very seldom. However, the damage observed in the outer layer of steel-aluminium earth wires, in the vicinity of the suspension clamps, is considered a direct result of differential pulls caused by unbalanced ice loads (compensating movement). No such damage has, however, occured on the steel-reinforced aluminium alloy earth wires, which have since been installed.

By far the largest proportion of failures due to ice or wet snow are caused by conductors clashing together or by flashover from live parts to tower structures. The resulting short circuits as well as earth faults and double earth faults caused conductors to start melting and strands to break. Characteristically, most of these failures always occurred in the same line sections and were largely confined to a few spans. Ascending winds, which are frequently observed in these sections favour the growth of ice coats, moreover, reinforce the motion impulses of the conductors. The tendency towards sag displacements as a result of unbalanced ice deposits is still higher in long stringing sections with many intermediate suspension towers, due to the mobility of the suspension strings. The most reliable remedies found so far are subsequently increased conductor spacing by means of lengthened tower crossarms and, in the latter of the above cases, subdivision of long stringing sections by providing intermediate tension towers. By way of trial insulating rods have lately been installed as spacers between the condutors.

Finally it may be interesting to note that even in mountainous regions altitudes of up to 25oo m above sea level, coalescence of ice coats on subconductors of a bundle, as has been apprehended by some experts abroad, has not been observed yet.

Only in the flat area around Vienna, the combination of rime load and gusty wind has caused in a few cases horizontally arranged twin bundle conductors to be "turned over". After the rime coat had melted, they more or less automatically turned back to their original position. Still, this incident appears to be significant enough to stress the advantage of a vertical twin bundle conductor arrangement.

Reference:

H. Krautt, CIGRE-Report Nr.219,1937

"Leiteranordnung und Phasenabstände bei Hochspannungs-Freileitungen, Beurteilung vom Standpunkt der Betriebssicherheit".

ANNEX:

ABSTRACT OF FAILURE STATISTIC OF VERBUNDGESELLSCHAFT AS REGARDS EHT-LINE FAILURES DUE TO ICE LOADINGS.

| Year | Total route lengths km | | | Description of failure |
|---|---|---|---|---|
| | 11o kV | 22o kV | 38o kV | |
| 1948 | 826 | 114 | - | no failures occured |
| 1949 | 89o | 343 | - | no failures occured |
| 195o | 1o13 | 551 | - | November: 11o kV line, designed 195o for ice load 1o kg/m, crest section, altitude 25oo m: crossarms of tension towers collapsed due to ice load 14 kg/m. |
| 1951 | 1o13 | 551 | - | December: in above crest section torsional collapse of one tension tower ; at adjacent tower conductor clamp damaged by sliding ice crust. |
| 1952 | 1o48 | 551 | - | no failures occured |
| 1953 | 1o52 | 551 | - | no failures occured |
| 1954 | 1172 | 619 | - | December: three tension towers collapsed in above crest section; two further tension towers damaged by pulls resulting from unbalanced ice (estimated 18 kg/m). |
| 1955 | 1174 | 619 | - | February and April: Shortcircuits and double earth fault on two 11o kV lines. |
| 1956 | 1236 | 619 | - | October: five 11o kV concrete pools, designed 1939 for ice load appr. 1 kg/m collapsed due to wet snow and storm acting simultaineously. |
| 1957 | 1296 | 637 | 63 | no failures occured |
| 1958 | 1296 | 868 | 63 | November, Jannuary and March: Short circuits and double earth faults on 11o kV lines.<br>November: A total of 64 11o kV towers collapsed or heavily damaged by wet snow rolls of 17 cm diameter. This line was designed 1952 for o,83 kg/m ice load and is running at the bottom of a valley. When the deadend tower failed, cascading effect started. Even intermediate tension towers were not able to stop cascading because of lacking loading assumptions for heavy longitudinal pulls. Adjacent line sections were free from ice! |
| 1959 | 13o2 | 9o3 | 63 | November, Dezember, March: Short circuits and earth fault on 11o kV lines. |
| 196o | 1354 | 1o46 | 63 | no failures occured |
| 1961 | 1358 | 1o87 | 63 | Jannuary: earth wire peaks of three 22o kV suspension towers damaged by longitudinal pulls resulting from unbalanced wet snow loadings; strands of outer layer of earth wire broken due to earth wire slip. |
| 1962 | 1358 | 1298 | 63 | November: spacer of insulator string heavily damaged by ice crust sliding down the crest section (same 11o kV line |

| Year | Total route lengths km<br>11o kV | <br>22o kV | <br>38o kV | Description of failure |
|---|---|---|---|---|
| | | | | as notified in the column for the year 1950).<br>Dezember, February: short circuits in a few 11o kV lines, partly resulting in breakage of strands caused by arc stream of clashing conductor (11o kV lines). |
| 1963 | 14o8 | 1455 | 11o | November, Dezember: Short circuits and breakage of strands as mentioned before (11o kV lines). |
| 1964 | 14o8 | 1384 | 18o | Jannuary: Short circuits on 11o kV lines as before |
| 1965 | 1412 | 1388 | 18o | no failures occured |
| 1966 | 1443 | 1388 | 18o | November: Short circuits on a 22o kV line. |
| 1967 | 1443 | 1436 | 18o | no failures occured |
| 1968 | 1443 | 1529 | 18o | February: Flashovers on insulator strings during ice melting process and short circuits between phases (11o kV lines). |
| 1969 | 1463 | 166o | 18o | Jannuary, February, April: Short circuits (11o and 22o kV lines). |
| 197o | 1463 | 1689 | 18o | Jannuary, February,April: short circuits (11o and 22o kV lines), partly resulting in breakage of strands. |
| 1971 | 1463 | 16o5 | 18o | April: Flashover on iced insulator strings (22o kV line). |
| 1972 | 1463 | 16o5 | 18o | Dezember, February: Flashover on iced insulator strings and short circuits between phases (11o kV lines). |
| 1973 | 1463 | 16o6 | 18o | Jannuary: double earth faults (11o kV). |
| 1974 | 1463 | 1687 | 18o | Jannuary: earth faults caused by freezing rain (11o and 22o kV lines). |
| 1975 | 1346 | 1733 | 224 | November, Dezember, March: earth faults and short circuits between phases resulting from wet snow rolls up to 25 cm diameter (11o and 22o kV lines). |
| 1976 | 1371 | 1786 | 278 | no failures occured |
| 1977 | 1285 | 1786 | 5o1 | Jannuary: conductor breakage (old 11o kV line) resulting from arc stream (clashing conductors) |
| 1978 | 1284 | 1786 | 573 | April: Short circuit (11o kV line). |
| 1979 | 1446 | 1786 | 573 | March: Total of 17 towers of 11o kV line designed 1952 for ice load 1 kg/m, collapsed due to heavy wet snow loadings and storm acting simultaineously. Short circuits and earth wire damaged, partly broken on 12 other 11o and 22o kV lines. |
| 198o | 11o8 | 1786 | 573 | Jannuary: Earth faults and short circuits on several 11o and 22o kV lines. |
| 1981 | 11o8 | 1786 | 573 | no failures occured |

AD P001704

# METHODS OF CALCULATING ICING LOADS ON OVERHEAD LINES AS SPATIAL CONSTRUCTIONS

T.N. Golikova  All-Union Research Institute of
B.F. Golikov  Energetics, USSR
D.S. Savvaitov

## Abstract

The paper deals with the method used in design practice for calculating icing loads on OH line conductors. Relationship between the probability of exceeding the standard icing load on OH lines and the length of the latter is analyzed.

To calculate this relationship the method is used, which considers the line length and the width of the zone $\theta$ with simultaneous exceeding of the design ice load. It is shown that to determine the probability of exceeding the design ice load on the whole line (P), we should account for relation in time between the cases of exceeding the design load and the probability characteristics of the zone width $\theta$.

The conclusion is drawn, that the value of probability P is more than probability of exceeding the design load in individual line points (p), and that P increases with the line length. This relation might be neglected only for the lines with lengths less than 10% of the width of zone $\theta$. It is found, that with a given return period of design load for the whole line, the return period of this load for an individual line point is a function of the line length, and for long lines it is proportional to the line length.

The proposed method may be used for the calculations of ice and ice-wind loads.

## Paper

When designing overhead transmission lines the standard values of ice loads (which correspond to conductor stress equal to about 40% of the breaking value) are determined by the ice-zone maps, each zone corresponding to a certain ice thickness value (in mm). These maps have been compiled using statistical treatment of ice observations data from meteorological stations.

The ice observations are made using two 5 mm diameter conductors rigidly fixed at 2 m above the ground, one oriented North-to-South and the other West-to-East. The results obtained are reduced by correction factors to a reference line with 10 mm diameter conductor suspended at 10 m above the ground.

The standard ice loads with a given return period or given security are determined by distribution function of year maximums of ice thickness.

The Fisher-Tippet function is taken as approximating one:

$$F(b_1) = e^{-\left(\frac{b_1}{\beta}\right)^{-\mu}} \qquad (1)$$

where $\beta$, $\mu$ - parameters characterizing average load value and dispersion.

The distribution function is drawn up on probability paper, $F(b_1)$ being plotted on bilogarithmic scale and $b_1$ on logarithmic scale, which results in flattening the distribution function.

The standard ice load $b_1$ is a function of the given return period of cases with exceeding standard load or a function of the given security $F(b_1)$.

The value of $F(b_1)$ equal to 90% corresponds to the return period of 10 years. Each point on the map of standard ice zones meets the above condition.

When compiling ice load maps the effects of phisical and geographical conditions are considered, such as particular features of relief, absolute and relative altitude elevations, slope exposure, character of synoptical processes causing icing formation, as well as other factors which influence ice load distribution over a certain area, but the line length is not considered. Therefore the maps don't allow to determine the load return period along the whole line of sufficient length, since it is unknown whether cases of exceeding the standard load over different line sections are related with time or occur independently.

The data from observations show that at weather stations located hundreds and even tens kilometers apart, cases of exceeding the standard ice loads have been obsrved more often during different years, i.e. they occured independently of one another and have been caused by different ice formation processes.

The relationship between the probability of exceeding the rated ice loads and the line length has been determined by the method involving consideration for the size of the zone with simultaneous exceeding of the rated ice load and correlation of the line length with the zone size.

The paper presents the results of theoretical studies.

The zone with simultaneous exceeding of the standard ice load should be distinguished from the zone with simultaneous ice covering. With the same synoptical processes the rated load may be achieved or not achieved in spite of the large size of the zone of simultaneous ice covering, but sizes of the zone with simultaneous exceeding of the rated load may be extremely small.

It is believed that the zone sizes depend on character and range of atmospheric processes, and also on physical and geographical features.

The zone of exceeding the rated loads, being a random variable, is characterized by possible values of its sizes and law of their distribution.

Analysis of the relationship between the probability of exceeding the rated load on the OH line and its length $P_1 = f(l)$ is carried out providing the zones distribution being random with the constant density both over the given area and with time. The following values were assumed to be known: the probability of exceeding the rated load at any point of the given area over a year (p), determined from long term observations at weather stations, and the size of the zone: with the presence of ice carrying flow - the zone width $\beta$ and in the absence of the flow - the zone diameter D.

At the first stage of calculation the sizes of the zone were considered to be constant.

In the absence of the ice carrying flow a weather station or a point of the line falls within the zone of the simultaneous exceeding ice load with diameter D, if the zone center falls into the circle with the same diameter and with the centre at the same point (Fig.1a).

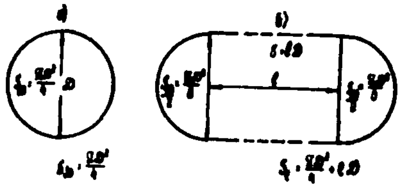

Fig.1. Area of the zone with diameter D (a) and area $S_1$ (b)

The exceeding of the rated load on the OH line with length l will occur in the cases when the zones with diameter D fall into the area $S_1$ around the OH line (Fig.1b).

In calculation the zones with simultaneous exceeding with diameter D are replaced by the points which meet the above conditions of distribution with space and time, and the points of the line are, quite the reverse, replaced by circles of diameter D and with centres coinciding with the line points.

The entry of the point into the circle of diameter D around the line point results in exceeding the rated load at the line point with probability p.

The area of the territory, $S_l$, including the circles with the radius D/2 around all line points is equal to:

$$S_l = \frac{\pi D^2}{4} + lD \qquad (2)$$

and this area is $n = 1 + \frac{4l}{\pi D}$ times more than the area of the circle of diameter D (Fig.1b).

If the probability of the point entry into the circle of diameter D in a year equals p , then the probability that such event will not occur equals 1-p, and the probability that the point will not fall into the area $S_l$ equals

$$\bar{P} = (1 - p)^n \qquad (3)$$

Then the probability of the point entry into the area $S_l$ in a year (i.e. the probability of entry of the zone with diameter D even on one point of the line) equals

$$P_l = 1 - (1 - p)^{1 + \frac{4l}{\pi D}} \qquad (4)$$

Provided that $p\frac{4l}{\pi D} \ll 1$ the following is obtained:

$$P_l = p\left(1 + \frac{4l}{\pi D}\right) \qquad (5)$$

With the presence of the ice carrying flow it has been found using the similar method that

$$P_l = 1 - (1-p)^{1 + \frac{l}{\theta}} \qquad (6)$$

and with $p\frac{l}{\theta} \ll 1$

$$P_l \cong p\left(1 + \frac{l}{\theta}\right) \qquad (7)$$

where $\theta$ - the width of the zone with simultaneous exceeding of the rated ice load.

It is advisable that formula (7) should be used for most practical cases. Comparison between the relationships $P_l = f(l)$ given on Fig.2 and determined from (6) and (7) shows the boundaries where it holds true.

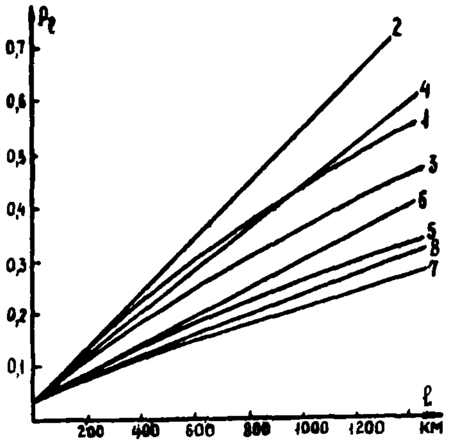

Fig.2. Relationship between probability of exceeding the rated ice load $P_l$ and the line length with p = 0.04

$$\left.\begin{array}{l}1 - \text{eq.}4\\ 2 - \text{eq.}5\end{array}\right\}D=100\text{km} \qquad \left.\begin{array}{l}5 - \text{eq.}4\\ 6 - \text{eq.}5\end{array}\right\}D=200\text{km}$$

$$\left.\begin{array}{l}3 - \text{eq.}6\\ 4 - \text{eq.}7\end{array}\right\}\theta=100\text{km} \qquad \left.\begin{array}{l}7 - \text{eq.}6\\ 8 - \text{eq.}7\end{array}\right\}\theta=200\text{km}$$

Thus, the probability $P_l$ is always more than probability p and increases with an increase in the line length. The degree of the increase (curve steepness) grows with the decrease of the width of the zone with simultaneous exceeding of the rated ice load.

Formula (7) allows to determine the maximum line length at which the probability $P_l$ (for the whole line) is more than the probability p (for the line point) by 10%, i.e. at which these probabilities may be considered approximately equal. This length, $l_{max} = 0.1\,\theta$ . If $\theta$ =200 km, then $l_{max}$ = 20 km.

It can be shown that for a 500 km OH line the probability $P_l$ will exceed p also by 10% only in case when the width of the zone $\theta$ equals 5000 km, that is when the zone is so large that it crosses all line sections practically simultaneously.

Under condition that the probabilities p and $P_l$ don't exceed 0.2 (the probabilities are equal with 10 percent accuracy to frequencies of cases of exceeding the rated load in a year), one may consider, that the return periods of the rated loads for the line points $T_p$ and for the whole line $T_l$

are related with the probabilities p and $P_1$ by the following relationships:

$$T_1 = \frac{1}{P_1} \quad \text{and} \quad T_p = \frac{1}{p} \qquad (8)$$

Taking into account (9) and using formula (7) one may obtain:

$$T_1 = \frac{T_p}{1 + \frac{1}{\theta}} \qquad (9)$$

This formula determines the relationship between the period $T_1$ and the OH line length with a given or calculated return period of the rated load at each point of the line. This task may be formulated in other way, namely, with a given return period for the whole line to determine the corresponding return period of the rated load for each line point, that is the following expression may be obtained from (9):

$$T_p = T_1 \left(1 + \frac{1}{\theta}\right) \qquad (10)$$

or in case if $1 \gg \theta$

$$T_p = T_1 \frac{1}{\theta} \qquad (11)$$

i.e. the return period of the rated load at the line point with the given return period $T_1$ for the whole line, is proportional to the line length. Relationships $T_p = f(l)$ determined from (10) are shown on Fig.3.

Comparing OH line construction costs and the costs of failures, and considering formula (10), one can find the optimal return period of the rated load for the whole line, $T_1$.

Thus two approaches to presetting the design ice loads may be used:

1. To determine the return period of the rated load for the whole line with the given return period of the load for the line point.
2. To determine the period of the rated load recurrence at the line point by presetting the return period of the rated load for the whole line.

The second approach is preferable in design process, since the reliability of components of any construction (line sections) should be determined based on the requirements imposed upon the whole construction (the whole line).

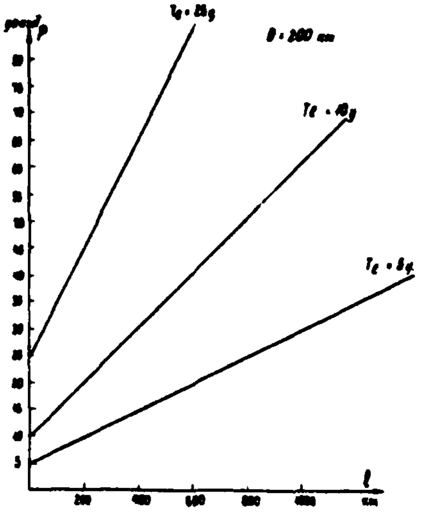

Fig.3. Relationship between return period of the rated ice load at the line point $T_p$ and the line length with the given return period for the whole line $T_1$.

With the known density of distributing the width of the zone with simultaneous exceeding the rated load, the probability of exceeding the rated ice load for the whole line will be equal

$$P_{1\Sigma} = \int_0^\infty \psi(\theta)\, P_1(\theta)\, d\theta \qquad (12)$$

where $P_1(\theta)$ is determined from the formulae (6) or (7).

Taking into consideration a variety of physical, geograhpical and synoptical conditions over the region or the country, one of the major problems whose solution is necessary for determination of the relationship between the probability of exceeding the rated ice load and the line length is to establish the law of distribution of of sizes of the zone with the simultaneous exceeding of the rated ice load.

The results obtained may be also used for calculations of wind and ice-wind loads. It should be noted that an increase in the probability of exceeding the rated ice and wind loads with an increase in the line length is supported by the experience of OH lines operation: the more is the line length, the more is the number of failures due to effect of climatic loads.

## Conclusions

1. The probability of exceeding the rated ice load on overhead lines is more than probability of exceeding the load at some points (sections) of the line and increases with the line length.

2. In designing OH line it is advisable that the return period of rated ice load for the whole line should be set, and then the rated loads for the line points should be determined.

3. The major task is the determination of distributing the sizes of the zone with simultaneous exceeding of the rated ice load.

# SESSION 5: PLANNING OF FUTURE ATMOSPHERIC ICING RESEARCH

## SESSION 5

Summary. The final session was devoted to an assessment by all participants of the content of the workshop and to a discussion of future research needs and mechanisms for information transfer. The needs of the varied constituencies represented at the workshop: utilities (powerline icing), aircraft operators and designers (airfoil and helicopter rotor blade icing), marine operators and designers (superstructure, or sea spray, icing) differ in detail but it was the consensus that it was valuable to include all these groups. The need for prompt establishment of standards for acquiring field meteorological and ice data for unambiguous comparison of all data on an international scale was stressed. The example was given of the many ways ice loading is presently recorded. Though utilities in the United States and their counterparts around the world have acquired vast quantities of data, in general this information is buried in files, and it was recommended that this be published, or transferred to a central repository, or both. The World Meteorological Organization (WMO) and the International Energy Agency (IEA) were mentioned as candidates. EPRI is coordinating the archiving of U.S. utility meteorological data. The participants agreed that four areas require further attention: development of improved instrumentation, especially an anemometer that will not be disabled by icing; ice accretion modeling; improved knowledge of the climatology of icing events; and the statistical analysis of icing data. Participants also agreed that a loosely-knit association of active workers and organizations would be desirable for future interchange of data and methodology. A second workshop is planned for 1984, to be hosted by The Norwegian Research Institute of Electricity Supply. In the meantime, CRREL will produce a directory of individuals and organizations working on the various aspects of structural ice accretion.

Pohlman - The purpose of this discussion today is to assess what we have been talking about the last couple of days, and maybe make a shopping list of future research needs. I hope that before we part company that we will have a clear-cut idea about what the next step is, who's going to take it, etc. One of the first things I would like to encourage the group to do is to discuss the needs for future research activities that were identified in the papers presented here. We came up with four categories and tried to sort the papers out into those categories for the program. However, if someone has better categories that we could confine the discussion to for a short period of time, I would be glad to do so now. Unless someone has some better ones, I suggest that we address each of these general areas one at a time and see what kind of shopping list we can develop. Before we get started on that let me make on announcement - all of you who are going to take the tour through the lab this afternoon, stay here, have lunch in the CRREL cafeteria, then go on the tour. Those of you who are going to Mt. Washington this afternoon, take the bus back to the hotel as soon as our meeting is over. After lunch, the CRREL van will pick us up for the trip to the mountain.

Question: How long will the tour of the lab take?

Minsk - An hour and a half, although it can be shortened if necessary.

Pohlman - I would like to open up the discussion with the first category, the physics of ice accretion. Would someone like to start the discussion? What do we need to do, what should we do in the future, what kinds of things do we need to undertake to give us a better idea of the physics?

Ervik - I do not feel quite happy about discussing this according to sessions, and an observation I think I have made is although we have the same final goal, to ameliorate difficulties we have due to icing, our intermediate goals do not seem to be the same. As for transmission lines, we realize that we have to live with ice and we try to cope with the ice coatings that we know we will have. As for other constructions, the solution is not to live with the ice, but rather to get rid of it. So at the outset I think there are some differences in the goals, and that might affect the way we attack the problem from the outset.

Pohlman - What you are saying is that our interest divides. Some say here is a problem and we have to live with it. Others are looking for preventive means to get rid of it. Is that the idea?

Ervik - Yes, it is. I think we have common interest but I think it is a good idea that we realize that our goals differ a bit, and if we realize this we can avoid some misunderstanding.

Pohlman - Nevertheless it all has to start some place. There is one thing I think I have heard said over the last two days: it's that we don't know everything we need to about icing, regardless of whether we can live with it, we don't know how much or whether we can get rid of it. Which means there are certainly needs for future research activities in this basic area of defining the icing mechanism and that sort of thing.

Krishnasamy - I have a problem of personal interest. On the icing model we have very much field data available and it would be a good idea if we could put all of these ideas together and in a short period of time, so that the designers can come up with a realistic model in as short period of time as possible, so the designers can have something to help out. So I would suggest first of all that we improve our data.

Olsen - I wonder if before we get into the areas it wouldn't be a good idea if we should discuss what groups we should be concerned with. For example, there's aircraft icing, powerline icing, and something that we haven't really discussed at all, splashing on oil derricks and such. I'm sure I am forgetting other things. The physics of ice accretion is all the same--just a little difference in the spreading of the technology, and how you balance one thing against another. Some things are covered by meetings in some areas, and others are not. We're not too bad off in aircraft icing so I think our needs are being met but I think some of these other areas might not have any particular conference. I would think that is almost the kind of thing you would want to define.

Pohlman - The question, then, and we'll ask the same question of others, is - you have a very specific interest in aircraft icing. Was it of interest to you - was it helpful to you, to hear discussions on some of these other applications like transmission lines? There is benefit to you from these other applications?

Olsen - Right. But the point I am making is that aircraft icing would always be so minor as to be trivial, but you need a liaison. We're not too bad off [with respect to] conferences on aircraft icing.

Jellinek - I think a lot of work on the transmission lines could be done in the laboratory so you can sort out the parameters. I think there are too many parameters in nature. You take a wind tunnel, for instance, and you can sort out these parameters much better and get some fundamentals ideas about the effects of these various parameters rather than have them all together and then sort them out.

Power - As far as transmission lines are concerned, I personally feel that agreement of the data and theory is adequate for freezing rain. I think we can handle freezing rain reasonably well. Where we have data we can come up with realistic design loads for the periods that engineers are interested in, 50 years. I think we can do a reasonable job for rime where we have data. We're lacking droplet sizes and liquid water contents in certain areas - that's a matter of observations. The one problem that gives me the biggest concern relating to theory is wet snow accretion. From our experience wet snow accretion is the limiting load in Pennsylvania and I know it is further down the coast as far as Washington (D.C.). I suspect that for most of the eastern states, within a couple hundred miles of the coast, that wet snow is going to be the limiting load. I don't think we're in very good shape at all as far as the accretion equations are concerned, and actually what goes on the line. I would certainly encourage the people at CRREL to continue their work, and I think we should all think about that.

Pohlman - I think had some of the Japanese researchers been able to attend they would have brought some of the results of their work. They have been very extensively studying wet snow and the attendant problems. For your general information, I am going to write them again inasmuch as we have received some papers from other countries and the authors were not able to attend to present them personally. We're going to print them in the proceedings anyway. So I'm going to contact the Japanese again and encourage them to submit their papers also, so we will have some input from them.

Minsk - Some needs were shown on a Vuegraph yesterday, and I think one that covers pretty much all the needs, is better instrumentation. Accurate measurement of ice accretion, functioning under all conditions without ice bridging, which is one of the major factors now on some commercial devices, is needed. I think this points out the lack of confidence in present instrumentation and points to the need for development of better devices. Also, better anemometers that will function under extreme icing conditions that sometimes occur are needed.

Franklin - I'd take that a little further. I think that one of the things you could cover in a discussion is instrumentation and communications, communications being [...] by the data storage or data transmission. I think it would be a definite asset. It would be to us.

Minsk - What are some of the failures of the present set-up?

Franklin - Anemometers are the worst thing we have. Sometimes we get no readings - it doesn't work. Also, communicating data. When you're dealing with -55 or -60° weather - that's where our problems come in, and sites are inaccessible six months of the year.

Ervik - I will come back to the sketch I made yesterday. I think this could be a base for seeing what we have in common. What I have called the "core model" is something we all would like to know something more about. Apparently in this way we can use in building up the ice and then define how we get this out. Linked to this we have all the problems of measurement of icing that we

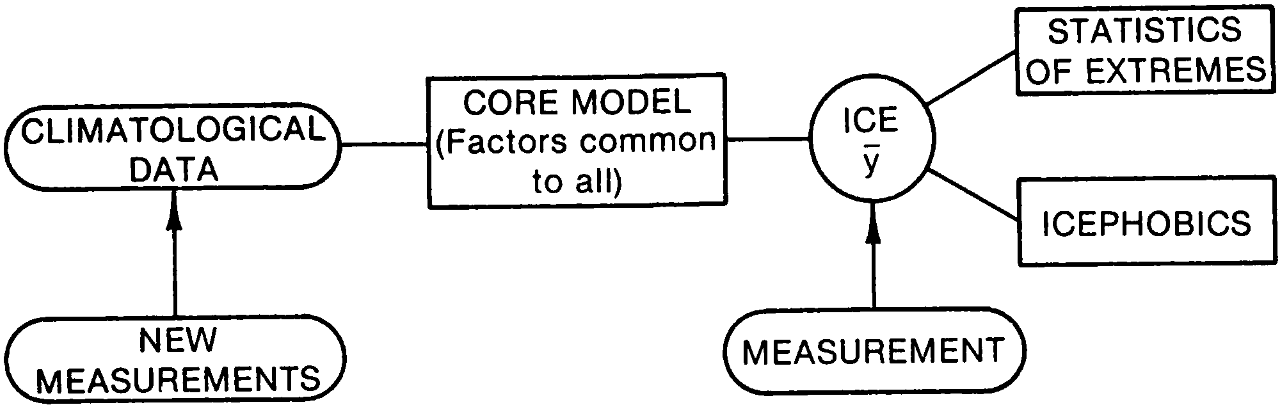

have in common. Also, how do we get the climatological data - how reliable are these data? What's not reliable? Should we encourage meteorological institutions to make new measurements? I mean such things as droplet sizes and liquid water. Is that realistic, to think that these could be future parameters to measure? And then out of this ice, we will have it in different ways. We will use maybe for transmission lines extreme statistics and pick out one extreme value at a site each year or more - that could be discussed. And others would handle it with some icephobic coating to get rid of the ice. So, maybe this might be a structure for seeing what we have in common and how we could look at these different parameters - do we measure this base the same - what is the difference when we are changing knowledge from one place to another? The problems in measurement - for instance, to measure wind during an icing storm, we know we cannot rely on these measurements we get from our meteorological stations, se we do not really know exactly what we have. So there are a number of problems we can discuss that we all have in common.

Jellinek - In my view that is the wrong way around. I would go first to the laboratory and study all the parameters which I can control singly and then go out with that knowledge and study icing in nature because you need some fundamental information on this whole business and you can do this only step by step when you can control the parameters. So I would plead for some fundamental work first.

Minsk - In the best of all possible worlds time is not a factor. But the collection of field data, I think, in order to obtain any reliability, requires many years of record and so I don't feel that the collection of field data should be delayed but should go along simultaneously with laboratory work, refining the methods of obtaining the data as you go along. But the basic field data have to be reliable.

Pohlman - I agree. I think we have considerable momentum going in many directions. In my own case, we have a very extensive experiment going on in the field at the moment. Now I think I identified certain needs that I would like to have to shorten the length of time that we have to work in the field. In that particular problem area, laboratory work has not really helped us to simplify our work in the field. But I agree with you that we should go in and throw away the excess baggage.

Rawlins - I think it's good to bear in mind that there are several constituencies involved here. Within transmission lines there are utilities that approach this in different ways. Beyond transmission lines there's aircraft icing, there's marine icing - I think they all should be looked at in connection with that model there because each constituency has a different data base to spring from, and a different set of answers it seeks; it tries to connect the two with this core model that Magnar referred to, but the management of the core model would be different depending on these input-output situations. I think there would be a thrust to focus too narrowly, to try to arrive at the North American Standard Core Model and to simplify down to something that could be codified right away. I know there is an impulse for this everywhere. Given the various constituencies, however, I think that would be a mistake. I think that we ought to think loose in terms of what's one of the core models - we need more technology to be reshaped to fit these different input-output demands.

Ackley - I just have a comment on the instrumentation question. At CRREL we currently have a graduate program with Dartmouth's Thayer School of Engineering and we have a graduate student working right now on a low-power instrumentation package specifically designed for cold regions work, something very applicable to these icing studies. The idea is that these would be in remote locations, would use low power and would transmit using digital multiplexing on a phone line, by microwave link, or by satellite communication. This is currently under construction and we expect prototype testing this summer and then installation on Loon Mountain next winter where we've had a continuous site for earlier work and where there is a weather station on top of the mountain. So maybe by this time next year we will have some results and some progress on instrumentation. The package will take any suite of sensors - whatever you want to hook up to it, since all this does is get the information in a format that you can burst out in the form of a digital stream. We're planning to put it directly in the computer at CRREL with an automated option so certain flags will be shown out and the thing will be self-calibrating. We'll get some alarm off the CRREL computer system if in fact something is going wrong with the data systems. That is one of the big problems with remote sites, and that is that by the time you've figured out something has gone wrong you've missed about 6 weeks worth of data. Right now what we have to do is send someone up every week or two to change strip charts or mag tapes or whatever, and I don't think anybody has really gotten around that problem.

Krishnasamy - EPRI is developing an instrumentation system to do the same thing - not on such a broad scale, but a data logging system.

Pohlman - We do have a very specially designed compact completely self-contained instrumentation package for measuring wind direction, velocity, air temperature, atmosphere pressure, and that sort of thing. This had to be ruggedly designed and it had to be portable because what we intend to do is anticipate the landfall of a hurricane and get into that area and deploy our instrumentation on transmission structures, arraying these so we have some packages along the coast line and some further inland. The purpose is to get extreme wind data, and a hurricane is a good source for that. These are completely self-contained packages which turn themselves on at a preset wind speed and then the battery pack will allow them to run approximately two days. Once it shuts down we don't want it to start up again because we don't want to lose any of the data we have taken. What we have been thinking about and hope to have underway soon is to change the power supply characteristics so that we can take data for a long period of time.

Krishnasamy - The Canadian Electrical Association has sponsored a project to do the same thing so that we can use these instruments at remote sites without any maintenance. That's a project that's just started and it's probably two or three years away.

Landers - I might mention about the data acquisition system Joe was talking about. It holds 23 Mb internally.

Ackley - I think a crucial question about remote systems is the failure of sensors - we have to have some indication of that, when that happens. Having some sort of a communication downlink is maybe an important component of these things.

Félin - At the present time, we have one remote station. It's updated every three hours. We're very satisfied with it, and we'll get most of our stations on [line]. We have other systems - microwave systems - that collect data, but some of our stations are on telephone lines, and all of our data, if we wanted it, could come in in real time. The problem is not there - the problem with us is in the sensors. We don't have the sensors.

Ervik - I don't think there is any conflict between what I said earlier and all the things that have been said later. I think that laboratory work will enter into the solution almost everywhere, for instance, as to the core model, and also to test instruments to be used. As I see it now, we should try to structurize this discussion and several speakers have already touched the problem of measuring. Therefore, I suggest that we should maybe set up a list and start with discussing measurements. This is obviously very interesting to several people - the kind of measurements to be made.

Félin - I would also be interested in a discussion of the physics of ice accretion.

Ervik - If you would once again allow me [to write on the blackboard], let's discuss measurements. What should we measure? [List] Wind measurements. We know that's an important quantity. Droplet size, LWC, precipitation measurements. Problems with icing measurements. Icing physics, in the field, the laboratory and theoretical studies. I think we could discuss according to this list. Those who are interested in particular things can state where they can make a contribution.

Félin - I have a comment. When you consider the measurement problem, what you need is icing wind loads for ground structures. Looking at this, if you measure droplet size and liquid water content, you still have to go through a model to get your load point. Now the direct measurement simply means you take some icing measurements and wind measurements which are the basic inputs to the load calculations. Once you start getting into the droplet size and LWC, you're really getting into the physics of ice accretion and you still have to go through the model and validate it which isn't very easy. We've heard a lot about models from several people; I think we should tackle one thing at a time. If we want a large scale observation program for icing, well let's measure direct icing in any way that's possible so that we can get long-term data and an icing system which will measure icing for us. And relative to the business of ice accretion, of course what we want is to validate these models, and droplet size and LWC are two important parameters and we have very little information on these. I would be very interested to know if anybody has some data. I've heard a lot about this Moscow tower in the last few days and I would like to know if their data would be useful to validate any of these models.

Laflamme - I agree with all of this. I just want to stress one point, something that was not discussed is this large scale field observation. We are getting ice intensity, we are getting the macrostructure of the ice, we look at the small portion of a cloud, but a transmission is not something small - it is very long, sometimes 1000 km, so there is a need for better field observations of storms. If you want to get some detailed measurement you have to be really careful because you have to take hundreds of measurements before you get something because this is too small a scale. We have a glaze storm, for example, this is a rather small scale. We should try to get a better knowledge of the space destruction. I agree with the extreme value analysis - this is very good. But when you have a grid network that's 200 miles apart, if there's a storm you don't see anything at the weather stations. This is very difficult because you have to run after a storm, like you're trying to do with galloping or high wind. What we need is a very simple passive ice meter. Because transmission line design engineers are getting more sophisticated now, they aren't happy with safe designs any more, they are looking at risk assessment and costs so I think we will need better statistical tools if you want to use extreme value techniques and you have to improve the basic analytical tool.

Pohlman - We have identified several areas. I have the same problem - when David Minsk, Jean Laflamme and I were putting this program together we had the same problem of having to categorize your papers that we're having now, and we're trying to categorize this discussion now. There are these subject areas - let's call them that - there are experiments that should be run in the laboratory, there are experiments that should be run in the field. We need to measure for the purpose of developing basic information like droplet sizes and that sort of thing, but we also need to take measurements of the ice build-up as it exists. We need to verify our models, we need to do all these things. And these are individual little links in a chain, and the chain is slightly different depending upon what your interest is - whether it's a transmission line, an airplane wing or whatever. Let me shift gears for a moment. I detect that there is a general interest here in some kind of a cooperative effort where we can share the results of our research work, and information, and so forth. Any one of these tasks cannot be tackled by any one company or any one person - it's got to be done on a cooperative basis, but somebody has to run it, somebody has to be the motivator. Somebody has to inventory internationally who all is doing work or is interested in doing work in that area and then trying to come up with some division of activity. I would like to ask for some comments from the floor - does anybody have any ideas about an arrangement whereby an organization could create this atmosphere of information exchange? The only one that I know of that seems to be working reasonably well is an organization of some 5 or 6 countries in Europe called CORECH. They banded together because they felt galloping was receiving inadequate attention in CIGRÉ and the other organizations they belonged to, so they formed their own. Dr. Dienne from Belgium, with the state laboratory there, volunteered to act as secretary, and they defined future programs, have assignments that each is supposed to look into and bring their contributions to the next meeting. I can see such an organization of people interested in the atmospheric icing problem in its many facets. I can see several secretariats in this room, and I would like to see some volunteers. But first let me ask for some specific comments on the desire to have some sort of a communications system or organization or such. I don't think we can sit in this room today and list the instrumentation needs, or something like that, and say who is going to do what.

Fikke - I certainly agree with you - we have to have some kind of umbrella and we must have a kind of loose organization that we can keep in contact with. There aren't many aspects within atmosphere icing, there are many fields of work as we have had many examples in these two days. The transmission line problem has been stressed as one big area, but even within this problem there are also specific fields. I think that the direction that we're working, the methods we use are different depending on the problems we have. In the United States there is the extreme of the ice accretion giving loads between 1 and 7.7 kg/m; 7.7 kg/m is almost where we start in Norway. We have a completely different problem in this respect. In Norway, we have much in common with the Canadians. Among us here we are not so many so we don't need a strong and rigid organization, but we have now the possibility to contact each other.

Ervik - I would like to clarify something. I don't think there is any disagreement between Béatrice Félin and myself. Of course, I see that you all the time have to have somebody to pull everything together. But I am concerned, from the work that has been presented here, that some of the work has been much confined to some of these separate ideas which I also listed here. So what I thought would be that those who are intested in a specific field, they might be encouraged to continue to do so and to contribute in their way. If I can say some comments also about the kind of organization, I am a little afraid [of] a new organization because we already have [some for] icing; this could be discussed within CIGRÉ or within IEC and maybe the contacts should be kept more informal. We do not necessarily start to build this organization now but we should plan a new workshop, for instance, in about two years.

Pohlman - I see a similarity between your comments and Mr. Fikke's in that you're talking on the utilization of this technology, and I agree on the differences in your service areas in the case of transmission [lines which] are going to dictate what is useful to you. Your problems and those of Jean Laflamme are somewhat similar, they're somewhat similar to isolated pockets in southern California. I don't think that this particular group should be involved in any way trying to duplicate or get involved in the work that's going on in IEC TC11 or in CIGRÉ Committee 22 or anything like that. I think there are several areas where we all recognize we know precious little about and we are trying to determine how to attack, and no one country or no one utility wants to subscribe to coming up with answers to all the questions that we have. And I think that's what we're trying to identify.

Olsen - I think the comment of Mr. Ervik is quite correct. If you generate an organization you have to get funding for it. Now basically what he is saying is a meeting every other year, [and that] makes a certain amount of sense. People are going to be attacking things in their own way. Anytime they find an instrument that works, everybody else is going to be using that instrument unless it's tied up. What I'm saying is if we hang together loosely and every two years get together and talk about it, by merely transferring information, I think you will get precisely what you want without any extreme organization. It's the same sort of thing that's done with aircraft icing.

Minsk - We should recognize that only a fraction of the organizations, individuals, countries, interested in atmospheric icing are represented here. The railroads, for instance, have problems that aren't represented, also the PT&T's in various countries; the question is where can they now go to get information that they may not know even exists. There needs to be a central clearing house, some central point of contact where those unfamiliar with the problem can write. And in particular perhaps a world data center where the information is collected and made available would I think reduce quite a bit of the problem of providing most efficient contacts.

Franklin - I think if you try to make a formalized organization you're going to wind up with a core of people who are interested in one specific area. It's going to be one of two: either the petroleum industry where you have structural icing problems on drill rigs, or the utility industry. Anyone else with any ideas would be pushed to the side. That would bother me since I would be interested in seeing other facets of engineering than utilities which I'm primarily interested in.

Pohlman - Let's assume for a moment that the best future step for us to take is to look forward to having another workshop or symposium in say two years. Let's hear some critique of the format that we used in this particular workshop to help those who will be planning the next one.

Lozowski - Could I mention something else that I personally would find helpful? I'm a supporter of this notion of an informal arrangement and it would certainly be helpful to me if we could induce someone like CRREL to publish a directory of people who are involved in this area. We do have something like that in the list of participants but we all know that not everybody interested in atmospheric icing is here. Some kind of a directory - it wouldn't have to be a fancy book - could be published along with a short listing of the types of interest that the people have and their capabilities, their areas of expertise, and also their needs. Distributing this would certainly facilitate the interaction among various groups. We would then know who all the modelers are, who all the transmission line people are ...

Pohlman - You are suggesting that an organization such as CRREL might be encouraged to produce a kind of reference book listing sources of information and of people who are doing work in the general areas of icing so that if someone had a specific question, he could look in the little directory and perhaps find someone to talk to about it?

Minsk - Are you going to answer that?

Pohlman - No, you are (laughter). Is this possible?

Minsk - Yes. One of the functions of CRREL is to act as an information clearing house. We do try to keep track of the research going on around the world in our fields of interest. As many of you are aware, we have the continuing bibliography project at the Library of Congress which searches the world's literature in cold regions engineering and publishes the Bibliography on Cold Regions Science and Technology. If you're not familiar with that I'll show you a copy. It's available to the public for purchase. We have practically everything that is in the public domain in either hard copy or microfiche, and it does represent a resource that is invaluable and available to anyone. In that sense, we do already act as a clearing house, a central repository of world-wide knowledge on cold regions problems. Therefore, it would not be out of line for CRREL to provide a directory of workers in the field.

Pohlman - Let's have some discussion of the format we used for this particular meeting. Were the sessions too broad, too narrow?

Thowless - In answer to your question, and with regard to what is on the board under application areas - though my interest is sea spray icing, I would recommend you do not include marine structures - you have more than enough problems with just atmospheric icing. It's not that there isn't a commonality between the two - it's true that someone interested in sea spray icing is interested in atmospheric icing and vice versa - I feel you have more than enough. The physics of saline icing is a bit different from freshwater icing, hence my recommendation you stay away from that sphere.

Pohlman - We did, as a matter of fact, reject some papers dealing specifically with sea spray icing because I was somewhat apprehensive this would make the subject matter too broad. I don't know if there would be quite the interest in that as there is in atmospheric icing.

Minsk - We should recognize that there is some commonality of interest in measurements, for instance, and in protection methods, so I don't think they should be completely divorced.

Rawlins - I think I would agree with that because the work that was described on the prevention of icing on canal locks certainly has application for prevention of icing on radomes and all sorts of structures. I feel it would be a mistake to exclude that. I think that's one of the things that struck my interest.

Minsk - That's marine icing rather than atmospheric icing and thus would be excluded if we stuck only to atmospheric icing.

Olsen - As a practical matter, let's assume you have a meeting in two years. Would it not be logical to in fact have those subjects and if there was the interest or apparent separation - the sea structure people don't have a place to meet, is that correct?

Pohlman - I don't think they have had a meeting specially directed towards this.

Olsen - Ok, it strikes me that at the next meeting you ought to include them and then if their interest is all that separate then they can go their own way. Now aircraft is already separated out. There's always overlap, and you don't want to lose this overlap.

Power - I agree with this. The basic physics of ice accretion came out of aircraft icing, and it's all founded on that, so I don't think we should split up too soon.

Nauman - For that matter, though, it seems to me you could have a joint meeting where you could have discussions on sea spray icing and transmission line icing going on simultaneously.

Minsk - No, I think that cross fertilization is the value to be gained from a joint meeting.

Berry - I have two comments, one addressing the immediate topic of critiquing the meeting format. I suspect that this last phase might have been better handled by using a divide-and-conquer-tactic and splitting into some smaller working groups.

Pohlman - We talked about that, and talked ourselves out of it about 20 minutes ago.

Berry - Ok, the other point I have is certainly one of my big interests - data on ice accretion and the supporting meteorological data. The best data sets tend to be the longest and not the quality ones, and I suspect that if some sort of recognized coordinated data collection program and archiving center is not formed soon, then in two years you're all going to meet and say again we need more data, and then you'll meet two years again and say the same thing, if nothing happens. So I would like to put a plug in for somebody to consider setting up a recognized data collection point. There may be organizations that can handle this - the World Meteorological Organization (WMO) is something you may not know about, but it plays a large role in coordinating data gathering activities internationally already for meteorological purposes. So it is a possibility we can try to squeeze in there somehow. There's an International Energy Agency that may or may not have an interest here.

Howe - Nobody's mentioned it - to go out and find possible organizations or people interested or have a contribution to make. For instance, I don't believe this workshop was announced in the AMS [American Meteorological Society] Bulletin. I'm sure there are quite a few people out there who have a contribution to make, but how do you find them?

Pohlman - That's a very good question. I would like to tell you the thinking that went into the decision to do what we did. Inasmuch as this was the first one, we purposely tried to collect participants, and among us - CRREL, Jean Laflamme in Canada, Magnar Ervik in Europe, and myself, we certainly know from the utility standpoint who is doing work around the world. But we tried to identify as best we could sources of information and people who are interested in this and get them here, and I think that we were reasonably successful. We unfortunately didn't give the Japanese time enough to prepare and that was a bit of a loss since I think they would have brought a wealth of information on wet snow and that would have been a timely subject for many of you. Speaking for myself, I'm very gratified with the attendance here and I haven't seen very many people sleeping which indicates to me that [this is of great interest]. Perhaps whoever is going to arrange the next workshop may want to scatter the publicity a lot wider.

Félin - I have leafed through the CRREL bibliography on icing problems and I notice that half of the articles are in Russian.

Minsk - 65%.

Felin - Unfortunately very few of us know Russian and there are no Russians here today and I sort of miss the contribution of the Russian people to our subject.

Pohlman - I really don't know why they're not here. Their papers are here but the authors aren't.

Makkonen - I have some comments on international aspects. I don't want to criticize the arrangements for this meeting - I'm sure everything was done to reach as many people working on ice accretion as possible. But I just want to point out that we have several types of meetings on ice accretion problems, and here are several examples: one of special interest was a symposium that was in the German Democratic Republic in 1967 and was a meeting for this same purpose. If we look at the countries that are represented in this meeting you can see that there is nothing in common except in the subject of the meeting. So there is no one here at this meeting represented at that meeting [GDR] and vice versa. We have heard so many important and interesting papers presented here that we might start to think that perhaps it is not that serious for us here but I would like to point out that [in terms of] quantity of papers published on ice accretion problems in recent years the conclusion would be that actually more research on ice accretion is done by those countries than by the countries represented here now. That's one conclusion that you can make from the number of papers published.

Landers - This is the second meeting of this type [on a specialty subject] - the first one was on winds. The reason these meetings came about was because we realized that the utility industry can't do it all and that there is more interest across the world and in those areas that can be addressed in a common thrust instead of everybody going in his own direction - that's not going to solve this major problem. So from a selfish standpoint I would like to see us come up with a recommendation as to what the priorities are of the work that needs to be done, that each one of us can benefit from and then we can go ahead and split off into the groups we have. We have more talent sitting in this room than I think has been pulled together on this subject before. If we can come out with a direction - just to begin interfacing that work, too - Beatrice's [Félin] comments [on the subject] if you have icing problems go out and measure the icing load. But approach it from a common data base. I agree with the comment that two years is a long time - we can miss a lot of data in two years. In the United States just look at the meteorological data stations we have - we use a total of 125 in our loading base, now we find out there's 8-9000. Maybe we're coming at this from the wrong side. Let's figure out what we need and get it, then we'll worry about how we'll fracture it off... The first priority I would say is data, basic data, field meteorological data.

Félin - For basic field data you need sensors.

Landers - What doesn't exist that needs research dollars to develop?

Tattelman - It seems there is a lot of interest in these icing events that the utilities have observed and they certainly have a lot more experience in this area than perhaps the National Weather Service, which doesn't observe icing. But yet I've never seen any published results of these icing occurrences. So the utility companies are like the rest of us who are in design from the other side and would like to see more data but they aren't publicizing the data that they have, and they're also not publicizing the research efforts that they have underway. These results seem to get distributed to a very small group and they never make it into the open literature. I think therefore that the priority would be to have the utilities take the extra step and pay the page charges for getting this information out. It would be of use to us all. Even from the standpoint of statistically analyzing what there is available and making estimates of what could happen out there in the environment.

Pohlman - That's very true in the U.S. - utility people publish for each other but a lot of these things do not appear in the open literature and therefore are not generally accessible. Is that true in other parts of the world?

Howe - It would be nice if all this data could be published in the open literature but that's not going to happen in the real world - it's too difficult. I know it would be a lot of work for somebody, but I'm wondering if a semi-annual newsletter [would be appropriate] - not with data but just telling who's doing what.

Landers - Let me mention something we're getting set to undertake. We realize that there is not good archiving today, or even a good idea of where the data is. What we [the utility industry] are undertaking now is an inventory of all the meteorological data that exists. I don't think this has ever been done - now remember, we're getting hints there are some 8 or 9000 out there. So we'll be using the massive labor base of the utilities and let them do the archiving for us, find out what's useful and what's not. I would recommend that maybe that's the first undertaking. Let's find out what we've really got to work from and then see what we need to shore up.

Pohlman - Phil, when this information is available, will EPRI issue some sort of report and analysis of it?

Landers - Yes, definitely. That's great for the United States, but I'm recommending that maybe we take this a little bit further, and that world meteorological data archiving sounds like it might be a good place to put it.

Ervik - I think we have fairly good meteorological data in Norway - I think it goes at least 25 years back. We have such data that we can use, and if we were able to convert these into icing in a reliable way then we would have time series that we could use for statistics of extremes. It may seem a little selfish, but we don't see a very great need for us to do anything more than we have in this direction. But I would be very interested in discussing maybe if there is any other meteorological parameter that should be measured and that other meteorological institutions have that we do not have. For instance, information on liquid water content.

Bilello - One of the problems associated with field meteorological measurements, or the availability of such data in the literature, is site-specific. In other words, in a review of available climatic records one can probably obtain anywhere from five to possibly 100 years of data for many locations, but the problem is that they are of sites that are not directly applicable to your needs. The information you require is often site-specific, as for example, the top of a mountain, where no measurements have ever been made. In some cases, if your area of interest is environmentally uniform - with respect to topography, vegetation, exposure, etc. - interpolation and/or extrapolation of available climatic data from nearby stations will provide good estimates of the climate at your particular location. However, if your point of interest is somewhat isolated or environmentally unique, then it might be necessary to obtain at least a year or two of meteorological measurements at the site. With these on-site values then, an analogy study can be conducted in which the data are compared with those given at the nearest weather station with 20 or more years of record.

Franklin - We defined instruments as one of the things we really need but we should take it one step further than that because if you want to measure, for example, you can specify it in miles per hour, but how are you going to specify ice loading - is it going to be kilograms per square meter, or kilograms per meter length of cable, and if so we've seen already that ice accretion is a function of wind speed, cable diameter, etc? What I would like to see is some specification we can all have for a common input - one thing we're all going to measure since there is no way I can compare my readings with someone else's.

Pohlman - Yes. In the matter of wind there is the little thing of averaging time. You can get 40 years of data but you don't know the averaging time, you don't know what instrument was used or where it was located - things like that which make it difficult to use the data. And it's even worse in icing.

Nauman - Just a comment on what was said earlier on data collection. In Alaska we don't have as much data as you other folks have, but I've heard this in a number of papers given in the last two days that what data was being collected wasn't where you needed it. That's particularly true in Alaska. We're getting meteorological data but it's always at the airport.

Rawlins - Analogy between a transmission line that's 100 miles long and has three stations along it to get your data from, the analogy between that and trying to get the 100th harmonic for a Fourier series we've taken three data points for the record. It gets to be a futile exercise - there's a certain amount of futility involved in getting more data because you realize how much data you need and you realize you can't have it. There's a hole in the technology here which I think that people like Rich Richmond and other crystal ball gazers - well, they'll take these few points and then you've got super Fourier that runs along there in an airplane or a car and from his own data bank, makes these little interpolations and fills in those higher harmonics. This is a region - the crystal ball region, if you want to call it that, that is part of the missing technology. I had to get that analogy off my chest before the break.

Power - I wouldn't agree that it's crystal-balling. Let's take a simple example - wind, for example. The problem in specifying wind for transmission lines over a wide area of varied terrain has been solved pretty well. You don't have to have wind measurements for every little hole and corner. We have general approaches whereby we can take the wind above the friction level and using roughness values go down and get the wind for transmission line purposes perfectly well except for certain areas. Now I agree there is a problem in icing, but I think that for glaze icing we're getting to the point where we can specify glaze icing over varied areas. We can for rime, and we certainly can for snow. It's not all up in the air - we've been working on this for the last 15 years and we've made a lot of progress.

Olsen - Perhaps you should use the example of aircraft icing - the game as played by the FAA. Out of 256 isolated data points, the whole FAR 25 criteria which is an extreme value probability kind of thing, was generated. Now it's got problems, of course - events might get a worse liquid water content, or a colder temperature, or whatever. Anyway, it's the same parameters you deal with except you're on the ground, and his point of extrapolating to the ground is in order. Now the FAA is in the process of taking a much larger data base - about 1000 times larger, running it through a statistical model, and they want to have it as a function of altitude. They will want to get, I might add, some ground measurements - see how they all tie together. So in a way you've got this blanket cover over you that is going to be statistically handled with its uncertainties - but you're predicting 25 years in advance, and you have a worst case thing anyway, so I don't see where that is disturbing. So I think that the package is there if you can put together the data package that you have and maybe follow it with the Russian example, where they seem to have many weather stations with 5-mm cylinders at 90° and 2 m off the ground and get some measurements on these every once in a while and get an idea of the ice loading in a gross sense. I appreciate that this is a simplistic approach - but it's practical.

Félin - Glaze storms have very limited extent though some are very wide. You're lucky if the synoptic stations are 150 miles apart and in remote areas maybe 2-300 miles apart [so if a storm occurred] between stations you'd never see it so you're extrapolating between two stations and maybe using data from stations which haven't seen real glaze storms for maximum intensity. That's one problem. In Quebec we have 150 of these simple instruments with at least 100 concentrated in the St. Lawrence Valley. Even with 100 we miss a lot of storms.

Pohlman - It looks to me, the way the discussion is going, we're going to be able at best to single out two or three of the most critical areas for attention. We're talking about taking more field data, and developing specifications for sensors.

Let's review the subjects:

1. Sensor development.
2. Development of core model.
3. Climatology.
4. Statistical analysis.

Ervik - I think it's too early to establish these working groups. We should start discussing if and when and where we should meet next time because we have to digest what we have learned at this workshop and think over the possibilities for participating in the things you have listed.

Pohlman - How about having a small cross section of talent with various expertise, background, countries, etc., who would collectively try to analyze what progress we've made during this meeting and come up with a recommendation - definitions of these working groups, etc?

Assur - Not only during this particular meeting but the present state of the art since some people unfortunately couldn't come here, the Japanese for example.

Pohlman - We don't seem to be moving in any direction here and maybe it could be accomplished in a smaller group, when people can sit down and think about this, each in his own way, scratch some things on a piece of paper and exchange the papers. Does that make any more sense?

Franklin - I disagree with that violently because with meteorological data, time is of the essence. I think leaving it for two years of sensor development, or anything like that, we're two years further behind than we are now.

Assur - We have data now. There are some organizations which have a lot of data which require analysis. You don't have to collect more over 10 years - the data are available. For example, not a very good one, but the German government put a lot of money into icing research on ships. They financed two research ships, and they just collected data, data, data. All we have to do is smoke it out.

Franklin - Assuming there's something there to smoke out.

Assur - Oh yes. Those people are trained meteorologists - not too good as physicists, but at least the observations are there. Then the Norwegians have data - probably the best in the world. We also have a lot of data on microfiche at CRREL - these are Soviet data. We have data. We don't need 10 or 20 years to collect them.

Mozer - From a practical aspect I'm not sure how much this group, or for that matter any other group, is going to be able to accomplish in two years as far as impacting on the way how things are being measured today, just based on the inertia that organizations have - how they do things. I would like to suggest that we continue along the line you've started, Joe, and identify those areas and try to get people to express an interest in those various areas and come prepared, either with a preprint by the next meeting two years from now with the state of the art and the definition of needs. I don't see how you can accomplish much more than that.

Howe - Nobody has much data on wind during icing because there are no sensors to measure that. We have a lot of data on Mt. Washington but that's not much help in British Columbia. So please, somebody develop an all-weather anemometer.

Assur - What you said is entirely correct - we need an anemometer which works under those conditions. You're right that a lot of data have been obtained from Mt. Washington - it's a beautiful site - you are not correct that information would not help in British Columbia - it would. Someone made the suggestion - why not at the next conference announce that we would primarily accept papers on the state of the art. In other words, each country would do their best to present whatever they have to offer for the state of the art. If you announce it now, it can just about be done in two years. We have to invite someone from each country to go in that direction. There's a lot available - it just requires some digging.

Rawlins - I was going to say much the same. I can't remember the exact name of the organization - the Symposium on Wind Loading and Building Construction - but it's a symposium held every four years. I think its a good model for this group. Oh yes, it's the Wind Engineering Association. Part of their activities are to invite theme papers from established authorities to present the state of the art. You don't necessarily aim at a country but at an individual, or a group of individuals who will do this.

Assur - It just happens that there are certain strengths in certain countries - Japan has a tremendous strength in icing on ships, for example, so they could be invited to cover that topic. The Russians have a strength in their observational network - they have the best in the world, so you invite them to present that. The Canadians of course have tremendous strengths and interests so you invite some Canadians.

Pohlman - We're going to have to get some working groups started. The other suggestion is that we leave it up to whoever is going to host the next meeting and see that the invitations go out for the state of the art type papers in these various areas.

Ervik - I would strongly support the last way. Maybe if only an organization, I would be in favor of a small group to prepare the next meeting.

Pohlman - An advisory group that would in fact set the flavor and the format for the next meeting. Is that what you're saying?

Ervik - Yes, and to list it in a way that ...

Landers - I don't want to lose two years - two years is a long time. We have struggled with the damn thing for a hundred years or more, and everybody has been very pleased to shove it off two more years. If we shove it off two more years in getting the framework developed and the momentum behind it, we'll shove it off two years beyond that. Look at our national electric safety code - we've patched that blamed thing for 40 years now and that's exactly how: leave it to the next group. If we don't do something now we will have lost the momentum.

Ervik - We can vote on it - one year or two years for the next meeting. I have no strong feelings one way or the other.

Assur - You can't do it in one year. Two years is the minimum to make the next step.

Pohlman - It took us six months to organize this but we had an untapped source of information because many of you have been doing work for years and it was just necessary to bring it to your attention. If we're going to make requests that are very specifically oriented, that we want you to come and give us a state of the art paper in this particular field, then I would agree that you're going to have to give those authors, those researchers, more time to prepare.

Tattelman - I get the impression that somebody anticipates getting an objective measure of icing, wind speed, and perhaps some of these other meteorological elements to be made in the harshest of environments sometime within the next year or two. There's no reason why we can't accomplish that. I think we have two diverse groups - those who want all this information and those who could be involved in doing that particular work. But it's very hard for one research organization to justify doing research to help a number of individual special interest groups. If you're talking about instrument development and testing and that sort of thing you're talking about a lot of money. So I think when you say - let's have something accomplished in a couple of years, I think you're being totally unrealistic.

Landers - All I'm saying is, let's not wait ten years to get started. It's going to take a lot of money, a lot of time, but unless we as a group define the starting point then we [stagnate].

Tattelman - We would go a long way if we added to what we've heard in the last couple of days the information that I think is available that has not been presented. We could probably go on for another couple of days presenting data that has been collected and not publicized, methods that have been tried and not publicized. Each individual may have 15 minutes perhaps to express one aspect of their work. That is not really adequate to cover that area of interest. If you can get all this information that is stuck in the files out in some published form or as a directory as somebody mentioned earlier, of individuals and what area of expertise they have, what information they hold, then you're starting to get this information out where it can be used.

Olsen - Let's hold a meeting say in two years - let's get a volunteer to do that, let's organize into five groups which will be the groups for next time. Those people who are going to be head will write a status report - this is the state of the art as we see it from what we've learned this time and you or CRREL or somebody will put this out separately or with the published documents you have here and there will be an overview from the chairman which is you. The state of the art suggestion is the key and that will invite out the kind of stuff you're going to get in the shortest possible effort because that's the incentive people want.

Minsk - We should consider some of the logistics of it - the earliest that the proceedings will be out, I would guess, will be October or November this year and that, once distributed worldwide, is going to announce the fact that there is such an interest and those we haven't reached will be so notified. Then there has to be time for digestion of the papers so the earliest I feel that it would be practicable to consider a follow-on workshop would be August or September of next year, but I would certainly opt for two years as the ideal time even though there is the delay in setting up the modus operandi. Secondly, I think that immediately we could try to fill the gap and this could be accomplished by CRREL with the assistance of all the others in providing a specialized bibliography including in particular the unpublished material from utilities, from the national organizations that have been working on it, and then disseminate that worldwide. That along with the listing of workers in the field would provide the structure for further work.

Krishnasamy - I support the idea of having this working group start now and at the same time plan for a meeting in two years. These two things can go on side by side.

Ervik - I'm prepared to invite you to Norway to Trondheim, for the next meeting [applause]. We may discuss when, but I think the best time would be May or June. That's in 1984. I think that most people here think that one year is too early.

Assur - I would also suggest to send out the invitations to alert the professional circles very early. If you do it late you don't get as good papers. We have to approach those people who are not here, so they have time to prepare their material.

Pohlman - Would you like some volunteers to serve as advisors to you on this activity? You'd probably want some contact in the other countries.

Ervik - Yes. I said that the only organization I would be in favor of at this time is a small group to prepare the next meeting.

Pohlman - Yes, I know that. But I was thinking that - I know that Phil has offered EPRI's support to you from the States' standpoint and I'm sure that CRREL would cooperate in that effort, and maybe some of the Canadian friends could volunteer to help you and the other countries as well. Ok, we finally settled something, now let's get back to the working groups. We have identified four areas of activity. Are there any more?

Olsen - I guess I argue that 3 and 4 are really the same because for the short term the statistical analysis of existing data is really the key issue, and you want to get a paper that addresses that.

Mozer - I was looking at it from the point of view of Magnar's diagram that the item 3 is the identification of climatological data that needs to be collected and how it should be collected and what kind of information is needed, whereas under statistical analysis I was looking at that more from the aspect of say, for example, wind and ice loadings, combined with extreme value analysis or whatever kind of analysis.

Pohlman - The simplest thing would be to put it together and then if you can't get along you can sit on opposite sides of the room.

Jellinek - Maybe we could have ice adhesion.

Pohlman - Any more?

Nauman - Question. About this meeting scheduled in two years - are we talking about including all these application areas?

Pohlman - I assume that will be a decision that our host and his advisors will reach when they set the format for the meeting. Do you have a recommendation?

Nauman - At this point my recommendation is to include all of them.

Thowless - I'm surprised it hasn't been mentioned - standardization of some of the measurements.

Pohlman - Yes, that's right. We couldn't decide what to call it so we put this - the core model - in lieu of it. But that doesn't really say what you just said.

Minsk - I would enlarge item 4 to be a little more comprehensive and call it the physics of ice accretion which would have as a subheading statistical analysis. All of these feed into that [modeling] but as identified subjects for further investigation.

Makkonen - What does this no. 2 now include?

Pohlman - I don't know. I just wrote it down.

Minsk - The core model is the synthesis of all these others. All of these feed into the core model. The core model really should not be listed separately - it's the consequence of everything.

Landers - What I would like to see is each of the chairmen of each of the sessions provide a summary that would go in front of that for the proceedings, something of a state of the art review so everybody wouldn't have to wade through the entire proceedings to get the flavor.

Minsk - The abstracts should serve that purpose.

Assur - Somebody mentioned the need for standardization of observations. The only network we know about where things are standardized and data are being systematically collected is the Soviet network. Nobody [from there] showed up here, but we have the data here at CRREL. What they have essentially is a completely standardized way of measuring ice accretion. They do it in their entire network in the more important stations - all over the entire network the same way. It may not be the best way of doing it, but it is a way. Essentially they place cylinders horizontally, of various diameters, at well-defined sites. Since they take meteorological observations anyhow it's just an add-on, and then record when icing occurs, under what conditions and so forth. They have special studies where they relate the data they've obtained, which of course are biased since they are near the ground, to powerlines. Icing on powerlines is more severe simply because the wind is stronger at a higher elevation. All of it is systematically observed so whenever they have to design powerlines in a given location, they do have the data. Furthermore, if you compare the icing results with the weather observations you develop a technique - how to predict it for those places where you don't have the icing information. Something on this line may be useful to look into. Perhaps the device you mention - the Rosemount detector, would be a more elegant way to do it and maybe the Canadian network could be talked into a similar approach. It's missing in other countries.

Minsk - Are you suggesting an interim, ad hoc agreement to adopt the Russian technique?

Assur - No, I'm not suggesting to adopt the Russian technique - I'm suggesting to have a fundamental network but perhaps with better gages.

Minsk - Yes, but if the gages aren't available now, and a cylinder is..

Assur - Yes, in that case it's a very simple way - let's do it.

Minsk - In order to start collecting data with some common basis for comparison.

Assur - Yes, and negotiate with the meteorological network in Canada and the United States.

Olsen - Here's my scheme [placed on blackboard]:

Application areas

- Ground structures
    - Transmission lines
    - Towers (powerlines, TV)
    - Transportation
- Sea structures
    - Ships
    - Drill rigs
- Aircraft

1. Climatological
2. Instrumentation
3. Ice accretion and its consequences
4. Mitigation of effects
5. Applications
6. Modeling

Ervik - What is listed is a lot of good ideas. I think everybody should look at this and then it should be left to the advisory group to ask for papers. In addition it should be left open to give contributions which do not fit in anywhere.

Pohlman - In the meantime, if we are to get anything started before the meeting in Norway, we still need someone to take on these various working group activities, define a scope for them, perhaps try to identify and prioritize the sub-activities under each of these general categories.

Franklin - I'm volunteering for the instrumentation group.

Pohlman - Very good.

Makkonen - I think there is one question before we decide to volunteer for some group; perhaps it could be modeling because we have a lot of good data of ice accretion. We have more or less good models but we should compare these, we have little for verification of the models. That's a really important thing, we should collect data and make data analysis not in a statistical sense but in the sense that we compare the field data with the models.

Félin - We've obtained some funds to develop an ice-free anemometer. I'm involved in this as well as Samy. I know that EPRI has some ideas. It's already going and it's going to be field tested next winter. We're also working on Rosemount ice detectors quite actively ourselves with our research institute of Hydro Quebec. Whatever happens here we're going to continue, and if anybody is interested or would like to know what we are doing, we could have a committee working group on this. We have obtained funds from the research and development group of the Canadian Electrical Association for development of a model, and this is going; if anybody wants to get into this, we might as well exchange information. I know Norway is interested. It could be very informal, but we can communicate and exchange ideas and information.

Krishnasamy - I think I would be able to help, because I'm on two projects to develop an ice-free anemometer and an instrument package for a meteorological tower.

Pohlman - There is a working group under the COECH banner trying to find out what people are doing on instrumentation worldwide. Weicker of Holland is the chairman, and I think the work is just starting. Certainly he would be delighted to find out what your experience has been ... I'm going to suggest this - everybody make a list of these items, think about it, and if someone would like to head up one of these activities drop me a line, call me, send me a telex, or something. If I don't hear from anybody volunteering to take one of these things over before our next major communication to you, which is the transmittal of the proceedings, then I'm going to be after some of you and twist your arm a little bit.

Patnaik - May I make a suggestion, maybe we can just join the groups you've listed here and then you can pick up a chairman. But at least you have a list of those who are interested in the subjects. I would like to be in the application group.

Pohlman - Dave Minsk graciously volunteered CRREL to be a clearing house.

Minsk - I think it is more appropriate for industry to do it, but then we have "what industry", but I think it should ultimately become industry's responsibility. But to get this started I think that CRREL can do it.

Pohlman - So if you have anything for the good of the organization, I think if you send it in here then you can spray it back out.

Minsk - Yes, a current awareness type of thing - work that Hydro-Quebec is planning to do next winter for instance, the results from last winter's work, work planned in Finland or Norway - that would be of interest to everyone here.

Pohlman - While you're working up your score cards I would like to take this opportunity to thank the Chairmen of the sessions who did such a good job of keeping us on schedule for the last two days, and I'd like to thank each of you authors, and I thank all of you for participating in what I feel has been a very effective and useful two days of discussion about a problem area that we all have an interest in.

☆ U. S. GOVERNMENT PRINTING OFFICE: 1983--601-774--106

END

FILMED

9-83

DTIC